Aspects of beach sand movement, at Gibraltar Point, Lincolnshire.

by

Howard R. Fox, B.A. (Hons.)

Thesis submitted to the Department of Geography, University of Nottingham, for the degree of Doctor of Philosophy.

October 1978.

CONTENTS

	Page
Abstract	i
Acknowledgements	iii
List of Plates	v
List of Figures	vi
List of Tables	xiii
Chapter 1 : Introduction and background	
1:1 Introduction	1
1:2 General physical background	6
1:3 Waves and wind	10
1:4 The offshore zone	18
1:5 The beach	20
Part 1	
Chapter 2 : Data collection	
2:1 Introduction	43
2:2 Tracer production	44
2:3 Preliminary experimental procedure	51
2:4 Measurement of process variables	56
2:5 Sampling techniques	60
2:6 Problems and efficiency of field procedure	68
Chapter 3 : Data analysis and presentation	
3:1 Introduction	76
3:2 Tracer grain counts	77
3:3 Data presentation	84
3:4 Numerical description of sand movement	89
3:5 Data rejection	96

	Page
Chapter 8 : Evaluation of the model	
8:1 Introduction	287
8:2 The predictive model	287
8:3 Summary of findings	297
8:4 Conclusion	300
Appendix 1 : Instrumentation	305
Appendix 2 : Maps and diagrams not referred to in the text	320
Bibliography	345

ABSTRACT.

In this study fluorescent sand tracer techniques were used to investigate sediment movement on the foreshore at two sites on the south Lincolnshire coast. Working over one tidal cycle, low water to low water, tracer release at different points across the beach revealed a complexity of sand movement in this strongly tidal environment. It was found that sand moved both at different rates and in contrasting dominant directions on different parts of the beach over the same tidal cycle. At Gibraltar Point there was confirmation from the tracer experiments of the importance of tidal generated currents on sand movements on the lower foreshore.

Tests conducted to study the patterns and rates of movement of different grain sizes produced inconclusive results largely due to low recovery rates for the tracer. However, from the evidence available, it appeared that sorting of sediment was taking place only in the sense that finer material was moved away from the release point at a faster rate than coarse material and not because different sized grains were moved in different directions.

In a consideration of models for the prediction of longshore sand transport two of the most commonly used models were tested using data collected during the tracer experiments. The results confirmed the success of the two models, one based on the wave power equation and the other on an energetics approach, and coefficients produced were in close agreement with those obtained by Komar (1969) in a previous study.

Finally, field measurements of a series of variables such as wave height, wave period and longshore current velocity were combined with measures of sand movement and direction in a linear multiple regression analysis to study the associations present and to produce a simple

predictive model of sand movement. Using both stepwise and combinatorial methods of regression it was found that 80% of the variation of amount of longshore sand movement could be accounted for by the 'best' equation. Wave height alone explained 61.3% of the variation but beach slope, water temperature and longshore current velocity were also of importance. 59% of the variation of average distance moved by sand grains normal to the shore was explained by beach slope, whilst wave period was seen to be the major factor in determining the direction of sand movement onshore or offshore. A set of equations was produced which together with longshore current flow direction, could be used to predict the average position of tracer on the beach face after one tidal cycle. At the same time individual equations could be used to model specific aspects of sand movement.

ACKNOWLEDGEMENTS

Sincere thanks are due to the many people, colleagues and friends, who have assisted me throughout this project. Members of the staff in the Geography Department have helped in a variety of ways. Professor C.A.M. King read and commented upon the typescript of this thesis and as my joint supervisor provided valuable advice at different times during the study. Dr. R.E. Dugdale and Dr. M.J. McCullagh provided expertise in the field of instrumentation and tracer techniques in addition to maintaining a nautical presence at Gibraltar Point. Professor J.P. Cole encouraged and cajoled on many occasions and also subjected himself to the rigours of fieldwork. However, any merit contained in this piece of work is due almost entirely to the friendly advice and encouragement of my supervisor, Dr. P.M. Mather. Frequent discussion produced much needed boosts to flagging morale as well as a wealth of suggestions and ideas on all aspects of the work. Furthermore, Dr. Mather provided many of the computer programs used in the study and gave a great deal of constructive criticism of the thesis itself.

In a physical geography project such as this a large amount of effort is expended in the field and this study would not have been possible without help with fieldwork. In this respect I gratefully acknowledge the invaluable help of my fellow researchers at Gibraltar Point, Mr. Richard Russell and Mrs. Elizabeth Fraser, who endured the horrors of night sampling and winter sea bathing with great good humour. Without their contribution to the corporate spirit little would have been achieved. Many others have willingly given of their time in helping with fieldwork and to them all I extend my deepest gratitude. Mr. George Evans and more recently Mr. Peter Bain gave every assistance as wardens of the Lincolnshire Trust and Nature Conservancy Field

Station at Gibraltar Point, which on more than one occasion was a welcome haven during bad weather.

I must also thank Dr. F. Palmer of the Chemistry Department and Dr. C.J. Paull of the Electrical Engineering Department who gave information and help with fluorescent tracers and electronic circuitry. Mrs. Morley and the staff of the Science Library were friendly and efficient in obtaining the more exotic literature and the technical staff of the Geography Department provided help at every stage of the study. In particular Mrs. E. Pyper gave much assistance with laboratory analysis. Mrs. E.O. Wigginton deserves much credit and grateful thanks for the deciphering of my handwriting and the able typing of this thesis.

Finally, I must thank my wife, Kathryn, who has patiently endured the completion of this study over the past three years and has never ceased to be a source of encouragement and support.

LIST OF PLATES.

Plate No.		Page
1.1	Skegness is bracing	17
1.2	Aerial view of H2 profile, Gibraltar Point May 1978 ..	24
1.3	View down the line of H2 profile from backshore March 1978	25
1.4	View up the line of H2 profile from lower ridge March 1978	25
1.5	Aerial view of E1 profile Skegness May 1978	26
1.6	View down the line of E1 profile from backshore March 1978	27
1.7	View up the line of E1 profile from lower beach March 1978	27
2.1	Emplacement of tracer into beach face	57
2.2	Portable ultra-violet lamp	61
3.1	Spray glue and black sugar paper used in counting procedure for each sample	81
3.2	Spraying the paper with thin coat of glue	81
3.3	Sample tipped onto sprayed surface	82
3.4	Sand residue removed	82
3.5	Paper square with thin coating of sand from sample ...	83
3.6	Fluorescent grains counted using cotton grid and Honovia hand held fluorescent lamp	83
A1.1	Detail of completed wave pole (foreground). Pole fixed to beach surface with concrete base and guy ropes (background)	306
A1.2	Strainguage current meter	311

LIST OF FIGURES.

Figure No.		Page
1.1	Study area and location of profiles	2
1.2	Dynamic beach zones	5
1.3	Beach terminology	5
1.4	Geological section of coastal margin	8
1.5	Percentage exceedance graph for wave height and wave direction rose taken from Inner Dowsing records 1974.	11
1.6	Percentage exceedance graph for wave height and wave direction rose taken from Inner Dowsing records 1975.	11
1.7	Percentage exceedance graph for wave height and wave direction rose taken from Inner Dowsing records 1976.	12
1.8	Wave fetch diagram for Gibraltar Point	14
1.9	Surface wind roses 1975 and 1976 for Gibraltar Point...	16
1.10	Comparison of offshore profiles for Skegness and Gibraltar Point	21
1.11	H2 profile surveyed 6.10.75 and 18.3.76	29
1.12	H2 profile surveyed 17.5.76 and 10.8.76	30
1.13	H2 profile surveyed 22.9.76 and 23.10.76	31
1.14	E1 profile surveyed 18.5.76 and 25.8.76	32
1.15	E1 profile surveyed 21.9.76 and 22.10.76	33
1.16	Sweep zone for H2 profile October 1975 to October 1976.	34
1.17	Sweep zone for E1 profile May 1976 to October 1976 ...	35
1.18	Sketch of cusp features of upper ridge face H2 profile during 28.2.76 tracer experiment	39
2.1	Effect of tracer coating on natural sand grains ...	48
2.2	Comparison of grain size distribution for natural sand and commercially produced tracer sand 28.2.76 experiments	50
2.3	Layout of guide pegs for sampling grid	52

Figure No.		Page
2.4	Techniques for measurment of depth of disturbance ...	54
2.5	Tracer map for 6.10.75 H2, an example of poor sampling caused by predetermined grid layout	62
2.6	Schematic diagram of typical sampling grid	64
2.7	Tracer map for 21.9.76 E1 experiment, lower ridge: an example of poor sampling	66
2.8	Phases of sedimentation during a single tidal cycle ...	70
2.9	Tracer map for 18.3.76 H2 experiment upper ridge. Pink tracer released for one tidal cycle. Note distance moved by centre of gravity	72
2.10	Tracer map for 18.3.76 H2 experiment upper ridge. Yellow tracer released for two tidal cycles. Compare with previous map	73
2.11	Tracer map for 7.9.76 H3 experiment lower ridge. First sample after one tidal cycle	74
2.12	Tracer map for 8.9.76 H3 experiment lower ridge. Second set of samples collected on same site as 7.9.76 tracer injection after two tidal cycles. Compare with previous map	75
3.1	Boundary line presentation of tracer dispersion used by Yasso (1962)	85
3.2a	Basic grid of data points before interpolation	87
3.2b	Expanded grid of data points after interpolation ...	87
3.3	Generation of mid point/grid values for mesh rectangles in contouring procedure	90
3.4a	Extreme values for length of mean vector r and angular deviation s : maximum concentration	93
3.4b	Extreme values for length of mean vector r and angular deviation s : maximum dispersion	93
4.1	E1 profile levelled 25.8.76	100
4.2	H2 profile levelled 18.3.76	101
4.3	Tracer map: 18.3.76 Grid 1 berm H2 Y	102

Figure No.		Page
4.4	Tracer map: 18.3.76 Grid 3 lower ridge H2 Y	103
4.5	H2 profile levelled 22.9.76	110
4.6	Tracer map: 22.9.76 lower ridge H2 Y	111
4.7	Tracer release equipment for injection at high water 22.9.76 experiment	113
4.8	Tracer map: 22.9.76 lower ridge H2 P, tracer released at turn of tide	114
4.9	Tracer map: 22.9.76 upper ridge H2 O	116
4.10	H2 profile levelled 6.10.76	118
4.11	Tracer map: 6.10.76 upper grid H2 Y	119
4.12	Tracer map: 6.10.76 lower grid H2 O	120
4.13	H3 profile levelled 7.9.76	122
4.14	Tracer map: 7.9.76 upper grid H3 P	123
4.15	H2 profile levelled 28.2.76	124
4.16	Tracer map: 28.2.76 lower ridge H2 P	125
4.17	H2 profile levelled 15.7.76	127
4.18	Tracer map: 15.7.76 lower ridge H2 Y	128
4.19	Tracer map: 25.8.76 upper ridge E1 Y	129
4.20	Tracer map: 25.8.76 lower ridge E1 P	130
4.21	E1 profile levelled 21.9.76	132
4.22	Tracer map: 21.9.76 upper ridge E1 P	133
4.23	E1 profile levelled 22.10.76	134
4.24	Tracer map: 22.10.76 upper ridge E1 P	135
4.25	Tracer map: 22.10.76 lower ridge E1 Y	136
4.26	E1 profile levelled 7.10.76	137
4.27	Tracer map: 7.10.76 upper ridge E1 Y	138
4.28	Tracer map: E1 7.10.76 lower ridge E1 P	139
4.29	E1 profile levelled 12.8.76	141
4.30	Tracer map: 12.8.76 lower ridge E1 Y	142
4.31	H2 profile levelled 2.11.75	149

Figure No.		Page
4.32	Tracer map: 2.11.75 upper ridge H2 Y	150
4.33	Tracer maps: 2.11.75 upper ridge H2 fine Y and 2.11.75 upper ridge H2 coarse P	151
4.34	H2 profile levelled 17.1.76	152
4.35	Tracer map: 17.1.76 upper ridge total	153
4.36	Tracer maps: 17.1.76 upper ridge H2 Y (coarse) and 17.1.76 upper ridge H2 pink (fine)	154
4.37	Tracer map: 7.10.76 upper ridge 0.3mm	156
4.38	Tracer map: 7.10.76 upper ridge blue 0.46mm	157
4.39	Tracer map: 7.10.76 upper ridge pink 0.65mm	158
4.40	Tracer map: 12.8.76 lower ridge E1 blue 0.25mm	160
4.41	Tracer map: 12.8.76 lower ridge E1 pink 0.5mm	160
4.42	Tracer map: 7.10.76 lower ridge E1 yellow 0.3mm	161
4.43	Tracer map: 7.10.76 lower ridge E1 blue 0.46mm	161
4.44	Tracer map: 7.10.76 lower ridge E1 orange 0.66mm ...	162
4.45	Conceptual arithmetic model of Price (1969) on diffusion of tracer	168
4.46	The Price (1969) model applied to the tidal situation ...	169
5.1	The asymmetry of wave orbital motions causing a net shorward transport of sediment	180
5.2	Comparison of water motions in theories of mass transport	180
5.3	Relationship between immersed-weight sand transport rate (I_ℓ) and wave power (P_ℓ), equation 5.14	193
5.4	Relationship between immersed-weight longshore sand transport rate and the model of equation 5.19 as deduced by Inman and Bagnold (1963)	194
6.1	Summary of regression models for amount of sand movement with the selected independent variables	211
6.2	Summary of regression models for amount of sand movement with the dimensionless variables	215

Figure No.		Page
7.1	Zig-zag motion of sediment along beach under action of swash/backwash	252
7.2	i) Longshore currents of cell circulation, ii) current formed by oblique wave approach and iii) summation of previous two diagrams to give resultant observed current patterns	252
7.3	E1 profile levelled 1.7.76	258
7.4	Tracer map: 1.7.76 upper ridge E1, Y	259
7.5	E1 profile levelled 8.9.76	261
7.6	Tracer map: 8.9.76 upper ridge E1, P	262
7.7	Plot of index of net movement (Ψ) against bottom orbital velocity (u_m)	264
7.8	Plot of index of net movement (Ψ) against mean grain size	264
7.9	Breaking wave types	270
8.1	Predicted and observed position of centre of gravity of tracer distribution for test data	292
8.2	Plot of predicted longshore movement versus residuals from equation 8.3	295
8.3	Plot of predicted onshore/offshore movement versus residuals from equation 8.6	295
8.4	Plot of predicted coefficient of onshore/offshore movement versus residuals from equation 8.11	296
8.5	Conceptual process-response model of sediment movement on the tidal foreshore	302
A1.1	Internal details of wave pole	306
A1.2	Schematic layout of wave pole system	308
A1.3	Example plot of wave data from wave pole system. Recording made at Skegness at 13.3.78	309
A1.4	Details of straingauge current meter	312

Figure No.		Page
A1.5	Schematic field layout of current meter system	312
A1.6	Plot of tidal currents measured on the lower foreshore at Skegness, 4-5.2.77. Recording height 15cm above the bed. Tidal heights 7m and 6.9m	314
A1.7	Plot of tidal currents measured on the lower foreshore at Skegness 4-5.2.77. Recording height 34cm above the bed. Tidal heights 7m and 6.9m	315
A1.8	Plot of tidal currents measured on the lower foreshore at Gibraltar Point, 18-19.1.77. Recording height 34cm above the bed. Tidal heights 6.6m and 6.6m ...	316
A1.9	Plot of tidal currents measured on the lower foreshore at Gibraltar Point, 22-23.11.76. Recording height 34cm above the bed. Tidal heights 7.4m and 7.4m. Instrument disturbed after 4 hours	317
A1.10	Plot of currents measured in the main runnel on profile H2, 21.9.76. Note all flow to north	318
A1.11	Plot of tidal currents measured on the lower foreshore at Gibraltar Point, 6.10.76. Instrument swamped after 5 hours in heavy sea. Tidal height 6·6m ...	318
A1.12	Calibration curve for current meters. Relates current speed to the force applied to the instrument sensors.	319
A2.1	H2 profile levelled 6.10.75	321
A2.2	Tracer map: 28.2.76 upper ridge H2 Y	322
A2.3	Tracer map: 28.2.76 upper ridge H2 B	322
A2.4	Tracer map: 28.2.76 lower ridge H2 B	323
A2.5	H2 profile levelled 17.5.76	324
A2.6	Tracer map: 17.5.76 lower ridge H2 P (A)	325
A2.7	H2 profile levelled 30.6.76	326
A2.8	Tracer map: 30.6.76 lower ridge H2 Y	327
A2.9	H2 profile levelled 10.8.76	328
A2.10	Tracer map: 10.8.76 H2 lower ridge Y	339
A2.11	Tracer maps for grain size test 7.9.76 lower ridge H3, first sample, one tidal cycle	330

Figure No.		Page
A2.12	Tracer maps for grain size test 8.9.76 lower ridge H3, second sample, two tidal cycles. Compare dispersions with Figure A2.11	331
A2.13	H2 profile levelled 23.10.76	332
A2.14	Tracer map: 23.10.76 H2 lower ridge P	333
A2.15	Tracer maps for grain size test 23.10.76 lower ridge H2	334
A2.16	H3 profile levelled 23.10.76	335
A2.17	Tracer map: 23.10.76 lower ridge H3	336
A2.18	Tracer maps for grain size test 23.10.76 H3	337
A2.19	E1 profile levelled 18.5.76	339
A2.20	Tracer map: 18.5.76 lower ridge E1 P	340
A2.21	E1 profile levelled 14.7.76	341
A2.22	Tracer map: 14.7.76 lower ridge E1 Y	342
A2.23	Tracer maps grain size test 21.9.76 upper ridge E1 ...	343
A2.24	Tracer map grain size test 21.9.76 upper ridge E1 ...	344

LIST OF TABLES.

Table No.		Page
1.1	Average figures for grain size and beach slope on H2 and E1 profiles for all tracer experiments	39
1.2	Variation of sediment characteristics down E1 profile .	41
1.3	Variation of sediment characteristics down H2 profile .	41
2.1	Grain size characteristics for experiments 28.2.76 and comparison with commercially produced tracer sand ...	49
4.1	Mean angle, mean angular deviation and index of concentration (r) for all tracer experiments	106
4.2	Mean figures for sand movement and selected variables for tracer experiments at Gibraltar Point and Skegness	144
5.1	Bulk sand transport rates (S_ℓ) and immersed-weight sand transport rates (I_ℓ)	195
5.2	Wave and wave power quantities	197
6.1	Dependent variables: amount of sand movement	216
6.2	Process variables Gibraltar Point and Skegness sites ..	217
6.3	Dimensionless variables Gibraltar Point and Skegness sites	219
6.4	Wind speed variables for onshore/offshore sand movement regression	221
6.5	Wind speed variables for alongshore sand movement regression	222
6.6	Longshore current variables for alongshore sand movement regression	223
6.7	Independent variables in regressions of distance sand moved in alongshore direction	224
6.8	Results of stepwise regression of amount of alongshore sand movement: 16 independent variables	225

Table No.		Page
6.9	Correlation matrix of independent variables in alongshore sand movement regressions	230
6.10	Results of combinatorial regressions for average distance of alongshore sand movement: All X's minus X4, X5, X6, X7 and X9	232
6.11	Most frequently occurring variables in the best of the combinatorial regression equations	233
6.12	Dimensionless independent variables used in regression of distance sand moved in alongshore direction ...	236
6.13	Results of stepwise regression of amount of alongshore sand movement: dimensionless variables	237
6.14	Results of combinatorial regression for average distance of alongshore movement: dimensionless variables ...	238
6.15	Independent variables in regressions of distance sand moved in direction normal to shoreline	240
6.16	Results of stepwise regression of amount of onshore/offshore sand movement: 15 independent variables ...	241
6.17	Correlation matrix of independent variables in onshore/offshore sand movement regressions	244
6.18	Results of combinatorial regression for average distance of onshore/offshore sand movement: all X's minus X3, X4, X6 and X14	245
6.19	Most frequently occurring variables in the best of the combinatorial regression equations	246
6.20	Results of stepwise regression of amount of onshore/offshore sand movement: dimensionless variables ...	248
6.21	Results of combinatorial regression for average distance of onshore/offshore sand movement: dimensionless variables	248
7.1	Comparison of general direction of sand movement with wave, wind and current characteristics	255
7.2	Wave characteristics and onshore/offshore index of sand movement	265

Table No.		Page
7.3	Contingency table of wind direction against onshore/ offshore/ index of net movement (Ψ)	267
7.4	Results of stepwise regression of concentration index of onshore/offshore sand movement (direction): 15 independent variables	273
7.5	Results of stepwise regression of concentration index of onshore/offshore sand movement: dimensionless variables	277
7.6	Results of combinatorial regression of concentration index of onshore/offshore sand movement: dimensionless variables	278
7.7	Results of combinatorial regression for concentration index of onshore/offshore sand movement: all X's minus X5, X6, X8 and X9	281
7.8	Most frequently occurring variables in 'best' combinations of combinatorial regression, Table 7.7 .	282
7.9	Results of combinatorial regression for concentration index of onshore/offshore sand movement: all X's minus X1, X5, X6 and X8	284
7.10	Most frequently occurring variables in the best combinations of combinatorial regression, Table 7.9 .	285
8.1	Best predictor equations from regression analysis ...	289
8.2	Comparison of best predictions with observed values ...	290

CHAPTER 1

INTRODUCTION AND BACKGROUND

1:1 Introduction

Beach studies can be grouped into those that emphasise beach attributes, those that emphasise processes operating on the beach and those that consider both. This study falls into the last category. It is concerned with the movement of sand on the beach over one tidal cycle and as such involves the consideration of the direction and amount of sand movement as a response to measured process variables such as wave height and period or longshore current velocity. In addition, more specific topics are considered such as the differential movements of contrasting grain size and differences between patterns of movement on various parts of the foreshore between high and low water mark.

Changes in the morphology of beaches cannot be properly understood until details of sediment movement both parallel to and normal to the shoreline are themselves understood. Much attention has been given to the transport rate of material alongshore because of the importance of this particular aspect of movement to coastal engineering and also because the amount of sediment movement normal to the shore is often much less than that alongshore. However, in terms of the impact on overall morphology, movement in both directions is of equal importance. Consequently, in this study attention is given to onshore/offshore sand movement as well as longshore movement.

In order to measure the movement of sand directly on the beach, fluorescent tracers were produced which were used on the beach along two profiles established on the south Lincolnshire coast, Figure 1.1. Their movement was monitored over one tidal cycle in a series of experiments between September 1975 and October 1976. Radioactive tracers were

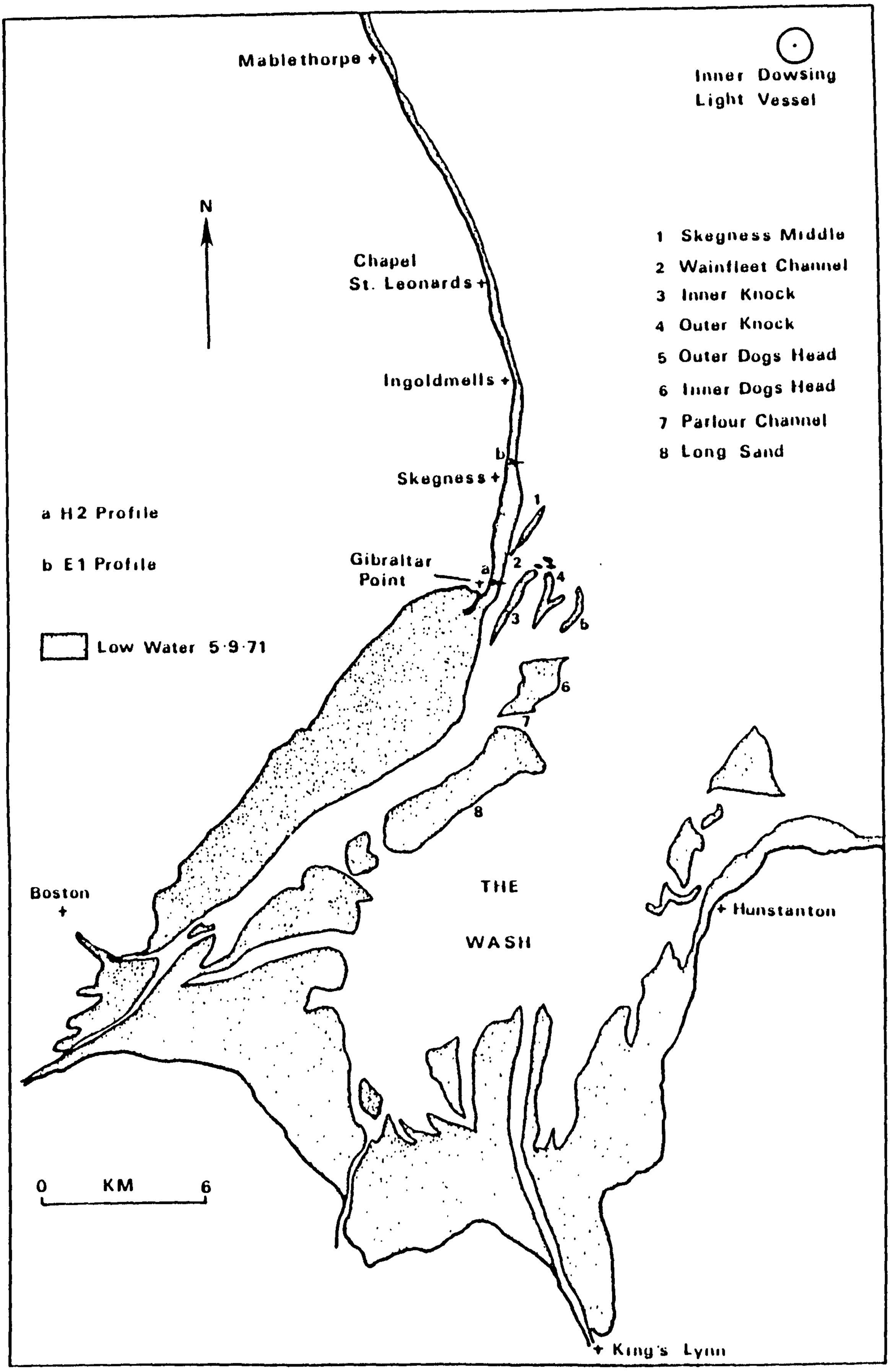

Figure 1.1. Study area and location of profiles.

rejected on the grounds of cost and health hazard and general inflexibility in their usage. As an indirect method of measuring movement, bedload traps, were also rejected because of their uncertain efficiency. Thornton (1973) estimates their efficiency at between 40% and 100%.

Measurements of selected hydrodynamic and meteorological parameters were made whilst the tracer was being dispersed and this information was used in a multiple linear regression analysis to gain an insight into the relationships present between sand movement responses and processes acting in the nearshore. The approach adopted, therefore, was empirical, with the least squares regression model being used as an exploratory tool. The general approach follows that employed by Harrison et al (1964) with the regression equations produced by the analysis being tested in their capacity of simple predictive models.

Harrison (1970) suggests that prediction within the beach/ocean system is made very difficult by the following three factors:

1. Short memory - process variables are constantly changing so that in nearly all cases the magnitude of a given process variable changes before a full beach response takes place.

2. Feedback - the 'explanatory' or process variables are interlocked to various degrees, that is, they are interdependent, so that a change in one variable induces change in others.

3. Range of process variables - process variables may fluctuate in frequency, magnitude and duration through large ranges and therefore a large number of combinations of these variables is possible, each producing a unique beach response.

However, because this study is not dealing with a geometric property of the beach subject to the short memory effects, but rather with the net effect of instantaneous responses to processes at work, problems of time lag with variables do not occur in the analysis. Nevertheless the analysis is subject to the problems of the complexity of the system and

hence the predictive efficiency of the models is limited. Despite this it is hoped that this exploratory study may form the basis of further work and lead to the development of a simulation type model of beach sand movement.

Before considering the characteristics of the study area, the lack of standardised nomenclature for the beach environment makes it necessary to outline the terminology used in this study. This is done diagrammatically in Figures 1.2 and 1.3. Moving from the offshore zone inland the first dynamic zone encountered is the shoaling wave zone. This is defined as that part of the offshore in which waves are 'feeling' the bottom and having a significant effect on sediment movement through the stress exerted on the sea bed. The seaward limit of this zone is indeterminate as the point at which waves begin to affect the bottom will depend upon wave characteristics. As far as this study is concerned, the shoaling wave zone will be thought of as the region immediately seaward of the breaking wave zone. The breaker zone itself will be defined as the area of the nearshore in which waves arriving from the offshore through the shoaling wave zone reach final instability and break. Wave characteristics and beach form determine the width of this zone. On steep beaches the breaker zone may be compressed, whilst on a wide flat beach an extended breaker zone may be present. The slope of the beach also determines the existence of the surf zone. Beaches with a steep slope do not exhibit a surf zone because deep water close inshore allows waves to break close to the shoreline and the breakers collapse directly into a swash/backwash zone. Gently shelving beaches, on the other hand, generally exhibit well developed surf zones as waves break some distance from the shore. The surf zone, therefore, is that portion of the nearshore through which solitary waves in the form of bores pass following the breaking of waves. It is an important zone in that longshore currents may develop as a result of wave energy dissipation or rip

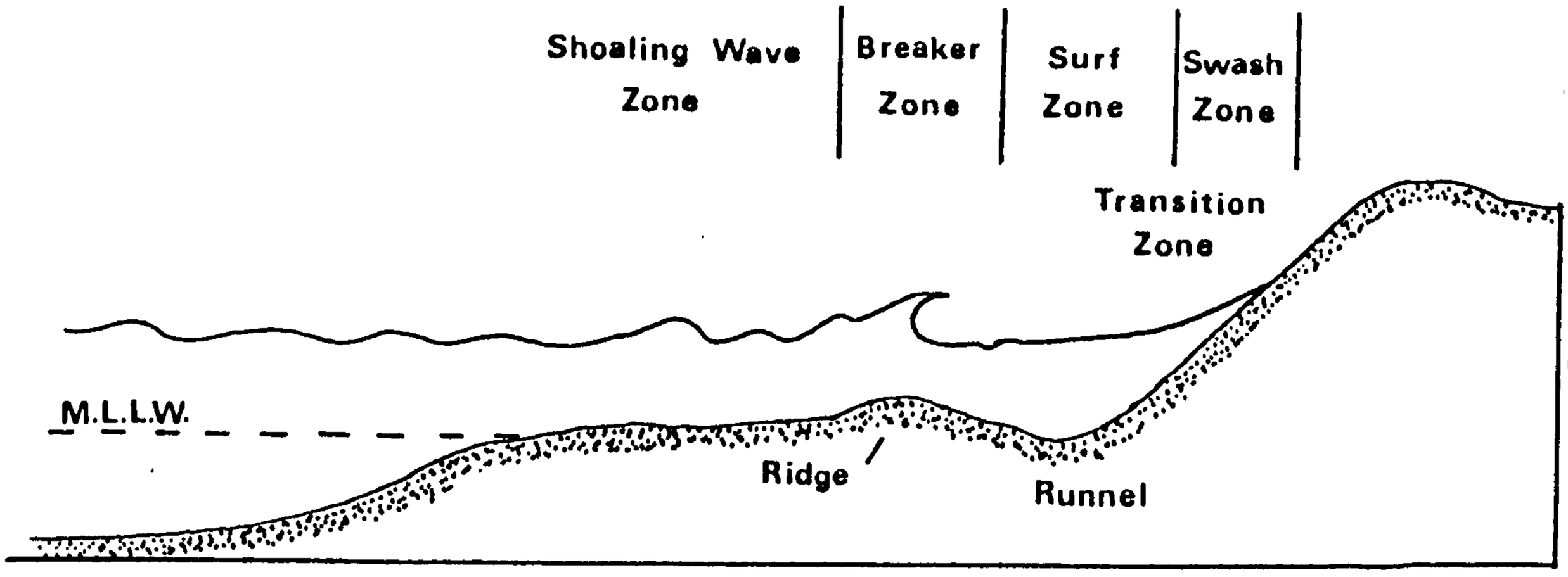

Figure 1.2. Dynamic beach zones.

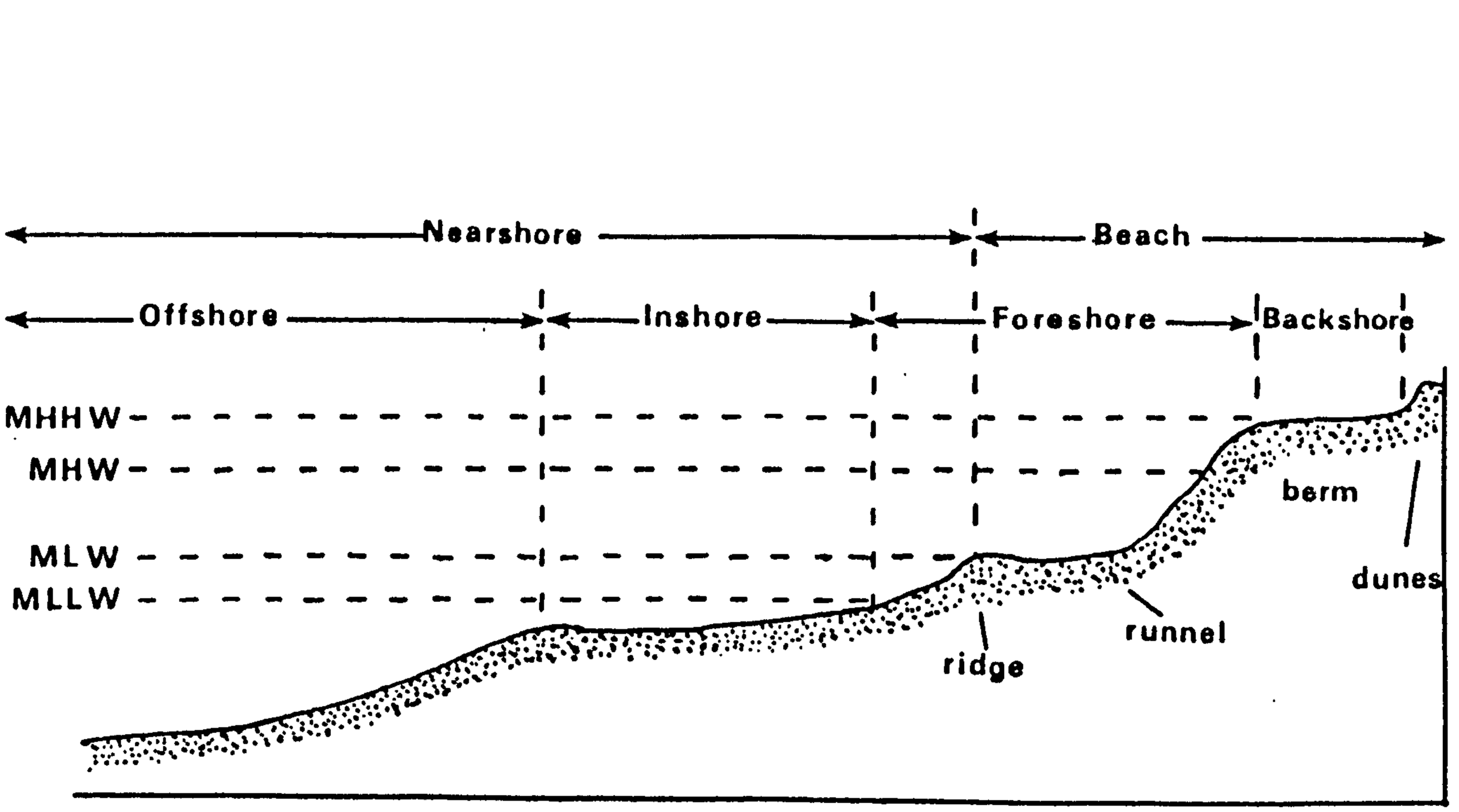

Figure 1.3. Beach terminology.

current cell circulation. Finally, the swash zone is that part of the beach face which is alternately covered by the uprush of water and exposed by the backwash. It is in this zone that the traditional zig-zag motions of water and sediment take place. In addition to these four zones Schiffman (1963, 1965) has identified a fifth zone known as the transition zone in which backwash collides with the oncoming bores of the surf zone and forms a band of high energy turbulence. This zone has been amalgamated with the surf zone for the purposes of this study.

The simple picture of dynamic zones depicted in Figure 1.2 is greatly complicated by the presence of a medium to large tidal range and relatively complex beach topography. In this situation the zones are moved backwards and forwards across a wide beach face and, dependent upon the beach slope at various points, either change their appearance or disappear altogether. The features of the different zones on the ridge and runnel beach of Gibraltar Point and Skegness are described in Section 1:5.

Figure 1.3 gives further divisions of the coastal environment which in general are more loosely defined and in consequence cause most confusion. The nearshore, for example, is an indefinite zone extending from M.L.W. mark on the shoreline to a point somewhere within the shoaling wave zone where waves are changing their form from the sinusoidal or trochoidal deepwater form to the shallow water solitary form. In addition, more than one name may be given to the same zone in the literature. Thus, for example, the foreshore may be known as the beach-face and the backshore as the back beach. As far as possible the terminology used in this study will be that shown in Figure 1.3.

1:2 General physical background

The geological history of eastern Lincolnshire has been outlined by Swinnerton and Kent (1949) and Swinnerton (1936). It is a relatively uncomplicated geology with Cretaceous rocks overlain by glacial and post-

glacial deposits. The basic structure of the coastal zone comprises a wave cut platform cut into the chalk of the Cretaceous with the inland margin finding a surface expression in the eastern edge of the Lincolnshire Wolds. Covering the wave cut platform, which is now below sea level, having been formed during an earlier interglacial period of lower sea level, is a deposit of boulder clay approximately 25m thick. This in turn is overlain along the coastal margin by a series of post-glacial deposits from a variety of environments, Figure 1.4.

The sequence of events in the post-glacial period is summarised by Dugdale (1977) based on Swinnerton's earlier work. Low sea levels at the end of the glacial episodes allowed the development of forests on the boulder clay. Later sea level rises caused the destruction of these forests and the resultant deterioration in the drainage of the coastal strip led to the production of peat deposits. Fluctuation in sea level during the period 2000-3000 years B.P. created conditions for the development of a series of salt marsh deposits, peat deposits and freshwater marsh clays. Swinnerton (1931) suggests that the necessary calm conditions for the deposition of clays and silts were provided by the protection of a morainic barrier located some miles east of the present shoreline and which was probably finally destroyed during the stormy period of the 14th and 15th centuries. However, recent work by Robinson (1968) has cast some doubt on the inference that remnants of the proposed barrier are seen in the present day Protector and Theddlethorpe Overfalls, 2.5 miles east of Theddlethorpe, and the Inner Dowsing Bank, 8 miles seaward of Chapel St. Leonards. Hydrographic surveys indicate that some of these banks are more likely to be of marine origin.

From more recent, historical, times documentary evidence of frequent flooding and erosion along the coast has been collected by Owen (1952). These problems have not been as severe as on the Holderness coast to the north but at least five coastal settlements in Lincolnshire

Figure 1.4.

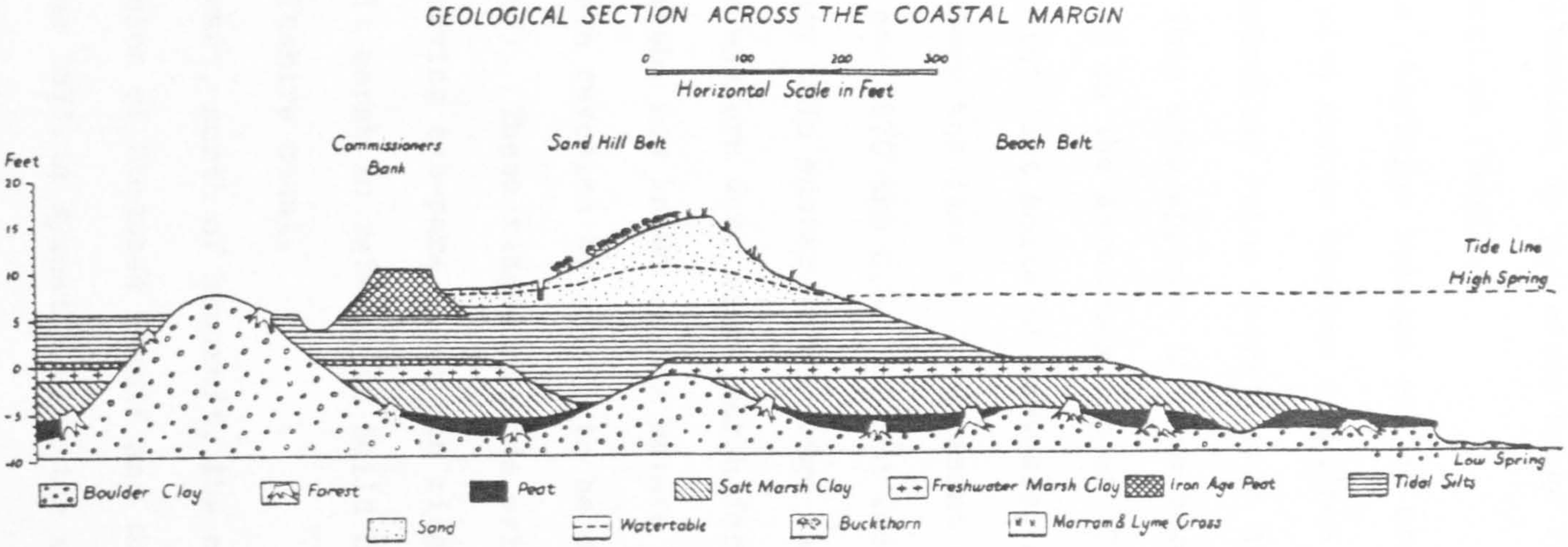

(After Swinnerton, 1936)

have had to develop new sites in the last 700 years and Skegness itself has suffered in this way.

In the last 150 years improved sea defences and reclamation have largely curtailed serious property damage but sea incursions are still a danger as witnessed by the storm surge flooding of 1953 and more recent less serious flooding.

Today the coastline remains one of erosion between Mablethorpe and Skegness with narrow beaches sometimes stripped of sand but from Skegness to Gibraltar Point accretion is now the dominant process. Accretion in this area appears to have begun in the late 18th and 19th centuries since on the Armstrong map of 1779 the coastline between Seacroft, a point just south of Skegness, and Gibraltar Point can be seen to lie along the line of the present day western dune ridge. Between 1824 and 1870 the O.S. 1st and 2nd edition 1:63360 maps indicate that the present day main eastern dune ridge was developed and between this and the older western dune ridge marsh formation took place. Contained within the marsh, now known as the Mature Marsh, are low ridge features which have been revealed by boring to be shingly beach ridges (Barnes and King, 1961). These ridges provide evidence of the way in which the gently curving sub-parallel beach ridges successively develop with strips of salt marsh in between to build out this southernmost section of the Lincolnshire coast.

In contrast, north of Seacroft, the coast has mainly been stabilised by the expansion of Skegness itself and the construction of sea defences. However, since 1871, in sympathy with the movement of a ness of accretion (Section 1:4), the beach has shown erosional tendencies and the backing dunes have been subjected to destructive attack due to the limited amount of protection afforded by the beach.

Thus the three mile section of coastline between a point just north of Skegness pier and Gibraltar Point at the north western corner of the

the Wash, which forms the section of coast of particular interest to this study, is a zone of transition from erosion in the north to accretion in the south.

1:3 Waves and wind

Davies (1964) classifies the east coast of Britain as a medium energy wave environment. This classification is confirmed by wave records from the Inner Dowsing Lightship which is situated 10-15 miles north of Skegness but provides the nearest point to Skegness from which deepwater wave data is available (Figure 1.1). A consideration of three years' records (1974, 1975 and 1976) covering the period of fieldwork for this study confirms that "waves in the North Sea are short and that high waves are rare" (Draper, 1968). The range of wave height for the three year period was from less than one foot to 25.5 feet but on only 7 days were waves greater than 16 feet observed. From Figures 1.5, 1.6, 1.7 of percentage exceedence of significant wave height it will be seen that waves were less than five feet in height for 70% of the time and were less than three feet for 40% of the time. For 1975 these figures were respectively 75% and 50% whilst in 1976, when much of the fieldwork for this study took place, the figures reflect the good summer and are 77% and ~~80~~ 85%. Waves greater than 8 feet were recorded only 8.7% of the time in 1974, 7.8% of the time in 1975 and in 1976 for 6.1% of the time.

As might be expected, a seasonal characteristic is present in the wave observations with a generally higher frequency of large waves occurring in the stormier weather of autumn and winter. In 1974 during the months of May, June, July, August and September waves of less than 3 feet accounted for 70% of the period whereas during the rest of the year the figure was 38%. Again in 1975 the waves were less than 3 feet for 60% of the time in the summer whilst in the winter they occurred only 28% of the time. The contrast is even greater for 1976 when waves were

Figure 1.5.

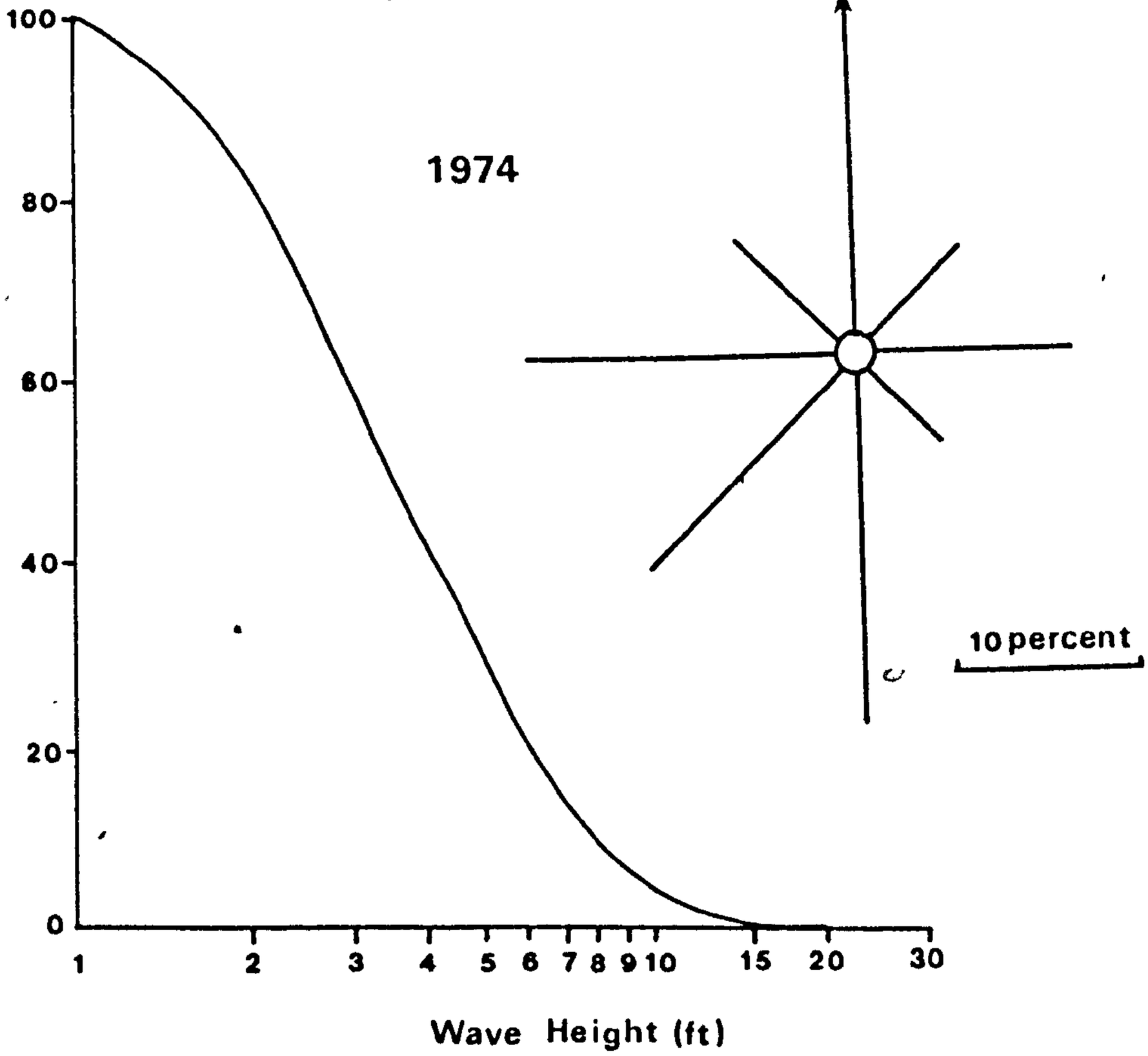

Figure 1.6.

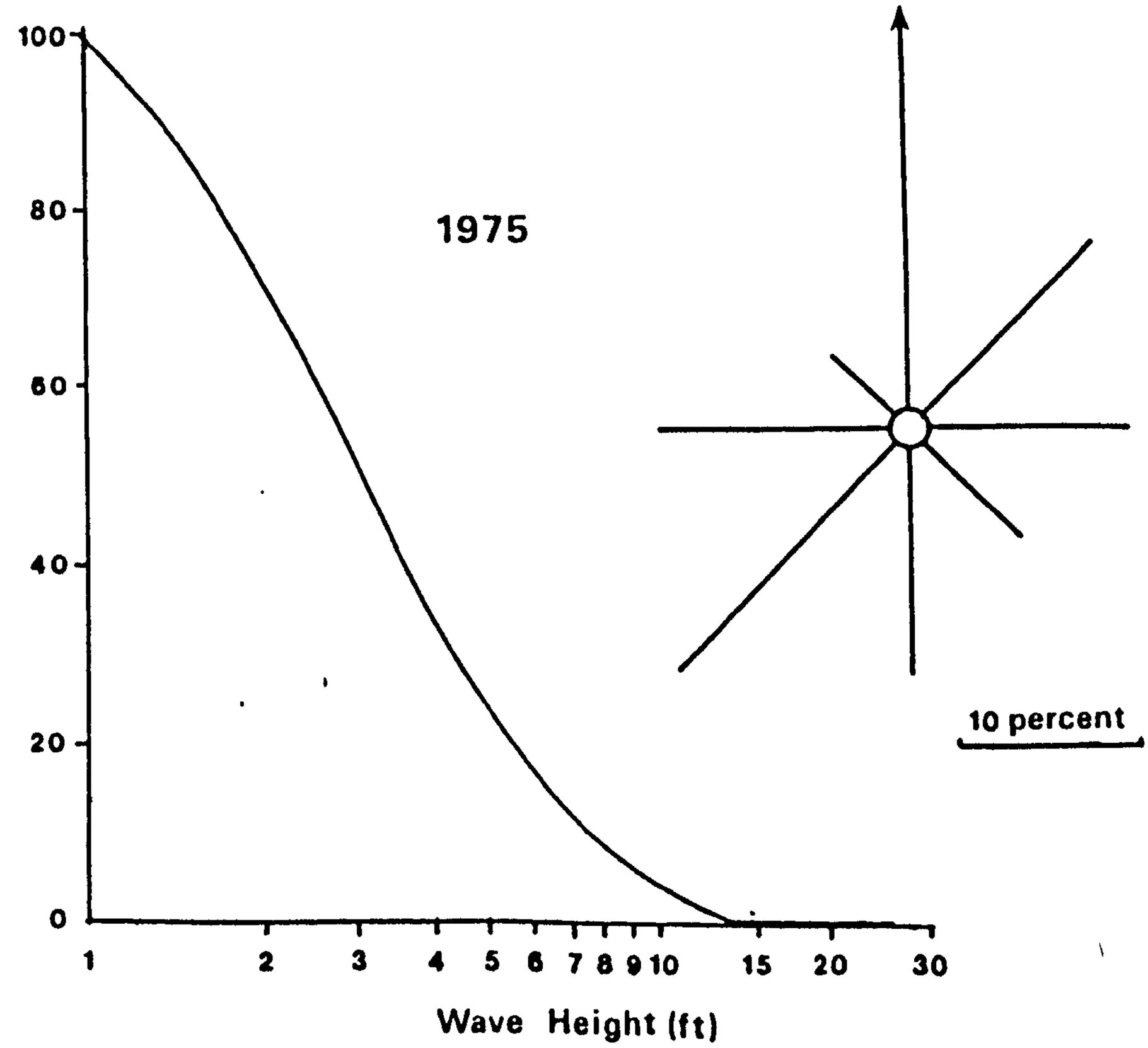

Figure 1.7.

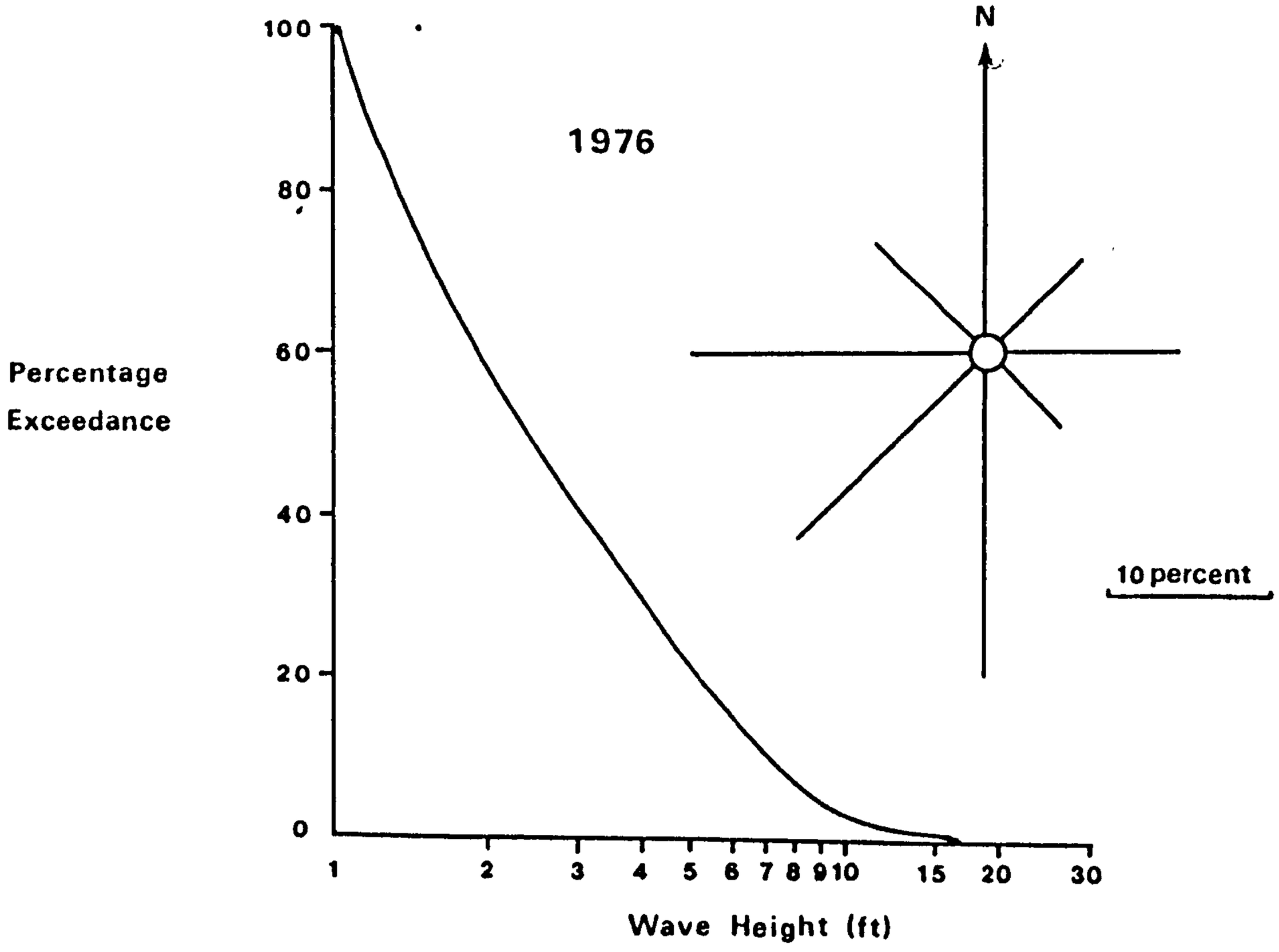
1976
Percentage
Exceedance
100
80
60
40
20
0
1
2
3
4
5
6
7
8
9
10
15
20
30
Wave Height (ft)
N
10 percent

less than three feet in height for 78.9% of the time in summer but for only 43% of the time in winter.

Wave periods for the whole of the time 1974-6 were 5 seconds or less except for the odd occasions when large waves had wave periods of 6 seconds. The 17th November 1975 was the only occasion when 7-8 second waves were observed and this was in conjunction with the largest waves recorded during the three years, of 25.5 feet in height.

These findings agree with Draper's (1968) reports of wave observations from Smith's Knoll Light Vessel in the North Sea, 22 miles E.N.E. of Great Yarmouth. He gives the most common wave conditions as being those where the significant wave height was between 2 and 3 feet and the wave period between 5 and 6 seconds. The highest wave recorded at this vessel was 24 feet in height with a period of 8.4 seconds. Draper also found that most of the waves were of local origin and suggested that the absence of waves with periods of 10 seconds or more was evidence of the lack of waves which may have been generated in distant waters such as the Norwegian Sea. Nevertheless, the Inner Dowsing records do show that the largest waves were associated with the longest fetch distance between N.W. and N.E. In 1974, of waves larger than 9 feet, 75% came from directions between N.W. and N.E. In 1975 this figure was 67% but for 1976 was only 10%. The wave direction diagrams, Figures 1.5, 1.6 and 1.7 indicate the variability of wave approach at the Inner Dowsing vessel.

However, deepwater wave observations are to a certain extent unhelpful when considering the foreshore between Skegness and Gibraltar Point. As may be seen from the map of fetch distances (Figure 1.8) waves may approach this stretch of coastline from directions between N.N.E. and S.S.W., 25^{o} and 225^{o}, with maximum fetches between N.~~W.~~ N.E. and N.E. However this map applies only to the period when the tidal plane reaches a level such that waves may approach the coast without first breaking on the

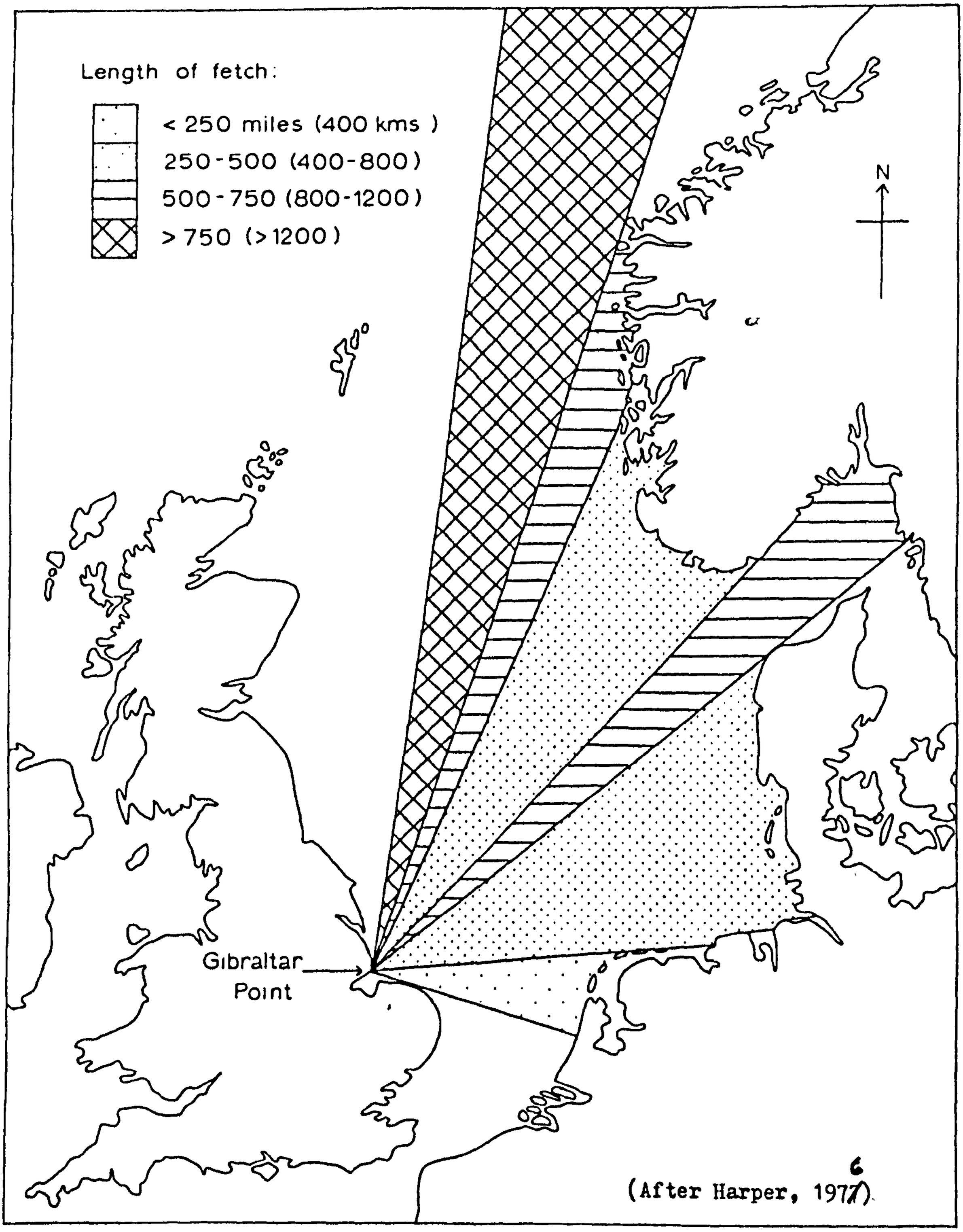

(After Harper, 1977)

Figure 1.8. Wave fetch diagram for Gibraltar Point.

complex offshore bank system. This protective aspect of the offshore banks is considered in the next section but it must be noted here that the banks only afford protection to the foreshore at the southern of the two experiment sites, the Gibraltar Point site (Figure 1.1).

Significant breaking wave heights ($H^{\frac{1}{3}}$) actually measured during tracer experiments ranged between 0.18m and 0.78m at Gibraltar Point and between 0.22m and 0.76m at Skegness. Breaking wave period for Gibraltar Point was between 2.8 and 5.4 seconds and between 2.6 and 5.4 seconds at Skegness. Only on two occasions, 6.10.76 and 23.10.76, were tracer experiments conducted when wave records from the Inner Dowsing Light Vessel indicated wave heights of more than two metres. On these two dates beach wave heights at Gibraltar Point were respectively 0.4 metres and 0.55 metres. This is an indication of the nature of protection afforded by the Inner Knock and other banks just offshore.

The surface winds for the study area are summarised in the annual wind rose diagrams for 1975 and 1976, Figure 1.9. These were compiled from readings taken at Gibraltar Point Field Station on equipment installed by Binney Ltd. during their feasibility study for the proposed Wash Barrage Scheme. The diagrams representing only two years wind data cannot reflect long term variability but nevertheless indicate the principal features of wind records in this area. A notable characteristic is the prevailing southwesterly direction of the winds. King and Barnes (1964) have suggested that these winds may have an important influence on the changes in the beach morphology. They postulate that they may generate onshore bottom currents, counter currents, and thereby encourage onshore sediment movement. They also suggest that these winds reduce the height of the constructive northeasterly swells, thus enhancing their constructive nature. An interesting point is the relatively low percentage of calm days and very light winds accounting for the bracing reputation of this coast! Plate 1.1.

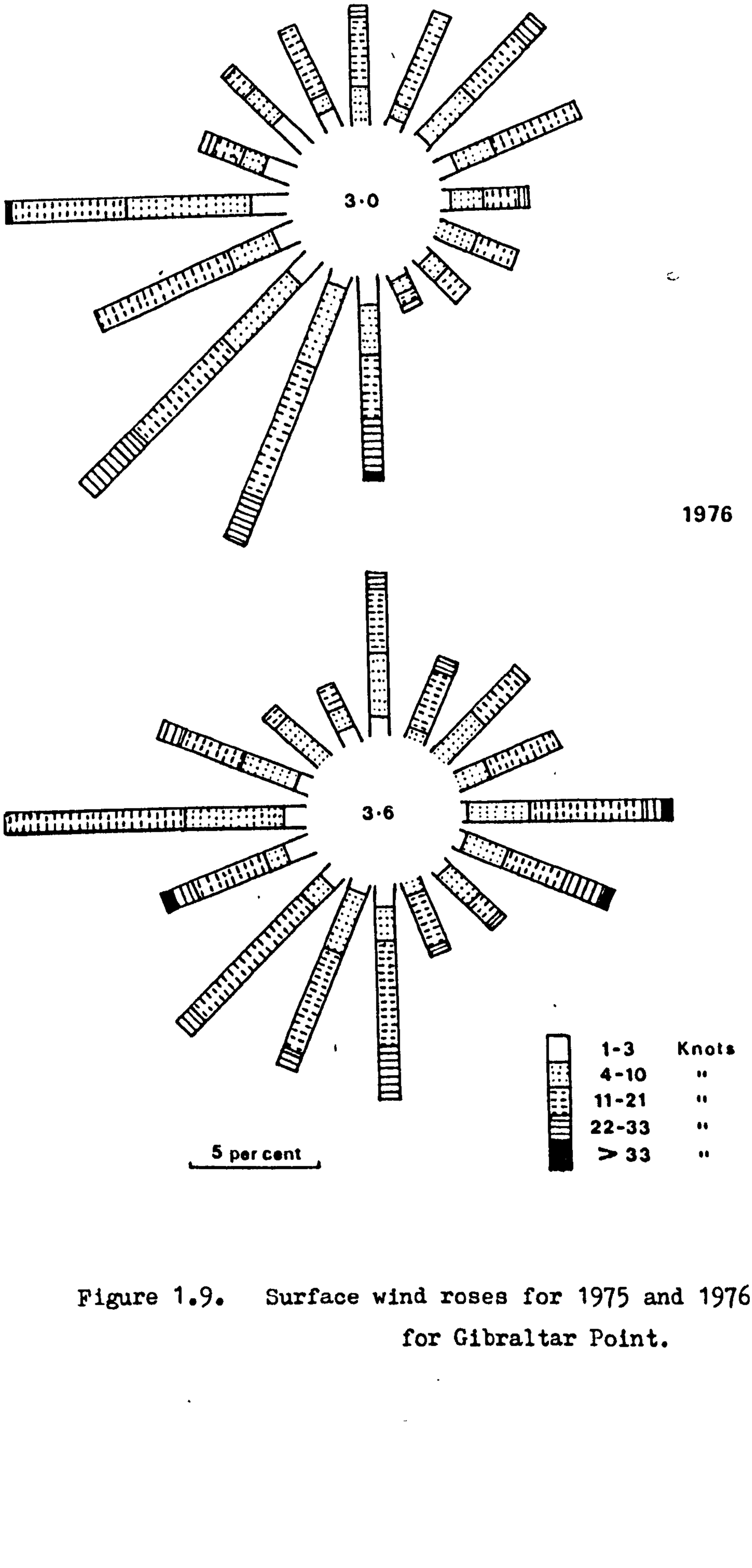

Figure 1.9. Surface wind roses for 1975 and 1976 for Gibraltar Point.

Plate 1.1. Skegness is bracing.

1:4 The offshore zone

Offshore bathymetry directly to seaward of the coast between Skegness and Gibraltar Point comprises a complex system of tidal banks and channels. This area is shown in Figure 1.1. Because of the large tidal range on this part of the coast, which may reach 7.5 metres on spring tides, the sandbanks are exposed at low water. The area of drying sand varies according to the stage of the fortnightly neap/spring tidal cycle and that found on average spring tides is indicated in Figure 1.1.

This complex offshore zone has an important influence on the nearshore zone in three ways:

1. The bank system provides a great deal of protection from wave attack to the lower for shore. Evidence of this is provided by the occurrence of very fine silts and mud on the lower parts of the beach, in particular around low water spring tide mark (L.W.S.T.). Furthermore direct observation of wave heights on the lower beach gives a measure of the protection of the banks. At low water wave heights may be as little as 5-10cm but as the tidal plane rises and the depth of water over the offshore banks increases so wave height increases until a point is reached when waves move directly from deepwater offshore across the submerged banks without significant deformation and break on the beach. For example, during the tracer experiment of 18th March 1976 the significant wave height ($H^{\frac{1}{3}}$) on the beach face increased from 26cm at quarter tide to 40cm at half flood tide. On the falling tide the process is reversed and breaking waves on the beach decrease in height.

2. Because of the large tidal range, strong tidal currents are found in the area. Currents flowing north-south along the Wainfleet Channel (Figure 1.1), the channel between the beach and the closest of the offshore banks, the Inner Knock, affect the lower foreshore since, as the tide rises, the flow in the channel impinges more and more on the

beach. Measurements of currents taken on the beach close to L.W.S.T. mark suggest that tidal currents may reach a maximum velocity of 40 to 60 cm/sec, Figure A1.9. This represents a value roughly 30% of the maximum current velocities offshore which in the main occur over the sandbanks themselves and are probably associated with large scale turbulence effects. Nevertheless these currents may be important in terms of sediment movement particularly when considered with turbulence possibly caused by wave effects. Evidence from tracer experiments for the importance of tidal generated currents on the lower foreshore is discussed in Chapter 4.

3. Recent work by Dugdale (1977) in the development of a descriptive model of sediment transport for the offshore zone at Gibraltar Point has confirmed earlier suggestions by King (1964) that the flood channel between the Skegness Middle bank and the foreshore (Figure 1.1) is a major route for sediment migration from the offshore to the foreshore. Beach and offshore morphology supports this view.

Robinson (1966), in a study of the coast of East Anglia, found that nesses or bulges on the foreshore were closely associated with tidal current ridges extending obliquely from the coast. The channels shoreward of the ridges were found to be routes along which the sand moved from the offshore circulation to the nesses. A bulge in the line of the foreshore seemingly related to the Skegness Middle has moved south since 1871 in sympathy with the Middle suggesting a situation similar to the cases in East Anglia described by Robinson. Further evidence is provided by the Woodhead seabed drifter experiments conducted by Robinson (1964) and again by Dugdale in 1975 which showed preferential strandings in the area of the foreshore between Skegness pier and the site where the line of the Skegness Middle meets the foreshore. Therefore, it seems reasonable to postulate that the accretion of the coast

south of Skegness has been the result of this sediment supply from the offshore reaching the foreshore along the Skegness Middle and its associated channel. Without this supply of sediment it is unlikely that the protection of the beach at Gibraltar Point by the offshore bank system would by itself have resulted in the outward growth of the coast which has taken place.

As already mentioned (Section 1:2), at the same time that there has been accretion on the beach south of Skegness, so north of the pier at Skegness there has been a tendency for erosion. Although an extension of the Skegness Middle bank may be discerned in offshore profiles taken seaward along the line of Skegness pier, this only forms a small rise on the sea bed and hence cannot afford the same protection for the foreshore as at Gibraltar Point. The comparison between the offshore profiles at Skegness and Gibraltar Point may be seen in Figure 1.10. Furthermore, movement of sediment from the offshore is not aided by the offshore bathymetry as at Gibraltar Point and tidal currents on the lower foreshore are slower. Measurements of the tidal currents on the lower foreshore at Skegness taken on 4th-5th February 1977 show them to be of the order of 20-30 cms/sec, roughly half of those at Gibraltar Point, Figure A1.7.

1:5 The beach

The intertidal beach zone of the coast between Skegness and Gibraltar Point has a well developed ridge and runnel morphology. The number and size of the ridges varies from place to place and on any one profile the form and position of the ridges changes with time. In plan, the ridges south of Skegness diverge slightly from the coast. They also have an arcuate form which is related to the stabilisation of the ridges. King (1972), who has studied the development of the beach morphology in this area over the last 25 years, suggests that the plan shape of the ridges

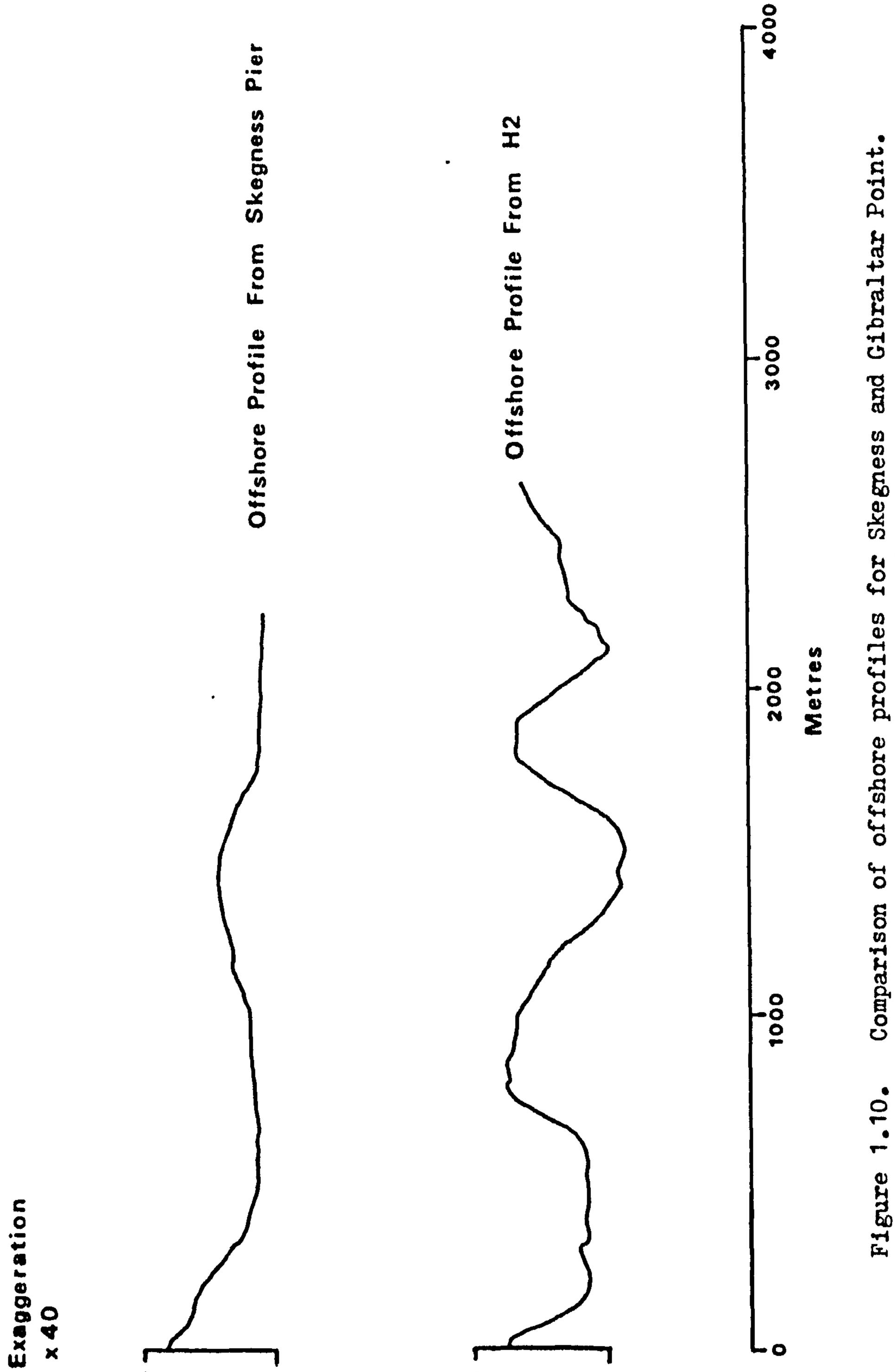

Figure 1.10. Comparison of offshore profiles for Skegness and Gibraltar Point.

is due to their construction by the flatter waves of maximum fetch approaching from the north and north east. These ridge building waves approach the coast at a slight angle after refraction and this is reflected in the alignment of the ridges. Because of the general southerly movement of the ridges they also appear to move steadily inland on any one profile. The part of the ridge nearest the top of the beach becomes stabilised first due to protection from wave attack by the growth of new ridges on the lower foreshore. However, at the southern, distal, end of the ridge landward movement continues and this causes the convex plan shape of the ridges. King (1971) suggests that the ridges represent the attempt by the waves to build up an equilibrium gradient on a foreshore slope which is too flat in overall gradient. Since the supply of sand to the foreshore south of Skegness pier is much greater than to the north, as discussed in the preceding section, the overall gradient is flatter and hence ridges tend to be larger. The average overall gradient on the two main profiles established at Gibraltar Point and Skegness for this study were respectively 0^{o} 55' and 1^{o} 28'. However, it appears that a surplus of beach sediment is not a prerequisite for ridge growth as ridge and runnel morphology is well developed north of Skegness in an area susceptible to erosion and with limited sediment supply.

In cross section the form of the ridge shows a firm, straight slope facing the sea. This is the swash-backwash face constructed by these processes in establishing their equilibrium gradient. The ridge crest is usually flattened and consists of much less consolidated sand with some coarser material, whilst the landward slope is shorter and steeper. The landward face may either merge gradually into the next landward runnel, as often occurs on the lower foreshore, or may be very steep as a result of gravity, slip-face construction and erosion by the water draining from the landward runnel. The bottom of the runnels themselves

is composed of very fine sediment, often with a mean phi size of less than 2.0, and frequently contains assemblages of micro-features ranging from wave-formed ripples to current-formed megaripple features.

In the short term surveys of beach changes reveal a stability of features (King,1968). Measurements on pegs along a profile every 3-4 days between March 1961 and August 1962 exhibited a slow and regular pattern of changes with slow ridge growth and movement. Only 22 out of 582 observations indicated changes in level of over 5cm during the summer period whilst this figure was 42 out of 480 observations for the winter period. Total changes did not exceed 10cm in the summer period and in the main any large changes that occurred were the result of runnel formation.

However, catastrophic changes can also occur in a short period with the recurrence of large storms and storm surge conditions. At these times much of the beach material is removed to the immediate offshore zone and the ridge and runnel morphology disappears. The normal beach profile rapidly returns after such events but complete recovery, particularly of the backshore, may take much longer. King and Barnes (1955) describe the beach changes along the Lincolnshire coast following the 1953 storm surge but conditions of less severity have produced similar 'planing away' of the ridge and runnel topography. Where the sediment cover is thin, particularly north of Skegness, the clay base beneath the beach may be exposed during the catastrophic events. The tidal cycle of spring and neap tides was found to have relatively little influence on the short term beach changes under normal conditions (King, 1968) but may be related to the more general location of beach ridges. On all profiles from Skegness and Gibraltar Point the two main ridges present seem related to the mean high spring tide and mean high neap tide levels.

The location of the two profiles used in this study is indicated in Figure 1.1. Plates 1.2 to 1.7 give aerial and ground views of the two

Plate 1.2. Aerial view of H2 profile, Gibraltar Point, May 1978. Note trend of ridges and runnels at angle to trend of coast.

Plate 1.3. View down the line of profile H2 from backshore, March 1978. Note line of breakers on Inner Knock bank in middle distance.

Plate 1.4. View up line of H2 profile from lower ridge, March 1978.

Plate 1.5. Aerial view of E1 profile, Skegness, May 1978.
Note insignificant effect of groynes.

Plate 1.6. View down line of E1 profile from backshore, March 1978.

Plate 1.7. View up line of profile E1 from lower ridge, March 1978.

profiles. A selection of surveys along these profiles at Gibraltar Point and Skegness (Figures 1.11 to 1.15) reveal the changes in the shape and position of ridges and runnels during the period of study, September 1975 and October 1976. It is difficult to say from the limited number of surveys completed on H2 and on E1 how much the changes are due to any cyclical effect, seasonal or tidal, but it seems likely that on the longer term trend of steady landward movement of ridges, shorter term patterns will be superimposed.

The sweep zones for the two profiles indicate the height and size of the ridges and the magnitude of the changes that have taken place over the period./ Some differences between Skegness and Gibraltar Point Figures 1.16 and 1.17. may be discerned but it must be remembered that ridge height is also a function of size of material (King, 1971). The average slope of the seaward face on the main ridge at Skegness was greater than on the upper ridge at Gibraltar Point because much coarser material was involved, Table 1.1. Parker (1971), working on a ridge and runnel foreshore at Formby Point north of the Mersey Estuary, has described the succession of environments across the foreshore during the rise and fall of the tide. The morphology of the beach, especially on the lower foreshore, is somewhat different to that at either Gibraltar Point or Skegness and consequently timing of events may be different, but nevertheless the general sequence of events remains roughly the same.

Broadly speaking, during spring tides the period between low water to 3 hours flood tide on the incoming flood tide sees much of the lower ridge covered by the tide as it advances over a surface of plane bed and current lineation. Breaker heights generally increase during this period at Gibraltar Point and tidal currents are effective on the beach near the low water mark. By the third or fourth hour of the flood tide water flows up the runnel landward of the lower ridge and begins to enter the runnel across the top of the lower southerly part of the ridge.

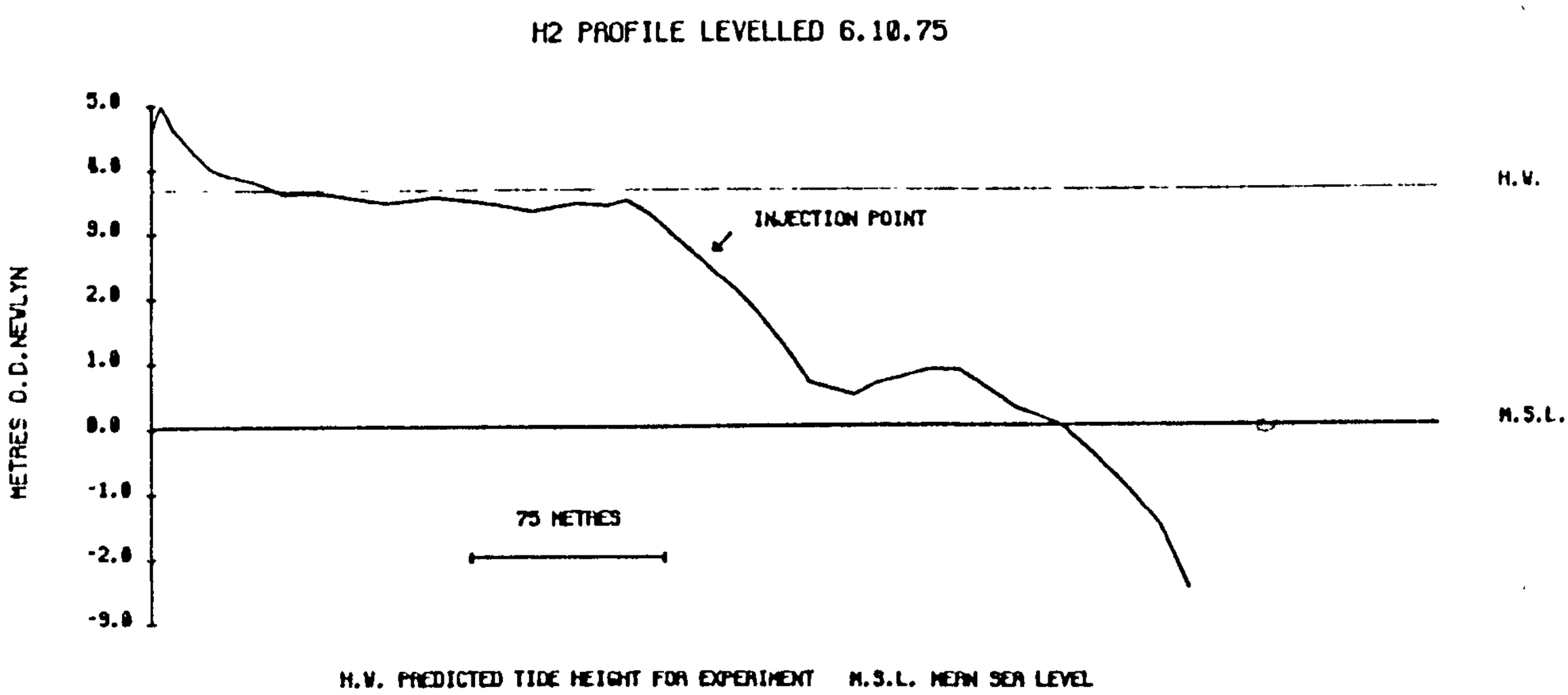

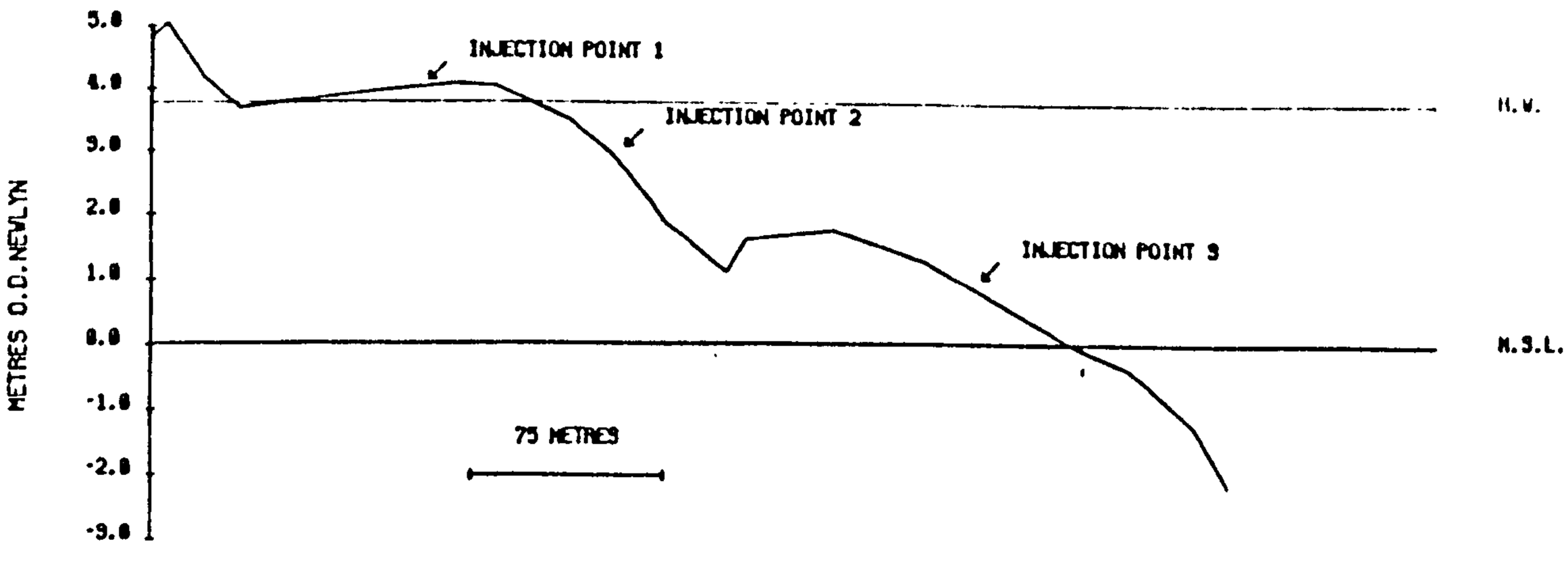

Figure 1.11. H2 profile surveyed on 6.10.75 and 18.3.76.

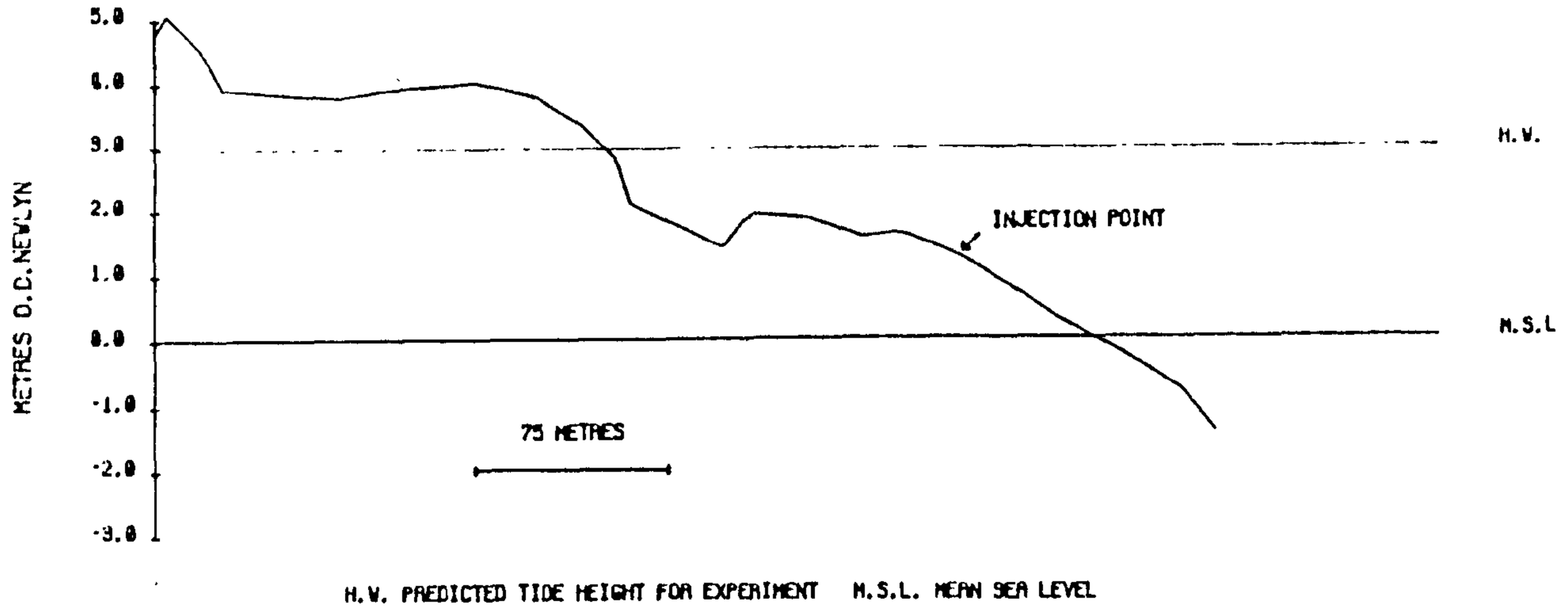

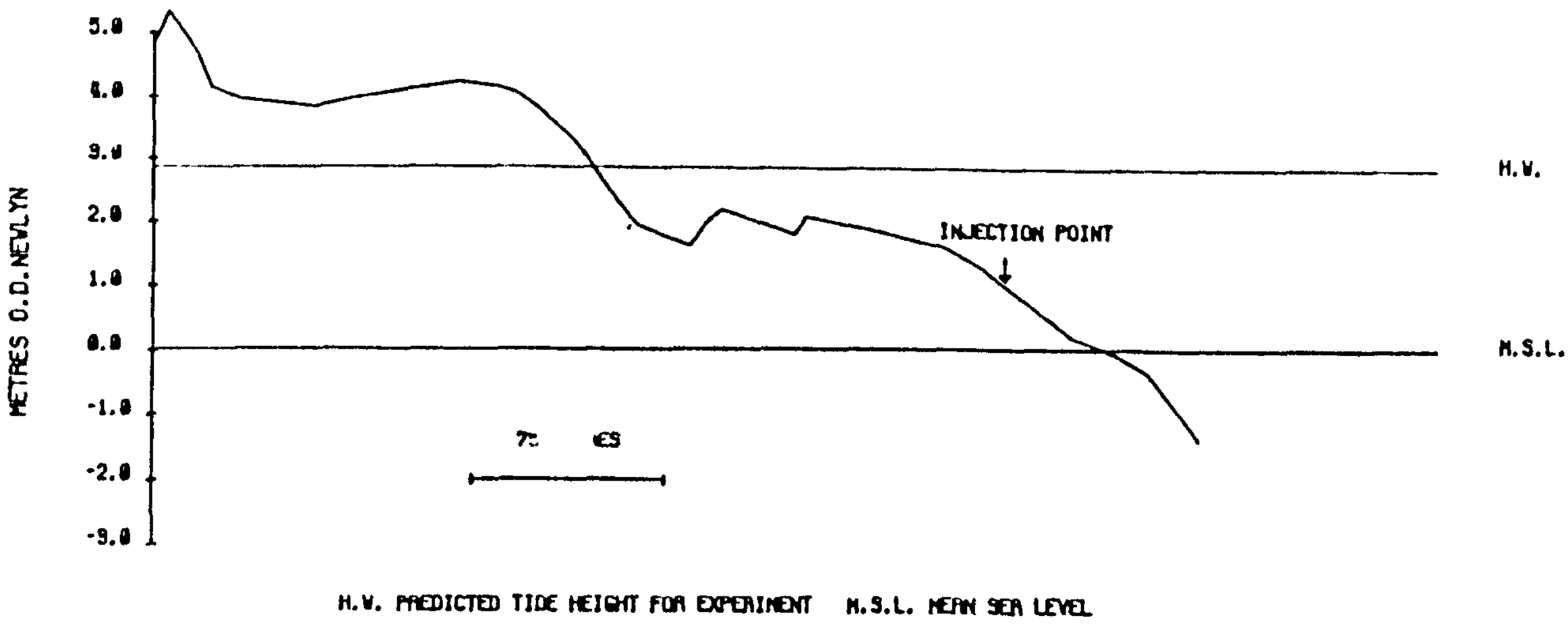

Figure 1.12. H2 profile surveyed on 17.5.76 and 10.8.76.

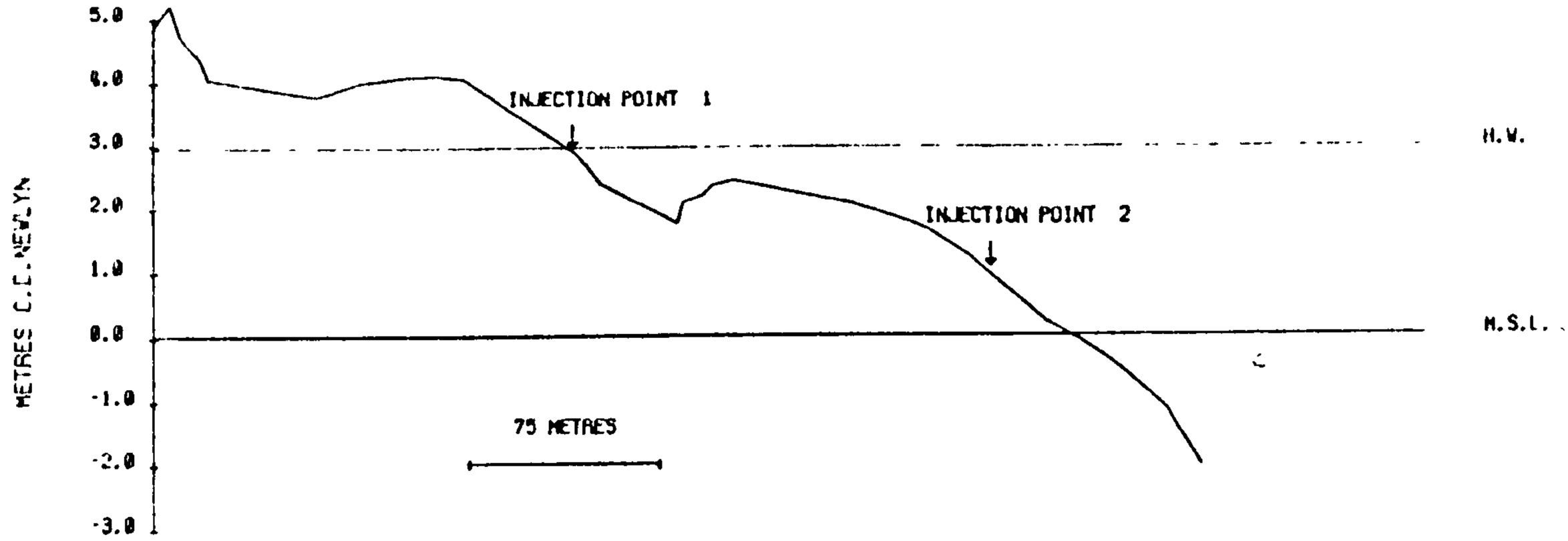

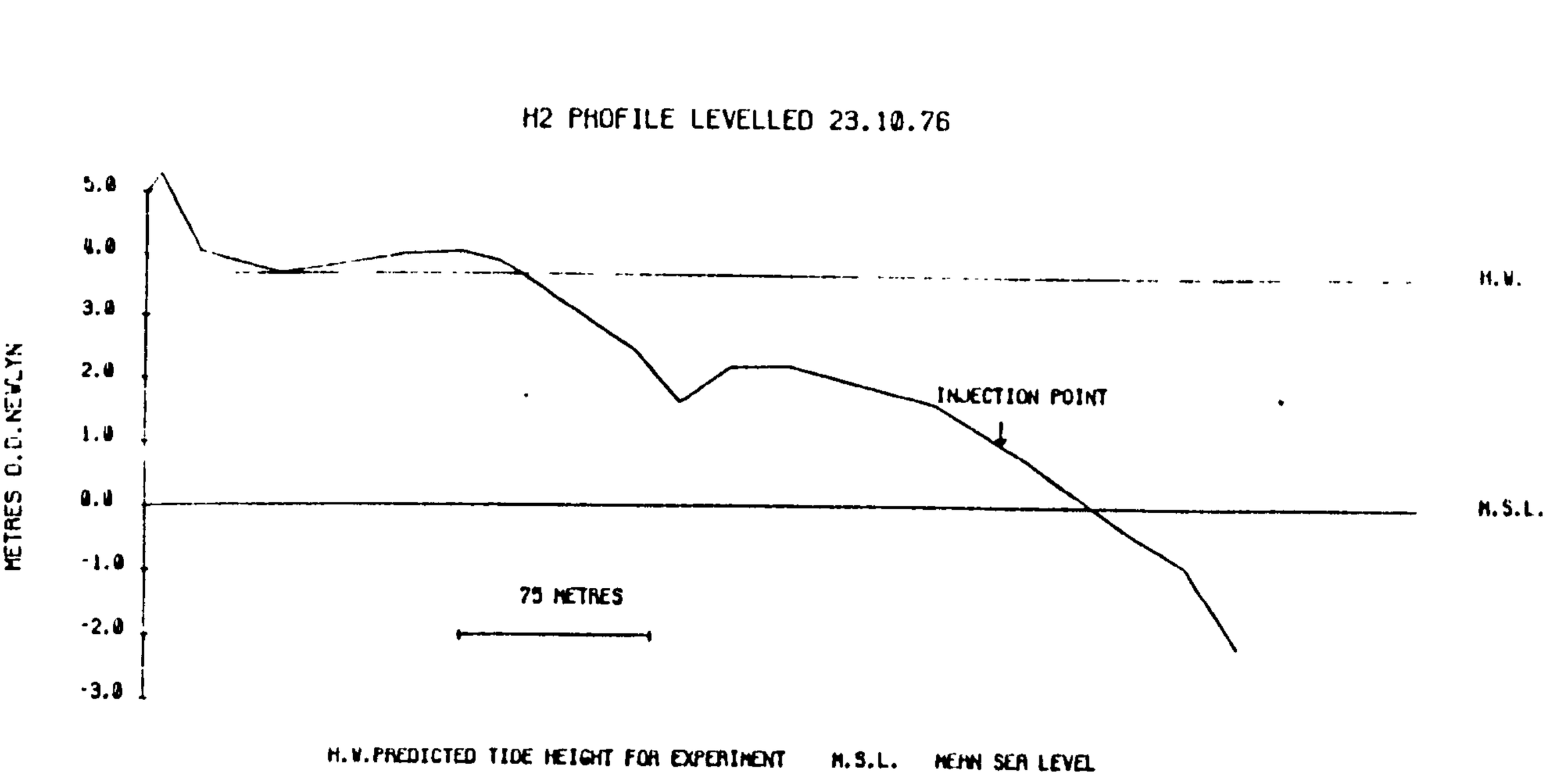

Figure 1.13. H2 profile surveyed on 22.9.76 and 23.10.76.

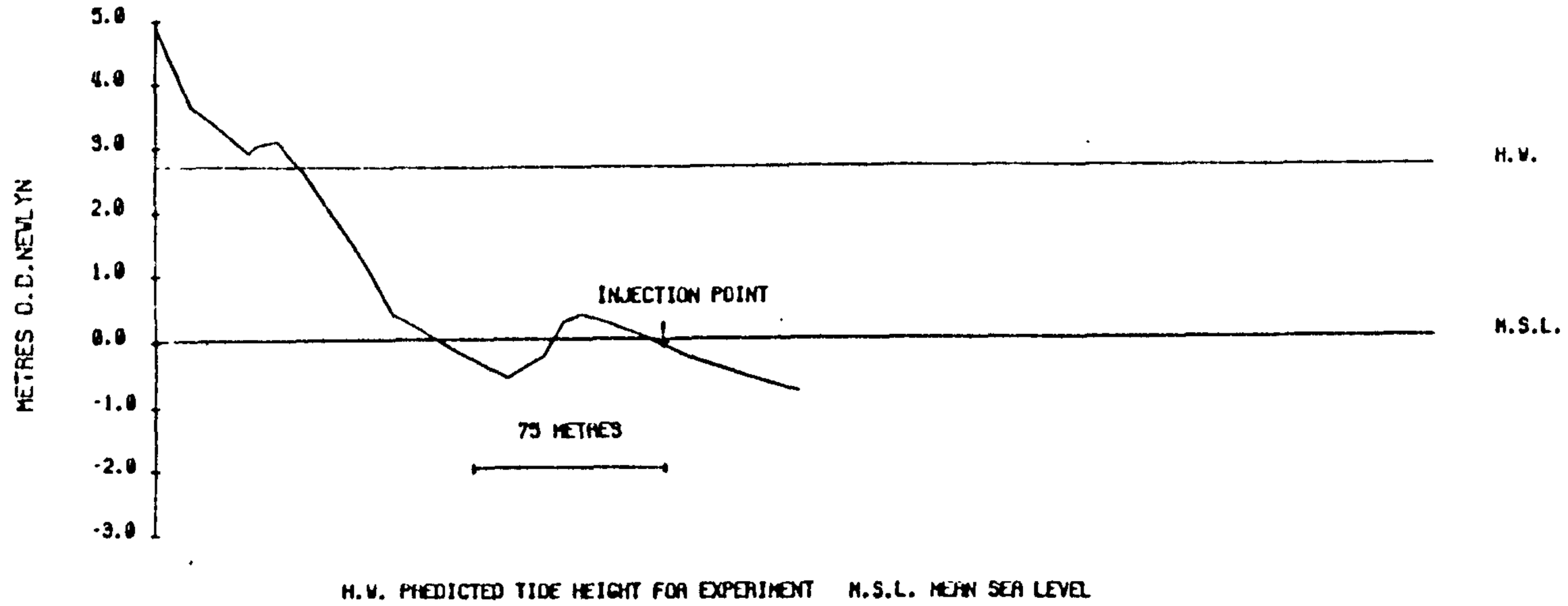

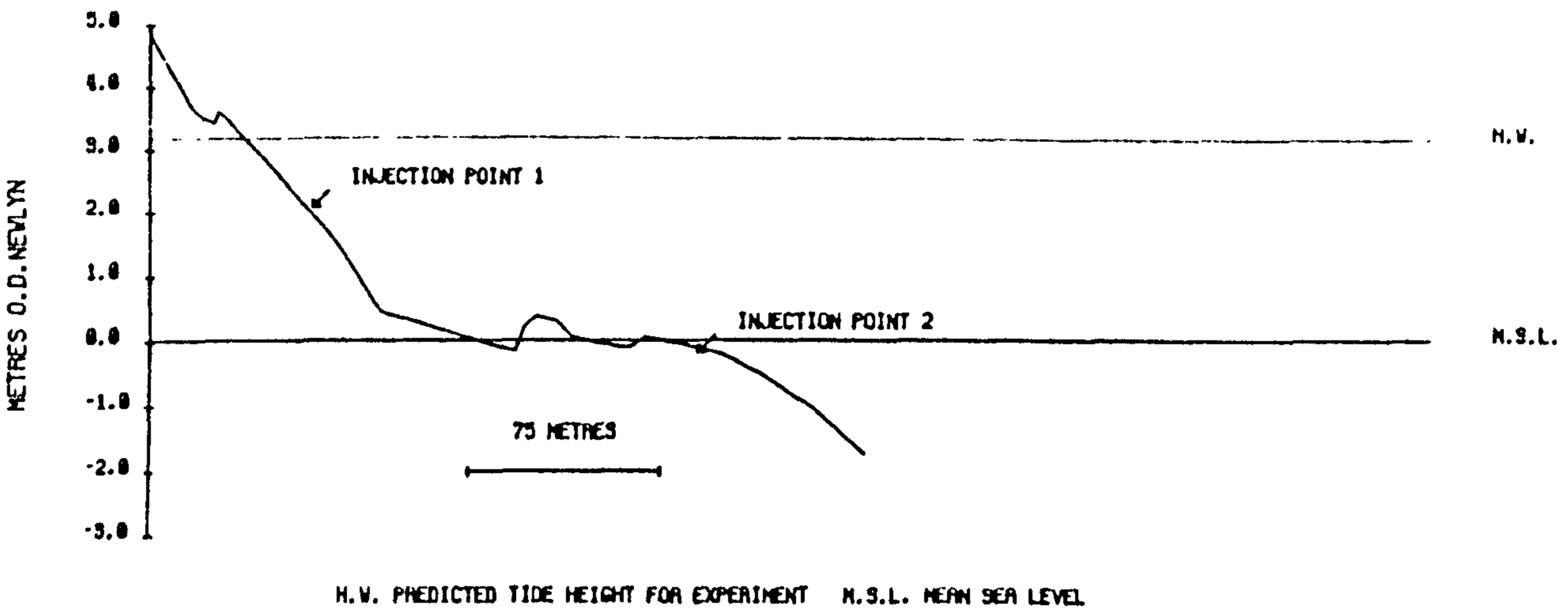

Figure 1.14. E1 profile surveyed on 18.5.76 and 25.8.76.

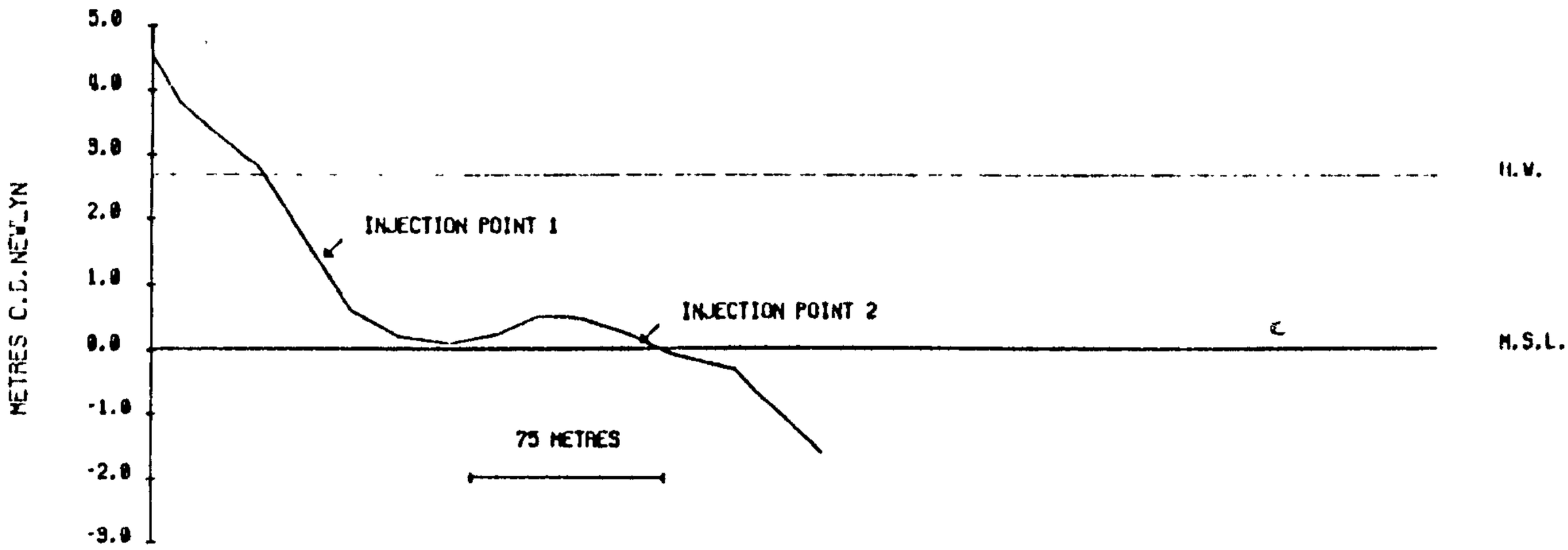

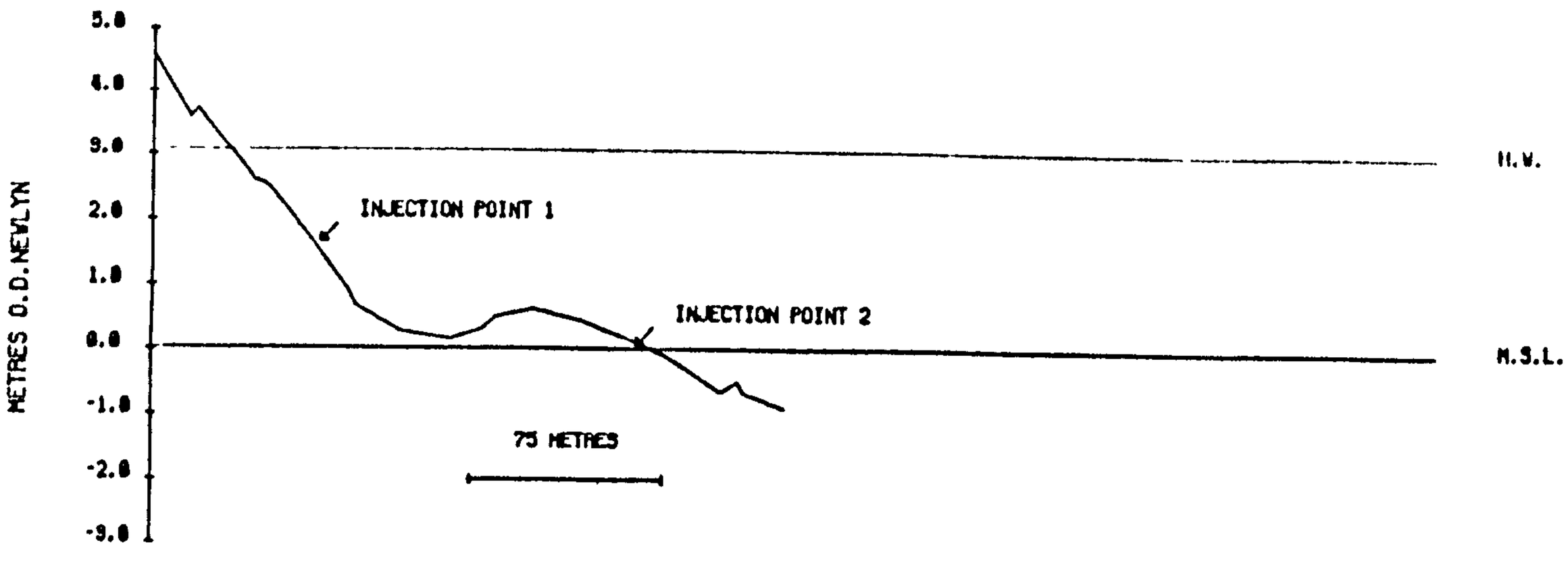

Figure 1.15. E1 profile surveyed on 21.9.76 and 22.10.76.

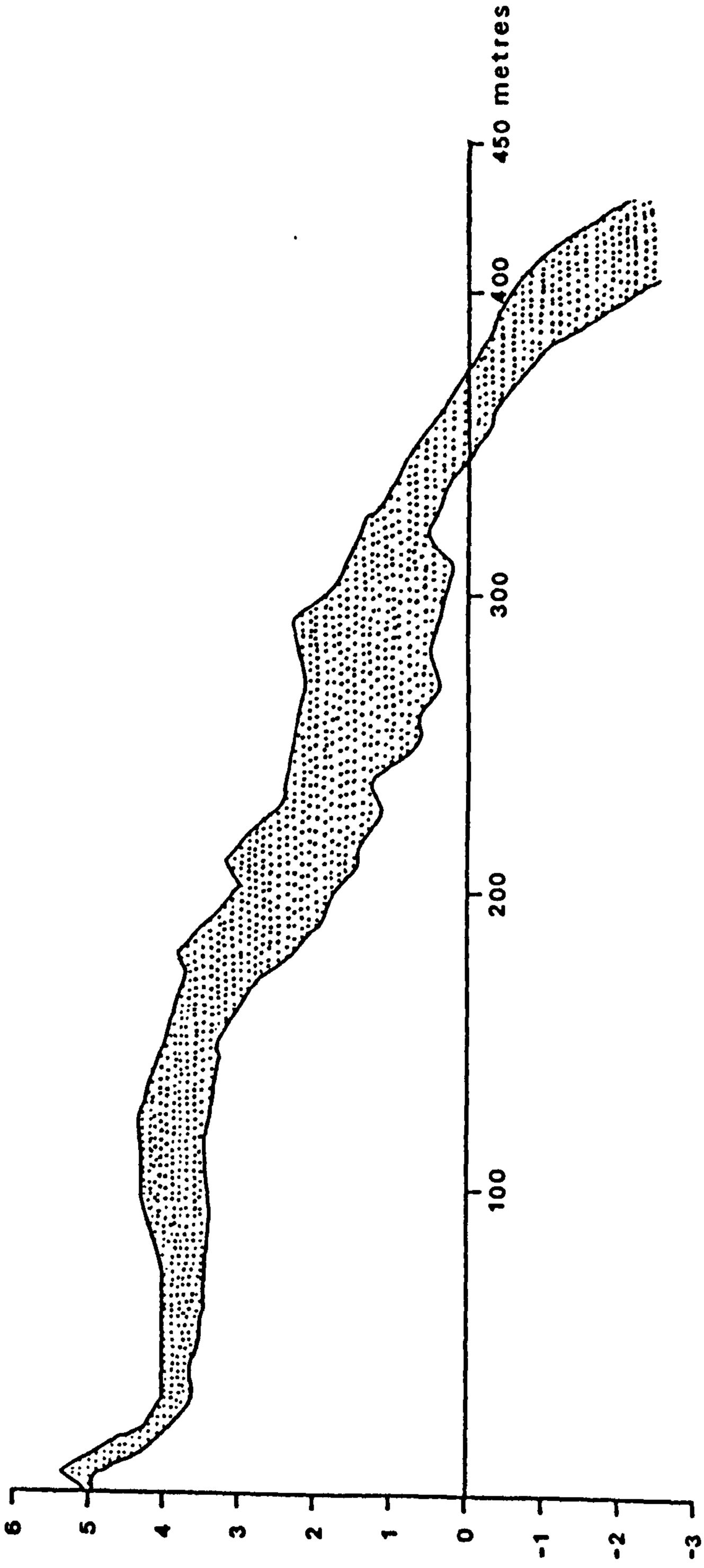

Figure 1.16. Sweep zone for H2 profile, October 1975 to October 1976.

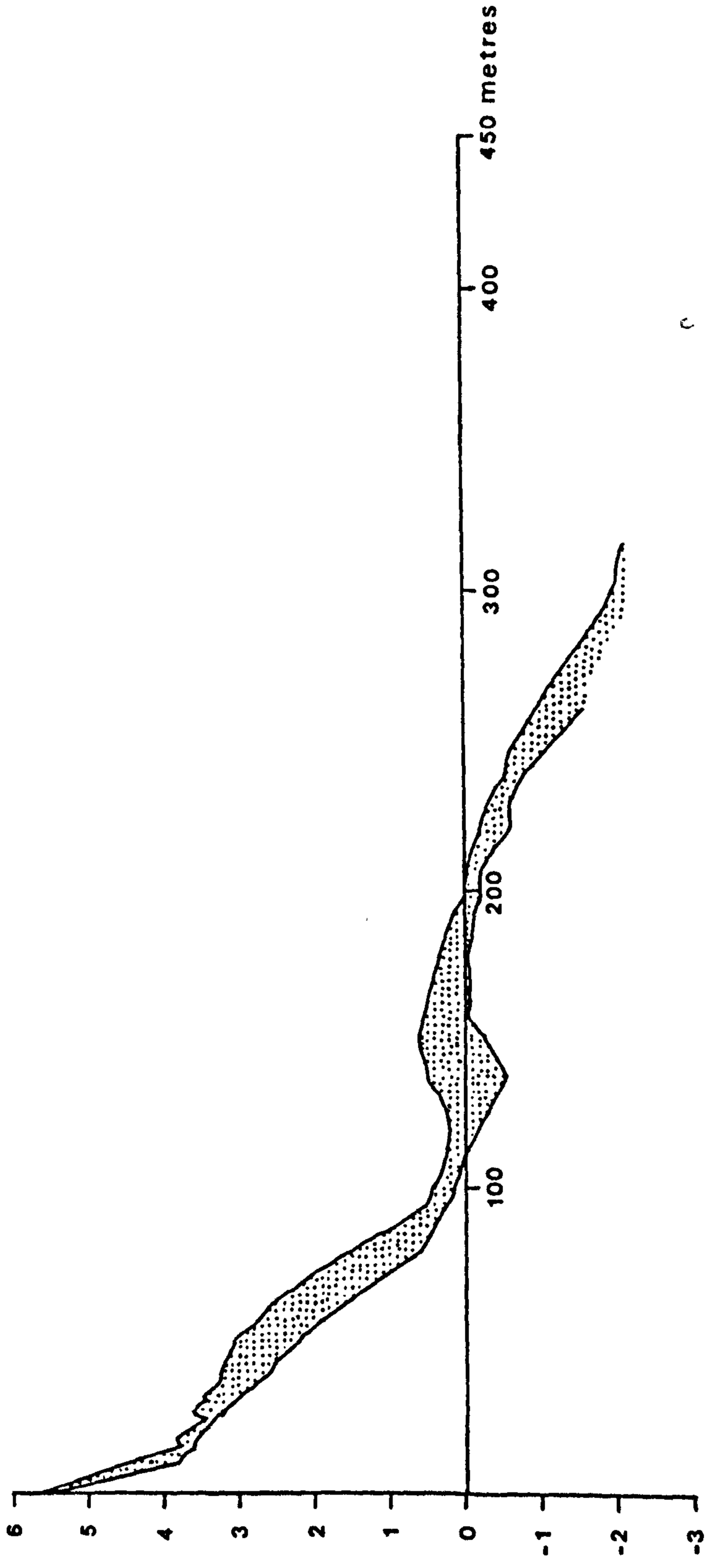

Figure 1.17. Sweep zone for E1 profile May 1976 to October 1976.

As the water level rises up the swash-backwash face of the lower ridge water begins to flow over the higher parts of the ridge crest and into the runnel, causing standing waves to develop in the very shallow water on the ridge crest. Short lived currents of high velocity occur in the runnel as water flows into the runnel filling it rapidly. At the Skegness site incipient seaward drainage channels across the less massive lower ridge stream the flow into the runnel and very strong northward flowing currents are produced for a short period.

As the breaker zone approaches the ridge crest longshore currents are generated in the new completely filled runnel, flowing in a direction dependent upon the direction of wave advance. The duration of the currents is governed by the continued existence of the breaker zone over the ridge seaward of the runnel, which in turn depends upon the heights of the incoming waves and their critical depth for breaking. The rate of rise of the tide will also play an important part in this. Moreover, with large waves or lower tides the dominant breaker zone may remain over the lower ridge crest for much of the tidal cycle, with a secondary breaker zone formed on the seaward face of the next ridge. On the other hand, with small waves and on spring tides the breaker zone may remain over the lower ridge crest for only thirty minutes before the water reaches sufficient depth for the waves to cross the ridge without breaking and break on the seaward face of the next ridge. In this latter case, when the breaker zone 'jumps' across the runnel the currents within the runnel die down. (Figure A1.10).

During the last two hours of the flood tide the breaker zone gradually moves up the face of the upper ridge and, where they exist, runnels on the upper beach fill slowly from the south. At Gibraltar Point, on the H2 profile, the runnel forming the backshore in front of the easternmost dunes is often filled on the high spring tides and the breaker zone reaches the upper ridge crest. However, it is only under storm conditions

or when spring tide levels have been raised above predicted height that waves break on the dune face. Similarly at Skegness it is only under severe conditions that the water level reaches the base of the dunes. The origin of H2 profile is located in the easternmost dune line at Gibraltar Point and this dune line represents the stabilised crest of a recently formed beach ridge. At high spring tides it becomes isolated from the main dune line further inland by the filling of the intervening strip marsh area. (Plate 1.2)

The ebb tide sees a reversal of the sequence of events with the breaker zone gradually moving down the swash/backwash face of the upper ridge, crossing to the lower ridge crest and reaching low water mark with much reduced wave heights at Gibraltar Point.

No specific study of the distribution of bedforms on the beach was made but from observations during tracer experiments it was apparent that at both Gibraltar Point and Skegness the upper flow regime of the swash/backwash zone provided the dominant planar bedform. Seaward ridge faces exhibited planar bed surfaces and also the whole of the lower beach to low water mark. On the other hand, the runnels frequently contained a whole suite of both upper and lower flow regime bedforms. Small sandwave type features or megaripples were sometimes found, as for example on the 22.9.76. On this occasion these features were very pronounced in the main runnel on H2 profile with amplitudes of 35-45cm and chord lengths of 6-7 metres. These features are formed by strong currents flowing in the runnel. Other smaller asymmetrical ripples formed by draining currents were also often present. In addition, small wave-generated ripples were sometimes in evidence. The survival of these lower flow regime bedforms, in particular the smaller features, is due to the protection of the runnel by the ridge to seaward, a process termed by Parker (1971) 'topography controlled survival.' Swash/backwash and breaker zones do not affect the runnel when the tide is falling and

consequently the lower flow regime bedforms in the runnel are not destroyed. The breaker zone 'jumps' from ridge to ridge very quickly because of the depth of water in the runnel which prevents wave breaking.

Occasionally at Gibraltar Point the repeated occurrence of the breaker zone close to the upper ridge crest, given the correct tidal height, leads to the formation of cusp like features along the crest of the ridge with associated channels down the ridge face, (Figure 1.18). On the 28.2.76, for example, these features had an amplitude of 20-30cm and an average wavelength of 15-20 metres. Shingle patches were often associated with the seaward limit of the ridge face channels and in one particular case this lag deposit was 20 metres from the beginning of the trough at the ridge crest.

More frequently occurring were large scale megaripples on the landward side of the lower ridge at Gibraltar Point and on the ridge crest. Aligned in a longshore direction they reflected the strength of alongshore flowing currents on this section of the beach. These features were usually present under high energy wave conditions and on spring tides. These large scale features were notably absent from the lower ridge at the Skegness site E1, reflecting considerably calmer conditions at this site. Bedforms on the lower ridge at Skegness consisted largely of small wave formed ripples, present in slight depressions, and planar bed.

Studies of sedimentary characteristics at Gibraltar Point by Davies (1963) and King (1970) have shown that mean grain size decreases down the beach to the low water mark, with variations on this general trend related to the morphological units of the foreshore. Mean grain size for the tracer experiments carried out on profile H2 at Gibraltar Point on the seaward face of the upper ridge was 1.65 ϕ compared with 2.24 ϕ for the lower ridge face. On the lower foreshore between MLNT and MLST very fine sand occurs with mud and silt also present so that mean grain

Figure 1.18. Sketch of cusp features of upper ridge face H2 profile during 28.2.76 tracer experiment.

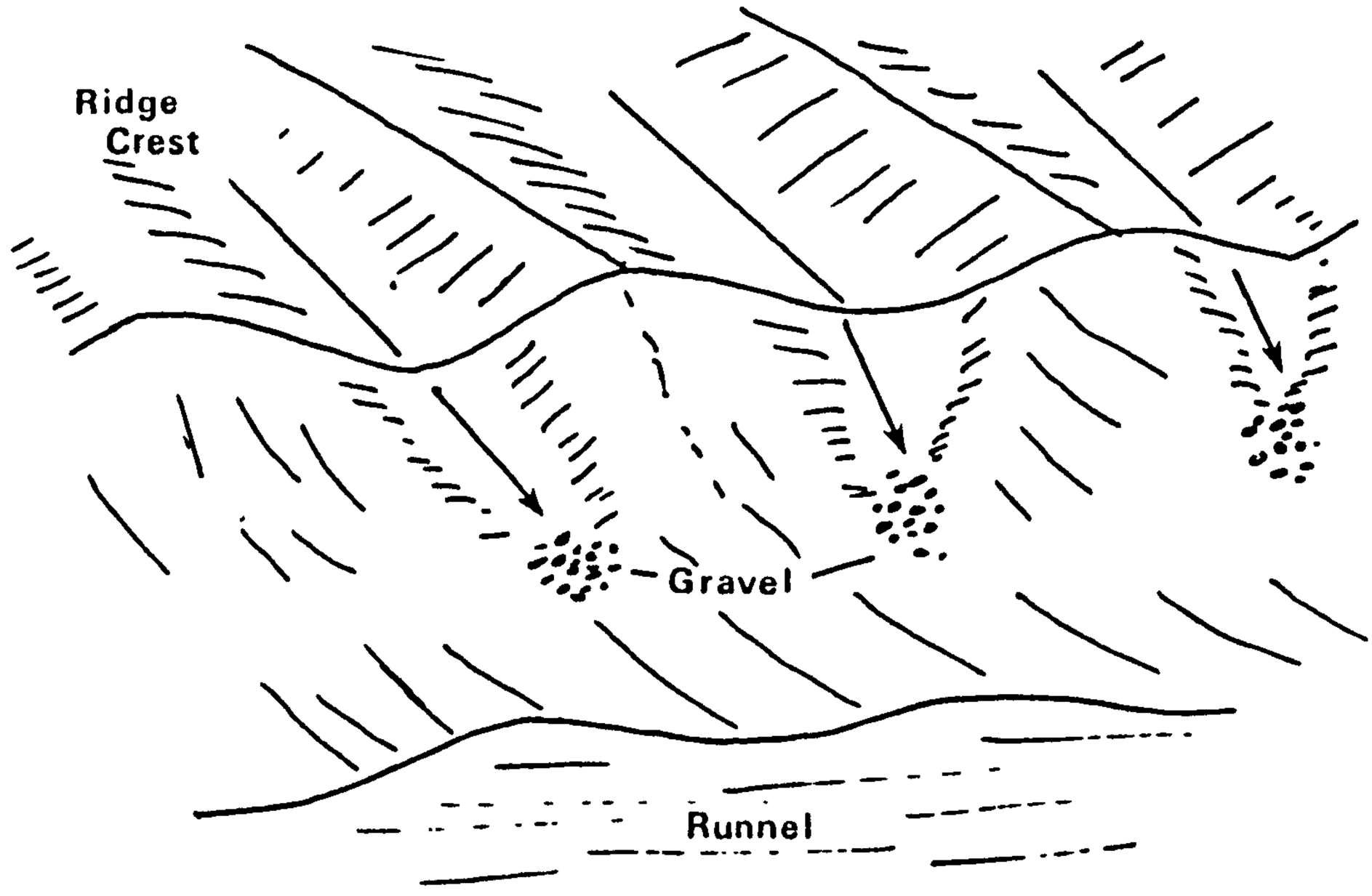

Table 1.1 Average figures for grain size and beach slope on H2 and E1 profiles for all tracer experiments.

	GIBRALTAR POINT (H2)	SKEGNESS (E1)
Mean grain size upper ridge seaward face Ø	1.6457	0.5194
Mean grain sorting upper ridge seaward face Ø	0.8615	1.8223
Mean grain size lower ridge seaward face Ø	2.2380	2.1412
Mean grain sorting lower ridge seaward face Ø	0.8849	0.6538
Mean beach slope upper ridge (degrees)	2.26	3.28
Mean beach slope lower ridge (degrees)	1.36	0.78

size may be smaller than 3.0 Ø. Mud is deposited at low water under calm conditions when the offshore bank system provides protection from wave attack. Mud and silt are also found in the runnels on the foreshore and here again sediment size may be as fine as 3.0 Ø. Commonly mean grain size on the seaward face of a ridge is coarser than on the crest although the difference may only be slight.

At Skegness on the E1 profile the contrast between the upper and lower ridges in terms of the mean grain size of the seaward face is even more striking with much coarser material being found on the upper ridge (Table 1.2). Comparisons with Gibraltar Point can also be made with Table 1.3. Table 1.1 shows the mean grain size figures for the tracer experiments. The coarser material forming the upper ridge at Skegness compared with Gibraltar Point is reflected in the steeper average slope of this ridge (Table 1.1) as already mentioned.

Because of the complex morphology of the beach at both Skegness and Gibraltar Point and the large tidal range of this part of the North Sea Coast, it is implied that a complex pattern of sand movements takes place across the foreshore. Parker (1975) has described an open cell-like pattern of movement between ridges and runnels based on the idea that the ridges are forms through which sediment passes from one runnel to another. With runnels acting as barriers to landward movement of material Parker suggests that landward transport paths are generally short with most of this movement taking place on the crests of ridges. The patterns of sand movement on various parts of the foreshore were examined in this study with fluorescent tracer and these will be discussed in a later chapter.

Table 1.2 Variation of sediment characteristics down E1 profile.

	Location	Distance Down Profile (M)	Mean Grain Size (Ø units)	Sorting (Ø units)
1	Backshore	0	1.663	0.534
2	Backshore	22	1.960	0.529
3	Top of upper ridge	56	-1.706	1.566
4	Runnel	130	2.115	0.873
5	Top of lower ridge	162	2.000	1.009
6	Low water terrace	264	2.309	1.066
7	Low water mark	336	2.798	0.491

Table 1.3 Variation of sediment characteristics down H2 profile.

	Location	Distance Down Profile (M)	Mean Grain Size (Ø units)	Sorting (Ø units)
1	Backshore	25	1.227	1.302
2	Middle of top runnel	50	2.164	0.540
3	Landward face of top ridge	60	1.636	1.017
4	Top of upper ridge	110	0.810	1.522
5	Seaward face top ridge	160	0.359	1.529
6	Middle of second runnel	210	2.193	0.593
7	Seaward face bottom ridge	260	2.034	1.000

PART 1.

Part 1 consists of three chapters. Field methods and the production of the fluorescent tracer sand are dealt with in the first of these chapters. The discussion is concluded with a brief section examining the major problems encountered during fieldwork. The second chapter, Chapter 3, describes the laboratory techniques employed in sample analysis and the mode of presentation of the data. The simple numerical descriptors of the tracer dispersion used in the study are also outlined. Finally, in the third chapter a qualitative consideration of the results of the tracer experiments is made. Specific experiments designed to test particular aspects of sand movement are examined together with more general features arising from the field studies.

CHAPTER 2

DATA COLLECTION

2:1 Introduction

Following Ingle and Gorsline (1973), methods of employing fluorescent tracer in the nearshore and foreshore environments can be divided into three broad categories:

1. The time-integration, or Eulerian, method. This involves the release of a known quantity of tracer sand at a point source and the continuous sampling of the moving bed load at a certain distance from the source. The variation of tracer concentration with time at the sampling point is then analysed to give an estimate of the velocity of grain movement.

2. The dilution method. Tracer grains are injected at a constant rate such that the concentration of tracer grains as sampled at a point 'downstream' will become stabilised. Velocity of grain movement can then be calculated from the distance to the sampling point and the time taken for tracer concentrations to become stabilised.

3. The space integration, or Lagrangian, method. A known quantity of tracer grains is released and areal sampling is carried out over the resultant tracer cloud. Movement of the centre of gravity of the tracer cloud in a given time period can then be used to calculate the velocity of tracer grains.

Discussing these methods in more detail, Crickmore and Lean (1962A, 1962B, 1966) describe their use in flume experiments.

A notable disadvantage of both the time integration and dilution methods is that they are, in effect, linear methods since they are suitable only for assessing rates of sand transport in one general direction. On the other hand space integration methods are more flexible being, by definition, of an areal nature. They facilitate the study of tracer

dispersion patterns and other features of grain movement in addition to the calculation of transport rates. Because of this a variant of the space integration method was the technique eventually employed in this study.

In all 23 successful tracer experiments were carried out in the period September, 1975 to October, 1976. In the light of experience gained from each experiment, especially the earlier studies, the field techniques used were gradually developed and experimental redesign took place as the series of tests progressed. This chapter will consider the field procedure adopted for the later experiments in the series, the procedure found to provide the most useful results. Any relevant major variations from this procedure will also be discussed.

2:2 Tracer production

The primary requisite of a sediment tracer is that it must be physically similar to the grains occurring at the study site in the field or in the wave tank in order that it reproduces as closely as possible the transport characteristics of the unmarked particles. Artificial materials such as pulverised coal, broken brick and magnetic concrete, which have all been used in sediment movement studies, are unlikely to fulfil this requirement. Apart from the fortuitous cases in which naturally occurring tracers can be used, such as heavy minerals as used by Cherry (1966) in his study of longshore movement of sand on part of the Californian coast, tagged natural grains are used as tracers in most present day studies of sediment movement.

There are two main approaches to tagging natural sand, using radioactive isotopes or fluorescent paint. Induced radioactivity brings with it problems of safety risk and lengthy preparation times in addition to the high cost of production of such tracers. Perhaps the most serious of these problems is the length of time radioactive tracer production

takes. The sand requires careful preparation before, and a lengthy cooling period after, bombardment in an atomic pile. There is therefore, a considerable time lag between removal of sand from the study area and its reintroduction as radioactive tracer. Since there is a constant change in foreshore sand and grain size distribution the tracer released may bear little resemblance to in situ sand in terms of grain size and sorting characteristics because of the time lag. On the other hand one major advantage of radioactive isotope tagging is that small grains can be marked successfully whereas fluorescent paint can only be used on coarse silts and coarser grains. However, because of the problems involved with radioactive tracer methods briefly outlined, fluorescent tracer was used in this study.

Fluorescent tracers are defined by Teleki (1966) as "olastic particles coated with selected organic or inorganic substances which upon excitation of 3650Å or 2537Å wavelengths ultraviolent light emit fluorescence of variable wavelength and intensity in the visible region of the spectrum." Teleki goes on to describe several methods of producing these tracers using a variety of combinations of colouring matter and coating materials. Yasso (1965) also provides details of several coating formulations and the results of laboratory tests on these coatings. A summary of many of these techniques is given in Ingle (1966). Ingle also lists the following advantages which all fluorescent dyeing methods have over radioactive techniques:

1. Naturally occurring coarse silt, sand or gravel from a study site can be readily marked.

2. The majority of dyes employed present no legal or health hazards.

3. Different fluorescent hues can be used to differentiate between successive tests at one locality or to trace the movement of different size fractions.

4. The solubility of binding media can in some cases be adjusted so

that it will adhere to grains for a period of from several days to many months.

5. The cost of dyeing is relatively low.

6. Dyeing can be accomplished anywhere and can in fact be carried out at the study site.

7. The time required for dyeing sand is often short sometimes entailing only minutes.

8. The sand to be dyed in most instances does not require special preparation other than drying.

9. The sensitivity of the fluorescent technique is at least equivalent to radioactive techniques.

10. Dyes do not appear to affect the hydraulic character of labelled sand grains.

In the experiments carried out in this study a variation of the coating formulations put forward by Yasso (1965) was employed. Three parts of Day-Glo spray or brush fluorescent paint were mixed with two parts of xylol solvent. This was then mixed with the natural beach sand taken from the selected study site. The only preparation of the sand prior to dyeing was a thorough drying. Attempts to tag the sand whilst it was still wet were notably unsuccessful. A small concrete mixer was used to gain a complete coating of all grains. The use of the mixer also speeded up the drying process after coating and largely eliminated the problem of 'clumping'.

Aggregation of individual particles during the coating process, or 'clumping', was much less of a problem with the coating formulation described because a binding agent was not used. Many of the techniques developed by Yasso and others involve the use of a resin binding agent to attach the fluorescent coating firmly to the grains. This undoubtedly lengthens the life of the coating but also causes serious 'clumping' problems. Since the tracer coating on grains used in this study was

required to last only a maximum of two tidal cycles the binding agent was found to be unnecessary.

Yasso (1965) found that the thickness of a single coat using the method followed in this study was 0.000591 mm on grains between 0.84 and 0.99 mm in diameter. He also found that the percentage weight loss due to abrasion, simulated by rolling marked material in a 24 oz screw cap jar at 120 r.p.m. for 18 hours, was 0.15%. Similar tests carried out during this study also revealed little significant loss of grain coating. However, such tests on coating loss due to abrasion, tend to be inconclusive as it is virtually impossible to simulate adequately the abrasive processes at work in the nearshore. Nevertheless field tests did indicate that grains coated by the method described retained some if not all of their coating for much longer periods than actually required in the tracer experiments. Tracer immersed in the sea for two weeks, in general, maintained its fluorescent coating but it is not possible to state that all grains remained perfectly coated during this period.

As a further test of the effect of coating the grains a mechanical sieve analysis was made of sand samples before and after coating. It can be seen from the average cumulation percentage curves (Figure 2.1) that there is a slight upward shift of the distribution throughout the range of sizes. This is the effect of the coating itself, albeit very thin, on each individual grain and the clumping of grains during the coating process. The larger shift of the curve at the fine end of the range, that is greater than 3.0 ϕ, reflects the inefficiency of fluorescent coating techniques for fine grain sizes due to aggregation of the individual grains. These effects of coating on the grain size distribution were unavoidable but when carefully minimised were deemed sufficiently small to be acceptable.

A wide range of colours is available in the Day-Glo spray and brush paint range, but it was found that many of the colours, although

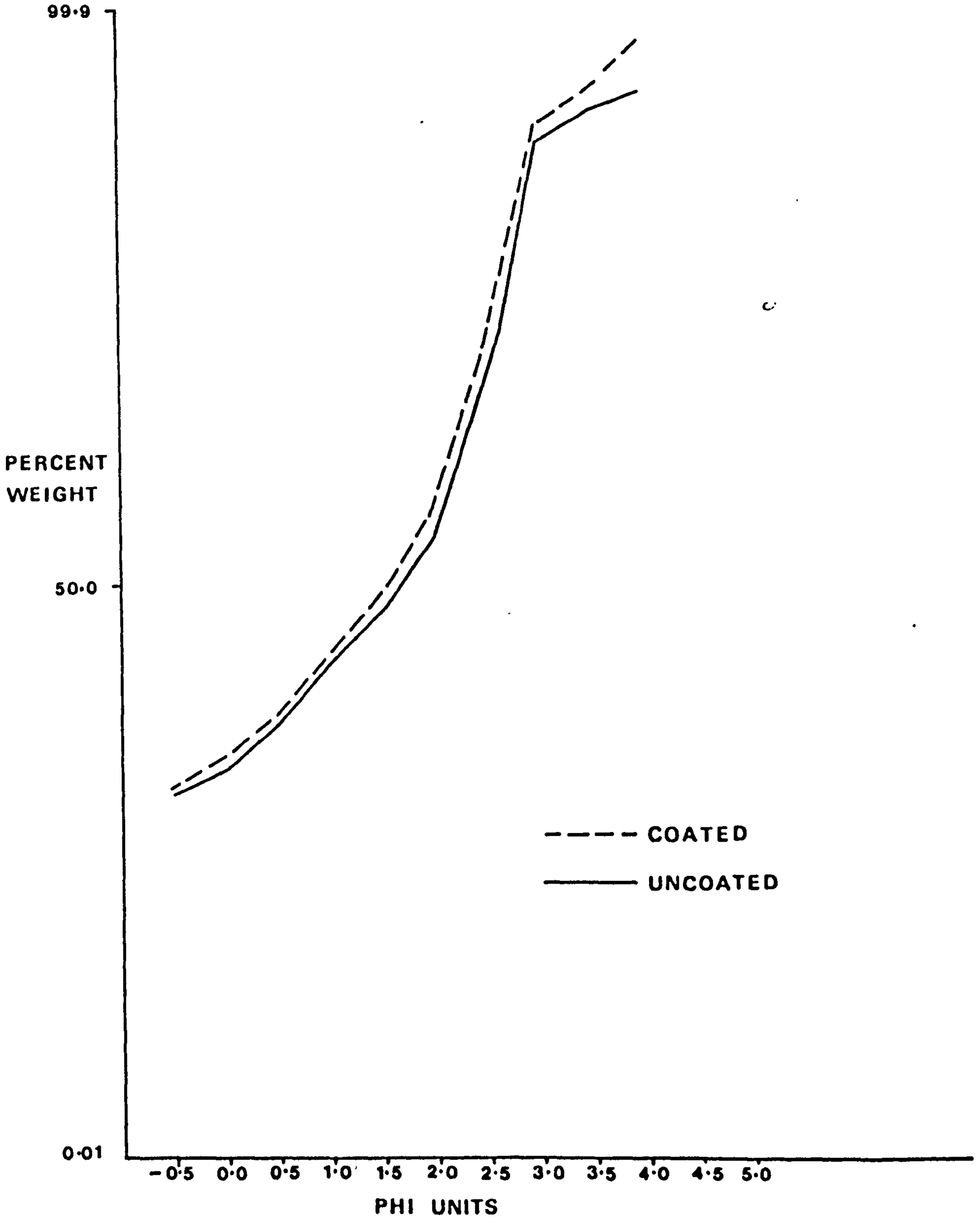

Figure 2.1. Effect of tracer coating on natural sand grains.

distinctly different in ordinary daylight were quite similar in their fluorescent colour in ultra-violet light. Teleki (1967) discussed this problem of overlap of transmission curves for fluorescent dyes in connection with the difficulties which may arise in distinguishing between several colours of tracer in the same sample. By careful selection two colours when chosen, Saturn Yellow and Aurora Pink which fluoresce yellow and orange respectively. These were found to be quite easily distinguishable when present in the same sample.

A third colour, blue, was also used in some grain size tests but this was in the form of commercially produced fluorescent sand. This colour was used sparingly, however, since it was sometimes difficult to distinguish between this tracer and naturally occurring blue fluorescing particles on the beach such as, for example, skeletal remains of marine organisms.

Commercially produced sand, available from British Industrial Sand, was not used for the main tracer experiments in this study because of the lack of agreement between the grain size distribution and hydrodynamic characteristics of this sand and the sand of the test sites. Figure 2.2 and Table 2.1 give a good example of these differences for the experiment of 28.2.76. The high cost of the industrial sand was also a factor in its rejection for this study.

Table 2.1 Grain size characteristics for experiment: 28.2.76. and comparison with commercially produced tracer sand.

	Mean	Standard Deviation	Skewness	Kurtosis
28.02.76 Upper Ridge	1.673	1.032	-1.155	3.285
28.02.76 Lower Ridge	2.431	0.577	-1.443	11.020
Industrial Sand	1.891	0.634	-0.054	2.954

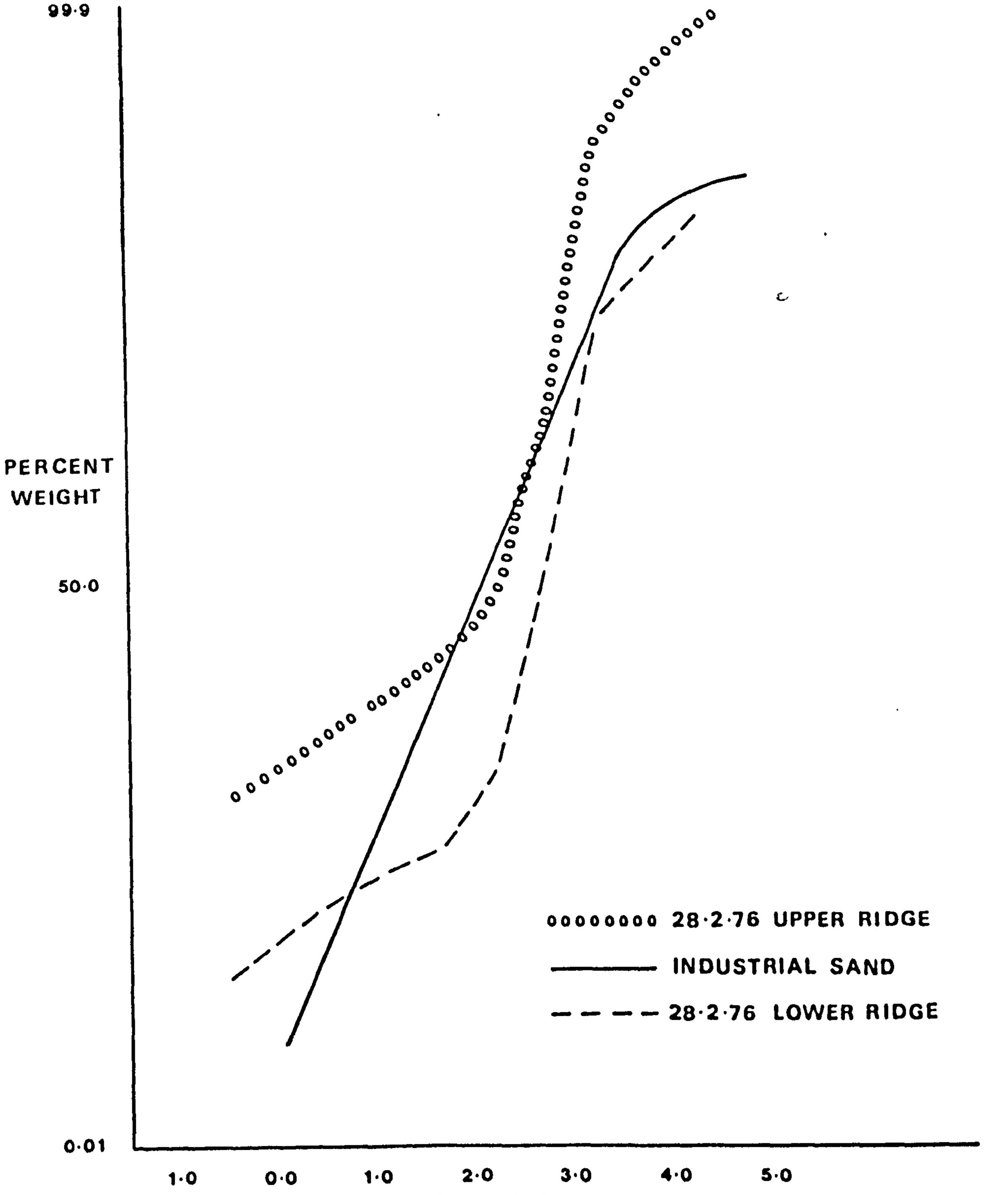

Figure 2.2. Comparison of grain size distribution for natural sand and commercially produced tracer sand 28.2.76 experiments.

In order to minimise the change in grain size characteristics between collection, coating and reintroduction of sand onto the beach face the sand was collected so as to leave as short a time as possible between collection and reintroduction as tracer. In some experiments this period was as short as two tidal cycles, that is 24 hours (17.1.76, 28.2.76, 18.3.76), but in others it was a matter of several days. However, in all experiments the tracer released contained large proportions of the predominant sand grains at the field site. Problems arising from areal differences in foreshore grain size distributions were avoided by collection of sand for each experiment from as near as possible to the selected tracer release point.

2:3 Preliminary experimental procedure

The majority of tracer experiments were carried out on two selected beach profiles (Figure 1.1) but a third profile (H3) was located approximately 500 metres north of H2 at Gibraltar Point. Before the tracer was placed on the beach the profile in use was surveyed using an Autoset Level or Dumpy Level and metre staff so that the position of the tracer injection points could be fixed for later analysis. The profile survey also allowed estimates of beach slope in the vicinity of the release points to be made. In early experiments a slope pantometer was also used to measure slope angles on the beach but this was discontinued as the accuracy of the pantometer was found to be low especially under difficult handling conditions, notably in strong winds.

While the profile was being surveyed a line of marker pegs was placed in the beach down the line of the profile with the central peg marking the injection point. The pegs were spaced at five metre intervals and usually seven pegs were used (Figure 2.3). In addition pegs were inserted perpendicular to the top and bottom pegs of the profile line at a distance of 10 metres. All these pegs were put in as a guide for the layout of the sampling grid at a later stage in the experiment. Since sampling took

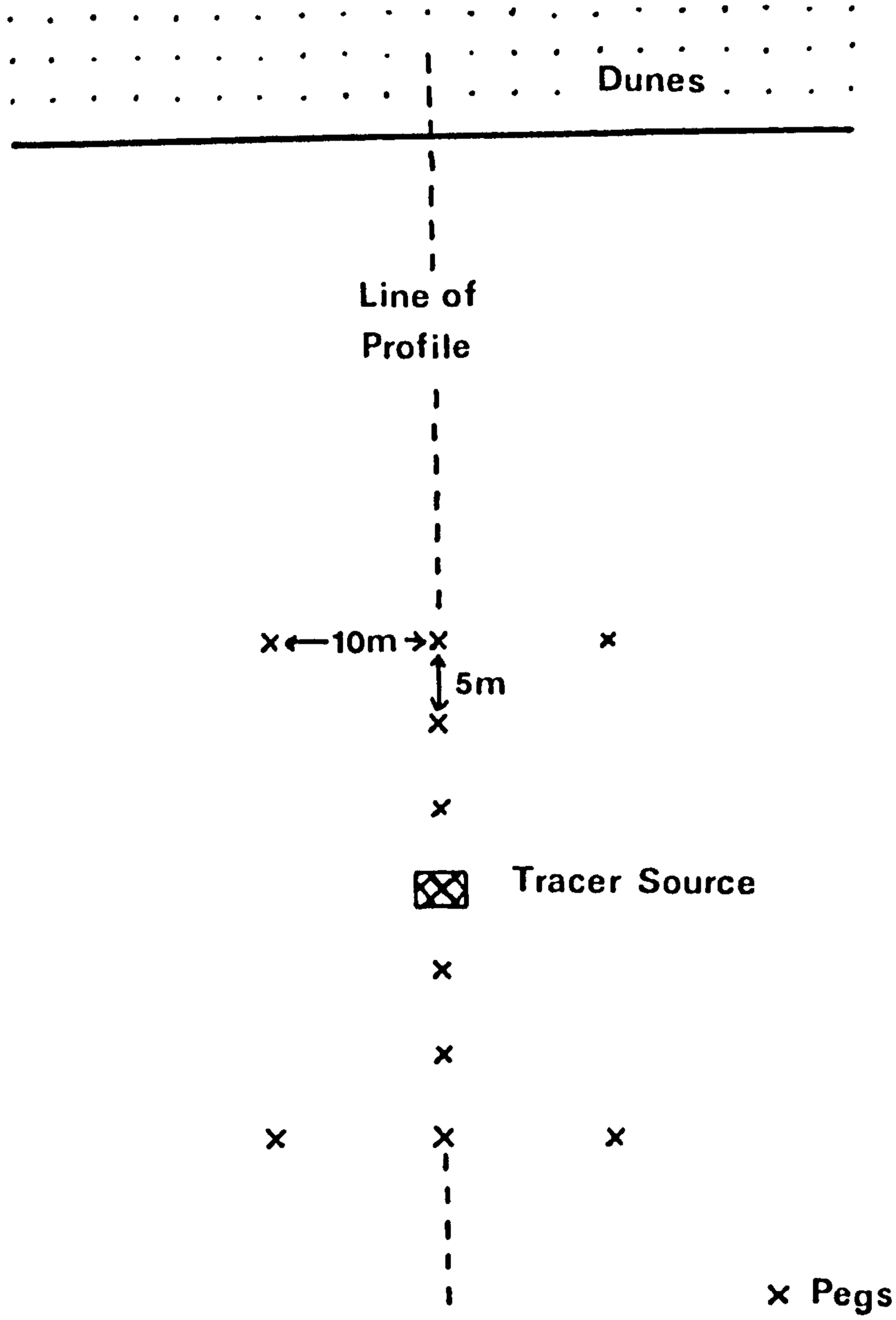

Figure 2.3. Layout of guide pegs for sampling grid.

place during the night the pegs were found to be particularly useful in maintaining the regularity of the sampling grid shape.

In addition to this the pegs placed in the beach face also served as marker points for the places at which depth of disturbance of the upper layers of the beach was measured. The importance of these measurements is discussed in the next section but the techniques of measurement will be briefly described here.

In early experiments the method formulated by King (1951) was employed. This involved the formation of a hole 10 cm deep in the beach surface with a piece of dowelling of 1 cm radius. The hole was then filled with sand coated with indian ink so that a core of black sand 10 cm long was produced. Figure 2.4 indicates the means by which the effects of the sequence of sedimentary events taking place during the tidal cycle can be measured. As erosion takes place the top of the sand core is removed to a depth consistent with the total depth of erosion, 2 cm in Figure 2.4. With final deposition a layer of clean sand covers the top of the core. Therefore, the length of the black sand core remaining gives an indication of the amount of erosion, bearing in mind that its original length was 10 cm, and the amount of clean sand on top of the core represents the final amount of deposition. The net change at that point is the difference between the two.

However, it was found that this method was not altogether satisfactory. It had two main drawbacks. Firstly, it was found to be very time-consuming locating and measuring the core lengths especially since great care was necessary to avoid damaging the cores. Secondly, and more importantly, the cores could not be used at all on particularly damp sections of the beach, where the water table was very close to the beach surface. This was because the thixotropic character of the sand in these locations prevented successful emplacement of the cores.

As a result of these difficulties an alternative method was sought

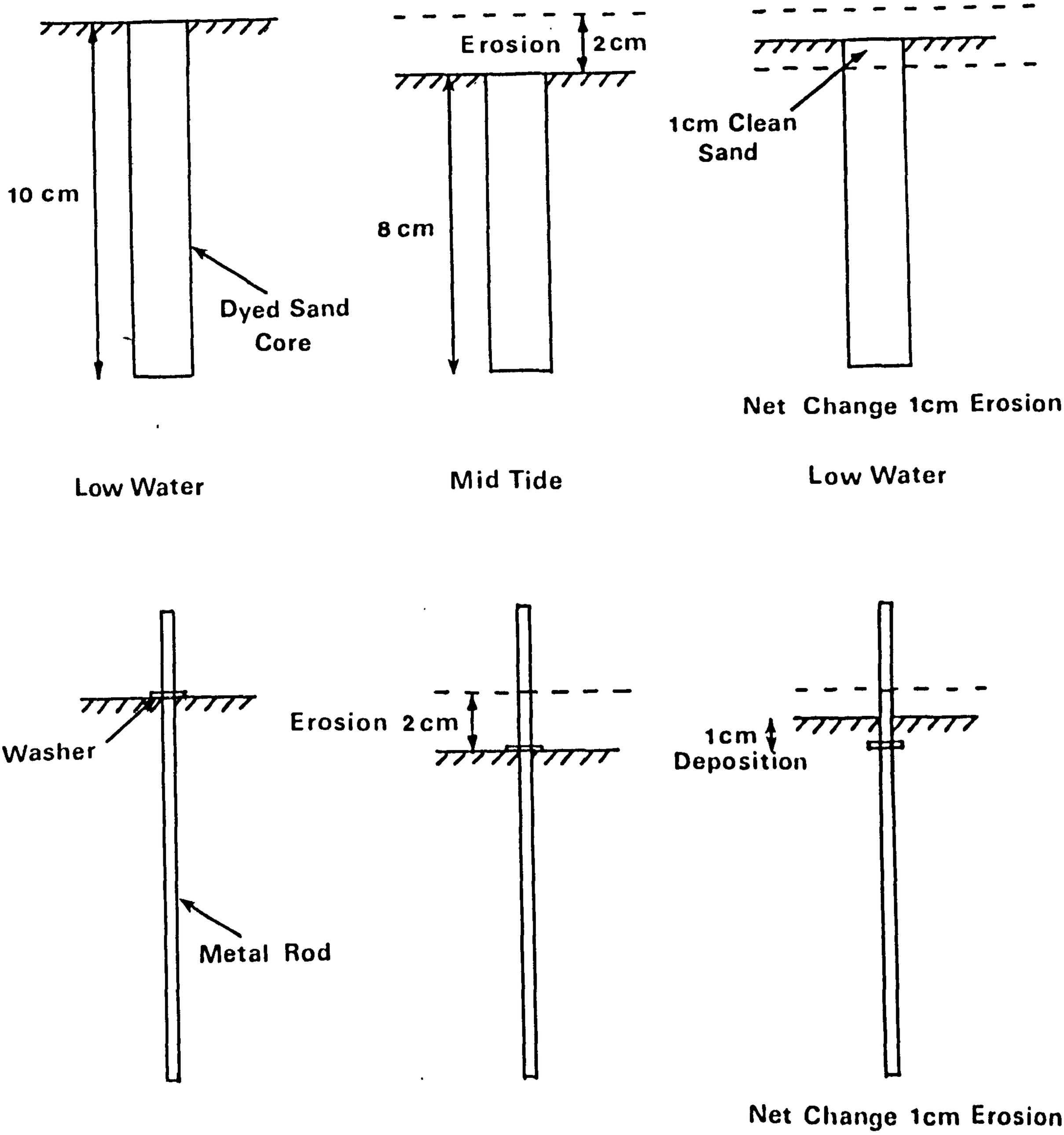

Figure 2.4. Techniques for measurement of depth of disturbance.

and eventually a technique outlined by Otvos (1965) was employed, using steel rods and washers. The rod is pushed into the beach plane to a marked depth, Figure 2.4, and a washer then placed over the rod to lie on the beach surface and also level with the mark on the rod. With erosion the metal washer falls down the rod and the depth of erosion is given by the distance from the mark on the rod to the washer. Deposition during the tidal cycle covers the washer and hence the amount of accretion is given by the distance from the washer to the new beach surface.

This method was found to be more reliable than that using sand cores since finding the rods, even at night, was a simple matter and in addition it could be employed in damp areas of the beach. The rods, painted to prevent rust, were between 15 and 20 cm long and were tapped into the beach face to a depth such that 4-5 cm was visible above the surface. Despite this scour was not a problem and a test of the two methods showed that comparable results were obtained. Some rods were lost under particularly severe wave conditions but nevertheless the retrieval rate was better than with the cores.

With the completion of the profile survey and the introduction of the depth of disturbance cores or rods the next stage in the preliminary experimental procedure was to put down the tracer. As tracer release was at low water and not directly into the surf zone this was a relatively straightforward matter but nevertheless certain precautions had to be taken. In particular the tracer was well wetted before laying on the beach surface. Stuiver and Purpura (1968) point out that if the tracer material is not wetted it will float on top of the water due to surface tension and this may cause misleading results. Consequently, the tracer was mixed in a bucket with detergent and water to break down the surface tension. A section of the beach surface was then removed over an area of about 0.75 sq. metres and to a depth of two to three centimetres. The wetted tracer was placed in the resultant depression and the surface levelled

(Plate 2.1).
to the surface of the surrounding beach face. / This was done so that as little disturbance as possible was caused to the overall beach face. Only one injection point was used for each grid in order to cut down sampling area but several experiments were conducted (e.g. 18.3.76, 6.10.76) in which more than one part of the beach was studied over the same tidal cycle and two or three injection points and grids were established.

The amount of tracer released at each injection point varied between 20 and 40 kg, although when several colours were being used in studies of specific grain size fractions quantities as small as 0.5 kg were used for some of the colours. No more than three different colours were used in a single tracer release in order to avoid the problems of differentiation as discussed earlier, (Section 2:1). Where small quantities of different colours of tracer were used these were mixed in with the main bulk of the tracer sand containing all beach grain sizes coated with the same colour.

2:4 Measurement of process variables

During the period from just before the time the tracer release point was covered by the incoming tide to approximately one hour after this, measurements of selected 'process' variables were made.

Wave height was measured using a metre staff held in the surf zone. Trough-to-crest distances of a series of between 20 and 30 breaking waves were read off on the staff and from these the significant wave height, $H^{\frac{1}{3}}$, calculated. Values of $H^{\frac{1}{3}}$ ranged from 0.18 to 0.79 metres although individual wave heights were sometimes in excess of one metre.

Wave period was measured by counting the number of waves passing a fixed point in a given time period. Values of wave period range from 2.6 to 5.4 seconds for all the experiments.

Wave height and period were measured in this relatively crude fashion for all tracer experiments but for some of the later experiments (e.g.

Plate 2.1. Emplacement of tracer into beach face.

6.10.76, 23.10.76) attempts were made to improve the accuracy of such data and increase the length of record through the introduction of electrical staff wave gauges. Designed and constructed by members of the Geography and Eleotrical Engineering Departments, including the author, these gauges were not available in time to facilitate use of the results from them in this study. Details of these gauges may be found in Appendix 1.

Following Krumbein's (1961) statement that the angle of wave approach measured in the sea area between initial refraction and final breaking would provide a more meaningful value of wave angle than deep water wave direction, measurements were taken just beyond the breaker and surf zones. This was done as accurately as possible using a compass and ranging rod, but Galvin and Savage (1966) suggested that this method may easily produce an error of $\pm$ 2 degrees. Such variability can result in considerable error in calculation of sediment transport as well as long-shore current velocity given the importance of angle of wave approach in predictive equations. Galvin and Savage also estimated a $\pm$ 25% accuracy for purely visual methods of wave height measurement.

Longshore currents were measured by means of drogues or fluorescein dye. In early experiments a plastic bottle filled with sea water to give it slight buoyancy was used as a drifter and timed over a measured distance. However, the bottle proved too heavy and too susceptible to surface winds to act as a satisfactory drogue and fluorescein due was used instead. The dye was placed in a polythene bag which was partially filled with sea water to create a concentrated solution. This was then released in the surf zone and the resultant dye patch timed over distance of between five and fifteen metres. Repeating this procedure at least four times, an average velocity for longshore current was calculated. The average values thus obtained ranged from 5 to 84 cm/sec. It must be remembered that these values represent surface current velocities and

hence reflect wind effects as well as wave generated currents.

Attempts were also made to improve the methods of measuring nearshore currents using automatic current recording devices. These instruments, again developed in the Geography Department at Nottingham University, were designed for use in the offshore zone but after several tests were found to be unsuited, in their present form, for the measurement of long-shore currents. They did, however, provide valuable proof of the existence of relatively strong tidal currents on the lower foreshore at various stages in the tidal cycle. Further details of these current gauges can be found in Appendix 1.

Water temperature was also measured for each experiment with measurements taken in the surf zone showing a range of between 2°C and 21°C. The upper end of this range reflects the heat gained by the shallow water of the surf zone from the warm sand of the beach face, as well as seasonal temperature changes. Initially it was hoped that the temperature data could be used in conjunction with water density estimates as this has been shown to be an important factor in suspended sediment movement (Harrison and Krumbein, 1964). However, at a later date the study was restricted to bedload movement and water density measurements, which had been relatively unsatisfactory anyway, were discontinued.

Meteorological data, in particular wind speed and direction was obtained from the weather station located at the Lincolnshire Trust and Nature Conservancy Reserve Field Station at Gibraltar Point. Wind records from this station were supplemented by measurements made with a hand held anemometer at the test site as the tide was coming in.

Other measurements, which were taken for only a proportion of the experiments and hence could not be used fully in later analysis, included swash/backwash velocity and wave thrust through the surf zone.

It was found that the procedure outlined so far in the preceding two sections took some three hours to complete with two people involved although

this time would vary a little dependent upon weather conditions and transport availability.

2:5 Sampling techniques

Sampling procedure was one of the fieldwork aspects of this study that passed through a process of development and improvement as the study progressed. Initially during the preliminary experimental procedure, as described in Section 2:3, a complete sampling grid was laid out around the tracer injection point using marker pegs. The pegs laid out along the profile, as described earlier, formed the middle column of the sampling net, with the injection point the central point, and further columns of pegs, spaced at five metre intervals, were laid out. The rectangular grid pattern so formed was aligned so that the longest side was parallel to the low water mark. However, it was quickly discovered, after early tracer tests, that this procedure was unsatisfactory as the sampling grid invariably did not cover the whole of the dispersed tracer cloud. This was because the grid was laid down without prior knowledge of the dominant direction of tracer movement and many sampling points were wasted being located in the opposite direction to tracer movement. A good example of this problem can be seen in Figure 2.5, the tracer map for the experiment of 6.10.75, showing the truncated tracer cloud and blank map area to the north of the injection point.

Since prediction of direction of tracer movement could not be performed with any confidence a new sampling procedure was devised which allowed construction of a sampling framework <u>after</u> dispersion of the tracer, that is immediately prior to the physical sampling. This procedure necessitated the construction of a portable ultra-violet lamp, Plate 2.2. The lamp was constructed from an adapted fluorescent lamp fitting attached to a wooden handle, with power supplied from a 12-volt car battery or dry cell rechargeable pack which could be carried in a heavy duty plastic bucket.

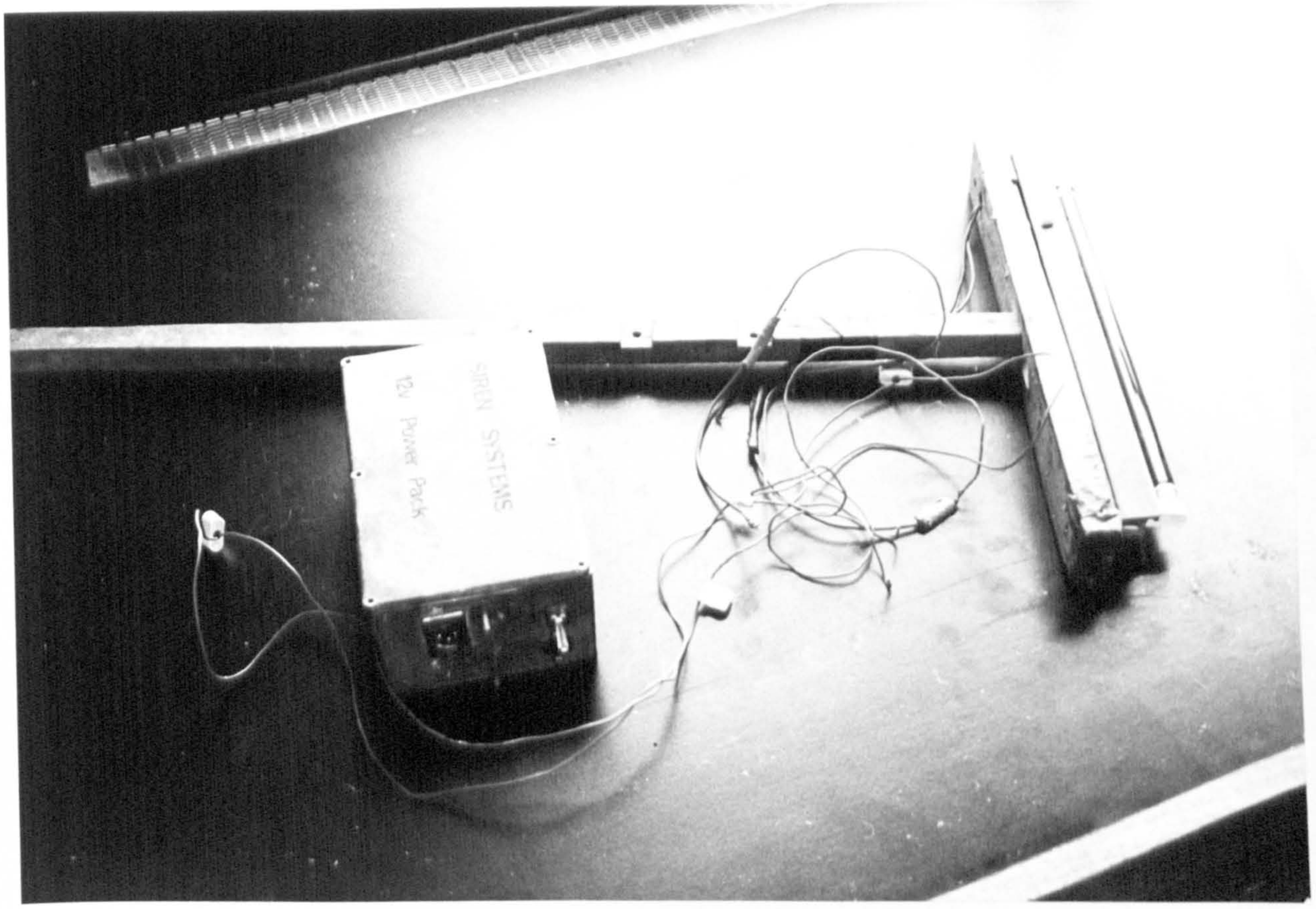

Plate 2.2. Portable ultra-violet lamp.

Figure 2.5. Tracer map for 6.10.75 H2, an example of poor sampling caused by pre-determined grid layout.

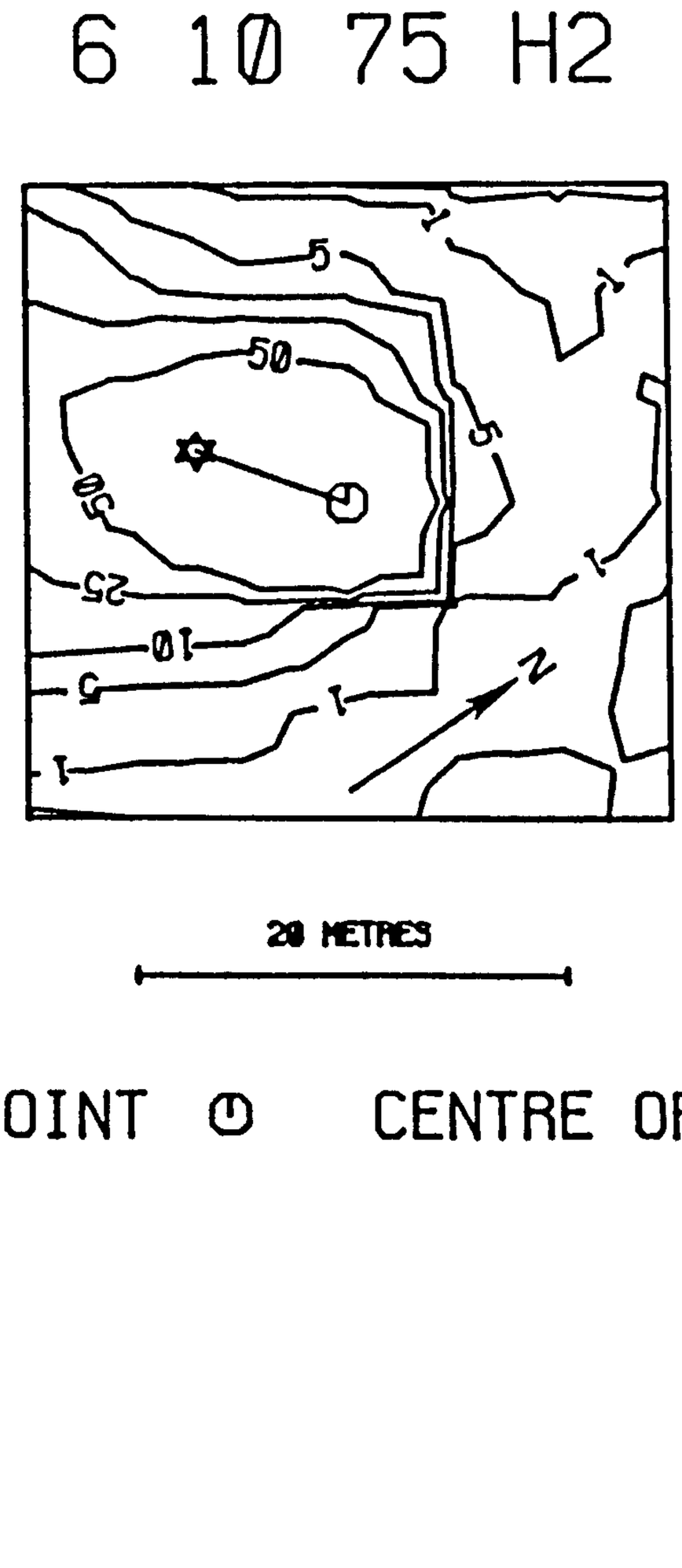

The fluorescent tube was replaced with an ultra-violet tube of similar dimensions and the lamp then used at night, that is during the low water period after tracer dispersion. With a little field experience the limits of dispersion could be roughly established in a matter of minutes. The extremities of the tracer cloud were then marked with flashing yellow hazard lamps. Using the marker pegs laid out along the profile line during the setting up of the experiment, four flashing lamps were aligned in a straight line along the beach perpendicular to the profile line. Samples were then taken along the line of lamps at intervals dependent upon the rate of decrease in surface tracer concentration, estimated whilst using the ultra-violet lamp. When all samples had been taken along this line the lamps were moved up or down the beach and aligned again. Samples were again taken and the whole procedure repeated until a grid of samples had been taken covering the whole area of the dispersed tracer cloud.

This was found to be a far more efficient method of sampling than that involving fixed grids established at the time of tracer injection. Much greater flexibility was achieved in the layout of the grid in terms of sampling interval such that a highly concentrated patch of tracer, identified with the ultra-violet lamp, could be sampled on a finer mesh than the less concentrated areas. Furthermore, sample collection in areas with no tracer present could be avoided - this being especially true of the collection of samples on the 'wrong' side, the updrift side, of the tracer release point. From field experience with this sampling procedure it was found that the simplest method to adopt was first of all to sample over a coarse rectangular mesh, with sample interval of five or ten metres and then infil with more sampling points on a finer mesh in areas of relatively high concentration, usually close to the injection point. Figure 2.6 indicates the typical sample plan. The greater the dispersion the coarser the initial grid. In certain cases tracer dispersion was more than 100 metres alongshore and hence a 10 metre sample interval was used. The

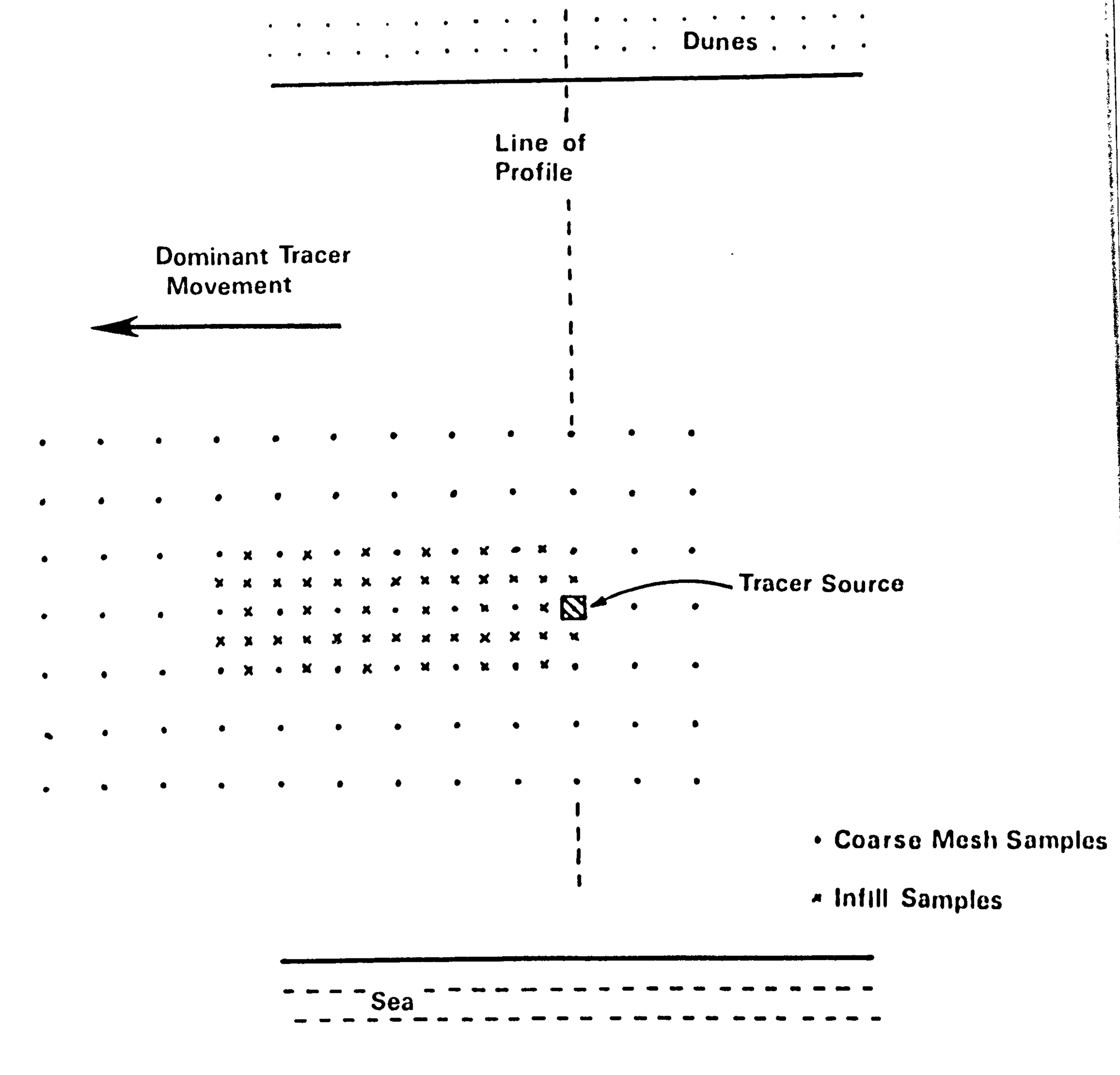

Figure 2.6. Schematic diagram of typical sampling grid.

number of samples collected per grid varied between 40 for the early 'fixed grid' experiments and 140 for the later tests.

A regular rectangular sampling plan was used because of the relative ease of location of points on the ground and later on a map. A random sampling pattern is very difficult to locate accurately at night. Other types of sampling plan which have been used in tracer studies include the radial net as used by Boon (1968) but this was thought to be less flexible than the rectangular mesh.

Thus, sampling at night with a portable ultra-violet lamp proved to be the most satisfactory method for this study but nevertheless was not always successful.

The map of tracer dispersion for the experiment on the 21.9.76 on the lower ridge at Skegness (Figure 2.7) shows that mistakes were sometimes made and some of the tracer cloud not sampled. Difficulties chiefly arose when weather conditions were poor during sampling or when the beach surface was very wet causing problems of tracer identification due to reflected blue, ultra-violet light.

To turn to the actual method of collection of individual samples is to bring into consideration the question of collecting a representative sample and the question of depth of tracer dispersion in the surface layers of the beach.

Ingle and Gorsline (1973) outline three basic methods of sample collection:

1. "In situ" analysis of tracer material by scanning the sediment surface with ultra-violet light (see Section 3:2).

2. Collection of bulk samples either by grab, if in the offshore zone, scoop or small corer.

3. Collection of surface and near surface grains only, utilising grease-coated cards or plastic strips.

However, as methods 1) and 3) refer only to surface concentrations

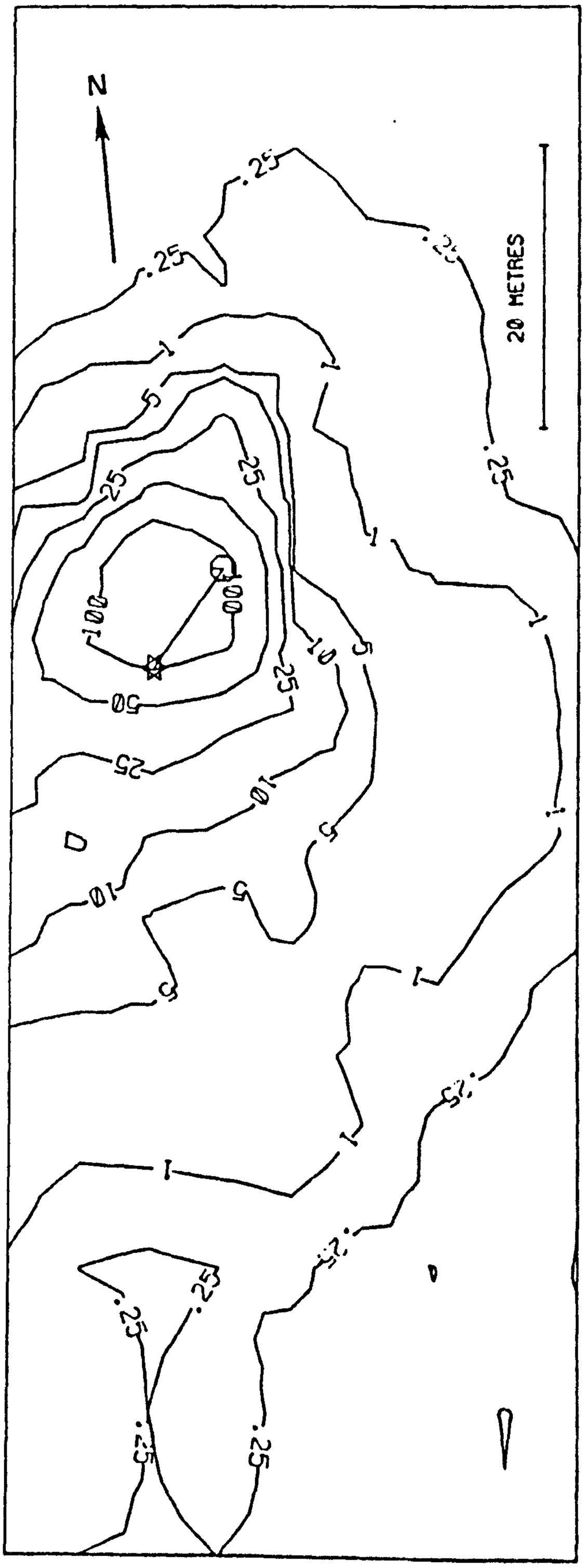

Figure 2.7. Tracer map for 21.9.76 experiment, lower ridge: an example of poor sampling.

and disregard the concentration of tracer with depth, they should not be used where quantitative analysis is to be carried out. James (1970) describes the distribution of tracer with depth in the following way "the concentration on the surface is finite but not maximal. The concentration increases with depth to some point where a maximum is reached and then diminishes in a long-tailed fashion." Therefore, with this complex depth/ tracer concentration relationship it is unlikely that purely surface sampling will produce meaningful results. Depth samples must be taken and in addition constancy of sample size by weight, area or volume is often useful in quantitative studies.

The most commonly used method of collecting depth samples in tracer studies involves the use of coring devices. Komar (1969), Murray (1967), Yasso (1965) and Boon (1968) all used corers of greater or lesser sophistication. However, cores were not taken in this study because of the slowness of collection and the large number of samples collected in each experiment. Instead the technique adopted was simply to sample using a stainless steel laboratory shovel of side $2\frac{1}{2}$ cm and approximately 100 sq.cm in area. Although a crude way of collecting depth samples the method was used because of the speed with which large numbers of samples could be collected. Chief among the disadvantages of this simple method is the relative lack of ability to control sample depth. As sampling too deep can cause dilution of the tracer concentration the ability to control the depth of sampling is crucial. Nevertheless, with practice, a reasonable amount of accuracy can be achieved.

One other drawback of the sampling technique which must be noted is that of sample contamination due to small amounts of sand adhering to the shovel during the sampling process. This can be reduced to a minimum by thorough cleaning of the shovel between each sampling station.

With two people, sampling time varied from two to four and a half hours, dependent upon the amount of tracer dispersion and the number of

grids being sampled. Weather conditions also affected the length of time taken for sampling.

2:6 Problems and efficiency of field procedure

A significant problem encountered in using the tracer techniques described in the previous sections of this chapter was the lack of information on the amount of tracer actually dispersed from the injection point. During any one experiment this will depend upon the following factors:

1. mode of injection of tracer
2. severity of wave conditions
3. cycle of erosion and deposition.

Several methods of placing the tracer on the beach face are described in the literature. Most commonly the tagged sand is laid either in a trench across the beach or at a single point, patch, location, in a shallow hole. Since it is important that the sand surface remains 'natural' over the beach face simply building a mound of tracer is not satisfactory. Equally, raking the tracer into the beach surface layers would appear to cause unacceptable disturbance. However, if, as in this study, the tracer is placed in a hole in a patch 2-3 cm thick and levelled with the surrounding beach face the tracer may be covered by clean sand by the incoming tide and hence not removed in large enough quantities during the tidal cycle. Wave conditions will play a large part in determining the exact amount set in motion. Under very slight wave conditions the depth of disturbance, that is the depth to which the surface layers of the beach are affected by the waves, may be small and as a result little tracer moved. On the other hand, severe wave conditions may cause the whole of the released tracer body to be moved and dispersed over a very wide area. Complete loss of the tracer occurred during the experiment of 31.1.76 at Gibraltar Point when waves were 66 cm in height and again on the 23.8.76 when wave heights were more than 80 cm on average.

Otvos (1965) and Strahler (1966) outlined three main phases of tidal cycle sedimentary changes: initial swash deposition, scour in the face of swash and backswash and step deposition under the breaker zone. As can be seen from Figure 2.8 the phases are reversed on the outgoing tide. This sequence was confirmed by Schwartz (1967) in a depth integrated tracer study. Thus, if the erosional phase of the cycle is not very significant then only a small part of the tracer may be moved over the beach. Since, according to Strahler's model, the amount of scour and deposition will decrease down beach, the point at which tracer is released with respect to the height of the tide will also be important in determining how much tracer is actually released. Close to the high water mark only small amounts of erosion may take place and hence release only small amounts of tracer, whilst larger scale changes may occur closer to the low water mark.

However, it must be pointed out that Strahler's cycle of beach changes was suggested for the equilibrium beach and for beaches with simple morphology. Beaches not in equilibrium, that is experiencing erosion or accretion, and beaches with complex morphology, may exhibit a considerably more unbalanced sequence of events. Also under these circumstances the amount of tracer dispersed might vary a great deal. On a prograding beach deposition may cover the tracer for the majority of the tidal cycle and allow only a small amount of tracer to be dispersed. Low tracer concentrations may then make the results unsuitable for analysis. On the other hand, low sample tracer concentrations may be caused by the complete removal of tracer from the area on a rapidly eroding foreshore.

Despite these problems it was found that usable results were obtained from sampling on 90% of occasions and as a test of the overall procedure two experiments were conducted in which sampling was undertaken over two consecutive tidal cycles. Assuming relatively constant environmental conditions the movement of sand on the beach should follow the same pattern

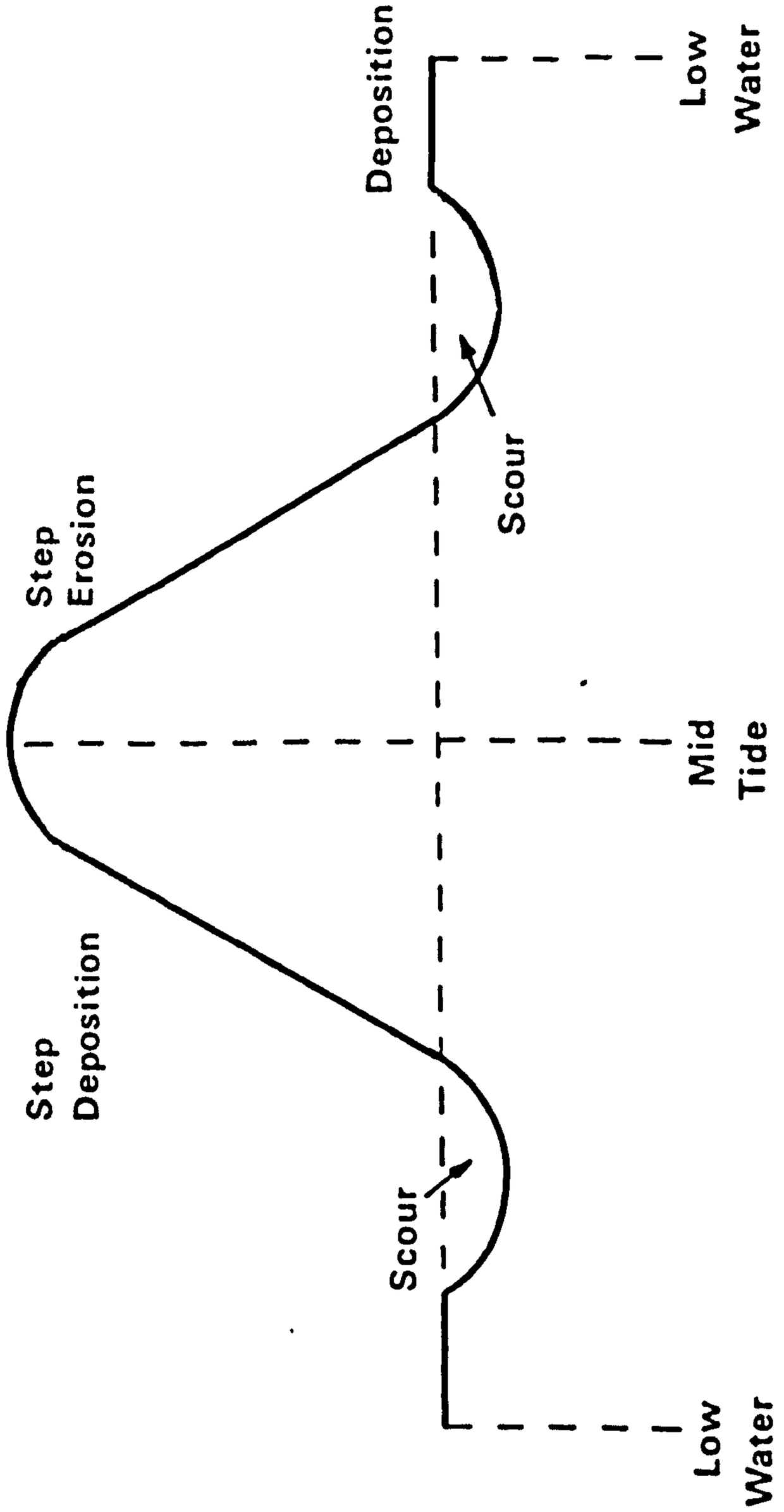

Figure 2.8. Phases of sedimentation during a single tidal cycle.

and with the same magnitude for two tidal cycles. Therefore, if the tracer is acting as a good surrogate of the in situ sand similar tracer patterns should be obtained.

On 17/18 March 1976 two injections of different coloured tracer were made and both sampled at the same time, whilst in the experiment of 7/8 September 1976 the same tracer was sampled twice. On both occasions wave and weather conditions remained relatively constant for the two days. Figures 2.9 - 2.12 show the results of these experiments and reveal encouraging similarities. The distance moved by the centre of gravity of the tracer cloud for one tidal cycle on 17/18 March was 27.67 metres and was 57.52 metres for two tidal cycles. Again on the 7/8 September the figures were respectively 9.6 metres and 13.5 metres. For both tests dominant vectors of motion were the same over both time periods.

18 3 76 GRID 2 UPPER RIDGE H2 P

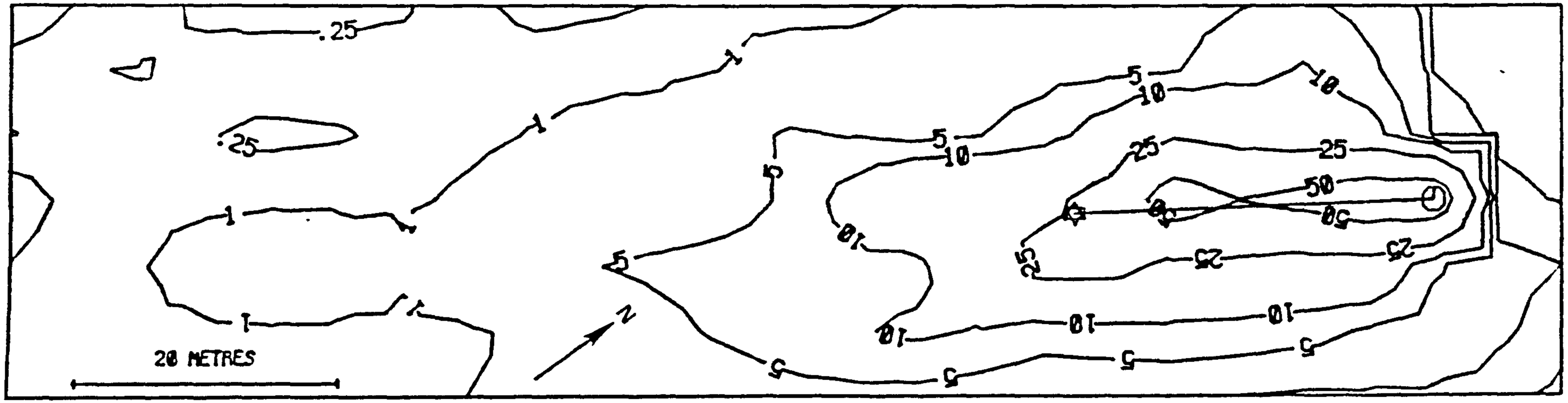

INJECTION POINT ⊙ CENTRE OF GRAVITY ✡

Figure 2.9. Tracer map for 18.3.76 H2 experiment, upper ridge.
Pink tracer released for one tidal cycle.
Note distance moved by centre of gravity.

18 3 76 GRID 2 UPPER RIDGE H2 Y

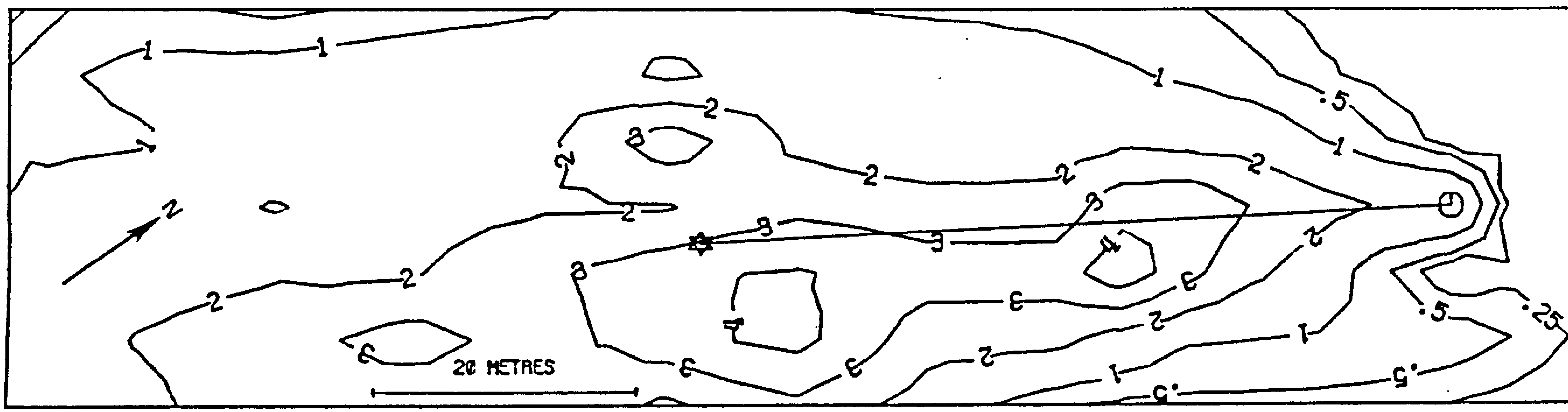

INJECTION POINT ⊖ CENTRE OF GRAVITY ✡

Figure 2.10. Tracer map for 18.3.76 H2 experiment, upper ridge. Yellow tracer released for two tidal cycles. Compare with previous map.

7 9 76 LOWER GRID FIRST SAMPLE

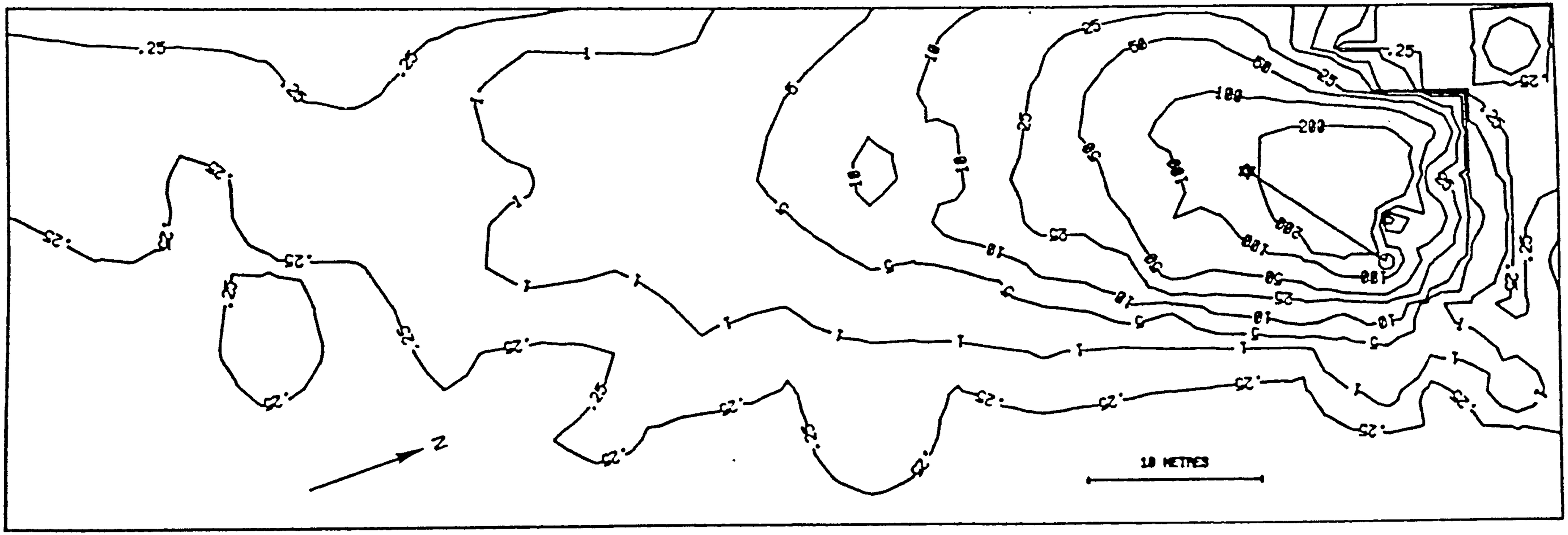

INJECTION POINT ⊙ CENTRE OF GRAVITY ✡

Figure 2.11. Tracer map for 7.9.76 H3 experiment, lower ridge.
First sample after one tidal cycle.

8 9 76 LOWER RIDGE H3 2ND SAMPLE

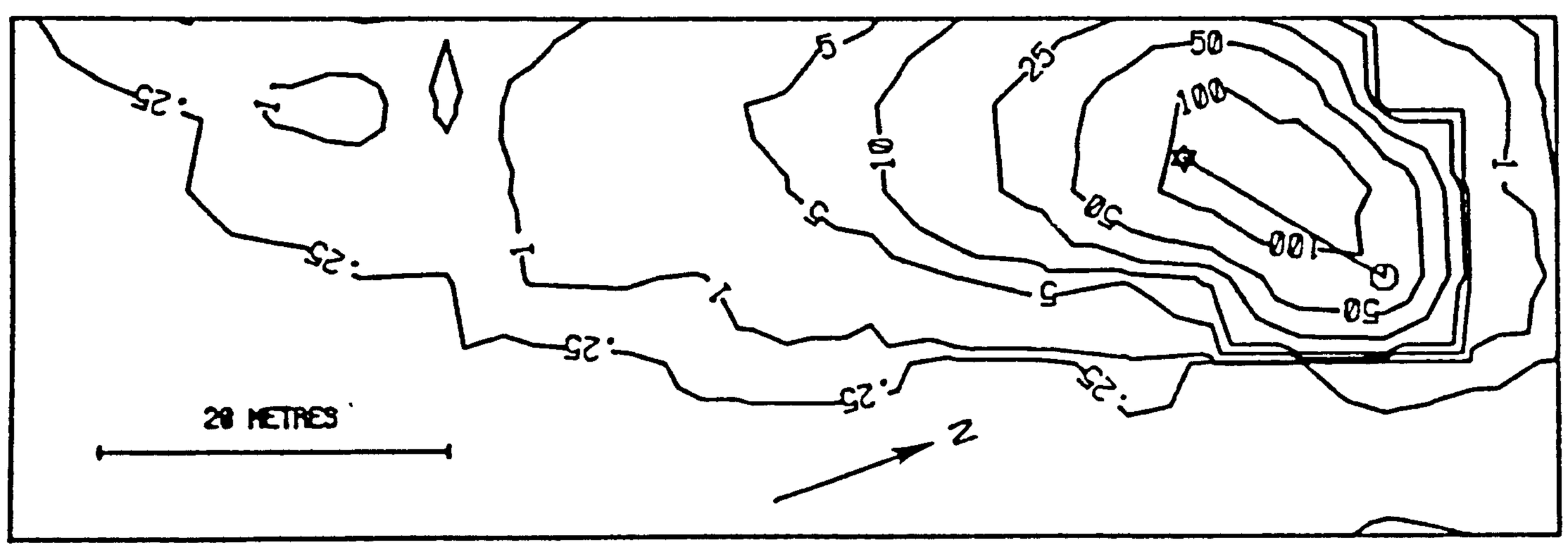

INJECTION POINT ⊙ CENTRE OF GRAVITY ✡

Figure 2.12. Tracer map for 8.9.76 H³ experiment. Second set of samples collected on same site as 7.9.76 tracer injection after two tidal cycles. Compare with previous map.

CHAPTER 3

DATA ANALYSIS AND PRESENTATION

3:1 Introduction

This chapter describes the methods of laboratory analysis of the data collected by the procedures outlined in Chapter 2. Also included are details of the graphical methods used to display the relationships present in the data. However, the numerical and computational aspects of the methods of analysing these relationships are dealt with in a later chapter.

One of the advantages of radioactive tracer techniques is that sampling and subsequent laboratory analysis to produce tracer concentration estimates are unnecessary. Direct measurements of tracer concentrations can be taken in the field with a scintillation or Geiger-Muller counter. Some workers have attempted to devise similar methods for use with fluorescent tracer, with varying degrees of success.

Yasso (1962), for example, developed a photometric technique using the principle of measuring visible light emission from coated particles under ultra-violet excitation. Laboratory calibration of the battery-operated, portable photometer constructed for use in the field indicated that 5% differences in areal concentrations of marked particles at a given sampling location could be determined. Initially this instrument was designed for field use in darkness, but in later work Yasso (1965) outlined modifications to facilitate its use in daylight. Sensitivity adjustments and changes for shallow and deep-water use were also suggested.

On a less sophisticated level, Camber (1973) used a portable ultra-violet lamp at night simply to count fluorescing grains on the beach surface. Field experience in this study suggests that this scanning procedure must inevitably produce inaccurate results since it was found to be very difficult to distinguish individual tracer grains on the beach surface even under the most favourable conditions.

Tests were also made of a third method of field counting, the use of standard sample cards. Again problems of discrimination between different concentrations were encountered but variation of tracer concentration with depth also invalidated the use of this method, which deals exclusively with surface concentrations. Thus, field counting procedures were rejected and as described in the previous chapter samples were collected for subsequent laboratory analysis.

3:2 Tracer grain counts

The laboratory methods of producing estimates of fluorescent grain concentrations can be placed into three broad categories:

1. Automatic counting procedures. Most electronic counting instrumentation involves the principle of photometric counting whereby light from an ultra-violet light source is passed through a filter cutting out all but the ultra-violet wavelengths, 4.5×10^{-5} cm to 10^{-6} cm. This is then incident on the sand grains as they pass in a stream of one grain thickness. Fluorescent light of the required frequency dependent upon the colour is then emitted by the grains and this is passed back through a further filter to a photomultiplier. The signal is then treated electronically and a counter activated. A good example of an instrument incorporating this principle is the Automatic Fluorescent Particle Counter (A.F.P.C.) as described by Teleki (1967). This machine, developed by the Coastal Engineering Laboratory of the University of Florida and the Budd Company of New York, allows the simultaneous counting of several colours of tracer particles. In addition, size analysis of the samples is carried out during the counting process. It is claimed that the A.F.P.C. can handle sand grains with a median grain size of 250 microns at a rate of 55,000 particles/second and can count specially distinct fluorescent colours at a maximum rate of 200 particles/colour/second.

Not all automatic counters are as sophisticated as the A.F.P.C. Yasso's photometer, described in the previous section, is a simpler example and de Vries (1973) gives details of a similar instrument. However, apart from the relatively high cost of such counters one drawback of the photo-

multiplier system is that stringent environmental conditions have to be maintained for effective operation due to the sensitivity of photomultipliers to changes in temperature and humidity. Despite this, automatic counting methods can alleviate a major problem inherent in tracer studies, that of keeping sample analysis in step with field work. In this study, because automatic counting methods were not available it was found that experiments in the field had to be conducted before analysis of samples obtained during the course of previous experiments had been made and, therefore, the use of information gained from these earlier experiments was inhibited.

2. Standard samples. This involves the use of a series of cards possessing a known tracer concentration in comparison with collected sand samples. As mentioned in the previous section, this method was tested as a field procedure but was found to be unsatisfactory. Furthermore, other workers have discovered that this technique may lead to inaccurate results even under laboratory conditions, because in general the human eye is unable to discriminate between different concentrations accurately. De Vries (1973) estimates that it is only possible to discriminate visually between concentrations which differ by a factor larger than about two. The problems are compounded when more than one colour of tracer is used.

3. Direct counting. Various procedures for the counting of fluorescent grains by eye have been devised. Murray (1967), for example, counted the total number of grains in each equal volume sample by placing the sample in a beaker of water which was kept agitated, thus putting the grains in suspension. The water-sediment mixture was then passed out of the bottom of the beaker through a valve and then over a rippled pan. The fluorescent grains were then counted as they moved past and the concentration expressed as the number of grains per sample.

On the other hand, Boon (1968), simply removed each fluorescent grain from split core samples using a fine brush and expressed these concentrations

as tracer grains per specific volume. More recently, Komar and Inman (1970) expressed tracer concentrations in terms of grains per kilogram of sample by spreading out volume samples to a thickness of one grain layer on a dull black table and scanning with a hand held ultra-violet light.

All the direct counting procedures are necessarily time-consuming and possibly inaccurate especially where more than one tracer colour is contained in each sample, where the number of dyed grains present is high or where the mean grain size of the sample is small. Teleki (1967) points out that " ... while it is possible to see one tracer grain among ten million natural sand particles it becomes quite difficult for the eye to perceive accurately concentrations of 10^{-4} and higher." He also estimates that the 'ability of keen differentiation' between different colours of tracer in the same sample will cease upon the addition of a fifth or sixth colour. Small grain size exacerbates the difficulties.

Despite the problems, a direct counting method was used in this study, although unsuccessful attempts were also made to develop a semi-automatic photographic counting procedure. The actual counting method used is outlined by Dugdale (1977). The initial weight of each sample was taken after air drying. A square sheet of black sugar paper with an area of 22 cm^2 was sprayed with "Spray 77" adhesive and the sample was then passed over the paper. The surplus sand was then tipped off the paper square leaving a thin coating of sand attached to the paper. The remaining sand was re-weighed in order to give the weight of the sand on the paper.

After drying a grid was laid over the paper square and the number of grains in the whole of, or a part of, the grid was then counted whilst scanning with a Hanovia Fluorescence 16 hand-held,ultra-violet lamp. When the number of dyed grains visible was greater than fifty only a part of the grid was used and a uniform distribution of tracer over the square

assumed. The concentration of tracer grains was then expressed as grains per gram of sample with a slight correction being made for the difference in area between grid and paper. The whole procedure, which assumes a thorough mix of tracer grains within each sample, is shown in Plates 3.1 to 3.6.

Boon (1969) using a similar method found that with care counting error could be kept to less than three per cent and although difficult to estimate it is thought that counting error was reasonably low in this study. Most error was present in counts of samples with high concentrations. The time taken to deal with each individual sample was three to four minutes from initial weighing to completion of counting but where large concentrations of tracers and two or more tracer colours were present counting times alone were as much as six to eight minutes. In all, more than 2,500 samples were analysed over a period of three months.

After drying, certain samples collected during each field test were also sieved to ascertain grain size characteristics. Mean grain size, sorting, skewness and kurtosis were calculated from the following formulae based on the method of moments and described by McBride (1971):

$$\text{Mean} \quad \bar{x}_\phi = \frac{\Sigma\, fm}{n} \qquad \text{Eq. 3.1}$$

$$\text{Sorting} \quad S_\phi = \left(\frac{1}{100}\,\Sigma\, fm^2 - \bar{x}_\phi\right)^{\frac{1}{2}} \qquad \text{Eq. 3.2}$$

$$\text{Skewness} \quad Sk_\phi = \frac{\frac{1}{100}\,\Sigma\, fm^3 - \frac{3}{100}\,\bar{x}_\phi\,\Sigma\, fm^2 + 2\bar{x}_\phi^3}{S_\phi^3} \qquad \text{Eq. 3.3}$$

$$\text{Kurtosis} \quad K_\phi = \frac{\frac{1}{100}\,\Sigma\, fm^4 - \frac{4x_\phi}{100}\,\Sigma\, fm^3 + \frac{6}{100}\,\bar{x}_\phi^2\,\Sigma\, fm^2 - 3\bar{x}_\phi}{S_\phi^4} \qquad \text{Eq. 3.}$$

Plate 3.1. Spray glue and black sugar paper used in counting procedure for each sample.

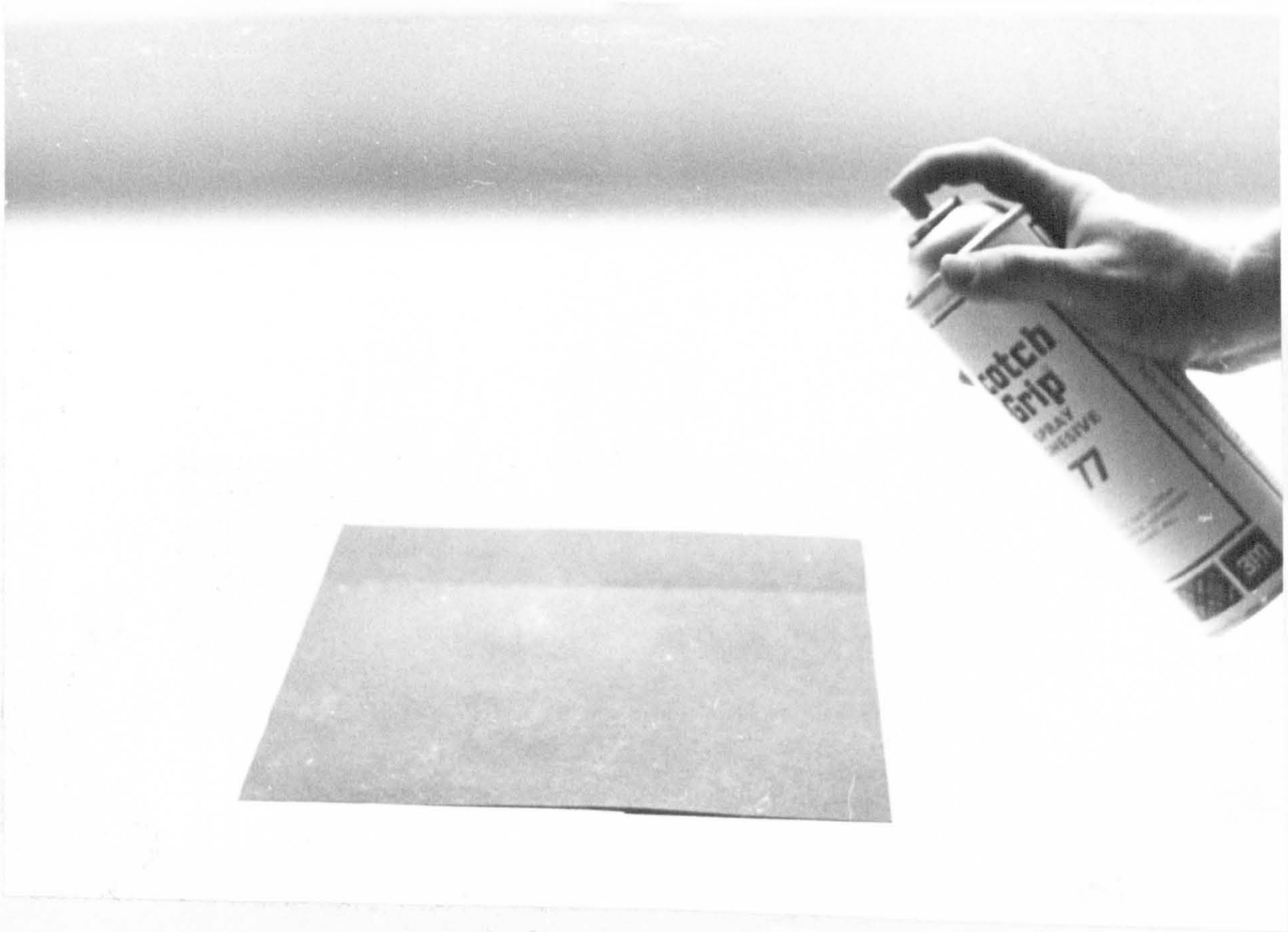

Plate 3.2. Spraying the paper with thin coat of glue.

Plate 3.3. Sample tipped onto sprayed surface.

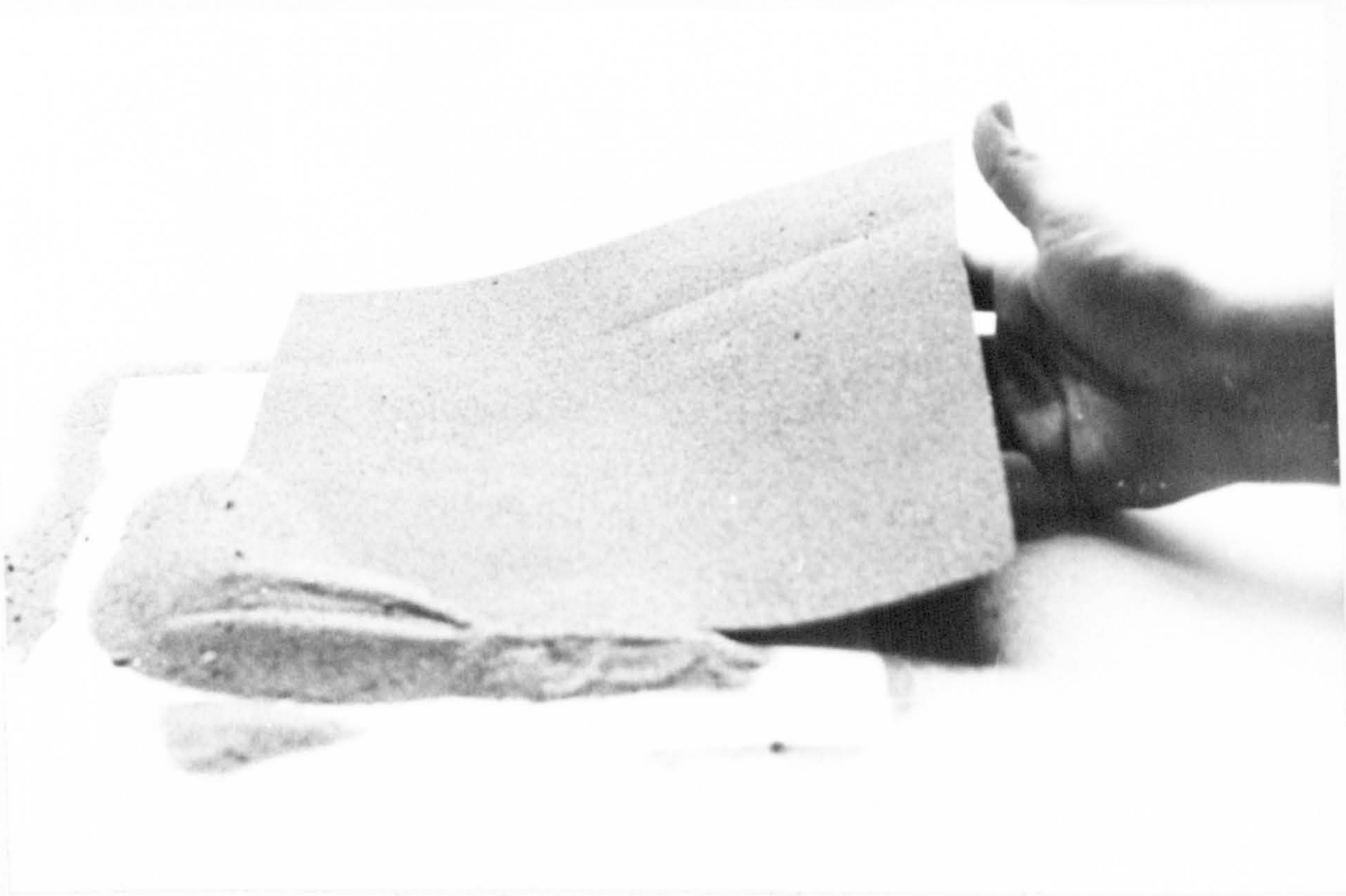

Plate 3.4. Sand residue removed.

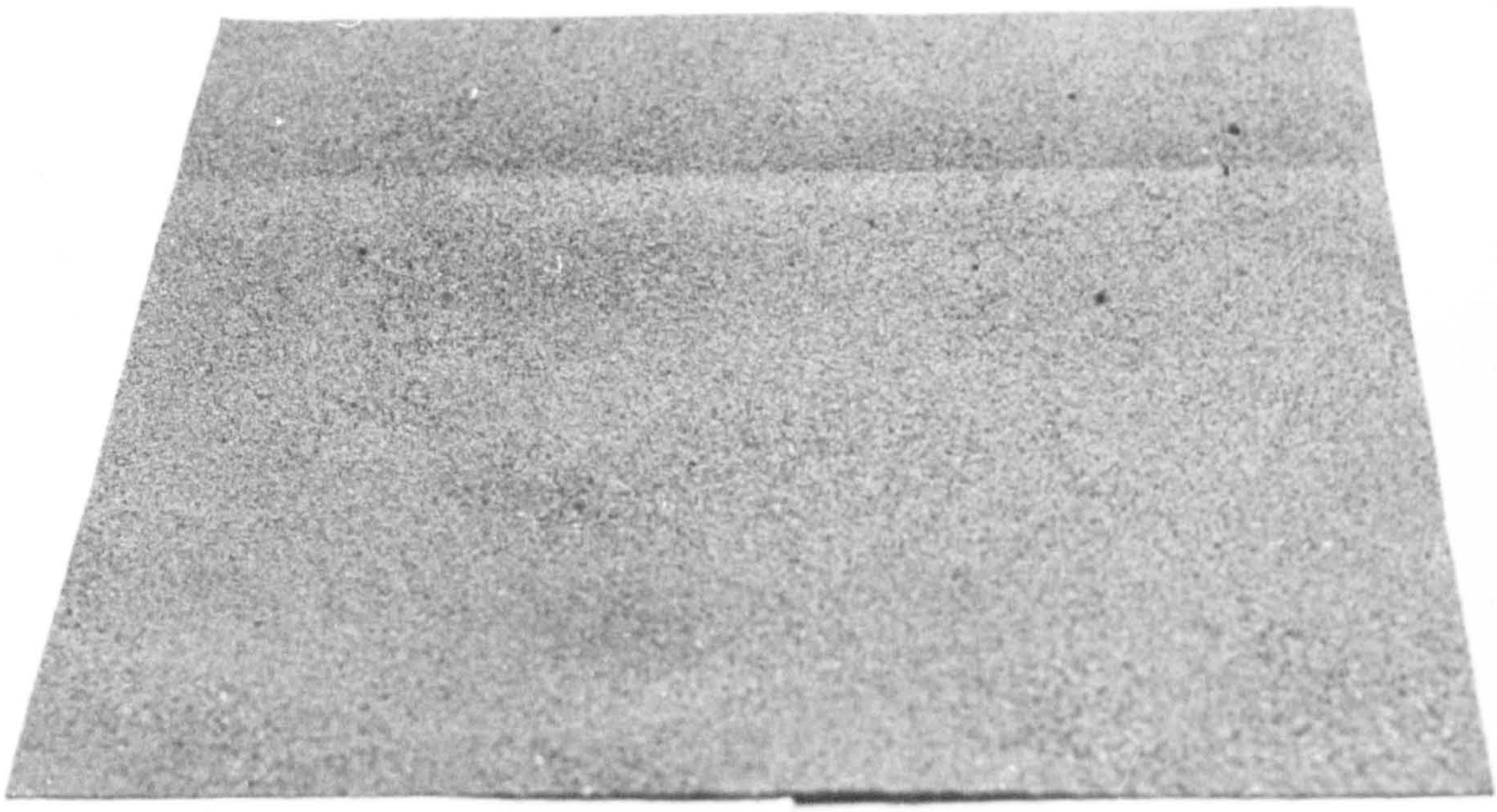

Plate 3.5. Paper square with thin coating of sand from sample.

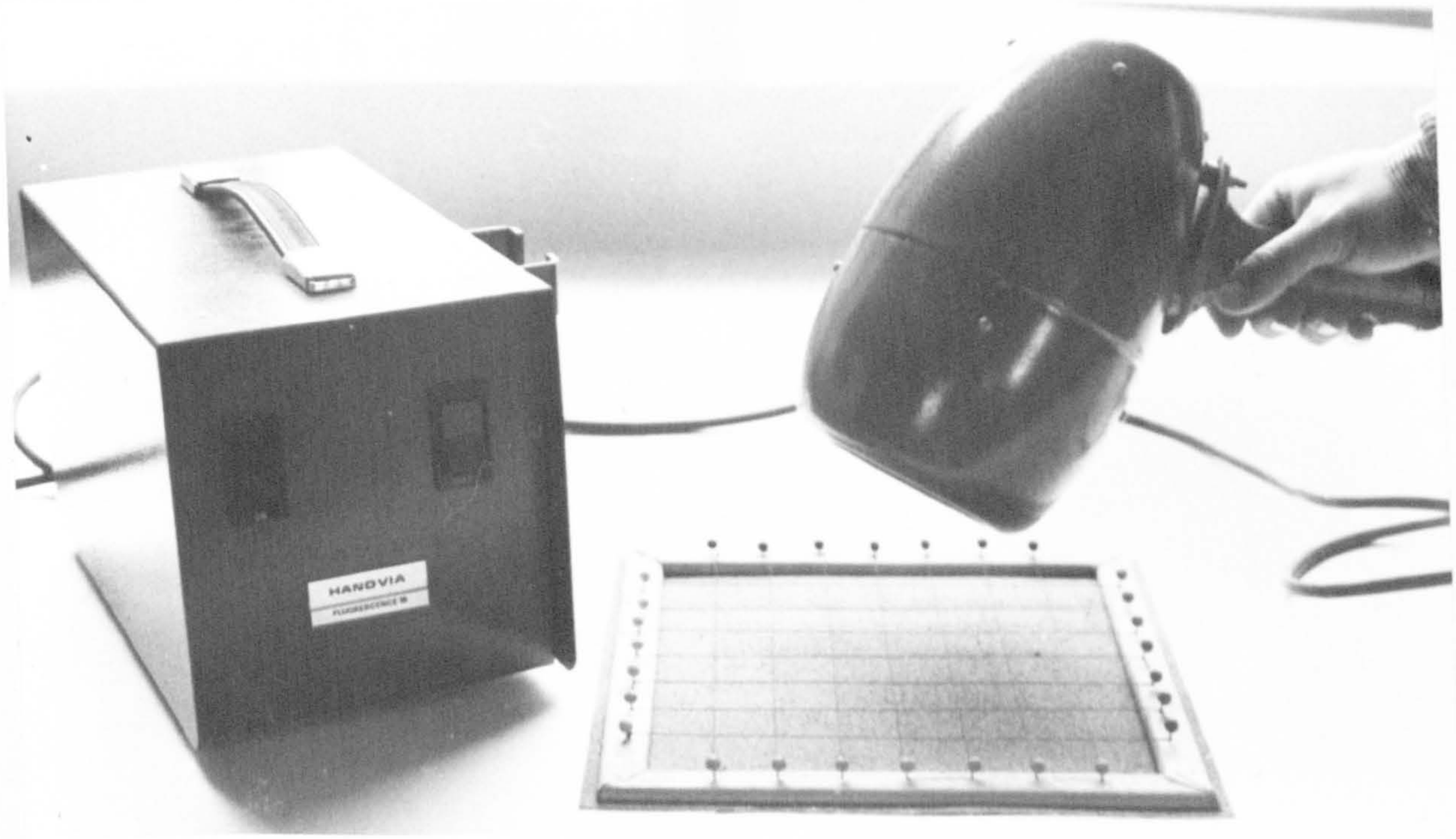

Plate 3.6. Fluorescent grains counted using cotton grid and Hanovia hand-held ultra-violet lamp.

where f = weight (% frequency) in each size class;

m = mid point of each class in phi (ϕ) units.

n = total number in sample (100 when f in %).

All grain size measures were expressed in phi (ϕ) units.

3:3 Data presentation

The way in which tracer dispersion can be described depends initially upon the recovery rate of dyed grains and the number of samples collected. Yasso (1965), in his field tests at Sandy Hook, New Jersey, found that particle recovery was low, 0.059% of tracer emplaced, and was insufficient to produce contour maps of the dispersion pattern. Instead, he produced boundary lines of dispersion by linking the point at which the tracer was placed on the beach with the nearest and furthest points of the tracer cloud. These were referred to as minimum and maximum transport vectors. The angles between the surveyed profile line on which the tracer was laid and the two vectors were, respectively, the minimum and maximum transport angles, and the angle between the two vectors was defined as the dispersion angle (Figure 3.1). This series of vectors and angles represents a minimum two dimensional expression of the tracer dispersion. At the other extreme, Boon (1968) used trend surface analysis to treat the concentration data more objectively, producing second and third order trend surface maps. This was made possible by good tracer recovery and a relatively large number of samples (40).

Where sampling results allow, the most commonly used form of representation of tracer patterns is the hand-drawn or machine-drawn contour map. Since tracer recovery was adequate in the majority of cases, as evidenced by the contour values on the maps themselves, contouring was used in this study and contour maps were produced using automated computer mapping

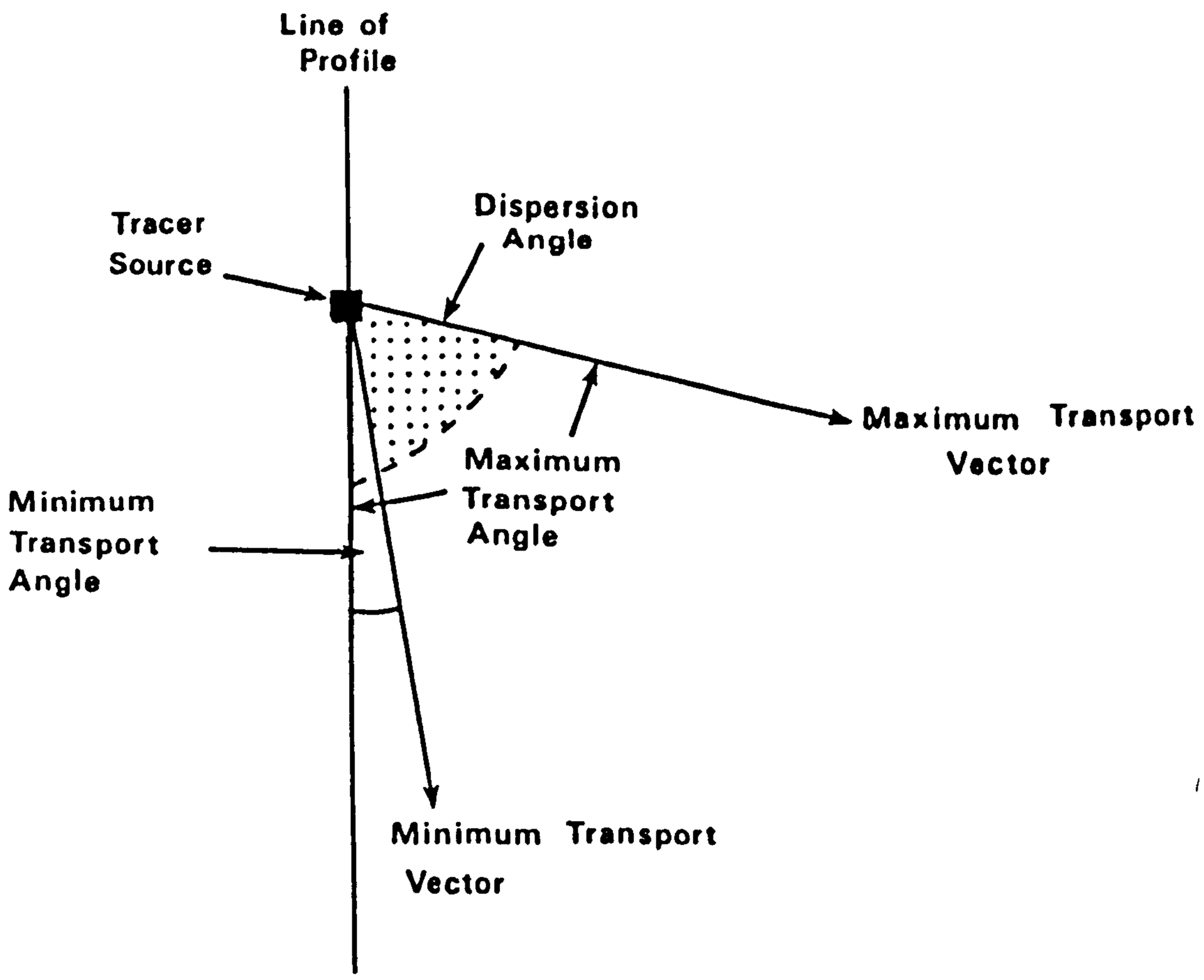

Figure 3.1. Boundary line presentation of tracer dispersion used by Yasso (1962).

techniques. Programs, developed principally by Dr. P.M. Mather, consisted of interpolation, contouring and plotting routines.

Field sampling was carried out on a rectangular grid pattern in all cases but sampling distances and areal extent of the grids varied for each grid. Frequently, as outlined in Section 2:3, sampling point patterns consisted of a coarse sampling mesh supplemented by infil sampling on a finer mesh, Figure 3.2a. In order to produce a regular pattern for the contouring routine with equal sampling interval in both X and Y directions, spatial interpolation was necessary.

The main aim of all methods of two-dimensional interpolation is to produce a smooth, acceptable representation of a surface, assuming the surface is known, from any set of data points either regularly or irregularly distributed over the surface. Problems are increased where data is irregularly spaced or of variable density and the major consideration of most methods is computation time as a function of ease of calculation and efficiency of algorithm.

Crain (1970) in a review of spatial interpolation methods defines two broad groups of methods: those which generate surfaces for which a closed mathematical expression exists and numerical methods which generate a surface from an algorithm whose end product is a numerical array of values. Of the mathematical methods, piecewise procedures, involving the fitting of a low-order polynomial to parts of a surface and combining them to produce a continuous surface are often preferred to the direct use of continuous surface fitting. At the same time, weighted averaging procedures provide advantages of speed of calculation, ease of programming and acceptable results with many types of data. In this study an algorithm, subroutine SFCFIT, developed by Akima (1974A & B), was used. This employs local or piecewise procedures and involves the generation of a local third order polynomial in X and Y directions, based on the thirteen closest data points, for each rectangle of the grid. The

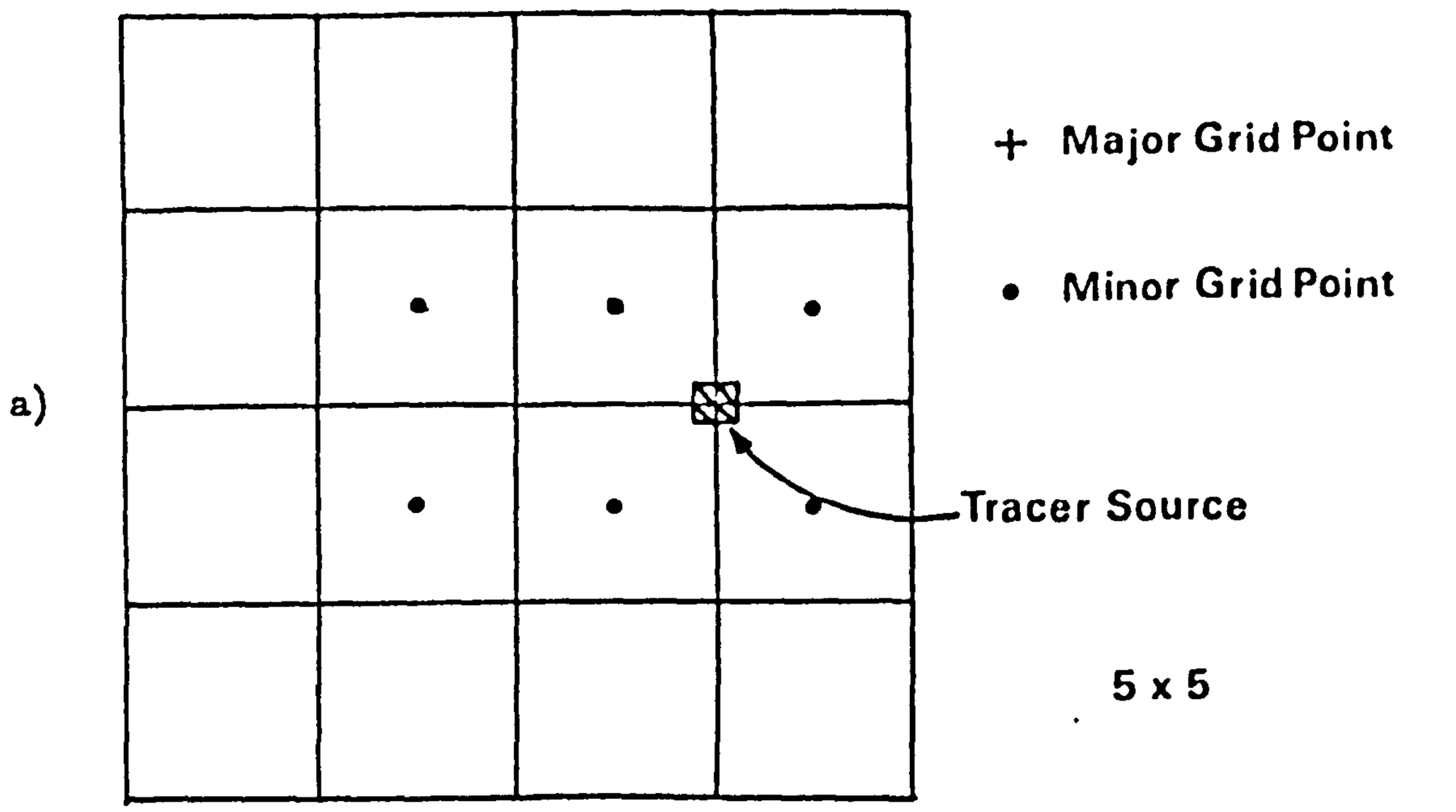

Figure 3.2a. Basic grid of data points before interpolation.

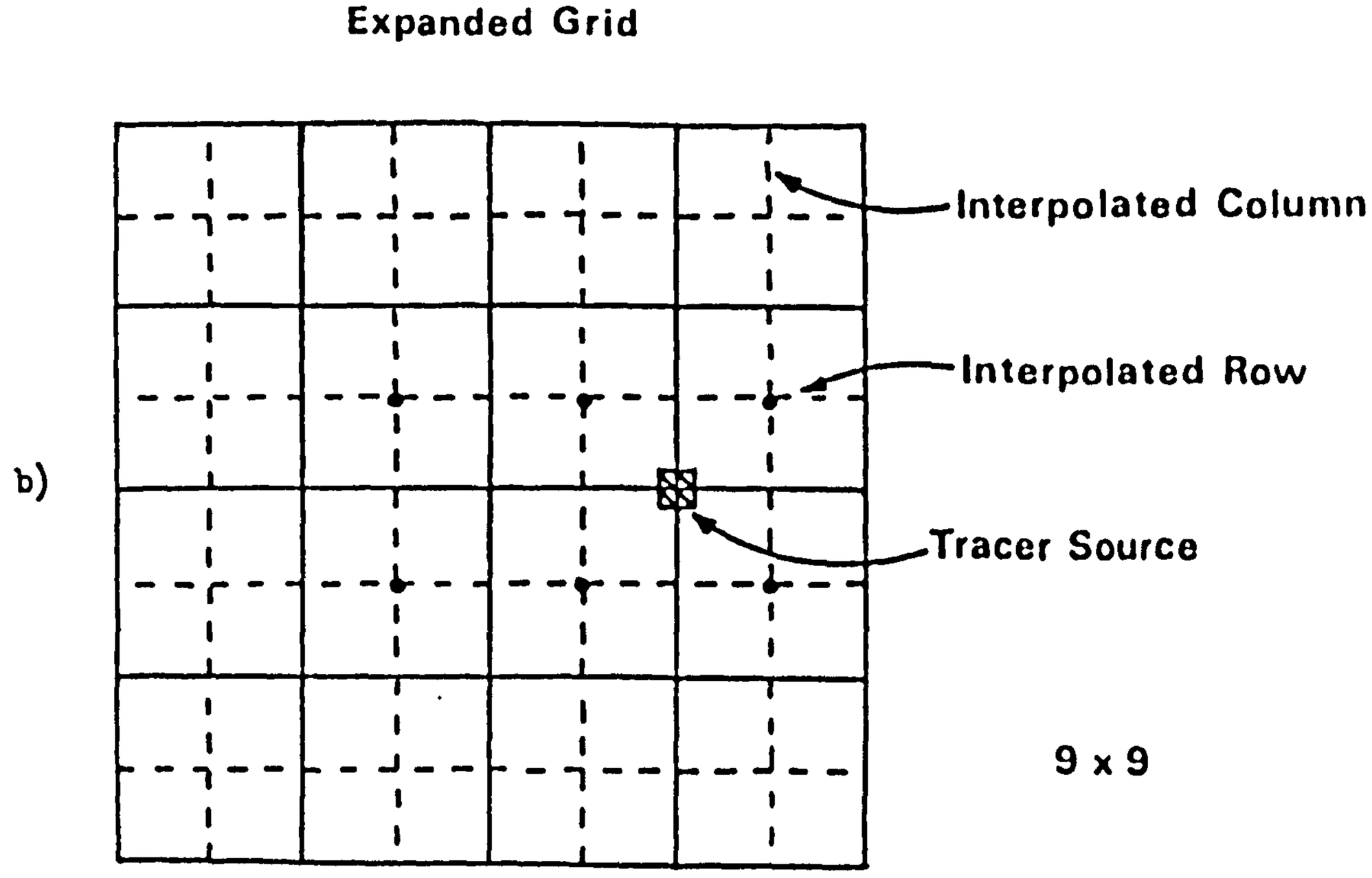

Figure 3.2b. Expanded grid of data points after interpolation.

polynomial is then used to determine values of Z_p at any point (X_p, Y_p) within that rectangle. The individual rectangles or patches of the interpolating surface are then forced to join smoothly giving a continuous surface. This method was found to provide visually the most pleasing results when compared with other methods tested.

Therefore, using the primary grid, that is consisting only of the major grid points, Figure 3.2a, without the intercalated points near the injection point, a finer mesh grid was produced, Figure 3.2b. For example, in the case of a 7 (rows) x 12 (columns) sampling grid of five metre sampling interval with infil sampling at 2.5 metres, the expanded matrix would have an overall size of 13 (rows) x 23 (columns) with additional point estimates at 2.5 metre intervals where these were lacking. Unwanted values generated because of minimum interpolation conditions included in the algorithm were removed. Also, where possible the interpolated points were replaced by intercalated values so that all concentration values gained from sampling were used. Problems due to irregular point spacing were not encountered in this study.

Akima's interpolation algorithm was chosen in preference to other possible methods on the grounds of relative simplicity and subjective appraisal of the results. An algorithm described by McLain (1972) based on a distance-weighted least-squares approach was also tested. In this method each interpolated point was computed from a weighted linear combination of all known values. However, purely on an intuitive basis, the values produced by this global fitting method were less reasonable than those produced by the Akima algorithm.

Once interpolated, each data set was mechanically contoured using a procedure based on the method previously published by Heap (1974A & B) and Heap and Pink (1969). The basic method was to take each selected contour height in turn and trace it through the data mesh using inverse linear interpolation to find the points where the contour crossed the mesh

lines. Ambiguity as to which way the contours turn on entering a mesh rectangle was avoided by the generation of further surface heights at the centre of each rectangle, (Figure 3.3) by assuming simply that the height at the centre of the grid was equal to the average of the heights of the four corners. Heap's (1974A & B) basic algorithm was extended by Dr. P.M. Mather to provide for numerical annotation of the contour lines and the addition of specific items of information to the resulting maps.

3:4 Numerical description of sand movement

In later analyses attempts to predict the direction and amount of grain movement were made (Chapters 6 and 7). It was therefore necessary to describe numerically the relevant characteristics of the patterns displayed by the contour maps. Simple average measures were adopted despite the problems arising from generalisation which can occur when spatial information is expressed in a single number or series of numbers.

Direct use of the contour maps themselves, such as in the calculation of contour areas, was avoided because of the problems of contour closure and complex contour shape. Instead, calculations were carried out on the matrix of concentration values from which the maps were produced.

The centre of gravity or weighted mean centre of the dispersed tracer was calculated using the following equation:

$$\bar{X}W_i = \frac{\Sigma x W_i}{\Sigma W_i} \qquad i = 1, n \qquad \text{Eq. 3.5}$$

$$\bar{Y}W_i = \frac{\Sigma y W_i}{\Sigma W_i} \qquad i = 1, n \qquad \text{Eq. 3.6}$$

where x and y = X and Y coordinates of data points

W_i = tracer concentration at each data point

n = number of data points (ie samples)

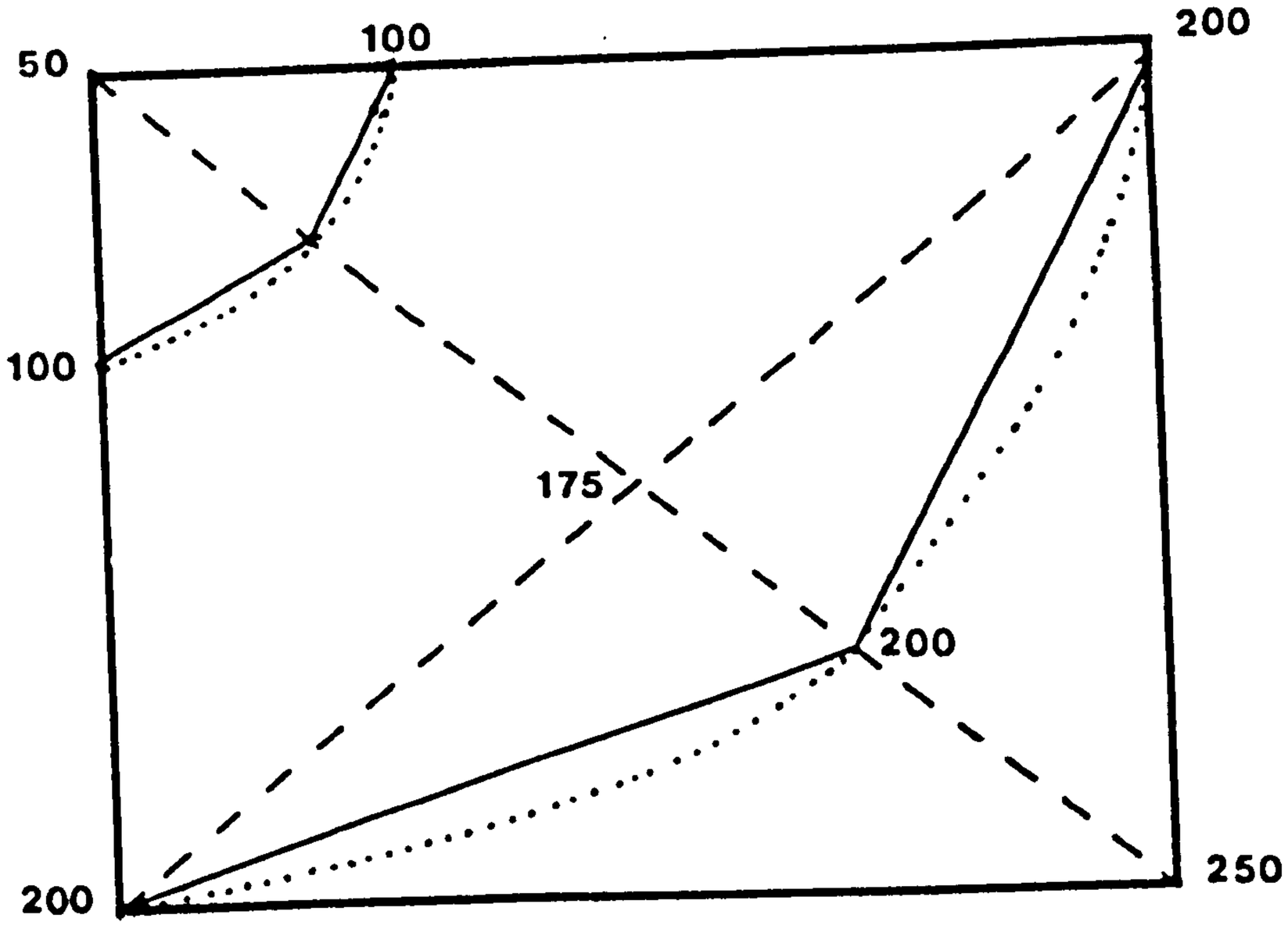

Figure 3.3. Generation of mid point grid values for mesh rectangles in contouring procedure.

This point, indicated on all the tracer maps, may be interpreted as the net position of all individual particle movements from the injection point, in all directions and over all distances. The fact that this is the weighted mean centre of the tracer cloud implies that it will suffer from the disadvantages of the mean. Therefore, for example, its position could mask two strong movements of tracer in opposite directions. This can be clearly seen in the map of the experiment conducted at Skegness on the lower ridge on the 22.10.76, Figure 4.25. Nevertheless, in most cases the centre of gravity provides an adequate summary of the tracer dispersion direction and amount. The distance between the injection point and the centre of gravity of the tracer cloud is a commonly used figure in transport rate studies when it is used to give an indication of average speed of sediment movement, Section 5:5. In this study, however, this distance, calculated by simple coordinate geometry and Pythagoras, was used to represent the average amount of movement in the dominant direction of movement.

The mean direction of movement, as indicated by the position of the centre of gravity with respect to the injection point, was calculated by trigonometric methods from the X and Y coordinates of the two points. This was also calculated using orientation statistics in order that a measure of the dispersion might also be gained. Batschelet (1965) provides an excellent description of orientation statistics and a brief summary of some of the methods is also given by Norcliffe (1977).

In analysing the data, each data matrix derived from the field sampling was treated as an empirical circular distribution by centering a set of coordinates on the injection point with the origin (0^{o}+ 360^{o}) coinciding with the 'easting' of conventional compass directions. By means of trigonometric functions the rectangular coordinates were re-expressed as polar coordinates. The X and Y components of the mean vector of the coordinates were calculated from:

$$x = \frac{\cos \alpha_i W_i}{W_i} \qquad i = 1, n \qquad \text{Eq. 3.7}$$

$$y = \frac{\sin \alpha_i W_i}{W_i} \qquad i = 1, n \qquad \text{Eq. 3.8}$$

where α_i = angle between the line from the mean centre to each data point and the East line, measured in an anticlockwise direction.

W_i = tracer concentration at each data point;

n = number of data points (ie samples).

with r, the length of the mean vector, being found from:

$$r = (x^2 + y^2)^{\frac{1}{2}} \qquad \text{Eq. 3.9}$$

Since the direction of the mean vector with components X and Y is uniquely determined by the configuration of the masses, i.e. weighted data points, on the circular distribution it may be regarded as the mean direction. Hence, the polar angle of the mean vector calculated from either:

$$\cos \alpha = \frac{x}{r} \qquad \text{Eq. 3.9}$$

$$\text{or} \qquad \sin \alpha = \frac{y}{r} \qquad \text{Eq. 3.10}$$

can be regarded as the mean angle. Continuing, the concentration or dispersion of vectors around the mean vector, that is angles around the mean angle, is given by:

$$s = (2(1-r))^{\frac{1}{2}} \qquad \text{Eq. 3.11}$$

where s = mean angular deviation in radians.

Clearly, this measure depends upon the value of r which ranges between 1 and 0. When $r = 1$ the total mass is concentrated in one point on the circle, Figure 3.4a, and s then takes the value 0. At the opposite extreme, when $r = 0$, no mean direction exists, Figure 3.4b,

a)

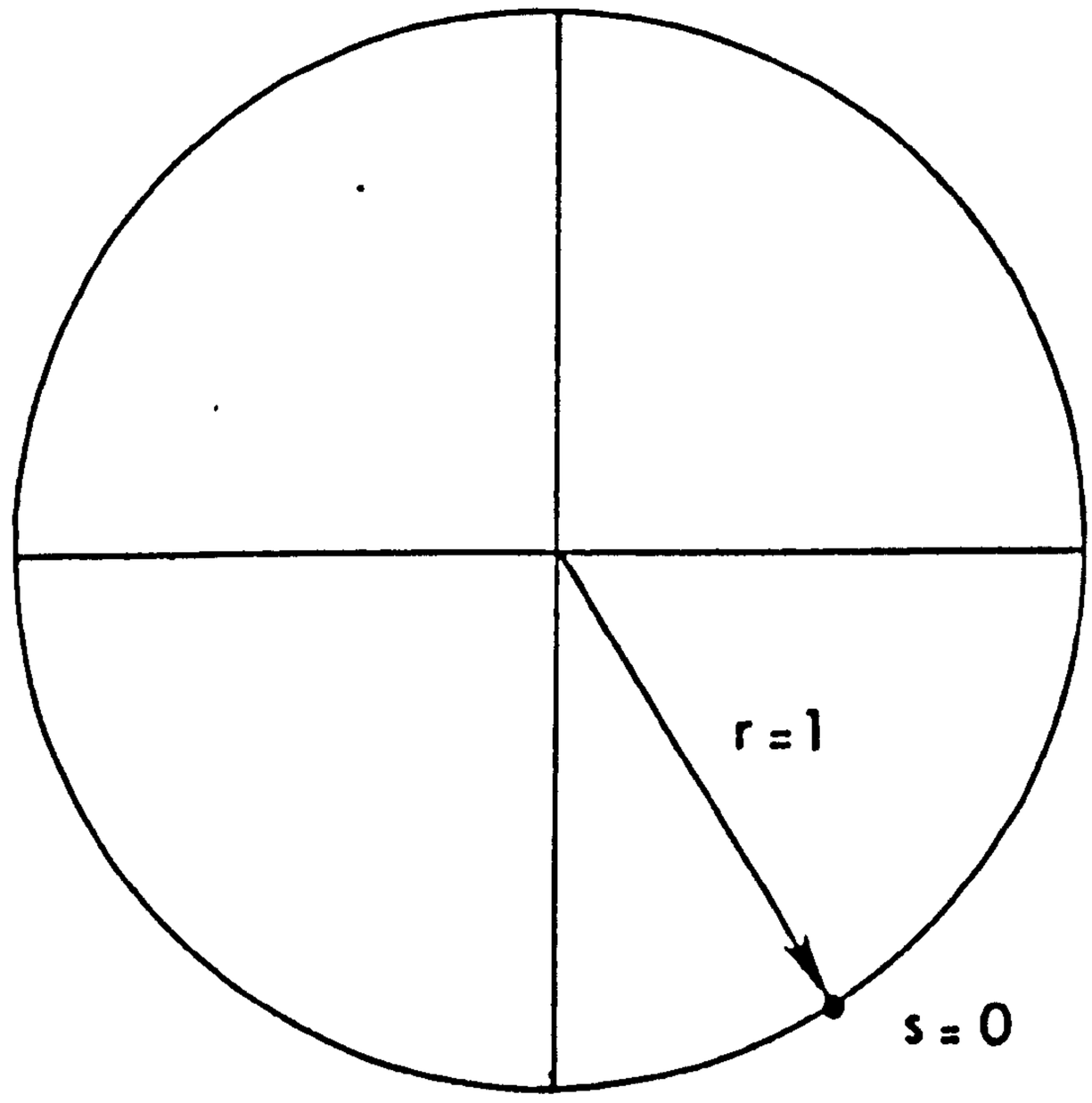

Figure 3.4a. Extreme values for length of mean vector r and angular deviation s: maximum concentration.

b)

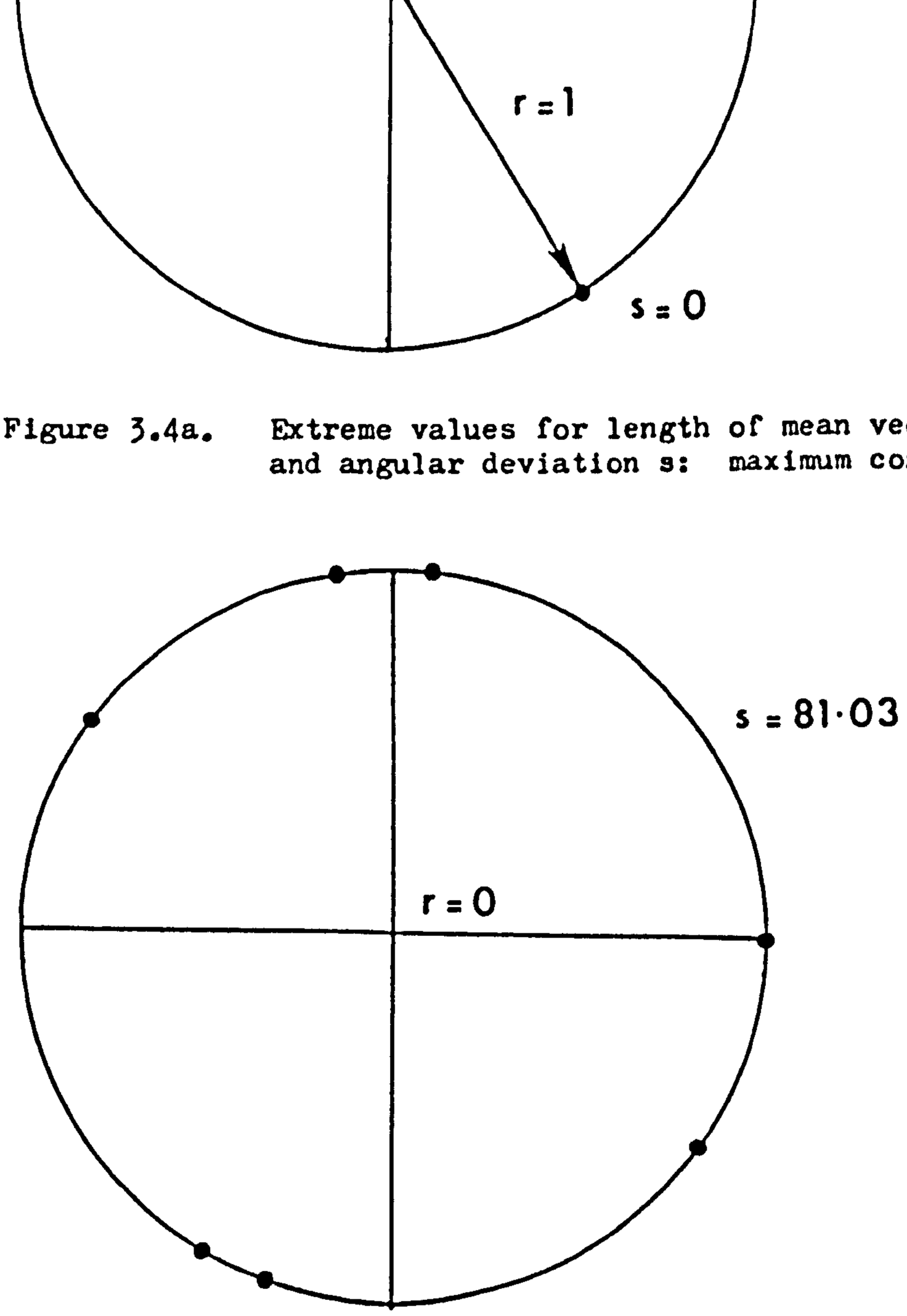

Figure 3.4b. Extreme values for length of mean vector r and angular deviation s: maximum dispersion.

and s takes its maximum value $(2)^{\frac{1}{2}}$ radians or 81.029°. This value has no intuitive meaning.

In addition to the simple mean direction of, and mean distance moved by, the centre of gravity a separate index was used to quantify relative amounts of onshore or offshore sand movement. This index was adapted from an index devised by Murray (1967) in his study of the effects of grain size and wave state on particle dispersion in the shoaling wave zone. Murray proposed a dimensionless parameter Ψ determined by:

$$\Psi = \frac{\Sigma_i A_{i\ell} C_i}{\Sigma_i A_i C_i} \qquad i = 1, 10, 100 \text{ contour of tracer concentration} \qquad \text{Eq. 3.12}$$

where A_i = total area contained by ith contour

$A_{i\ell}$ = component of the total area of the ith contour landward of a line drawn through the tracer source and parallel to the wave crest line.

C_i = concentration of the ith contour.

As this index depends on the calculation of contour areas it could not be adopted directly for reasons mentioned earlier (p.89). Because of this a slightly modified version of the index was used employing data point values rather than contour areas. Therefore:

$$\Psi = \frac{\sum_{i=1}^{L} W_i D_{i\ell}}{\sum_{i=1}^{n} W_i D_i} \qquad \begin{array}{l} n = \text{total no. of points} \\ i = 1, n \\ L = \text{no. of points to landward} \end{array} \qquad \text{Eq. 3.13}$$

where $\Sigma W_i D_{i\ell}$ = the sum of distance weighted concentration values landward of a line drawn through the grain source and parallel to shoreline orientation (i.e. alongshore side of sampling grid)

$\Sigma W_i D_i$ = total distance weighted concentrations.

N.B. Values along the line through the tracer source were omitted.

Therefore Ψ becomes the ratio of the sum of the landward distance weighted concentrations to the sum of all distance weighted concentrations for each map and so defined varies between 0 and 1. If all grain movement is landward from the source $\Psi = 1$ and if it is all seaward $\Psi = 0$. Values of Ψ between 0 and 0.5 indicate a net seaward movement of the grains whilst values between 0.5 and 1.0 indicate a net landward movement. This implies that decreasing values of Ψ indicate an increasing tendency for seaward motion. In this way the relative strength of onshore/offshore movement could be quantified.

Other measures were investigated, in particular the standard deviational ellipse. The calculation of this two dimensional figure which produces a series of measures and was devised originally by Lefever (1927) is discussed by Yuill (1971) and Ebdon (1977). It involves, principally, the summary of dispersion in weighted point patterns in terms of an ellipse fitted around the mean centre. It holds an advantage over more commonly used measures of dispersion such as standard distance, in that the variation in spread of points in different directions around the centre of gravity is taken into account. In effect, the standard deviational ellipse provides a two dimensional standard deviation which means that the orientation of the fitted ellipse as expressed by the orientation of the long axis of the ellipse gives the direction of dominant dispersion from the mean centre. The area of the ellipse, which gives a relative measure of the total amount of dispersion, is calculated from:

$$A = a\,b \qquad \text{Eq. 3.14}$$

where a = half the length of the major axis

b = half the length of the minor axis

In addition the eccentricity of the ellipse, c, as given by:

$$e = \frac{c}{a^*} \qquad \text{Eq. 3.15}$$

where c = length of the focus or minor axis

a^* = length of the major axis

may be used as an indication of the shape of the dispersion pattern, reflecting the dominance of unidirectional movement away from the release point.

However, after extensive appraisal of the results produced by these measures they were found to be unsuitable for this study. Problems of inaccurate description of dispersion pattern characteristics arose largely because of the use of the weighted mean centre as origin for the fitted ellipse rather than the tracer source. Nevertheless, the measures provided frequent cause for checking of results and in this respect were extremely useful.

3:5 Data rejection

Apart from early tests, thirty separate tracer experiments were conducted at the Gibraltar Point and Skegness sites during the fieldwork period of this study, September 1975 to October 1976. On three occasions sea and weather conditions were such that all the tracer was removed from the site and hence no samples were taken. On three other occasions, although samples were taken, the results could not be used because process measurements were unsatisfactory. Finally, confusion of sand sample labelling and poor process measurements meant that data from one other experiment could not be used.

From the remaining 23 experiments good field data was gleaned and this produced a total of 34 grids which could be mapped. This figure arises from the fact that on several occasions more than one tracer injection was made along the beach profile. For example, three sources of tracer were placed on different parts of the profile H2 during the experiment of the 18.3.76 at Gibraltar Point.

Of the 34 finished maps, five of these were rejected for further quantitative analysis either because the tracer cloud had not been sampled properly, as shown by Figure 2.5 and mentioned in the previous Chapter, or because too little of the tracer was found to remain when the map was produced. This latter case is illustrated by Figure 4.22 which shows the small amount of tracer recovered for the experiment on the upper ridge at Skegness on the 21.9.76. Visual inspection of the contour patterns and their values provided sufficient discrimination for the rejection of maps on the grounds of insufficient tracer recovery.

Therefore, in all 29 maps were used in later numerical analysis although some of the five rejected maps were used in purely descriptive sections of the study.

During some of the field experiments tests of the effects of grain size on the particle movement were also made through the use of quantities of different grain sizes coated with different tracer colours, Section 4:2. This data was not used in quantitative analysis because of very low tracer recovery rates. The low recovery rates were themselves due largely to the small volume of the quantities of tagged grains actually used. Of five such specific grain size tests only one produced good results.

CHAPTER 4

TRACER EXPERIMENT CASE STUDIES

4:1 Introduction

As pointed out in Chapter 1, previous tracer work on ridge and runnel type beaches is limited. Ingle (1966) found that ridges and runnels of varying depth and width, which were common features of the test sites, had varying effects on tracer patterns. Narrow and shallow runnels of less than two feet deep had essentially no detectable effect on the direction and rate of tracer movement but a deeper cobble-lined runnel present during a tracer test on Santa Monica beach had a marked effect. The runnel acted as a sink for the tracer which was swept alongshore and out of the runnel by low velocity runnel currents and the turbulence from the slopping of wave bores into the runnel. In one of the few other pieces of work on irregular nearshore morphology, Zenkovitch (1960, 1967) has established that maximum sand transport on undulating foreshore-inshore surfaces commonly takes place on topographic highs in conjunction with breaking waves.

In this chapter the tracer experiments conducted for this study are considered as separate case studies. Most of the experiments were designed to test specific aspects of sand movement in addition to providing a larger data set for further analysis. Some of the experiments were conducted to compare rates of movement and dispersion patterns on different parts of the beach profile during a single tidal cycle whilst others were specific to the study of the effects of tidal currents on the lower part of the foreshore. The results of these experiments are considered in the next section, 4:2, with respect to the two beach sites at Gibraltar Point and Skegness, Figure 1.1. Comparisons between the two sites are also made and possible reasons for the major differences put forward. Other experiments, attempting to study the effects of grain

size on tracer sand dispersion, are discussed in Section 4:3.

4:2 Cross beach differences and Gibraltar Point/Skegness comparisons

It was expected that, because of the complex nature of the beach morphology at both Gibraltar Point and Skegness sites, there would be some variation in patterns and rates of sand movement across the beach width. Furthermore it has also been suggested that tidal currents play an important role in sediment movement on the lower foreshore, Section 2:5. In order to gain some insight into these aspects of beach sand movement as far as possible different positions on the beach profiles were chosen for each experiment and also several experiments were conducted in which two or more injections of tracer were made across the beach face on the same tidal cycle. For example on the 25.8.76 tracer was laid on the upper ridge seaward face and on the lower ridge seaward face on the profile at Skegness, Figure 4.1 and similarly on 18.3.76 tracer was released from three locations along profile H2 at Gibraltar Point, Figure 4.2.

Gibraltar Point

A consideration of the results of the tracer experiments at Gibraltar Point provides some interesting evidence of differences in sand movement rates and patterns of dispersion between the upper and lower beach ridges and between different points on the same ridge. The experiment of 18.3.76 gave results which highlight the contrasts on both these scales. Figure 4.2 indicates the position of the tracer injection points on the profile H2 and the resultant tracer patterns are shown in Figures 4.3, 4.4, 2.9 and 2.10. The most landward release point, 1, Figure 4.2, was located on the landward face of the upper beach ridge, on the gently dipping slope from the crest of the ridge down into the shallow runnel at the back of the beach. Source 2 was placed on the much steeper seaward ridge face of the upper ridge whilst the third tracer injection, 3, was made on the

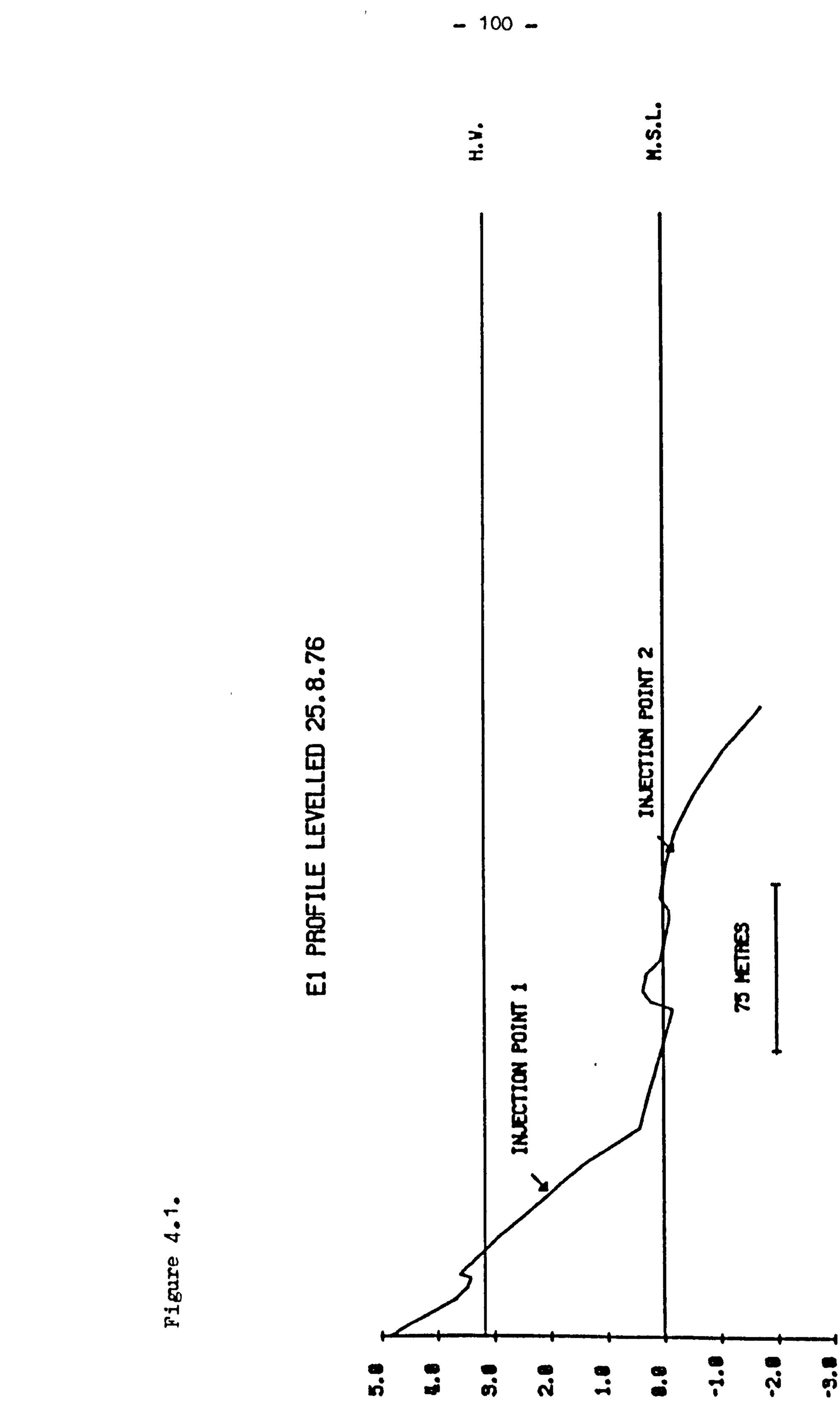
H.W.
M.S.L.
E1 PROFILE LEVELLED 25.8.76
INJECTION POINT 2
INJECTION POINT 1
75 METRES
H.W. PREDICTED TIDE HEIGHT FOR EXPERIMENT M.S.L. MEAN SEA LEVEL
5.0
4.0
3.0
2.0
1.0
0.0
-1.0
-2.0
-3.0
METRES O.D.NEWLYN

Figure 4.1.

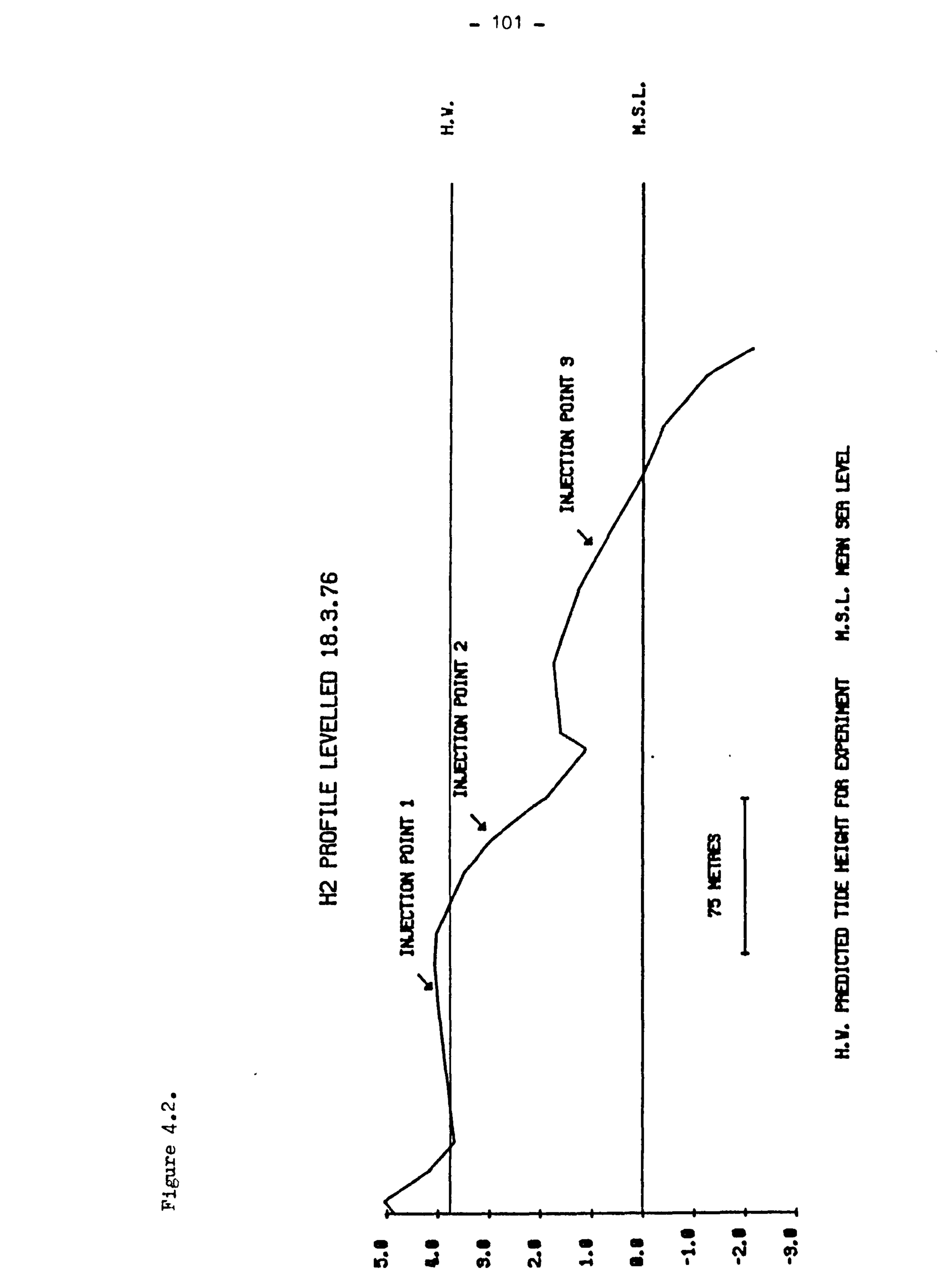
H.W.
M.S.L.
H2 PROFILE LEVELLED 18.3.76
INJECTION POINT 1
INJECTION POINT 2
INJECTION POINT 3
75 METRES
H.W. PREDICTED TIDE HEIGHT FOR EXPERIMENT
M.S.L. MEAN SEA LEVEL
5.0
4.0
3.0
2.0
1.0
0.0
-1.0
-2.0
-3.0
METRES O.D.NEWLYN

Figure 4.2.

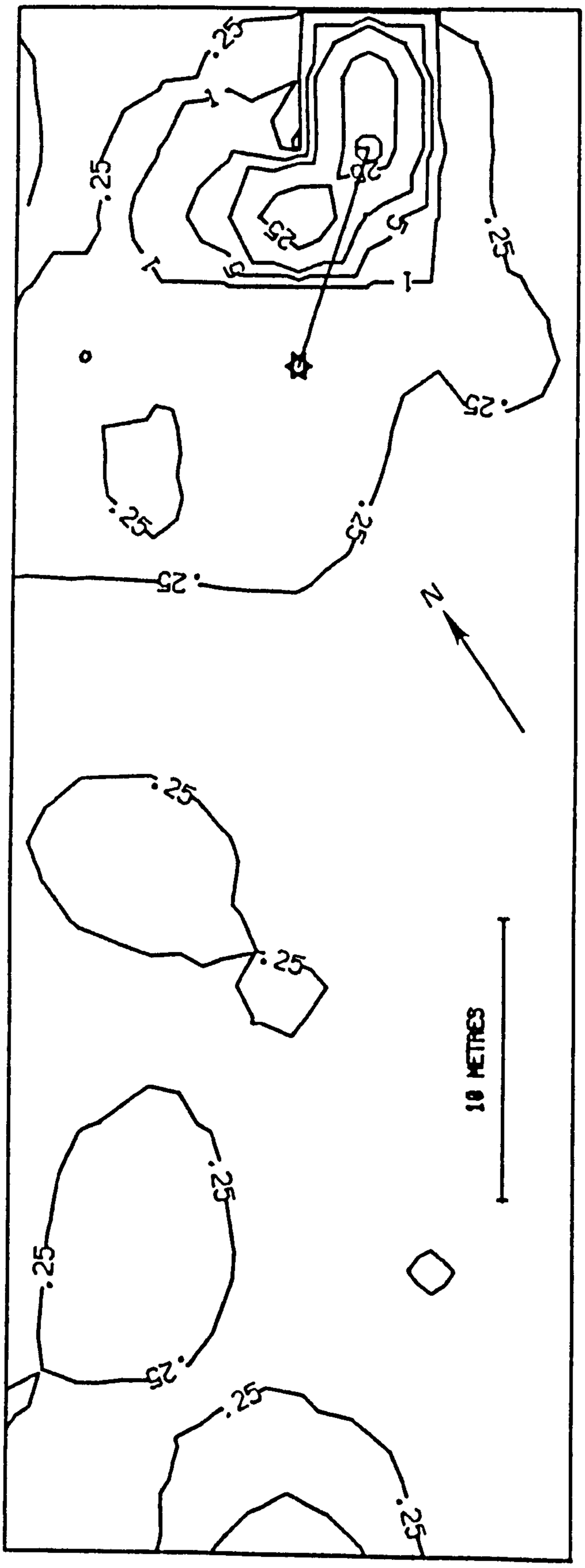
18 3 76 GRID 1 BERM H2 Y
INJECTION POINT ⊖ CENTRE OF GRAVITY ✡
10 METRES
N
.25
.5
1
2
5

Figure 4.3.

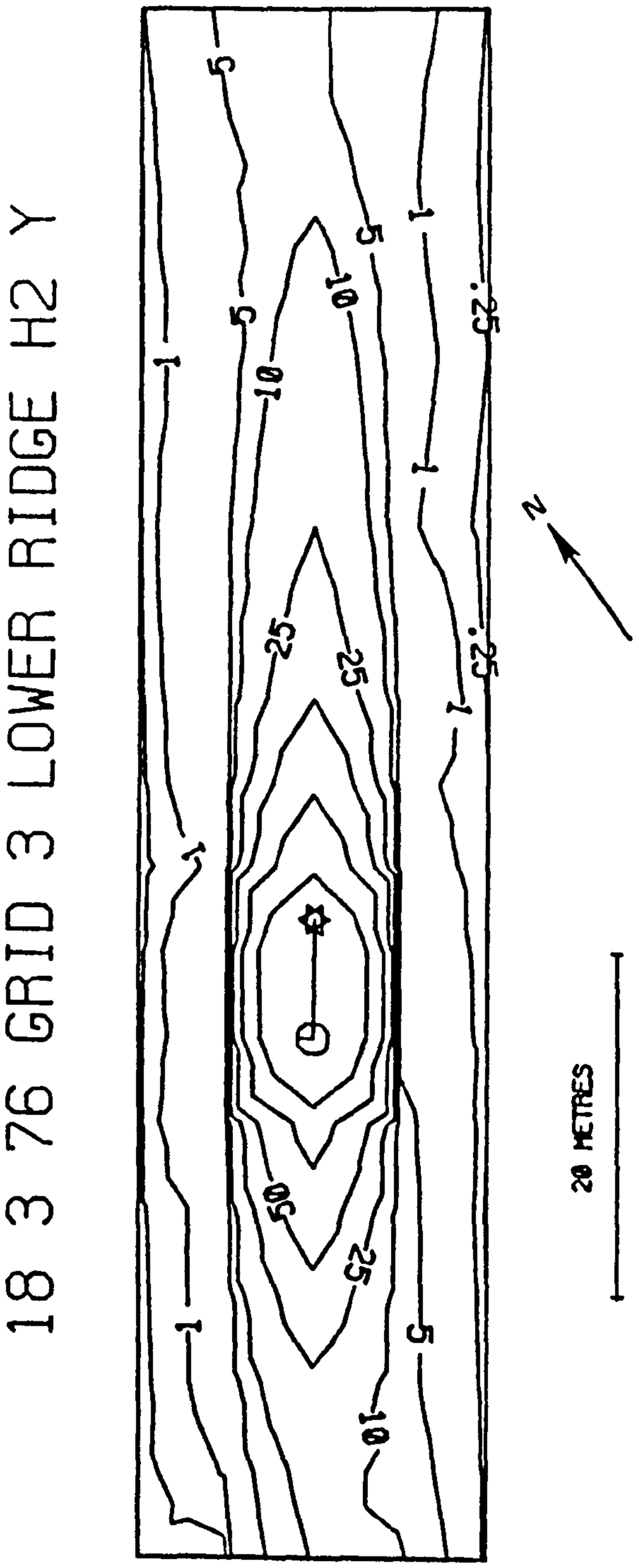
18 3 76 GRID 3 LOWER RIDGE H2 Y
1
5
10
25
50
INJECTION POINT
CENTRE OF GRAVITY
N
20 METRES

Figure 4.4.

seaward face of the lower ridge at a distance of about 320 metres from the top of the beach. The predicted tide height was 3.75m O.D. (7.5m C.D.) which was one of the largest spring tides of the year.

The tracer pattern emanating from release point 1 mapped in Figure 4.3 illustrates the calm conditions which prevailed at this location and the influence of very slight runnel currents. Breaking waves did not directly affect this tracer source as the breaking wave zone was situated at the crest of the upper ridge at the maximum point of the tide. The contours show that little movement of tracer took place and indeed the tracer injection patch was seen to be little disturbed when sampling was carried out. Most of the tracer was left at the injection point and was still quite clearly visible despite a thin covering of clean sand. The low-energy nature of this runnel was confirmed by the existence of mud deposits slightly to the south of the profile line. It is only on the very high spring tides, above about 3.5m O.D. (7.25m C.D.), or in conditions producing abnormally high tides, that this runnel does become filled with water and even then only for one or two hours. Waves rarely cross the runnel to break on the dune face and in fact very often the runnel is filled gradually from the south rather than by water entering the runnel across the seaward ridge crest. The line of profile cuts across the runnel 10 metres from its northern end and consequently the depth of water in the runnel at this location cannot be in excess of 30-40 cms. except under the combination of storm conditions and a high spring tide. The low value contours on the map indicate some tracer was moved south along the runnel by currents draining the runnel in this direction. On the other hand the high value contours close to the tracer source also reveal an onshore trend, which would be imparted by the landward surge of the occasional surf bore passing across the tracer source from waves breaking to seaward and enhanced by the slight landward slope into the runnel. Dispersion southwards and onshore are the main movement

directions. The position of the centre of gravity in relation to the injection point indicates well the dominant movement direction of the tracer but on the other hand the average distance moved by the grains,which this also shows,perhaps slightly over-exaggerates the true picture.

The pattern revealed by Figure 2.9 for Grid 2 on the seaward side of the upper ridge is very different from that of Grid 1. Much more dispersion is evident from the tracer pattern, the scale of the map being half that of Figure 4.3 and a dominant direction of movement along the beach face in a southerly direction is clearly shown. A little onshore/offshore diffusion of tracer is also present but the overall pattern is consistent with that which might be expected to occur as a result of the combined effect of wave drifting and longshore currents. The southerly sawtooth effect of the swash-backwash drift of material was probably caused by the relatively oblique, 11^{o}, angle with the line of the ridge face, at which the waves broke. Furthermore, the longshore current generated in the runnel to the seaward of the ridge face was also flowing southwards at a velocity of roughly 6 cm/sec and this, therefore, would enhance the southerly movement of sand grains. An indication of the amount of movement of individual particles is given by the average distance moved which was over 25 metres in a longshore direction, Table 6.2.

The unidirectional nature of the tracer movement is reflected in the value of 21.4^{o}, Table 4.1 for the mean angular deviation which indicates a very narrow spread of dispersion around the mean direction of movement. When this is converted to the 0-1 index the value is 0.93, Table 4.1 again indicating the high degree of concentration of vectors of movement in one dominant direction.

This strong southerly movement of tracer on the upper ridge face is not repeated on the lower ridge face, indeed the position of the centre

Table 4.1. Mean angle, mean angular deviation and index of concentration (r) for all tracer experiments.

G I B R A L T A R P O I N T

			Mean Angle	Mean Angular Deviation	Concentration Index (r)
2.11.75	Total	UR	42.2	42.6	0.72
2.11.75	2ϕ	UR	44.6	23.0	0.92
2.11.75	2ϕ	UR	43.5	22.2	0.92
17.1.76	Total	UR	174.9	16.3	0.96
17.1.76	2ϕ	UR	175.8	15.6	0.96
17.1.76	2ϕ	UR	173.8	15.4	0.96
28.2.76	Pink	LR	99.6	51.0	0.60
28.2.76	Blue	LR	78.1	58.2	0.48
18.3.76	Grid 1	UR	129.9	36.6	0.80
18.3.76	Grid 2 P	UR	-178.1	21.4	0.93
18.3.76	Grid 3	LR	-0.8	57.3	0.50
17.5.76		LR	1.6	45.58	0.68
30.6.76		LR	-166.4	28.8	0.87
15.7.76		LR	-0.51	49.6	0.63
10.8.76		LR	-177.4	67.6	0.30
7.9.76	H3	UR	-94.6	73.5	0.18
7.9.76	H3	LR	136.7	30.7	0.86
22.9.76		UR	179.8	34.2	0.82
22.9.76		LR Y	-177.6	17.7	0.95
22.9.76		LR P	-18.9	49.1	0.63
6.10.76		UG	-12.6	19.2	0.94
6.10.76		LG	6.9	54.1	0.55
23.10.76	H2	LR	-1.7	9.8	0.99
23.10.76	H3	LR	-6.9	26.3	0.89

Continued overleaf

Table 4.1 continued.

		SKEGNESS		
		Mean Angle	Mean Angular Deviation	Concentration Index (r)
18.5.76	LR	179.5	73.9	0.17
1.7.76	UR	-118.9	57.7	0.49
14.7.76	LR	174.1	20.4	0.94
12.8.76	LR	179.5	42.1	0.73
25.8.76	UR	163.6	63.4	0.39
25.8.76	LR	164.9	30.9	0.86
8.9.76	UR	140.2	31.2	0.30
21.9.76	UR	63.9	67.8	0.30
21.9.76	LR	130.0	49.8	0.62
7.10.76	UR	42.9	32.6	0.84
7.10.76	LR	-177.9	29.9	0.86
22.10.76	UR	5.7	22.4	0.92
22.10.76	LR	-109.9	74.5	0.15

N.B. Concentration index vectoral re-expression of angular deviation.

of gravity for the dispersed tracer cloud from release point 3 reveals a net movement to the north. The contour pattern of Grid 3 shown in Figure 4.4 has a very pronounced linear shape with onshore-offshore movements very restricted. This pattern suggests the existence of a current-dominated environment and its position on the beach, close to the low-water mark, allows the possibility of its tidal current generation to be considered. This seems to be confirmed by the way in which tracer has dispersed in both directions alongshore since this pattern would be expected to occur with a reversing current. Longshore currents generated in the nearshore zones could not have produced the pattern of Figure 4.4 in one tidal cycle as they would produce movement in one major direction only as in the pattern displayed by Grid 2. Furthermore, longshore current velocities measured during this experiment on this section of the beach were found to be very low. Although tidal currents were not measured during this particular experiment, Figure A1.8 gives an idea of the velocities which can be achieved on this lower part of the beach. The tidal currents shown in Figure A1.8 were in fact recorded on a lower tide than that of 18.3.76 and hence it may be that the currents affecting tracer release point 3 were even stronger than those represented.

It has certainly been observed that strong winds blowing longshore can cause a significant quickening of tidal current velocities. The longer duration, albeit lower velocity of the ebb current in the Wainfleet Channel flowing to the north would explain the net movement of tracer to the north, assuming that current velocities were sufficient to exceed the critical velocity and actually cause movement. Dugdale (1977) has found that tidal current velocities at the sea bed in the Wainfleet Channel are sufficient to cause sand movement and so the above explanation is a strong possibility. The only alternative explanation of the contour pattern displayed in Figure 4.4 with a strong movement in both longshore directions, is a complete change in wave and weather conditions during the tidal cycle

but this may be quickly rejected. Weather records showed that no dramatic change took place, winds remaining light and from the east, and no large changes in wave conditions during the incoming tide were observed.

Thus, the three maps of tracer dispersion for the experiment of 18.3.76 show that over the same tidal cycle a complex series of sand movements is taking place on different parts of the foreshore above L.W.M. and that net sediment movements on particular parts of the beach can be highly contrasting. Also it seems that under low energy wave conditions, significant wave height for Grid 3 of the experiment on 18.3.76 was measured at 0.26 metres, sediment movement on the lower beach can be dominated by tidal current flows. However, under higher wave energy conditions or with lower velocities of tidal currents, wave parameters might be expected to be the dominant process and if this is so similar patterns of tracer movement might be expected for both the upper and lower ridges. This seems to be confirmed by the experiment of 22.9.76 on profile H2. Two tracer injections were made, Figure 4.5, one on the upper ridge face and one on the lower ridge. Breaking wave heights were measured as 0.79m at the lower ridge site and 0.55m at the upper ridge site and under these relatively severe conditions large movements of sand took place. Average figures for depth of erosion were 3.26cm on the upper ridge and 4.97cm on the lower ridge compared with a mean of just over 2.7cm for all the experiments at Gibraltar Point. Distances moved alongshore by the centre of gravity of the tracer cloud were respectively 18.59 metres and 43.95 metres for the upper and lower ridges, Table 6.1. Wave approach was from the north at an angle of 11^{o} to the line of the beach at both sites and the effect of this may be seen in the dominant southerly movement of tracer alongshore on both ridges. The two-directional movement of the Grid 3 map for 18.3.76 is absent from the lower ridge map of 22.9.76, Figure 4.6, and it seems that on this occasion the flood tide current to

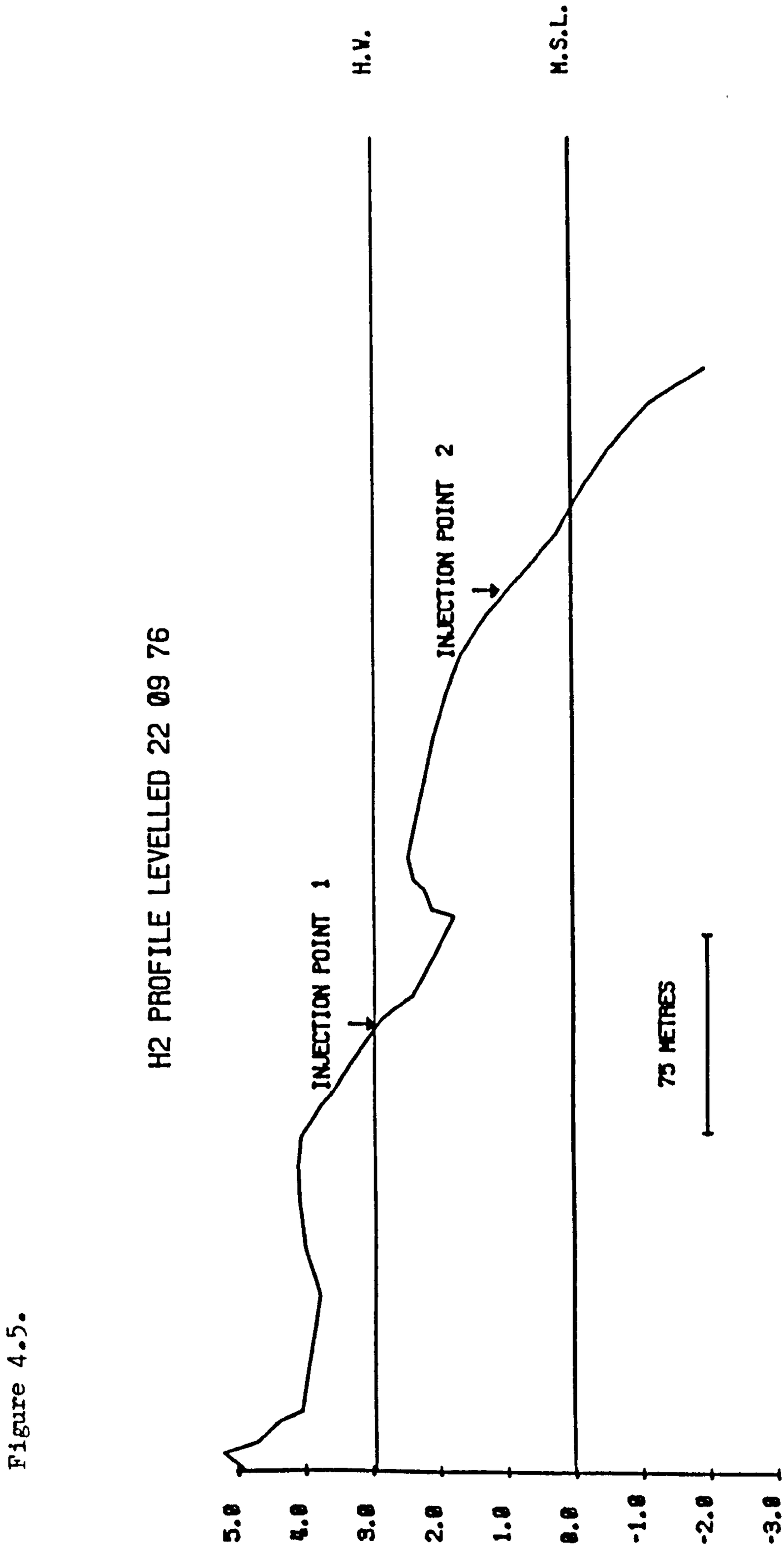
H2 PROFILE LEVELLED 22 09 76
H.W.
M.S.L.
INJECTION POINT 1
INJECTION POINT 2
75 METRES
H.W. - PREDICTED TIDE HEIGHT FOR EXPERIMENT
M.S.L. - MEAN SEA LEVEL
5.0
4.0
3.0
2.0
1.0
0.0
-1.0
-2.0
-3.0
METRES O.D.NEWLYN

Figure 4.5.

Figure 4.6.

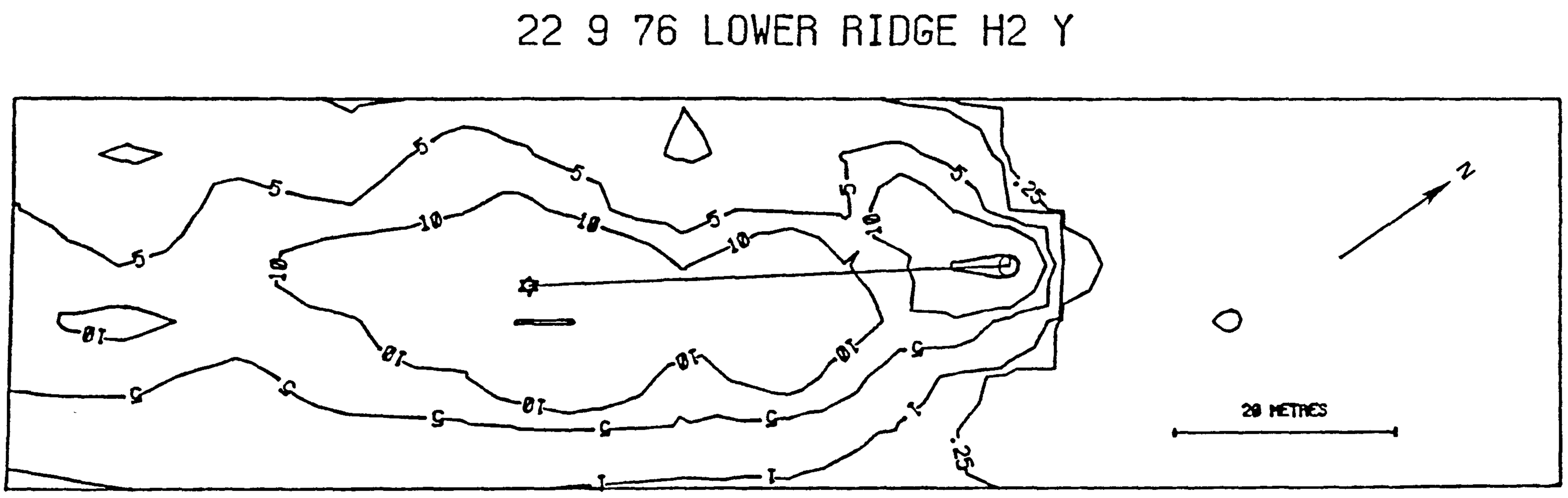
22 9 76 LOWER RIDGE H2 Y
N
20 METRES
INJECTION POINT
CENTRE OF GRAVITY

the south was complemented by the very strong wave generated southerly flowing longshore current and by wave drift such that any ebb effect is not apparent in the final pattern. However, this experiment was also specifically designed to study the influence of tidal currents on the lower beach and two injections of tracer were made at the same spot on the lower ridge.

The first tracer release was made as usual at low water and the results of this have just been discussed. The second was made at high water, when the tidal currents slacken and reverse. This was achieved by driving a boat out through the surf and breaker zones, lowering a weighted bucket of tracer to the submerged beach surface and then tipping out the tracer onto the beach face by means of ropes attached to the bucket, Figure 4.7.

Release of some tracer into the water column by this method was unavoidable but was considered acceptable in the absence of more efficient methods of tracer release in this situation. An abortive attempt was made to lay the tracer by digging it into the beach face at low water and then covering it with a wooden box hammered firmly into the beach surface which was to be removed at the appropriate time. However, this method proved totally unsuccessful because of the difficulty of keeping the tracer covered.

It was hoped that the tracer released at the turn of the tide would respond to ebb tidal current and hence move northwards, thus confirming the fact that tidal currents do influence sand movement high up the lower beach. The resultant tracer dispersion does indeed show a dominant movement northwards with the centre of gravity having a mean angle of 341^{o}, Figure 4.8. This map contrasts strongly with the map of dispersion of the tracer released for the whole tidal cycle which, as stated, reflects the strong southerly longshore currents and southerly wave drift caused by the large waves, mean 0.79m, together with the southerly flood current.

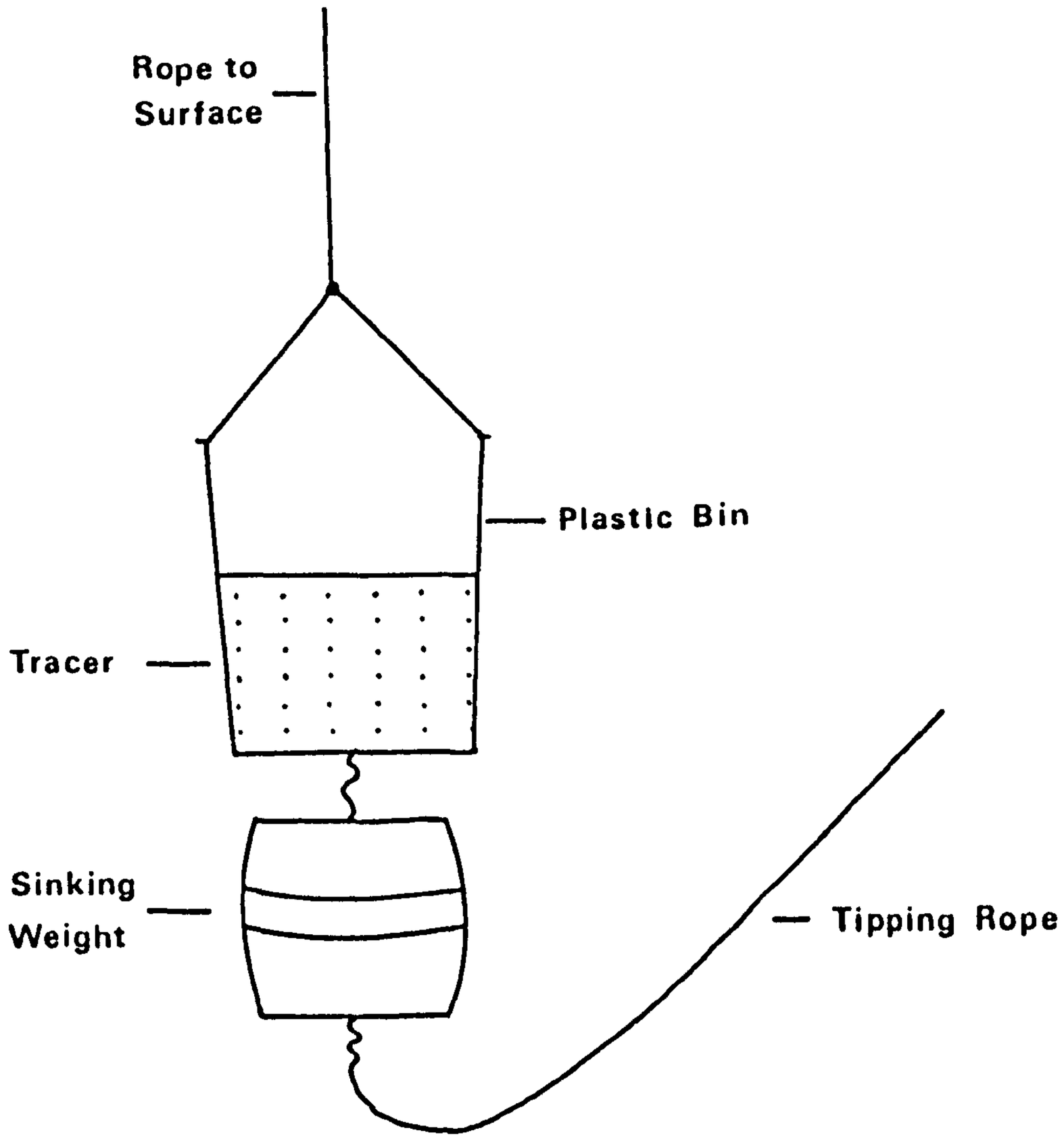

Figure 4.7. Tracer release equipment for injection at high water 22.9.76 experiment.

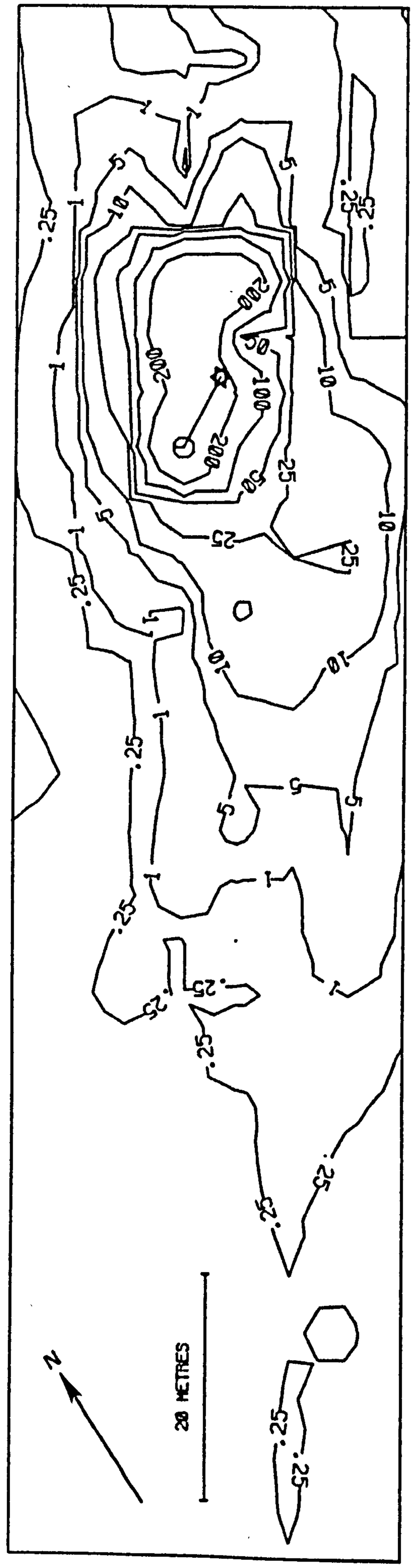

N.B. Tracer released at turn of tide.

Figure 4.8.

It is difficult to say how much the dispersion of tracer in Figure 4.8 overemphasises the actual bedload movement of sand by the ebb tidal current. Tracer grains suspended in the water column for any considerable time after release would be rapidly moved northwards by the accelerating ebb current but at the same time it is likely that these finer grains would have moved a long way outside the sampling area and hence would not be considered in calculations. The much greater overall dispersion of tracer reflected in the concentration index of 0.63 is probably the result of the method of release. Despite the problems, though, Figure 4.8 does show that tidal currents do affect sand movement on the lower foreshore. Their importance in relation to other processes is difficult to assess and requires much more study.

It is interesting that there is seemingly no ebb tidal current effect on the tracer released at low water, Figure 4.8,but this may partly be explained by the model of the sequence of erosional and depositional events during a tidal cycle described in Section 2:6. During the time when the influence of the ebb current might be expected to be at its greatest, the tracer source was probably covered by accretion and effectively cut off. Any tracer available for movement northwards would already have moved south from the tracer source and hence probably would not actually move back past the release point. Although erosion was considerable during this experiment because of the large waves, accretion was equally large and resultant net changes were relatively small. The comparable figures for the 18.3.76 experiment when the tracer was dispersed in both longshore directions, presumably by the tidal current, reveal that erosion was much greater than accretion and hence the tracer probably remained a source throughout the whole of the tidal cycle.

Although the overriding vector of movement is alongshore in both the maps for the upper and lower ridges of the 22.9.76 experiment, a difference in dispersion pattern can be discerned, Figures 4.9 and 4.6. The contours

Figure 4.9.

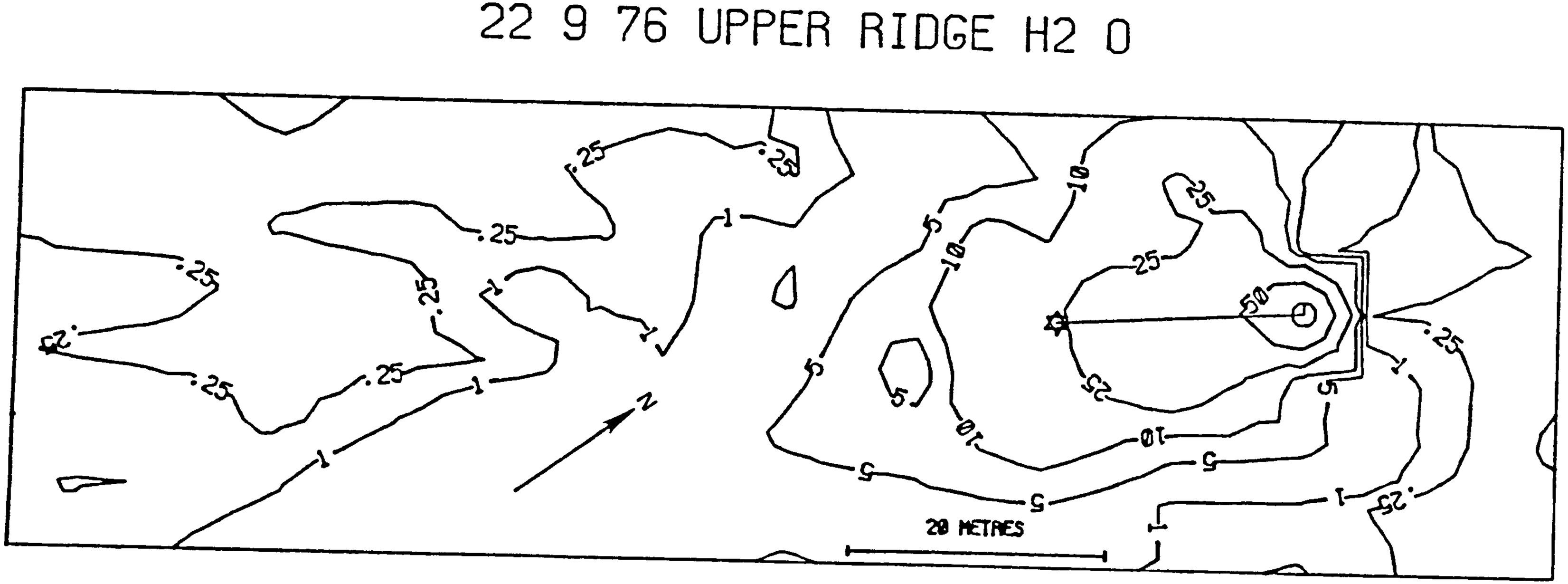
22 9 76 UPPER RIDGE H2 O
.25
1
5
10
25
50
20 METRES
INJECTION POINT ⊙ CENTRE OF GRAVITY ✡

on the lower map are more definitely elliptical and suggest longshore movement whilst more of a circular pattern is evident for the upper ridge map. This is reflected in the angular deviation and concentration index figures, Table 4.1,which reveal a more unidirectional pattern for the lower ridge map. Greater current effect on the lower ridge is probably the cause of the differences.

Similar differences have also been noted earlier for the 18.3.76 experiment but because of the bimodal nature of the vectors of sand motion on the lower ridge the angular dispersion figures do not represent the differences very well.

Parker (1976) has postulated that on the crests of ridges on a multi-barred foreshore, location and swash are dominant processes causing a landward movement of material whilst on the seaward faces of ridges swash and backwash are most important and lead to predictable directional dependence on wave approach. Results of two tracer experiments conducted at Gibraltar Point to test these ideas seem to suggest that they may be an oversimplification of a complex situation.

Figures 4.11 and 4.12 are the maps for the 6.10.76 experiment in which two lots of tracer were released on the lower ridge, Figure 4.10. Comparison of these two maps reveals a conflict with Parker's (1976) suggestions. Both show strong longshore movements to the north caused by the southerly wave approach and northward flowing longshore current of 40.5 cm/sec but the map of tracer released from the lower of the two injection points is the one which has a strong onshore component and not the upper ridge crest map. Indeed, the tracer map for the upper release point has a slight offshore tendency rather than the landward component predicted by Parker's thesis. However, it must be noted that the upper release point was located just below the ridge crest on the seaward face and not actually on the crest itself, Figure 4.10. Movement alongshore was much greater on the

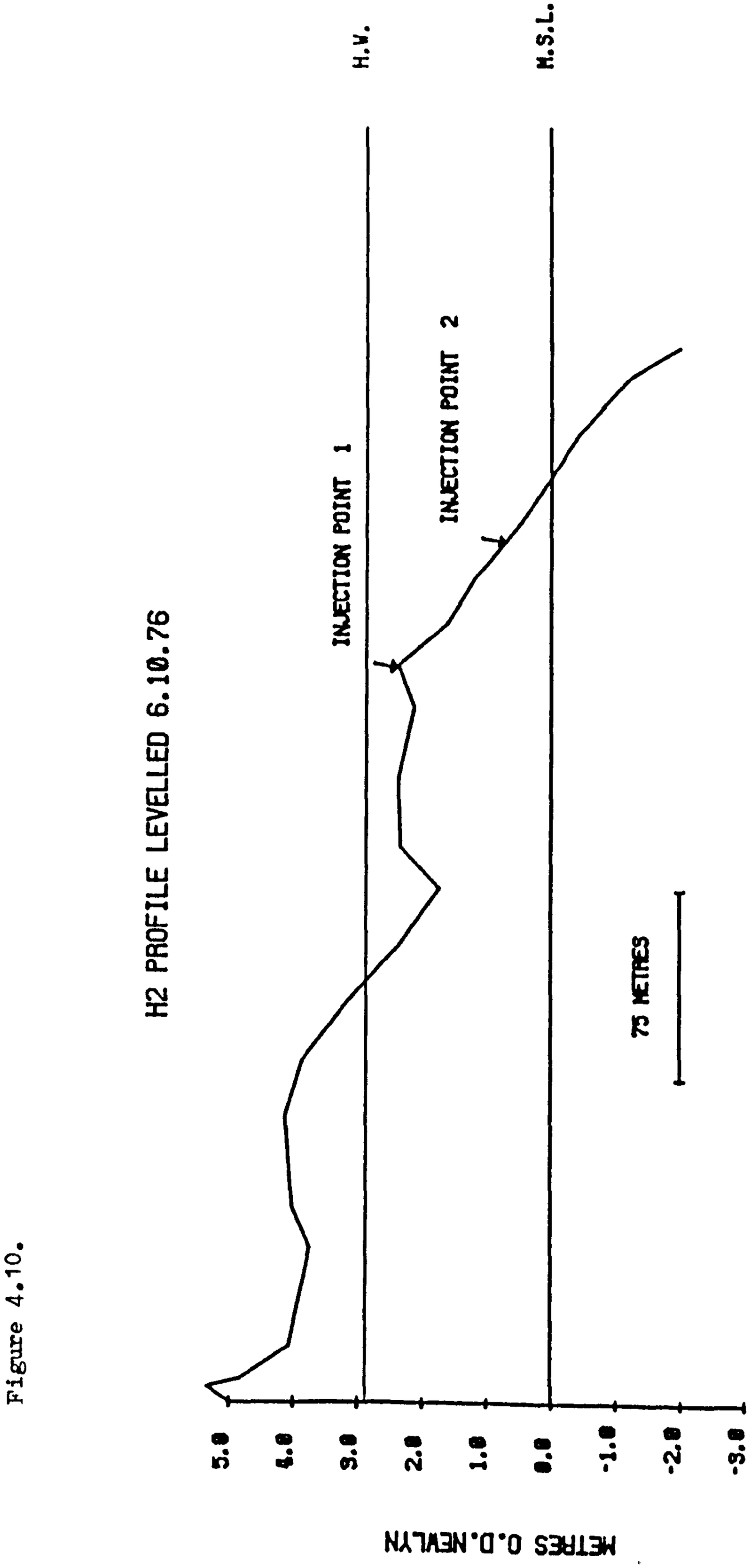
H.W.
M.S.L.
INJECTION POINT 1
INJECTION POINT 2
H2 PROFILE LEVELLED 6.10.76
75 METRES
M.S.L. MEAN SEA LEVEL
H.W. PREDICTED TIDE HEIGHT FOR EXPERIMENT
5.0
4.0
3.0
2.0
1.0
0.0
-1.0
-2.0
-3.0
METRES O.D.NEWLYN

Figure 4.10.

Figure 4.11.

6 10 76 UPPER GRID H2 Y

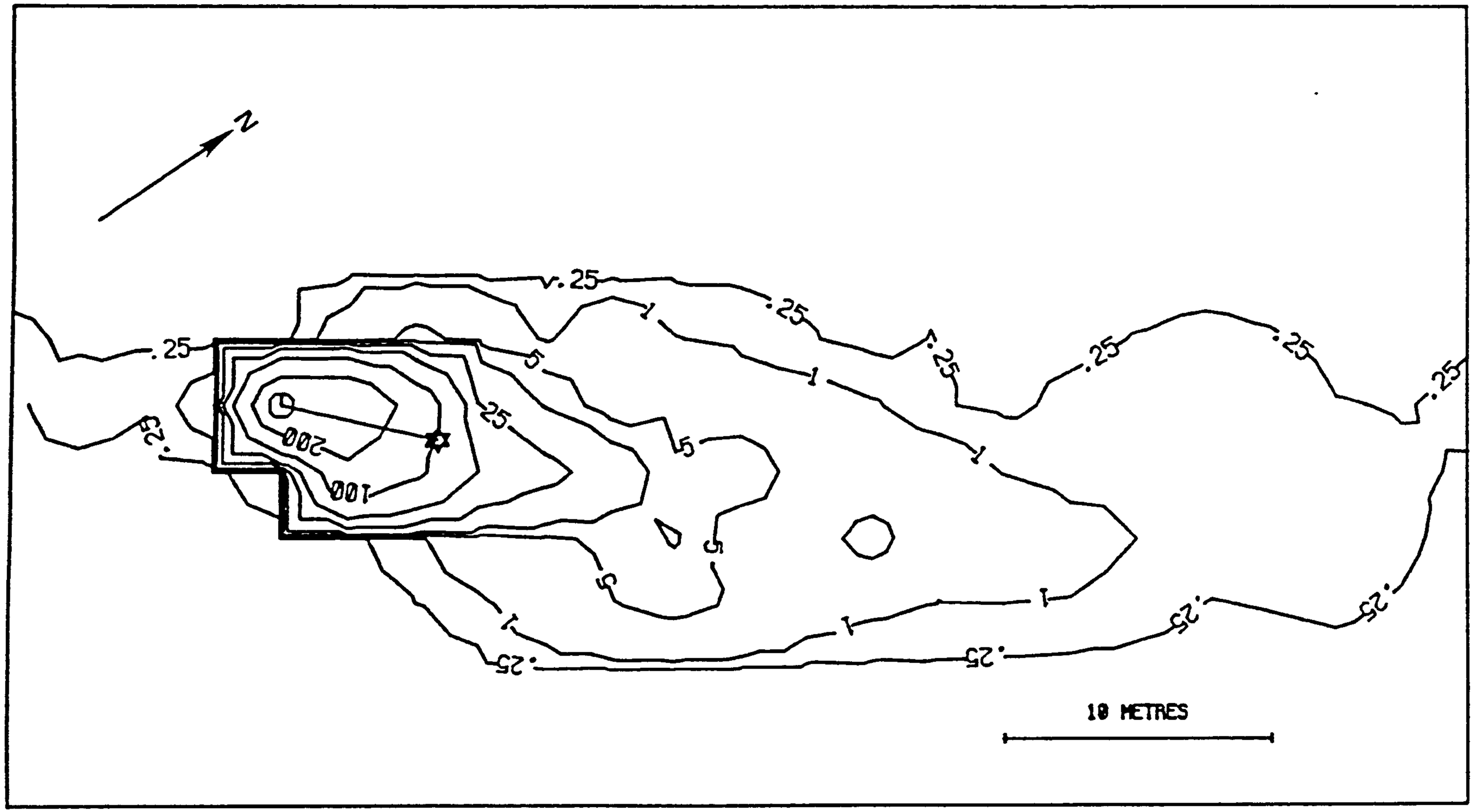

INJECTION POINT ⊙ CENTRE OF GRAVITY ✡

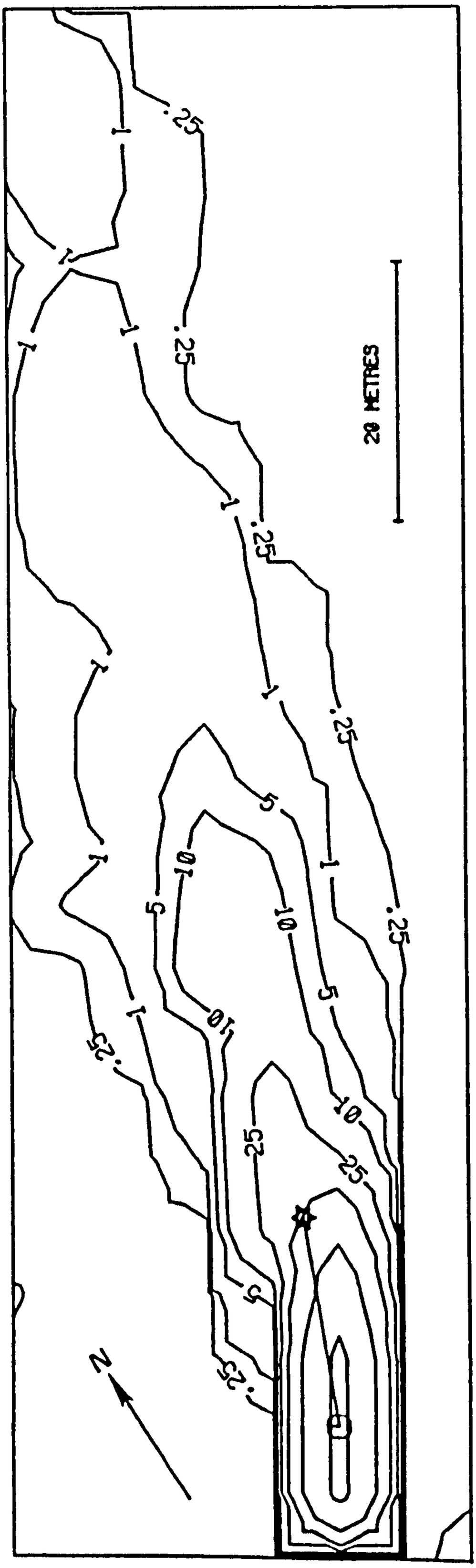
6 10 76 LOWER GRID H2 O
INJECTION POINT Θ CENTRE OF GRAVITY ✡
20 METRES
N

Figure 4.12.

lower part of the ridge than from the upper release point as evidenced by the scales of the two maps and this might again be the result of a tidal current factor.

The patterns of movement for the experiment carried out on profile H3 on 7.9.76 conform more closely to Parker's ideas, Figure 4.14 and 2.11. The two maps are quite contrasting, with the dispersion from the upper release point, on the landward side of the ridge crest, showing a circular diffusion pattern. This is indicated by the angular deviation of 73.5^{o}, concentration index of 0.18, for the map. The centre of gravity would appear to show very slight offshore movement but this represents the 'resolved' position of the two main arms of movement diagonally onshore and offshore shown by the contours themselves.

Thus, landward movement took place on the ridge crest but a slightly stronger offshore movement occurred which may possibly be explained by the presence of the rippled surface of the beach in the vicinity of the release site. Inman and Bowen (1963) found that in deep water a strong current superimposed on near-bottom water motions produced by waves reduced the symmetry of ripples by increasing effective onshore orbital velocity and decreasing orbital velocity in the offshore direction. The resulting asymmetric ripples generated asymmetric vortices and when these were thrown up from the bottom the stronger vortices became directed in an offshore direction. A similar mechanism may well have caused the offshore vectors of sand movement in Figure 4.14.

The tracer dispersion pattern seen in Figure 2.11 shows a strong longshore component but also has a strong landward tendency. This onshore tendency is difficult to explain in terms of wave approach since the angle of the breaking waves to the line of the beach was oblique, at about 26^{o}. A similar but more extreme example of this onshore movement can be seen in Figure 4.16 of the tracer experiment on the lower ridge on 28.2.76 and once again satisfactory explanation of the pattern is difficult. In

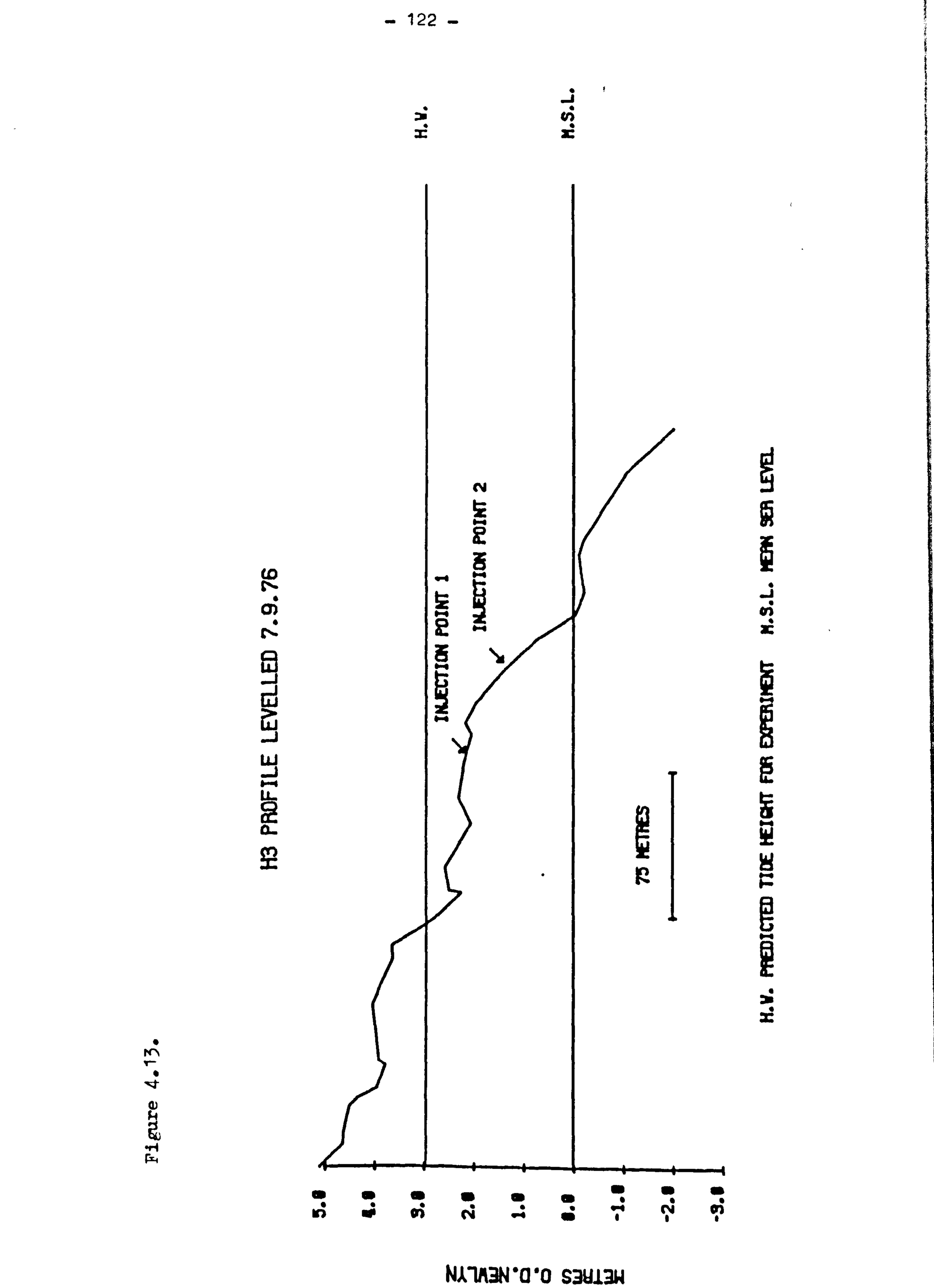
H.W.
M.S.L.
H3 PROFILE LEVELLED 7.9.76
INJECTION POINT 1
INJECTION POINT 2
M.S.L. MEAN SEA LEVEL
75 METRES
H.W. PREDICTED TIDE HEIGHT FOR EXPERIMENT
5.0
4.0
3.0
2.0
1.0
0.0
-1.0
-2.0
-3.0
METRES O.D.NEWLYN

Figure 4.13.

Figure 4.14.

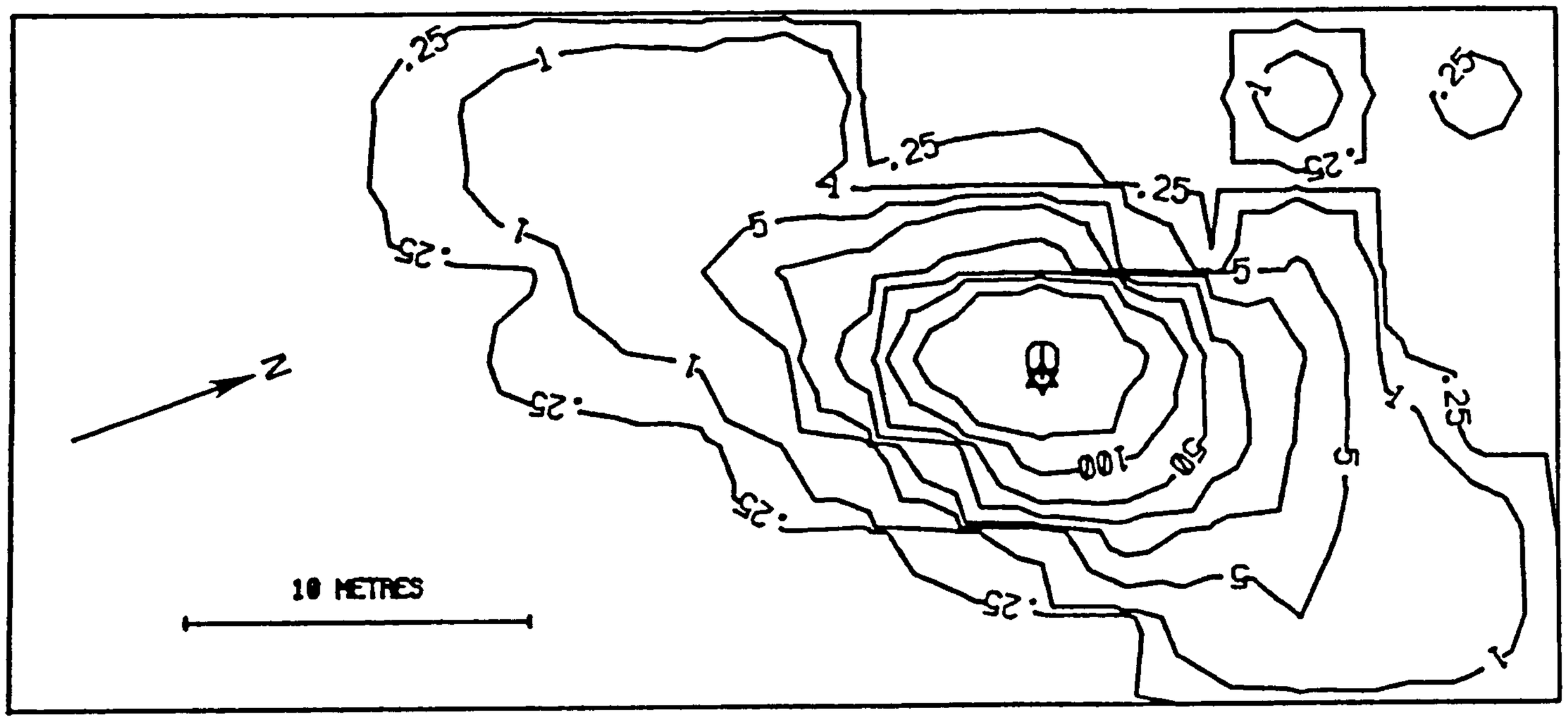

INJECTION POINT ⊙ CENTRE OF GRAVITY ✡

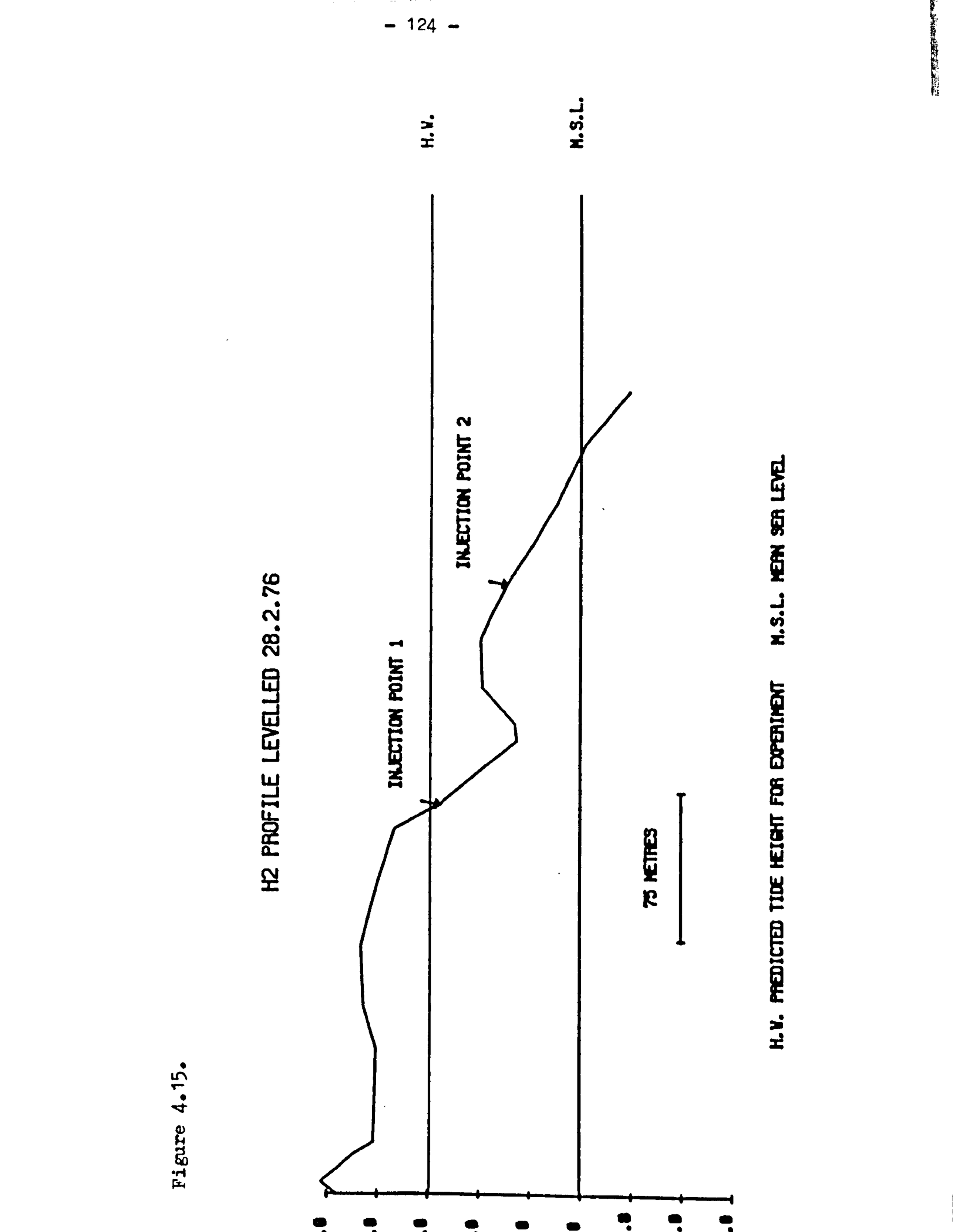
H2 PROFILE LEVELLED 28.2.76
H.W.
M.S.L.
INJECTION POINT 1
INJECTION POINT 2
M.S.L. MEAN SEA LEVEL
75 METRES
H.W. PREDICTED TIDE HEIGHT FOR EXPERIMENT
METRES O.D.NEWLYN
5.0
4.0
3.0
2.0
1.0
0.0
-1.0
-2.0
-3.0

Figure 4.15.

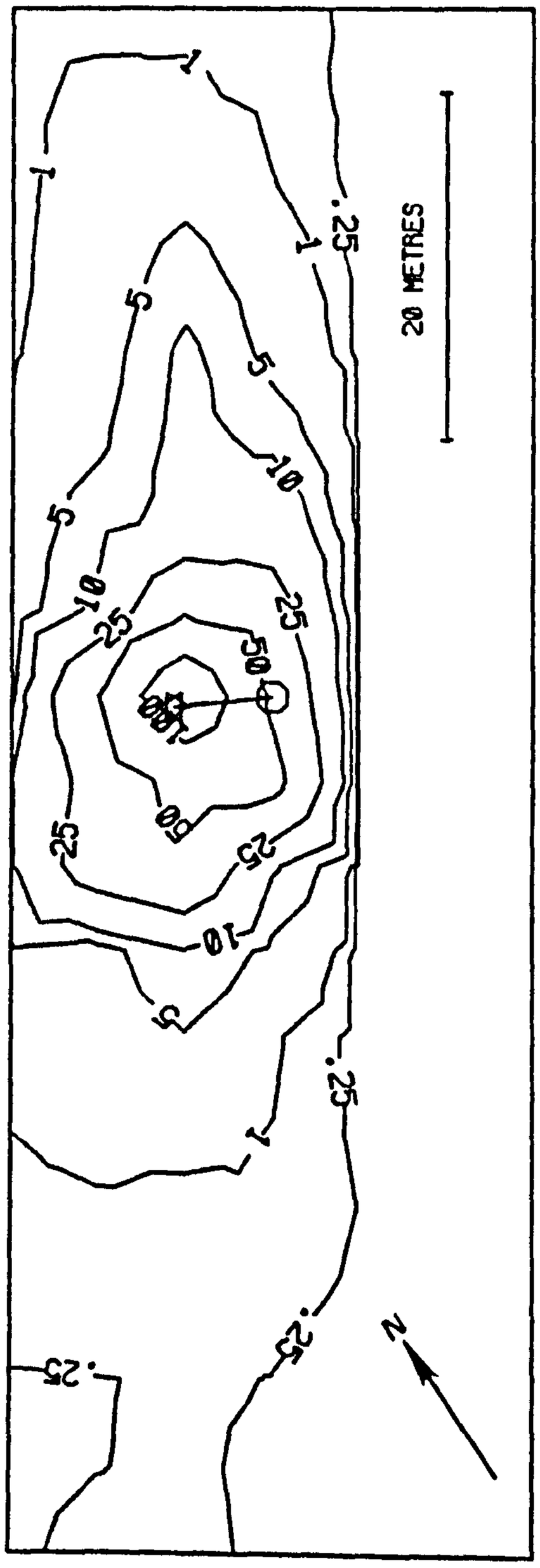
28 2 76 LOWER RIDGE H2 P
INJECTION POINT
CENTRE OF GRAVITY
20 METRES
N

Figure 4.16.

Figure 4.16 some longshore dispersal is apparent and this interestingly is in both directions. This perhaps is another example of the tidal current effect but the pattern lacks the strong linearity which might be expected of a current caused pattern and which is present in Figure 4.18 The major component of the pattern in Figure 4.16 though, is the landward movement. Angle of wave approach was small, 4^{o}, with waves from the north-east which probably reduced wave drift,and longshore currents were relatively slight with a speed of just over 16 cm/sec, but there is no obvious cause of the dominant landward vector of movement other than the wave type and other wave characteristics. Causes of onshore/offshore movement are considered further in a later chapter.

The complexity of interaction of the processes causing the tracer dispersion patterns is evidenced by the fact that with a very similar combination of conditions on 15.7.76 the tracer map, Figure 4.18, of dispersion from the single lower ridge release point gives a markedly different picture than that for the 28.2.76 experiment, Figure 4.16.

Skegness

Fewer experiments were conducted at the Skegness site and 13 successful maps were produced. On four occasions tracer was laid on both the beach ridges simultaneously and these experiments provide some interesting results.

The two maps for the experiment of the 25.8.76, Figures 4.19 and 4.20, show relatively similar patterns, at least in terms of the dominant vectors of movement. The position of the centre of gravity relative to the tracer injection point on both maps has an onshore direction of about 20^{o} but the subsidiary southerly alongshore components of movement are also present on both maps and in particular the upper ridge map. The amount of dispersion appears larger on the lower ridge with a greater displacement of the centre of gravity and this contrasts with findings from other experiments at Skegness in which the greater dispersion was usually on the upper

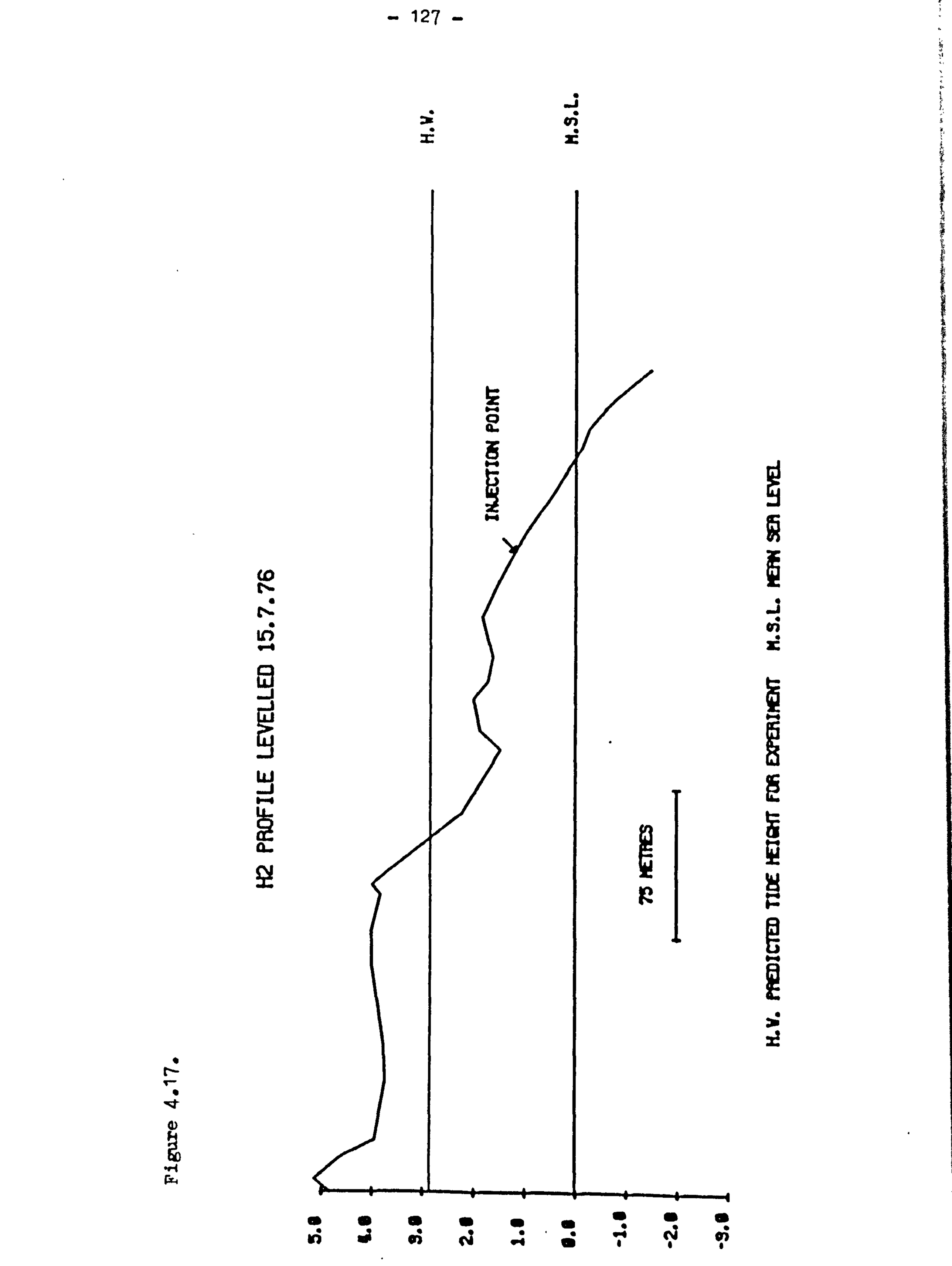
H.W.
M.S.L.
INJECTION POINT
M.S.L. MEAN SEA LEVEL
H2 PROFILE LEVELLED 15.7.76
H.W. PREDICTED TIDE HEIGHT FOR EXPERIMENT
75 METRES
5.0
4.0
3.0
2.0
1.0
0.0
-1.0
-2.0
-3.0
METRES O.D.NEWLYN

Figure 4.17.

Figure 4.18.

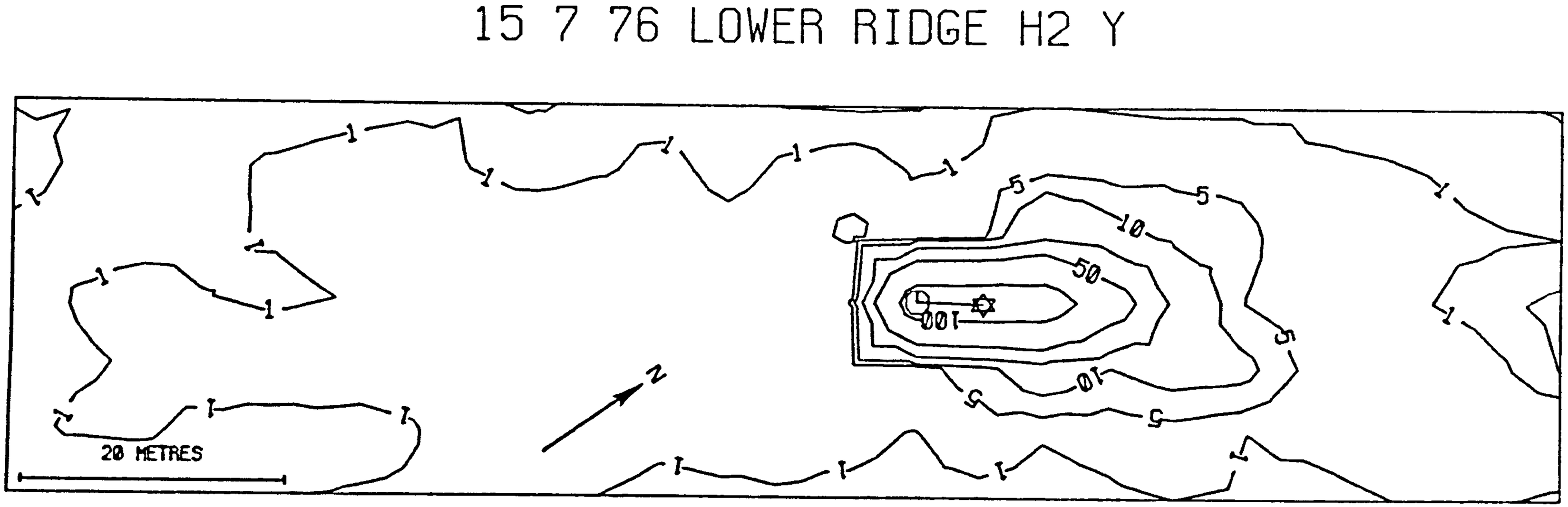

INJECTION POINT ⊙ CENTRE OF GRAVITY ✡

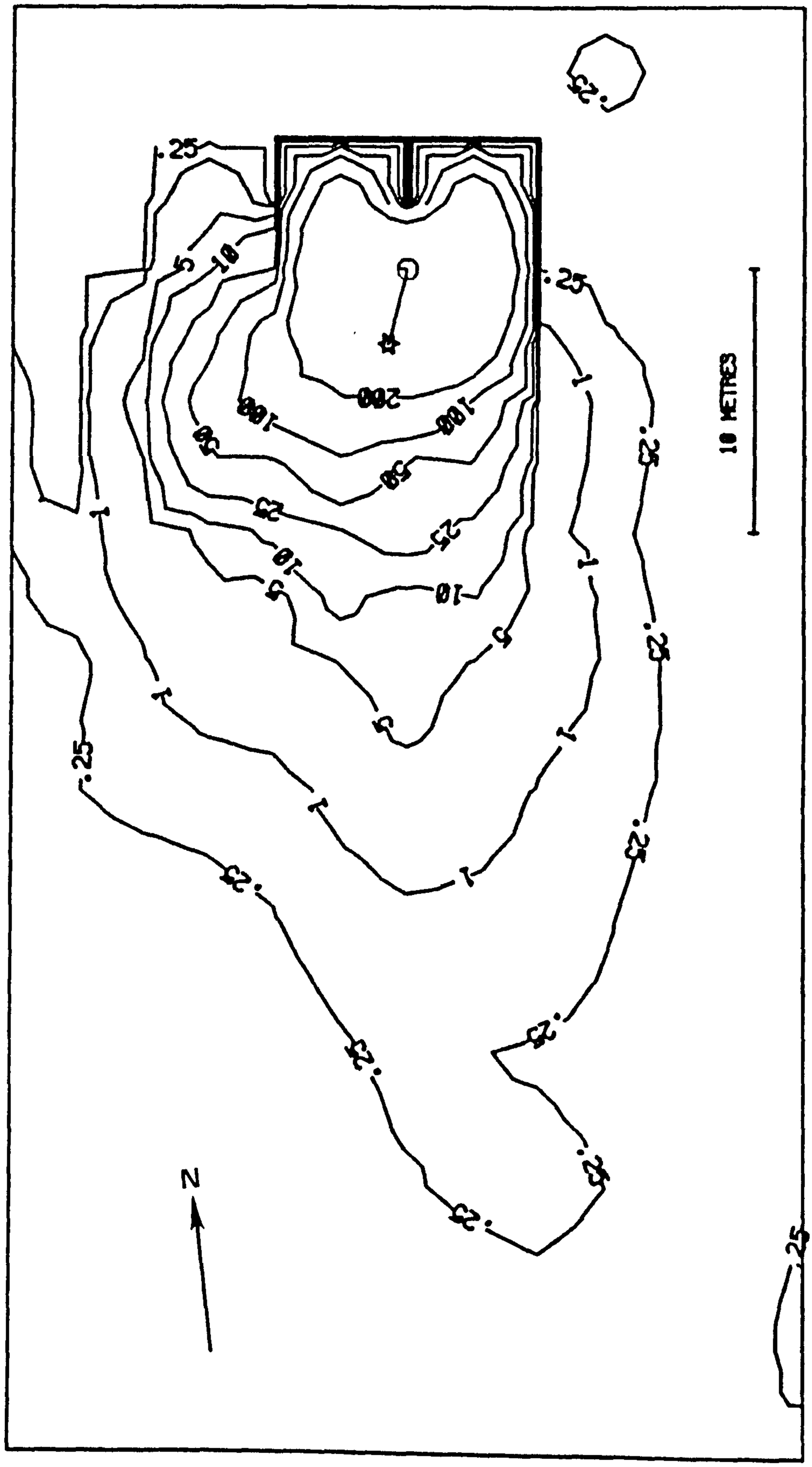
25 8 76 UPPER RIDGE E1 Y
INJECTION POINT
CENTRE OF GRAVITY
10 METRES
N

Figure 4.19.

Figure 4.20.

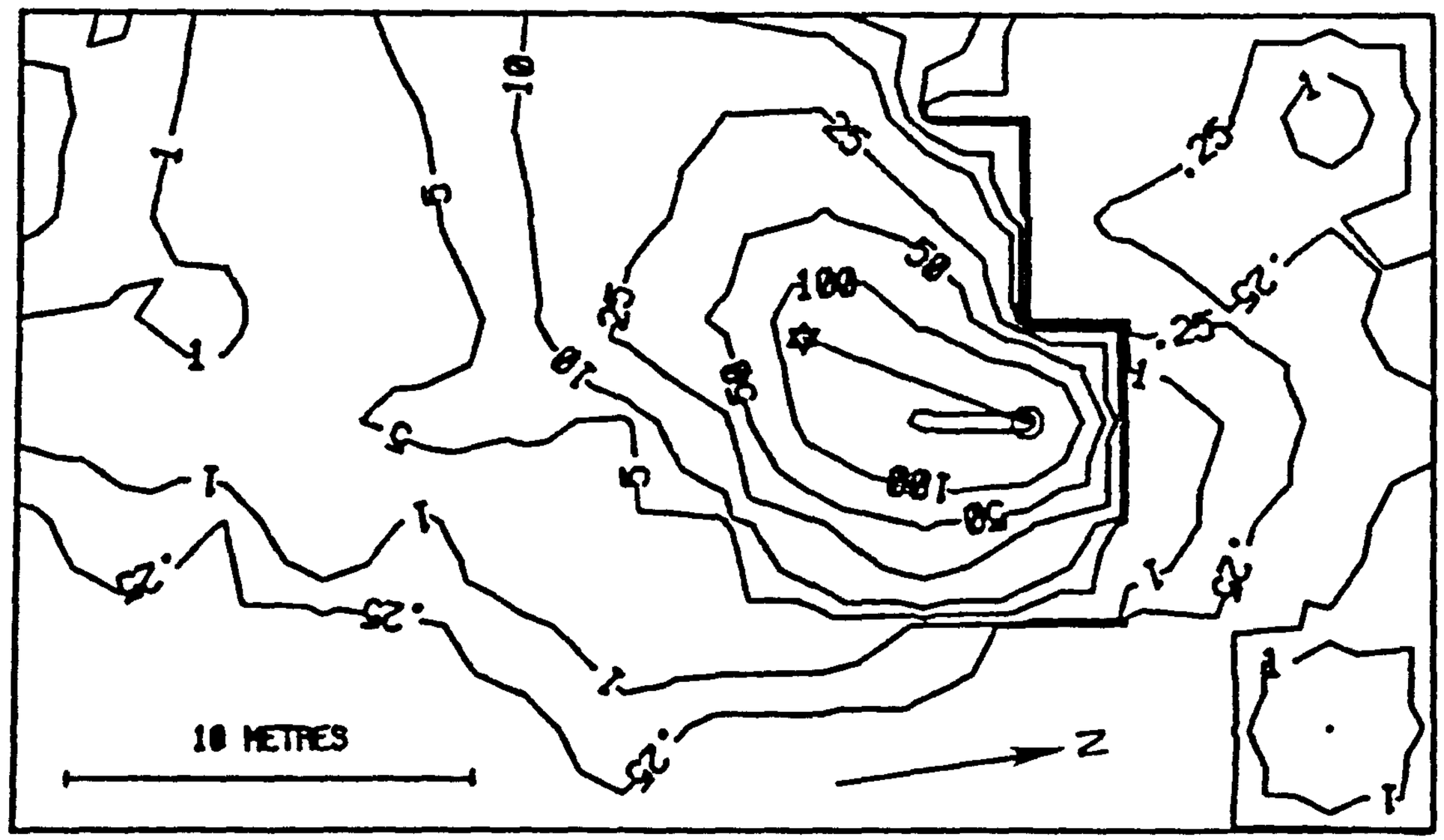
25 8 76 LOWER RIDGE E1 P
10 METRES
N
INJECTION POINT ⊙ CENTRE OF GRAVITY ✡

ridge. However, on this occasion wave heights were slightly higher on the lower ridge and longshore currents markedly stronger, 32.4 cm/sec compared with 4.7 cm/sec and this probably accounts for the anomalous situation.

On the 21.9.76 wave conditions were relatively severe with $H^{\frac{1}{3}}$ of 0.75cm and these large waves led to considerable dispersal of tracer on both ridges. Indeed, much of the tracer on the upper ridge was lost completely, Figure 4.22, whilst on the lower ridge, Figure 2.7, landward transport was the dominant trend of a widely diffused pattern. Again on 22.10.76 under smaller wave attack, dispersion on the upper ridge was considerably greater than that on the lower ridge as evidence clearly by the scales of the two maps, Figures 4.24 and 4.25, and the relative distances moved by the centre of gravities. The upper ridge/lower ridge contrast in dispersion and amount of grain movement was also repeated for the experiment of 7.10.76 when $H^{\frac{1}{3}}$ was 0.36m on the upper ridge and 0.32m on the lower ridge and longshore currents were respectively 9.1 cm/sec and 13.3 cm/sec. When tests were being made with the standard deviational ellipse as a measure of overall dispersion, the area of the fitted ellipse for the upper ridge was 82 compared with 35 for the lower ridge.

In general, therefore, it appears that at Skegness the dispersion and rates of grain movement are greater on the upper ridge face than on the lower ridge. This may in part be due to the length of time that the more turbulent zones of the nearshore operate on a particular part of the beach but further consideration will be given to this later in this section.

Not only do contrasting amounts of dispersion take place on the two ridges but directions of movement also showed significant differences and even, sometimes, completely opposite vectors. For example, the maps of the experiment of 7.10.76, Figures 4.27 and 4.28, reveal immediate differences. The overall direction of movement was to the north on the upper ridge and to the south on the lower. A secondary landward vector is evident on the

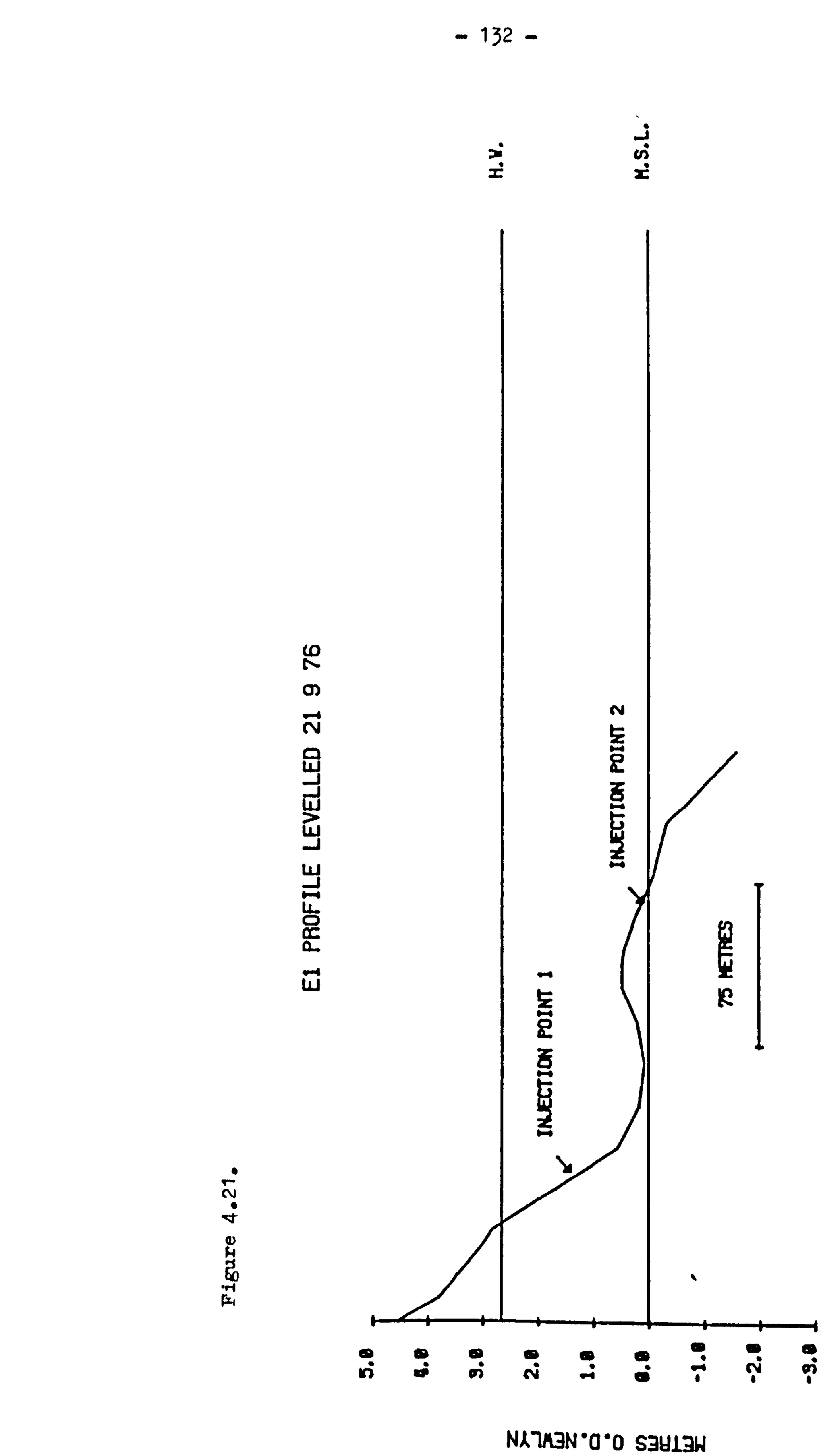
E1 PROFILE LEVELLED 21 9 76
H.W.
M.S.L.
INJECTION POINT 1
INJECTION POINT 2
75 METRES
H.W. PREDICTED TIDE HEIGHT FOR EXPERIMENT
M.S.L. MEAN SEA LEVEL
METRES O.D.NEWLYN
5.0
4.0
3.0
2.0
1.0
0.0
-1.0
-2.0
-3.0

Figure 4.21.

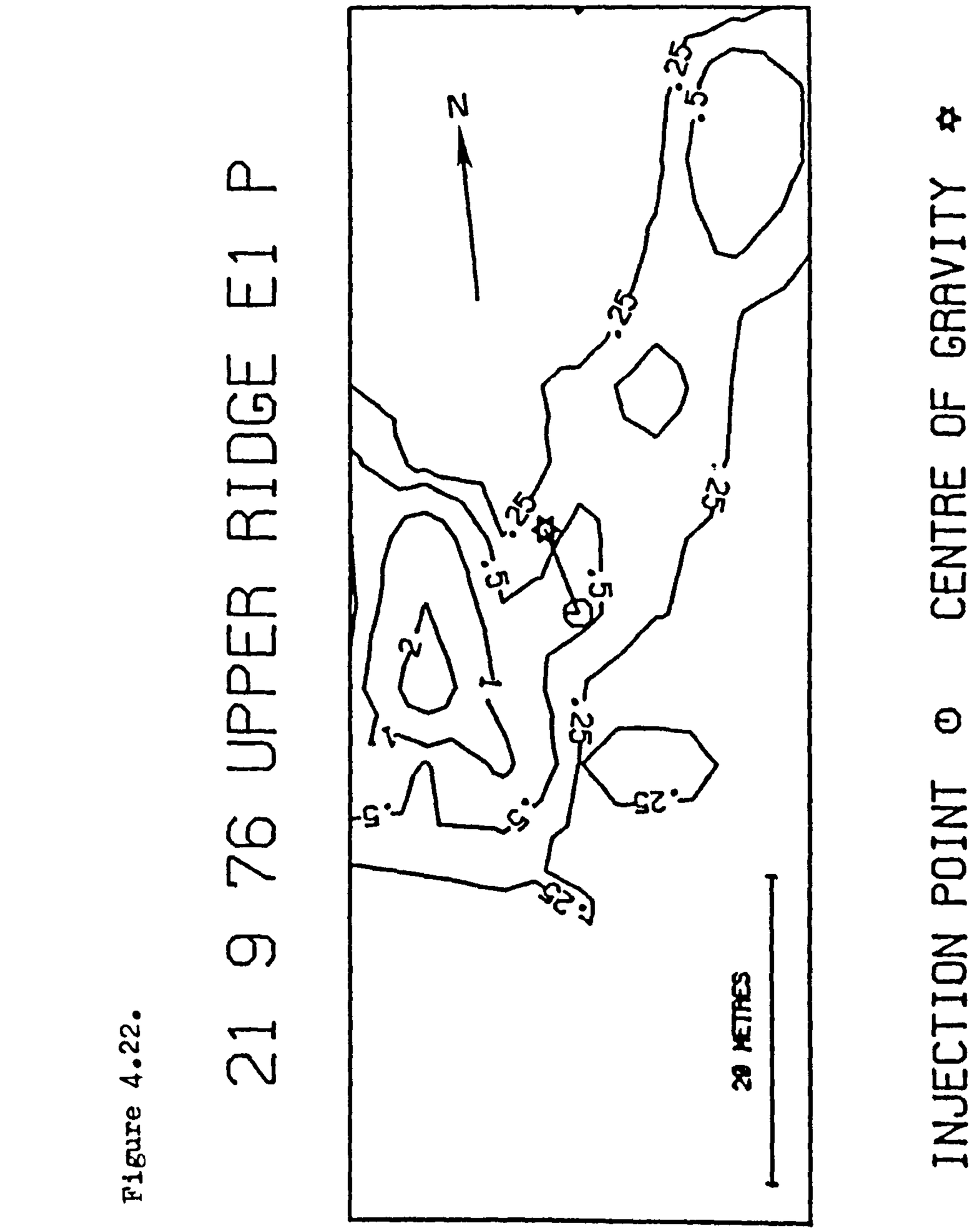
21 9 76 UPPER RIDGE E1 P
N
.25
.5
1
2
20 METRES
CENTRE OF GRAVITY ✡
INJECTION POINT ⊙

Figure 4.22.

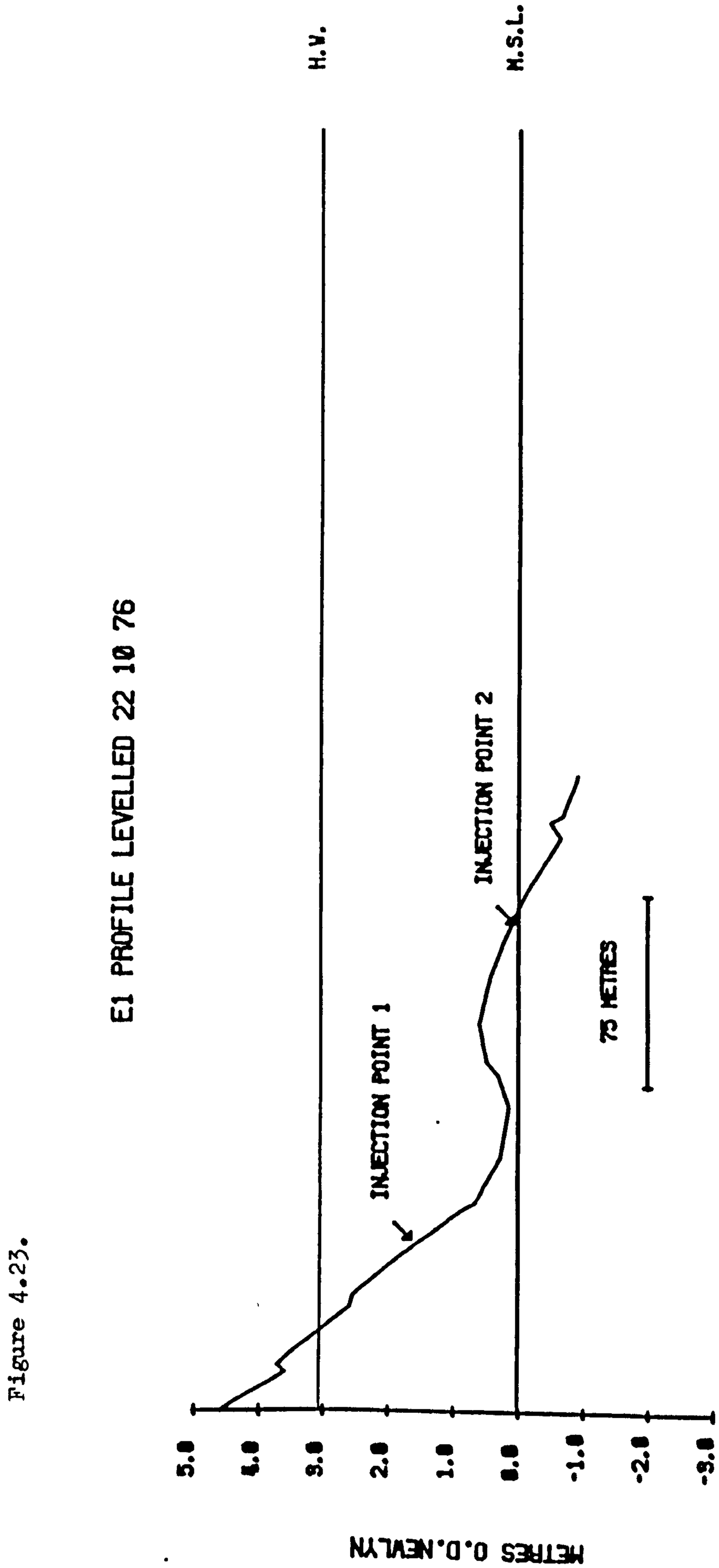
E1 PROFILE LEVELLED 22 10 76
H.W.
M.S.L.
INJECTION POINT 1
INJECTION POINT 2
75 METRES
5.0
4.0
3.0
2.0
1.0
0.0
-1.0
-2.0
-3.0
METRES O.D.NEWLYN
M.S.L. MEAN SEA LEVEL
H.W. PREDICTED TIDE HEIGHT FOR EXPERIMENT

Figure 4.23.

Figure 4.24.

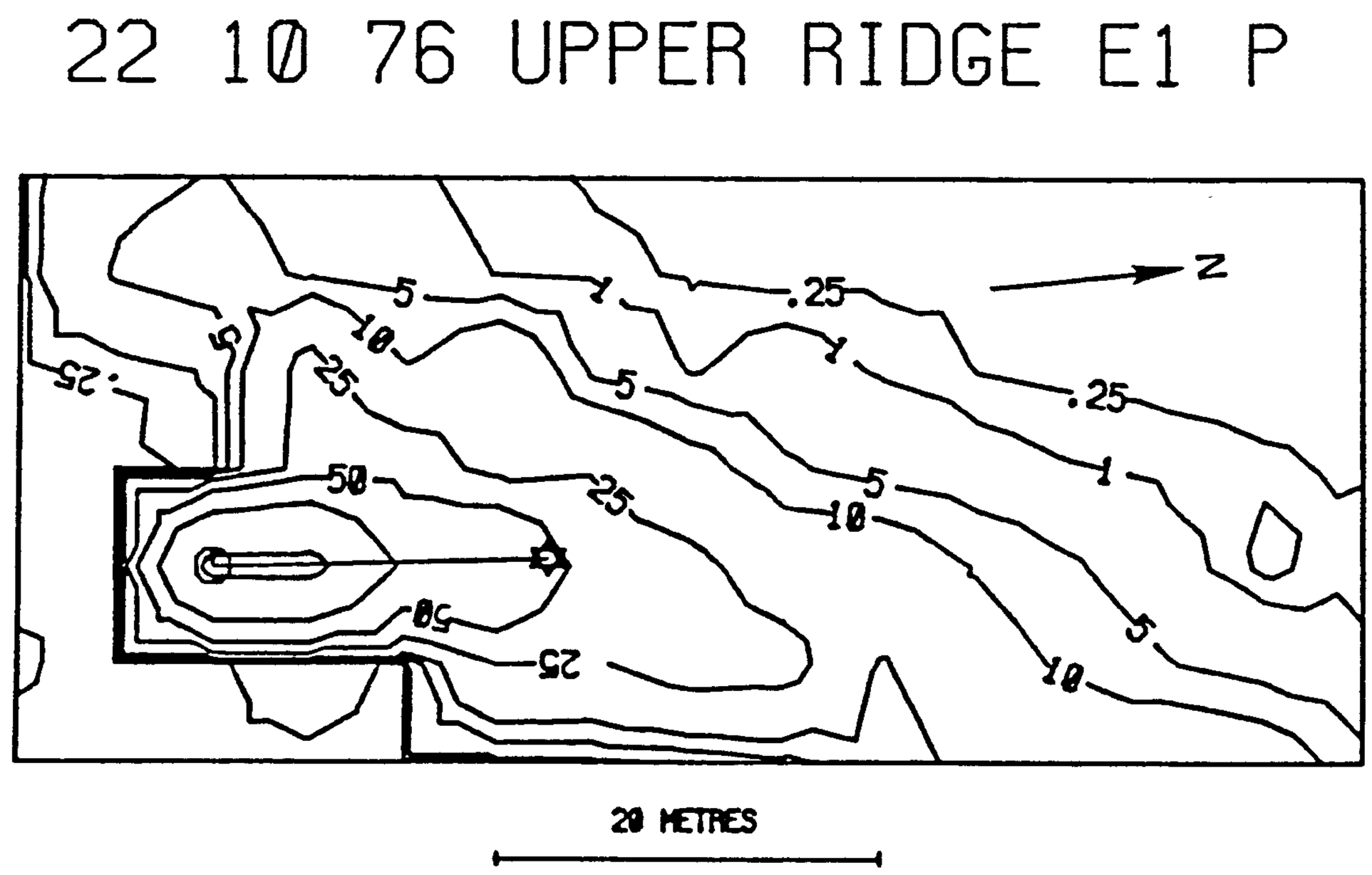
22 10 76 UPPER RIDGE E1 P
N
5
1
.25
5
10
25
1
5
.25
50
25
5
10
1
5
10
50
25
20 METRES
INJECTION POINT
CENTRE OF GRAVITY

Figure 4.25.

22 10 76 LOWER RIDGE E1 Y

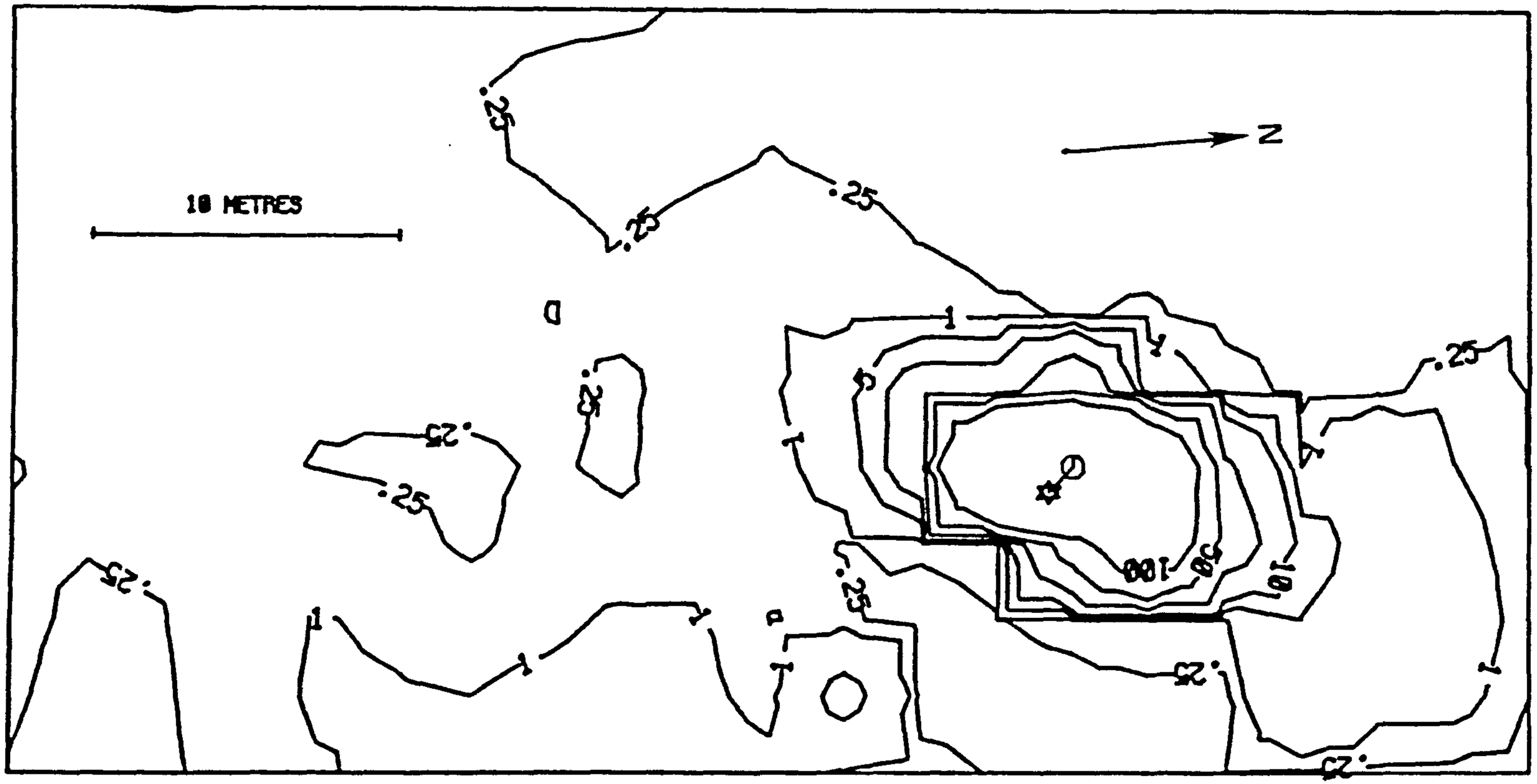

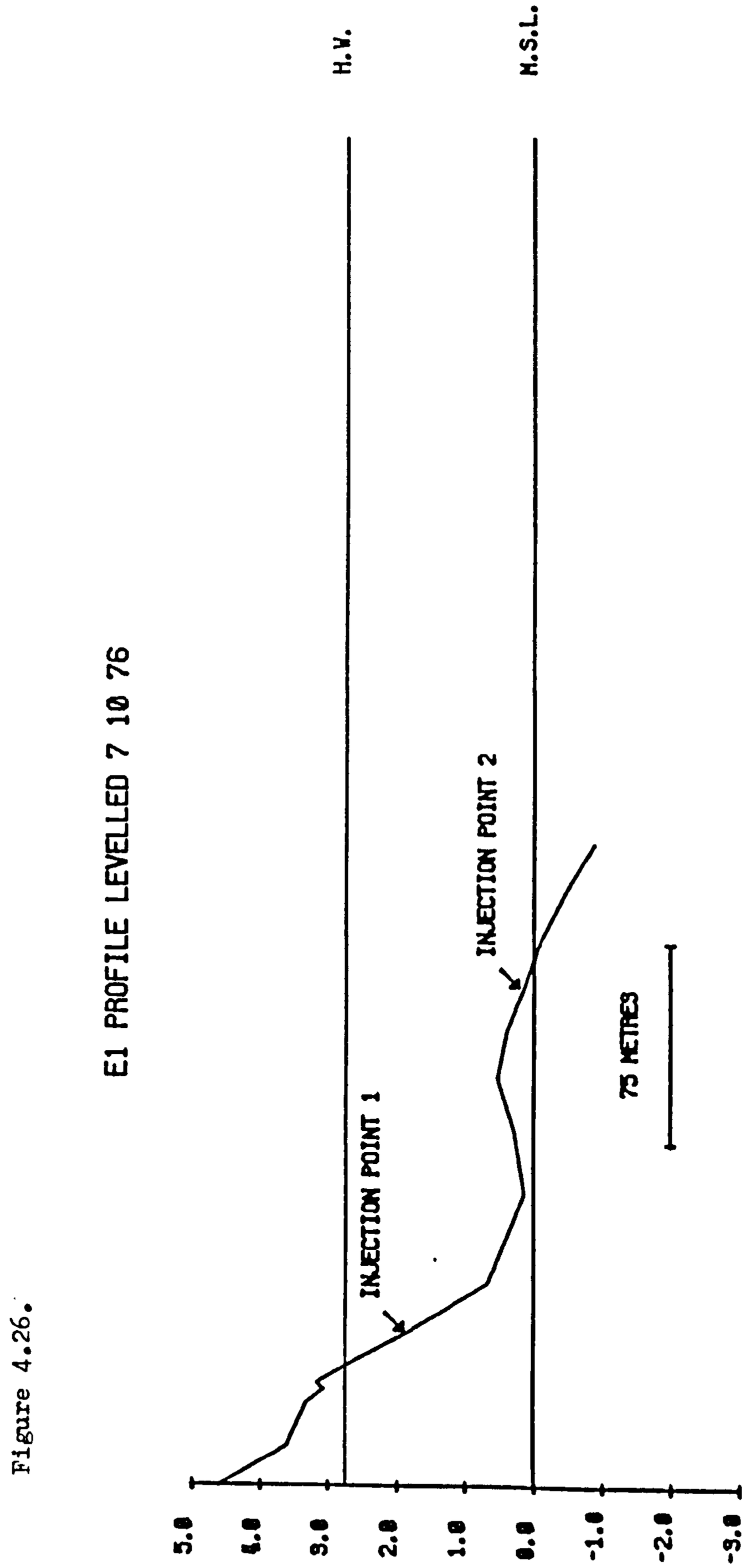
E1 PROFILE LEVELLED 7 10 76
H.W.
M.S.L.
INJECTION POINT 1
INJECTION POINT 2
75 METRES
5.0
4.0
3.0
2.0
1.0
0.0
-1.0
-2.0
-3.0
METRES O.D.NEWLYN
H.W. - PREDICTED TIDE HEIGHT FOR EXPERIMENT
M.S.L. -MEAN SEA LEVEL

Figure 4.26.

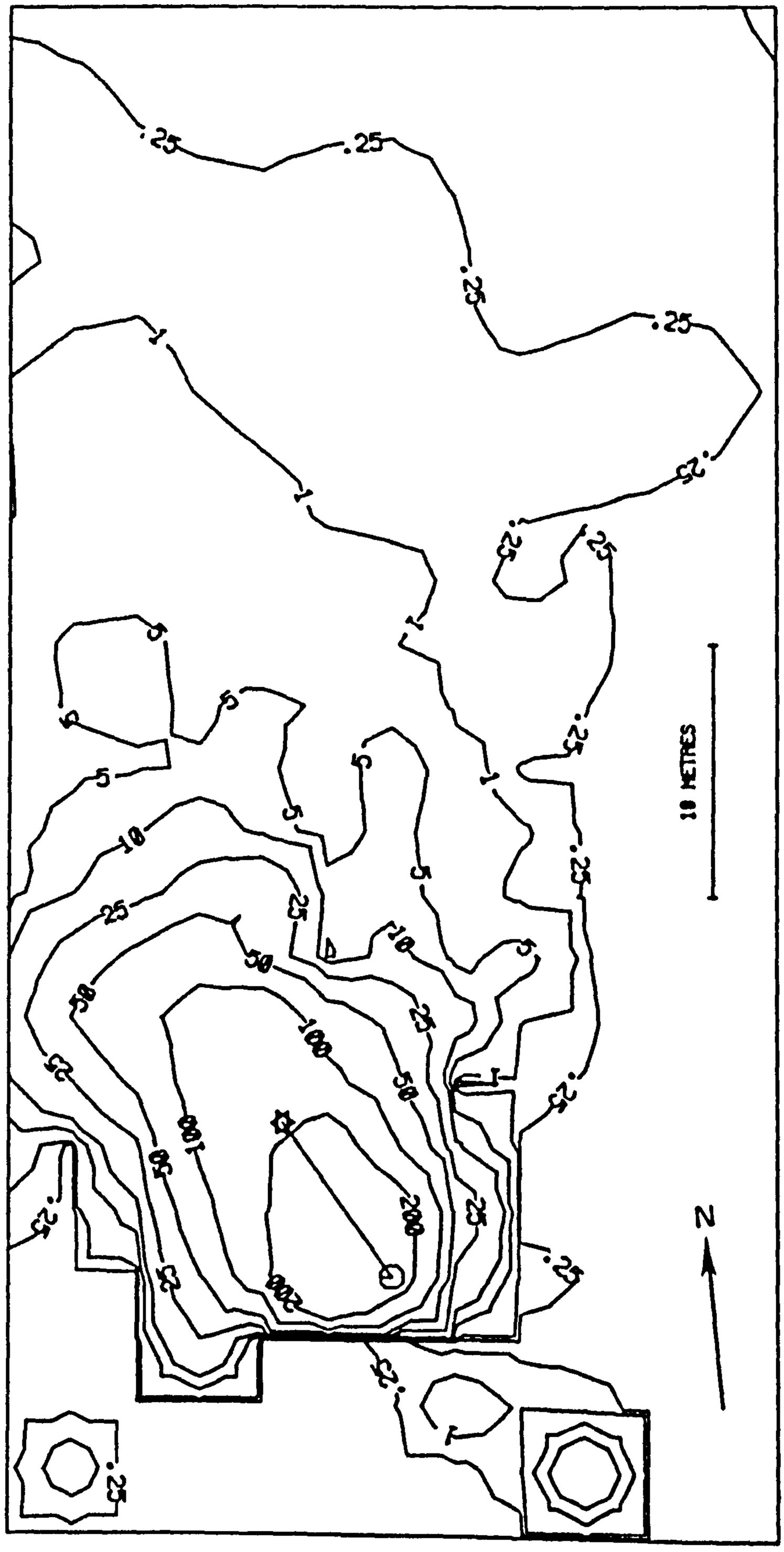
7 10 76 UPPER RIDGE E1 Y
INJECTION POINT ⊙ CENTRE OF GRAVITY ✡
10 METRES
2

Figure 4.27.

Figure 4.28.

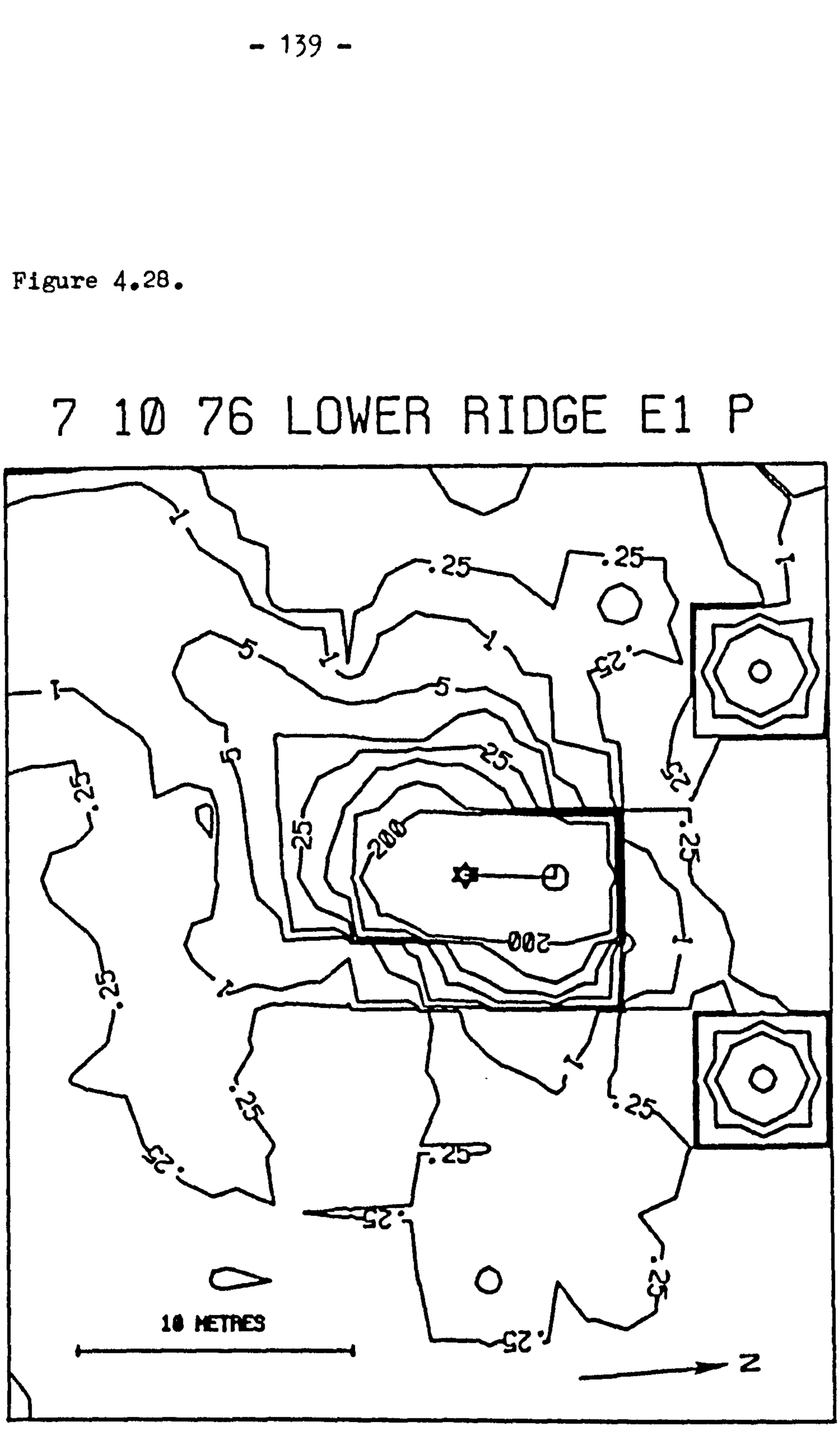
7 10 76 LOWER RIDGE E1 P
1
.25
5
200
10 METRES
N
INJECTION POINT ⊙ CENTRE OF GRAVITY ✡

lower ridge where the mean angle indicates a longshore average direction of movement, whilst on the upper ridge the mean vector of movement is diagonally onshore. These contrasts would appear to be the result of progressive refraction of waves across the beach with the rising phases of the tide. Wave approach was from the north-east on the lower beach, resulting in the southerly trend of the tracer. With the rise of the tide over the lower ridge, refraction of the wave fronts caused them to meet the upper ridge face at a very slight angle. Since longshore currents were weak, 9 cm/sec, it seems swash backwash wave drift was responsible for the northerly components of movement on the upper ridge.

A similar explanation may be applied to the experiment results of 25.8.76 when a stronger onshore trend was apparent on the lower ridge than the upper. However, the maps produced from the experiment of 22.10.76, Figures 4.24 and 4.25, provide problems of explanation.

The maps show quite different patterns of tracer movement on different scales. On the upper ridge a strong longshore and slightly offshore movement took place, probably caused by wave drift, but on the lower ridge two dominant arms of movement are present diagonally landward and seaward. A diffusion of grains in all directions away from the release point has taken place on the lower ridge as indicated by the angular deviation of 74.5^{o}, 0.15, Table 4.1 , and current effects seem to have been minimal. A similar pattern can be seen in Figure 4.30 for the 12.8.76 experiment on the lower ridge, which was produced even though much stronger longshore currents were measured, 41.3 cm/sec. This type of pattern was found by Murray (1967) in his experiments in the shoaling wave zone and is typical of work in deeper water offshore. It would appear, therefore, that the patterns in Figures 4.25 and 4.30 are largely the result of shoaling wave zone processes. On both occasions, more than three metres of water covered the release point at high water and therefore, given significant wave heights of 33.9cm abd 33.5cm respectively, the

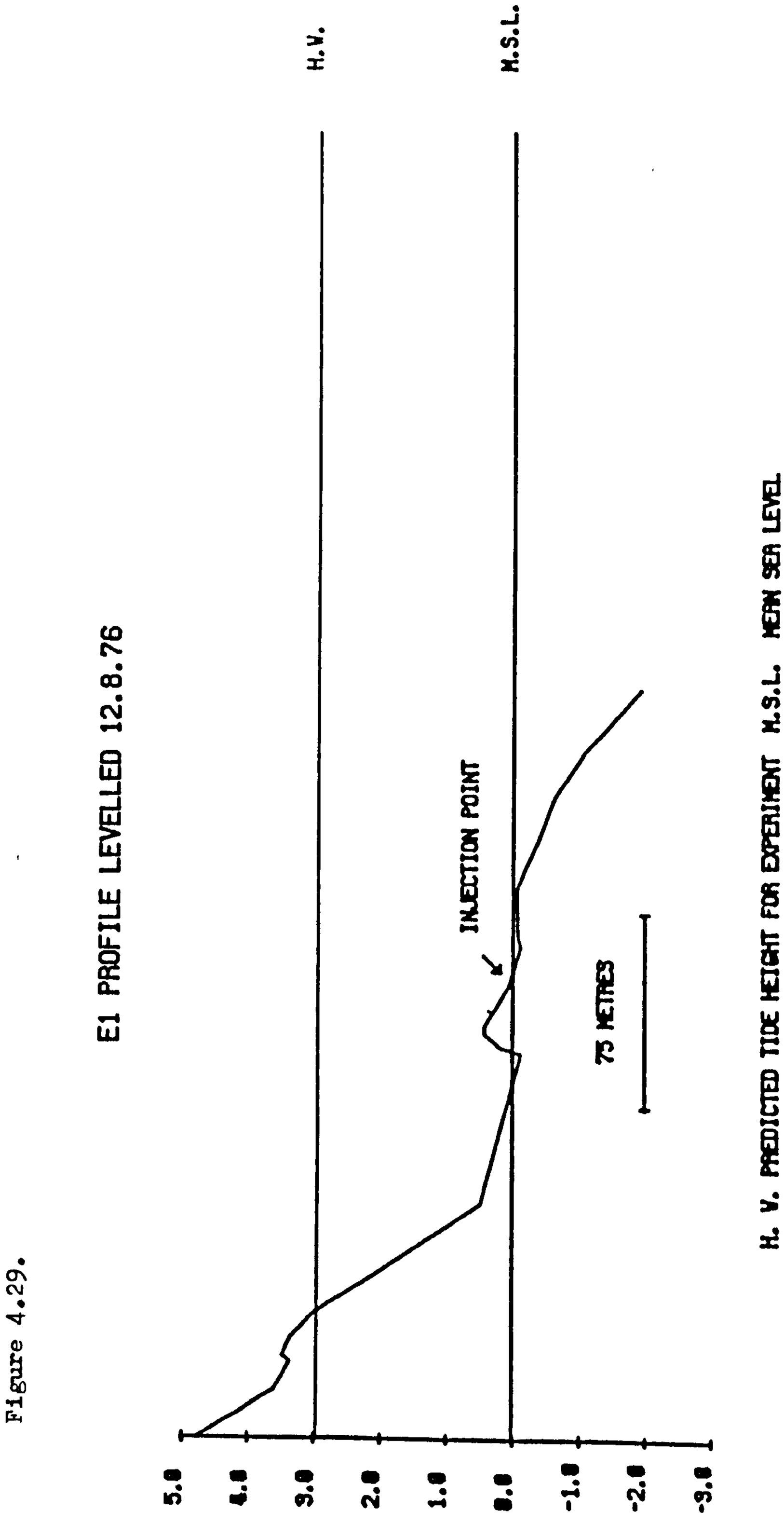
H.V.
M.S.L.
E1 PROFILE LEVELLED 12.8.76
INJECTION POINT
75 METRES
H. V. PREDICTED TIDE HEIGHT FOR EXPERIMENT
M.S.L. MEAN SEA LEVEL
5.0
4.0
3.0
2.0
1.0
0.0
-1.0
-2.0
-3.0
METRES O.D.NEWLYN

Figure 4.29.

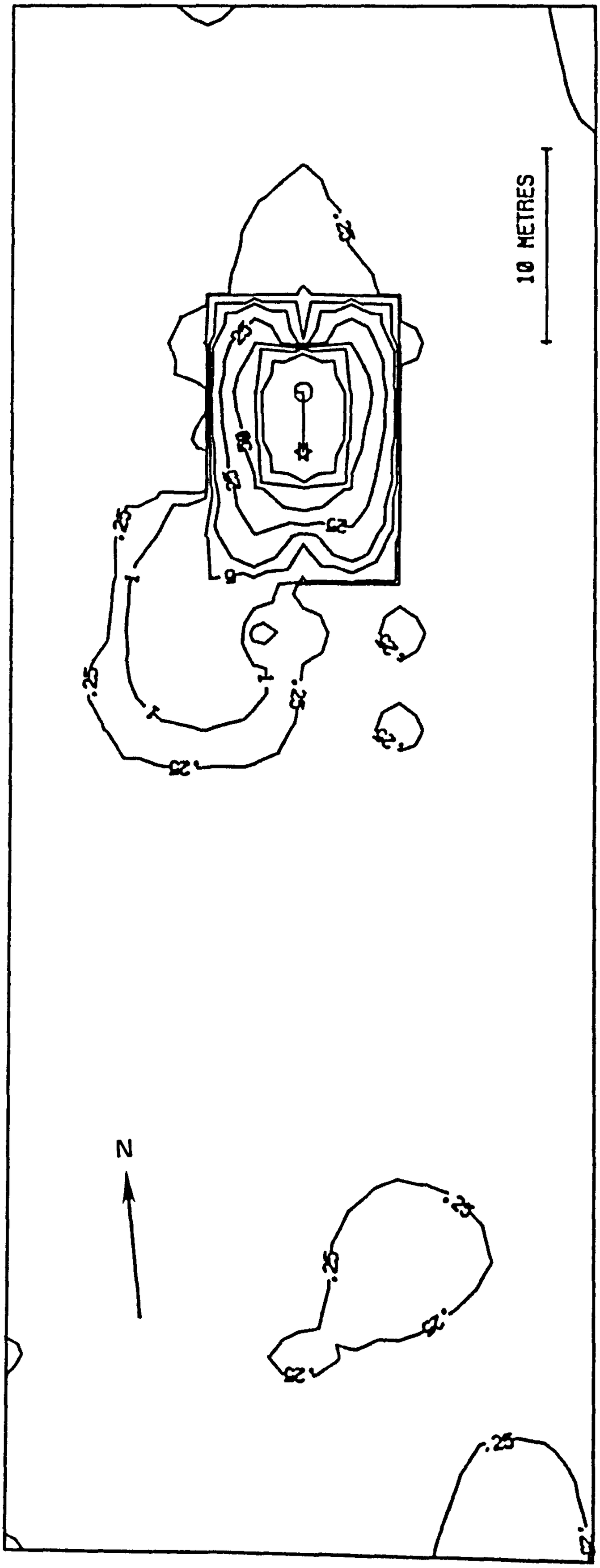
12 8 76 LOWER RIDGE E1 Y
10 METRES
CENTRE OF GRAVITY ✡
INJECTION POINT ⊖
N
.25
.2

Figure 4.30.

tracer would certainly have been affected by shoaling waves for a major part of the tide.

Discussion

At both sites, onshore/offshore and longshore movement of sand, as indicated by the respective components of the centre of gravity of the dispersed tracer cloud and average speeds of particle movement, were greater on the upper ridge than the lower ridge, Table 4.2. However, wave heights on both ridges at the two sites are similar and, indeed, at Skegness the lower ridge wave heights were on average slightly larger than on the upper ridge. Furthermore, the steep seaward face of the upper ridge at both Gibraltar Point and Skegness provided relatively deeper water close inshore, restricting surf zone development, and hence much weaker longshore currents were measured during the upper ridge experiments. Because of these factors it might have been expected that lower ridge sand movements would have been the greater, but this was not the case largely because of the variation in the length of time processes were operating on different parts of the beach width.

The lower beach is affected by the breaker zone for a relatively short period as this zone crosses the more gently shelving lower foreshore rapidly on both the incoming and outgoing tides. This is particularly true at Skegness. Only topographical highs on the lower foreshore, such as the beach ridges, remain under the influence of the more turbulent breaker and surf zones, until the tidal plane has risen sufficiently to allow the waves to cross without breaking. The steeper upper beach ridge face suffers wave attack for a much longer period as the water level rises causing greater sand movements. Actual lengths of time the near-shore zones operate on different parts of the beach will depend upon the stage of the fortnightly spring/neap cycle and wave heights as discussed in Chapter 1.

In comparing results from Gibraltar Point and Skegness, generally

Table 4.2 Mean figures for sand movement and selected variables for tracer experiments at Gibraltar Point and Skegness.

	Gibraltar Point	Skegness
Mean movement of centre of gravity: all experiments (m)	16.12	7.15
Mean movement of centre of gravity longshore: all experiments (m)	14.78	6.12
Mean longshore component of movement: upper ridge (m)	20.92	8.62
Mean longshore component of movement: lower ridge (m)	12.50	3.90
Mean onshore/offshore component of movement: all experiments (m)	1.85	3.04
Mean onshore/offshore component of movement: upper ridge (m)	2.26	5.46
Mean onshore/offshore component of movement: lower ridge (m)	1.72	1.31
Mean speed of grain movement: all experiments (cm/sec)	0.129	0.029
Mean speed of grain movement: upper ridge (cm/sec)	0.17	0.046
Mean speed of grain movement: lower ridge (cm/sec)	0.087	0.014
Significant wave height $H^{\frac{1}{3}}$: all experiments (m)	0.45	0.39
Significant wave height $H^{\frac{1}{3}}$: upper ridge (m)	0.47	0.41
Significant wave height $h^{\frac{1}{3}}$: lower ridge (m)	0.45	0.38
Mean longshore current velocity: all experiments (cm/sec)	36.71	26.56
Mean longshore current velocity: upper ridge (cm/sec)	12.55	18.18
Mean longshore current velocity: lower ridge (cm/sec)	44.11	41.14

speaking, there was more longshore movement and less movement normal to the beach at Gibraltar Point than Skegness, Table 4.2. The stronger longshore movements on the upper ridge at Gibraltar Point compared with Skegness, despite only slightly different wave heights and longshore current velocities, probably reflect the effects of a larger average angle of wave approach at Gibraltar Point and a coarser average grain size at Skegness. The angle of wave approach determines the amount of longshore sand movement to a certain extent through the action of longshore drift, and the greater the angle the greater the sweep of particles alongshore. The mean angle on the upper ridge at Gibraltar Point was 9^{o} compared with 5^{o} at Skegness. At the same time, coarser beach material at Skegness would not be expected to move as far as the finer material at Gibraltar Point, given the same conditions, although some studies show that coarser material moves faster than finer as will be seen later.

The very low longshore movements measured on the lower ridge at Skegness were partly the result of the duration of process operation as discussed earlier, but also partly the result of the much weaker tidal currents in this vicinity, Chapter 1. These factors would also account for the smaller upper ridge/lower ridge differences at Gibraltar Point despite higher absolute values for longshore movement.

Movements normal to the shore were greatest on the upper ridge at Skegness, which reflects the effect of refraction in causing wave approach to be much more parallel to the beach face. The steepness of this particular seaward ridge face was also probably important, although strong offshore vectors of motion were less common. The low value for the average onshore/offshore component of movement for experiments on the lower ridge at Skegness is partially a function of the shortcomings of the use of centre of gravity as a measure of movement. Relatively strong onshore/offshore movements of material were masked by the balancing of nearly equal tendencies. As mentioned earlier, the experiments on this ridge show strong evidence of shoaling wave effects and diffusion of grains in

in all directions away from the release point.

Lower values for shoreward or seaward transport of material at Gibraltar Point are undoubtedly the result of the stronger alongshore acting processes in this area.

Much more work is required on the contrast in sand movement patterns between the Skegness area and Gibraltar Point site and in particular the simultaneous release of tracer, at both places, on both ridges, would provide valuable information. This type of experiment was attempted in this study but shortage of manpower meant that no worthwhile results were achieved.

4:3 Sorting and the movement of different grain sizes

The movement of different grain sizes is the basis of the process of sorting, which involves the rearrangement of particles of varying size on a sloping beach face in response to particular physical parameters such as wave height or current velocity. The sorting of grains of differing diameter and/or specific gravity ultimately dictates the basic changes and indeed the existence of any given sand beach, Ingle and Gorsline (1973). As a result, the differential movement of various grain sizes may be considered a fundamental process in beach formation and development.

Fluorescent tracers lend themselves very well to the study of differential grain movement because of the many colours available and their ease of application to a wide range of particle sizes. In an effort to investigate the effects of grain size on the patterns of sediment movement, several experiments were conducted in this study in which different grain sizes were tagged with different fluorescent colours. Two approaches were adopted:

1. Bicolour tests. Sand was collected from the beach and then dry-sieved into two fractions, less than 2ϕ and greater than 2ϕ. The 2ϕ cut off was chosen because it represents the boundary between fine sand and

medium sand on the phi scale of grain size description. Thus all grains coarser than fine sand were labelled with one colour and all grains of fine sand and smaller were coated with a second colour. This follows a method used by Ingle (1966) although a slight change was that in this study no attempt was made to equalise the weight of sand in each fraction, whereas Ingle used equal weights. It was felt that this slight change was more likely to make actual grain numbers in each fraction equal, since the number of grains in a particular weight increases rapidly with decrease in grain size.

2. Specific size tests. Small amounts of sand within a narrow size range were coated with different colours in such a way that roughly equivalent numbers of grains were placed on the beach. Murray (1967), working in the shoaling wave zone, stated that the area over which a quantity of a particular grain size tracer will spread is a function of the initial concentration, so that to compare movements of different grain sizes all sizes should initially have an equal number of grains. Assuming sphericity, the number of grains of one size in a specific weight of sand will vary inversely as the cube of the radius and hence the weight of sand released should take account of this relation. In certain experiments in this study, this was achieved by using particular amounts of sand in each grain size selected and thus correcting the sampled concentration by multiplying by particular factors. For example, in the experiment of 7.10.76 conducted on the upper ridge at Skegness 1.0kg of sand in the range 0.6 - 0.71mm, 0.5kg in the range 0.42 - 0.5mm and 0.25kg in the range 0.25 - 0.355mm were used. The concentration of the medium sized sand, tagged blue, were multiplied by 1.75 and those of the largest fraction, tagged pink, multiplied by 2.5. The smallest grains were coated orange.

Two successful bicolour tests were conducted on 2.11.75 and 17.1.76 both at Gibraltar Point. The grain size distribution was split at 2ϕ (0.25mm.) but for the 2.11.75 experiment the mean size of the coarse fraction was

0.389ϕ and of the fine fraction 2.371ϕ whilst for 17.1.76 these values were 1.341ϕ and 2.422ϕ respectively. Therefore, for the earlier experiment each fraction was coarser. The results of these tests as shown in Figures 4.31 to 4.36 illustrate the fact that spatial sorting was not taking place as a result of different vectors of motion for different grain sizes. Dominant vectors of motion for the two halves of the grain size distribution were similar in each experiment. However, in both tests the average distance moved by the finer grains and overall dispersion of the finer grains was greater than for the coarser fraction and in this way sorting did occur. The average distance moved by the coarse fraction for 2.11.75 and 17.1.76 experiments were 4m and 24.5m compared with 6m and 30m for the fine fraction. This probably reflects the movement of finer particles partly in suspension and partly as bedload leading to larger distances and areas covered whilst the coarser fraction moved more as bedload and hence distances of movement are shorter.

However, these results conflict with Komar's (1977) findings for longshore transport rates of different grain sizes. He found that average distances moved were greater for the coarser grains and decreased for the finer sizes. Following Evans' (1939) work on transportation and sorting of material in the swash zone, Komar suggested that the finer material moved more slowly because it swashes higher up the beach face whilst coarse grains remain nearer the breaker zone and hence are transported by stronger, steady longshore currents. Komar's measurements were made at El Moreno, Baja California, Mexico where, because of the steep beach face, an intense swash zone is found and hence swash transport forms a higher proportion of total transport than on 'normal' Atlantic type beaches with a wider surf zone. The average beach slope was 8^{o} compared with 2.53^{o} and 2.48^{o} for the two tests of this study and this morphological difference and the resultant hydrodynamic differences probably account for the contrast in findings.

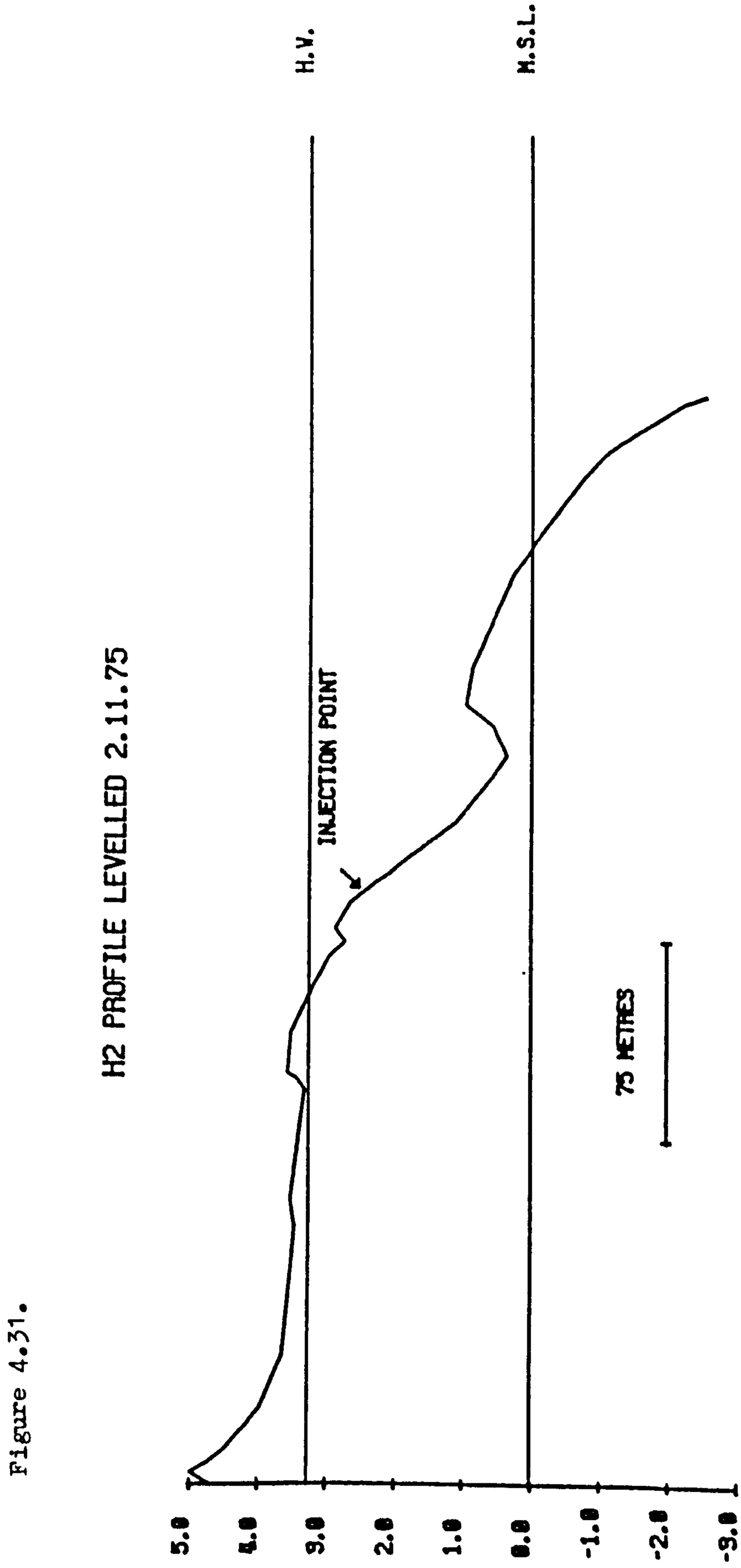
H2 PROFILE LEVELLED 2.11.75
H.W.
M.S.L.
INJECTION POINT
75 METRES
H.W. PREDICTED TIDE FOR EXPERIMENT M.S.L. MEAN SEA LEVEL
5.0
4.0
3.0
2.0
1.0
0.0
-1.0
-2.0
-3.0
METRES O.D.NEWLYN

Figure 4.31.

Figure 4.32.

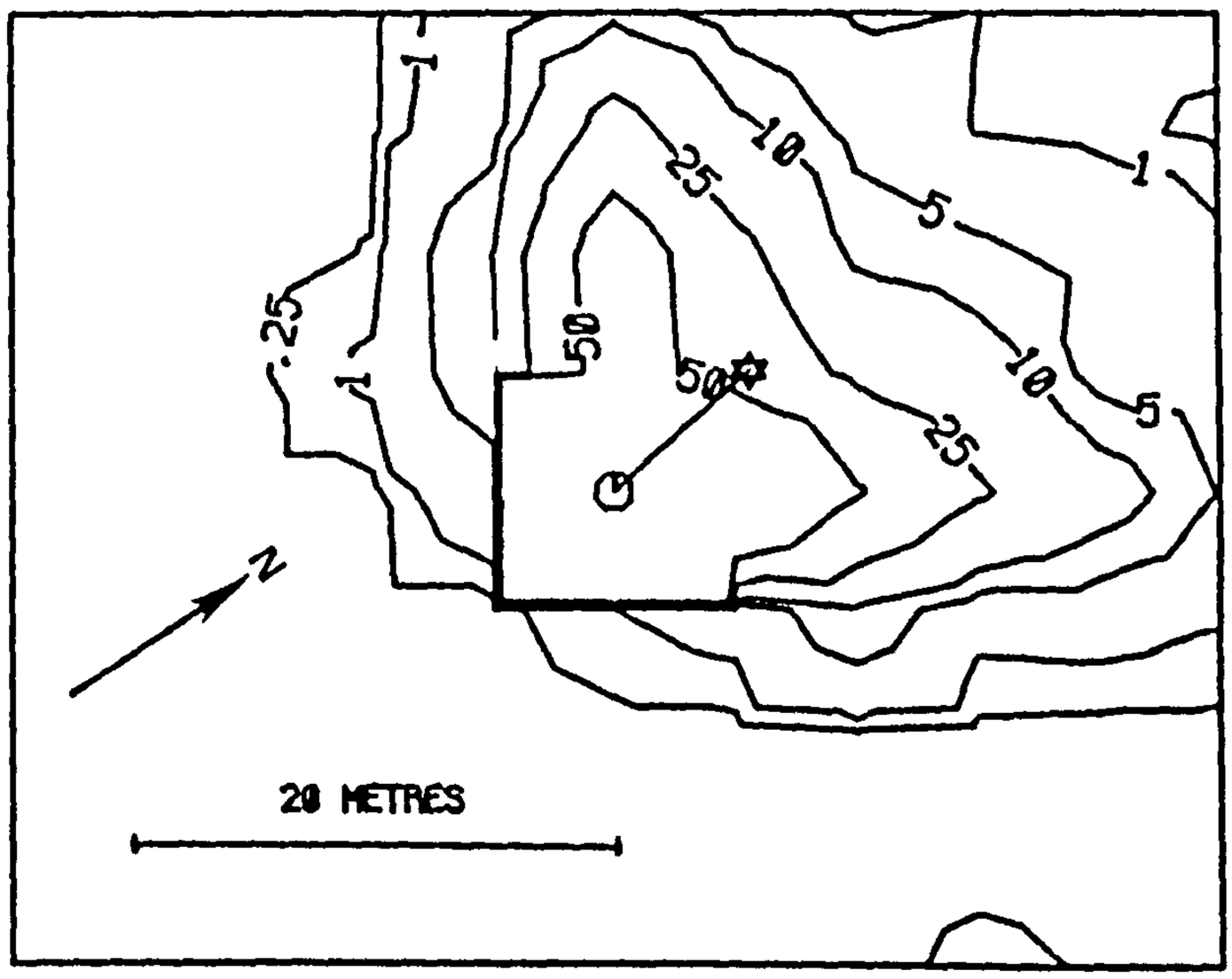
2 11 75 UPPER RIDGE H2 Y
T
.25
1
50
50
25
10
5
1
10
5
25
N
20 METRES
INJECTION POINT ⊙ CENTRE OF GRAVITY ✡

Figure 4.33.

2 11 75 UPPER RIDGE H2 FINE Y

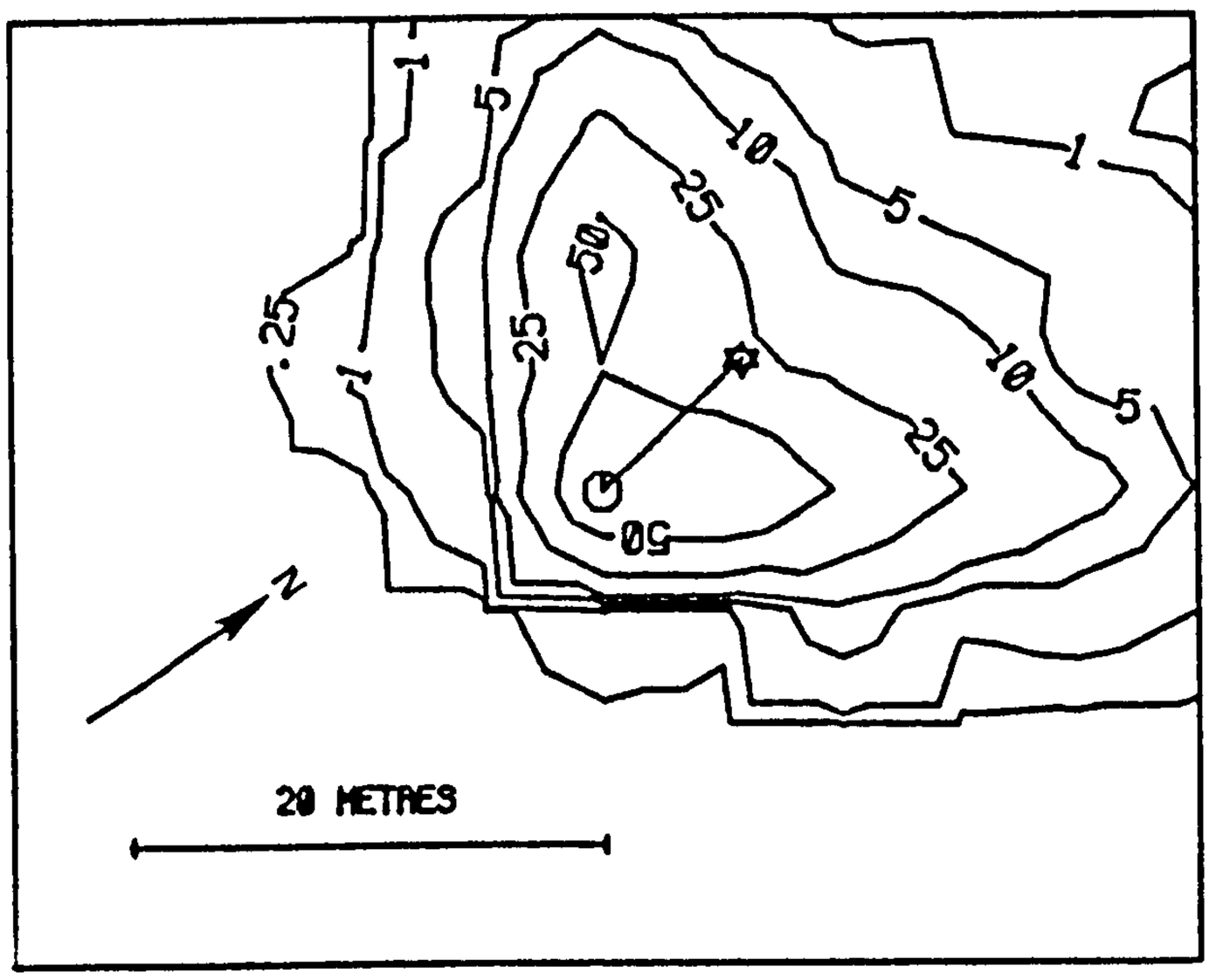

INJECTION POINT ⏲ CENTRE OF GRAVITY ✡

2 11 75 UPPER RIDGE H2 COARSE P

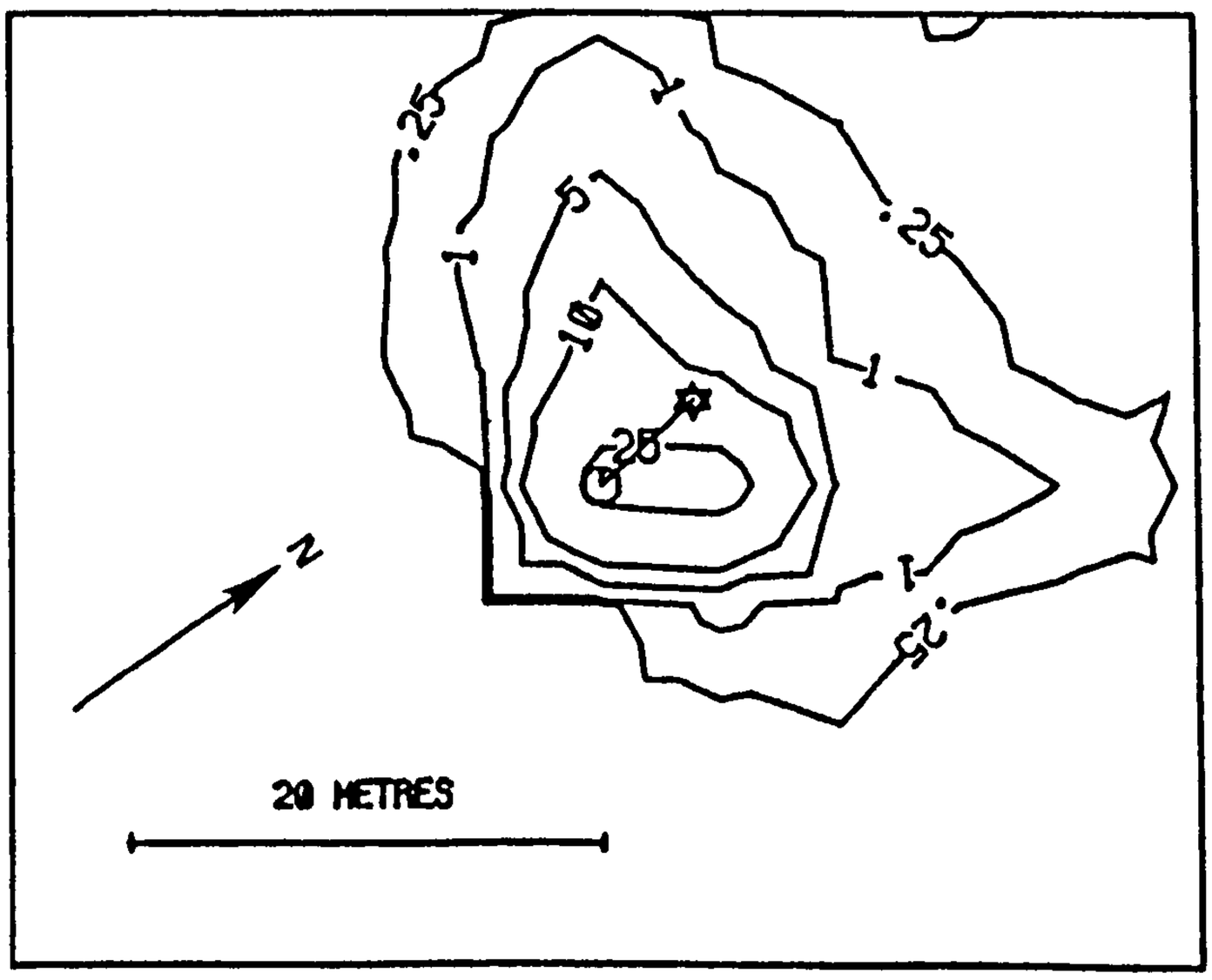

INJECTION POINT ⏲ CENTRE OF GRAVITY ✡

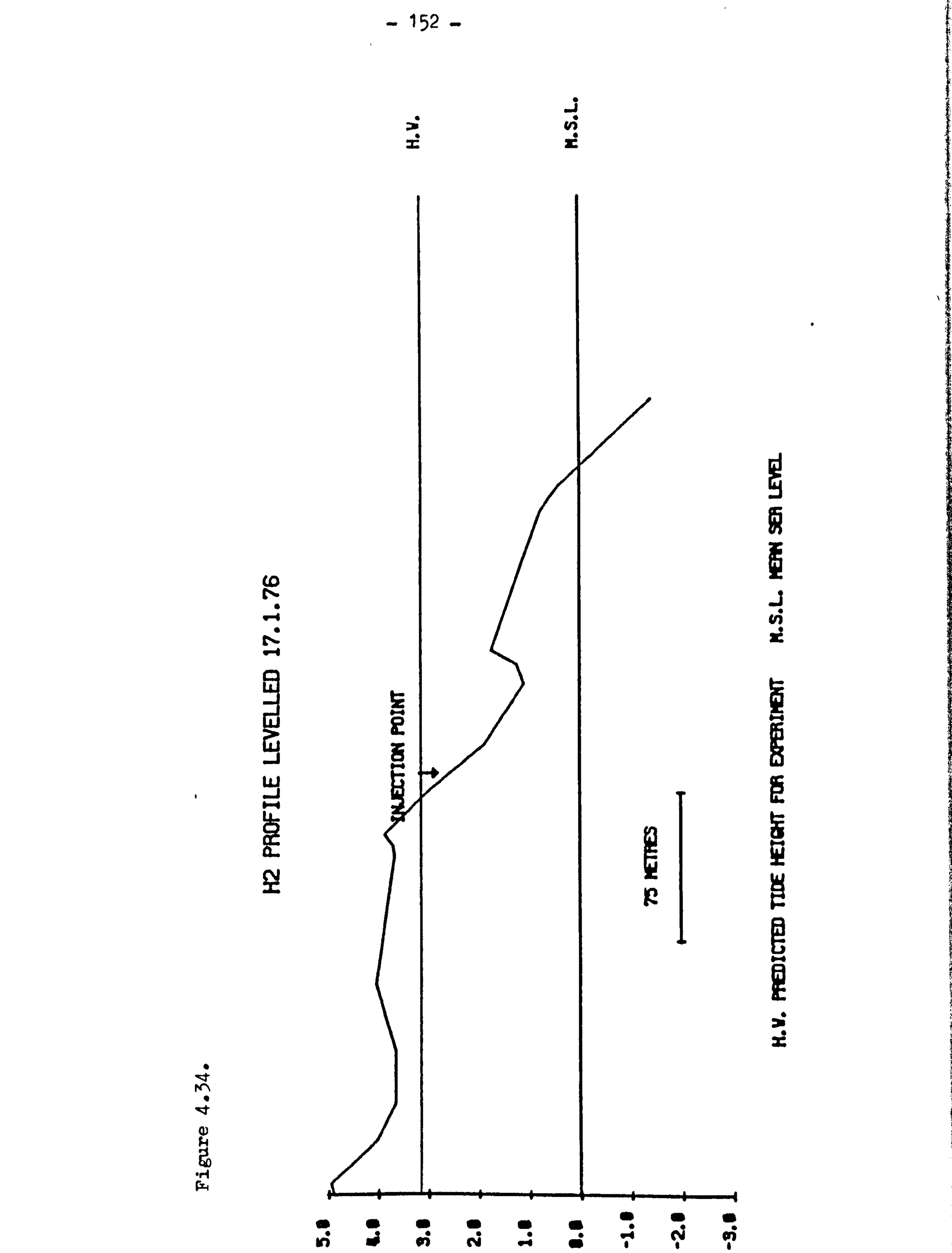
H.V.
M.S.L.
H2 PROFILE LEVELLED 17.1.76
INJECTION POINT
M.S.L. MEAN SEA LEVEL
75 METRES
H.V. PREDICTED TIDE HEIGHT FOR EXPERIMENT
5.0
4.0
3.0
2.0
1.0
0.0
-1.0
-2.0
-3.0
METRES O.D.NEWLYN

Figure 4.34.

Figure 4.35.

17 1 76 UPPER RIDGE TOTAL

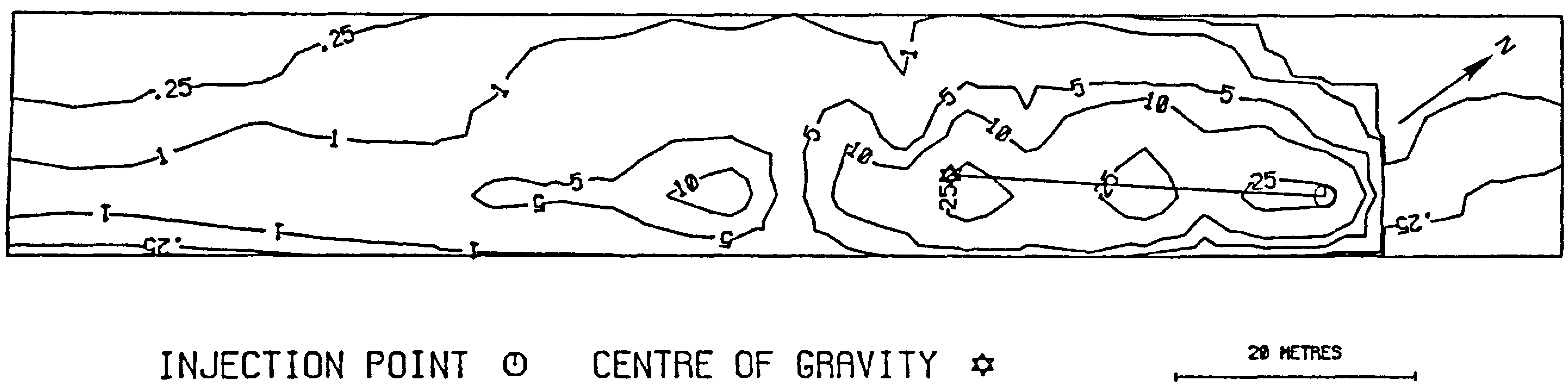

Figure 4.36.

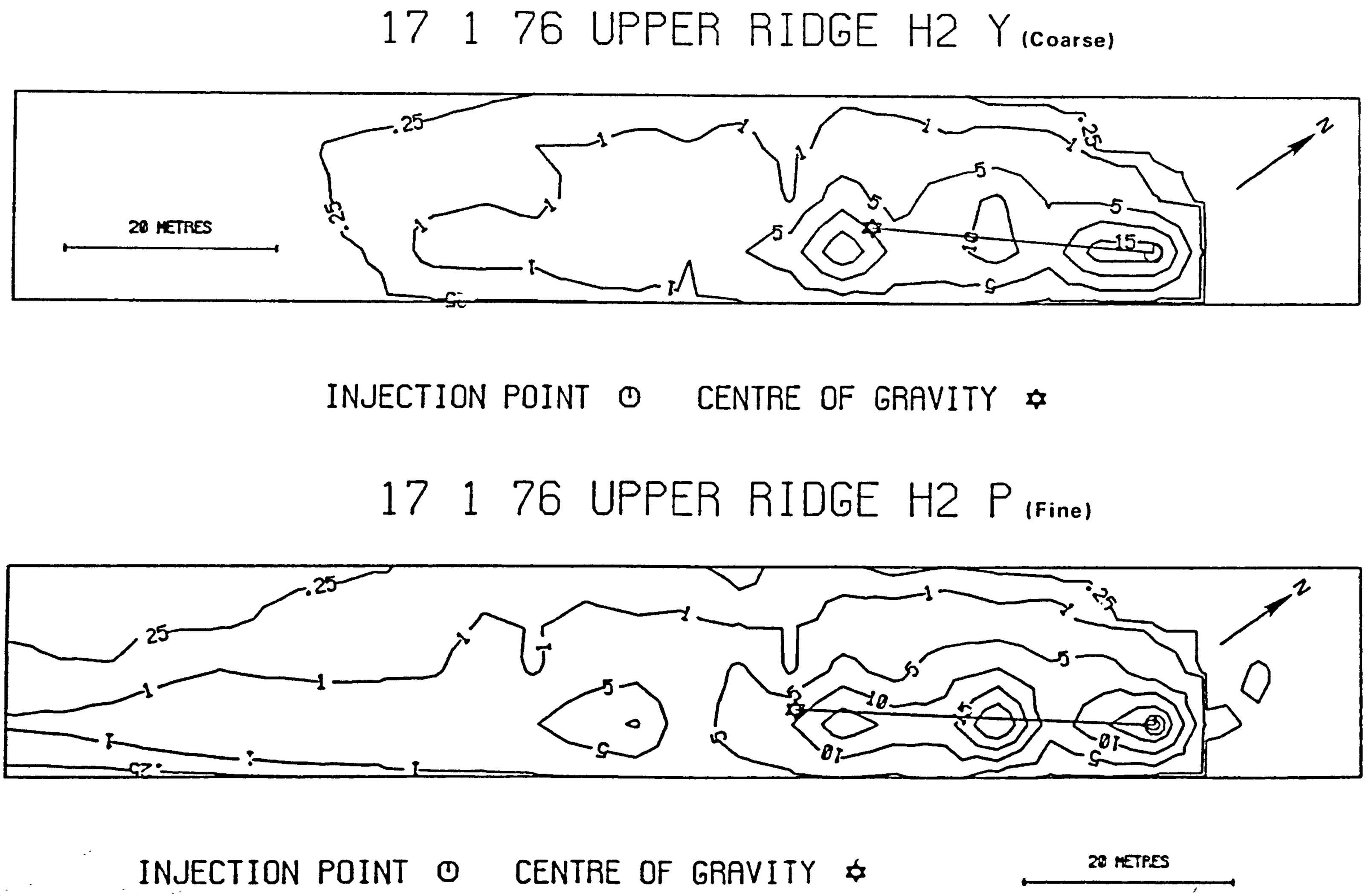
17 1 76 UPPER RIDGE H2 Y (Coarse)
20 METRES
INJECTION POINT
CENTRE OF GRAVITY
17 1 76 UPPER RIDGE H2 P (Fine)
INJECTION POINT
CENTRE OF GRAVITY
20 METRES

The significant difference between average distances moved for both fractions of the two tests is a reflection of the stronger conditions prevailing for the 17.1.76 experiment compared with the 2.11.75 and also perhaps the difference in average grain size between the two tests as already noted. Significant wave heights were 0.18m for 2.11.75 and 0.39m for 17.1.76 whilst longshore current velocities were 6 and 12 cm/sec respectively.

The usefulness of this type of bicolour test is limited since each division of the grain size distribution contains a wide range of sizes and variation in the position of the split in the distribution will affect the average distance figures for each division. Consequently the tests with more specific, narrower size ranges were made. However, because only small quantities of each fraction were used recovery rates from these experiments were very low and in the majority of cases too low to reveal significant trends. Only the 7.10.76 experiment on the upper ridge at Skegness provided results which could be realistically contoured and these are shown in Figures 4.37, 4.38 and 4.39. The finest fraction, 0.3mm displays a stronger onshore vector of movement whilst the coarser fractions show more alongshore components. Comparison of the three maps of the different fractions with Figure 4.27, the map of the whole distribution, suggests that the finer fractions in fact form a major constituent of the overall pattern. It is interesting to note that average distances moved by each fraction confirms the findings of the bicolour tests that the finer grains move furthest. In fact average distances moved alongshore are very similar but the medium fraction 0.46m moved furthest at 12m compared with 10.25m for the 0.3mm fraction and 9.75m for the coarsest size 0.65mm.

Results of all the other specific grain size tests were mapped on dot type maps with actual numbers of grains counted per fraction of sample entered at each sample site. Although in the main little can be

Figure 4.37.

7 10 76 UPPER RIDGE 0.3 MM

INJECTION POINT ⊙ CENTRE OF GRAVITY ✡

Figure 4.38.

7 10 76 UPPER RIDGE BLUE 0.46 MM

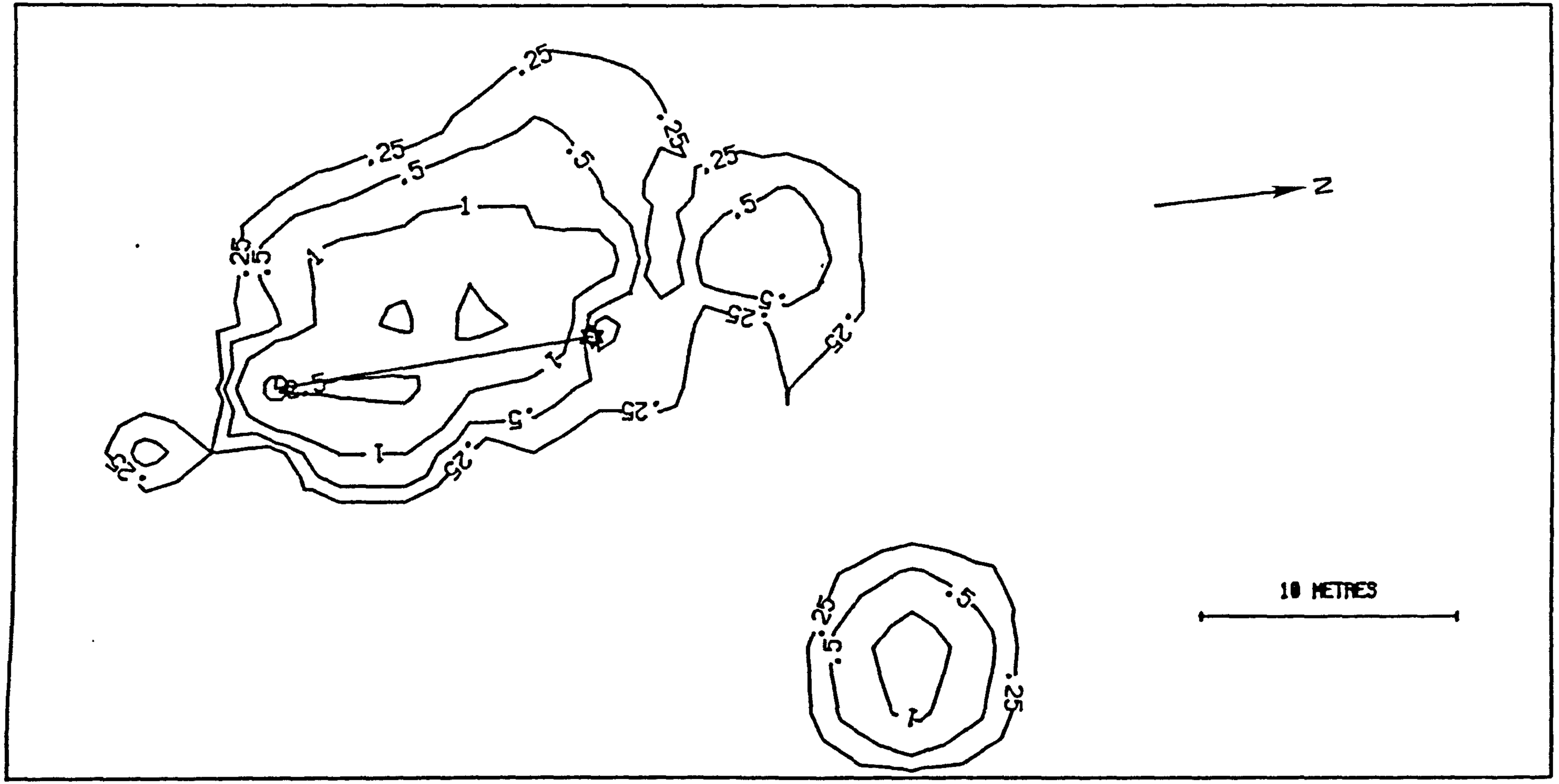

INJECTION POINT ⊙ CENTRE OF GRAVITY ✡

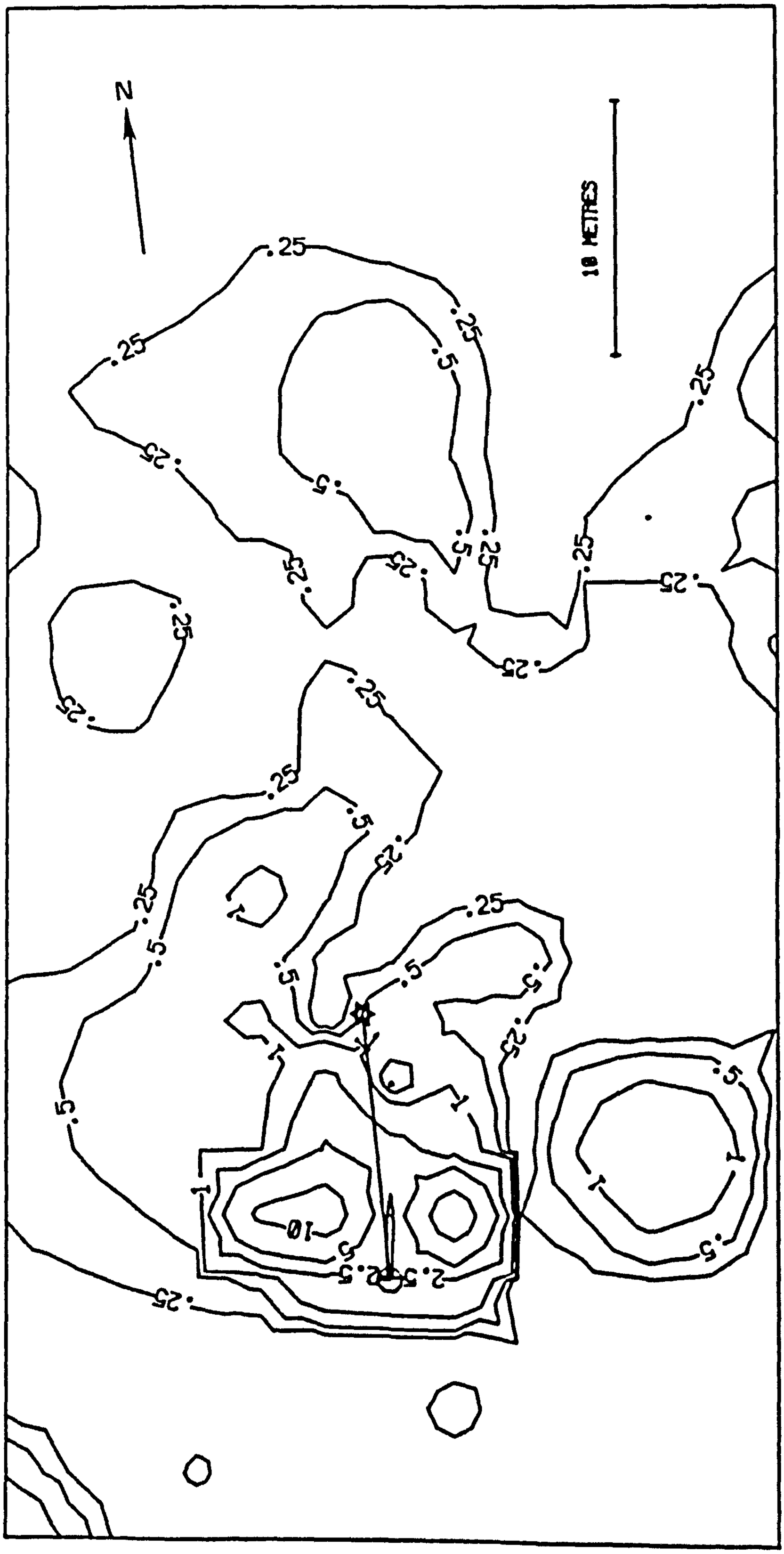
N
10 METRES
7 10 76 UPPER RIDGE PINK 0.65 MM
CENTRE OF GRAVITY ✱
INJECTION POINT ⊙

Figure 4.39.

gained from these the general pattern revealed by some maps shows interesting features. For example contamination of the tracer site from previous experiments is clearly visible on the upper part of the map for 12.8.76 experiment at Skegness with pink tracer for the 0.5mm fraction (Figure 4.40) and on the lower part of Figure 4.42,the map for 7.10.76 lower ridge with yellow tracer for the 0.3mm fraction. Such contamination reflects the efficiency of grain coating and also the calmness of conditions between some field tests but may also, of course, constitute a sampling problem. From the series of maps Figures 4.40 to 4.44 it will be seen that recovery of finer grains was usually greater than for coarse simply because of the larger number of grains in a particular weight of each fraction. In general the dot maps confirm the findings of the bicolour tests in that very different dominant directions of movement are not distinguishable for different size fractions.

The distinct lack of success of the specific grain size tests was due to the use of quantities of tracer too small to give sufficiently large recovery rates. Because of the experimental timetable this fact was not discovered until laboratory analysis of all test samples had been completed. In future tests larger quantities would be necessary but an alternative technique used by Komar (1977) would give more information. This method involves using a single colour for all grain sizes in the beach sediment,sieving each sample collected into selected size fractions and then counting the number of tracer grains present in each fraction. In this way data on the movement of nearly all grain sizes on the beach can be gained rather than for just two or three sizes tagged with different colours and in addition the different size fractions are in their correct proportions since the complete grain size distribution is coated.

Previous work on sorting and differential grain movements using fluorescent tracers has produced conflicting results although the

Figure 4.40.

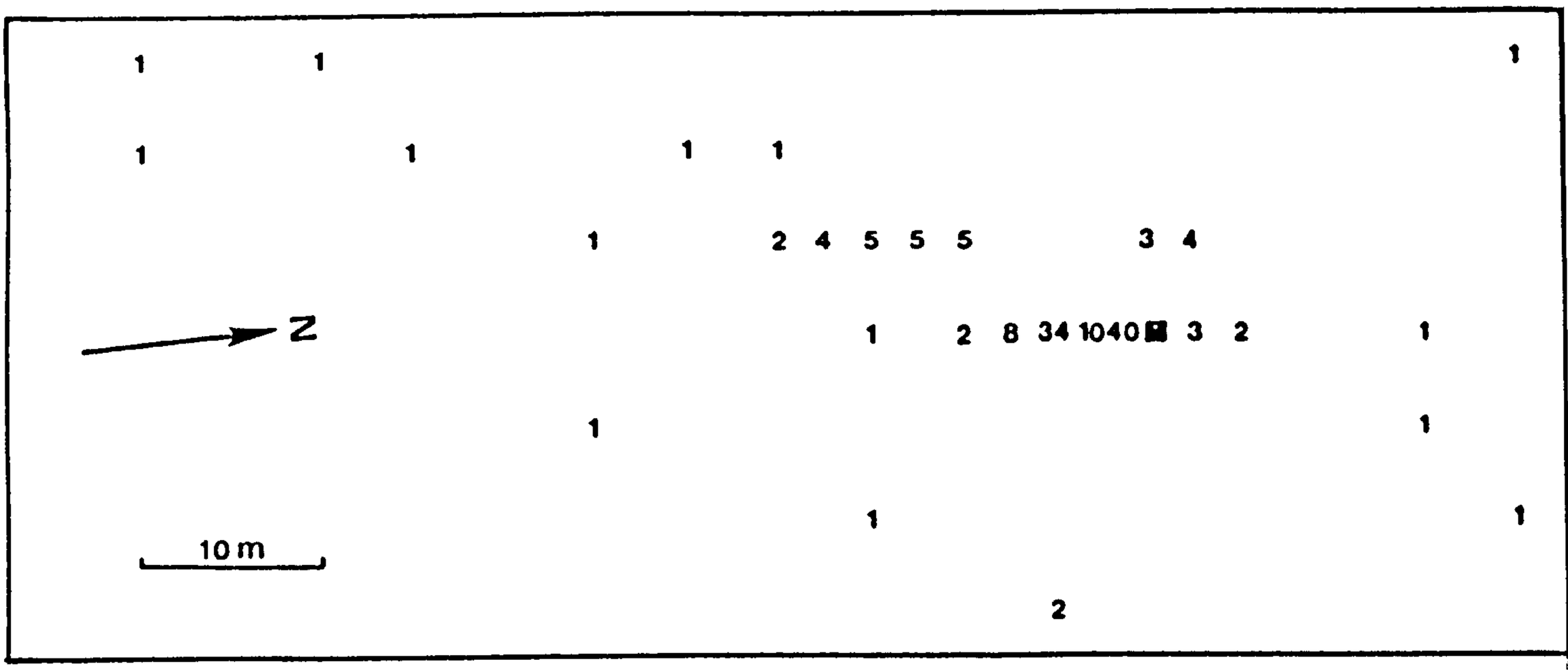

Figure 4.41.

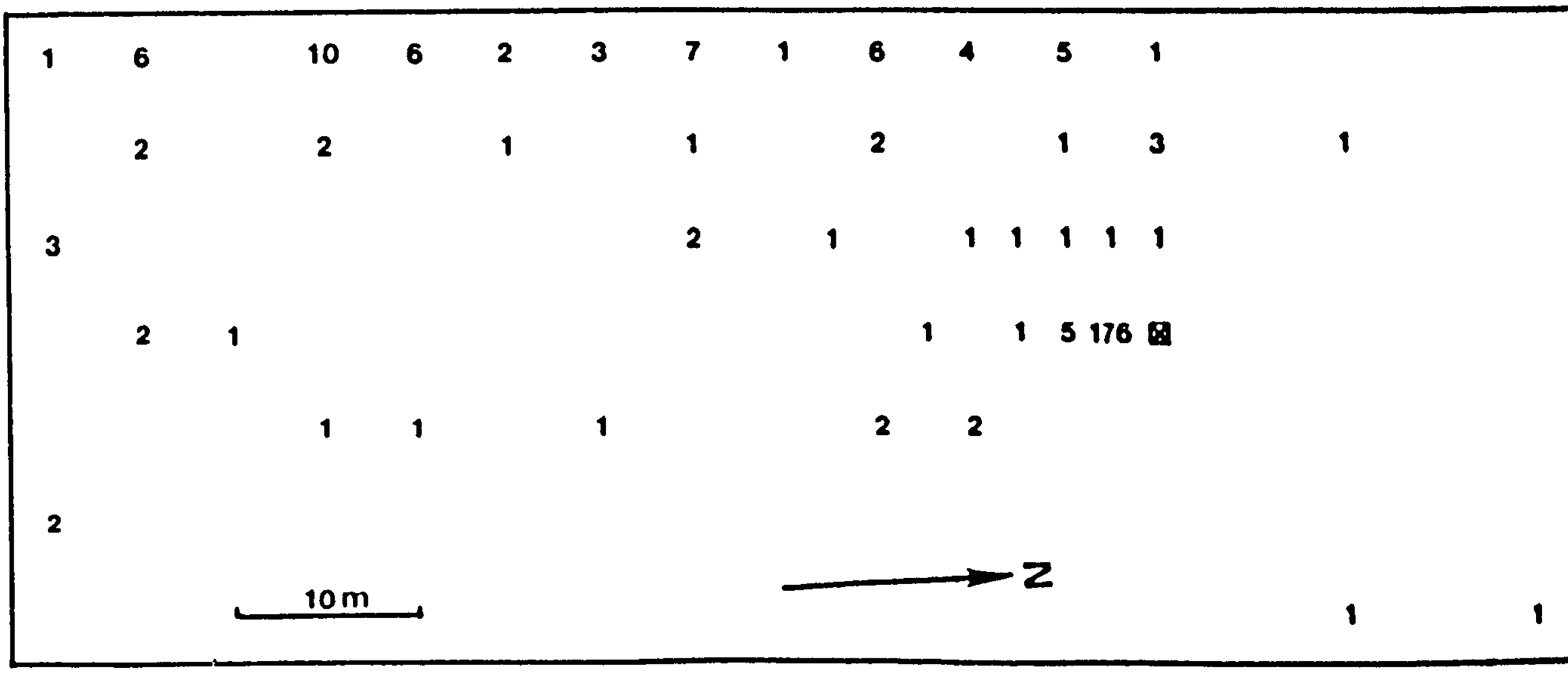

Figure 4.42.

7·10·76 Lower Ridge El Yellow 0·3 mm

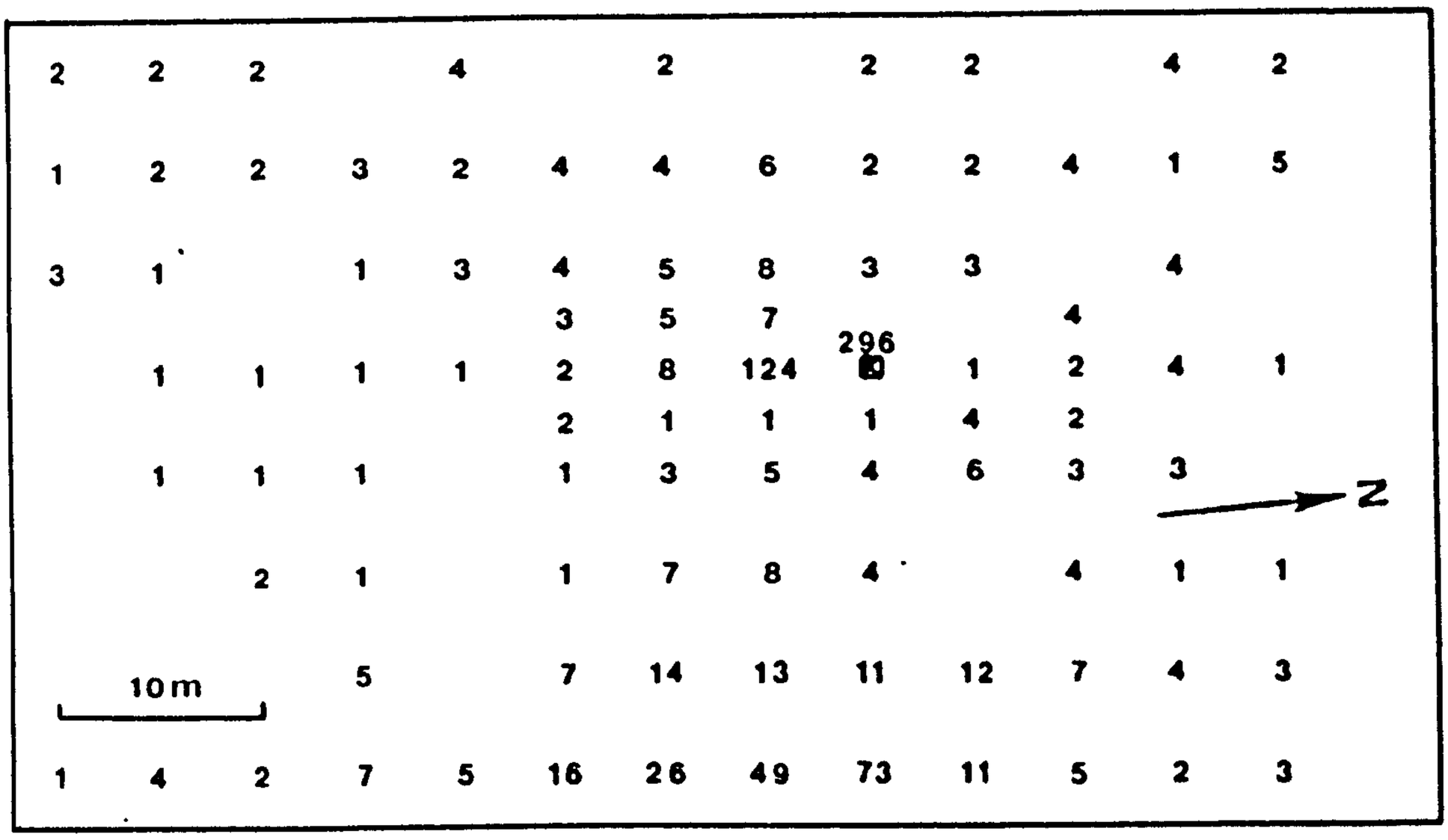

■ Tracer Release Point

Figure 4.43.

7·10·76 Lower Ridge El Blue 0·46mm

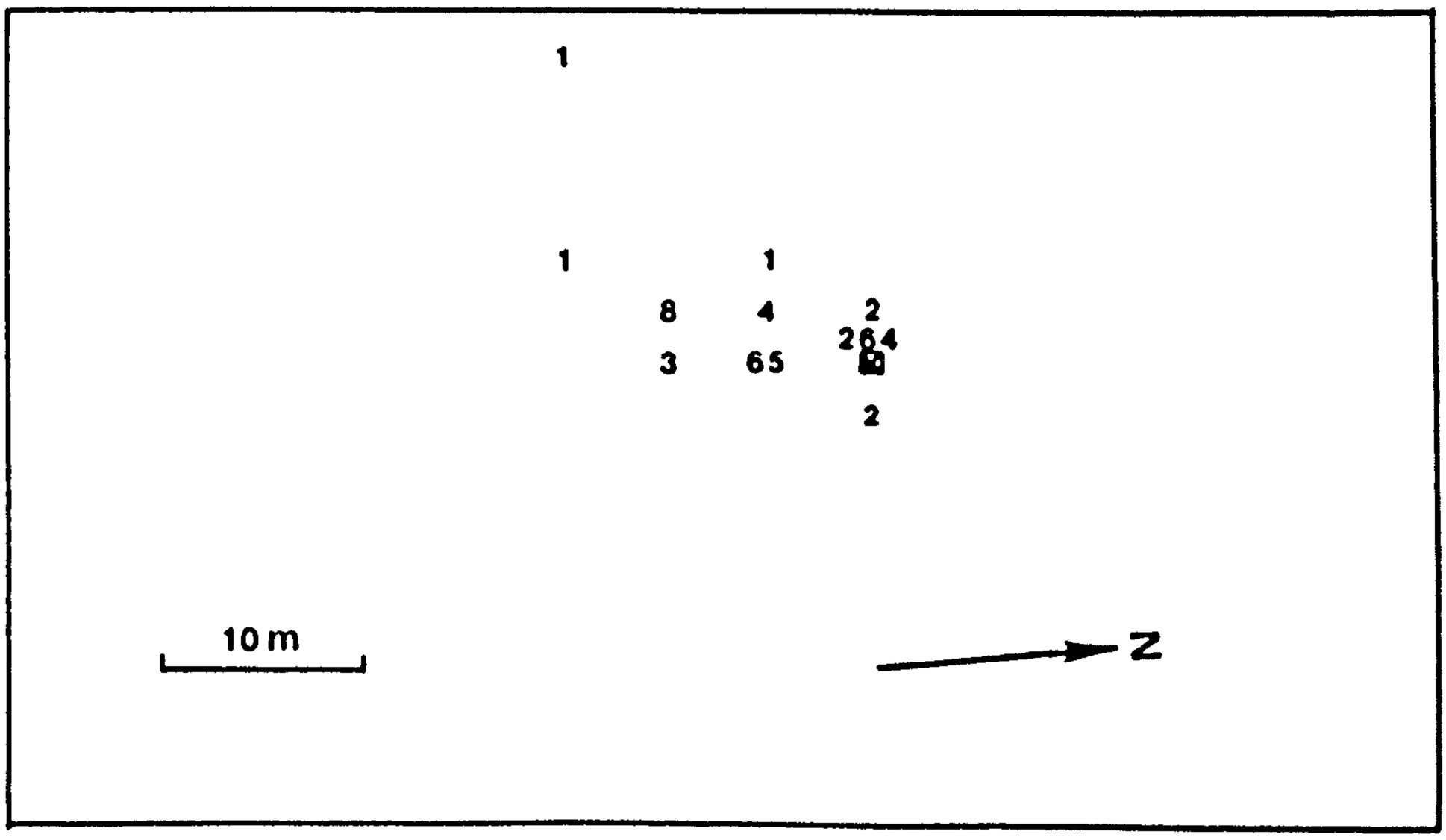

■ Tracer Release Point

Figure 4.44.

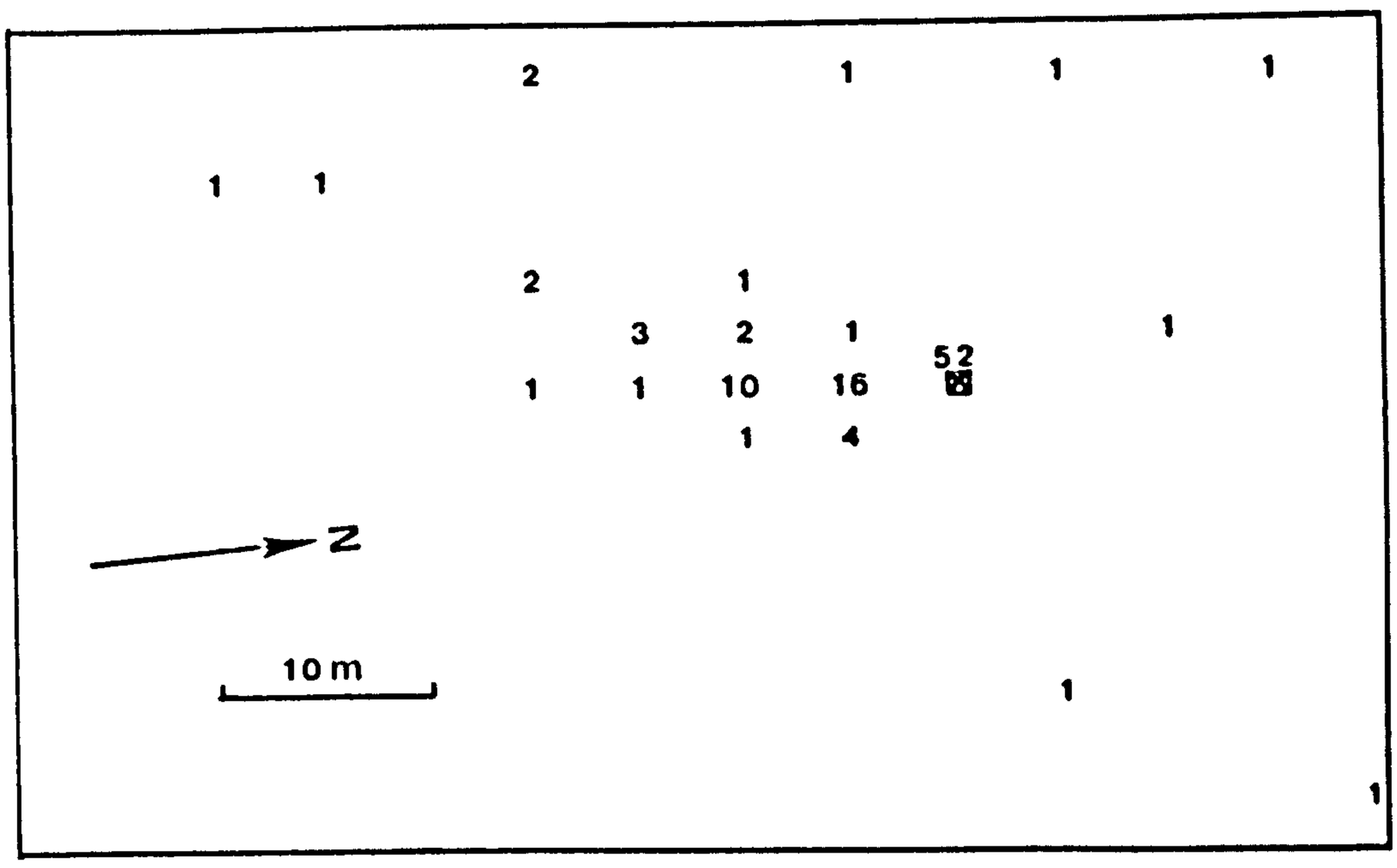
7·10·76 Lower Ridge El Orange 0·66mm
2
1
1
1
1
1
2
1
3
2
1
1
52
1
1
10
16
1
4
N
10 m
1
1
Tracer Release Point

bulk of the evidence from field tests suggests differential rates of movement forms the main mechanism by which sorting takes place and not directional factors. Boon (1968) used trend surface analysis to describe the tracer patterns from an experiment he conducted in the British West Indies. Assuming synchronous areal distributions he suggested that any tendency for grains to be sorted into, and travel along in, discrete bands parallel to the shore would be reflected in distinctly different isopleth patterns for the trend surfaces. However, testing the orientation of orthogonals to the trend surface contours he found that over a tidal cycle no clear cut differences developed between the patterns of tracer particle distribution representing different sizes and shapes. Similarly, Ingle and Schnack (1971) reported from work carried out at Moss Landing Beach, California, that with major grain size fractions of greater than 0.35mm, 0.35mm to 0.25mm and less than 0.25mm mean vector paths were essentially the same over short time periods. They also found, though, that grains finer than 0.25mm left the sampling areas 20-50% faster than grains 0.35mm and coarser. However, Ingle's (1966) earlier work indicated a tendency for coarser grains to move seaward out of the surf zone, whilst the finer grains remained within the surf zone producing sorting in this way. Yasso (1962) also had previously found that grains of varying diameter exhibited a variety of maximum and minimum onshore transport vectors in experiments at Sandy Hook, Virginia. Working in the shoaling wave zone Murray (1967) found that under the same hydrodynamic conditions the finer grain sizes have a greater tendency to move offshore than coarser grains and that, in general, finer grains disperse into quasi-circular concentration contours while coarser grains form more elongated isopleths.

Miller and Zeigler (1958) built up a model of sediment patterns in the shoaling wave zone, the breaking wave zone and the swash/backwash zone based upon the differential movement of different grain sizes as

the mechanism of sorting. In the shoaling wave zone they concluded that sand movement was in accordance with a modified form of Cornaglia's null point theory. This theory states that there are two opposing forces acting on sediment in shallow water:

1. the onshore drift associated with wave motion and

2. the offshore gravitational forces produced by the bottom slope.

For each grain of a given density, size and shape there is a line of equilibrium between the opposing forces whose net movement onshore/offshore is zero. The larger the particle the closer to shore the null point. Shoreward of the null point a particle will move onshore, whilst offshore of it, it will move seaward. If many different sizes are present, only one of the sizes can be at its null point. Using Ippen and Eagleson's (1955) empirically-derived equations for null points, Miller and Zeigler suggested that median sediment size increases towards the shore and sorting improves in the same direction, in the shoaling wave zone. Gravity was assumed to play little part in moving material offshore. In the breaker zone, improved sorting and larger mean grain size was postulated as a result of turbulence, causing winnowing of the finer sediment from the coarser fraction. On the other hand, in the swash/backwash zone they expected a band near the top of this zone to show a rapid increase in size on a traverse downslope and a rapid improvement in sorting. Continuing downslope they envisaged a regular rise in median size but poor sorting and an irregular contour pattern. Field observations at Falmouth beach, Massachusetts, confirmed the model but only in the situation where wave crests advanced parallel to the shoreline over a plane bottom with a gentle seaward slope. In addition, the study area was small to reduce the effect of longshore currents, and strong tidal currents were absent. In later work, application of the model to more complex beach topography and strong current action proved much more difficult.

For the tidal situation, Miller and Zeigler suggested that as the tide rises the well sorted band of finer material is continually erased or covered and appears higher on the beach, while the other zones take over a larger portion of the beach. With the fall of the tide the well sorted band of finer sediment increases in width, reaching a maximum at low tide.

Ingle (1966) extended the Miller and Zeigler model by postulating additional sorting processes for the surf zone. He suggested that for any given slope and spectrum of bottom velocities active beneath the surf zone, a relatively wide band of oscillating equilibrium would exist for particular grain diameters. These grains he envisaged as being most susceptible to transport by longshore currents and hence would exhibit the strongest vectors of longshore movement. At the same time, grains of lower than a critical diameter would travel in suspension with the greatest density in the swash/surf boundary area and the breaker zone, whilst larger grains would move in a sheet flow towards the breaker zone or towards the swash/surf boundary, depending on their point of origin. This simple scheme, which it was acknowledged would be greatly modified by irregular topography and rip currents, was partially confirmed by Ingle's (1966) bicolour grain size tests but later more detailed work produced results not in agreement with it.

The results of the grain size tests of this study indicate the complexity of the problem of modelling differential grain movements. Given simple beach topography and steady state wave and tidal conditions it seems likely that an equilibrium sand surface in terms of grain sorting and size patterns would develop, but the inherent variability of hydrodynamic and sediment characteristics means that the actual surface at any given moment probably represents a dynamic equilibrium. Furthermore, in the strong tidal environment this dynamic equilibrium becomes a transient, oscillating feature related to the movement of

different nearshore zones backwards and forwards across the beach with the rise and fall of the tide. With the inclusion of complex beach topography the picture is even more complicated and its description in any type of model even more difficult. Therefore, from the tracer dispersion patterns mapped in this study, representing the net effect of a series of sorting processes operating throughout the tidal cycle, it is likely that particular sorting patterns would be indistinguishable. Multiple sampling of tracer dispersion at different times throughout the tide might be expected to yield more information on the processes of grain sorting, but even this approach has not produced consistent results, as indicated by Ingle's conflicting results.

A consistent feature of the grain size tests conducted in this study was the greater dispersal of the finer sizes and the larger distances moved by these grains. On the other hand, examples of differences in dominant direction of movement were few. Onshore-offshore sorting patterns were not present because of the strong longshore operating processes, but sorting alongshore was evident in the differential rates of movement. Further analysis of selected sets of samples from this study may throw more light onto the problem of sorting patterns and differential movements. One approach already noted would be to sieve each sample collected into different size fractions and count the number of tracer grains present in each fraction. However, as previously suggested, multiple sampling might provide better results in future field tests.

4:4 Note of caution

Price (1969) introduces a note of caution into the interpretation of tracer maps, in particular with reference to the onshore-offshore sediment transport. In a simple arithmetic model, Price has shown that on a stable beach on which, by definition, no net transport of material normal to the beach is occurring, an apparent net transport may be indicated by a tracer

map using the usual 'centroid' or centre of gravity method of analysis. By looking at sand movement in terms of the exchange of particles between ripples, the apparent movement is shown to be due to the tendency of tracer to move towards the area of maximum diffusion in the breaker zone. Figure 4.45 is a diagrammatic representation of the model.

Beginning with two tracer sources of 1,000 particles, one seaward and one landward of the breaker zone, the number of particles exchanged between ripples for each wave stroke is shown. It is assumed that because wave orbits and general lack of turbulence are greater as the breaker zone is approached, so seaward of the breaker zone the number of particles exchanged between successive ripples increases in the onshore direction. In the diagram, 40 grains are exchanged with the next ripple seaward of the tracer and 50 shoreward. With each successive wave stroke, more tracer is moved onshore than offshore but there is no net transport since the particles are replaced by untagged grains. Thus, despite the fact that the centroid of the tracer distribution is moving onshore from A and offshore from B indicating a net transport, there is no net transport and the beach is stable.

Applying the model to the tidal situation, Price contends that the misleading tracer results for the part of the beach between high and low water become time dependent. The dispersion with tides is shown in Figure 4.46. On the part of the beach below low water the dispersion activity will increase towards the breaker zone. Shorewards of the low water level, because the time at which water stands at the various levels decreases when moving from low water to high water, the cumulative effect of the dispersion also decreases. This means that tracer placed seaward of the low water level will move landwards, while that placed shoreward will move seaward.

It is difficult to say how well this model can be applied to the tracer dispersion maps discussed in this chapter. Onshore and offshore

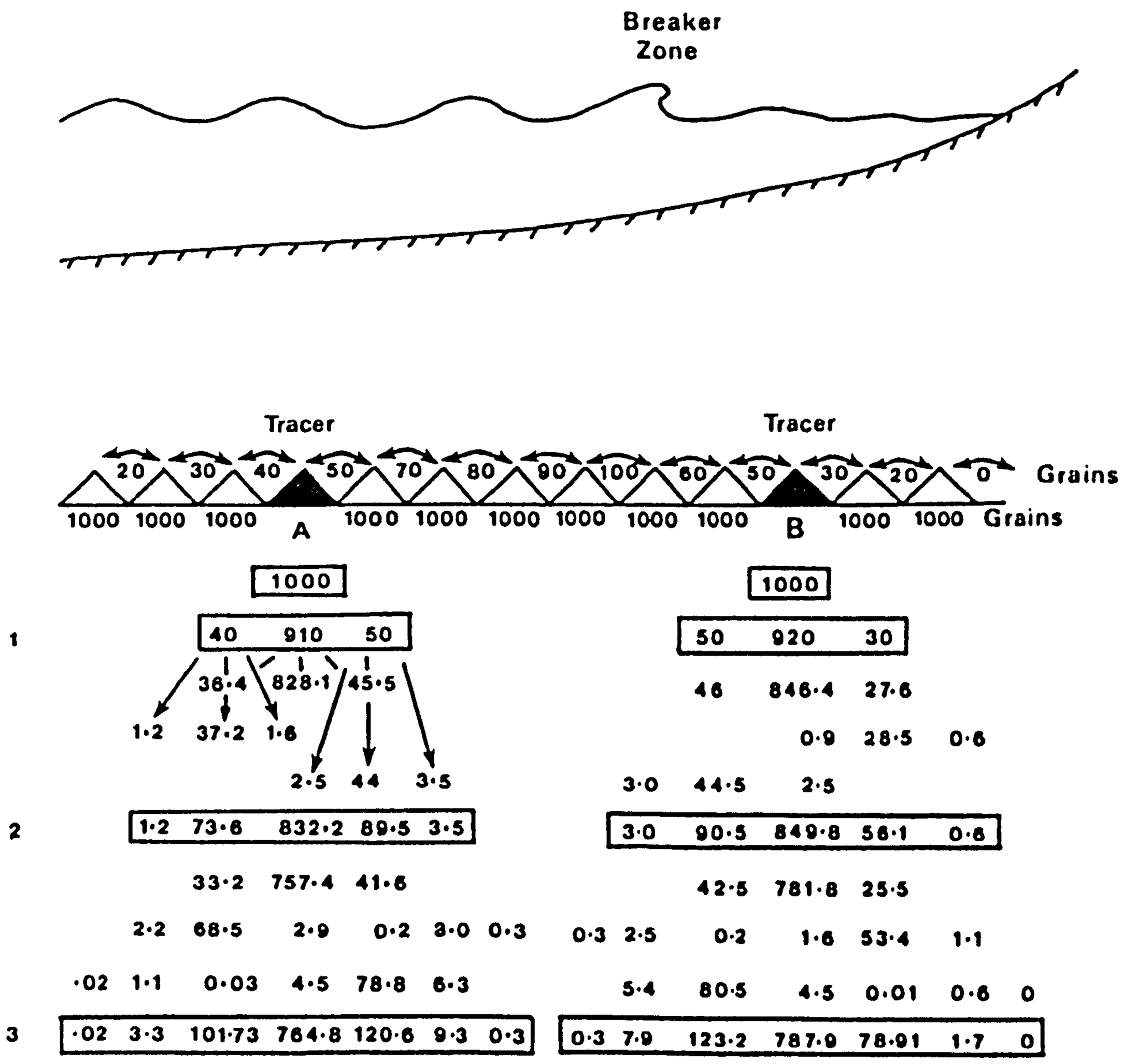

Figure 4.45. Conceptual arithmetic model of Price (1969) on diffusion of tracer.

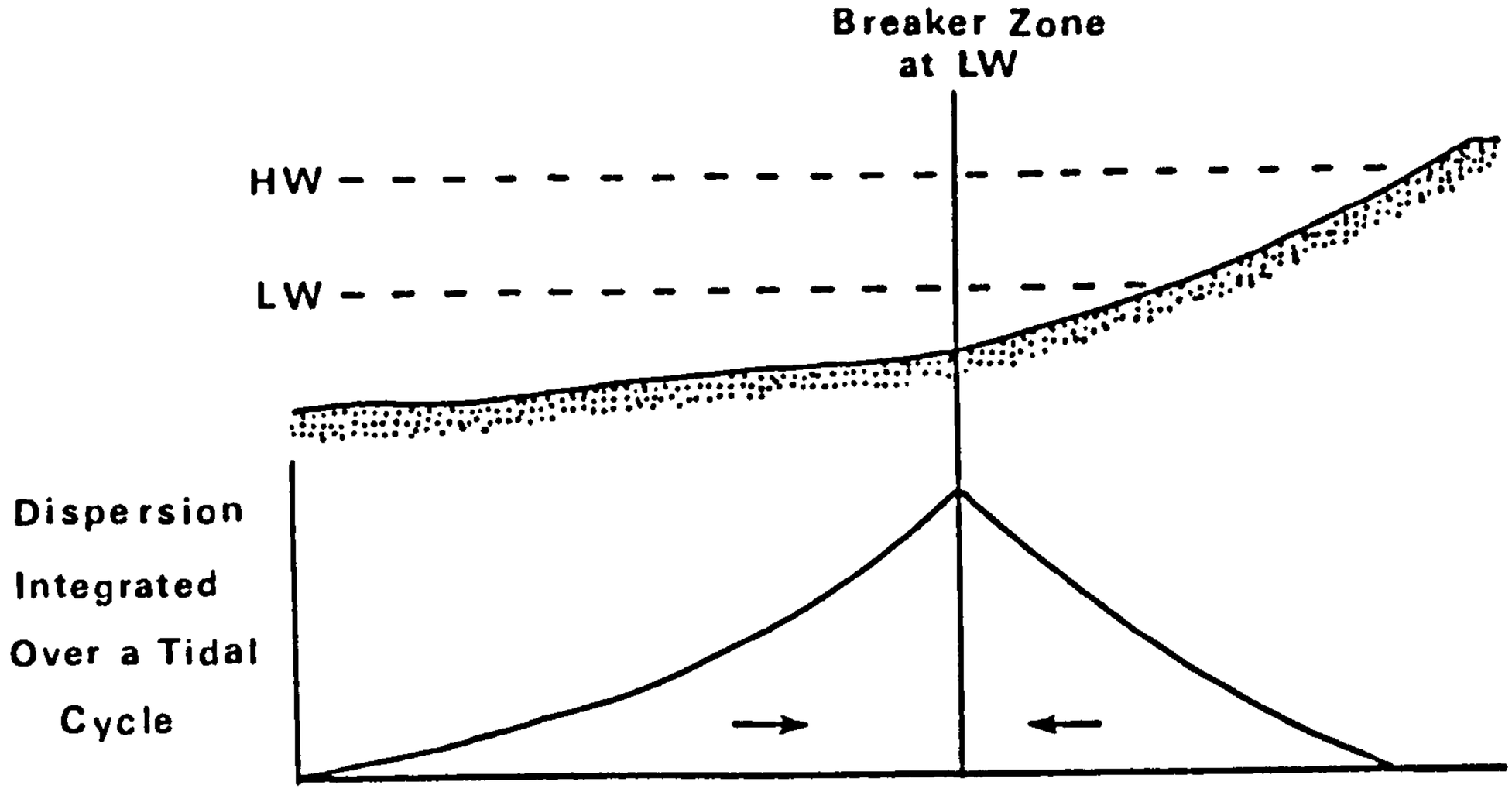

Figure 4.46. The Price (1969) model applied to the tidal situation.

movements of material are indicated by the maps from locations in the zone between the high and low water levels and some of these movements are quite strong, which does not conform to the tidal version of the model. However, Price (1969) does point out that such a simple model could not represent the movement of beach material completely.

Nevertheless, the model is valuable in that it demonstrates how misleading tracer results could be if care is not taken in interpretation. In particular, caution must be exercised before net movements of material are proposed on the basis of tracer dispersions. An example of the usefulness of Price's model in explaining seemingly anomalous sand movements is to be found in Ingle's (1966) tracer results. Some of these tests were conducted on stable beaches on the Californian coast on which it was known that no accretion or erosion was taking place. The tracer maps indicated consistent onshore/offshore movements but virtually no profile changes occurred. However, if no net movement is assumed from the map evidence the anomaly may be explained.

PART 2.

In the four chapters of Part 2 a more quantitative approach to the results of the tracer experiments is adopted. The first of the chapters, Chapter 5, is a brief consideration of some of the aspects of the mechanics of sediment movement together with physical models proposed by previous workers. Two of the most popular models of long-shore sand transport are field tested with data from this study. Following this the remaining chapters deal with the use of multiple linear regression techniques to construct a statistical model of sand movement.

Regression techniques were adopted because of the complexity of the interrelationships in the system under study but at the same time data inadequacies introduced an element of caution. Since the sample of observations on the variables involved totalled 29 the wide range of possible combinations of the variables has not been covered. In addition, the quality of data in terms of measurement error may also be open to improvement and strong interrelationships between independent variables caused problems of interpretation of results. Nevertheless, as a search procedure multiple regression method can be of great value and in this case of particular usefulness since little field data is available on short term sand movements and the system involved is far from being well understood. Krumbein (1976) points out that the standard statistical models such as stepwise regression help the geologist "to identify the more important variates to be included in his conceptual model."

In this study regression techniques are used to describe and predict the amount and direction of sand movement. Although it is possible to consider these two aspects as distinct response or dependent variables, directional and magnitude components of process variables are difficult to separate without considerable partitioning of the data set. Therefore,

the two basic parts of the sand movement model took the form

1) Amount of sand movement = f (magnitude of processes) + f (direction of processes);

2) Direction of sand movement = f (direction of processes) + f (magnitude of processes).

The model is further split into onshore/offshore and longshore aspects and for example individual consideration is given to the average distance moved by grains normal to the line of the beach and also along the beach.

Linearity does not always occur in the relationships between variables but in the absence of any theoretical basis for relationships the general linear model is the simplest of many possible hypotheses. From the point of view of interpretation of results and the computational aspects of the regression technique, the linear model is least complex. Furthermore, non-linear models are often intractable, no general method for their calculation and use is available and they are often only suited to particular situations. However, the linear approach can provide a first step towards further non-linear analysis and indeed it is hoped that the exploratory nature of the use of regression in this study may form the basis of further modelling work.

CHAPTER 5

MODELS OF SAND MOVEMENT

5:1 Introduction

Before going on to develop a model of sand movement based upon regression techniques a brief consideration is made in this chapter of some aspects of the fundamental mechanisms of sediment motion and also of some of the previously proposed models. Sediment movement is of interest to research workers in a wide range of disciplines, including hydraulic engineering, coastal engineering, geology, hydrology and geography and as a result there is a profusion of published material. It is not attempted to review this literature here but rather to deal with particularly relevant work.

In general most attention has been focussed on the problem of providing an efficient formula for the rate of sediment transport, usually as bedload, caused by moving fluid. Less success has been achieved for the coastal environment than for the fluvial largely due to the complexity of interaction of the many processes operating in the littoral zone. The tendency has been to concentrate on the longshore movement of sand on beaches because of the implications for coastal engineering construction but in morphological terms sand movements orthogonal to the beach are equally important.

Section 5:2 of this chapter deals with the initiation of sediment movement. This is the starting point of most of the theoretical work on the mechanics of sediment motion and involves the examination of flow characteristics, shear stresses and friction factors. Following this in Sections 5:3 and 5:4 the processes involved in some of the models of sand movement normal to the shore and alongshore are considered. Finally in Section 5:5 data from this study is applied to two of the most well known equations of longshore sand transport on beaches. These equations have

only recently been field tested by Komar (1969). He states that "additional measurements are required from other beaches when waves are small enough or tidal range is sufficiently large that measurements of sand transport include the breaker zone as well as the surf zone." Thus the use of these equations with data from this study to a certain extent achieves this and provides a reflection of their general applicability and efficiency.

5:2 Initiation of sediment motion

One of the first questions to be asked when dealing with sediment movement caused by a moving fluid is: when does the sediment start to move? Water flowing over a loose boundary, that is a cohesionless granular bed on which the particles are available for transport, will exert forces on that boundary. As these forces are increased a stage is reached at which they are sufficient to cause particles to move from the bed and be transported. This stage is variously known as the threshold of sediment movement or the critical stage for erosion or entrainment. The forces acting on the particles, produced by the flowing water, give rise to shear stresses between the particles in motion and those forming the stationary boundary, with the fluid between the particles taking part in the shearing. (Raudkivi, 1967). This shearing force is known as the boundary shear stress and the critical boundary shear stress is the level of the threshold of sediment motion. Also the water flow related to the boundary shear stress has a velocity known as the shear velocity.

Instead of using the critical shear stress alone to define the threshold of movement it is more usual to employ a dimensionless form of the stress. Often this takes the form of Shields Criterion (Shields, 1936) a widely accepted, though still empirical, criterion which determines the initiation of sediment motion on a plane-bed under unidirectional steady flow. The relationship is as follows:

$$\Theta_{(crit.)} = \frac{\tau_{(crit.)}}{(p_s - p)gD} \qquad \text{Eq. 5.1}$$

where $\Theta_{(crit.)}$ = dimensionless threshold criterion;
$\tau_{(crit.)}$ = critical boundary shear stress;
g = constant of gravitation;

D = grain diameter;

p_s = density of sediment;

p = density of water.

Fluid and sediment properties are taken into account as well as flow characteristics as can be seen and equation 5:1 expresses the critical value of the ratio of entraining forces to stabilising forces acting on a sediment grain in the sediment/fluid interface.

The Shields Criterion has general applications so long as the sediment is cohesionless and the fluid flow is unidirectional and steady. In the nearshore beach environment, however, oscillatory flows are experienced due to wave action and under these conditions determination of a general criterion for the onset of sand movement is more difficult.

Many equations have been put forward. Silvester and Mogridge (1971) present thirteen different equations from the literature but these equations are largely of limited applicability. The main problem encountered is the correct evaluation of the boundary shear stress which depends upon the use of friction factors or drag coefficients and which are themselves difficult to evaluate. Under steady current conditions boundary shear stress, τ_o , may be derived from the Darcy-Weisbach relationship:

$$\tau_o = \frac{f}{8} p U^2 \qquad \text{Eq. 5.2}$$

in which U = depth-averaged current velocity;

f = Darcy-Weisbach friction factor;

p = water density.

In this relationship the drag coefficient, f, is a function of the Reynold's number of the flow and the relative rougnness of the boundary. Boundary effects are assumed to extend over the full depth of the flow. However, under oscillatory flow, boundary effects are confined to the region immediately above the bottom and hence a different relationship is required. Other friction factors which have been used include Chezy's

c and Manning's n and in 1968 Jonsson introduced the concept of a wave friction factor, $f_{(w)}$. Using this, which is analogous to the Darcy-Weisbach f , the magnitude of shear stress exerted on the bottom, τ_{om} is calculated from:

$$\tau_{om} = \frac{1}{2} f_{(w)} \rho U_b^2 \qquad \text{Eq. 5.3}$$

where U_b^2 = maximum fluid velocity relative to the bed just outside the boundary layer.

Madsen and Grant (1976) devised a Modified Shields Criterion for use under oscillatory flow conditions based on this formula. However, all the friction factors have been determined in laboratory experiments and have been found to be fixed under certain flow conditions and for particular bed configurations, mostly flat bed. On the other hand, under natural conditions total roughness may be comprised of effects not only from grain roughness but also from other elements such as ripple marks and larger scale bedforms such as megaripples and sand waves. Little is known of the influence of bedflows on shear stresses and the operation of friction coefficients but Carstens et al (1969 and Silvester and Mogridge (1971) do provide some experimental evidence to suggest that threshold conditions may be lower on a rippled bed than a flat bed. Since both the Shields Criterion and Madsen and Grant's modified version of it, apply only to flat bed situations their use under rippled bed conditions may well produce misleading results.

In the offshore zone large scale bedforms may be encountered and here drag coefficients fall outside the narrow range of experimental conditions. Ludwick (1974), for example, found that with a movable bed and bedforms as large as sandwaves the drag coefficient ranged through four orders of magnitude. Because of the problems involved in the use of friction factors Ludwick concludes that " ... it appears that velocity profile methods are required for the accurate evaluation of boundary shear stress

in the ocean." These methods involve the use of velocity-defect formulae from which it is possible to infer shear stress without the direct use of a friction coefficient. However, these formulae are also empirically derived.

Dugdale (1977) provides a good example of the velocity profile methods in the calculation of shear stresses. Using tidal current velocities measured over the submerged sandbanks and intervening channels offshore from Gibraltar Point, Figure 1.1 , he calculated boundary shear stress from the parabolic form of the velocity defect law (Hama, 1954)

$$\frac{U-u}{u_*} = 9.6\ (1-\frac{d}{D})^2 \qquad \text{Eq. 5.4}$$

where U = velocity of flow at surface;

u = flow velocity at distance d above the bed;

u_* = shear velocity;

D = boundary layer thickness (water depth for fully developed flow).

This gave $\frac{u}{U_*}$ which was then substituted in equation 5.5:

$$\tau_o = u_*^2 p \qquad \text{Eq. 5.5}$$

Critical values of shear stress could then be ascertained from a Shields curve for Skegness and from this it was ascertained that sediment motion occurs at all states of the tide except for a short period around low and high water. Dugdale concluded that tidal currents at Gibraltar Point were competent to transport available sediment for a minimum of 75 per cent of the time.

In a similar vein the practical difficulties surrounding the use of friction factors caused Komar and Miller (1975) to propose a simpler approach to the problem of predicting grain threshold under waves. They suggested the use of near bottom velocity, u_m , alone rather than shear stress because u_m can be estimated from wave height and water depth

using the following:

$$u_m = \frac{\pi H}{T \sinh (2\pi h/L)} = \frac{\pi d_o}{T} \qquad \text{Eq. 5.6}$$

where H = wave height;

T = wave period;

h = water depth;

d_o = orbital diameter of water motion;

L = wave length.

Two equations were put forward to calculate threshold values for grain diameters: below 0.5mm , medium sands and finer, equation 5.7 and for those grains larger than 0.5mm , coarse sands and coarser, equation 5.8. The critical size 0.5mm is related to the transition from laminar to turbulent flow in the boundary layer.

$$\theta_t = \frac{p u_m^2}{(p_s - p) g D} = 0.21 \left(\frac{d_o}{D}\right)^{\frac{1}{2}} \qquad \text{Eq. 5.7}$$

$$\theta_t = \frac{p u_m^2}{(p_s - p) g D} = 0.46\pi \left(\frac{d_o}{D}\right)^{\frac{1}{4}} \qquad \text{Eq. 5.8}$$

where D = grain diameter.

Despite the similarity of these equations to the velocity defect relationship the equations are only of limited value because they assume pure sinusoidal wave motion and do not take account of asymmetric wave motions in deep water and shallow water waves.

This brief discussion of the problems of predicting sediment movement thresholds provides ample evidence of the fundamental difficulty, that of accurate field observation. Much work has been carried out in the laboratory but the empirical formulae so produced usually cannot be applied to the field situation. Models developed under conditions of unidirectional, laminar flow are of little value for study of oscillatory turbulent flow over a bed composed of ripples or even larger features. More work in the

field is required on all aspects of the problem of initiation of sediment motion, under 'natural' conditions.

5:3 Onshore-offshore sand movement

Full and complete models of sand movement normal to the shoreline are almost absent from the literature due largely to the complexity of the system. A large number of processes and effects is involved and those commonly accepted as the most important will now be considered.

Niederoda (1974), in a study of processes operating orthogonal to the beach, points out that a sloped sand bed subjected to uniformly oscillating wave orbital motions has only the tangential stress component of gravity which is capable of producing a net motion of sediment in an offshore direction. Under the wave crest the bottom shear stress acting up the slope is counteracted by the component of the submerged weight of the sand particle acting down the slope but under the wave trough the two forces act in the downslope direction. Therefore, a net sediment transport offshore might be expected from this asymmetry in the entraining forces. Arguing from this, Niederoda suggests that unless large amounts of material are being supplied to beaches in equilibrium by longshore transport then most natural beaches must be affected by onshore orthogonal processes if constant erosion is not to take place. Wave asymmetry and wave drift are put forward as the two processes that function uniformly in space and are capable of producing static equilibrium.

Wave asymmetry. Wave theory predicts that for a small amplitude wave progressing over a horizontal bed there will be a purely sinusoidal orbital velocity above the bed. This motion may cause sediment to be moved back and forth assuming the threshold velocity is exceeded but no net movement occurs. However, if finite amplitude, that is non-linear effects are considered the wave profile is no longer symmetric about the mean water level. Therefore, for non-linear waves the mean crests become

more peaked, higher and steeper, than the wave troughs which become shallower and flatter, Figure 5.1. This lack of symmetry is reflected in the near-bottom velocities which show a forward velocity of greater magnitude, but shorter duration, under the wave crests, and a lower backwards velocity of longer duration under the troughs, Figure 5.1. Under these conditions the time-average net rate of transport is in the direction of wave propagation. The differences in bottom velocities may be greater for long period waves than for short period waves but the situation is not clearly understood. Madsen and Grant (1976) point out that experimental data on the net sediment transport due to wave asymmetry velocity variation is not available and that predictions of these rates by Kamphuis (1973) were not encouraging. However, some success has been achieved with an equation for sediment transport developed from an approach based on instantaneous near bottom velocities.

Mass Transport. Longuet-Higgins (1953) discussed Stoke's classical treatment of mass transport or wave drift associated with the propagation of shallow water waves. When second and higher order terms are introduced it was demonstrated that the circular orbits of local water motion caused by the propagation of surface waves in deep water are deformed to an open geometric form in shallow water. This results in a net displacement of the water in the direction of wave movement with the passage of each wave, Figure 5.2. Longuet-Higgins then adjusted the model explaining mass transport by considering the interaction between the sediment and water boundary layer. An analytical solution was developed which provided for a mass transport in the direction of wave motion at the surface and along the bottom and a return flow at an intermediate level, Figure 5.2. Russell and Osario (1958) conducted wave tank experiments which essentially supported the current profile given by the Longuet-Higgins solution but their results were obtained with a slightly turbulent flow regime whilst Lonquet-Higgins' theoretical investigations were based on assumptions of

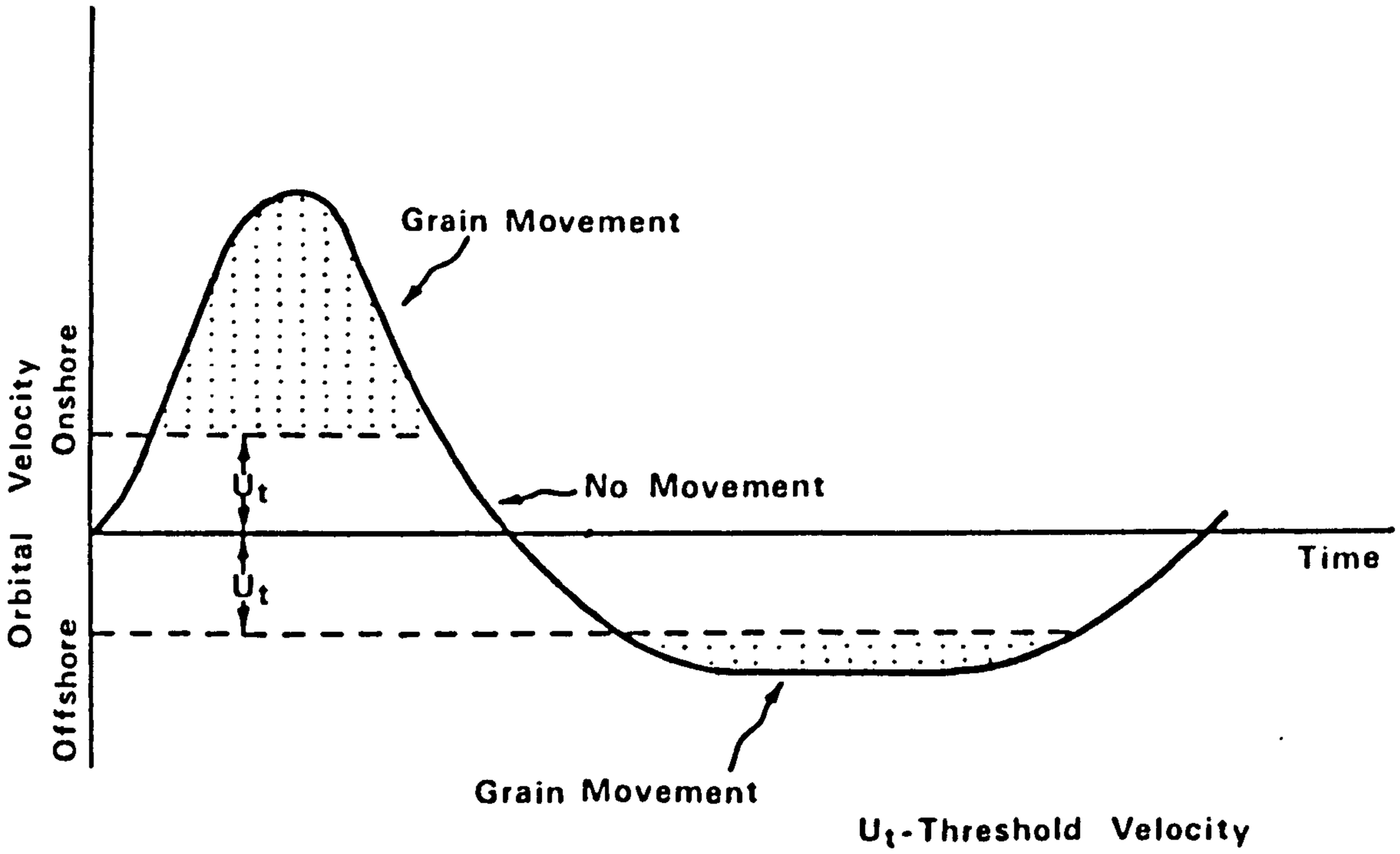

Figure 5.1. The asymmetry of wave orbital motions causing a net shoreward transport of sediment.

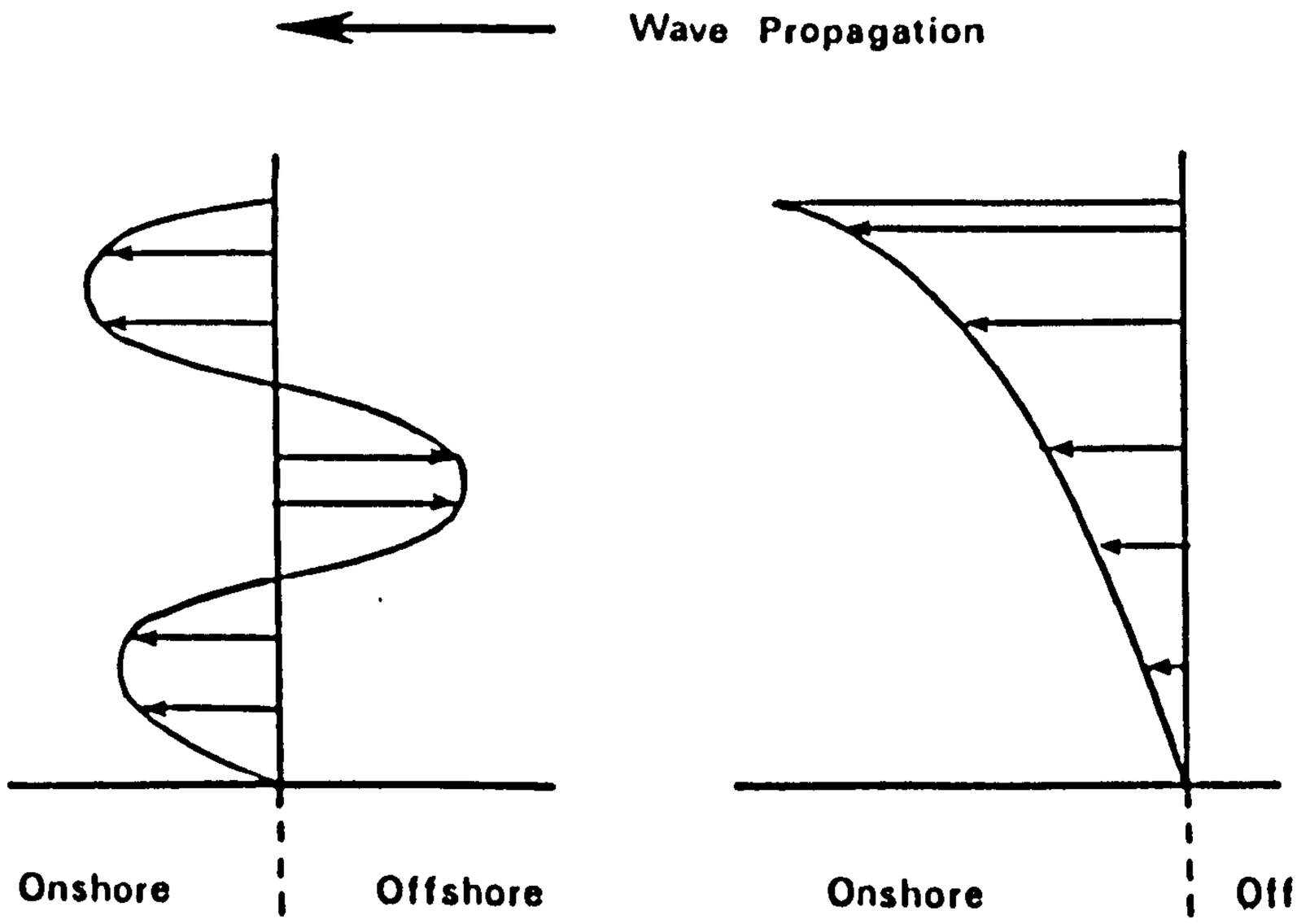

Figure 5.2. Comparison of water motion in theories of mass transport.

laminar flow. Longuet-Higgins (1968) explained this apparent contradiction by showing that given certain assumptions his model also applied to turbulent flows but more recent results reported by Bijker et al (1974) have cast doubts on this. Bijker et al conclude that more data are needed on mass transport under turbulent boundary layer conditions. King (1949) observed a transport pattern similar to that predicted by the Longuet-Higgins model but found that the forward thrust on the bottom was dependent upon the character of the bed. The forward thrust occurred only when the bottom was of smooth sand and disappeared when ripples formed on the bed.

Given the inconclusive evidence of wave tank studies it is difficult to state how important mass transport is in the sediment transport picture for the nearshore. Indeed, Russell and Osario (1938) noted that when the width of the wave tank channel was large compared with the water depth there was a tendency to develop a horizontal circulation with a vertical axis. Therefore, under these circumstances wave drift would be non-existent since the shoreward discharge would not be balanced by a return flow at mid depth because continuity would no longer be necessary in two dimensions. This type of horizontal circulation would, under 'natural' conditions, include longshore and rip current systems.

Bagnold (1963) developed a model of sediment transport, based on the coupling of wave action with superimposed currents, which he applied to sediment transport beyond the breaker zone as a result of wave drift. According to the model the stress exerted by wave motion supports and suspends sediment above the bottom without causing net transport since the wave orbits are closed. A unidirectional current superimposed on this to and fro motion causes the net transport in the direction of current flow. A current of any strength will cause net movement since wave power provides the cause of sand motion. The immersed weight sediment transport rate per unit of bed width, i_θ , is given by:

$$i_\theta = \frac{k' w \bar{u}}{u_o} \qquad \text{Eq. 5.9}$$

where u_o = horizontal component of orbital velocity at the bed;

w = wave power;

$\bar{u}_o$ = superimposed current;

k' = dimensionless coefficient of proportionality.

The mass transport velocity $\bar{u}$ is given by Bagnold as being related to the orbital velocity close to the bed by the following equation:

$$\bar{u} = \frac{5}{4} U_o^2 / c \qquad \text{Eq. 5.10}$$

where U_o = orbital velocity just above the boundary layer;

c = phase velocity (wave velocity);

H = wave height;

h = water depth.

Substituting this into the transport model, equation 5.9, gives the following for wave drift transport, i_θ:

$$i_\theta = k'' w U_o / c \qquad \text{Eq. 5.11}$$

$$\text{or } k'' w H / 2h$$

where k'' = proportionality coefficient, probably a function of wavelength.

Inman and Bowen (1963) made a wave tank study of this relationship but as with King's (1949) results found seemingly anomalous results when the sand bottom was rippled. They found that in some tests with rippled bed sediment movement was decreased by an increase in the superimposed current velocity and in one case there was actually a net transport offshore, opposite to the superimposed current. These results serve to indicate the complexity of any solution to the problem of modelling sediment transport under combined wave and current systems.

Complicating the use of the wave drift model under natural conditions is the effect of a surface wind. Bagnold (1963) suggested that this 'external' variable in the system would affect matters in two ways:

i. A direct wind drag on the water surface might be expected to create a circulation in the vertical plane if sustained such that at the surface with an onshore wind an onshore water movement might take place with, at the sea bed, a compensatory return flow. The latter seaward drift might reduce or even reverse the forward wave drift. Wave tank experiments conducted by King and Williams (1949) support this premise as does the more recent work by King (1953) at Marsden Bay and of Siebold (1963) in the Baltic. Murray (1967), on the other hand, discounts the importance of wind-induced currents.

ii. Under an imposed surface wind drag the water waves themselves have a different character. Considerable turbulence develops from the water surface downwards in addition to the turbulence due to friction and roughness factors. However, it is not known what the effect of this might be. The effects of wind on sand movement normal to the shore are considered further in Chapter 7.

As pointed out in Chapter 4, Section 4:3, the balance of the offshore effect of gravity through beach slope and the onshore effect of wave drift and wave asymmetry forms the basis of Cornaglia's null point theory. However, results of grain size tests in this study and previous work have produced conflicting evidence for the applicability of this theory.

So far the processes and models considered have been largely applicable to the region seaward of the breaker zone that is in the shoaling wave zone and beyond. Other orthogonal processes operate in the zones landward of the breaker zone and these must also be discussed briefly since the tidal fluctuations involved in this study area necessitate a consideration of all nearshore zones and the processes operating in them.

Offshore tendencies imparted to the movement of sand grains are provided by the force of gravity acting tangentially to the beach slope but

in the swash-backwash zone these tendencies are strengthened by the translational water movements. Inman and Bagnold (1963) produced an indirect model of sand transport when they applied the energy approach to the concept of an equilibrium beach slope. The orthogonal effects of swash and backwash processes/such that the equilibrium slope is a function of the ratio of local offshore and onshore dissipation rates (c). At balance, they suggest, there must be an equilibrium between the amount of sand carried up and down the beach under wave action. Frictional drag on the swash and water percolation into the beach removing water from the return flow of the backwash produce a net shoreward movement of sand. This is opposed by the local beach slope which through the effects of gravity aids backwash in moving material offshore and hence produces a balancing offshore tendency. The relationship given by Inman and Bagnold is:

$$\tan \beta = \tan\phi\left(\frac{1 - c}{1 + c}\right) \qquad \text{Eq. 5.12}$$

where $\tan \beta$ = local beach slope;

$\tan \phi$ = coefficient of internal friction in shearing of gramular media ≃ angle of repose of sediment.

In the surf zone, a highly turbulent zone, if it exists on the foreshore, (Section 1:1), the dynamic variables involved in causing grain movement normal to the shoreline include the shoreward moving bores formed after wave collapse and the seaward return flow at the bed. The layered type of flow suggested for wave drift is transformed in the surf zone to a surface fluid motion with the wave of translation passing through the zone from breaker to swash zones and a seaward return flow at the sea bed. Field measurements by Schiffman (1965) confirmed the existence of the layered flow but it is likely that it only occurs under certain conditions. The shoreward fluid motion of the turbulent bore for example must at times extend down to the sand surface. Furthermore, as pointed out earlier,

horizontal circulation may replace the layered vertical flow. Where horizontal circulation is present seaward return flow through rip currents is an important cause of sand movement perpendicular to the line of the beach.

Finally, it is necessary to point out the importance that has been attached by some workers to wave steepness as a factor in orthogonal sand movements. The C.E.R.C. Manual (1973) asserts "Onshore offshore transport is the result of wave steepness, sediment size and beach slope. High steep waves move material offshore and low waves of long period, (low steepness) move material onshore." Rector (1934) provides an empirical limiting relationship between sand size and wave steepness:

$$M_d / L = 0.0146\ H/L^{1.23} \qquad \text{Eq. 5.13}$$

where M_d = grain diameter.

When the ratio of diameter to wave-length is greater than the steepness side of the equation sand moves from the offshore to the foreshore whilst the reverse is true when the ratio is small.

Many wave tank studies have been conducted to study the onshore-offshore movement of sand and the related profile type associated with wave steepness changes. King and Williams (1949) for example found that a wave steepness of 0.012 was important in governing the direction of sand movement in the surf zone. However, field studies have not provided conclusive evidence of the role played by wave steepness, often because wave measurements were not sufficiently accurate.

The importance of wave steepness and indeed many of the processes mentioned briefly in this section will be discussed further in Chapter 7 when a regression type model of onshore/offshore sand movement is developed.

5:4 Longshore sand movement

The chief causes of longshore sand movement are longshore drift and

the effects of longshore flowing currents. Longshore drift is the zig-zag, sawtooth pattern of movement produced in the swash-backwash zone by oblique wave approach. Longshore currents, on the other hand, may operate in both the surf zone or seaward of the breakers dependent upon their mode of generation. Komar (1976) identifies two ways in which longshore currents are generated in the surf zone: (1) as part of a cell circulation of rip currents and associated feeding longshore currents which is normally produced by longshore variation in wave height, and (2) through oblique wave approach. In addition to these currents produced by various characteristics of the waves themselves, wind stress and tidal action may also result in longshore flowing currents in any of the near-shore zones, which in turn may result in sediment movements.

The longshore movement of beach material has been given much attention in the past because the ability to predict the amount of sediment moving along a section of beach in a given time or under certain conditions has been of major importance in coastal civil engineering projects. One of the most frequently used relationships has been an empirical correlation of sand drift and wave power which is expressed as follows:

$$P_\ell = (EC_g)_b \cos \alpha_b \sin \alpha_b \qquad \text{Eq. 5.14}$$

where P_ℓ = 'longshore wave power'

EC_g = wave energy flux at the breaker zone

α_b = angle of breaking waves with shore.

Because equation 5.14 was based on an intuitive understanding of the causes of sand movement in the nearshore zone and not on pure physical theory a conflict has arisen over the interpretation of the term 'P_ℓ'. Komar and Inman (1970) called this term 'the longshore component of wave energy flux per unit length of beach' and it has also been referred to as 'longshore power' but Longuet-Higgins (1972) suggested both these labels were nonsensical because of the inclusion of the term $\cos \alpha_b$.

Longuet-Higgins does,however,concede that equation 5.14 represents "the pioneers' first intuitive attempt at grasping the quantity H" where H is the lateral thrust of waves exerted on water and sediment inside the surf zone and is given by:

$$H = E(C_g / C) \cos \alpha_b \sin \alpha_b \qquad \text{Eq. 5.15}$$

when C = wave velocity in the surf zone.

This confusion over the expression 5.14 is perhaps understandable for an empirical approach of this nature but it is also unfortunate since equation 5.14 has provided the basis of many field and laboratory measurements of sediment movement. Watts (1953) obtained the first field measurements to provide the empirical relationship:

$$S_\ell = 0.0011 P_\ell^{0.9} \qquad \text{Eq. 5.16}$$

where S_ℓ = longshore volume transport rate of sand

P_ℓ = wave power.

Later work by Caldwell (1956) and Savage (1959) which produced similar relationships was then combined with Watts' results by Inman and Bagnold (1963) who produced the following equation with a wave power exponent of unity:

$$S_\ell = 125 P_\ell \qquad \text{Eq. 5.17}$$

Following a consideration of Shields' (1936) work on the natural threshold of sediment motion Bagnold (1963) put forward a refinement of the previously described relationships. By a conversion of the transport rate of sediment S_ℓ from a volume to an immersed weight basis he developed a more efficient formula for longshore sand transport. Therefore:

$$I_\ell = (p_s - p)\, g\, á\, S_\ell \qquad \text{Eq. 5.18}$$

where I_ℓ = longshore dynamic transport rate;

p_s = density of sand grains;

p = density of sea water;

g = constant of gravitation;

$\acute{a}$ = correction factor for pore spaces (taken as 0.6 for sand beaches).

Equation 5.18 has more general applicability than the crude volume transport rates because it takes into account the density of material actually moving. This means that transport rates for beaches composed of sediment other than quartz can be used in comparative studies. Furthermore, because I_ℓ and P_ℓ have similar units of power 5.18 allows the derivation of a dimensionless coefficient K in the relationship $S_\ell = K P_\ell$. This now becomes $I_\ell = K P_\ell$. Despite these physically meaningful adjustments, however, the fundamental relationship expressed in 5.14 remains empirically derived and intuitive and because of this Longuet-Higgins (1972) has attempted to provide a more rational explanation of the relationship by applying the thrust of the waves in the longshore direction directly to the sand transport. Through careful analysis and using empirical values obtained from the field, he was able to show that the relationship expressed in equation 5.14 does have a fundamental physical basis.

However, a second model employing a basic approach to the mechanics of sand transport has also been developed by Inman and Bagnold (1963). This model relates the amount of longshore sand transport to the effects of longshore currents and follows Bagnold's (1963) general model mentioned earlier, and expressed in equation 5.9. Applying this equation to the nearshore zone the following model was produced:

$$I_\ell = K' (EC_g)_b \cos \alpha_b \frac{\ell}{u_o} \qquad \text{Eq. 5.19}$$

where v_ℓ = longshore current velocity;

u_o = orbital velocity at the bed;

K' = dimensionless proportionality factor.

In this model, therefore, sand is placed in motion by the dissipation

of wave energy in overcoming bed friction and once it is in motion it becomes available for transport by the longshore current v_ℓ. The factor K' may be considered a coefficient of efficiency as it represents an index of the proportion of power dissipated in moving sediment. This arises because much of the energy available for sediment movement, represented by EC_g is used not in overcoming bottom friction but by other effects such as turbulence and viscous dissipation.

Since, in this model, the quantity of sand moved is a function of the energy available for transport the approach has been termed the 'energetics' approach. Longuet-Higgins (1972) considered this model less fundamental than the relationship expressed in equation 5.14. On the other hand, Komar and Inman (1970) demonstrated that both relationships were equally successful in explaining sand transport rates when field data was employed to test the models, but that equation 5.19 was the more flexible model. They concluded that both equations were effective because in their study the longshore current was generated by the waves through the relation:

$$v_\ell = 2.7\, u_m \sin \alpha_b \qquad \text{Eq. 5.20}$$

However, where longshore currents were not generated in this way, for example when the current was the result of the circulation of rip current cells, then the empirical relation 5.14 would not apply but equation 5.19 could be used successfully. Further, since the longshore current is introduced as a separate item to the relationship equation 5.19 could also be adapted for use in the offshore where tidal currents are important. Dugdale (1977) calculated bed-load indices for the offshore circulation system off Gibraltar Point using the energetics approach of equation 5.19.

At the same time, Komar (1971), using the radiation stress concepts defined by Longuet-Higgins and Stewart (1964), has derived the empirical model of equation 5.14 for longshore sand transport caused by the sawtooth motion of longshore drift in the swash-backwash zone. This is particularly

useful where no longshore current exists and equation 5.19 cannot be used, such as for example when waves break close to the shore on a steeply shelving beach and no surf zone is present.

Thus, dependent on the circumstances of the particular location, one or other of the two models of longshore sand transport can be applied to all zones of the nearshore. Equations 5.14 and 5.19 are two of the most frequently used models of sand transport and will be considered further in the next section when the data collected in this study will be used to test their general applicability. Nevertheless they are only two of many approaches to the problem of modelling sand transport. For details of the other main approaches such as those of Einstein and the Berkeley School, reference should be made to Yalin (1972) who also provides a detailed technical consideration of the mechanics involved.

5:5 Test of the models

Komar (1969) conducted tracer experiments to test the two models of longshore sand transport, equations 5.14 and 5.19, discussed in the previous section. Following his approach the two models will be tested with the data collected in this study.

A bulk sand transport rate was calculated from the following expression:

$$S_\ell = b\, X_b\, (V_\ell) \qquad \text{Eq. 5.21}$$

where b = measured thickness of sand movement;

X_b = width of beach face of experiment;

V_ℓ = mean speed of longshore sand movement.

The thickness of sand movement was estimated from the depth of disturbance measurements taken during each experiment. The amount of erosion indicated by the measurements was taken as the average depth of movement. In fact, it was noted earlier (Chapter 2) that this figure represents an average

for the depth of burial of the tracer which will decrease away from the injection point because of the length of time available to bury the grains diminishes as they move away from the tracer source.

V_ℓ , the speed of grain movement was calculated as follows:

$$V_\ell = d_x / t \qquad \text{Eq. 5.22}$$

where d_x = longshore component (i.e. in x direction) of distance between tracer source and centre of gravity of dispersed tracer cloud;

t = time tracer covered by sea.

Substituting S_ℓ into equation 5.5 the immersed weight transport rate, I_ℓ , was then calculated. The density of sand, p_s , and the density of sea water were taken as 2.65 gm/cm^3 and 1.2 gm/cm^3 , as evaluated by Dugdale (1977) from analysis of samples in the Skegness-Gibraltar Point areas. I_ℓ was then plotted against P_ℓ and $(ECg)_b \cos \alpha_b \frac{V_\ell}{u_m}$ as shown in Figures 5.3 and 5.4. The data for these plots is given in Tables 5.1 and 5.2.

In equations 5.14 and 5.19 Cg was calculated from:

$$Cg = (2g H_b)^{\frac{1}{2}} = 8.02 H_b^{\frac{1}{2}} \qquad \text{Eq. 5.23}$$

For all calculations involving breaking wave height, H_b , the significant wave height, $H^{\frac{1}{3}}$, as derived from field measurement was converted to an estimate of H_{rms} using:

$$H_{rms} = H^{\frac{1}{3}} / 1.418 \qquad \text{Eq. 5.24}$$

where H_{rms} = root mean square wave height;

$H^{\frac{1}{3}}$ = significant wave height.

This conversion was necessary in order to allow comparison of results with Komar's work and is based on the findings of Longuet-Higgins (1952) concerning the relationship of these wave parameters.

Wave energy density, E_b , was calculated from:

$$E_b = \frac{\rho g H_{rms}^2}{8} \qquad \text{Eq. 5.25}$$

and this was used to evaluate u_m, the maximum orbital velocity, from:

$$u_m = \left(\frac{2\ E_b}{\rho h_b}\right)^{\frac{1}{2}} \qquad \text{Eq. 5.26}$$

where h_b = the trough to bottom distance in front of the breaking wave (i.e. water depth).

Longshore current velocity v_l used in the energetics model was obtained from field measurements.

Figure 5.3 shows the plot of I_l against wave power, P_l, for the data collected at Gibraltar Point and Skegness. Also plotted on the log/log graph are the data points from Komar's (1969) tracer studies at El Moreno and Silver Strand beaches on the west coast of America and it will be seen that there is a greater scatter of points in the data set from the present study but that nevertheless a similar relationship holds. The equation of the best fit line for Komar's data was:

$$I_l = 0.77\ P_l \qquad \text{Eq. 5.27}$$

where the regression line passes through the origin. The coefficient of the best fit line for data from the present study was 0.525.

Again when I_l was plotted against the right hand side of the 'energetics' equation 5.19, similar comparisons were obtained (Figure 5.4). The scatter of data points produced by this study was again much greater than for Komar's study and the two coefficients were respectively 0.179 and 0.28.

The greater data scatter observed in this study, reflected in the low R^2 values for the best fit lines of 22% and 32% respectively for Figures 5.3 and 5.4, is probably accounted for by differences in fieldwork techniques. More sophisticated equipment was employed by Komar for measuring such things as wave characteristics and, furthermore, sampling was carried out three or four times during the tidal cycle giving a more

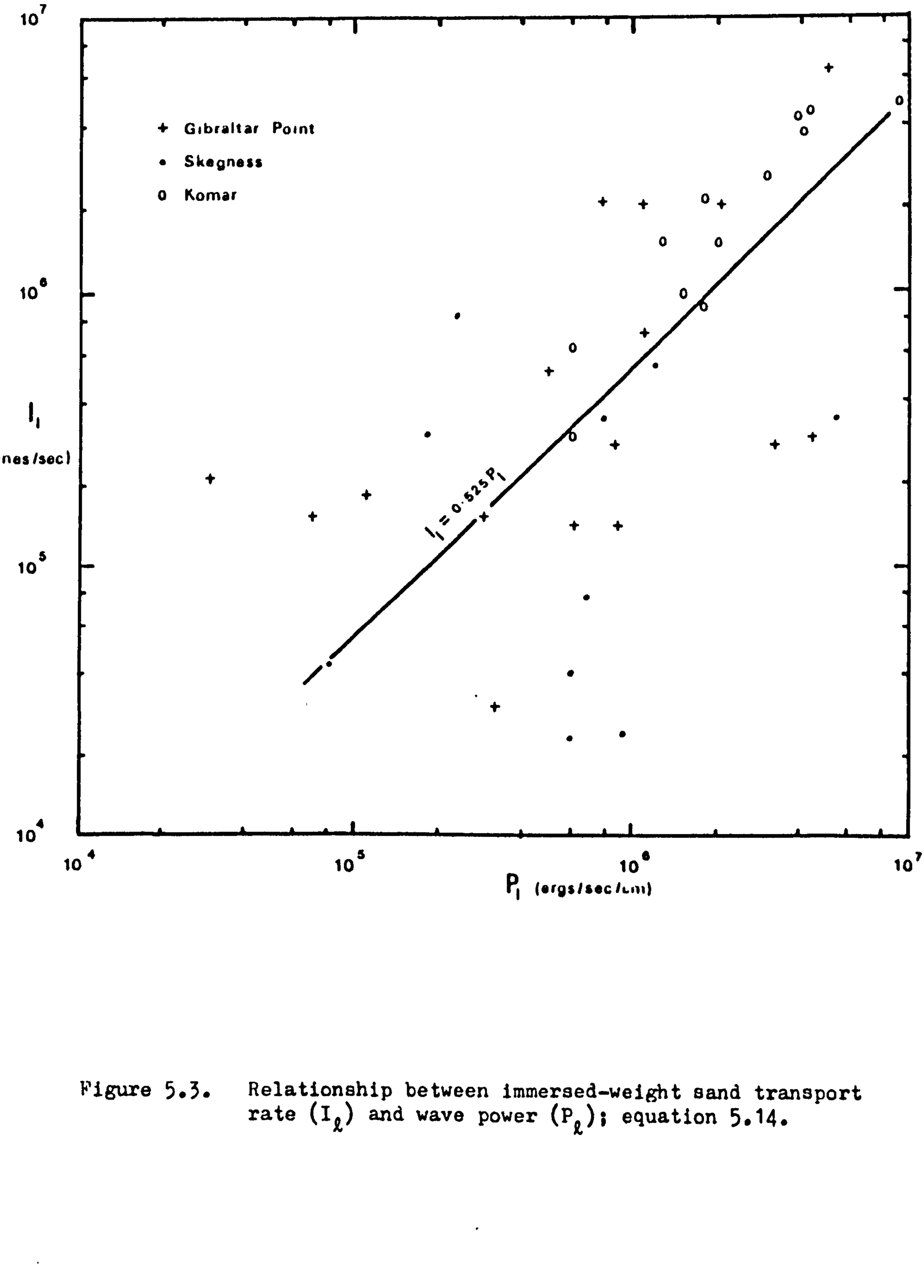

Figure 5.3. Relationship between immersed-weight sand transport rate (I_ℓ) and wave power (P_ℓ); equation 5.14.

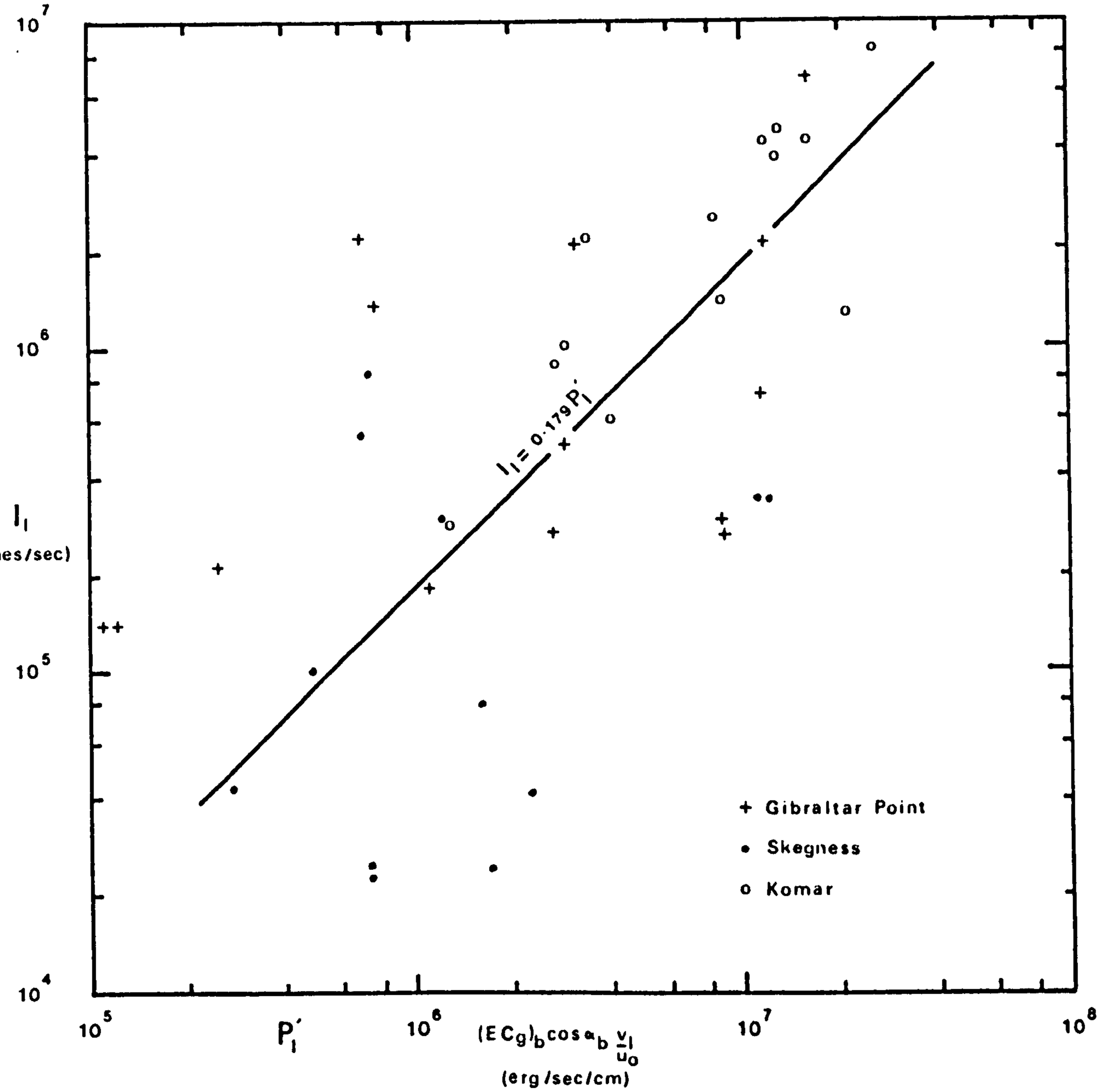

Figure 5.4. Relationship between immersed-weight longshore sand transport rate (I_l) and the model of equation 5.19 as deduced by Inman and Bagnold (1963).

TABLE 5.1 Bulk sand transport rates (sand advection rates) S_ℓ , and immersed weight sand transport rates I_ℓ

G I B R A L T A R P O I N T

Date			Average longshore distance of tracer movement (m)	t (secs)	V_ℓ (cm/sec)	b (cm)	X_ℓ (cm)	S_ℓ (cm^3/sec)	$I_\ell \times 10^5$ (dyne/sec)
2.11.75			5.61	10800	.052	1.12	3000	174.7	1.49
17.1.76			31.87	15600	.204	3.60	2200	1615.7	13.78
28.2.76			0.63	21600	.003	0.70	2000	4.1	0.03
18.3.76	U.R.		27.65	21600	.230	3.45	3100	2459.9	20.99
18.3.76	L.R.		6.95	19800	.035	3.55	2000	248.5	2.12
17.5.76			7.52	20400	.037	2.57	2200	209.2	1.78
30.6.76			12.82	19800	.065	2.18	2200	311.7	2.66
15.7.76			4.84	14400	.036	1.60	3000	172.8	1.47
10.8.76			7.62	18000	.042	3.00	2700	340.2	2.90
7.9.76	U.R.	(H3)	0.02	14400	.0001	2.56	2200	0.7	0.006 *
7.9.76	L.R.	(H3)	8.02	18000	.045	1.98	3500	311.9	2.66
22.9.76	U.R.		18.59	9000	.207	3.26	3500	2361.9	20.16
22.9.76	L.R.		43.95	9600	.458	4.97	3500	7966.9	67.99
6.10.76			15.88	20400	.078	2.33	3200	581.6	4.96
6.10.76			5.89	14400	.041	2.73	1500	167.9	1.43
23.10.76		(H3)	35.72	18000	.198	4.25	3000	2524.5	21.55
23.10.76		(H2)	17.67	18000	.098	2.84	3000	174.7	7.1

Continued overleaf

TABLE 5.1 continued

Date		Average longshore distance of tracer movement (m)	S K E G N E S S t (secs)	V_ℓ (cm/sec)	b (cm)	X_ℓ (cm)	S_ℓ (cm^3/sec)	$I_\ell \times 10^5$ (dyne/sec)
18.5.76		3.29	27900	.012	1.33	3000	47.9	0.41
1.7.76		6.87	18000	.038	3.36	5000	638.4	5.45
14.7.76		4.41	27000	.016	1.10	1500	26.4	0.23
12.8.76		3.06	22800	.013	1.07	2000	27.8	0.24
25.876	U.R.	2.22	15600	.014	1.41	2500	50.1	0.43
25.8.76	L.R.	5.55	25200	.022	2.10	2000	92.4	0.79
8.9.76	.	13.53	16800	.081	2.98	4000	965.5	8.24
21.9.76		6.97	25200	.028	3.97	4000	444.6	3.39
7.10.76	U.G.	5.93	22300	.024	1.85	2500	111.0	0.95
7.10.76	L.G.	3.25	34800	.009	1.02	3000	27.5	0.24
22.10.76	U.G.	17.59	19800	.089	1.32	3000	347.1	2.96
22.10.76	L.G.	0.80	19800	.00003	1.52	2000	.09	0.0008*

N.B. $I_\ell = (p_s - p)\, gaS_\ell$

* These two points were omitted from analysis since sand movement was overwhelmingly normal to the shore. See Figures 4.14 and 4.25.

TABLE 5.2 Wave and wave power quantities

G I B R A L T A R P O I N T

Date	$H_b^{\frac{1}{3}}$ (cm)	H_{rms} (cm)	ECg x 10^5 (ergs/cm sec)	α_b (degrees)	P_ℓ x 10^5 (ergs/cm sec)	h_b (cm)	u_m (cm/sec)	v_ℓ (cm/sec)	$(ECg)\cos\alpha_b \frac{v_\ell}{u_m}$ x 10^5
2.11.75	16.3	12.9	7.1	6.0	0.7	28.8	37.7	6.0	1.1
17.1.76	39.2	27.6	47.3	11.0	8.9	34.7	73.5	11.9	7.5
28.2.76	38.8	27.4	46.2	4.0	3.2	51.6	59.7	16.2	13.4
18.3.76 U.R.	40.0	28.2	75.4	9.0	7.7	41.4	69.7	6.4	6.9
18.3.76 L.R.	26.0	18.3	16.9	1.0	0.3	45.7	42.5	6.4	2.5
17.5.76	43.5	30.7	60.2	1.0	1.1	44.1	72.4	23.3	11.4
30.6.76	46.6	32.9	72.0	8.0	8.6	62.1	65.3	69.0	76.4
15.7.76	37.1	26.2	4.4	4.0	2.9	55.5	55.0	15.6	1.2
10.8.76	53.4	37.7	102.8	26.0	40.5	54.6	79.8	65.5	75.9
7.9.76 U.G.	49.2	34.7	83.7	26.0	33.0	39.4	83.4	30.1	26.2
7.9.76 L.G.	47.3	33.4	75.9	26.0	29.9	39.2	79.8	30.1	24.6
22.9.76 U.G.	55.3	39.0	112.0	11.0	21.0	48.3	87.9	25.9	32.4
22.9.76 L.G.	78.7	55.5	270.8	11.0	50.7	66.5	106.6	70.0	174.7
6.10.76 U.G.	39.1	27.6	47.1	6.0	4.9	44.2	64.9	40.5	29.2
6.10.76 L.G.	42.8	30.2	59.0	6.0	6.1	50.4	66.3	38.4	34.0
23.10.76 H3	55.0	38.8	107.8	6.0	11.2	60.0	78.4	83.8	115.9
27.10.76 H2	55.0	38.8	107.8	6.0	11.2	60.0	78.4	83.8	115.9

Continued overleaf

TABLE 5.2 continued

Date		S K E G N E S S $H_b^{\frac{1}{3}}$ (cm)	H_{rms} (cm)	$ECg \times 10^5$ (ergs/cm sec)	α_b (degrees)	$P \times 10^5$ (ergs/cm sec)	h_b (cm)	u_m (cm/sec)	v_ℓ (cm/sec)	$(ECg)\cos\alpha_b \frac{v_\ell}{u_m} \times 10^5$
10.5.76		39.6	27.9	48.6	8.0	5.9	47.1	63.7	30.4	23.0
1.7.76		60.0	42.3	13.7	4.0	12.0	61.0	84.8	43.1	6.9
14.7.76		21.9	15.4	11.6	1.0	0.01	30.0	44.2	29.0	7.3
12.8.76		33.9	23.9	33.0	18.0	9.2	23.9	76.6	41.3	17.0
25.8.76	U.R.	29.1	20.5	22.5	3.0	0.8	34.0	39.0	4.7	2.7
25.8.76	L.R.	31.6	22.3	27.7	16.0	6.9	43.6	52.8	32.4	16.4
8.9.76		44.5	31.4	65.1	3.0	2.3	21.1	88.1	9.6	7.1
21.9.76		76.3	53.8	250.8	14.0	54.9	62.7	106.4	51.3	118.0
7.10.76	U.R.	35.8	25.3	37.8	1.0	0.04	32.5	69.4	9.1	4.9
7.10.76	L.R.	32.3	22.8	29.2	13.0	6.0	44.6	53.4	13.3	7.1
22.10.76	U.R.	34.3	24.2	34.0	4.0	1.8	31.3	67.7	24.4	12.2
22.10.76	L.R.	33.5	23.6	32.0	1.0	0.03	26.1	61.6	13.7	7.1

N.B. $H_{rms} = H^{\frac{1}{3}} / 1.418$

$u_m = (2E_b / ph_b)^{\frac{1}{2}}$

$Cg = 8.02\, H^{\frac{1}{2}}_{rms}$

accurate picture of tracer movement. Despite this, as has been seen, a similar relationship amongst the data points can be identified.

Where possible comparable methods of calculation were used to produce the plotted data. However, one other source of discrepancy was envisaged arising from the contrasting nature of the tidal range in the study areas. Because of a limited tidal range Komar was able to concentrate solely on the surf and swash/backwash zones in his study. At Skegness and Gibraltar Point on the other hand, processes operating seaward of the breaker zone also affected tracer movement due to the much larger tidal range and the positioning of tracer release points. Therefore there are slight differences between the values of the constants for the two models produced by the data from this study and by Komar's earlier work. However, this might well be expected given the differences in experimental procedure and the fact that both data sets are only samples of the total population. The fact that the values of the derived coefficients are close confirms the validity of the two models.

A final point arising from Komar's (1969) test of the two models of sand transport concerns the importance of beach slope in the mechanism of sand transport. Komar's two study sites had quite contrasting slope characteristics but this did not lead to any significant differences when the tests of the transport models were conducted. This was explained by the equivalence of the two models given conditions of longshore current generation by oblique wave approach. By simultaneous solution of the two equations 5.14 and 5.19 Komar obtained the relationship expressed in equation 5.20 where 2.7 is the value of the relation K/K'. Substituting the values of K and K' obtained from this study into the relation K/K' the value 2.9 was produced, again reasonably close to Komar's result. Comparison of equation 5.20 with the following theoretical relationship for longshore current generation based on radiation stress concepts,

Longuet-Higgins (1970):

$$v_\ell = \frac{5\pi}{8} \frac{\tan \beta}{c_f} u_m \sin \alpha_b \qquad \text{Eq. 5.28}$$

where $\tan \beta$ = beach slope;

c_f = drag coefficient,

shows that it differs only by the presence of the factor $\tan \beta / c_f$.

From a plot of longshore current velocity with the expression $u_m \sin \alpha_b$ it was found that the best fit straight line closely approximated 2.7, the value given by the relation K/K' for the two proportionality coefficients of the transport equations. This was taken to indicate that:

$$\frac{\tan \beta}{c_f} \simeq \text{constant} \qquad \text{Eq. 5.29}$$

with the drag coefficient increasing proportionally with an increase in beach slope and hence explaining the lack of dependence of transport rate on beach slope. However, as pointed out earlier, longshore flowing current may be generated in several ways and so this lack of dependence of sand transport on beach slope may not always be the case. This question will be considered further in later chapters in light of regression analysis.

In summary, it may be said that the results of the test of the two sand transport models with data collected from this study have a high degree of agreement with the findings of Komar's field tests of the models and this may be taken as an indication of the efficiency of the two models in predicting longshore sand transport rates.

CHAPTER 6

REGRESSION MODEL OF SAND MOVEMENT : AMOUNT

6:1 INTRODUCTION

It was seen in Chapter 5 that much attention has been given to the production of longshore sand transport rates. However, in the model to be developed the amount of sand transport is not expressed as a volume or bulk transport rate, rather in simpler terms, as the average distance moved by sand grains during one tidal cycle. This is a more fundamental measure and seems to reflect more accurately the magnitude of sand grain movements of the small scale tracer experiments. Bulk sand transport formulae are based upon some measure of distance travelled by sand grains over a given time period but are also sometimes made less accurate by the inclusion of nominal or poorly measured variables such as disturbance depth or beach face width. For example, large errors can be introduced by the inaccurate measurement of the depth to which sand movement takes place. The sampling results of tracer concentration used in this study do contain some error due to non-core sampling methods but this error is not compounded by the separate entry of depth of disturbance in a sand transport equation. Since the contour maps of tracer concentration exhibit regularities and systematic patterns, it is assumed that sampling was generally adequate in defining the trend of movement and that any error arising from the lack of complete information on depth of disturbance did not have a large effect.

The distance moved by the centre of gravity of the tracer cloud during the tidal cycle is used to provide the measure of <u>average distance</u> of sand grain movement and the calculation of this from the tracer maps is described in Section 3:5. As this measure also has a directional component, which may be thought of as the <u>average direction</u> of sand grain movement,

it may be seen as a vector quantity. As such it may be resolved into two orthogonal components which are the x and y coordinates of the centre of gravity from the origin, the tracer source. These coordinates may then be taken to reflect average alongshore distance travelled by the tracer grains and average distance moved orthogonal to the line of beach. Thus in this way magnitude of sand movement alongshore and onshore/offshore are considered separately.

Description and prediction of the process-response system concerning the amount of sand movement in the two general directions is attempted using linear multiple regression techniques. Both stepwise and combinatorial multiple regression methods are used. Komar (1976) has criticised the use of regression type methods on three counts:

1 The results of this type of analysis are always dependent upon the data base and really apply only to that data;

2 No physical reasoning goes into their formulation;

3 The results depend upon the technique employed.

It is certainly true that extrapolation of predictive-type equations produced by regression analysis is dangerous and that the results are dependent upon the data base but this applies to every form of analysis and is not specific to regression techniques. Similarly, the assertion that the actual technique employed affects the results is also a very general point and is true of all experimental situations. Furthermore, the use of regression type methods does not preclude physical reasoning. Careful selection of variables for use in the analysis must necessarily take account of physical relationships in the interaction of sediment and fluid in the foreshore zone. It is also important to stress the exploratory role of these methods within the framework of scientific reasoning. The regression model is being employed in this study as an exploratory tool and any findings should form the basis of further study perhaps employing inferential methods. Finally, Harrison

(1964) justifies the use of regression analysis by referring back to physical equations. He found that sequential type linear multiple regression analysis reasonably duplicated " ... the expectable influence of combinations of important variables as suggested by theoretical and empirical approaches when studied by a straightforward least-squares procedure." (Harrison, 1964, p. 24).

6:2 The general regression model

Regression analysis involves the specification and identification of the type and nature of the dependence of a single variable upon a set of controlling, predictor or explanatory variables (Mather, 1976, p. 39). Underlying regression techniques is the basic postulate that the variations in a dependent variable (y term) is made up of two parts, one part of which is postulated to be deterministically related to the explanatory variables (x terms) and a second part which appears to be random. The deterministic part of the relationship may take any form but the linear model is the most frequently used, for reasons given in a previous discussion (p.171). The linear regression model describes the linear relationship between a random vector variable $[y]$ and a set of explanatory variables $[x_1]$, $[x_2]$ ... $[x_k]$. The general form of the relationship is:

$$[y] = \beta_o + \beta_1 [x_1] + \beta_2 [x_2] + ... + \beta_k [x_k] + [\varepsilon] \qquad \text{Eq. 6.1}$$

where $[\varepsilon]$ is the disturbance term or residual term associated with the observed values. If $[x_o]$ is a unit vector then this equation can be rewritten as:

$$y_i = \sum_{j=1}^{k} \beta_i [x_{ij}] + \varepsilon_i \quad (i = 1,2 .... n) \qquad \text{Eq. 6.2}$$

or in matrix notation as:

$$[y] = [X] [\beta] + [\varepsilon] \qquad \text{Eq. 6.3}$$

The β's are the parameters of the model which are to be estimated. The term β_o is the constant term or intercept. This term gives the value of y when all the x's are zero. It is the level of the dependent variable in the absence of any control by the explanatory variables. The remaining β_i's are the partial regression coefficients and they give the change in the corresponding x (independent of the level of the other x's) when y is increased by one unit.

When the regression equation contains an intercept term, β_o, the regression is said to pass 'through the mean'. However, in certain circumstances, in particular in physical geography, the existence of the constant term may not be consistent with the physical explanation of the regression. For example, in the simple case of regression of bedload sediment transport on fluvial discharge carried out through the mean, a strict interpretation of this would be that even when fluvial discharge is nil there is a sediment transport equivalent to the intercept term. This makes nonsense in physical terms, and so the regression must be constrained to pass through the origin so that when river discharge is zero the bedload also is nil. A similar situation arises in the case of beach sand movement and hence the regression model as used in this chapter also excludes the intercept term.

It is not proposed to enter into a detailed consideration of the mathematical and computational aspects of regression analysis in this chapter. Many texts have been produced, in a wide range of disciplines, on all aspects of regression. For a clear account of the practical application of regression techniques the reader is referred to Draper and Smith (1966) whilst a more mathematical treatment of linear models is given by Seber (1977). Mather (1976) deals with the computational problems of regression and provides many routines and programs.

Best linear unbiased estimates of the regression coefficients are calculated by least-squares methods and then because of scale problems these are usually standardised. At various stages tests are carried out

to determine how far certain conditions for the successful application of the regression model are being met. In general, the following assumptions are made when the regression model is applied:

1) The mean of $[\varepsilon]$ is zero.

2) The variances of the error terms are independent of the values of x .

3) Explanatory variables are non-random and are measured without error.

4) The explanatory variables are not perfectly linearly related, i.e. there is no multicollinearity within the x's.

5) The number of observations exceeds the numbers of x's.

6) No autocorrelation occurs in adjacent values of ε_i.

7) If statistical tests are to be used the conditional distribution of y given x should be approximately normal.

6:3 Choosing the 'best' regression

Two main methods of regression analysis were used in this chapter in order to provide the maximum amount of information on the optimum regression. These were the combinatorial method and the stepwise method.

The combinatorial method involves the computation of all possible regression equations including all combinations of the explanatory variables. This approach is sometimes known as sequential regression because it proceeds by taking the controlling variables one at a time, two at a time and so on until all combinations of the explanatory variables are included simultaneously. The number of combinations of k variables, that is the number of regression equations, it is necessary to calculate is 2^k-1. Consequently, it is only with the recent development of large, fast computer systems and efficient programs that this approach has been made possible. It is a very useful technique which provides a great deal of information on the regressions and allows the relative importance of individual variables to be traced at each stage. The program for the combinatorial regression used in this study is described by Grosenbaugh (1967).

On the other hand the stepwise method is far more economical as only selected regressions are calculated. Stepwise regression is in fact an improved version of the forward selection procedure whereby variables are added to the regression equation based on "partial F. tests". Hence, it provides a means of selecting automatically the 'best' regression equation containing the 'best' subset of variables. Draper and Smith (1966) believe this to be the best of what they term the "variable screening" procedures and recommend its use in preference to any of the alternative backward or forward elimination methods. Nevertheless it is not always successful as will be discussed in later paragraphs.

The stepwise procedure begins with the matrix of correlations between all the explanatory variables and the dependent variable from which the x that is most highly correlated with y is entered into the regression. Using partial correlation coefficients the next variable to enter the regression is selected and an F-test on the significance of the regression is calculated. At this stage the individual contribution of the included variables is examined by means of a partial F test to determine whether any should be deleted. This process continues with variables being added and/or deleted until a point is reached when next highest partial correlation in the subset of unentered variables is not statistically significant and no further variable is added or deleted. The existing combination of variable(s) then forms the 'best' regression equation. In this study low probability values of 2% are used in order to extend the exploratory nature of the analysis and increase the number of variables entered into the regression equation. Normally a much higher significance level is chosen but more information concerning the relative importance of the variables can be gained from the use of a low value.

Screening procedures, including the stepwise method, have been criticised by many workers on the grounds that the 'best' equation may not be

produced. Grosenbaugh (1967), for example, provides an illustration of this criticism and also considers invalid the tests of significance applied at each cyle of the procedure. In fact there may not be a single 'best' equation but several near optimal combinations of x's. Hauser (1974) contends that due to interdependence or multicollinearity amongst the independent variables several 'best' equations may exist. Examining this problem in detail he suggests that the existence of a number of different equations with similar explanatory content may be a serious problem when considering the theoretical implications of particular equations. On the other hand the problems may not be so serious for the derivation of predictive equations.

However, in the main the choice of the best regression will depend upon the details of each particular study and the reasons for the regression analysis. From a practical point of view the cost of measurement or ease of measurement of individual variables may be of great importance. In this situation it would be advantageous to know all the 'best' equations so that selection by inspection rather than statistical test might be made.

Computationally the estimation of the optimum regression may depend also on the measure of efficiency adopted. R^2 or the sums of squares criterion is the most commonly used measure of the explanatory value of a certain combination of variables. It is the test used in the stepwise procedure carried out in this study, the program for which is listed by Mather (1976). Also known as the coefficient of determination it measures the efficiency of each equation in explaining variation in the dependent variable (y). It is represented by the ratio of the sums of squares due to the regression to the total sums of squares and usually expressed as a percentage. However, Maddala (1977) points out that when regression through the origin is performed calculations of R^2 may be inaccurate unless the following equation is used:

$$R^2 = \frac{\hat{\beta}' S_{xy}}{S_{yy}} \qquad \text{Eq. 6.4}$$

where $S_{xy} = \Sigma x_i y_i$

$S_{yy} = \Sigma y_i^2$

$\hat{\beta}'$ = regression coefficients.

R^2 is generally most useful when the number of samples is several times the number of process variables. As the number of x's measured approaches the number of observations or cases, the sum of squares criterion tends to be forced closer to 100% and therefore may give the impression of explaining a greater part of the variability than is correct. Thus, for 10 variables the minimum number of observations should be 20-30. In some of the regressions carried out in this study a maximum of 16 variables is used with 29 observations. This is on the borderline of statistical acceptance and must be borne in mind when attaching significance to the results.

A further problem with R^2 is that it must increase with the addition of successive variables; it cannot fall in value because it is dependent upon the number of variables present. This may lead to difficulties when estimating the usefulness of particular regression. Because of these problems, the value of R^2 is often adjusted to give $\bar{R}^2$, termed "R^2 adjusted for degrees of freedom". This alternative measure is calculated from:

$$\bar{R}^2 = R^2 - \frac{k-1}{n-k}\ 1 - R^2 \qquad \text{Eq. 6.5}$$

where k = number of coefficients;

n = number of observations.

Thus $\bar{R}^2$ takes account of the number of variables and the degrees of freedom and hence does not always increase with the addition of more variables. $\bar{R}^2$ rather than R^2 should always be used when comparing equations with different numbers of independent variables. Both R^2 and $\bar{R}^2$ are calculated for regressions in this study.

A third measure used in the combinatorial regression procedure employed in this study is relative mean squared residual (R.M.S.R.). This is not a monotonic function as is R^2 but "fluctuates in an unpredictable manner depending upon both the sums of squares and degrees of freedom" (Grosenbaugh, 1967, p.12). Nevertheless, it is still partially related to the number of variables because degrees of freedom themselves are dependent upon the number of x's. R.M.S.R. is generated by the calculation of the mean squared residuals relative to the variance about the dependent variables and its minimum value indicates the best combination of variables.

6:4 Independent variables

The variables specified as explanatory variables in the analysis were selected on the basis of intuition constrained by the practicalities of field measurement. Fieldwork methods are described in Chapter 3. In the main the variables chosen were those found to be useful in previous field and laboratory studies. However, with the complex nature of the beach-nearshore tidal environment it is virtually certain that the variables measured will not account for all the systematic variations in any chosen dependent variable. For a variety of reasons it is possible that a significant variable will be omitted completely or that others that are included will exert little influence in the analysis. In this study limited fieldwork capability provided

the major constraint on the number of variables included. One possibly significant variable not measured was the height of the water table in the beach face. Duncan (1964) indicated the importance of the water table fluctuations to beach foreshore changes through its influence on the amount of erosion and deposition in the swash zone. Harrison (1969) attempted to quantify the relationship between changes in the water table level and foreshore sand volume and found that groundwater head was one of the strongest predictors of deposition or removal of foreshore sand over a tidal cycle. Groundwater head was defined as the vertical distance between the water table outcrop on the foreshore and the still water level in front of the breaking waves. In a later study Harrison et al (1971) suggested that the augmentation or diminution of the swash energy by groundwater flow through the lower foreshore or percolation into the upper foreshore must be taken into account when considering the available energy for sand grain transport.

In addition to lack of water table measurements, swash-backwash measurements were not taken regularly enough for their inclusion in the regression analysis. However, it is not clear how much of the explanatory value of these processes would be accounted for by variation in significant wave height which is the principal energy source of the swash-backwash processes.

All the variables used in the first series of regression analyses are shown in Figure 6.1 which summarises the models being fitted. Particular attention is drawn to the variables angle of wave approach and wind direction. Initially regression analysis was performed with these predictors expressed as bearings as measured in the field. However, due to the nature of directional data such as this and its underlying

Fig. 6.1 Summary of regression models for amount of sand movement with the selected independent variables.

(Y)		(X)
Amount of movement Alongshore	=	Wave height Wave period Longshore current Mean grain size Sorting Angle of wave approach
Amount of movement Offshore/onshore	=	Wind speed Wind direction Tidal height Average beach slope Water temperature Trough to bottom distance Period of inundation Depth of water at tracer injection point

circular distribution the results of the regressions were found to be uninterpretable. To avoid this problem, angle of wave approach and wind data were re-expressed. Wave approach was entered in all regressions as an angle with the line of the beach whilst the wind data was transformed according to the dependent variable of the regression. For example in the regression of sand movement alongshore three 'wind' variables were included: average wind speed in direction of sand movement, average wind speed opposite to direction of sand movement and wind speed onshore/offshore. To facilitate this wind directions were defined as alongshore if having a bearing making an angle of less than 20^{o} with the bearing of the beach, offshore for a wind with a direction deviating $\pm$ 20^{o} from a wind vector perpendicular to the shore and in an offshore direction and onshore for a wind with a deviation $\pm$ 70^{o} from the orthogonal wind vector and blowing in an onshore direction.

In addition, when dealing with alongshore sand movement, direction of longshore current flow was introduced by splitting this variable into current flow against sand movement and current flow in same direction as sand movement. Only on four occasions was current flow opposite to sand movement. When orthogonal sand movement was being considered, no account was taken of longshore current direction of flow. More attention will be given to the problem of multivariate analysis with directional data in the next chapter.

In multiple regression analysis it is important that the ratio of observations or cases to the number of independent variables is as large as possible. It was possible to use the results of only 29 of the tracer experiments in this study and with a maximum of 16 predictor variables some reduction of these was thought advisable. In this way

confirmation of the first phase regressions was felt might be possible and hence more reliable results achieved.

Dimensional analysis provides one means of reducing the number of variables in a problem without large information loss. Langhaar (1951) defines this technique as a method by which it is possible to deduce information about a phenomenon from a single premise that the phenomenon can be described by a dimensionally correct equation among certain variables. The analysis is conducted through the use of Buckingham's Pi Theorem which states that:

> If an equation is dimensionally homogeneous it can be reduced to a relationship among a complete set of dimensionless products.

However, a necessary condition of this technique is that all variables which influence a particular phenomenon are contained in the equation. Consequently this technique could not be used in this study since, as mentioned earlier, not all significant variables were measured. Instead, an approach retaining the idea of dimensionless variables and used by Harrison (1969) was adopted here. Harrison used dimensional analysis to produce empirical equations for geometrical foreshore changes over a tidal cycle and reduced 15 independent variables measured in a 26-day time-series to 8 dimensionless terms. However, it was found that the series of 8 terms had a commonality of the variable $\bar{H}_b$, mean wave height, which produced problems of multicollinearity between the dimensionless ratios when used in regression analysis.

To overcome this problem, Harrison specified a set of dimensionless variables which, although not part of a dimensionally homogeneous equation, were nevertheless dimensionless and were also devised such that commonality was completely removed. The variables were cast as ratios with physical significance based on an understanding of the processes involved. As an expression of average breaker steepness the dimensionless variable

$(\overline{H}_b / g\overline{T}_b^2)^{\frac{1}{2}}$ was used where $\overline{H}_b$ and $\overline{T}_b$ are average wave height and average wave period respectively and g is acceleration due to gravity. Galvin (1968) used this as an index of 'breaker steepness' in an attempt to develop a classification of breaker types on laboratory beaches but also included beach slope in the ratio. As it was felt important to assess the affect of beach slope itself this was removed from Galvin's ratio and entered as a separate variable. A further dimensionless term was produced by combining mean trough to bottom distance in front of the breaking wave $(\overline{Z})$ with mean grain size $(\overline{D})$ in the ratio $\overline{D} / \overline{Z}$. It was hoped this would reflect the interplay of grain size and swash characteristics in the movement of the beach sediment. Angle of wave approach and sea water temperature were also included as dimensionless variables in themselves. Hence the number of controlling variables was reduced to five dimensionless terms. These are shown in Figure 6.2. Regression analysis was conducted with these variables in exactly the same way as for the 'raw' variables. Results of the analysis are discussed in the next two sections. Raw data values for all variables are to be found in Tables 6.1 to 6.6.

6:5 Alongshore sand movement

Stepwise and combinational regression analyses were conducted using the mean distance of grain movement alongshore as the dependent variable (Table 6.2). Sixteen independent variables were included in the stepwise procedure but because of computer core capacity limitations only eleven X variables could be used in the combinatorial regression. Nevertheless, for ease of description the variable numbers shown in Table 6.7, the complete list of specific variables included in the stepwise program, were also used in the combinatorial method of regression. The omitted variables will be discussed later.

From Table 6.8 it can be seen that the first variable entered into the

Fig. 6.2. Summary of regression models for amount of sand movement with the dimensionless variables.

(Y)		(X)
Amount of Movement		Breaker type
Alongshore		Grain size/swash characteristics
	=	Wave approach angle
Amount of Movement		Beach slope
Offshore/onshore		Water temperature

Table 6.1 Dependent Variables : amount of sand movement

	GIBRALTAR POINT			SKEGNESS	
	Mean Distance of Grain Movement Alongshore (M)	Mean Distance of Grain Movement Onshore/Offshore (M)		Mean Distance of Grain Movement Alongshore (M)	Mean Distance of Grain Movement Onshore/Offshore (M)
1	5.61	5.18	1	3.29	0.64
2	31.87	1.74	2	6.87	10.54
3	0.63	5.62	3	4.41	0.85
4	27.65	1.03	4	3.06	0.02
5	6.95	0.07	5	2.22	0.77
6	7.52	0.10	6	5.55	2.07
7	12.82	2.39	7	13.53	11.30
8	4.84	0.16	8	6.97	4.88
9	7.62	0.26	9	5.93	4.26
10	0.02	0.58	10	3.25	0.12
11	8.02	5.33	11	17.59	0.43
12	18.59	1.10	12	0.80	0.60
13	43.95	1.77			
14	15.88	2.67			
15	5.89	1.29			
16	35.72	0.74			
17	17.67	1.36			

Table 6.2 Process Variables : GIBRALTAR POINT Sites

Sample No.	Description	Mean Wave Height (cm)	Mean Wave Period (secs)	Mean Grain size (units)	Grain Sorting (units)	Angle of Wave Approach (°)	Predicted Tide Height (M)	Average Beach Slope (tan β)	Period of Inundation (hrs)	Depth of Water at Injection Point (m)	Water Temp. (°C)	Trough to Bottom Distance of Breaking Wave (cm)	Longshore Current Velocity (cm/sec)
1	2.11.75 UR	18.3	3.24	1.155	1.007	6.0	7.0	0.0441	3.0	2.850	11.5	28.8	6.0
2	17.1.76 UR	39.2	2.86	1.931	0.682	11.0	6.9	0.0433	4.33	0.10	6.5	34.7	11.9
3	28.2.76 LR	38.8	3.66	2.319	0.659	4.0	6.7	0.0232	6.0	1.521	6.0	51.6	16.2
4	18.3.76 UR	40.0	3.75	1.177	1.184	9.0	7.5	0.0414	3.33	1.054	6.5	41.4	6.4
5	18.3.76 LR	26.0	3.91	2.185	0.789	1.0	7.5	0.0221	5.5	3.115	6.5	45.7	6.4
6	17.5.76 LR	43.5	3.43	2.208	0.716	1.0	6.7	0.0205	5.66	1.688	15.0	44.1	23.3
7	30.6.76 LR	46.6	2.73	2.455	0.436	8.0	6.6	0.0209	5.5	1.663	23.0	62.1	69.0
8	15.7.76 LR	37.1	3.33	2.418	0.469	4.0	6.5	0.0211	4.0	1.535	21.5	55.5	15.6
9	10.8.76 LR	53.4	3.6	2.439	0.615	26.0	6.8	0.0270	5.0	1.577	20.0	54.6	65.5
10	7.9.76 LR	49.2	5.36	1.862	1.049	26.0	6.7	0.0368	5.0	1.516	19.0	39.4	30.1
11	7.9.76 LR	47.3	5.36	2.156	0.621	26.0	6.7	0.0077	4.0	0.756	19.0	39.2	30.1
12	22.9.76 UR	55.3	5.0	1.919	0.573	11.0	6.8	0.0280	2.5	0.616	17.0	48.3	25.9
13	22.9.76 LR	78.7	4.29	2.184	0.648	11.0	6.8	0.0300	4.75	2.484	17.0	66.5	70.0
14	6.10.76 LR	39.1	4.93	2.337	0.517	6.0	6.6	0.0312	5.66	2.162	16.0	44.2	40.5
15	6.10.76 LR	42.8	5.0	2.198	0.676	6.0	6.6	0.0154	4.0	0.485	16.0	50.4	38.4
16	23.10.76 LR	55.0	3.75	2.214	0.648	6.0	7.4	0.0249	5.0	2.477	12.0	60.0	83.8
17	23.10.76 LR	55.0	3.75	2.119	0.656	6.0	7.4	0.0277	5.0	2.588	12.0	60.0	83.8

Table 6.2 continued. Process Variables : SKEGNESS Site

Sample No.	Description	Mean Wave Height (cm)	Mean Wave Period (secs)	Mean Grain Size (units)	Grain Sorting (units)	Angle of Wave Approach (°)	Predicted Tide Height (M)	Average Beach Slope (tanβ)	Period of Inundation (hrs)	Depth of Water at Injection Point (m)	Water Temp. (°C)	Trough to Bottom Distance of Breaking Wave (cm)	Longshore Current Velocity (cm/sec)
1	18.5.76 LR	39.6	3.0	1.935	1.005	8.0	6.4	0.0157	7.74	2.581	14.0	47.1	30.4
2	1.7.76 UR	60.0	3.37	1.259	1.523	4.0	6.5	0.0612	5.0	0.423	20.5	61.0	43.1
3	14.7.76 LR	21.9	3.53	2.163	0.780	1.0	6.7	0.0073	7.33	3.254	19.8	30.0	29.0
4	12.8.76 LR	33.9	2.61	2.097	0.873	18.0	6.7	0.0149	6.33	3.085	22.0	23.9	41.3
5	25.8.76 UR	29.1	3.16	0.831	1.720	3.0	6.9	0.0463	4.33	1.151	22.0	34.0	4.7
6	25.8.76 LR	31.6	3.08	2.328	0.668	16.0	6.9	0.0093	7.0	3.409	23.5	43.6	32.4
7	8.9.76 UR	44.5	4.74	0.066	1.846	3.0	6.8	0.0574	4.6	1.009	18.0	31.1	9.6
8	21.9.76 LR	76.3	5.17	2.112	0.940	14.0	6.4	0.0145	7.0	2.437	16.5	62.7	51.3
9	7.10.76 UR	35.8	5.43	-0.304	1.948	1.0	6.7	0.0679	6.25	1.116	14.5	32.5	9.1
10	7.10.76 LR	32.3	4.29	2.218	0.919	13.0	6.7	0.0146	8.37	2.803	14.5	44.6	13.3
11	22.10.76 UR	34.3	3.60	0.745	1.755	4.0	7.1	0.0507	5.5	1.573	12.0	31.3	24.4
12	22.10.76 LR	33.5	3.60	2.157	1.009	1.0	7.1	0.0190	7.0	3.157	12.0	36.1	13.7

Table 6.3 Dimensionless Variables : GIBRALTAR POINT

Sample No.	Description	$(\overline{H}_b/gT_b^2)^{\frac{1}{2}}$	$\overline{D}/\overline{Z}$	α (angle of wave approach)	$\overline{m}$ (beach slope)	t water temperature
1	2.11.75 UR	0.02334	1.559	6.0	0.0441	11.5
2	17.1.76 UR	0.03870	0.755	11.0	0.0433	6.5
3	28.2.76 LR	0.03008	0.388	4.0	0.0232	6.0
4	18.3.76 UR	0.02981	1.068	9.0	0.0414	6.5
5	18.3.76 LR	0.02305	0.481	1.0	0.0221	6.5
6	17.5.76 LR	0.03399	0.490	1.0	0.0205	15.0
7	30.6.76 LR	0.04420	0.293	8.0	0.0209	23.0
8	15.7.76 LR	0.03233	0.337	4.0	0.0211	21.5
9	10.8.76 LR	0.03588	0.337	26.0	0.0270	20.0
10	7.9.76 LR	0.02268	0.571	26.0	0.0368	19.0
11	7.9.76 LR	0.02313	0.698	26.0	0.0077	19.0
12	22.9.76 UR	0.02629	0.547	11.0	0.0280	17.0
13	22.9.76 LR	0.03656	0.331	11.0	0.0300	17.0
14	6.10.76 LR	0.02242	0.393	6.0	0.0312	16.0
15	6.10.76 LR	0.02313	0.433	6.0	0.0154	16.0
16	23.10.76 LR	0.03496	0.360	6.0	0.0249	12.0
17	23.10.76 LR	0.03496	0.383	6.0	0.0277	12.0

Continued overleaf

Table 6.3. continued.

Dimensionless Variables : SKEGNESS

Sample No.	Description	$(\overline{H}_b/gT_b^2)^{\frac{1}{2}}$	$\overline{D}/\overline{Z}$	α (angle of wave approach)	$\overline{m}$ (beach slope)	t water temperature
1	18.5.76 LR	0.03708	0.556	8.0	0.0157	14.0
2	1.7.76 UR	0.04112	0.685	4.0	0.0612	20.5
3	14.7.76 LR	0.02344	0.743	1.0	0.0073	19.8
4	12.8.76 LR	0.03945	0.979	18.0	0.0149	22.0
5	25.8.76 UR	0.03020	1.653	3.0	0.0463	22.0
6	25.8.76 LR	0.03229	0.456	16.0	0.0093	23.5
7	8.9.76 UR	0.02489	2.645	3.0	0.0574	18.0
8	21.9.76 LR	0.02985	0.368	14.0	0.0145	16.5
9	7.10.76 UR	0.01948	3.800	1.0	0.0679	14.5
10	7.10.76 LR	0.02344	0.482	13.0	0.0146	14.5
11	22.10.76 UR	0.02875	1.907	4.0	0.0507	12.0
12	22.10.76 LR	0.02841	0.620	1.0	0.0190	12.0

Table 6.4 Wind Speed Variables for Onshore/Offshore Sand Movement Regression

	GIBRALTAR POINT				SKEGNESS		
	X(i)	X(ii)	X(iii)		X(i)	X(ii)	X(iii)
1	0.0	3.5	0.0	1	4.0	0.0	4.0
2	3.0	3.0	3.0	2	0.0	7.0	0.0
3	4.0	0.0	0.0	3	0.0	4.0	3.0
4	0.0	5.0	0.0	4	3.8	0.0	2.0
5	0.0	6.0	0.0	5	3.5	0.0	0.0
6	0.0	7.0	7.5	6	4.0	0.0	0.0
7	0.0	6.0	6.0	7	0.0	9.0	6.0
8	5.5	5.5	5.5	8	4.0	0.0	0.0
9	6.5	6.5	6.0	9	0.0	5.0	3.5
10	0.0	4.0	1.0	10	0.0	6.0	4.5
11	0.0	4.0	1.0	11	6.5	0.0	3.0
12	0.0	4.5	0.0	12	0.0	6.5	4.0
13	0.0	5.5	0.0				
14	0.0	13.0	11.0				
15	13.0	0.0	11.0				
16	0.0	14.0	10.0				
17	0.0	14.0	10.0				

X(i) Mean wind speed onshore/offshore in direction of sand movement

X(ii) Mean wind speed onshore/offshore against direction of sand movement

X(iii) Mean wind speed alongshore

Table 6.5 Wind Speed Variables for Alongshore Sand Movement Regression

	GIBRALTAR POINT				SKEGNESS		
	X(i)	X(ii)	X(iii)		X(i)	X(ii)	X(iii)
1	0.0	0.0	3.5	1	4.0	0.0	4.0
2	0.0	3.0	3.0	2	0.0	0.0	7.0
3	0.0	0.0	4.0	3	0.0	3.0	4.0
4	0.0	0.0	5.0	4	2.0	0.0	3.8
5	0.0	0.0	6.0	5	0.0	0.0	3.5
6	7.5	0.0	7.0	6	0.0	0.0	4.0
7	6.0	0.0	6.0	7	0.0	6.0	9.0
8	5.5	0.0	5.5	8	0.0	0.0	4.0
9	6.0	0.0	6.5	9	3.5	0.0	5.0
10	1.0	0.0	4.0	10	0.0	4.5	6.0
11	1.0	0.0	4.0	11	0.0	3.0	0.0
12	0.0	0.0	4.5	12	4.0	0.0	6.5
13	0.0	0.0	5.5				
14	11.0	0.0	13.0				
15	11.0	0.0	13.0				
16	10.0	0.0	14.0				
17	0.0	0.0	3.5				

X(i) Mean wind speed alongshore in direction of sand movement

X(ii) Mean wind speed alongshore against direction of sand movement

X(iii) Mean wind speed onshore/offshore

Table 6.6 Longshore Current Variables for Alongshore Sand Movement Regression

	GIBRALTAR POINT			SKEGNESS	
	X(i)	X(ii)		X(i)	X(ii)
1	6.0	0.0	1	30.4	0.0
2	11.9	0.0	2	0.0	43.1
3	0.0	16.2	3	0.0	29.0
4	6.4	0.0	4	41.3	0.0
5	6.4	0.0	5	4.7	0.0
6	23.3	0.0	6	32.4	0.0
7	69.0	0.0	7	0.0	9.6
8	15.6	0.0	8	51.3	0.0
9	65.5	0.0	9	9.1	0.0
10	30.1	0.0	10	13.3	0.0
11	30.1	0.0	11	24.4	0.0
12	25.9	0.0	12	13.7	0.0
13	70.0	0.0			
14	40.5	0.0			
15	38.4	0.0			
16	83.8	0.0			
17	83.8	0.0			

X(i) Mean longshore current velocity in direction of sand movement

X(ii) Mean longshore current velocity against direction of sand movement

Table 6.7 Independent Variables in Regressions of Distance Sand moved in an Alongshore Direction

X1 : Mean wave height (m)

X2 : Wave period (secs.)

X3 : Longshore current velocity in direction of sand movement (cm/sec)

X4 : Longshore current velocity in direction opposite to sand movement direction (cm/sec)

X5 : Mean grain size (phi units)

X6 : Mean wave angle (^{o})

X7 : Mean wind speed in direction of sand movement (cm/sec)

X8 : Mean wind speed in direction opposite to sand movement direction (cm/sec)

X9 : Mean wind speed onshore/offshore (cm/sec)

X10 : Predicted tide height (m)

X11 : Beach slope angle (^{o})

X12 : Length of time tracer covered (hrs)

X13 : Depth of water at injection point at high water (m)

X14 : Water temperature (^{o}C)

X15 : Grain sorting (phi units)

X16 : Trough to bottom depth in front of breaking wave (m).

Table 6.8 Results of Stepwise Regression of amount of Alongshore Sand Movement : 16 Independent Variables

ITERATION	REGRESSION EQUATION	$\bar{R}^2$	R^2	REGRESSION F TEST	PARTIAL F TESTS
1	Y = 27.303 X1	61.3	61.3	42.8 (99.9)	X1 42.8 (99.99)
2	Y = 48.633 X1 - 0.633 X14	67.0	68.2	27.9 (99.9)	X1 24.63 (99.99) X14 5.61 (84.03)
3	Y = 42.710 X1 - 0.703 X14 + 134.329 X11	68.3	70.6	20.0 (99.9)	X1 16.60 (99.53) X14 6.95 (89.99) X11 2.01 (42.19)
4	Y = 22.261 X1 - 0.721 X14 + 245.064 X11 + 0.200 X3	73.3	76.2	19.2 (99.9)	X1 2.96 (58.47) X14 8.64 (94.32) X11 6.16 (86.67) X3 5.61 (83.86)
5	Y = 21.629 X1 - 0.771 X14 + 217.561 X11 + 0.230 X3 + 1.626 X8	74.9	78.5	16.8 (99.9)	X1 2.97 X9 7.46 (58.49) (91.39) X14 10.32 X8 8.25 (96.65) (51.07) X11 4.99 (79.75)
10	Y = 33.68 X1 - 0.568 X14 + 388.759 X11 + 0.107 X3 + 2.549 X8 - 9.649 X15 + 4.769 X13 - 3.383 X12 + 2.218 X10 - 1.813 X2	81.4	87.4	12.5 (99.9)	X1 5.76 X15 2.25 (83.72) (46.41) X14 4.68 X13 3.22 (76.61) (61.47) X11 4.69 X12 5.14 (76.71) (79.98) X3 1.61 X10 2.37 (33.70) (48.56) X8 7.23 X2 1.08 (89.93) (21.76)

Continued overleaf

Table 6.8. continued.

INTERATION	REGRESSION EQUATION	$\bar{R}^2$	R^2	REGRESSION F TEST	PARTIAL F TESTS
15	Y = 46.46 X1 - 0.376 X14 + 418.192 X11 + 0.188 X3 + 1.992 X8 - 16.069 X15 + 2.333 X13 - 1.839 X12 + 3.441 X10 - 1.429 X2 - 29.406 X16 - 0.413 X6 - 0.644 X7 - 0.100 X4	80.0	89.3	8.3 (99.9)	X1 3.50 (64.51) X15 4.14 (71.0) X16 1.28 (26.18) X14 1.45 (30.12) X13 0.47 (7.64) X6 1.53 (31.79) X11 4.61 (75.08) X12 0.97 (19.23) X7 0.81 (15.30) X3 1.44 (29.81) X10 3.48 (64.06) X4 0.26 (3.42) X8 3.36 (62.50) X2 0.43 (6.81)

Variable X9: Unentered.

Variable X5: Entered at iteration 11. Removed at iteration 14.

regression equation in the stepwise procedure for regression through the origin was mean wave height (X1). This accounted for 61.3% of the variation in the dependent variable and may be interpreted as indicating the dominance of wave energy in this particular system. At the second iteration variable X14 (Water temperature) was entered with a negative relationship. This produced an increase of 5.7% in the measure of goodness of fit $\bar{R}^2$. The negative relationship indicates a smaller movement of grains alongshore with higher sea temperatures and may be explained through the close relationship between water temperature and water density. Harrison and Krumbein (1964) found that water density was of some importance in sand movement. They postulated that the rate of grain transport would be affected by the density of the water through fluid drag. Furthermore, wave tank experiments on beach slope modification at the Coastal Environment Research Council (C.E.R.C.) laboratories using warm and cold water have revealed that under constant increasing wave energies the slope modification was more rapid under cold water conditions. This implies greater sand movements under lower temperature conditions which would appear to be confirmed by this regression study.

Beach slope (X11) was the third variable entered into the equation which at this stage had an $\bar{R}^2$ value of 68.3%. It is interesting that beach slope is picked up early in the procedure indicating a certain amount of importance. This conflicts with the findings of previous workers, notably Komar (1969), who found that the amount of longshore sand transport was independent of beach slope but suggested that more refined measurements would show some relationship of beach slope to the proportionality factors introduced into his longshore sand transport formulae (Section 5.4). However, in later work Komar (1971) has shown through energetics and radiation stress concepts that beach slope does not influence sand transport rates. This regression analysis would suggest that there is in fact a connection between the two variables. The relationship is positive,

indicating greater mean grain movements alongshore with steeper slopes. Although addition of beach slope to the equation increases $\bar{R}^2$ by only 1.3%, its early selection suggests its importance.

Longshore current velocity in the direction of movement (X3), included at the next iteration, adds a further 5.0% to $\bar{R}^2$ confirming intuitive proposals that the stronger the longshore current the greater the mean distance moved. After this iteration the inclusion of a further eleven X's adds only another 13.1% to R^2 and the procedure is halted after the fifteenth iteration with an R^2 of 89.3%. $\bar{R}^2$ on the other hand continues to rise up to the eleventh iteration, 81.3%, and thereafter falls despite the addition of more variables. The two variables not entered were X5 (mean grain size) and X9 (onshore/offshore wind velocity). Grain size is a notable absentee from the regression as this might be expected to be important in accounting for the variation in the mean distance of grain movement in any direction. It was shown by the grain size tests discussed in Chapter 4 that different groups of grain sizes produced different average rates of movement. Reference was made to Komar's (1977) recent work and Ingle (1966) using tracer techniques also found a significant relationship between the alongshore component of wave energy, alongshore sand transport and average median grain diameter. However, Castanho (1970) points out that in fact the influence of grain size on sediment transport is not as straightforward as might at first seem and that different conclusions are often reached by workers in this field, in particular between field and laboratory studies. He suggests that much of the conflict in findings stems from the fact that the influence of grain size depends upon the flow conditions and how far from the beginning of movement attention is centred. For conditions near the beginning of sediment motion the grain size effect is working through threshold shear stress and bed roughness and hence will be very different from the effect of grain size, through settling velocities, on

fully developed movement. Thus the complexity of the problem and the fact that coarse average figures are used may explain the lack of dependence found in the regression.

A further explanation for the lack of a significant relationship between sand movement and grain size which ranges between 0.176mm and 1.235mm for the tracer tests, may be found in the strong correlations between this variable and beach slope (X11) and grain sorting (X15). These values are respectively 0.84 and 0.93 (Table 6.9). Beach slope was entered into the regression equation at the third step in the procedure and grain sorting at the sixth and hence may be incorporating much of the explanation which might otherwise have been introduced by the inclusion of grain size (X5). However, at the same time the correlations between grain size and the alongshore distance moved by the grains is - 0.08 and so it would appear that the lack of dependence shown by the regression procedure is real. A transformation of this variable may improve its contribution to the overall level of explanation of the model. Castanho, for example, quotes the work of L. Bajournas and his finding that littoral drift should increase with the square root of grain size.

Information on the relative importance of different variables can also be gained from an examination of the F ratio values for each of the variable coefficients and in this particular stepwise regression the value for wave height remains significant at a relatively high level throughout the procedure. This confirms the importance of wave height in the model. Beach slope (X11) also maintains a high significance level as does water temperature (X14) until the final iterations. Longshore current (X3) on the other hand loses importance with the inclusion of variables after iteration six.

As pointed out at the beginning of this section, a maximum of only 11 independent variables could be used in the combinatorial regression. Five variables, X4, X5, X6, X7, and X9 were omitted from the stepwise

Table 6. 9 Correlation matrix of independent variables in alongshore sand movement regressions

	1	2	3	4	5	6	7	8	9	10	11	12	13	14	15	16
1	1.00															
2	0.35	1.00														
3	0.60	0.03	1.00													
4	0.03	-0.14	-0.39	1.00												
5	0.18	-0.20	0.46	-0.12	1.00											
6	0.32	0.22	0.36	-0.27	0.32	1.00										
7	0.13	0.05	0.58	-0.26	0.33	-0.13	1.00									
8	-0.22	0.04	-0.34	0.18	-0.34	-0.14	-0.32	1.00								
9	0.22	0.21	0.49	-0.05	0.11	-0.26	0.80	-0.01	1.00							
10	-0.20	-0.15	0.09	-0.24	-0.11	-0.19	0.01	-0.11	0.27	1.00						
11	0.01	0.10	-0.32	0.21	-0.84	-0.29	-0.20	0.20	0.02	0.14	1.00					
12	-0.14	-0.14	0.01	0.12	0.19	-0.06	-0.02	0.20	-0.09	-0.27	-0.37	1.00				
13	-0.12	-0.22	0.28	-0.11	0.42	-0.04	0.07	-0.04	0.06	0.17	-0.57	0.73	1.00			
14	0.14	-0.02	0.20	0.14	0.08	0.33	0.05	-0.07	-0.10	-0.56	-0.17	0.08	0.08	1.00		
15	-0.17	0.12	-0.48	0.22	-0.93	-0.30	-0.39	0.35	-0.15	0.06	0.76	0.05	-0.25	-0.02	1.00	
16	0.48	0.01	0.43	-0.17	-0.01	-0.03	0.09	0.08	0.29	0.41	-0.21	-0.04	0.06	0.07	-0.46	1.00

N.B. Figures on axes correspond to the variable list, Table 6.7.

Correlations greater than 0.5 underlined.

regression list. Variables X5 (mean grain size) and X9 (mean wind speed onshore/offshore) were not entered into the stepwise equation, whilst X4 (mean longshore current velocity against direction of sand movement), X7 (mean wind speed alongshore in direction of sand movement) and X6 (angle of wave approach) were the last three variables entered into the equation. Table 6.10 shows the results of the combinatorial regression with the eleven remaining variables. The procedure produced the best combination of variables at the stage when ten variables are taken at a time. The combination of the first ten variables in the list of variables had the lowest R.M.S.R. of 0.3816 which represents an $\bar{R}^2$ of 81.4%. This exactly corresponds with the stepwise regression equation for the tenth iteration of that program (Table 6.8). Partial regression coefficients and their signs are the same for both regressions.

Wave height, X1, is picked out as the most important single variable and remains a constituent of most of the 'best' combinations of variable throughout the procedure. Up to and including the stage where variables are taken six at a time, wave height appears in 9 out of the maximum possible 16 combinations when the three best combinations at each stage are listed (Table 6.11). This again confirms the intuitive expectation that this variable is the dominant variable in the system, providing the main energy source for the model. However, as a general rule it is dangerous to infer the relative rank of certain combinations of variables from the ranks of variables when taken individually. For example, variable X16 (trough to bottom depth in front of the breaking wave) appears as the second most important single variable (Table 6.10) but this variable does not then reappear in any of the 'best' combinations until combinations of eight are considered. A further point to make at this stage is that one might intuitively expect that none of the variables occurring in the strongest combinations would appear in the weakest combinations, but this may happen. In the case of variable X14, for example, it occurs in as

Table 6.10 Results of Combinatorial Regression for Average Distance of Alongshore Sand Movement : All X's minus X4, X5, X6, X7 & X9.

Iteration	Best Three Combinations of X's	R.M.S.R.	Worst Three Combinations of X's	R.M.S.R.
	1	0.7932	8	1.8215
1	16	0.9001	13	1.3205
	3	0.9370	15	1.2810
	1 14	0.6767	8 15	1.3258
2	3 11	0.6909	8 13	1.3256
	1 12	0.7352	12 13	1.2851
	3 11 14	0.5922	8 12 13	1.3217
3	3 11 15	0.5994	12 13 14	1.3155
	1 11 15	0.6186	8 14 15	1.3032
	3 8 11 15	0.5334	8 12 13 14	1.3481
4	1 3 11 14	0.5482	8 12 14 15	1.3396
	3 8 11 14	0.5583	8 12 13 15	1.3341
	1 3 8 11 14	0.5150	8 12 13 14 15	1.3750
5	3 8 10 12 14	0.5158	2 8 13 14 15	1.1789
	3 8 11 14 15	0.5195	2 8 12 14 15	1.1754
	1 8 11 12 13 15	0.4411	2 8 12 13 14 15	1.1690
6	1 3 8 11 14 15	0.4582	2 8 10 11 13 14	1.0233
	1 3 8 10 12 14	0.4642	2 8 10 13 14 15	0.9755
	1 8 11 12 13 14 15	0.4059	2 8 10 13 14 15 16	0.8996
7	1 2 3 8 10 12 14	0.4361	2 8 10 12 13 14 15	0.8765
	1 3 8 11 12 13 15	0.4406	2 8 10 11 13 14 16	0.8696
	1 3 8 11 12 13 14 15	0.3921	1 2 3 8 10 13 15 16	0.7410
8	1 8 10 11 12 13 14 15	0.4039	1 2 3 8 10 11 13 16	0.7254
	1 8 11 12 13 14 15 16	0.4247	1 2 3 12 13 14 15 16	0.7208
	1 3 8 10 11 12 13 14 15	0.3843	1 2 3 8 12 13 14 15 16	0.6066
9	1 2 8 10 11 12 13 14 15	0.3949	2 3 10 11 12 13 14 15 16	0.6032
	1 2 3 8 10 11 12 13 14	0.4079	2 8 10 11 12 13 14 15 16	0.5991
	1 2 3 8 10 11 12 13 14 15	0.3816	2 3 8 10 11 12 13 14 15 16	0.4826
10	1 3 8 10 11 12 13 14 15 16	0.3950	1 2 3 10 11 12 13 14 15 16	0.4815
	1 2 8 10 11 12 13 14 15 16	0.3958	1 2 3 8 10 12 13 14 15 16	0.4754
	All X's	0.3845		

Table 6.11 Most Frequently Occurring Variables in the best of Combinatorial Regression Equations

Variable No.	Frequency of Occurrence in Three Best Combinations of X's (up to iteration 6 inc.)	Frequency of Occurrence in Three Worst Combinations of X's (up to iteration 6 inc.)
1	9	-
2	-	5
3	12	-
8	8	14
10	2	2
11	11	1
12	4	9
13	1	12
14	9	10
15	6	10
16	1	-

many strong combinations as X1 (Table 6.11) but also occurs frequently in the weakest combinations. This variable, water temperature, was also the variable included at the second iteration of the stepwise regression. This anomalous state of affairs may arise because the variable, by itself, may provide only a slight contribution to the explanation of variation in the dependent variable, say 1 or 2%. Although when combined with stronger variables its addition maintains the high explanatory value of the equation, its contribution to weaker combinations is only slight and hence does not raise the total contribution significantly. Variable X14 has a R.M.S.R. of 1.2706 which is the fourth worst single contribution of the eleven variables in the combinatorial regression.

The two other most frequently occurring variables are X3 and X11, longshore current velocity and beach slope. X3 is in fact the most frequently occurring variable in the strong combinations of all the eleven in the list and also has a R.M.S.R. individually of 0.9370, the third 'best'.

Beach slope, X11, on the other hand, taken individually, only has a R.M.S.R. of 1.0156 but nevertheless has its importance reflected in its inclusion in so many of the best combinations. The stepwise regression results are confirmed but the exact role played by beach slope in affecting longshore sand movement remains unclear.

Some of the unexpected results may perhaps be explained by intercorrelations amongst the independent variables as already discovered for grain size effects. Examination of the correlation matrix for the variables included in the regression (Table 6.9) show several strong linear correlations. The largest is that between X15 and X5, grain size and grain sorting (-0.93) but several others exceed $\pm$ 0.7. All those correlations greater than $\pm$ 0.5 are indicated. Where linear relationships exist among the explanatory variables it becomes difficult to sort out their separate contributions to the sums of squares of the dependent

variable, and the matrix inversions necessary in the technique may involve error. Variables X11 and X3 are both involved in three strong correlations with other variables and it may be that their seeming importance in the regressions is due to their absorption of the explanatory content of the variables with which they are correlated.

However, although one of the conditions for the use of the linear regression model is a lack of multicollinearity amongst the independent variables, as mentioned in Section 6.2, there is no direct link between the degree of collinearity and the correlation coefficients except in the case of perfect ($\pm$ 1.0) correlation between two variables (Kmenta, 1971). Hence, it is necessary to calculate a measure of collinearity and for each of the combinations in the combinatorial regression this is done. The measure ranges from 0 - 1 and a zero or near zero value indicates high collinearity and a null or nearly null correlation matrix of independent variables. High coefficient values occurred in this regression when few variables were entered but rapidly fell with the introduction of several variables. Nevertheless the lowest value for the coefficient was 0.35 E-10 with all eleven variables included which is comfortably inside the limit beyond which nullity prevents matrix inversion or severe errors in computation occur. This limit is roughly where the negative exponent is more than double the number of independent variables. Therefore, despite the presence of reasonably high multicollinearity which may lead to some problems of interpretation the computations were relatively easily performed.

In the main, the results of the combinatorial regression confirm the findings of the stepwise regressions and there is almost exact correspondence between the two procedures at several stages of the two programs. The most important variables would appear to be X1 (wave height), X3 (longshore current velocity in the direction of sand movement), X11 (beach slope) and X14 (water temperature).

Table 6.12 Dimensionless Independent Variables in Regression of Distance Sand moved in an Alongshore Direction.

X1 : Breaker steepness ratio $(H_b / gT_b)^{\frac{1}{2}}$

X2 : Grain size/swash characteristics $\overline{D} / \overline{Z}$

X3 : Angle of wave approach

X4 : Beach slope

X5 : Water temperature

Reducing the number of independent variables to five by the creation of dimensionless variables (Table 6.12) produced an $\overline{R}^2$ of 60.3% with the stepwise regression containing all variables (Table 6.13). The first variable selected was the breaker steepness (variable X1) accounting for 55% of the explanation. Komar (1969) found that alongshore transport rate did not correlate highly with wave steepness and suggested that if there is any dependence it is small enough to be masked by measurement error. However, this conflict may be partly resolved by the fact that Komar used deepwater wave steepness (H_∞ / L_∞) whilst in this study breaking wave steepness is used. Presumably the strength of the wave height variable in accounting for variation in Y is the main reason for the importance of this breaker steepness index. It does not, however, account for as much explanation as wave height by itself. At step two the water temperature variable (X5) was included. Again with a negative relationship this variable adds 6.2% to R^2. Beach slope (X4), included at iteration 3, added a further 2.5% but only 1.9% was added by the last two variables X3 and X2.

Again repeating the regressions with the combinatorial method and the same dimensionless variables produces a check on the results and maximum information. The 'best' combination was found to be X1, X4, X5 with R.M.S.R. of 0.794 and R^2 of 61.3%. Table 6.14 reveals the importance of X1 in terms of its frequency of occurrence in the strongest groupings.

Table 6.13 Results of Stepwise Regression Alongshore Sand Movement : Dimensionless Variables

INTEGRATION	REGRESSION EQUATION	$\bar{R}^2$	R^2	F TEST ON WHOLE REGRESSION	PARTIAL F TESTS
1	Y = 377.403 X1	55.4	55.4	33.47	33.47 (99.99)
2	Y = 734.466 X1 - 0.710 X5	60.2	61.6	20.87	X1 15.9 (99.46) X5 4.2 (73.89)
3	Y = 656.193 X1 - 0.800 X5 + 127-787	61.3	64.1	14.86	X1 11.79 (98.00) X5 5.32 (82.2) X4 1.71 (36.0)
4	Y = 624.777 X1 - 0.958 X5 + 162.894 X4 + 0.272 X3	61.2	65.4	11.32	X1 10.3 X4 2.4 (96.73) (49.74) X5 6.2 X3 0.89 (86.71) (17.30)
5	Y = 592.159 X1 - 0.916 X5 + 232.493 X4 + 0.269 X3 - 2.232 X2	60.3	66.0	8.94	X1 8.54 X4 0.86 (94.0) (16.5) X5 5.38 X2 0.45 (82.3) (7.1) X4 2.46 (50.3)

N.B. F tests on whole regressions are significant at the 99.99% level.

Table 6.14 Results of Combinatorial Regression for Average Distance of Alongshore Sand Movement : Dimensionless Variables

Iteration	Best Three Combinations of X's	R.M.S.R.	Worst Three Combinations of X's	R.M.S.R.
	1	0.9166	2	1.5693
1	4	1.1065	3	1.4640
	5	1.2710		
	1 5	0.8172	2 3	1.3482
2	1 4	0.9466	3 5	1.3056
	1 3	0.9503	2 0 5	1.3032
	1 4 5	0.7943	2 3 5	1.3305
3	1 2 5	0.8415	2 4 5	1.0961
	1 3 5	0.8430	3 4 5	1.0953
	1 3 4 5	0.7964	2 3 4 5	0.9639
4	1 2 4 5	0.8103	1 2 3 4	1.0713
	1 2 3 5	0.8846		
	All X's	0.8137		

It is also the most important variable taken singly (iteration 1). X2 (the combination of water depth and grain size characteristic) and X3 (angle of wave approach) were confirmed as the least important of the five variables.

In general terms then, the use of dimensionless variables reduced the explanatory value of the regression equation and provided little further information, except to confirm certain previous findings.

6:6 Onshore/offshore sand movement

Following the same procedures and techniques used in the previous section, the distance moved by sand grains normal to the shoreline was investigated. Table 6.1 indicates that in the majority of cases such movement was over much shorter distances than in an alongshore direction. Average distance moved onshore/offshore for all the experiments was 2.34m with a standard deviation of 2.88m compared with a mean of 11.19m and a standard deviation of 10.92m for average distance alongshore.

The variables used in the stepwise regression procedure are listed in Table 6.15 and the results of this analysis are contained in Table 6.16. It can be seen that in this case fifteen independent variables were included and the first variable entered into the equation was X10, beach slope. This has a positive relationship with the Y variable and explained 59.2% of its variation. At the second iteration alongshore wind velocity (X8) was entered with a negative relationship, indicating an increase in onshore/offshore distance moved with a fall in alongshore wind velocity. A physical interpretation of this might be that the slower the alongshore wind speeds the slower any consequent longshore currents might be and hence sand grain movement(s) normal to the shore are more likely. However, a similar relationship is not found for longshore current itself (X3) and indeed this is one of the variables not selected for the regression equation.

Table 6.15 Independent Variables in Regressions of Distance Sand Moved in Direction Normal to Shoreline

X1 : Mean wave height (metres)

X2 : Wave period (secs)

X3 : Longshore current velocity (cm/sec)

X4 : Mean grain size (phi units)

X5 : Mean wave angle (^{o})

X6 : Wind speed normal to shoreline in direction of sand movement (cm/sec)

X7 : Wind speed normal to shoreline in direction opposite to sand movement (cm/sec)

X8 : Wind speed alongshore (cm/sec)

X9 : Predicted tide height

X10 : Beach slope angle (tan. of angle)

X11 : Length of time tracer covered (hrs)

X12 : Depth of water at injection point at high water (metres)

X13 : Water temperature (^{o}C)

X14 : Grain sorting (phi units)

X15 : Trough to bottom depth in front of breaking wave (metres)

Table 6.16 Results of Stepwise Regression of amount of Onshore/Offshore Sand Movement: 15 Independent Variables

ITERATION	REGRESSION EQUATIONS	$\bar{R}^2$	R^2	F TEST ON WHOLE REGRESSION	PARTIAL F TESTS
1	Y = 86.51 X10	59.2	59.2	39.1 (99.99)	39.1 (99.99)
2	Y = 95.88 X10 - 0.107 X8	59.2	60.6	20.0 (99.99)	X10 32.25(99.99) X8 0.94(18.47)
3	Y = 84.117 X10 - 0.191 X8 + 0.156 X1	58.2	61.2	13.1 (99.99)	X10 10.75(97.2) X8 1.28(26.4) X1 0.38 (5.6)
4	Y = 106.714 X10 - 0.085 X8 + 5.114 X1 - 0.390 X9	60.6	64.8	11.1 (99.99)	X10 13.8 X1 12.61 (98.9) (52.96) X8 0.46 X9 2.49 (7.31) (51.00)
5	Y = 118.709 X10 - 0.091 X8 + 5.252 X1 - 0.744 X9 + 0.383 X11	61.4	66.9	9.32 (99.99)	X10 15.42 X9 3.71 (99.27) (68.1) X8 0.53 X11 1.40 (88.39) (29.3) X1 2.80 (55.86)
8	Y = 124.218 X10 - 0.124 X8 - 1.195 X9 + 0.323 X11 + 0.614 X2 + 0.068 X13 + 4.781 X15	61.3	69.6	6.96 (99.93)	X10 15.88 X2 1.41 (99.3) (29.2) X8 0.94 X13 0.63 (18.3) (11.2) X9 5.84 X15 1.47 (84.7) (30.6) X11 0.96 (19.0)

Continued overleaf

Table 6.16 continued

ITERATION	REGRESSION EQUATIONS	$\bar{R}^2$	R^2	F TEST ON WHOLE REGRESSION	PARTIAL F TESTS
11	Y = 82.666 X10 − 0.275 X8 − 0.987 + 0.749 X11 + 0.528 X2 + 0.098 X13 + 3.162 X15 + 0.196 X7 − 1.076 X12 − 0.042 X5	58.4	71.8	4.6 (99.75)	X10 2.91 (57.2); X2 0.82 (15.7); X12 1.02 (20.4); X8 2.11 (43.7); X13 1.03 (20.5); X5 0.29 (3.9); X9 3.14 (60.4); X15 0.53 (8.8); X11 1.90 (39.7); X7 1.04 (20.7)

X3, X4, X6, X14: Unentered.

X1: Entered at iteration 3. Removed at iteration 8.

Wave height is included at the third step but does not remain in the regression, being removed at iteration 8 when variable X15 (grain sorting) is included. The strong correlation between the two variables, Table 6.17, is probably responsible for this, X15 taking over the explanatory value of X1. Tide height and length of time the tracer was covered raise the coefficient of determination to 61.4% and the procedure was halted at the eleventh iteration when R^2 had a value of 71.8% and $\bar{R}^2$ 58.4%.

The only variables to maintain relatively highly significant F ratio values throughout the procedure were X10 and X9 suggesting their relative importance. It is interesting that beach slope accounts for much of the variation in the dependent variable but because of strong inter-correlation with other variables such as grain size it is not possible to say exactly how important it is. Of the variables not entered into the regression equation, variables X3, X4, X6 and X14 were omitted from the list of combinatorial regression X's. Hence,eleven explanatory variables were included and stepwise variable numbers were again retained to avoid confusion.

As can be seen from Table 6.18 the minimum R.M.S.R. value for the combinatorial regression procedure was 0.6978 for a combination of five variables. This had a corresponding R^2 value of 63.6% and the actual equation form was:

$$Y = 0.392\ X7 - 0.407\ X8 + 0.982\ X10 + 1.219\ X11 - 2.540\ X12 \quad \text{Eq. 6.6}$$

Taken as a whole there is a marked dissimilarity between the results of the stepwise and combinatorial regressions. When selected individually in the combinatorial regression X2, best accounted for variation in the dependent variable, followed by X1 and X9. On the other hand X10, which was the first variable selected for the stepwise regression equation, was found to be the worst of the variables taken singly and third worst in combination with other variables (Table 6.19). X12 (the estimated

Table 6.17 Correlation Matrix of Independent Variables in Onshore/Offshore Sand Movement Regressions

1	1.00														
2	0.35	1.00													
3	0.66	-0.29	1.00												
4	0.18	-0.20	0.45	1.00											
5	0.32	0.22	0.28	0.32	1.00										
6	-0.36	-0.09	0.03	0.14	0.11	1.00									
7	0.22	0.15	0.41	0.08	-0.18	-0.55	1.00								
8	0.04	0.07	0.42	0.20	-0.20	0.19	0.59	1.00							
9	-0.20	-0.15	-0.004	-0.11	-0.19	-0.26	0.36	0.004	1.00						
10	0.02	0.11	-0.26	-0.84	-0.29	-0.19	0.16	-0.12	0.14	1.00					
11	-0.14	-0.14	0.06	0.19	-0.06	-0.02	-0.13	0.06	-0.27	-0.37	1.00				
12	-0.12	-0.22	0.25	0.42	-0.04	-0.16	0.09	0.06	0.17	-0.57	0.73	1.00			
13	0.14	-0.02	0.28	0.08	0.33	0.11	-0.11	0.02	-0.56	-0.18	0.08	0.08	1.00		
14	-0.17	0.12	-0.44	-0.93	-0.30	-0.07	-0.18	-0.25	0.06	0.75	0.05	-0.25	-0.02	1.00	
15	0.74	0.06	0.68	0.48	0.06	0.05	0.31	0.20	-0.11	-0.21	-0.04	-0.05	-0.07	0.46	1.00
	1	2	3	4	5	6	7	8	9	10	11	12	13	14	15

N.B. Figures on axes correspond to the list of variables (Table 6.15).
Values greater than 0.5 indicated.

Table 6.18 Results of Combinatorial Regression for Average Distance of Onshore/Offshore Sand Movement : All X's minus X3, X4, X6 & X14.

Iteration	Best Three Combinations of X's	R.M.S.R.	Worst Three Combinations of X's	R.M.S.R.
	2	0.9489	10	1.6390
1	1	0.9500	15	1.5481
	9	1.0028	8	1.4513
	2 12	0.8637	8 9	1.5037
2	1 12	0.8959	8 15	1.4863
	2 8	0.9313	12 15	1.4199
	1 11 12	0.8562	8 12 15	1.4579
3	2 11 12	0.8588	8 10 12	1.4437
	11 12 15	0.8612	5 8 10	1.4011
	2 7 8 12	0.8247	5 8 12 15	1.4417
4	1 10 11 12	0.8362	5 8 10 12	1.4342
	1 5 11 12	0.8495	7 8 12 15	1.3057
	7 8 10 11 12	0.6978	5 7 8 12 15	1.2942
5	7 8 11 12 15	0.6987	5 7 8 10 12	1.2771
	2 7 8 11 12	0.7617	5 8 10 11 15	1.1644
	7 8 10 11 12 13	0.7124	5 7 9 10 11 15	1.1971
6	5 7 8 11 12 15	0.7127	7 9 10 11 13 15	1.1881
	5 7 8 10 11 12	0.7165	5 7 9 10 13 15	1.1768
	5 7 8 9 10 11 12	0.7071	5 8 9 10 11 13 15	1.1622
7	5 7 8 11 12 13 15	0.7106	2 7 9 10 11 13 15	1.1608
	1 5 7 8 10 11 12	0.7108	1 2 7 9 10 11 13	1.1424
	1 5 7 8 10 11 12 15	0.7190	2 5 7 9 10 11 13 15	1.1629
8	1 5 7 8 10 11 12 13	0.7203	5 7 8 9 10 11 13 15	1.1465
	2 5 7 8 10 11 12 13	0.7307	1 2 7 9 10 11 13 15	1.1302
	1 5 7 8 10 11 12 13 15	0.7221	1 2 7 8 9 10 11 13 15	1.1006
9	1 5 7 8 9 10 11 12 13	0.7442	1 2 5 7 9 10 11 13 15	1.0806
	2 5 7 8 9 10 11 12 13	0.7476	2 5 7 8 9 10 11 13 15	1.0702
	1 5 7 8 9 10 11 12 13 15	0.7550	1 2 5 7 8 9 10 11 13 15	1.0272
10	1 2 5 7 8 10 11 12 13 15	0.7592	1 2 5 7 9 10 11 12 13 15	0.9406
	1 2 5 7 8 9 10 11 12 13	0.7680	1 2 5 7 8 9 10 12 13 15	0.8990
	All X's	0.7895		

Table 6.19 Most Frequently Occurring Variables in the Best of the Combinatorial Regression Equations

Variable No.	Frequency of Occurrence in Three Best Combinations of X's (up to iteration 6 inc.)	Frequency of Occurrence in Three Worst Combinations of X's (up to iteration 6 inc.)
1	5	-
2	6	-
5	3	8
7	7	6
8	8	12
9	1	4
10	4	9
11	11	3
12	14	8
13	1	2
15	3	11

depth of water at the tracer inspection point at high tide) frequently occurs in the strongest variable groupings but as it is often found in weak combinations as well its importance is undetermined. Furthermore, it is not one of the variables 'picked up' early in the stepwise regression. Of the variables included in the 'best' combination of five variables only three X8 (alongshore wind speed), X10 (beach slope angle) and X11 (length of time tracer covered) were selected in the stepwise procedure by iteration five. Comparison of Tables 6.16 and 6.18 shows that variables X1 and X9 in the stepwise equation are replaced by X7 and X12 in the 'best' combination. The grouping of variables included at step 5 in the stepwise method gives a R.M.S.R. value of 1.0446 compared with 0.6978 and 1.2942 minimum and maximum values at this level. At the same time, the best regression as suggested by the stepwise program containing ten variables has a R.M.S.R. of 0.7867 compared with a minimum of 0.7550 and a maximum of 1.0272 where variables were considered ten at a time in the combinatorial program.

Therefore, despite the inconsistencies it would appear that X10 (beach slope), X11 (length of time the tracer was covered) and X8 (wind speed alongshore) are important variables in this regression model with X1 (wave height), X2 (wave period) and X9 (predicted tide height) of some lesser significance.

When the dimensionless variables were used as independent variables (Table 6.12) X4 (beach slope angle) was of most value. In the stepwise regression program it was selected at the first iteration with an $\bar{R}^2$ of 52.8% (Table 6.20) and in the combinatorial technique it had the smallest R.M.S.R. of 0.7834 with a similar $\bar{R}^2$ value (Table 6.21). The stepwise program was terminated at stage two with the addition of X2 and a concomitant rise in R^2 of only 0.4% but with a fall in $\bar{R}^2$ to 51.1%. This variable was also of some importance in the combinatorial procedure occurring in many of the 'best' groupings but even so its linking with X4

Table 6.20 Results of Stepwise Regression of amount of Onshore/Offshore Sand Movement: Dimensionless Variables

ITERATION	EQUATION	$\bar{R}^2$	R^2	F	PARTIAL F
1	Y = 75.64 X4	52.8	52.8	30.18 (99.99)	30.18
2	Y = 64.53 X4 + 0.404 X2	51.1	53.2	14.77 (99.96)	X4 5.67 (84.4) X2 0.23 (2.8)

Table 6.21 Results of Combinatorial Regression for Average Distance of Onshore/Offshore Sand Movement : Dimensionless Variables

Iteration	Best Three Combinations of X's	R.M.S.R.	Worst Three Combinations of X's	R.M.S.R.
	4	0.7834	3	1.3596
1	2	0.9459	1	1.0469
	5	1.0257		
	2 4	0.8053	1 3	1.0807
2	3 4	0.8101	1 5	1.0539
	4 5	0.8104	3 5	1.0444
	2 3 4	0.8331	1 3 5	1.0728
3	2 4 5	0.8337	2 3 5	0.9235
	1 2 4	0.8360	1 2 3	0.9231
	1 2 4 5	0.8652	1 2 3 5	0.9538
4	1 2 3 4	0.8657	1 3 4 5	0.8699
	2 3 4 5	0.8662		
	All X's	0.8999		

increases R.M.S.R. rather than reduces it and even when taken individually is more than 0.15 greater than the minimum R.M.S.R. for X4.

The increase in R^2, albeit small, with its inclusion in the stepwise regression equation, indicates the shortcomings of R^2 as an indicator of the level of explanation. As discussed in Section 6:3, provided the entered variable is significant at the selected probability level R^2 will always increase as it is related to the number of variables in the equation. R.M.S.R. on the other hand need not always increase. Furthermore the sensitivity of R^2 to the ratio of the number of variables and the number of observations in a particular regression is revealed by the difference in R^2 for the variable beach slope in the two stepwise regressions. As a dimensionless variable it is included with an R^2 of 52.8 whilst when used in the regression with fifteen independent variables the R^2 figure is 59.2%. As mentioned earlier, this is due to the tendency for R^2 to be pushed closer to 100% as the number of X's measured approaches the number of observations. $\bar{R}^2$ is also affected in this way as can be seen.

A further interesting point about the regressions with the dimensionless variables is the poor performance of X1, (the breaker wave steepness index). It is one of the worst of the five explanatory variables in the combinatorial regression and is not entered into the stepwise equation. Wave steepness, usually deepwater wave steepness, has been found to be of significance in sand movement normal to the shore by other workers, in particular King (1971). However, it has been related more especially to direction of movement than amount of movement. This relationship will be considered further in the next chapter.

The levels of explanation for onshore/offshore sand movement are lower than for alongshore sand movement indicating a poorer fit of the model to the data. Improvement may be brought about in several ways. Some of the variables already included could be transformed to improve

their individual contribution. Indeed, more variables could be used, replacing existing variables or simply adding to the list. In particular measurements of swash/backwash velocities and related percolation rates and water table levels would undoubtedly lead to an improvement in the model, whilst accurate estimates of orbital velocity beneath shoaling waves might also help. Alternatively a non-linear model might be adopted but interpretation of these models in terms of the physical system under study is often hazardous.

In summary, it can be said that wave height, accounting for 61.3% of the variation, appears to be the most important variable in determining alongshore sand movement when this was the dependent variable. Water temperature, with a negative relationship, and beach slope were also found to be important. On the other hand beach slope emerges as the most significant variable in accounting for the amount of onshore/offshore sand movement. However, in this latter case a far more confused picture is produced by the results of the regression analysis and lower levels of explanation are achieved. Strong intercorrelations between some of the independent variables provide problems of interpretation and may account in large part for the absence of mean grain size from the 'best' regression equations when intuitively its inclusion may have been expected.

CHAPTER 7

REGRESSION MODEL OF SAND MOVEMENT : DIRECTION

7:1 Introduction

Direction of sand movement should form the second major component of any sand transport model. In this chapter an attempt is made to account for this component with reference to the results of field data collected in this study.

Direction is not considered as a continuous variable ranging between 0^{o} and 360^{o} because of the problems of handling this type of data in regression analysis. Instead, simple distinctions are made between alongshore movement, north or south with respect to the beaches under study, and onshore or offshore movement. Since alongshore direction of movement is predicted more easily, less attention is paid to this aspect. On the other hand movement normal to the shoreline is more difficult to account for and consequently the greater part of this chapter deals with this problem. Initially bivariate relationships arising from previous work are discussed in Section 7:3. Section 7:4 then deals with the multivariate analysis conducted with the field data.

7:2 Alongshore sand movement

In the nearshore, two factors largely determine the direction of alongshore sand movement:

1. The direction of wave thrust.
2. The direction of alongshore flowing currents.

An oblique wave approach is translated into the zig-zag motion of wave drifting in the swash-backwash zone and hence produces sand movement in the direction of wave thrust, Figure 7.1. Alongshore flowing currents can be divided into those found shoreward of the breakers and those found to seaward. The longshore currents of the surf zone have been the subject of much theoretical and empirical study in the last decade but from the

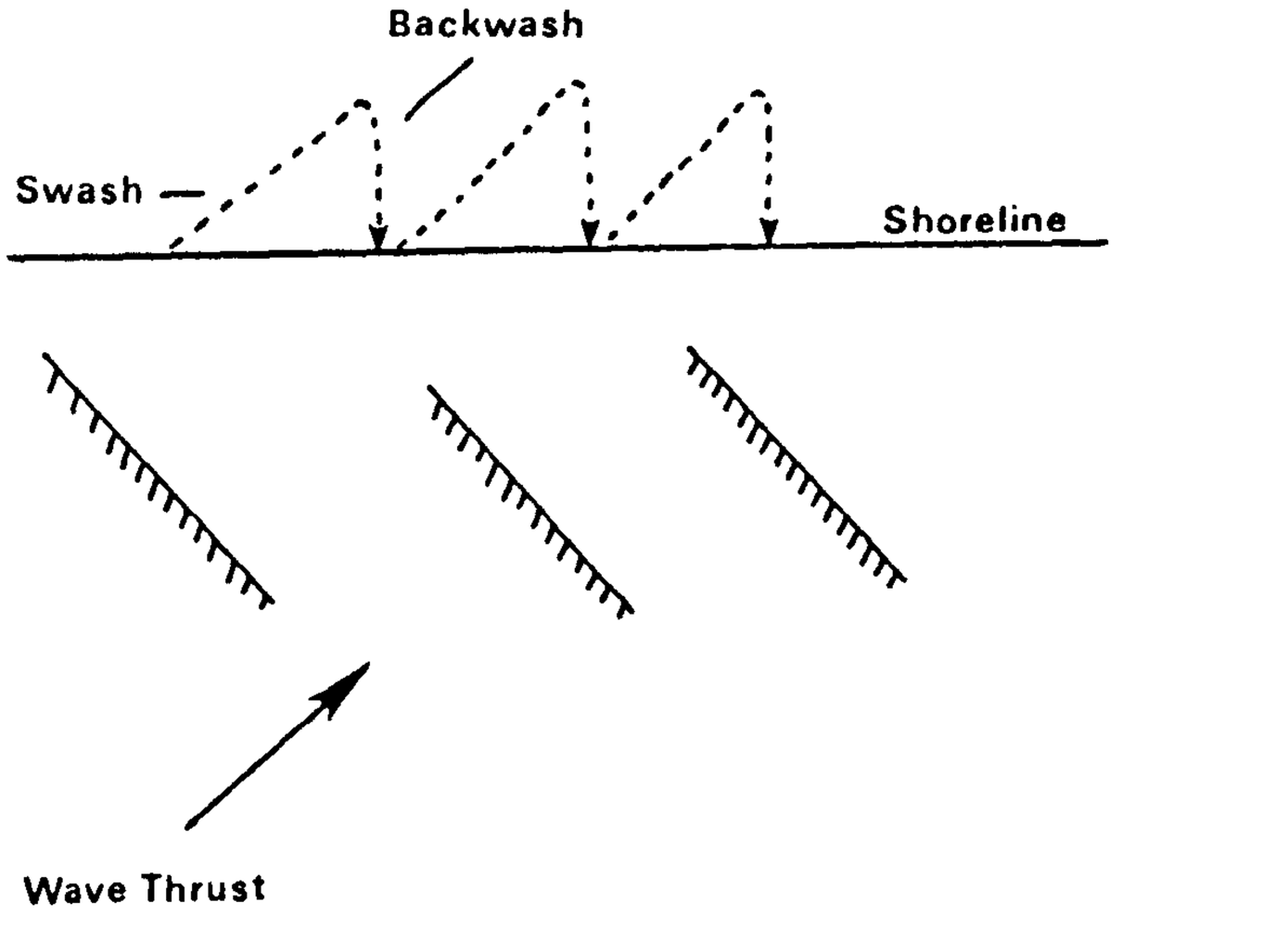

Figure 7.1. Zig-zag motion of sediment along the beach under action of swash-backwash.

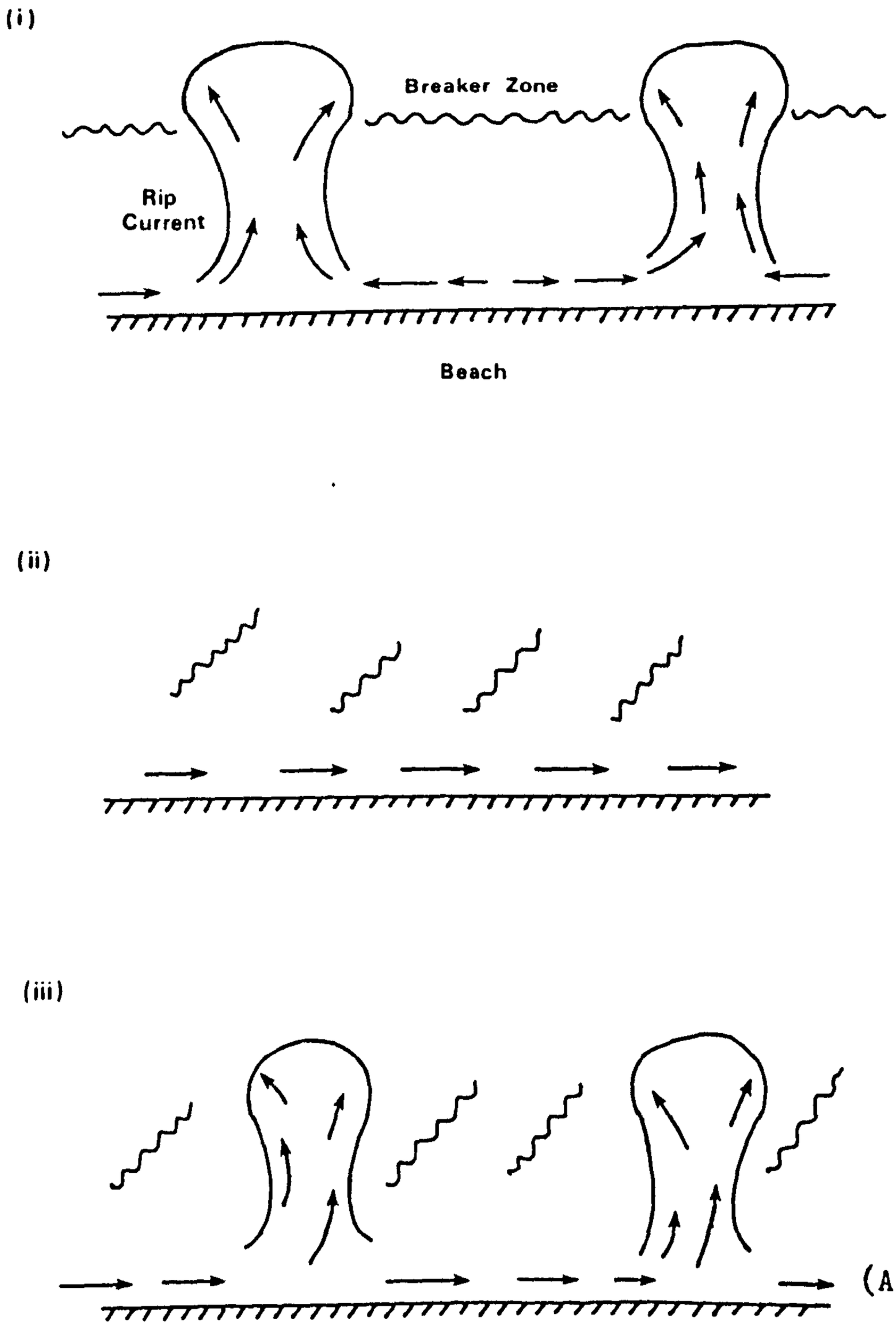

Figure 7.2. i) Longshore currents of cell circulation, ii) Current formed by oblique wave approach and iii) Summation of previous two diagrams to give resultant observed current patterns.

many ideas put forward two main mechanisms for their generation have been postulated:

1. Longshore variations in breaker height.
2. Oblique wave approach.

It has been suggested that variation in wave height alongshore, caused either by wave refraction or edge waves trapped in the nearshore interacting with swell waves, results in a variation in water levels shoreward of the breakers. This in turn causes water to flow from higher water levels to lower levels producing the longshore current. Where the water flows converge, near the location of the smaller breaking waves, the current turns seaward as a rip current. In this way a cell circulation is set up. (Figure 7.2i). Alternatively it is postulated that currents are produced by waves breaking at an angle to the shoreline. (Figure 7.2ii). Several theories have been put forward to account for this, notably those based on the shoreward mass transfer of water in solitary waves developed by Inman and Bagnold (1963), energy flux and momentum energy flux considerations suggested by Putnam, Munk and Trayler (1949) and radiation stress concepts produced by Lonquet-Higgins and Stewart (1963). Komar (1976) deals in some detail with all these approaches and discusses nearshore currents in general. He also states that " ... of all the equations formulated for the generation of these currents, those based on radiation stress (momentum flux) concepts have the firmest theoretical basis." (Komar, 1975).

Komar and Inman (1970) proposed that the observed current pattern in the nearshore may be the result of a combination of the two mechanisms of longshore current generation. This is shown in the bottom diagram (Figure 7.2iii). However, such a simplified picture may be complicated by irregular beach topography as indicated by the work of Sonu (1972). Nevertheless, it provides a useful general concept of longshore current generation.

Thus, generation of longshore currents in the surf zone is a complex

problem and it will be seen that, for example, a situation may arise where the effects of different mechanisms serve to offset one another and produce a small residual current. Equally a strong current may be formed when several processes act together. Bowen and Inman (1969) have also observed that when a cell circulation pattern does exist in conjunction with oblique wave approach, the cell system itself may move slowly alongshore. If this is the case then, at any point on the beach, variations in current strength with time might be expected, other factors remaining constant.

A further complicating factor which must also be taken into account is the wind. Shepard and Inman (1950) postulated that wind might be significant in producing longshore currents, but little empirical work has been carried out because of the difficulty of separating wind-generated and wave-generated currents. Using Table 7.1, a simple correspondence table, it would appear that wherever longshore current direction and the direction of wave thrust do not agree then wind stress may have been the cause of the current. On such occasions generation of the current through cell circulation is not precluded and measurement of wave and current was not detailed enough to allow identification of such cells.

Seaward of the breaking wave zone, alongshore flowing currents are generated by tidal forces. Except in strongly tidal environments, currents formed in this way will affect only the lowest parts of the beach face just above low water mark, if at all. Where they are important the tidal currents may be reversing in direction and hence cause sediment movement in both directions alongshore. A possible example of this was discussed in Section 4:2.

When alongshore flowing currents exist the direction of alongshore sand movement can be expected to be in the direction of current flow. However, where surf zone currents do not exist and tidal currents are unimportant, wave approach may become the dominant factor in direction of

Table 7.1 Comparison of general direction of sand movement with wave, wind and current characteristics

GIBRALTAR POINT.

Experiment (Date)		Sand Movement Direction	Longshore Current Direction	Direction of Wave Thrust	Wind Direction Alongshore
2.11.75		1	1	0	1
17.1.76		0	0	0	1
28.2.76		0	0	0	1
18.3.76	LR	1	1	1	-
18.3.76	UR	0	0	0	-
17.5.76		1	1	0	1
30.6.76		0	0	0	-
15.7.76		1	1	1	1
10.8.76		0	0	0	0
7.9.76	LG	0	0	0	-
7.9.76	UG	1	0	0	-
22.9.76	LR	0	0	0	-
22.9.76	UR	0	0	0	-
6.10.76	LG	1	1	1	1
6.10.76	UG	1	1	1	1
23.10.76	H3	1	1	0	1
23.10.76	H2	1	1	0	1

Continued.

Table 7.1 continued

SKEGNESS

Experiment (Date)		Sand Movement Direction	Longshore Current Direction	Direction of Wave Thrust	Wind Direction Alongshore
18.5.76		0	0	0	-
1.7.76		0	1	1	-
14.7.76		0	0	0	-
12.8.76		0	0	0	-
25.8.76	LR	0	0	0	-
25.8.76	UR	0	0	0	-
8.9.76		0	1	0	-
21.9.76		0	0	0	-
7.10.76	LR	0	0	0	-
7.10.76	UR	1	1	0	-
22.10.76	LR	0	0	0	-
22.10.76	UR	1	1	0	-

N.B.

1 refers to northerly movement and 0 to movement to the south.

Direction of wave thrust refers to direction in which waves are moving. Wind direction is represented as - when wind was dominantly blowing normal to the beach. Definition of onshore/offshore wind is as outlined in Section 6:4.

movement through longshore wave drift of material. This seems to be borne out by the results of the tracer experiments shown in Table 7.1 where on only three occasions are direction of alongshore movement, as indicated by the position of the mean centre of the dispersed tracer cloud and measured current direction,not in agreement.

On two of these occasions, the 7.9.76 experiment on the lower ridge at Gibraltar Point and the 1.7.76 experiment on the upper ridge at Skegness the tracer patterns reveal the possible influence of current flow within the runnels associated with each tracer release point, Figures 4.14 and 7.3.

The injection point for the 7.9.76 experiment was placed just on the edge of a runnel and the longshore component of two arms of movement of the tracer map probably represent the effects of currents filling and draining the runnel. The centre of gravity indicates an equality of dispersion in two main directions. Much rougher conditions for the 1.7.76 experiment seem to have caused a wide dispersion of tracer, much of which was affected by a southerly draining current emptying the runnel. The northerly flowing longshore current was strong at 43.1 cm/sec and the effect of this is seen in the northerly element to the map landward of the tracer source. It is important to note, however, that currents were not monitored for the whole tidal cycle during each experiment and hence it is difficult to interpret accurately the tracer patterns showing unexpected features. Interestingly though, on the single occasion when runnel currents were measured throughout the tidal cycle it was found that currents at a height of approximately 30cms above the bed were unidirectional and did not reverse as expected, Figure A1.10.

The third occasion when longshore current direction and sediment movement direction were not in accord was on 8.9.76 during the experiment on the upper ridge. In this case the main vector of movement was onshore as a result of an almost parallel wave approach to the beach. Slight

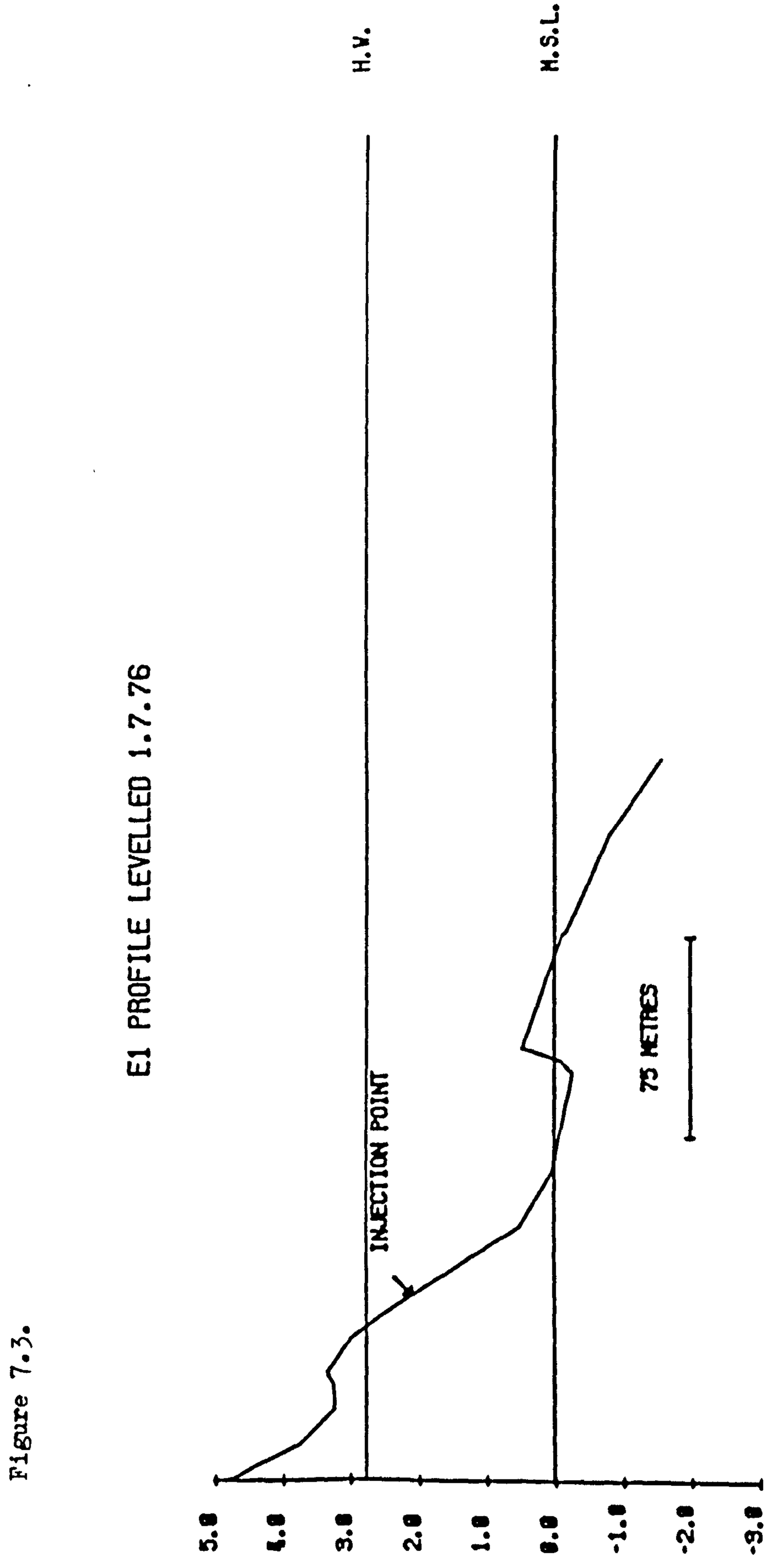
H.W.
M.S.L.
1.7.76
E1 PROFILE LEVELLED
M.S.L. MEAN SEA LEVEL
H.W. PREDICTED TIDE HEIGHT FOR EXPERIMENT
INJECTION POINT
75 METRES
5.0
4.0
3.0
2.0
1.0
0.0
-1.0
-2.0
-3.0
METRES O.D.NEWLYN

Figure 7.3.

Figure 7.4.

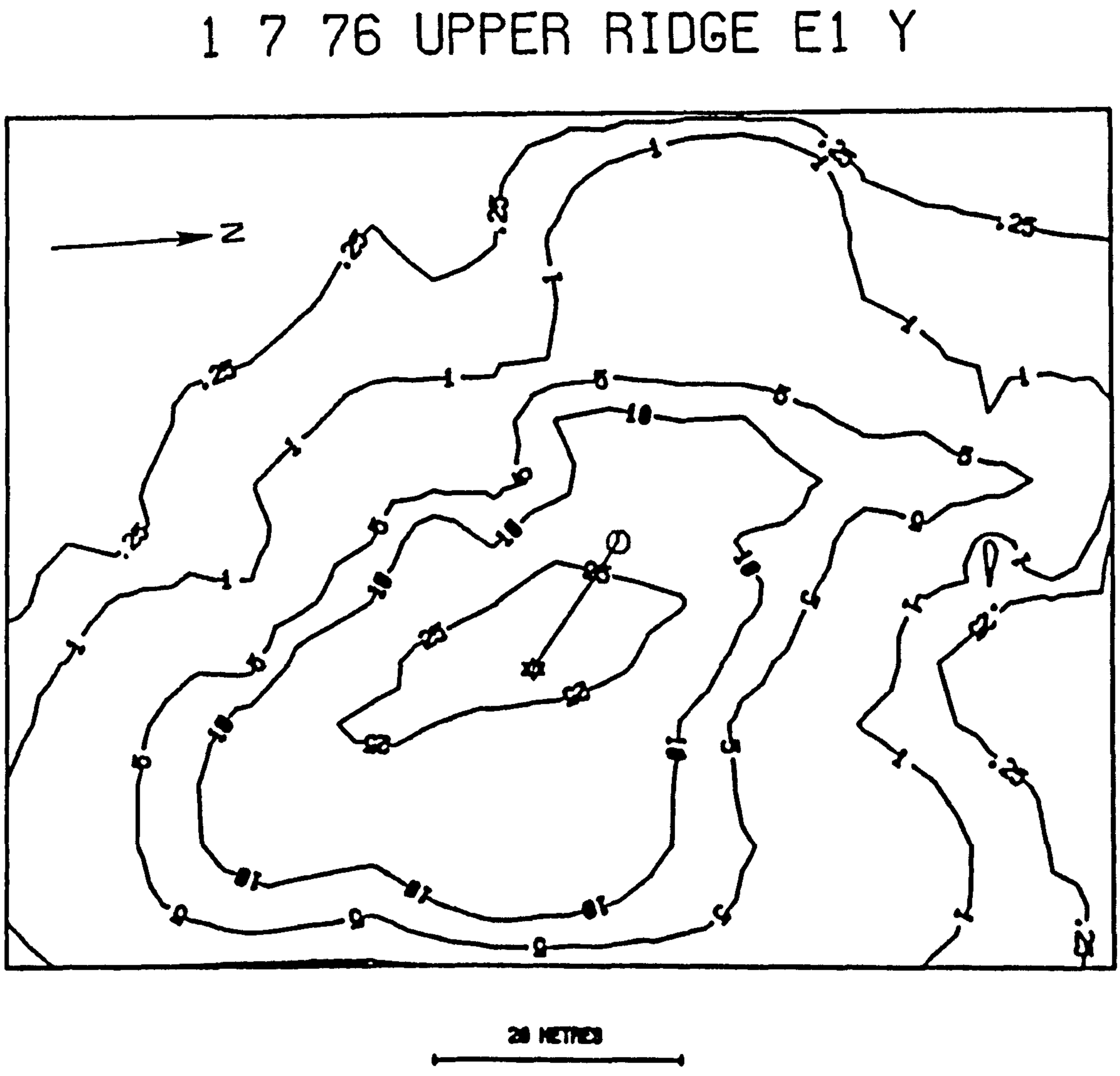
1 7 76 UPPER RIDGE E1 Y
N
20 METRES
INJECTION POINT
CENTRE OF GRAVITY

variation in angle of wave approach, combined with the effect of changes of wind direction during this experiment, were probably sufficient to override the influence of the slight northerly flowing current. (Figure 7.6).

Therefore, despite some slight disagreement, in general longshore current direction was found to be a good predictor of longshore sand movement direction. Although tidal currents were found to be important influences on sand movement on the lower beach at Gibraltar Point on some occasions, this did not cause serious difficulties in relating current and sediment movement direction.

7:3 Onshore or offshore : previous findings

Movement of sediment normal to the shoreline, in a tidal environment as outlined in Section 5:3, represents the net result of a balance of many forces. Much less work has been done on this aspect of sediment movement but investigations in the field and the laboratory by a number of workers have thrown up a series of suggestions which it is possible to test with the results of this study.

Murray (1967), dealing with the shoaling wave zone, found that there was a direct relationship between the maximum horizontal velocity over the bottom as given by:

$$u_m = \frac{\pi H}{T \sin h\,(2\pi h/L)} \qquad \text{Eq. 7.1}$$

(see also Eq. 5.6)

where H = wave height ;

T = wave period ;

L = wave length ;

h = water depth .

and his index of net movement normal to the beach (Section 3:5). He was able to show that least squares lines fitted to the data points had a negative slope indicating that as maximum horizontal velocity near the bottom increased there was an increasing tendency for offshore movement.

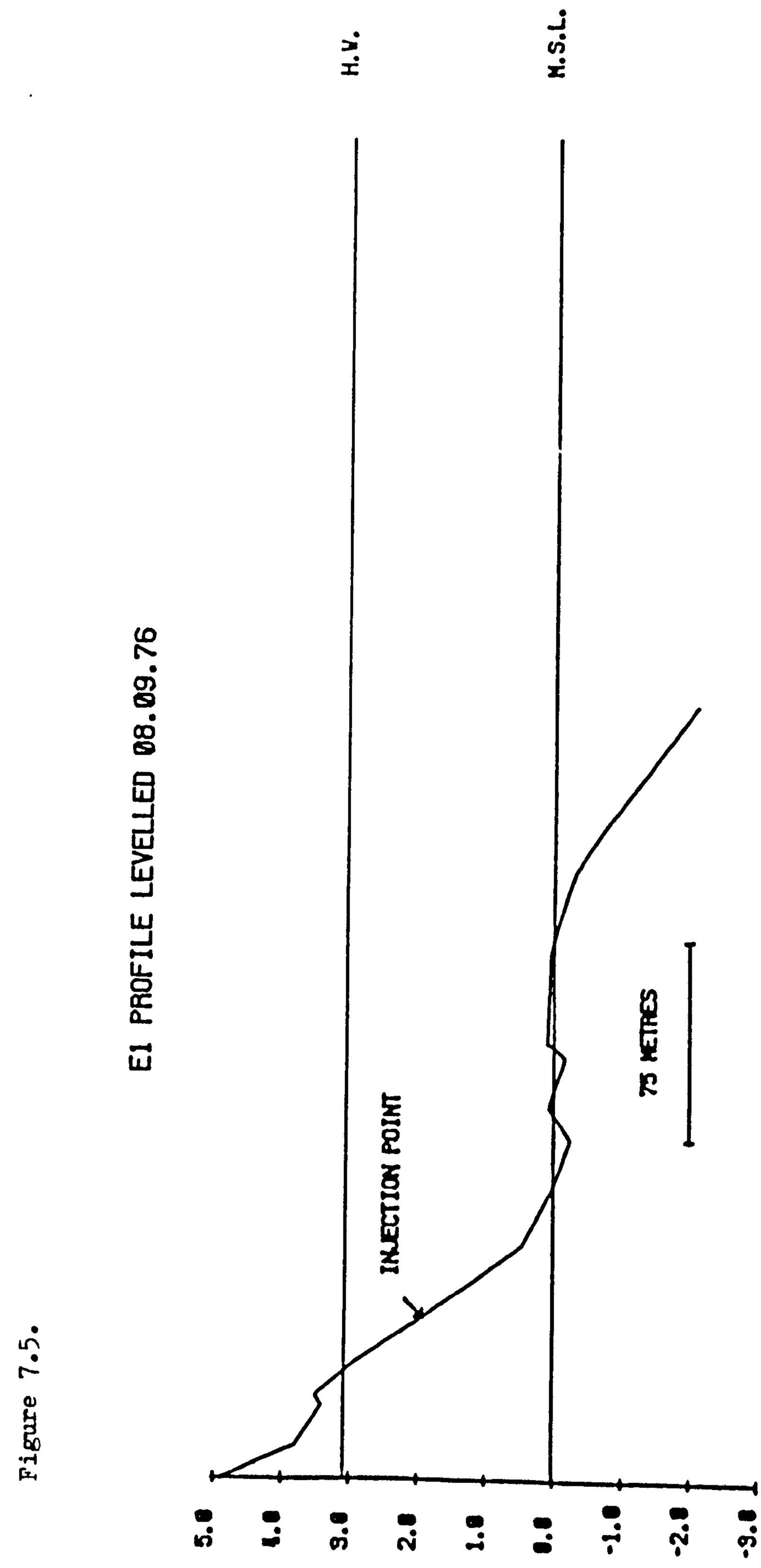
H.W.
M.S.L.
E1 PROFILE LEVELLED 08.09.76
INJECTION POINT
75 METRES
H.W. PREDICTED TIDE HEIGHT FOR EXPERIMENT
M.S.L. MEAN SEA LEVEL
5.0
4.0
3.0
2.0
1.0
0.0
-1.0
-2.0
-3.0
METRES O.D.NEWLYN

Figure 7.5.

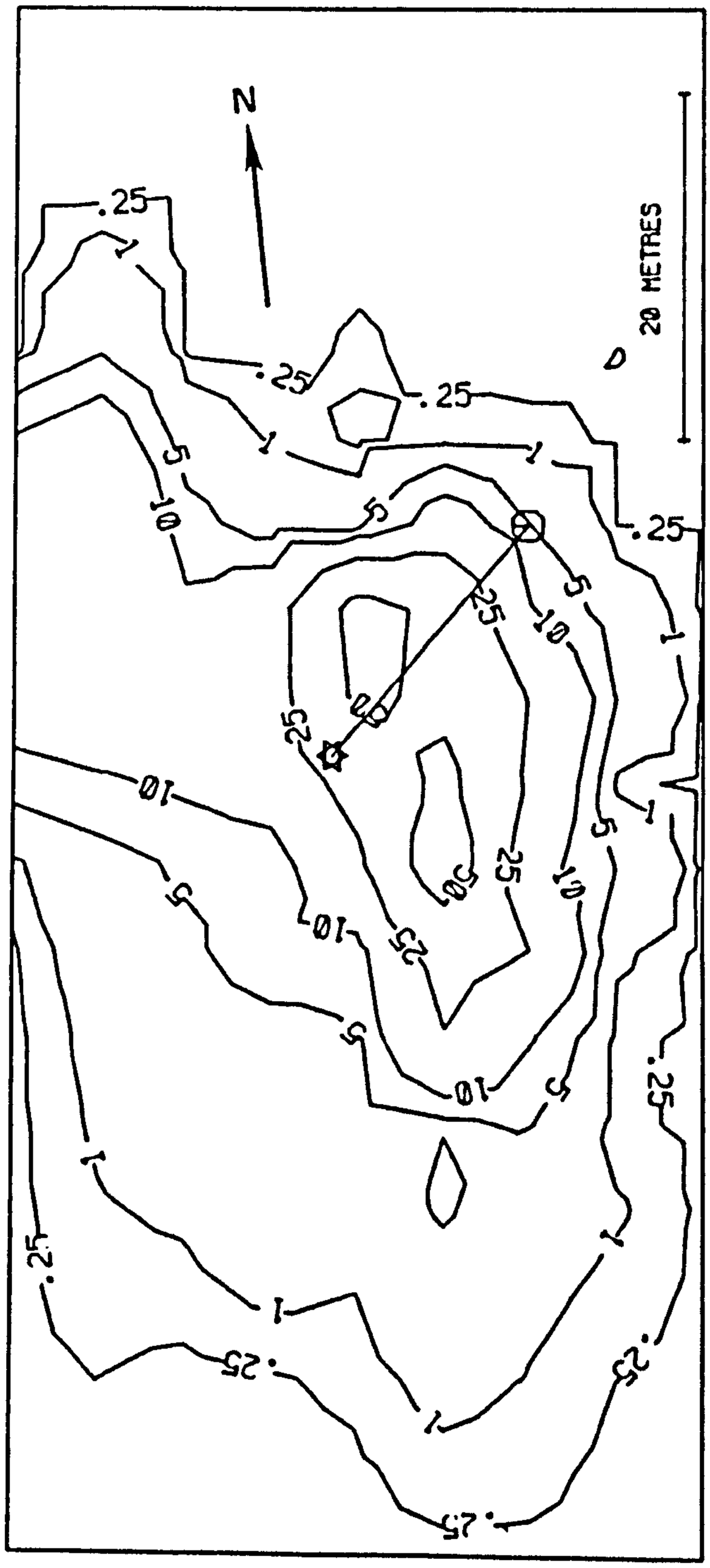
8 9 76 UPPER RIDGE E1 P
N
20 METRES
D
INJECTION POINT ⊙ CENTRE OF GRAVITY ✡
.25
1
5
10
25
50

Figure 7.6.

He also concluded that for any given value of u_m the finer grain sizes had a greater tendency for seaward motion. Murray explained these conclusions by assuming a mass transport system of currents as suggested by Longuet-Higgins (1953). (Figure 5.2). Finer grains thrown higher off the bed by the turbulence associated with strong bottom velocities would be affected by the offshore mid-depth flow and hence be carried offshore or less onshore.

Murray was concerned solely with sediment movement in the shoaling wave zone whilst the results of tracer experiments in this study represent the operation of processes in three or four distinct nearshore zones, swash-backwash, surf (if present), breaker and shoaling wave zones, (Figure 1.2). Consequently comparisons are not very easy. Nevertheless, it is interesting to test Murray's findings.

Because deepwater wave statistics are not available for this study equation 7.1 was not used. Instead maximum orbital velocity was substituted given by equation 5.26. A plot of this against net movement index Ψ as calculated for each of the tracer maps (Table 7.2) is shown in Figure 7.7. As will be seen, there is a very wide scatter of points and no obvious relationship exists. The best fit line does indicate that as the orbital velocity increases there is an increasing tendency for offshore movement. However, the correlation coefficient between the two variables is very low at 0.145 and, indeed, at the 95% significance level it is not significantly different from zero. A slightly more successful result was obtained from the plot of Ψ with grain size (Figure 7.8). It was found that the correlation was 0.352 and the best fit line produced by simple linear regression methods explained 12.4% of the variation. The slope of the line, however, is positive, suggesting that as grain size increases there is a greater tendency for onshore movement, agreeing with Murray's findings.

In his model of sand movements under shoaling waves Murray discounts the importance of wind induced bottom currents. However, other evidence

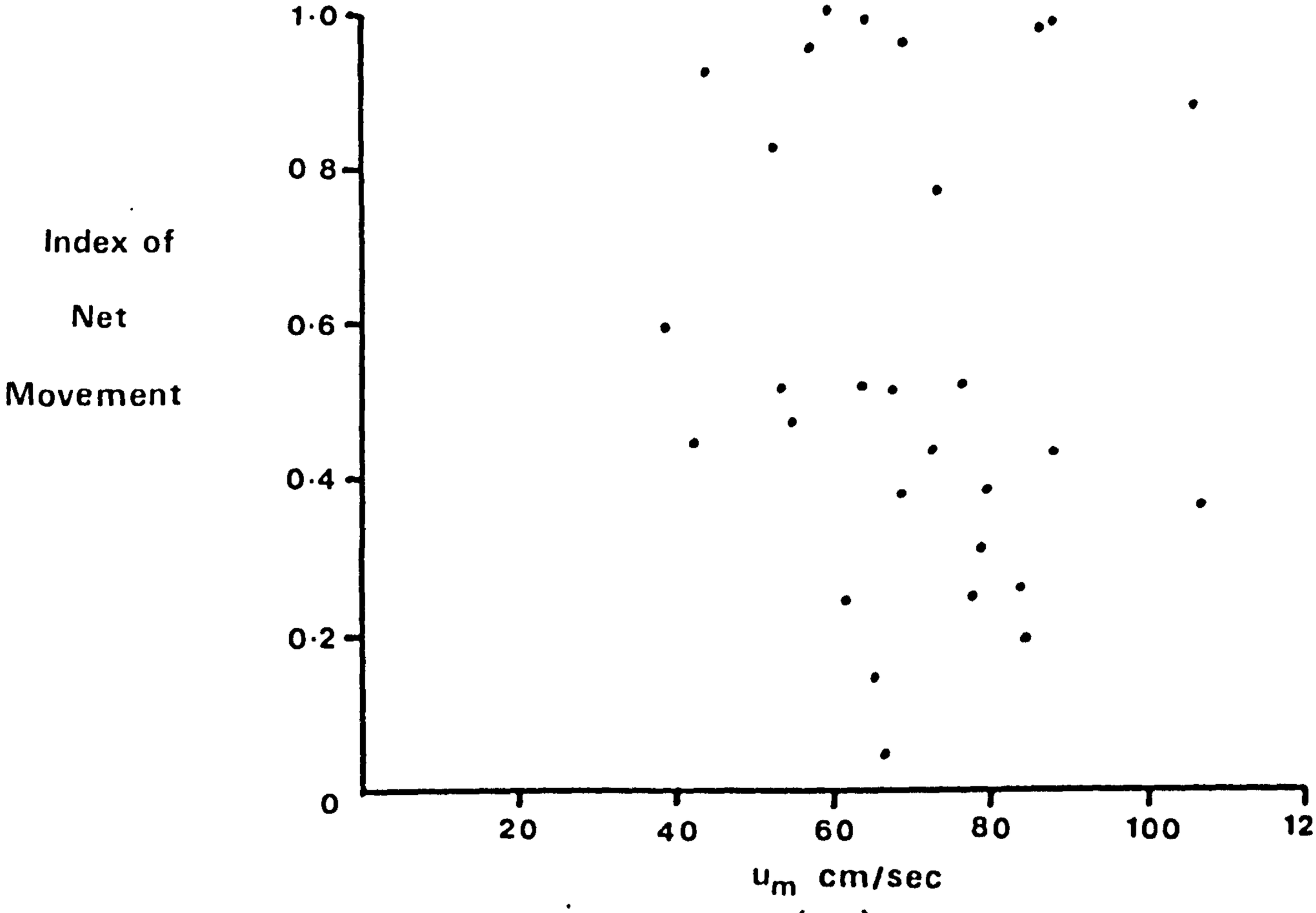

Figure 7.7. Plot of index of net movement (Ψ) against bottom orbital velocity (u_m).

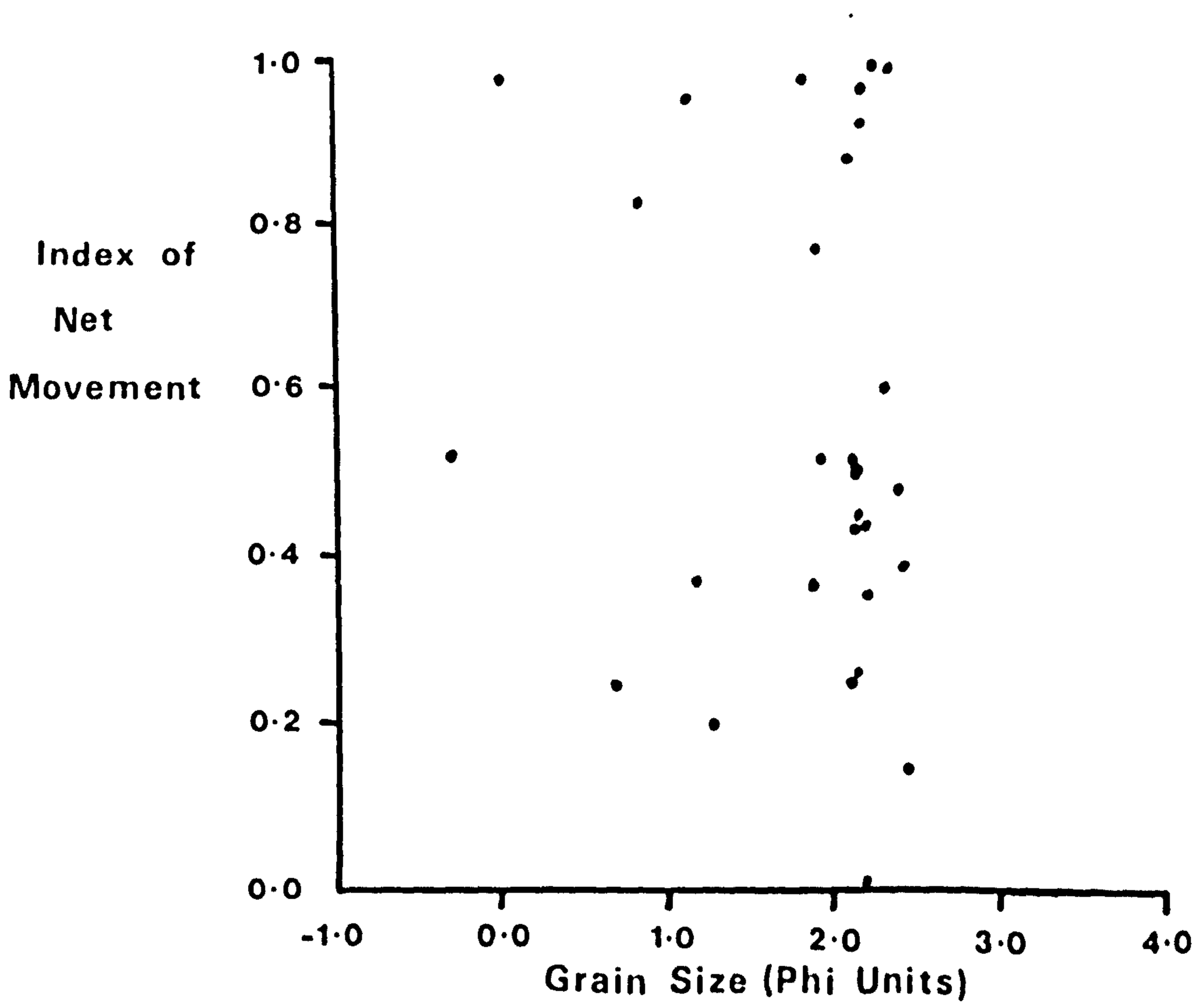

Figure 7.8. Plot of index of net movement (Ψ) against mean grain size.

Table 7.2 Wave Characteristics and Onshore/Offshore Index of Sand Movement (Ψ)

	Breaker Steepness (H_b/L_b)	Breaker Type Index	Max. Orbital Velocity Beneath Breaking Waves (u_m)	Ψ
		G I B R A L T A R P O I N T		
1	.0336	.0402	37.7	0.950
2	.0743	.113	73.5	0.768
3	.0471	.127	59.7	0.996
4	.0529	.0700	68.7	0.367
5	.0314	.0788	42.5	0.444
6	.0610	.184	72.4	0.436
7	.0692	.305	65.3	0.141
8	.0478	.162	55.0	0.473
9	.0641	.156	79.8	0.382
10	.0467	.0474	86.6	0.975
11	.0450	.218	83.4	0.259
12	.0508	.0805	87.9	0.428
13	.0718	.145	106.6	0.360
14	.0381	.0526	64.9	0.985
15	.0385	.113	66.3	0.049
16	.0605	.160	78.4	0.310
17	.0605	.144	77.6	0.249
		S K E G N E S S		
1	.0614	.164	63.7	0.514
2	.0728	.088	84.8	0.193
3	.0363	.246	44.2	0.922
4	.0849	.341	76.6	0.516
5	.0505	.0642	39.0	0.594
6	.0360	.366	52.8	0.823
7	.0538	.0356	88.1	0.978
8	.0595	.201	106.4	0.874
9	.0369	.0182	69.4	0.959
10	.0360	.123	53.4	0.515
11	.0544	.0532	67.9	0.510
12	.0494	.139	61.6	0.240

N.B. Breaker type index: $H_b/(gm\ T_b^2)$ when H_b = breaking wave height, m = tan. of beach slope and T_b = breaking wave period.

has been produced which suggests that currents set up by wind stress can be important in onshore/offshore transport of sediment. Siebold (1963) for example, in a tracer study off the Baltic Coast, found that onshore movement took place during strong offshore winds. He calculated that a compensating undercurrent transported sand with a velocity of more than 5 m/hr in a direction opposite to the wind from depths of 12.2m and 11.5m to shallower regions. Grains larger than 0.6mm were not removed from the original site.

Much work on the question of effect of wind on the nearshore circulation has been done by King (1972). Wave tank experiments indicated a general seaward drift at lower depths and along the bottom with an onshore wind. Combining the effects of wind with wave effects King illustrated the importance of wave steepness. For runs in the wave tank made with steep destructive waves and a strong onshore wind the seaward sand movement was found to be much greater in volume at all depths than when no wind was blowing, but in particular was much greater inside the break point. Outside the break point the strong landward transport associated with the steep waves dominated the seaward wind current effect. With flatter constructive waves and no wind a landward transport of material took place at all depths. The introduction of a strong onshore wind caused the slight onshore movement of material in the deeper water of the shoaling wave zone to be reversed and a slight seaward transport occurred. Closer to the break point the landward direction of movement was maintained but was much reduced whilst inside the break point a fairly marked seaward sediment movement replaced the landward movement of no wind conditions.

King (1957) has collected evidence from the field to support these wave tank findings. At Marsden Bay, Co. Durham, beach surveys showed that with an offshore wind accretion took place on the upper beach on 13 occasions, whilst erosion occurred only three times. Similarly, with an onshore wind erosion took place 13 times whilst accretion was seen on

only four occasions.

Apart from the direct effect of the wind generated current King (1972) also suggested that sand movement will also be influenced by the action of the wind on the form of the waves. A strong onshore wind may cause steep locally-generated waves and,even without the contribution of the wind-generated current,cause offshore sand movement through the more destructive nature of these waves. At the same time, a strong offshore wind may reduce the approaching waves flattening them and causing them to be more constructive with the resultant onshore sand movement.

By eliminating all the experiments in which general wind direction for the tidal cycle was within 25° of the alongshore bearing, and hence concentrating on experiments with onshore or offshore winds, some of King's ideas were tested with the data of this study. The net movement index ψ was also divided into onshore and offshore at the 0.5 value for the particular experiments involved and a contingency table was constructed. (Table 7.3).

Table 7.3.

INDEX OF NET MOVEMENT	WIND DIRECTION: Onshore	WIND DIRECTION: Offshore
Onshore	A: 8	B: 5
Offshore	C: 10	D: 0

Using the Fisher exact probability test as given by equation 7.2;

$$p = \frac{(A+B)\,!\,(C+D)\,!\,(A+C)\,!\,(B+D)\,!}{N\,!\,A\,!\,B\,!\,C\,!\,D\,!} \qquad \text{Eq. 7.2}$$

where A+B C+D etc. are marginal totals, N = number of cases ,

the hypothesis of no association between the two variables was tested. The Chi Square test could not be used because of restrictions on its use with expected frequencies less than 5 (Siegal, 1956) and this also precluded the use of the contingency coefficient C to assess the strength of any relationship. Using Eq. 7.2 it was found that there was a probability of 0.038 that the null hypothesis, H_o, that there was no association between the two variables, was correct. It would appear, from this evidence, that wind effects are important in determining direction of sand movement onshore or offshore. However, it should be pointed out that the wind data obtained was not a detailed record of the whole tidal cycle and short term wind effects may be important in the water and sediment circulation of the nearshore. Nevertheless, in general terms it would appear that King's findings are confirmed by this study.

Taking wind speed into account as well as direction, speeds ranged from 1.5 to 6.0 cm/sec when winds were blowing normal to the shore. With wind speeds at the lower end of the scale sand movement, as indicated by the net index, appeared to be less strongly onshore or offshore.

Deepwater wave steepness could not be calculated since the necessary measurements were not available but breaking wave steepness, possibly a more meaningful measure anyway, was calculated in order to look at the relationship, if any, between wave steepness and sand movement onshore/offshore.

Breaking wave steepness was calculated from:

$$s = \frac{H_b}{L_b} \qquad \text{Eq. 7.3}$$

where H_b = breaking wave height

L_b = breaking wave length (calculated from $c = \sqrt{gd}$ and $c = L/T$, where c = wave celerity, d = water depth, T = wave period)

Breaker steepness ranged from 0.0314 to 0.0849 for the experiments with a mean of 0.0531 (Table 7.2). There is a correlation of 0.332 between steepness and the onshore/offshore movement index Ψ but when combined with wind direction it was found that the mean of the net movement index for the three experiments with steepest breaking waves and a strong onshore wind was 0.356. This represents a medium offshore tendency for movement. Also the mean of the three experiments with the flattest breaking waves and strong onshore wind was 0.556, showing a slight tendency for onshore sediment movement.

Extending this analysis to wave type, the nearshore version of a formula for wave classification given by Patrick and Wiegel (1955) and used later by Galvin (1968), was employed. This formula, discussed in the previous chapter (Section 6:3), was developed in laboratory experiments on slopes having a tangent of between 0.2 and 0.05. Transitional values for the three main types of waves (Figure 7.9) were given as 0.03 for the surge/plunge division and 0.068 for the plunge/spill transition. Plunging breakers, in which the shoreward face of the wave becomes vertical curls over and plunges downward onto the beach face as an intact water mass, might be expected to be destructive in nature and produce offshore movement of sediment whilst surging waves would be more likely to produce onshore movement.

As can be seen from Table 7.2 the calculated values of the breaker type parameter for the tracer experiments, all fall within the plunging or spilling wave categories. Surging waves, as defined by the Patrick and Weigel experiments are absent. This is probably due to the relatively low beach slopes encountered during the experiments because generally speaking spilling breakers tend to occur on beaches of very low slope with waves of high steepness value, plunging waves on steeper beaches with waves of intermediate steepness and surging waves on high steepness beaches with low steepness waves. From Table 7.2 it will be seen that when plunging waves occur the net movement index indicates an onshore

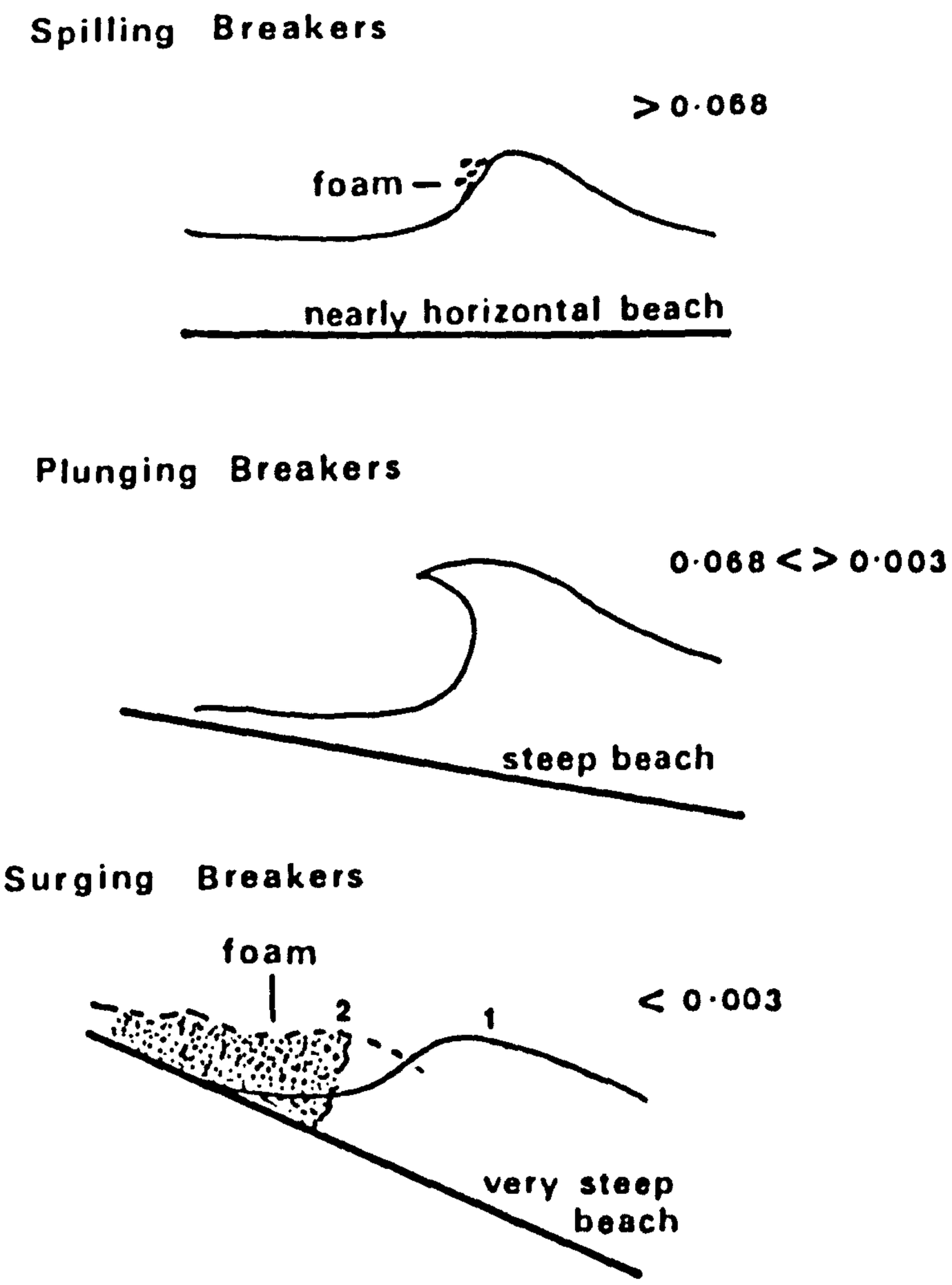

Figure 7.9. Breaking wave types. Transition values as given by $H_b/gm\ T_b^2$) where H_b and T_b are average wave height and average wave period and m is beach slope. After Calvin (1968).

movement of sand whilst on the four occasions when B_b had a value greater than the plunging/spilling transition value offshore movement of sand was indicated by the movement index Ψ. This conflicts with the expected results. Also, when combined with wind data, it was found that the mean of the net movement index for the combination of a wind blowing onshore with plunging waves was 0.509, or slightly onshore tendency, whilst for an offshore wind with spilling waves the index indicated a slight offshore movement, 0.480. Again this is in disagreement with King's suggestions (p.266) but it must be emphasised that in this strongly tidal situation several different nearshore zones may cross the tracer source. In this case wave effects in terms of net direction of sand movement differ, dependent upon the conditions present in each zone. Further, the length of time each zone affects the tracer will be important so that for conditions of steep waves and onshore wind the net picture of sand movement may still be onshore and not offshore as might be expected because shoaling waves in deeper water affect the tracer for a relatively longer period of time and hence form the dominant cause of movement. Also the transition values for the wave classification put forward by Patrick and Weigel may not be applicable to slopes flatter than 0.05 (Galvin, 1968) and many of the slopes encountered in these field experiments were flatter than this figure.

7:4 Onshore or Offshore : multivariate approach

The use of data which consists of observations of a directional nature precludes application of standard statistical measures and it is only recently that statistical developments in this field have taken place. Gould (1969) discussed an analogue of the normal linear regression model for circular variables, that is variables in which the data is expressed as two dimensional directions, but no regression method for the simultaneous handling of angular and non-angular variates is available. Consequently when data were expressed in angular terms, that is as a point on the circumferences of a circle, it was re-expressed. Independent variables were redefined as discussed in Chapter 6 and the concentration index Ψ of onshore/offshore sand movement, as described in Section 3:4 and 7:2, was used to

Table 7.4 Results of Stepwise Regression of Concentration Index of Onshore/Offshore Sand Movement (Direction): 15 Independent Variables

ITERATION	REGRESSION EQUATION	$\bar{R}^2$	R^2	F TEST ON WHOLE REGRESSION	PARTIAL F TEST
1	Y = 0.140 X2	78.5	78.5	98.5	X2 98.5 (99.9)
2	Y = 0.169 X2 - 0.004 X3	80.0	80.7	54.2	X2 58.86 (99.9) X3 2.91 (57.8)
3	Y = 0.096 X2 - 0.005 X3 + 0.064 X11	82.9	84.1	44.1	X2 6.70 (89.0) X3 5.59 (83.8) X11 5.46 (83.0)
4	Y = 0.063 X2 - 0.005 X3 + 0.065 X11 + 4.109 X10	83.4	85.2	34.6	X2 1.98 (41.5) X11 5.82 (85.0) X3 4.80 (78.4) X10 1.82 (38.2)
9	Y = 0.132 X2 - 0.003 X3 + 0.110 X11 + 17.552 X10 - 0.581 X14 - 1.177 X15 - 0.20 X8 + 0.007 X13 + 0.051 X12	85.9	89.9	16.9	X2 5.87 (84.5) X15 4.94 (78.8) X3 0.60 (10.5) X8 1.73 (36.3) X11 4.29 (73.5) X13 0.60 (10.4) X10 8.90 (94.2) X12 0.35 (5.1) X14 5.98 (85.1)

Continued overleaf

Table 7.4 continued.

ITERATION	REGRESSION EQUATION	$\bar{R}^2$	R^2	F TEST ON WHOLE REGRESSION	PARTIAL F TEST		
13	$Y = 0.132\ X2 - 0.003\ X3 + 0.121\ X11 + 20.03\ X10 - 0.942\ X14 - 0.870\ X15 + 0.010\ X13 + 0.095\ X12 - 0.021\ X7 - 0.214\ X4 + 0.055\ X9 - 0.009\ X8$	84.9	90.8	13.1	X2 4.61 (75.6) X3 0.68 (12.3) X11 2.90 (56.7) X10 5.86 (83.8) X14 4.52 (74.8)	X15 1.65 (34.5) X13 0.83 (15.8) X12 0.65 (11.6) X7 0.95 (18.7) X4 0.61 (10.7)	X9 0.25 (3.2) X8 0.20 (2.4)

X1, X5, X6: Unentered.

X8: Entered at iteration 7. Removed at iteration 11. Re-entered at iteration 13.

N.B. F Tests on complete regressions all significant at 99.99% probability level.

variable X1 is being made redundant by the presence of the other two variables in the regression. A further point is that as the regression continues the significance of variable X3 declines as indicated by the partial F test values and their probability levels. In particular the addition of X15 reduces the partial F test on X3 from 6.76, significant at the 89.1% probability level, to 1.172 which is significant only at the 23.9% level. Again this is due to the relatively strong correlation between X15 and X3 (Table 6.17).

At iteration three X11 (length of time the tracer was covered) was added to the regression equation with a positive coefficient. This indicates that the longer the tracer is immersed the more likely onshore movement is,or the lower offshore movement is likely to be. In a strongly tidal location such as this the length of time the tracer is covered will also reflect the position of the tracer release point on the beach and also the depth of water over the injection point. The lower down the beach face, the nearer to the low-water mark the longer the tracer will be covered and the deeper the water over the tracer at three-quarter and full tide. Under relatively deeper water the tracer is more likely to be beyond the breaker zone and hence more susceptible to shoreward acting processes. The addition of X11 increases $\bar{R}^2$ by 2.9%.

Beach slope (X10) is the fourth variable entered but only causes an increase of 0.5% in $\bar{R}^2$. The slope variable has a positive relationship which provides an unexpected interpretation since it implies that with steep beach slopes sand movement is more likely to be onshore or at least less offshore.

After the fourth iteration only a further 5.6% is added to R^2, whilst $\bar{R}^2$ reaches a maximum value of 86.5% at iteration 7. The final equation given at iteration 13 contains 12 variables and has an R^2 of 90.8 (Table 7.4). Of the variables included only X10, X2, X14 and X11 maintain relatively significant F test values throughout, whilst variable X8 (wind speed alongshore)

undergoes interesting changes. At iteration 7 it is entered for the first time with a partial F test of 2.26, significant at the 46.8% level. This falls gradually until with the addition of X7 to the equation its F value falls to 0.2 which is significant only at the 3% probability level. The addition of X4 at the next iteration causes X8 to be removed because the partial F value is significant only at a level less than 2%. However, at the last iteration X8 is re-entered with a marginally acceptable significance level. This is a good example of the way in which the contribution of a variable already in the regression may be duplicated by a second variable and lose its significance when that second variable is entered into the regression. The correlation between variables X7 and X8 is 0.59, (Table 6.17).

Three variables were not entered into the regression at all, X1, X5 and X6, wave height, wave angle and wind speed normal to the shoreline in the direction of movement. The last of the variables is a predictable absentee since winds causing counter currents have been suggested as being important, Section 7:3. On the other hand, the absence of both wave height and wave angle from the regressions is quite surprising. When combined with wave period in the breaker type variable of the set of dimensionless variables, wave height remains of relative unimportance. In the stepwise regression of the five dimensionless variables with the onshore/offshore concentration index variable X1 (the breaker type variable) is only entered at the fourth and final iteration and adds little to the R^2 value for the regression equation (Table 7.5). Similarly in the combinatorial regression with the same variables, X1 figures in few of the best combinations (Table 7.6). Wave angle(X3) on the other hand, is relatively important in the regressions, appearing in most of the best groupings in the combinatorial regression procedure and being the second variable added to the stepwise regression equation. X3 in fact adds 5.3% to the $\bar{R}^2$ value for the regression equation. It is interesting that wave angle

Table 7.5. Results of Stepwise Regression of Concentration Index of Onshore/Offshore Sand Movement : Dimensionless Variables

ITERATION	REGRESSION EQUATION	$\bar{R}^2$	R^2	F TEST ON WHOLE REGRESSION	PARTIAL F TESTS
1	Y = 15.126 X4	74.0	74.0	77.02	77.02
2	Y = 12.432 X4 + 0.016	79.3	80.0	51.97	X4 45.33 (99.9)
					X3 7.7 (92.4)
3	Y = 9.147 X4 + 0.016 X3 + 0.106 X2	79.5	81.0	35.46	X4 8.52 (94.2)
					X3 8.28 (93.7)
					X2 1.29 (26.7)
4	Y = 7.452 X4 + 0.013 X3 + 0.119 X2 + 3.101 X1	79.1	81.3	26.17	X4 2.99 (58.9)
					X3 2.84 (56.6)
					X2 1.52 (31.9)
					X1 0.49 (7.9)

Variable X5:Unentered. Calculated values of F ratio for whole regressions all significant at 99.99% probability level.

Table 7.6 Results of Combinatorial Regression for Concentration Index of Onshore/Offshore Sand Movement : Dimensionless Variables

Iteration	Best Three Combinations of X's	R.M.S.R.	Worst Three Combinations of X's	R.M.S.R.
	4	1.2149	3	2.5698
1	5	1.4327	2	1.8467
	1	1.4956		
	3 4	0.9714	1 3	1.5262
2	4 5	1.0278	3 5	1.4840
	1 4	1.0802	1 5	1.4164
	2 3 4	0.9592	1 3 5	1.4701
3	3 4 5	0.9902	2 3 5	1.0950
	1 3 4	0.9998	1 2 5	1.0870
	1 2 3 4	0.9778	1 2 3 5	1.0890
4	2 3 4 5	0.9780	1 2 4 5	1.0526
	1 3 4 5	1.0297		
5	All X's	1.0145		

should be important in regression with the dimensionless variables and not in the full regression with fifteen independent variables. The variable is not strongly correlated with any of the other variables (Table 6.17) and so its explanatory content is not being duplicated in the full stepwise regression. It is significant, however, that in the dimensionless context it is only important in combination with other variables and not by itself. Indeed, in the combinatorial regression of dimensionless variables when taken singly it is the worst variable with a R.M.S.R. of 2.5698 (Table 7.6).

The 'best' regression from the combinatorial regression with dimensionless variables is given as:

$$Y = 0.106\ X2 + 0.016\ X3 + 9.417\ X4 \qquad \text{Eq. 7.4}$$

with an R^2 of 80.97% and a R.M.S.R. of 0.9592. This agrees with the stepwise equation for iteration 3, but it can be seen that only variables X3 and X4 have strongly significant partial F values (Table 7.5). Water temperature (X5) is of little importance, not entered at all in the stepwise equation and occurring in many of the worst combinations in the combinatorial regression. However, individually in the combinatorial regression it is the second best variable. The importance of beach slope in the regressions with dimensionless variables is clear from Tables 7.5 and 7.6. It accounts for 74% of the variation in the dependent variable in the stepwise regression and figures in all the best groupings in the combinatorial procedure. It appears that in the absence of wave period as an independent variable this is the most significant variable determining direction of movement normal to the shore. However, this would not be immediately obvious from the other regression results (Table 7.4). With all fifteen variables beach slope was not entered until the fourth iteration and even then only added 0.5% to $\bar{R}^2$. Nevertheless, it is a variable which remains significant at a high probability level for the whole stepwise procedure which gives an indication of its importance. As has been

noted (Section 7.3), the positive relationship of beach slope which is present in all regressions is perhaps unexpected since intuitively a greater offshore movement of material may have been envisaged with steeper slopes.

Returning to regression analysis with the fifteen independent variables two combinatorial regressions were conducted with slight differences in the variables omitted from the full list (Table 6.15). In the first variables X5, X6, X8 and X9 were omitted and the results of the regression are shown in Tables 7.7 and 7.8. With regression through the origin the best combination of variables was found to be seven with an $\bar{R}^2$ of 87.1% and a R.M.S.R. of 0.6131. However, several combinations of 6, 8 and 9 variables all have R.M.S.R. values below 0.6400 (Table 7.7). Taken individually X2, X11 and X14 are the best variables and X3 the worst. X3 (longshore current velocity) is in fact selected second for the stepwise regression but does not retain its significance throughout the regression as indicated by the partial F values (Tables 7.4). Variables X2 and X11 are the two variables occurring most frequently in the best combinations of independent variables followed by X10, whilst X4 and X7 occur most in worst combinations (Table 7.8).

There is relatively close agreement between the stepwise and combinatorial results although variable X14, entered at iteration 5 in the stepwise procedure, has less prominence in the combinatorial groupings, occurring only six times in the best combinations. Wave height (X1) again is unimportant in the combinatorial regression. Indeed, it does not occur in any of the strongest combinations until sets of nine variables are taken. Comparing the best combination of variables from the sequential regression with the variables included in the stepwise equation at iteration 7, it will be seen that two variables are different. Variables X3 and X8 in the stepwise are replaced by variables X7 and X12 in the combinatorial equation. X3 and X8 are the two variables with lowest

Table 7.7 Results of Combinatorial Regression for Concentration Index of Onshore/Offshore Sand Movement : All X's minus X5, X6, X8 & X9.

Iteration	Best Three Combinations of X's	R.M.S.R.	Worst Three Combinations of X's	R.M.S.R.
	2	1.0069	3	2.9559
1	11	1.0452	7	2.8281
	14	1.2464	4	1.8735
	10 11	0.8833	3 7	2.7613
2	2 3	0.9392	4 7	1.9037
	2 11	0.9432	3 4	1.8977
	2 3 11	0.8006	3 4 7	1.8644
3	3 10 11	0.8057	3 7 12	1.7718
	2 11 15	0.8081	4 7 15	1.7554
	2 10 11 15	0.7438	1 4 7 15	1.7884
4	2 3 10 11	0.7741	3 4 7 12	1.6833
	2 3 10 12	0.7751	4 7 12 15	1.6000
	2 10 11 14 15	0.6707	4 7 12 13 15	1.4933
5	2 4 10 11 15	0.7418	1 4 12 13 15	1.4783
	2 3 10 11 14	0.7471	1 4 7 12 13	1.4770
	2 7 10 11 14 15	0.6323	1 4 7 12 13 15	1.5412
6	2 3 10 11 14 15	0.6645	1 3 7 10 14 15	1.2949
	2 7 10 12 14 15	0.6720	1 3 4 7 13 15	1.2879
	2 7 10 11 12 14 15	0.6131	1 3 7 10 13 14 15	1.2497
7	2 3 7 10 11 14 15	0.6494	1 4 7 11 12 13 15	1.1820
	2 7 10 11 13 14 15	0.6555	1 4 7 12 13 14 15	1.1685
	2 3 7 10 11 12 14 15	0.6224	1 3 4 7 11 12 13 14	1.1551
8	2 7 10 11 12 13 14 15	0.6372	1 3 4 7 12 13 14 15	1.1157
	2 4 7 10 11 12 14 15	0.6384	1 4 7 11 12 13 14 15	1.0737
	2 3 7 10 11 12 13 14 15	0.6388	1 3 4 7 11 12 13 14 15	1.0961
9	2 3 4 7 10 11 12 13 14	0.6463	1 2 3 4 7 12 13 14 15	1.0500
	1 2 3 7 10 11 12 14 15	0.6529	1 2 4 7 11 12 13 14 15	1.0274
	2 3 4 7 10 11 12 13 14 15	0.6513	1 2 3 4 7 11 12 13 14 15	1.0419
10	1 2 3 7 10 11 12 13 14 15	0.6707	1 2 3 4 7 10 11 12 13 15	0.8860
	1 2 3 4 7 10 11 12 14 15	0.6800	1 3 4 7 10 11 12 13 14 15	0.8308
	All X's	0.6867		

Table 7.8 Most frequently occurring variables in 'best' combinations of the combinatorial regression, Table 7.7.

Variable No.	Frequency of Occurrence in Three Best Combinations of X's (Up to Iteration 6 inc.)	Frequency of Occurrence in Three Worst Combinations of X's (Up to Iteration 6 inc.)
1	-	6
2	14	-
3	7	8
4	1	13
7	2	14
10	11	1
11	13	-
12	2	7
13	-	5
14	6	1
15	7	8

partial F test values and hence least significance in the stepwise equation and also X8, of course, is omitted from the sequential procedure.

In the second combinatorial regression X1 (wave height)was omitted and X9 (predicted tide height)reinstated. The results of this, shown in Table 7.9, reveal that the change had little effect on the regressions. The best combination was exactly as before as were most of the other significant combinations. X9 is the second best variable when the variables were taken singly and also occurs in the best bivariate set, but thereafter it does not occur. However, the inclusion of X9 instead of X1 does appear to have a slight advantage in that the worst combinations are not quite as bad in terms of their R.M.S.R. values. X1 occurs very often in the worst sets of variables (Table 7.10) and its omission improves the R.M.S.R. of these combinations. Furthermore, the R.M.S.R. of the set of all variables is 0.6797 with X9 but with X1 is slightly worse at 0.6867. X9, as indicated by its late inclusion in the stepwise equation and the results in Table 7.9, is relatively insignificant.

Summarising the findings of this chapter it can be said that, within the range of the wave conditions covered by the tracer experiments, wave period was the most important variable in determining direction of sand movement normal to the shoreline. It accounted for 78.5% of the variation in the dependent variable when stepwise regression was conducted through the origin with fifteen independent variables and this importance was confirmed by combinatorial regression. At the same time, beach slope was found to be a significant variable more especially when wave period was removed from the regression. Net alongshore direction of sand movement was found to be largely determined by the direction of longshore current flow but the direction of wave thrust through swash/backwash and longshore drift had an influence when longshore current was unimportant. Although a direct link was found between wind direction and the direction

Table 7.9 Results of Combinatorial Regression for Concentration Index of Onshore/Offshore Sand Movement : All X's minus X1, X5, X6 & X8.

Iteration	Best Three Combinations of X's	R.M.S.R.	Worst Three Combinations of X's	R.M.S.R.
	2	1.0069	3	2.9559
1	9	1.0412	7	2.8281
	11	1.0452	4	1.8735
	10 11	0.8833	3 7	2.7613
2	3 9	0.9230	4 7	1.9037
	9 15	0.9297	3 4	1.8977
	2 3 11	0.8006	3 4 7	1.8644
3	3 10 11	0.8057	3 7 12	1.7718
	2 11 15	0.8081	4 7 15	1.7564
	2 10 11 15	0.7438	3 4 7 12	1.6833
4	2 3 10 11	0.7741	4 7 12 15	1.6000
	2 3 10 12	0.7751	3 4 7 15	1.5372
	2 10 11 14 15	0.6707	4 7 12 13 15	1.4933
5	2 3 10 11 15	0.7418	3 4 7 12 15	1.3499
	2 3 10 11 14	0.7471	3 4 7 13 15	1.3114
	2 7 10 11 14 15	0.6323	3 4 7 12 13 15	1.2209
6	2 3 10 11 14 15	0.6645	4 7 11 12 13 15	1.1445
	2 7 10 12 14 15	0.6720	4 7 9 10 13 14	1.1269
	2 7 10 11 12 14 15	0.6131	4 7 11 12 13 14 15	1.1106
7	2 3 7 10 11 14 15	0.6494	3 4 7 12 13 14 15	1.1103
	2 7 10 11 13 14 15	0.6555	2 3 7 9 10 13 14	1.1029
	2 3 7 10 11 12 14 15	0.6224	3 4 7 11 12 13 14 15	1.0989
8	2 7 10 11 12 13 14 15	0.6372	3 4 7 9 12 13 14 15	1.0802
	2 4 7 10 11 12 14 15	0.6384	2 3 4 7 9 10 13 14	1.0534
	2 3 7 10 11 12 13 14 15	0.6388	2 3 4 7 9 12 13 14 15	1.0119
9	2 3 4 7 10 11 12 14 15	0.6463	2 3 4 7 9 10 13 14 15	1.0052
	2 3 7 9 10 11 12 14 15	0.6516	2 3 4 7 11 12 13 14 15	0.9918
	2 3 4 7 10 11 12 13 14 15	0.6513	2 3 4 7 9 11 12 13 14 15	0.9252
10	2 3 7 9 10 11 12 13 14 15	0.6665	3 4 7 9 10 11 12 13 14 15	0.8329
	2 3 4 7 9 10 11 12 14 15	0.8226	2 3 7 9 10 11 12 13 14 15	0.8226
	All X's	0.6797		

Table 7.10 Most frequently occurring variables in the best combinations of the combinatorial regression, Table 7.9.

Variable No.	Frequency of Occurrence in Three Best Combinations of X's (Up to Iteration 6 inc.)	Frequency of Occurrence in Three Worst Combinations of X's (Up to Iteration 6 inc.)
2	12	-
3	8	10
4	-	14
7	2	15
9	2	1
10	11	1
11	12	1
12	2	6
13	-	5
14	5	1
15	8	8

of sand movement normal to the shoreline, confirming King's (1972) suggestions, other analysis concerning breaker type, wave steepness and bottom orbital velocities provided conflicting results with previous findings. However, this may largely be accounted for by fundamental differences between the field tests in this study and those of previous studies, especially the fact that movement of sediment, as measured in this study, was the product of several dynamic nearshore zones and their respective dominant processes rather than one specific zone.

CHAPTER 8

EVALUATION OF THE MODEL

8:1 Introduction

In the previous two chapters selection procedures have been used to produce sets of variables which best explain the variation in a series of dependent variables describing direction and amount of sand movement. Amount of sand movement was divided into alongshore and onshore/offshore components and direction was also considered on the basis of the distinction between onshore or offshore and alongshore to the north or to the south with respect to the line of this part of the coast. Using the equations produced by the analysis it is possible to predict the nature of the various aspects of sand movement given the necessary input information. Each aspect can be treated separately so that, for example, it can be stated whether sand movement will be onshore or offshore given certain conditions over a tidal cycle. On the other hand, all the separate equations may be used together to predict the position of average tracer movement.

In this chapter the success of the regression equations as predictive models will be assessed and tested using data collected independently of this study. A summary of findings from the study is given in Section 8:3 and a final consideration of the exploratory nature of the study made in Section 8:4.

8:2 The predictive model

A distinction must be made between the prediction based upon theory and that based upon empirical modelling such as that employed in this study. Physical or mathematical models based on universally valid statements will predict responses that should arise from the physical processes specified in the model, whilst statistical models will predict responses

that are'true' within specified limits. Prediction from a statistical model is achieved through interpolation within, or extrapolation beyond, the range of values assumed by the variables within the model. Thus, the prediction of beach slope from the regression of this variable on mean grain size will only be legitimate within the range of values of grain size for that particular sample of points. On the other hand, it is possible to predict at what speed a freely falling object will hit the ground,after falling from particular heights,for any sample of heights because the law of gravity is universally applicable and derived from physical theory. Although prediction stemming from statistical inference is in some respects a more dangerous and a more limited affair it is nevertheless a valid and widely used technique.

The 'best' equations suggested by the regression analysis of the previous two chapters are shown in Table 8.1. It was noted in Section 6:3 that practical considerations such as ease of measurement or cost of measurement of certain variables may be important factors when considering the number or type of variables in a predictor equation and as a result equations are also shown in Table 8.1 other than those shown on the basis of $\bar{R}^2$ calculations. Data collected independently of this study is used to test the predictive efficiency of the models as this is probably the most practical and convincing test of significance. The data was collected during tracer experiments conducted on the 5.3.77 and 1.6.77 on the lower part of the beach at Skegness and values of independent variables were substituted in the listed equations. The 'best' results of this are shown in Table 8.2 along with the actual figures for sand movement as revealed by the dispersion of the tracer.

In general, all the equations tended to overestimate the amount of alongshore sand movement and underestimate the distance moved normal to the shoreline . In particular the alongshore movement for 5.3.77 was overestimated but the predictions for 1.6.77 were in the main far closer

Table 8.1 Best Predictor Equations from Regression Analysis

		Equation	R^2	$\bar{R}^2$
DISTANCE ALONGSHORE:				
Stepwise:	Eq. 8.1	$Y = 21.629X1 - 0.771X14 + 217.561X11 + 0.230X3 + 1.626X8$	78.5	74.9
	Eq. 8.2	$Y = 41.839X1 - 0.457X14 + 311.411X11 + 0.073X3 + 0.231X8 - 20.689X15 + 4.076X13 - 2.164X12 + 5.232X10 - 2.472X2 - 8.145X5$	88.1	81.5
	Eq. 8.3	$Y = 46.460X1 - 0.376X14 + 418.192X11 + 0.188X3 + 1.992X8 - 16.069X15 + 2.333X13 - 1.839X12 + 3.441X10 - 1.429X2 - 29.406X16 - 0.413X6 - 0644X7 - 0.100X4$	89.3	80.0
Combinatorial:	Eq. 8.4	$Y = 33.682X1 - 1.813X2 + 0.107X3 + 2.549X8 + 2.218X10 + 388.759X11 - 3.383X12 + 4.769X13 - 0.568X14 - 9.649X15$	87.4	81.4
DISTANCE ONSHORE/OFFSHORE:				
Stepwise:	Eq. 8.6	$Y = 118.709X10 - 0.091X8 + 5.252X1 - 0.744X9 + 0.383X11$	66.8	61.4
	Eq. 8.7	$Y = 82.666X10 - 0.275X8 - 0.987X9 + 0.749X11 + 0.528X2 + 0.098X13 + 3.162X15 + 0.196X7 - 1.076X12 - 0.042X5$	71.8	58.4
Combinatorial:	Eq. 8.8	$Y = 0.392X7 - 0.407X8 + 0.982X10 + 1.219X11 - 2.540X12$	63.6	57.2
DIRECTION ONSHORE/OFFSHORE:				
Stepwise:	Eq. 8.9	$Y = 0.129X2 - 0.001X3 + 0.136X11 + 15.975X10 - 0.535X14 - 1.165X15 - 0.022X8$	89.5	86.5
	Eq. 8.10	$Y = 0.132X2 - 0.003X3 + 0.121X11 + 20.03X10 - 0.942X14 - 0.870X15 + 0.010X13 + 0.095X12 - 0.021X7 - 0.214X4 + 0.550X9 - 0.009X8$	90.8	84.8
Combinatorial:	Eq. 8.11	$Y = 0.146X2 - 0.029X7 + 21.697X10 + 0.087X11 + 0.112X12 - 0.626X14 - 1.298X15$	89.7	87.1

Table 8.2 Comparison of best predictions with observed values

	Observed Value	Best Predicted Value	Confidence Limits (95%)	
Amount of movement alongshore (m)				
5.3.77	1.498	11.017 (Eq.8.3)	-13.817	35.850
1.6.77	10.585	16.479 (")	- 0.928	33.886
Amount of movement onshore/offshore (m)				
5.3.77	1.175	0.646 (Eq.8.6)	- 4.579	5.872
1.6.77	3.255	1.433 (")	- 3.949	6.815
Direction of Movement onshore/offshore (Dimensionless)				
5.3.77	0.989	0.945 (Eq.8.11)	0.298	1.592
1.6.77	0.951	0.606 (")	0.055	1.156

to reality. Of the equations for average distance moved onshore/offshore only equation 8.6 gave meaningful results since negative values were obtained from the other two equations. The prediction of direction in gross terms, onshore or offshore, was correct for both experiments when the equations for the index of direction were taken except when the stepwise equation with 5 X's was used. Precise values of the concentration index were, however, underestimated for both experiments with all equations. Equation 8.11 provided the closest predicted values. It must be pointed out that in prediction from a statistical model the predicted values should range from plus to minus infinity and be normally distributed. Consequently negative values are shown in Table 8.2. However, in reality values less than zero are meaningless and may be treated as zero.

When all the best predictions are combined it is possible to plot the predicted position of the centre of gravity of the dispersed tracer cloud for each test, Figure 8.1. Using the longshore current direction to predict the dominant alongshore vector of sediment motion and the concentration index equation 8.11 for the onshore/offshore direction, the correct quadrant of the graph for the location of the mean point is predicted. However, when the predicted average distances of movement are used as coordinates for the mean point within the quadrant the amount of error is clearly visible.

Since the regression model is a statistical one it is possible to place confidence limits around the predicted values. The predicted values given by the regression equation represent the mean of all possible values of the dependent variable given the independent variable inputs. Assuming that the forecast error, that is the difference between observed and predicted values, is normally distributed with a mean of 0 then an unbiased estimator of the variance of the forecast error, s_f^2, is shown by Kmenta (1971) to be given by:

Figure 8.1.

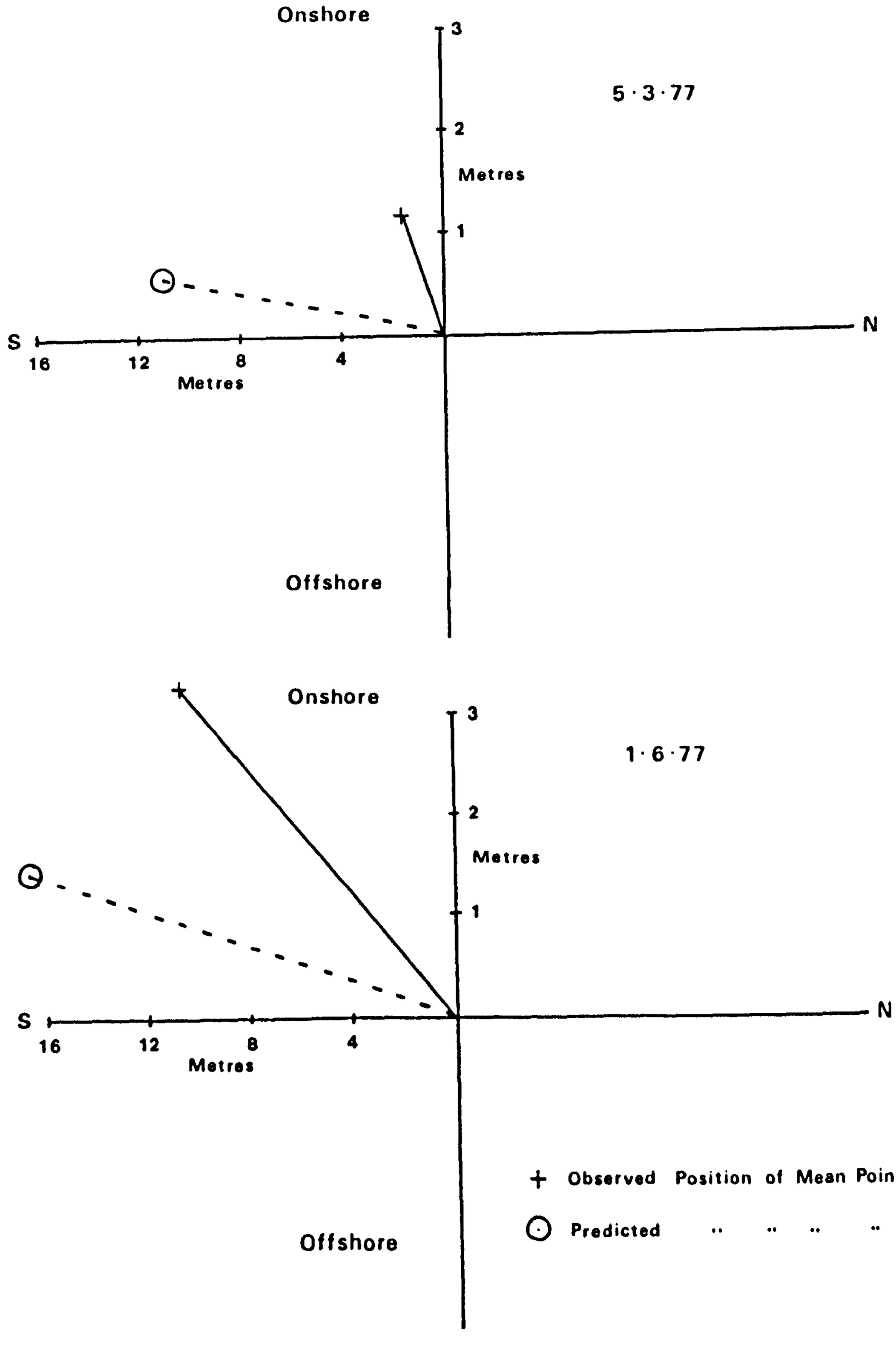
Onshore
3
5·3·77
2
Metres
1
N
S
16
12
8
4
Metres
Offshore
Onshore
3
1·6·77
2
Metres
1
S
N
16
12
8
4
Metres
Offshore
+ Observed Position of Mean Point
Predicted

$$s_f^2 = s^2 \left[1 + \frac{1}{n} + (X_o - \bar{X})^1 (X^1X)^{-1} (X_o - \bar{X})\right] \qquad \text{Eq. 8.12}$$

where s = unbiased estimator of observed Y values.

Then

$$\frac{Y_o - \bar{Y}_o}{s_f} \approx t_{n-k} \qquad \text{Eq. 8.13}$$

where n = number of observations, and

k = number of coefficients,

can be used to construct a forecast interval with any chosen probability level. The results of these calculations for the two sets of test data used in this section with the 'best' predictors are incorporated in Table 8.2. It will be seen that for all aspects of sand movement modelled by regression methods the actual observed value for the two experiments falls well within the 95% confidence limits placed around the predicted values. This is an indication of the relative efficiency of the equation band around any predicted points. At the same time, of course, a different sample may produce a different regression equation but it would be expected to contain the same explanatory variables with roughly the same importance. Improvement of the explanatory and predictive strength of the regression models would also be achieved through the use of more accurate data, that is by reducing the measurement error inherent in the data. In this context the improved methods of measuring some of the process variables such as wave height and period and current speeds using semi-continuous electronic instrumentation, as mentioned in Chapter 2 and described in Appendix 1, would be greatly beneficial to further study.

When dealing with simple linear regression it is usual to conduct an analysis of the residuals. Maddala (1977) states that "One of the most important and informative parts of the analysis in regression

equations is the analysis of residuals." However, with the multiple regression model a complete analysis is more difficult. Furthermore, since the data used in this analysis is not a time series in the sense of being regular observations on particular variables and the amount and direction of sand movement will not be affected by preceding values of these variables, in time or space, as measured in this study, it is unnecessary to test for autocorrelation amongst the disturbances. Nevertheless a plot of the residuals $(\hat{Y} - Y)$ against the predicted $(\hat{Y})$ values for each of the three best equations 8.3, 8.6 and 8.11 shows a random distribution of points (Figures 8.2 - 8.4). It would appear from this that the equations have been correctly specified and that the linear model is appropriate. This is not to say that further rearrangement and re-specification of the models could not be carried out. It has already been pointed out that some variables were not included because they were not measured or could not be measured consistently. Variables such as the height of the water table in the beach and swash/backwash velocities may add to the power of the models in the presence of the included predictors. In addition, the re-expression of some of the existing variables may also improve the explanatory content and predictive capacity of the equations. For example, the inclusion of a transformed grain size variable such as the root of mean grain size may improve the contribution of this particular predictor. Also re-expression of the time variable may improve the efficiency of the equations. Instead of the total length of time the tracer was covered by the tide this could be replaced by estimates of the time the tracer source was covered by particular dynamic zones. Thus, there is much scope for further investigation.

In a predictive sense it is dangerous to state that the equations listed are totally successful on the basis of two sets of test data. Nevertheless the models are encouraging as a first step and although the

Figure 8.2.

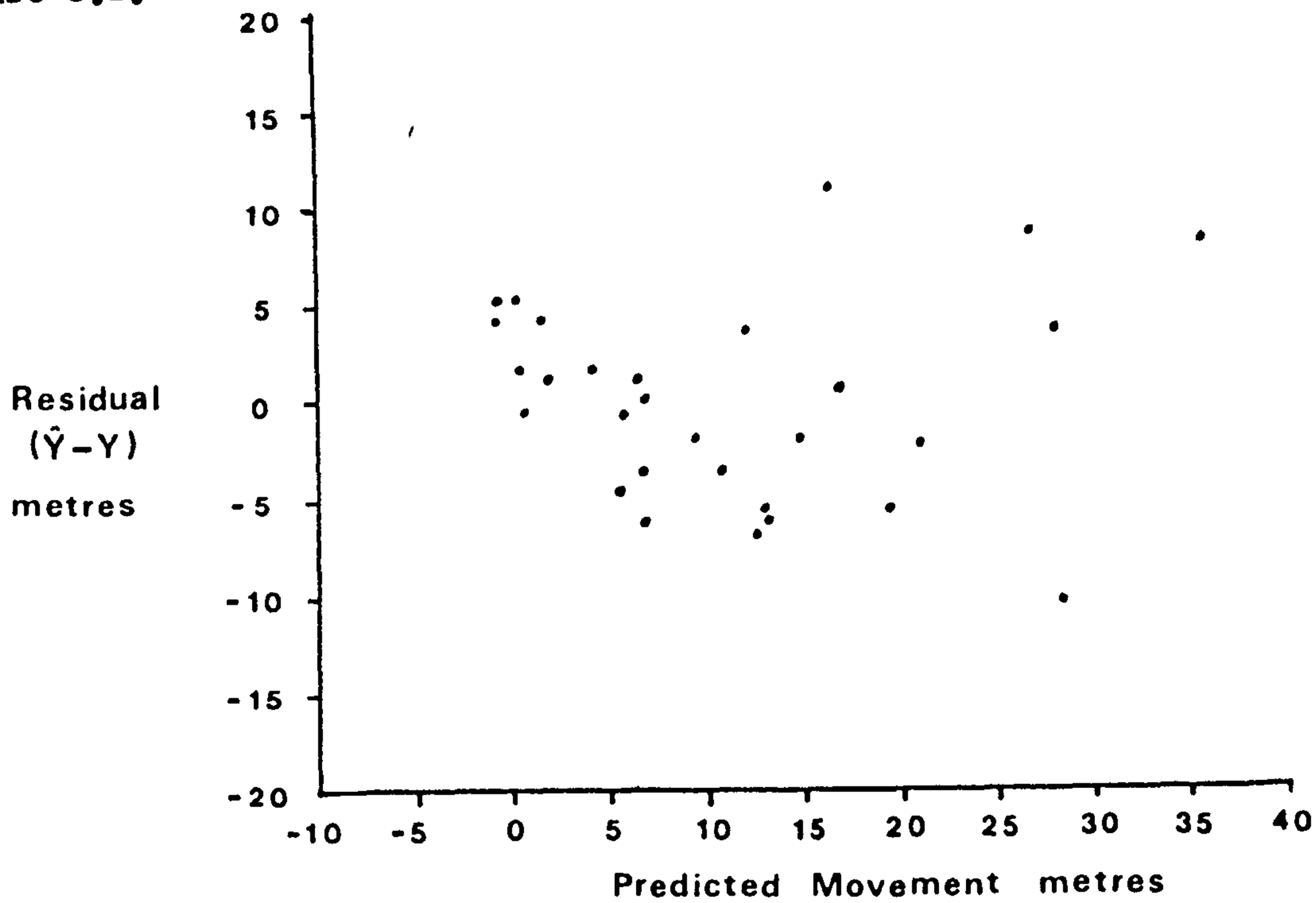

Figure 8.4.

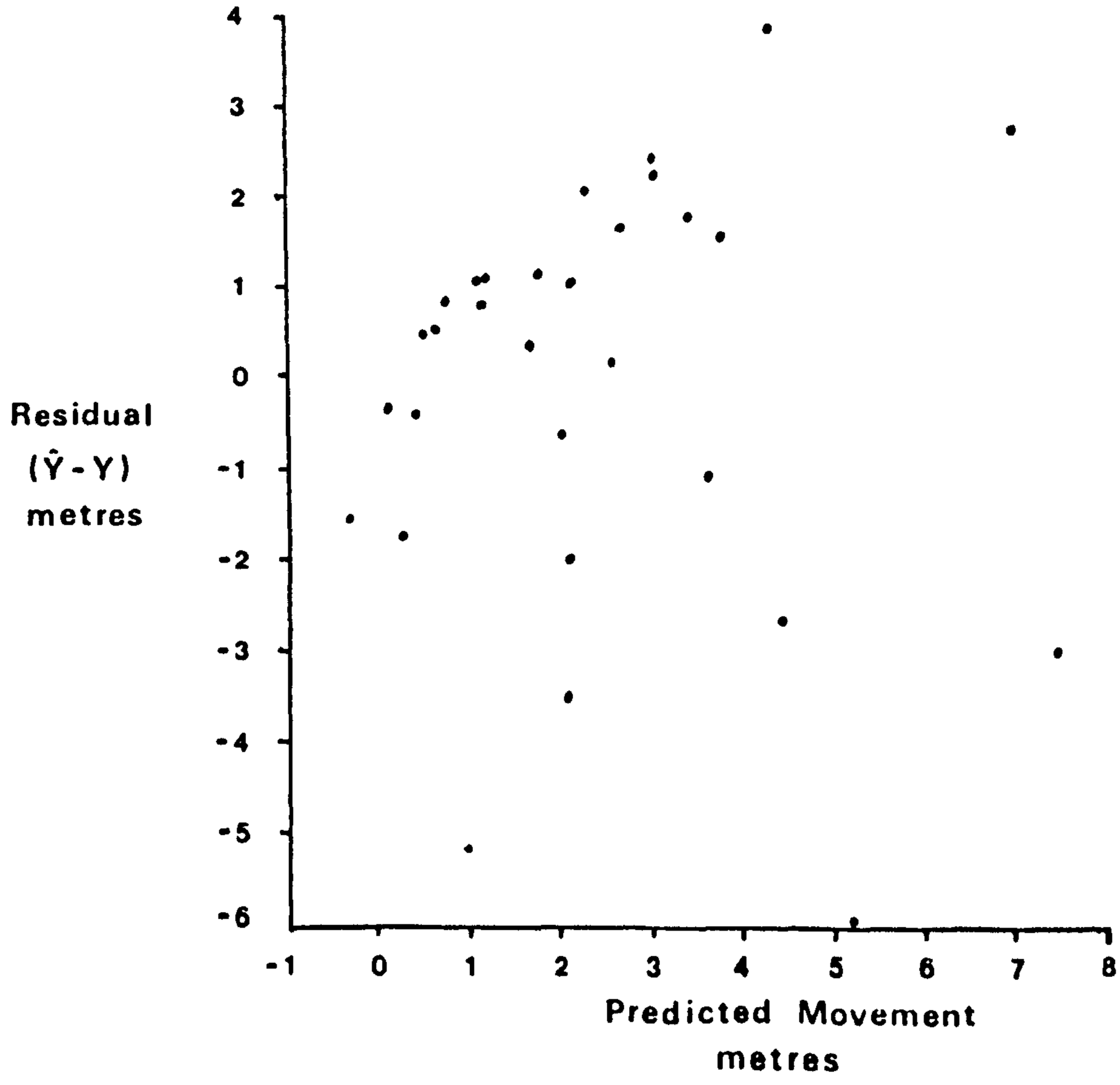

Figure 8.2.

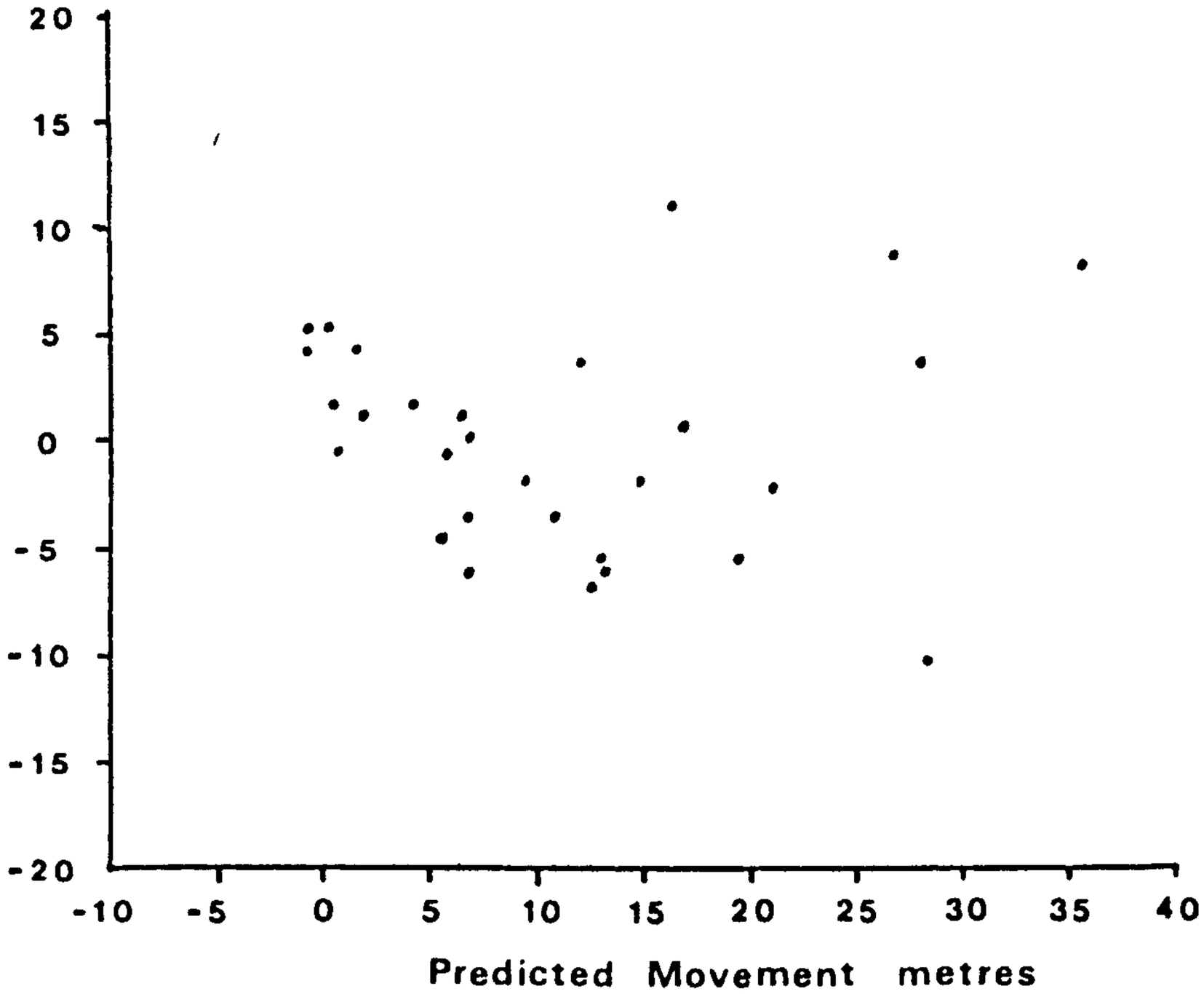

Figure 8.4.

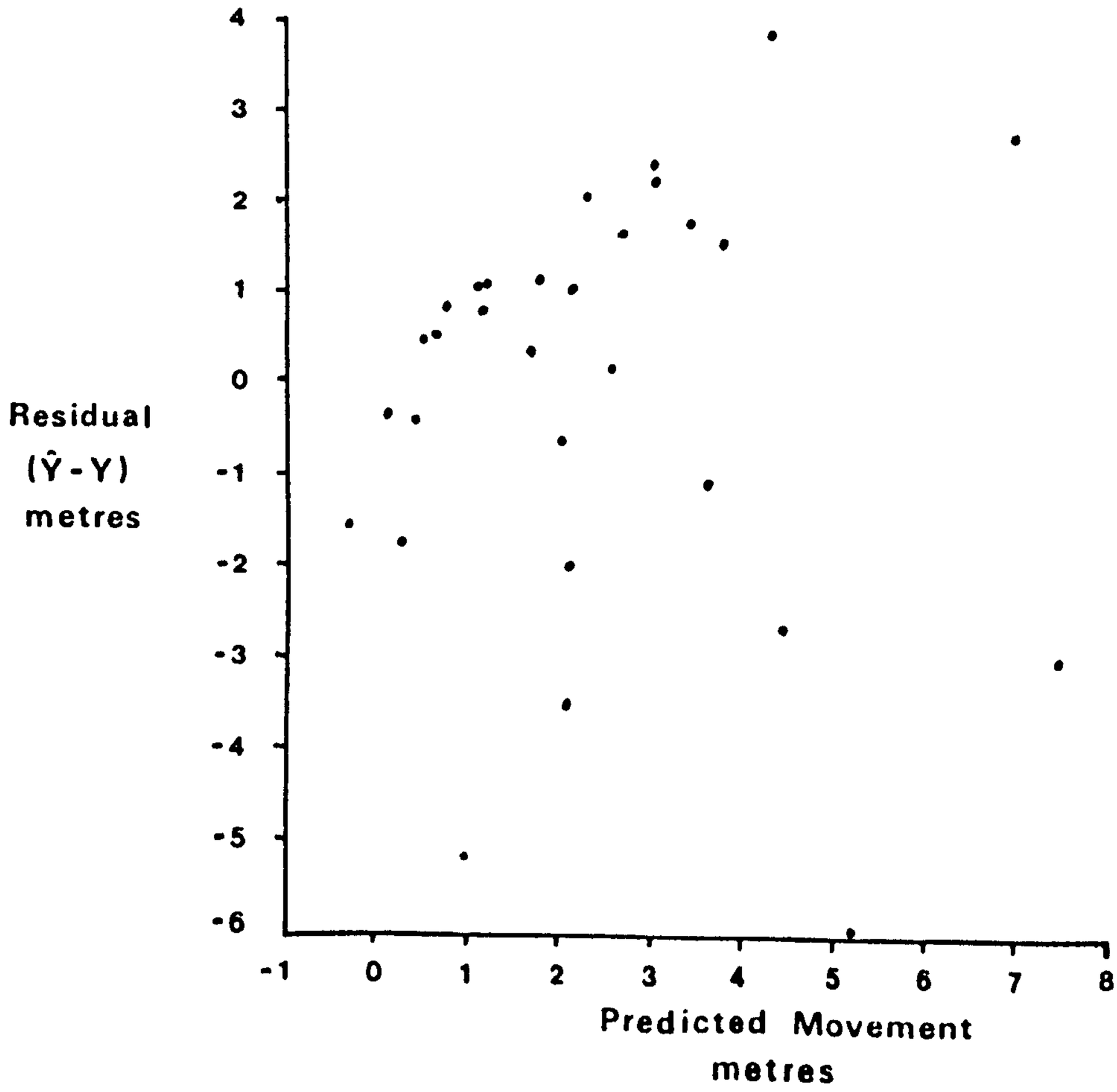

Figure 8.3.

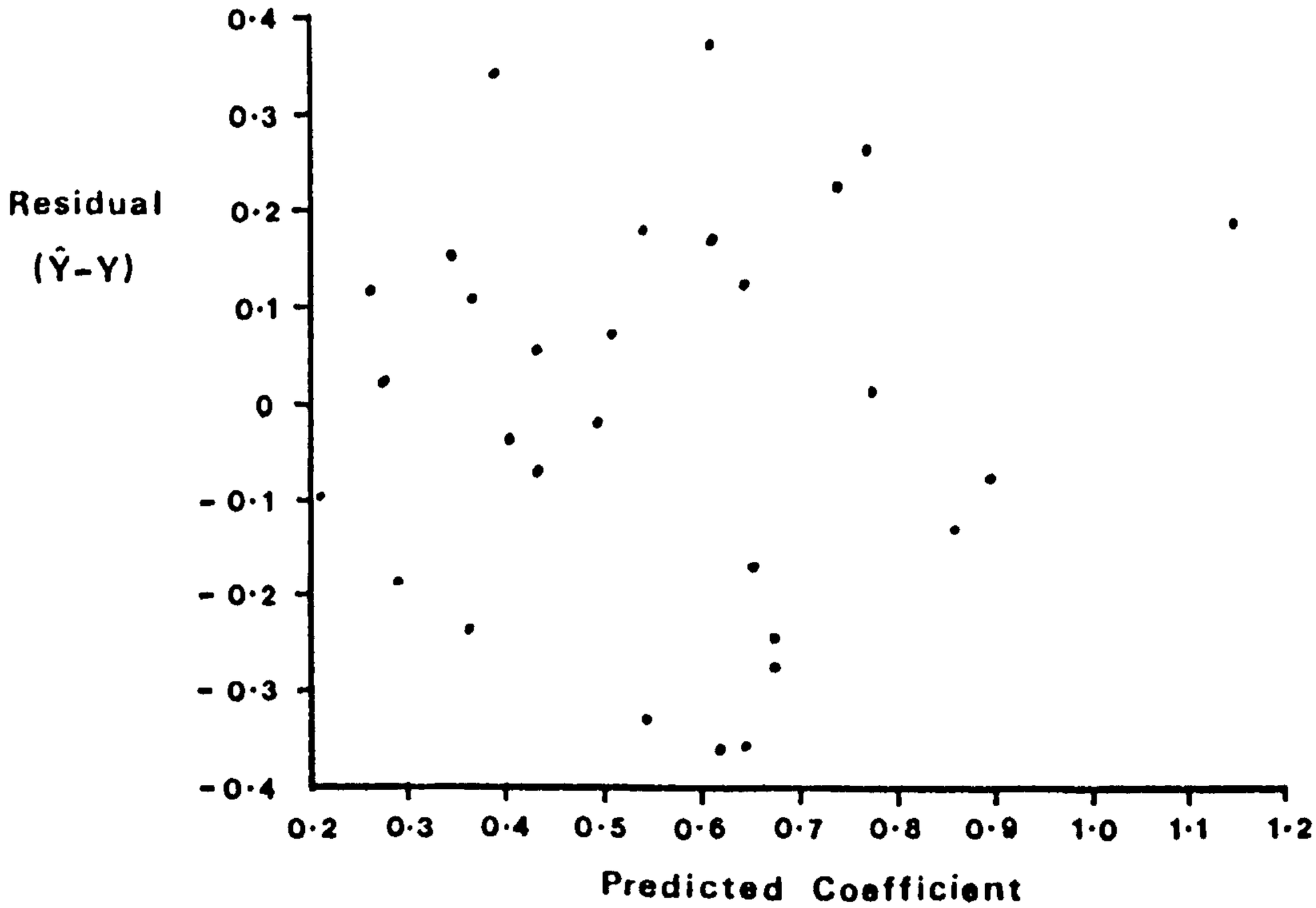
Residual
(Ŷ-Y)
0·4
0·3
0·2
0·1
0
- 0·1
- 0·2
- 0·3
- 0·4
0·2
0·3
0·4
0·5
0·6
0·7
0·8
0·9
1·0
1·1
1·2
Predicted Coefficient

equations were developed with data from the Lincolnshire coast this is not to say that they could not be applied more generally to beaches in other areas with similar conditions of beach morphology, tidal characteristics and wave climate.

Using the three predictor equations, plus direction of longshore current flow to estimate direction of movement alongshore, it is possible to derive the average direction and distance of movement of sand grains from a particular point on the beach. Further work may lead to the development of a simulation-type model of sand movement from these initial regression equations. Additionally, particular aspects of sand movement may be modelled separately as for example prediction of the net direction of movement normal to the shoreline. With respect to direction of movement the use of regression type methods with circular data would provide interesting comparisons.

8:3 Summary of findings

In this study a specific field procedure was developed for the use of fluorescent tracer techniques under macro-tidal conditions with limited manpower and equipment. The procedure was tailored to the needs of this study in the light of the problems encountered and under different circumstances may not be ideal. Indeed, with greater inputs of manpower and equipment two major improvements to the field method would be the use of core sampling devices and multiple sampling throughout the tidal cycle. One serious drawback to the general tracer method was found to be the lack of control over actual amounts of tracer released from the injection point due to the unpredictability of erosional and depositional episodes during the tidal cycle. Electronic instrumentation was developed to provide improved measurements of wave and current characteristics but this was not available for the fieldwork conducted in the present study.

Attention has been focussed solely on bed-load transport because

tracers are not amenable to the study of suspended sediment movement in the field. The relative importance of each mode of transportation in total sediment movement is a matter of controversy but recent direct observations over the entire surf zone by Brenninkmeyer (1975) suggested that suspended sediment movement is much less important than bed-load transport.

In the first part of this study the results of individual tracer experiments and specific tests were considered. Acknowledging any limitations of the field technique and working over the fundamental beach time unit of one tidal cycle, it was shown that in this strongly tidal environment sediment movement patterns across the foreshore were complex. Probably because of the differences in the period of operation of particular dynamic zones over specific parts of the beach considerable differences in the measured rates of sediment movement were discovered across the width of the foreshore. In addition to this it was found that general sand movement could be in opposite directions on different parts of the foreshore during the same tidal cycle. This was in part explained by the influence of tidal currents on the lower beach for which there was confirmatory evidence at Gibraltar Point. Morphological effects were also important in this respect through wave refraction. In general it was found that alongshore components of movement were far stronger at Gibraltar Point than further north at Skegness and that sand movement both alongshore and normal to the beach was greater on the upper of two beach ridges than the lower.

Tests conducted to study differential grain size movements were inconclusive but did show that sorting was not taking place through the movement of different sized grains in contrasting directions. However, different rates of movement were observed for different groups of size fractions. Grains of 2 ϕ and larger were found to move shorter distances on average than finer grains.

The data from the tracer experiments was used to test two models often employed in the prediction of longshore sand transport rates. The results supported Komar's (1969) findings that both wave energy flux and Inman and Bagnold's (1963) energetics model were successful in relating longshore sand transport to wave and current characteristics. Proportionality coefficients of 0.525 and 0.179 were produced from this study compared with 0.77 and 0.28 from Komar's results.

In the second part of this study, a more general model of sand movement was proposed using multiple regression analysis. This was successfully tested with independently collected data. Wave height, accounting for 61.3% of the variation in the dependent variable, was found to be the most important variable affecting the average distance moved by sand grains alongshore. Water temperature, beach slope and longshore current velocity were also found to be of significance. Beach slope was found to account for 59.2% of the variation of average distance of sand movement normal to the shoreline but the addition of later variables to the regression equation produced only slight improvements. The absence of mean grain size from predictor equations was thought to be the result of strong intercorrelations between certain independent variables but the complexity of the system under study and the complicated role of grain size within that system could also account for this. Direction of sand movement alongshore was seen to be determined largely by the direction of longshore current flow but normal to the shoreline wave period was found to account for 78.5% of the variation in the index of net movement, used as an indicator of movement direction onshore/offshore. At the same time beach slope was also found to be important, especially when wave period was omitted from consideration.

The three equations found to be the best predictors based on independently collected data were as follows:

a) Average distance moved by sand grains alongshore:

$$Y = 46.460\,X1 - 0.376\,X14 + 418.192\,X11 + 0.188\,X3 + 1.922\,X8 - 16.069\,X15 + 2.333\,X13 - 1.839\,X12 + 3.441\,X10 - 1.429\,X2 - 29.406\,X16 - 0.413\,X6 - 0.644\,X7 - 0.100\,X4 \qquad \text{Eq. 8.3}$$

N.B. For list of variables see Table 6.7

b) Average distance moved by sand grains onshore/offshore:

$$Y = 118.709\,X10 - 0.091\,X8 + 5.252\,X1 - 0.744\,X9 + 0.383\,X11 \qquad \text{Eq. 8.6}$$

N.B. For list of variables see Table 6.5

c) Direction of movement normal to shoreline:

$$Y = 0.146\,X2 - 0.029\,X7 + 21.697\,X10 + 0.087\,X11 + 0.112\,X12 - 0.626\,X14 - 1.298\,X15 \qquad \text{Eq. 8.11}$$

N.B. For list of variables see Table 6.5

Using these/together, in conjunction with longshore current direction equations to predict direction of alongshore sand movement, it was found possible to roughly predict the average amount and direction of grain movement from a particular point on the beach. Alternatively, specific aspects of sand movement could be modelled using the individual equations.

8:4 Conclusion

Field data concerning direct observation of sand movement is relatively scarce and in the past tracer techniques have largely been used to study individual aspects of sand movement such as, in particular, longshore sand transport rates. Alternatively, specific dynamic zones have been studied. Murray (1967) for example considered onshore/offshore sand movement in the shoaling wave zone and Siebold (1963) was concerned with the offshore zone. Ingle's (1966) work covered a wide range of topics relating to the various nearshore zones but only simple relationships were investigated largely in a qualitative manner. In this study the net results of processes operating in a succession of dynamic zones

(Figure 8.5) over the whole tidal cycle were observed and, following the assumption that the tracers employed were acting as efficient surrogates for the beach sand, the results of individual tracer experiments were scrutinised and an attempt made to model both amount and direction of sand movement. In this attempt the complex relationships of a complicated system were studied.

The empirical approach adopted was very much of an exploratory nature with multiple regression analysis employed as the means of investigating relationships within the data set. Since the period known as the 'quantitative revolution' in geography two opposing standpoints have been taken by users of multivariate methods and research workers in geography generally. On the one hand the use of deductive, scientific methods has been encouraged with investigation proceeding from hypothesis formulation based on existing theory, through testing using collected data relevant to the hypothesis, to final development of new laws. In this framework the role of multivariate analysis is seen as purely confirmatory. However, on the other hand the inductive or Baconian approach to scientific explanation is also widely used. In this approach empirical regularities are sought which can be transformed into postulated universal laws which in turn when linked will produce a body of theory capable of predicting the observed regularities (Harvey, 1969). Within this procedure, commonly used in disciplines where a firm basis of theory has not yet been established, multivariate techniques are employed in an exploratory manner, to suggest rather than confirm hypotheses. For example Krumbein (1976) proposes that in the framework of sequential modelling most standard least squares techniques are used as search models rather than end products.

The lack of a formal hypothesis as a base in the exploratory approach may in some cases lead to error but Tukey (1967) points out that " .... no conclusion or inference ever becomes knowledge without risk of error."

Figure 8.5 Conceptual process-response model of sediment movement on the tidal foreshore.

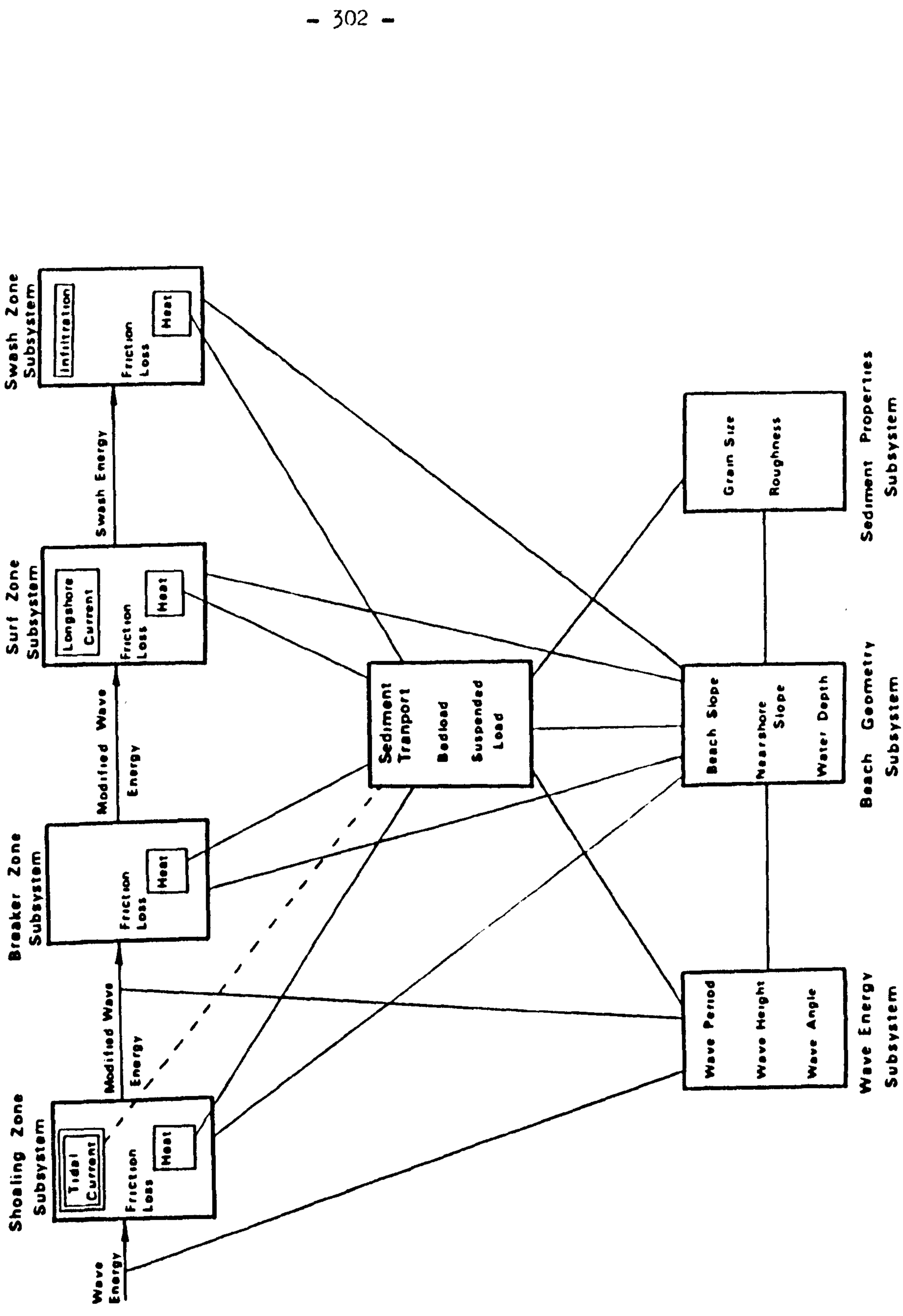

Tukey also stresses the need to view the two approaches to scientific explanation not solely as competing alternatives but as complementary paths to the creation of theory: "Both detection and adjudication play crucial roles in the progress of science as in the control of crime."

Although much work in physical geography follows the deductive model of the scientific method many examples of the valuable use of the exploratory, inductive approach do exist. In coastal studies Harrison's predictor equations of various aspects of the beach-ocean-atmosphere system produced by regression methods have already been discussed (Chapters 6 and 7). Work by Krumbein and others of a similar nature has also been mentioned and has played an important role in furthering the understanding of these systems. In hydrology the Stanford Watershed Model developed by Crawford and Linsley (1966) and the USDAHL model of watershed hydrology (Holtan et al, 1975) are just two examples of the results of the exploratory approach. The latter model is described by Holtan and Lopez as " ... a series of empiricisms selected to provide a mathematical continuum from ridgetop to watershed outlet in terms of input information readily available to the analyst." Finally, Melton (1957) provides an example of the exploratory approach in an analysis of relationships among elements of climate, surface properties and geomorphology.

In employing the multiple regression analysis in an exploratory design the problem of accounting for sediment movement in terms of amount and direction is viewed as a process response type system with complex relationships and feedback loops. This allows the sets of variables under consideration to be viewed as a whole rather than as a series of simpler relationships. Figure 8.5 demonstrates the complexity of the overall system and it is this very complexity plus the lack of a comprehensive body of theory to explain many of the observed relationships which suggests the utility of exploratory investigations which in turn may lead to the development of theory.

It is hoped that the exploratory analysis described in this study might form the basis of future work on sediment movement problems and that refined versions of predictive models may be produced. Dispersion of tracer with depth is at present being studied whilst movement of sand in suspension should also be considered if a model of total sand transport is required. This study was largely concerned with understanding and modelling the processes involved in short-term sand movements but building upon this type of work, probabilistic methods may be used to predict more accurately the longer term, larger scale foreshore sediment movements which are not only of academic interest but of great practical importance both to the engineer and the local community. Prediction of future trends at Skegness, for example, are greatly needed in view of the plans for the development of the foreshore and the importance of the beach as a tourist asset in what is at present an area of foreshore erosion.

Finally, in view of the complexity of the system studied in the foregoing discussion and the nature of the work conducted for this dissertation it is perhaps pertinent to recall the words of the following quotation:

> "I do not know what I may appear to the world;
> but to myself I seem to have been only a boy
> playing on the seashore and diverting myself
> and now and then finding a smoother pebble or
> a prettier shell than ordinary, while the
> great oceans of truth lay undiscovered before
> me."
>
> (Newton)

APPENDIX 1

INSTRUMENTATION

Because of the relative inaccuracy and discontinuous nature of wave measurements made with a metre staff held in the breaking wave zone an attempt was made to produce a semi-continuous wave recording system which would enable accurate measurements of wave height, wave period and angle of wave approach to be made.

The system devised consists of a resin moulded wave pole, a synchroniser, a power source and a tape recorder. In the field these are linked by a length of three core cable, from the measuring pole at the required point on the beach to the tape recorder in a 'dry' position in the dunes, at the back of the beach. Power supply for the system is provided by a 9 volt rechargeable power pack.

The pole itself is constructed from an inner polypropylene tube approximately 2.5 metres long and of 33mm diameter into which 2BA stainless steel bolts are driven at intervals of four centimetres. This distance represents the accuracy of wave height measurement and can be varied accordingly. The bolts are positioned so that on moulding the bolt heads are flush with the resin surface and hence able to act as electrical contacts. They are also positioned in rings of three around the tube, although again this number may be varied. At intervals, offset from rings of bolts inserted to act as 'live' contacts, rings of bolts to act as earth contacts are included. The poles built for experiments in this study contained 60 rings of live contacts and 10 rings of earth contacts and consequently were able to measure waves up to about 1.5 metres in height. Solid core wire is attached to each ring of bolts and linked to the top of the pole through the inner polypropylene tube. Details of the pole are shown in Figure A1.1 and also Plate A1.1.

Once tested the inner tube is then cast in polyester resin in a tube

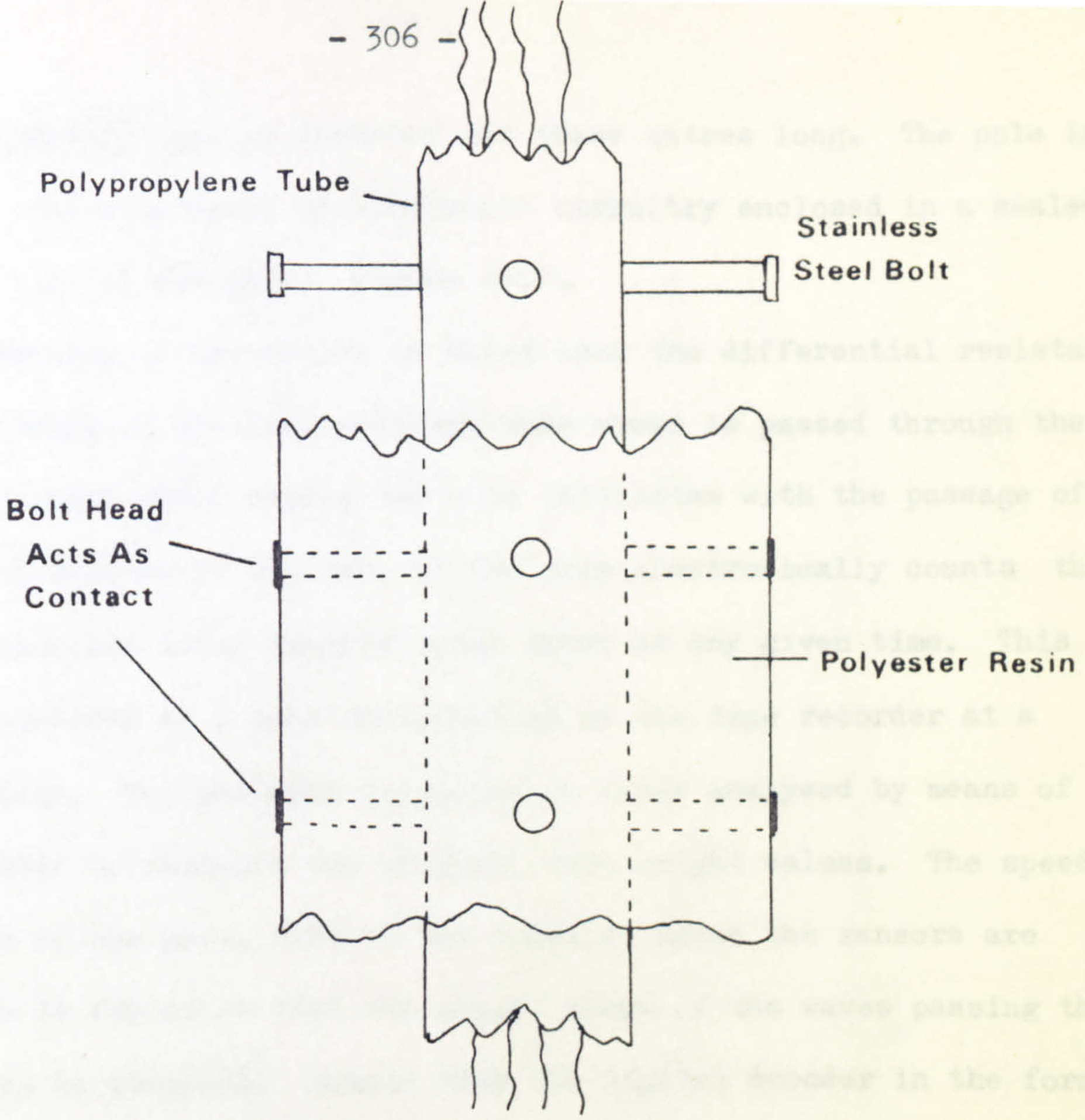

Figure A1.1. Internal details of wave pole.

Plate A1.1. Detail of completed wave pole (foreground). Pole fixed to beach face with concrete base and guy ropes (background).

mould approximately 50cm in diameter and three metres long. The pole is completed by the attachment of electronic circuitry enclosed in a sealed tube to the top of the pole. Figure A1.2.

The operation of the system is based upon the differential resistance changes occurring at the live contacts when power is passed through the pole and the water level around the pole oscillates with the passage of waves. The circuitry at the top of the pole electronically counts the number of stainless steel sensors under water at any given time. This number is converted to a tone and recorded on the tape recorder at a remote location. The recorded frequency is later analysed by means of a digital decoder to retrieve the original wave height values. The speed of operation of the pole, that is the speed at which the sensors are counted, can be varied so that the actual shape of the waves passing the pole can also be recorded. Output from the digital decoder in the form of paper tape is directly available for computer processing. Figure A1.3 is an example of the plot of wave recordings made with the system. The rising trend of the plot indicates the incoming tide upon which is superimposed the wave oscillations themselves. From plots of this nature wave height and period calculations can easily be made.

When in use in the field the pole is linked to the tape recorder through a tone synchroniser, Figure A1.2. Its function is to synchronise the signals from several poles so that recordings made on different tape recorders can be made exactly contemporaneous. This enables information on wave approach to be collected. Given a series of wave poles positioned accordingly on the beach face, the arrival of the same wave front at different points in space and time can be recorded and an exact time comparison made by means of curve comparison. The mode of operation of the synchroniser is to chop the signals from the poles into equal space periods and to transmit these periods to tape recorders at exactly the same time. The frequency of signal chopping can be varied to accommodate the period

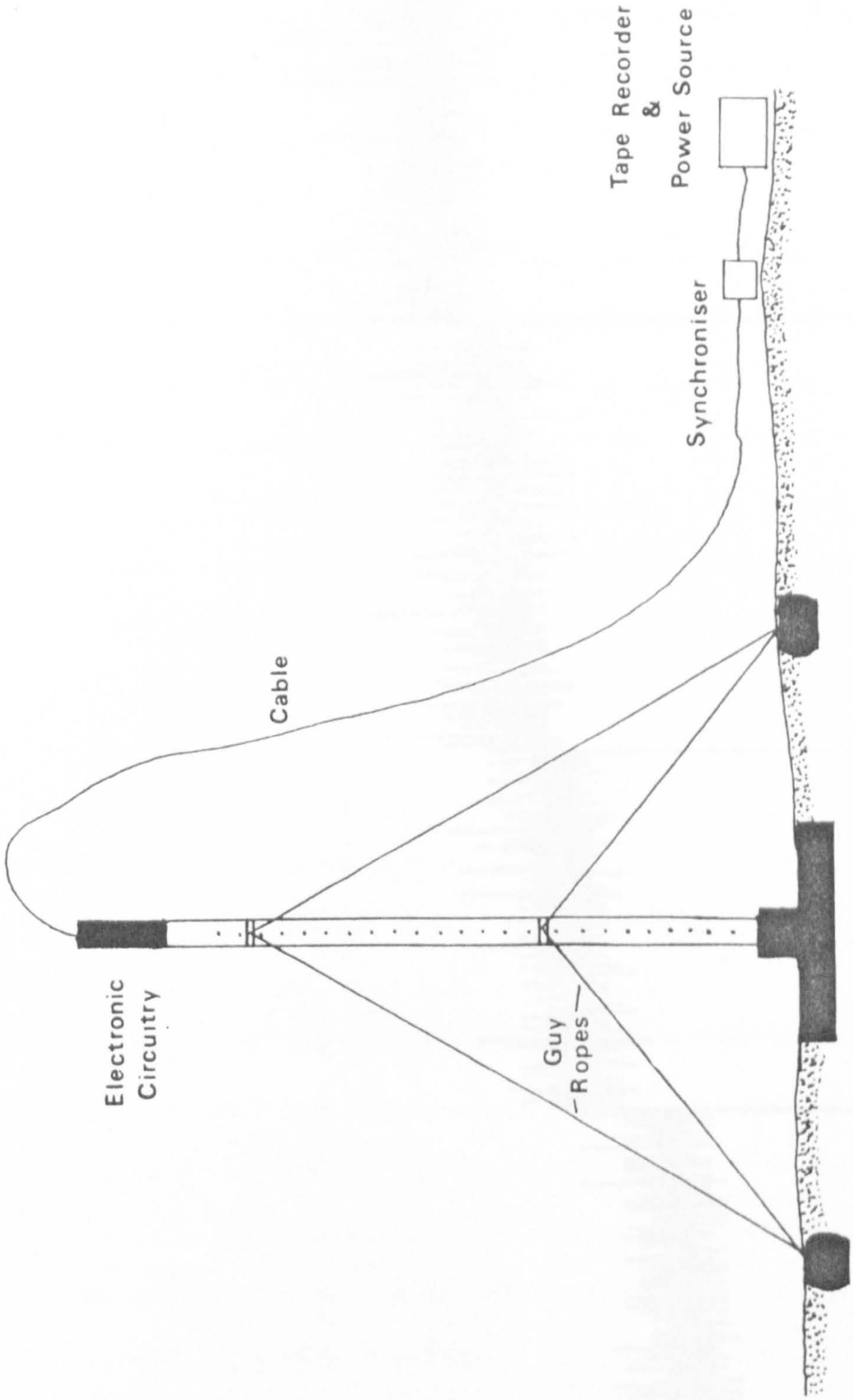

Figure A1.2. Schematic field layout of wave pole system.

Figure A1.3. Example plot of wave data from wave pole system. Recording made at Skegness on 13.3.78. Time of high tide (6.8m) 20.57. Note increase in underlying level of each burst of recording reflecting rise of tide. Tone bursts approximately 4 minutes in length.

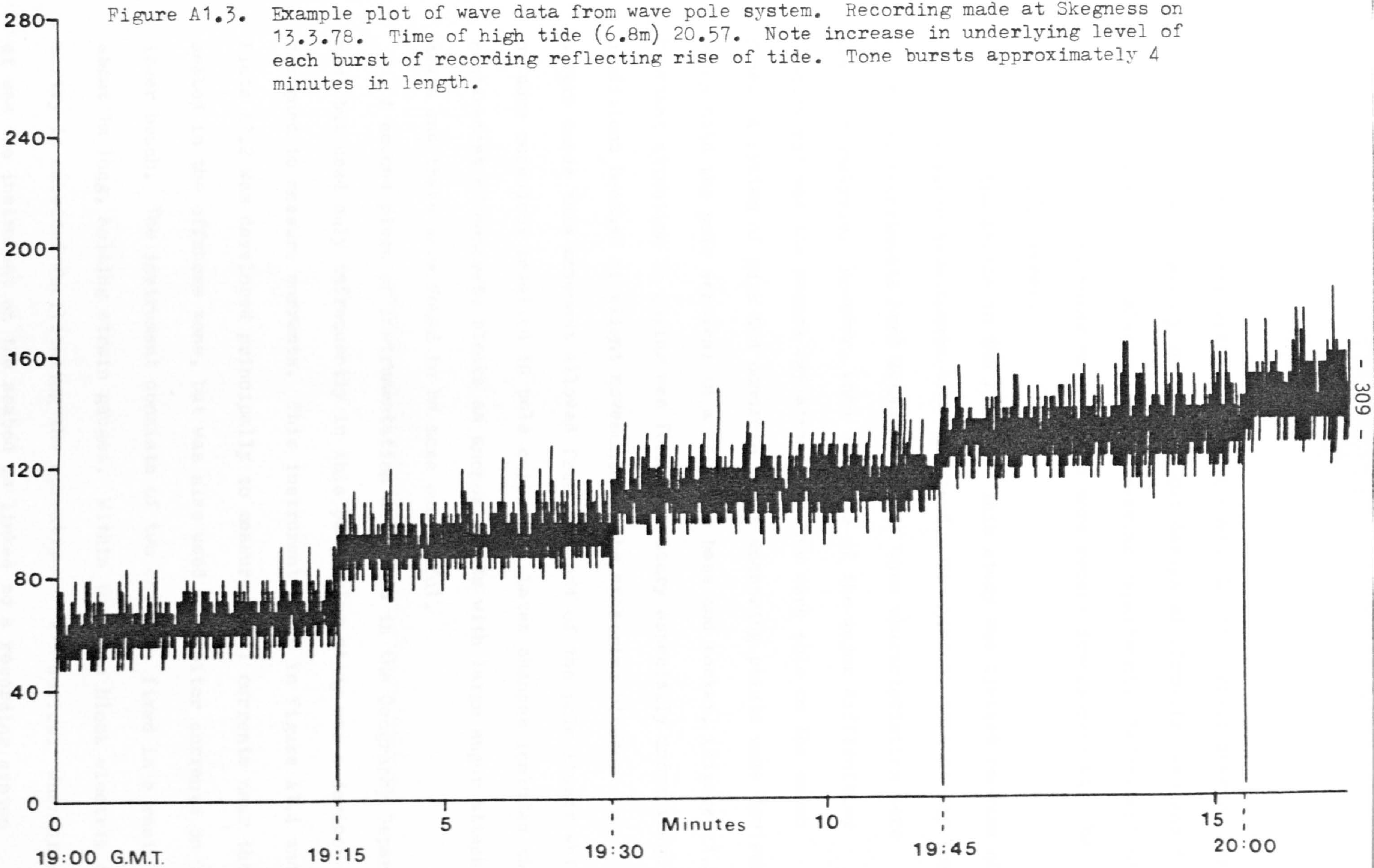

of different wave trains.

All electronic circuitry including custom built circuit boards, was assembled in the Geography Department but design of circuitry was assisted by Dr. C. Paull of the Electrical Engineering Department. Refinement of the system is a continuing process and more recent development will be detailed by E.J. Fraser.

Use of the system in the field in this study was limited because of the considerable development time involved. To maintain consistency for all tracer experiments hand measurements of wave characteristics were used for analysis. However, when used one of the major difficulties encountered was the secure emplacement of the wave pole on the beach face. A system of guys and concrete block anchoring points were devised which held the pole vertical in a concrete base and socket. (Figure A1.2). Constant attention to guying was found necessary especially under rough conditions because of slight movements of the anchoring blocks. In severe cases this movement allowed free movement of the pole itself which on some occasions resulted in pole collapse. Later changes included the replacement of concrete blocks as anchor points with large augur attachments and these were found to be more successful.

A second piece of instrumentation developed in the Geography Department but used only infrequently in this particular study was a device designed to measure currents. This instrument shown in Figure A1.4 and Plate A1.2 was developed principally to measure tidal currents near the seabed in the offshore zone, but was also used to monitor currents on the lower beach. The instrument consists of two columns, fixed in a resin block, about 1m long, holding strain gauges. Within the base block electric circuitry is embedded facilitating the operation of the device. When in use at sea the instrument on the seabed is linked to a recording system contained in a buoy at the surface by three core cable (Figure A1.5).

The operation of the instrument is based on the movement of the

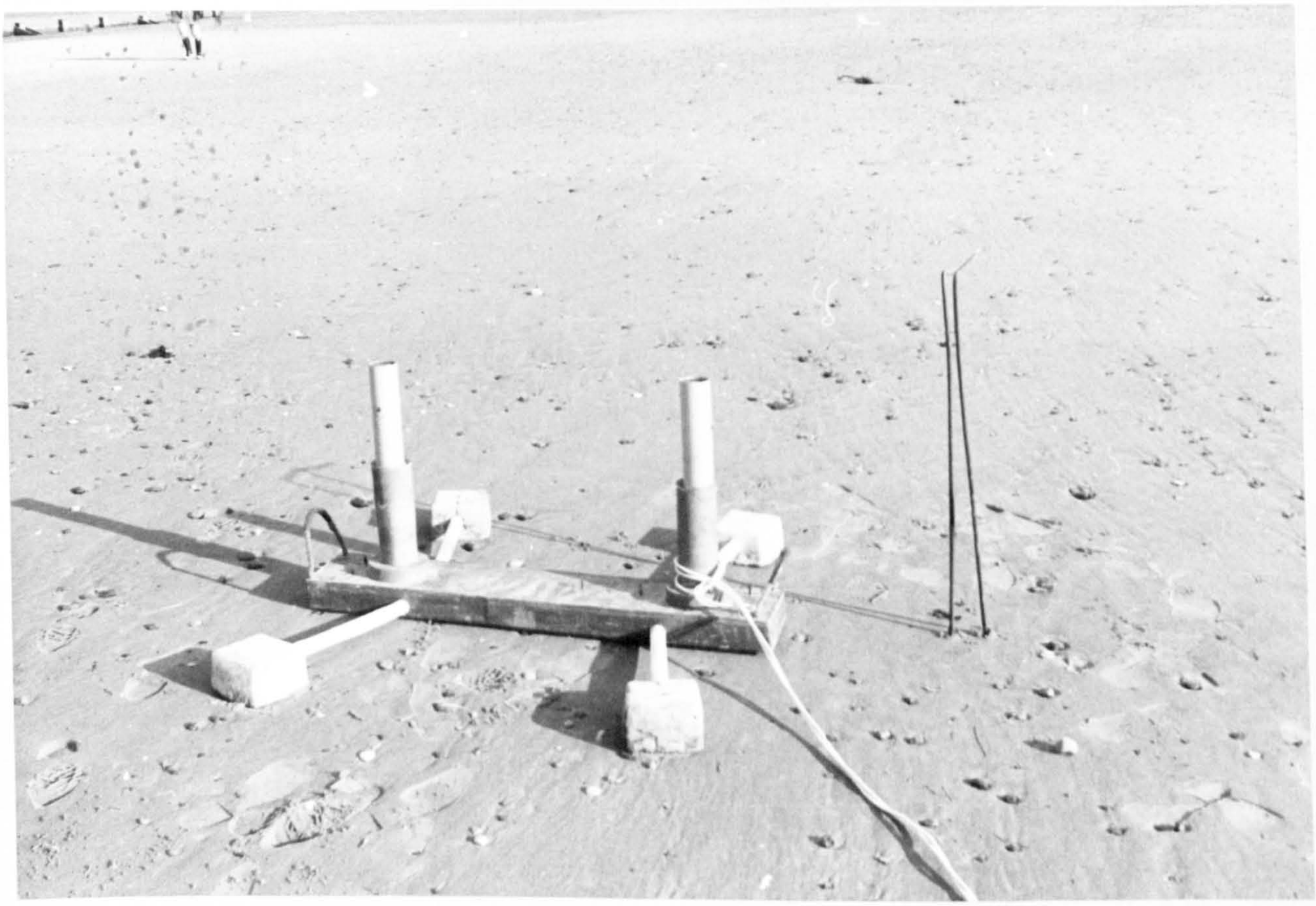

Plate A1.2. Straingauge current meter.

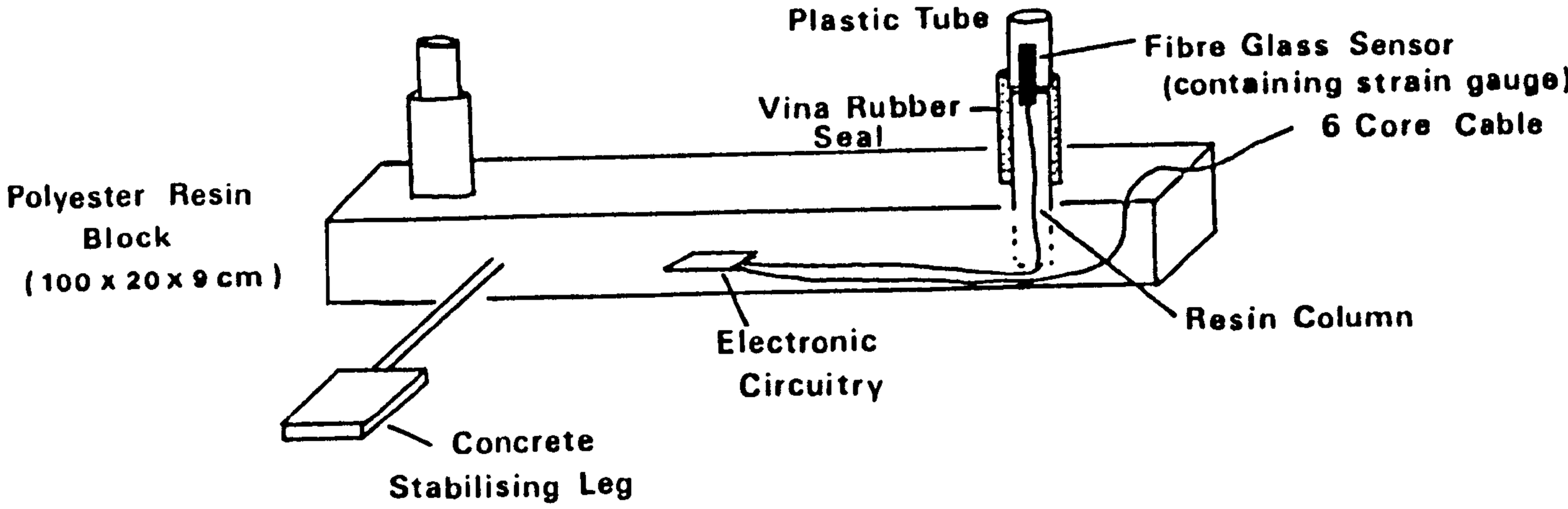

Figure A1.4. Details of straingauge current meter.

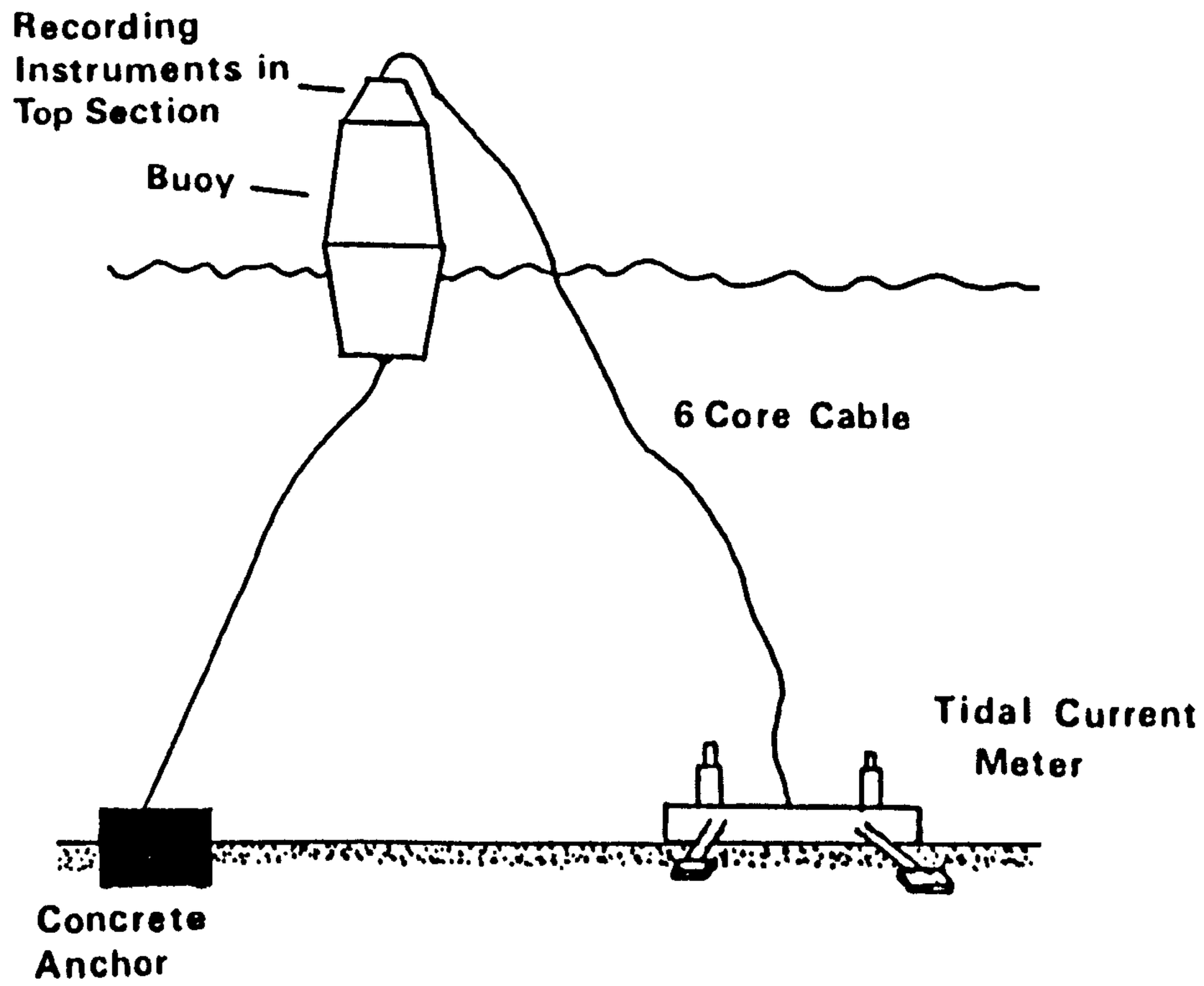

Figure A1.5. Schematic field layout of current meter system

strain gauges which causes a change in their electrical resistance dependent upon the pressure put upon them. The change in resistance is converted to a frequency or tone and hence any change in the tone given off by a sensor is proportional to the amount of bending of the gauges by the currents. Direction of change in frequency is related to the direction of pressure and two sensors were used to ensure that direction of flow as well as current velocity is measured. The actual recording procedure is as described for the wave pole system in that a chopped tone is held on cassette tape and then converted to digital form by means of a decoder. Because the device was designed to measure relatively slowly changing tidal currents intermittent sampling was used with a few seconds' burst of recording occurring at selected periods ranging from 2 to 16 minutes. A more detailed description of the design, construction and operation of this instrument can be found in Russell (1978).

Currents on the lower beach at Skegness and Gibraltar Point were recorded with this instrument and the results can be seen in Figures A1.6 to A1.11. The calibration curve for the instruments relating tone change expressed in gms. of force to current speed in cm/sec is shown in Figure A1.12 and from this current speeds can be obtained using the directional plot of the current meter records.

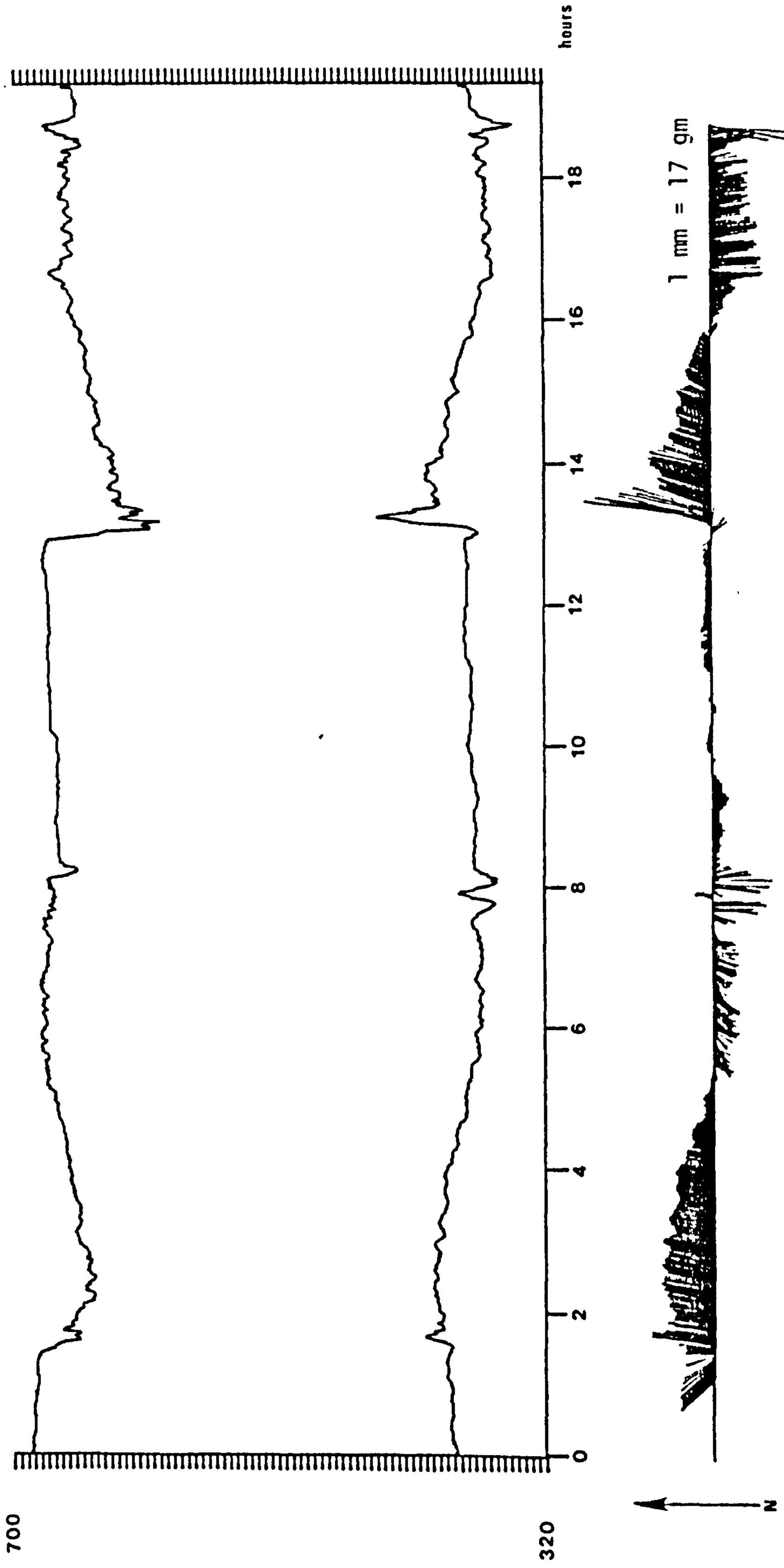

Figure A1.6. Plot of tidal currents measured on lower foreshore at Skegness, 4-5.2.77.
Recording height 15cm above the bed. Tidal heights 7m and 6.9m.

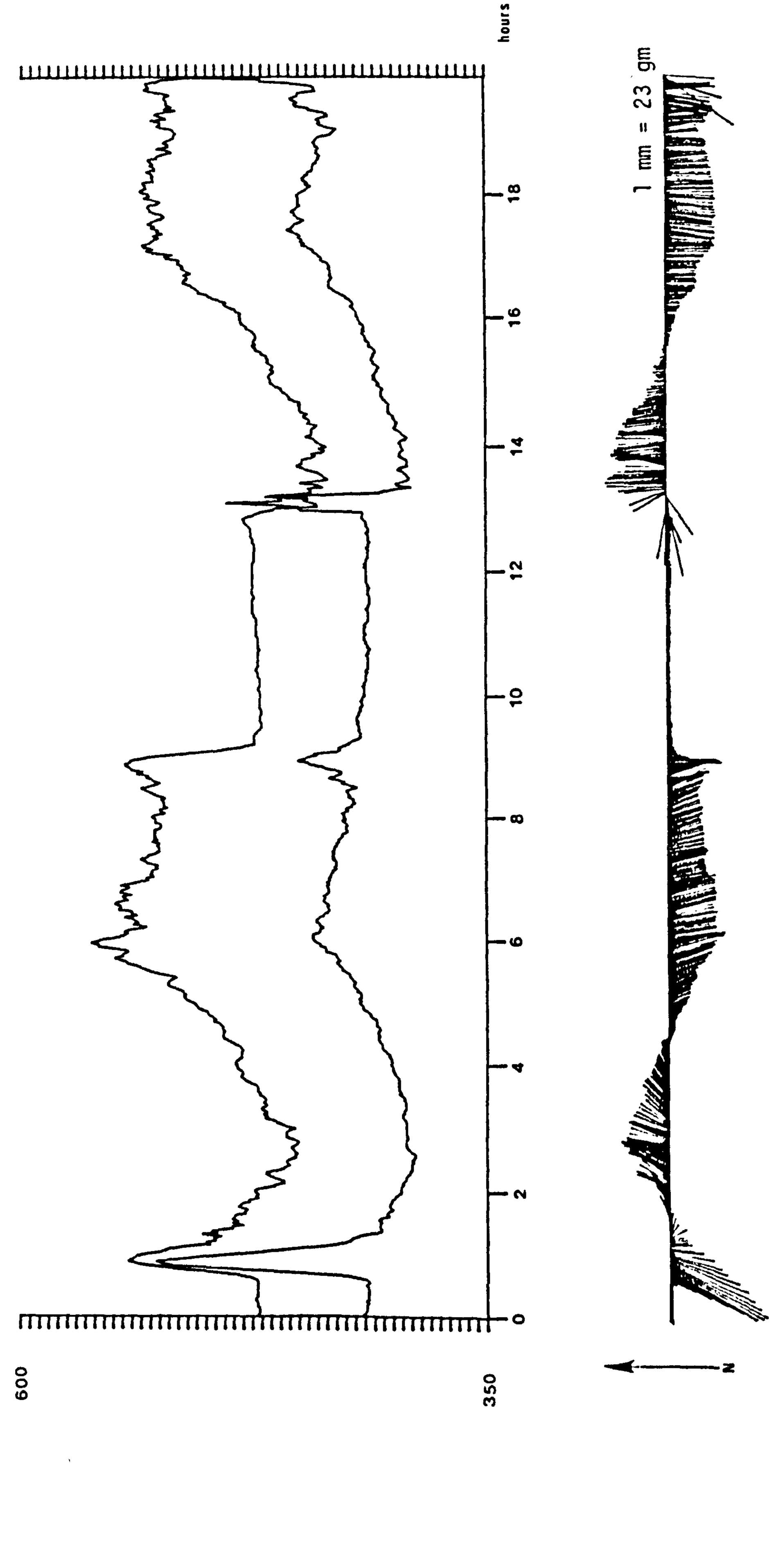

Figure A1.7. Plot of tidal currents measured on the lower foreshore at Skegness 4-5.2.77.
Recording height 34cm above bed. Tidal heights 7m and 6.9m.

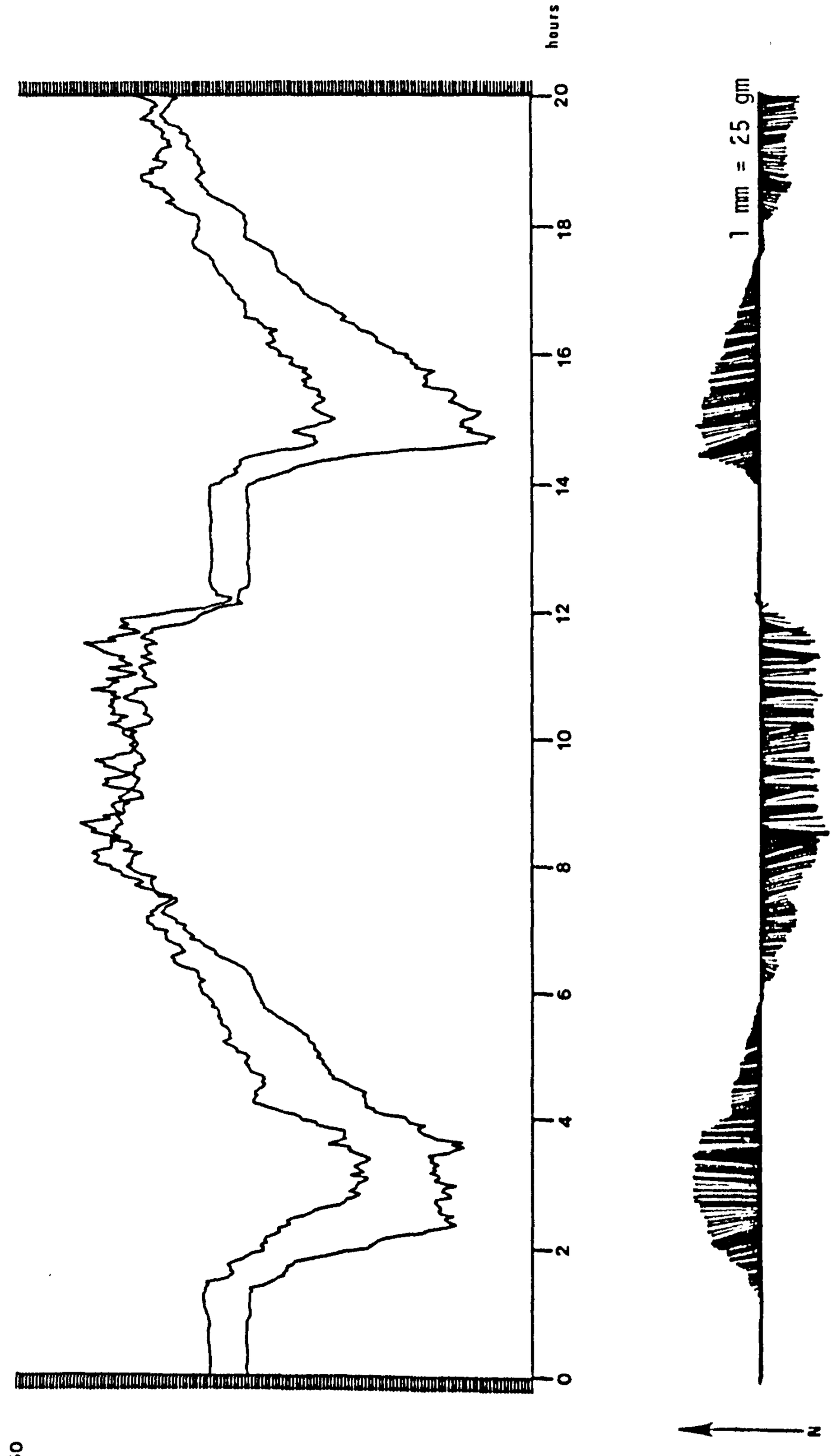

Figure A1.8. Plot of tidal currents measured on the lower foreshore at Gibraltar Point 18–19.1.77.
Recording height 34cm above the bed. Tidal heights 6.6m and 6.6m.

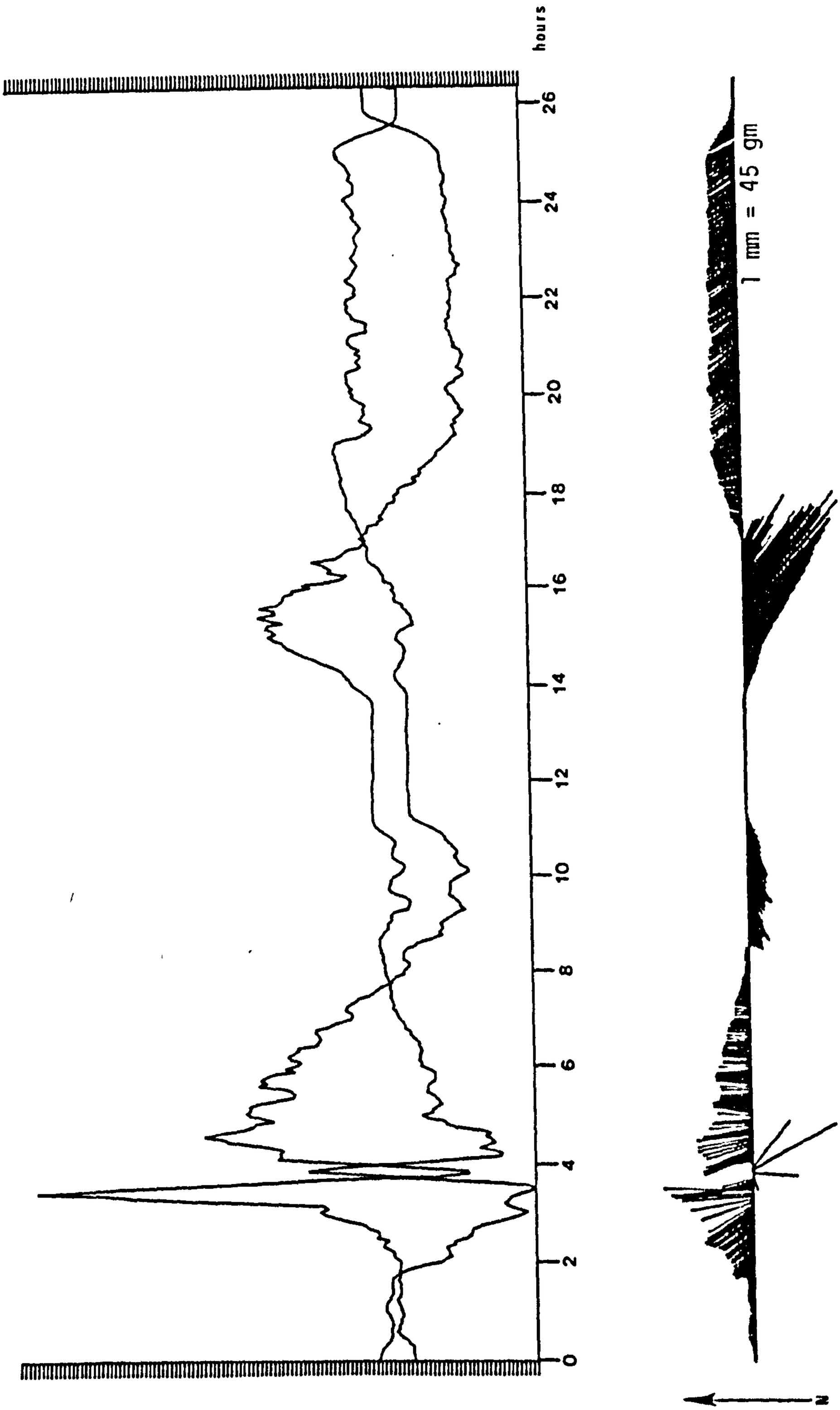

Figure A1.9. Plot of tidal currents measured on the lower foreshore at Gibraltar Point 22-23.11.76. Recording height 34cm above the bed. Tidal heights 7.4m and 7.4m. Instrument disturbed after 4 hours.

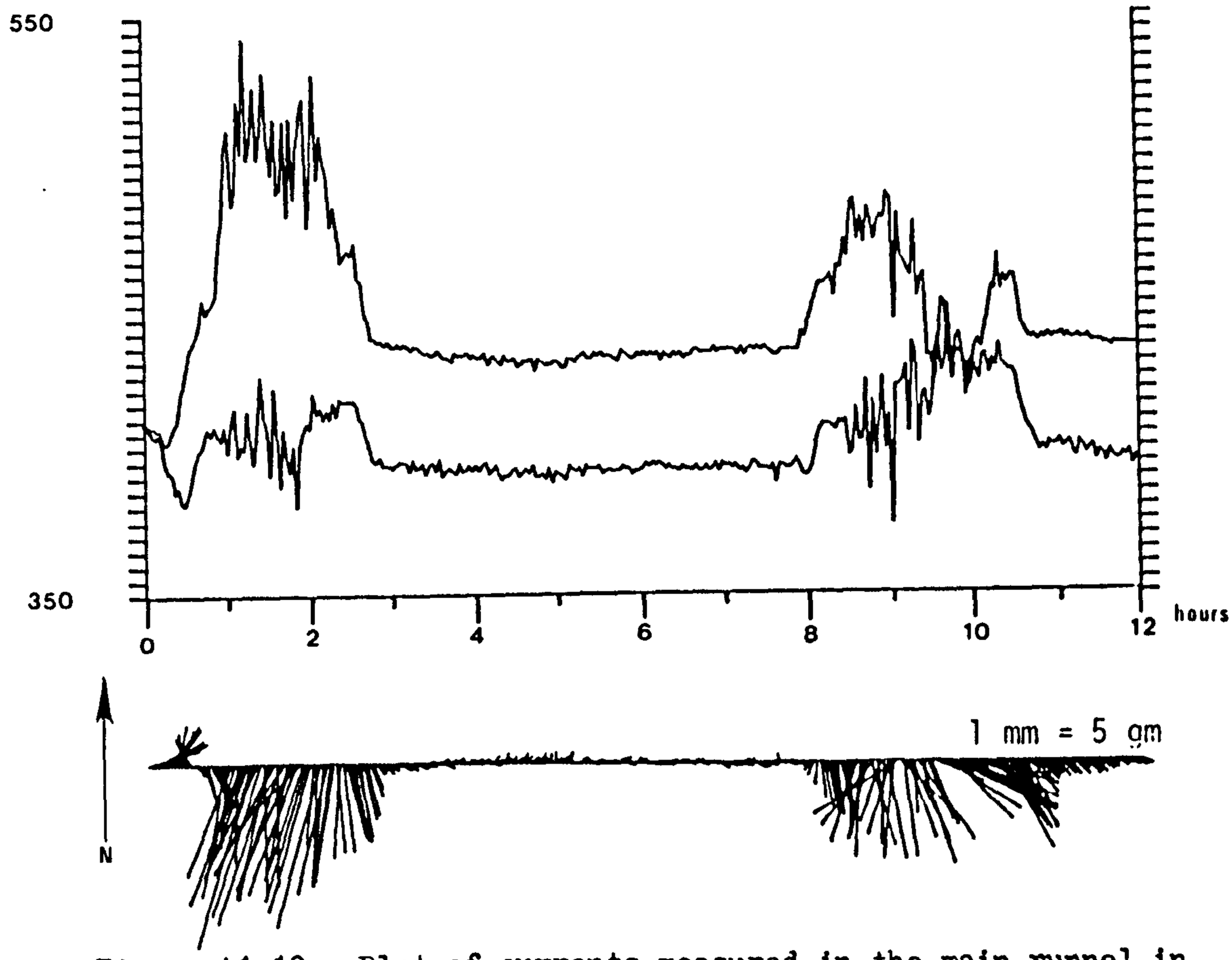

Figure A1.10. Plot of currents measured in the main runnel in profile H2, 21.9.76. Note all flow to north.

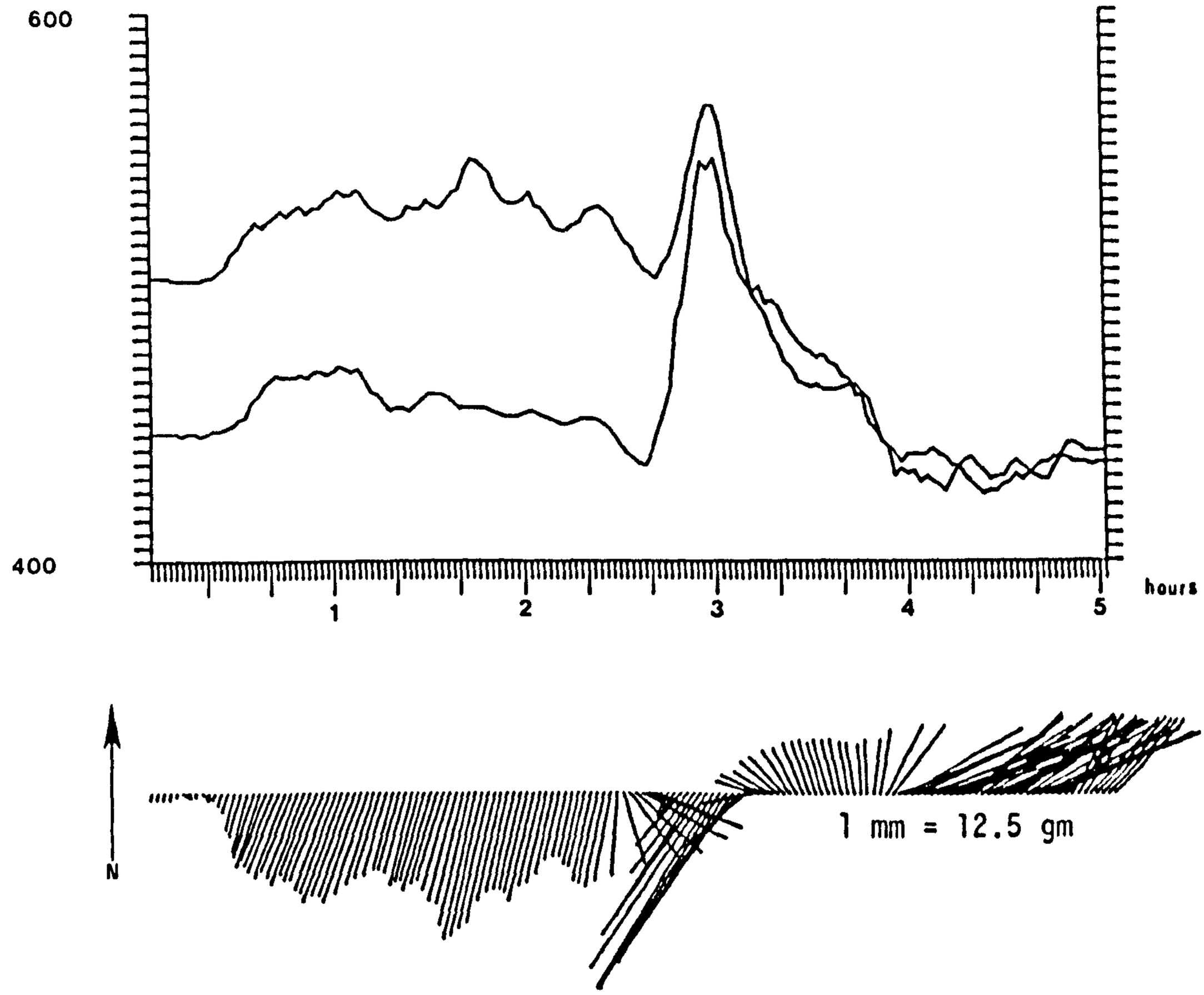

Figure A1.11. Plot of tidal currents measured on lower foreshore at Gibraltar Point, 6.10.76. Instrument swamped after 5 hours in heavy seas. Tidal height 6.6m.

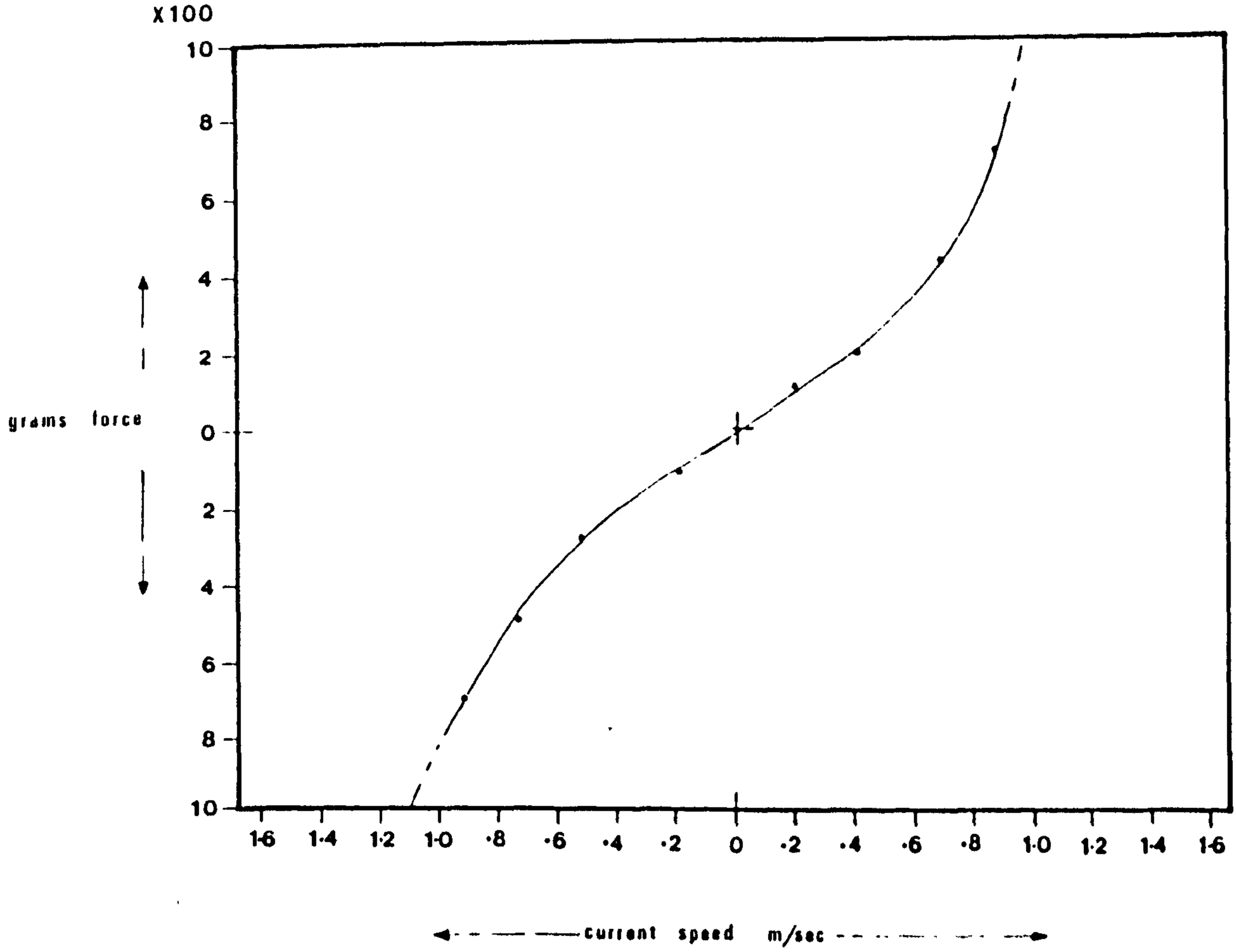

Figure A1.12. Calibration curve for current meters. Relates current speed to the force applied to the instrument sensors.

APPENDIX 2

Profiles and tracer maps for experiments not specifically mentioned in text: Gibraltar Point (H2 and H3 profiles).

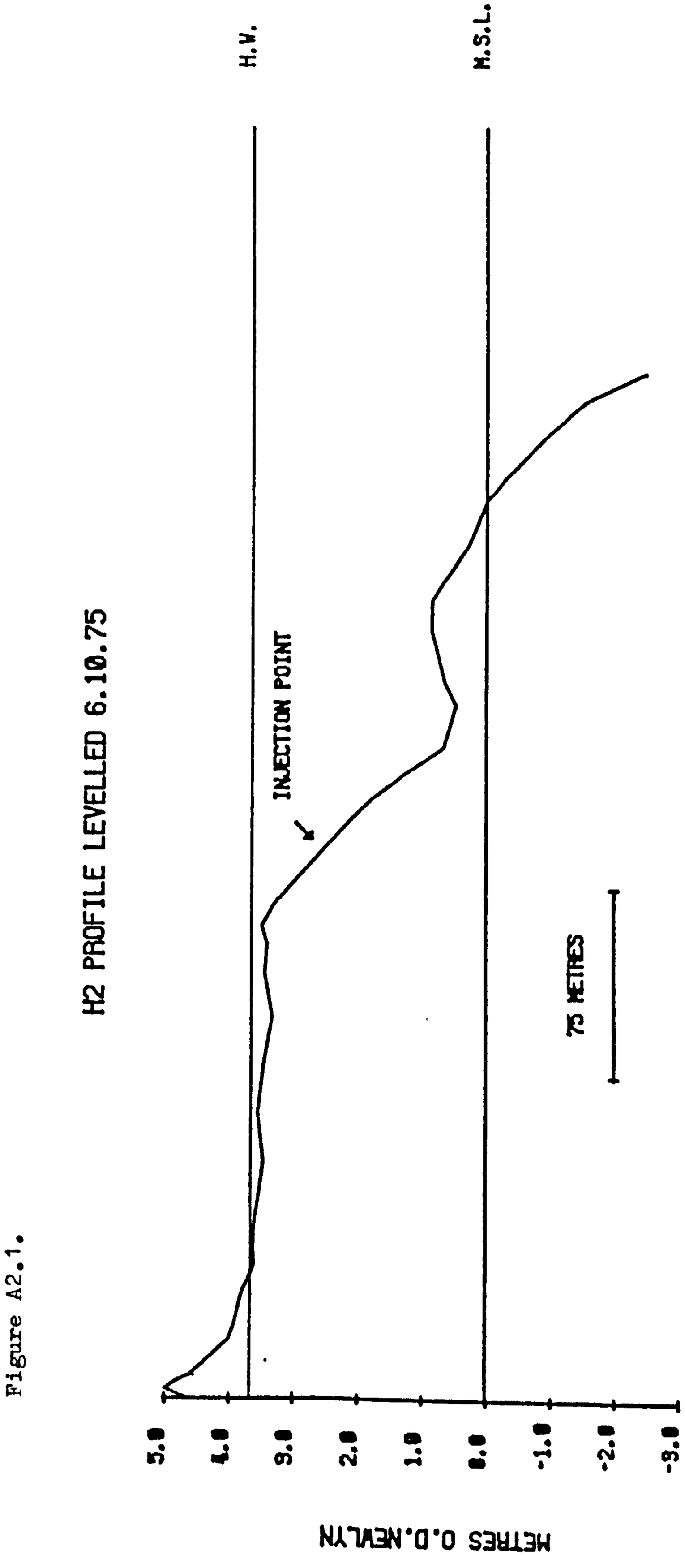
H.W.
M.S.L.
INJECTION POINT
H2 PROFILE LEVELLED 6.10.75
75 METRES
H.W. PREDICTED TIDE HEIGHT FOR EXPERIMENT M.S.L. MEAN SEA LEVEL
5.0
4.0
3.0
2.0
1.0
0.0
-1.0
-2.0
-3.0
METRES O.D.NEWLYN

Figure A2.1.

Figure A2.2.

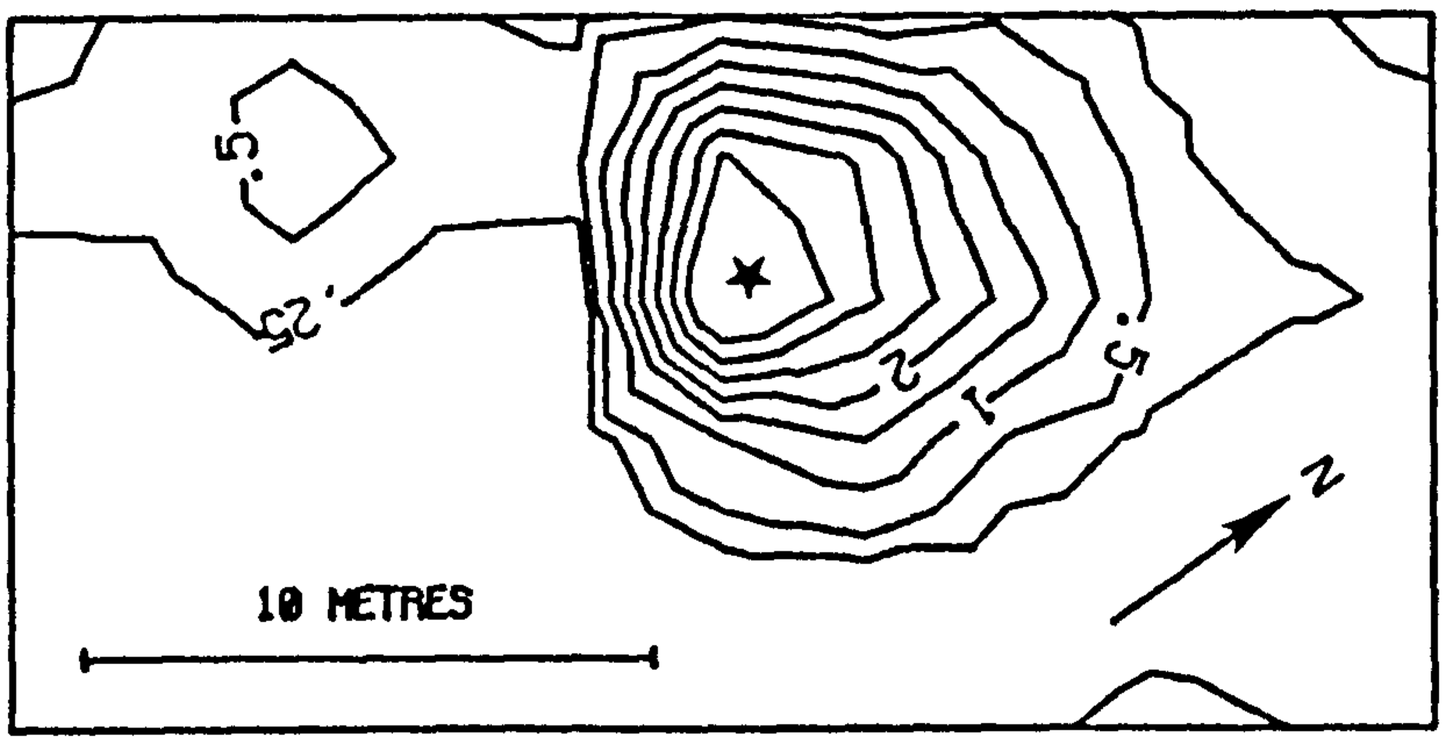

Figure A2.3.

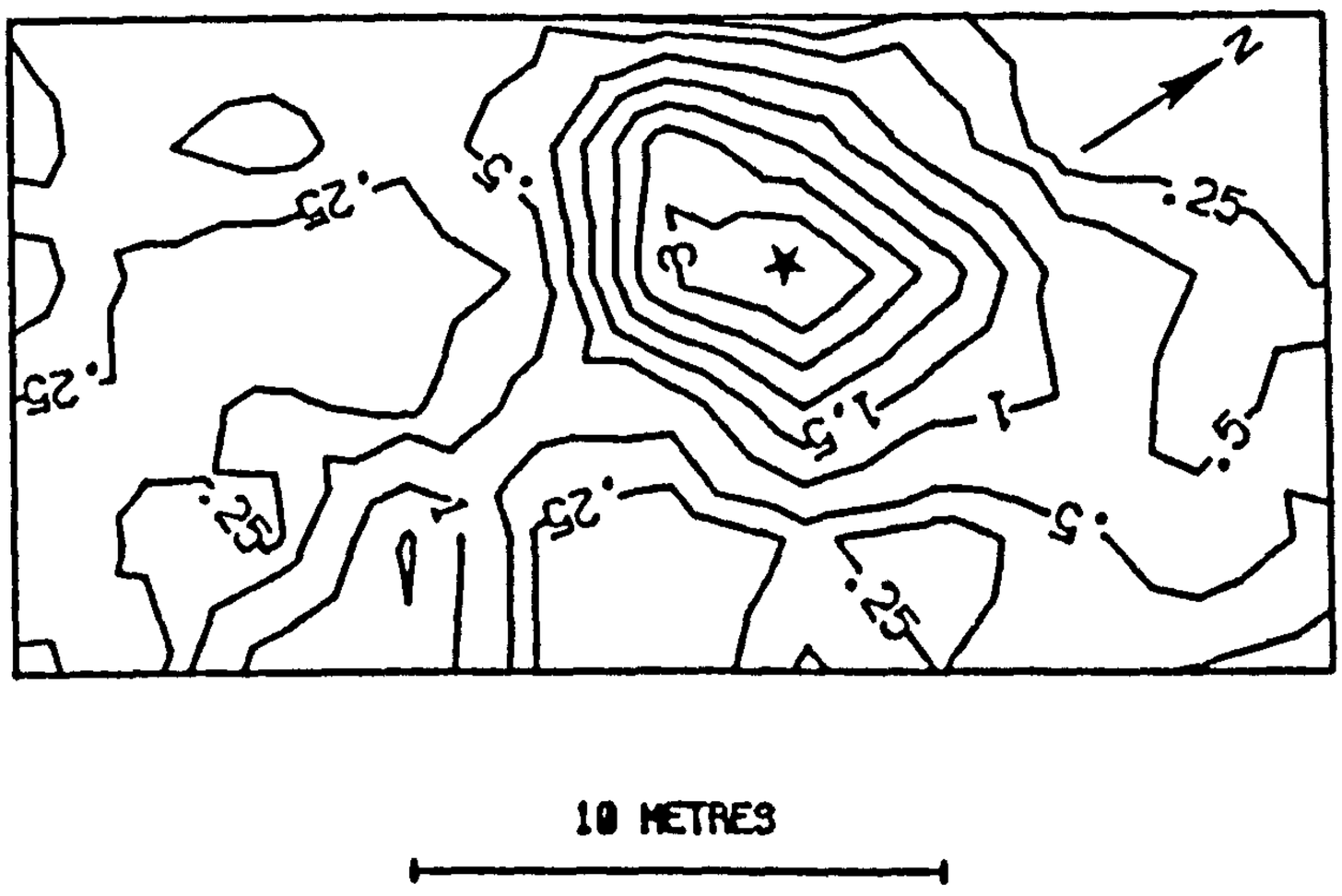

N.B.Comparison with above map shows difference between use of 'artificial' tracer (A2.3) and 'natural' tracer (A2.2).

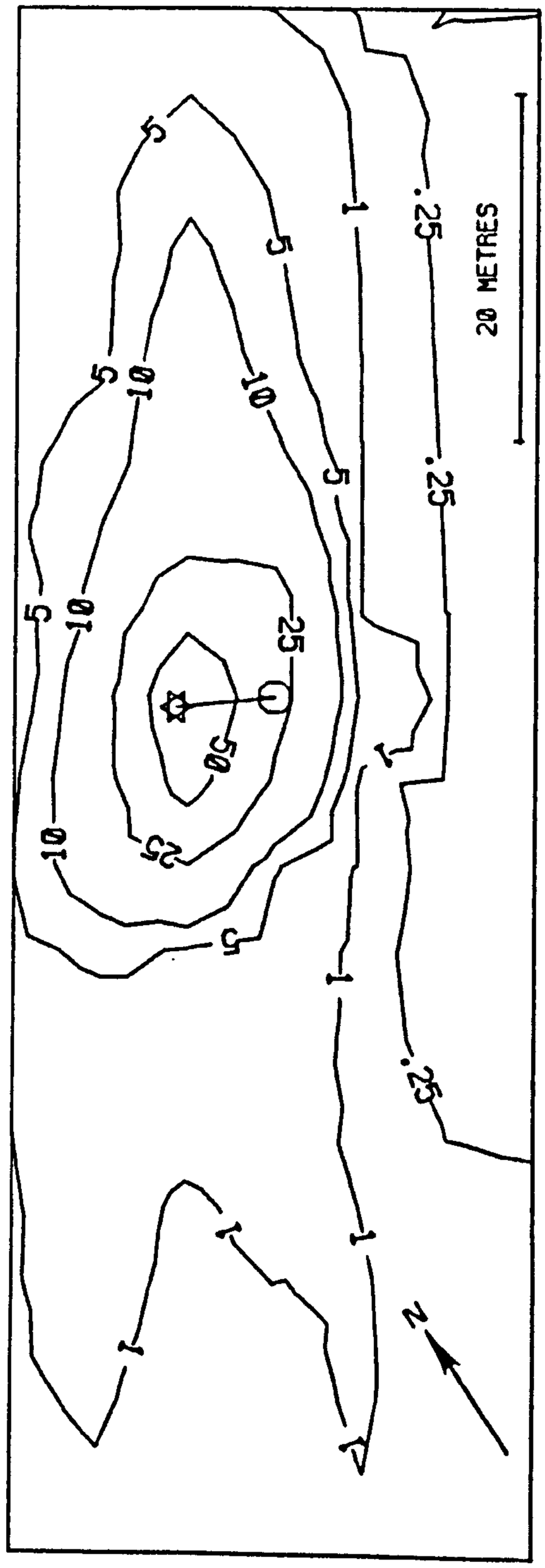

Figure A2.4.

N.B. Compare with Figure 4.16 to show effect of use of 'artificial' tracer instead of tagged in situ sand.

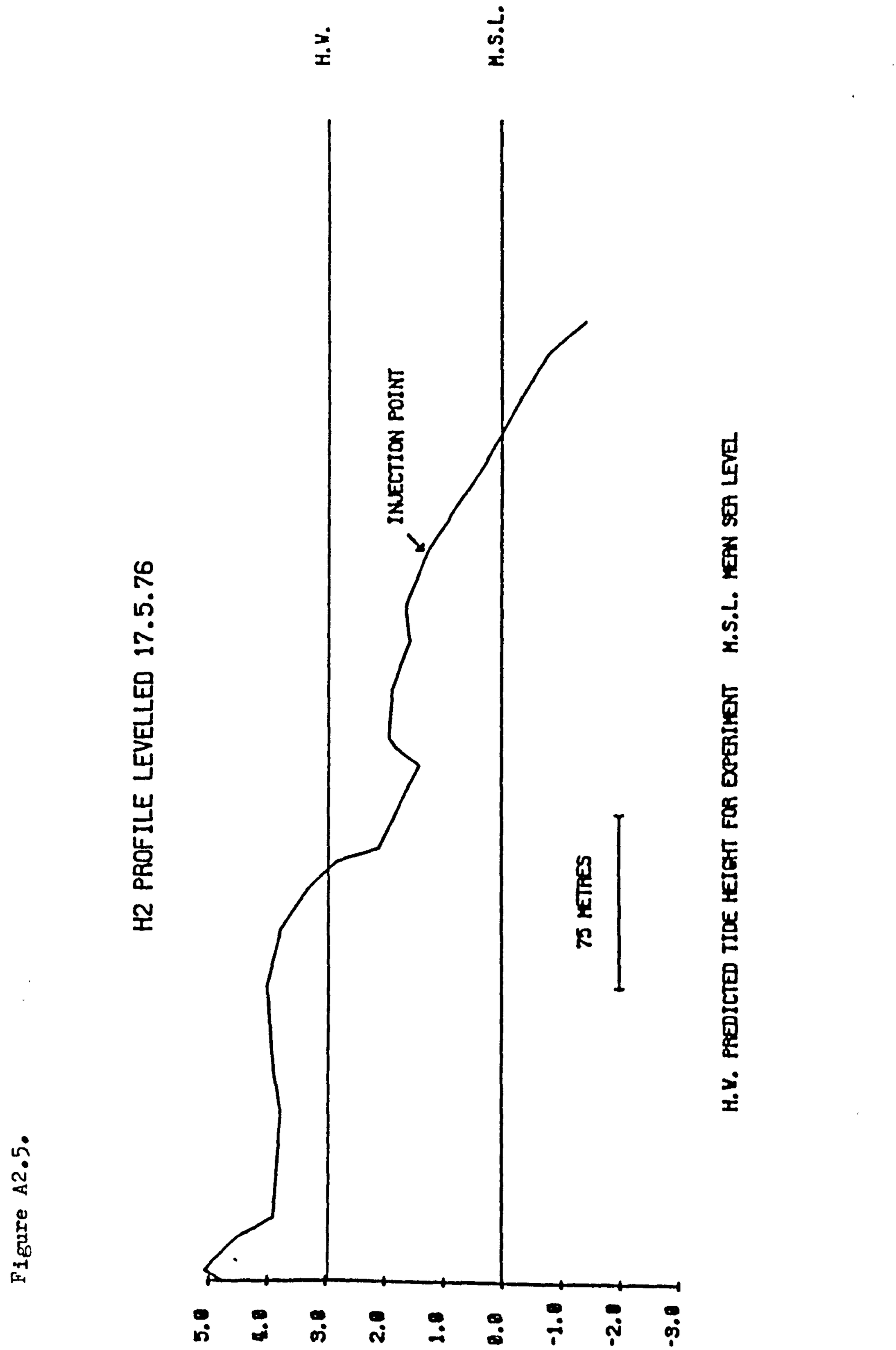
H.W.
M.S.L.
INJECTION POINT
H2 PROFILE LEVELLED 17.5.76
M.S.L. MEAN SEA LEVEL
75 METRES
H.W. PREDICTED TIDE HEIGHT FOR EXPERIMENT
5.0
4.0
3.0
2.0
1.0
0.0
-1.0
-2.0
-3.0
METRES O.D.NEWLYN

Figure A2.5.

Figure A2.6.

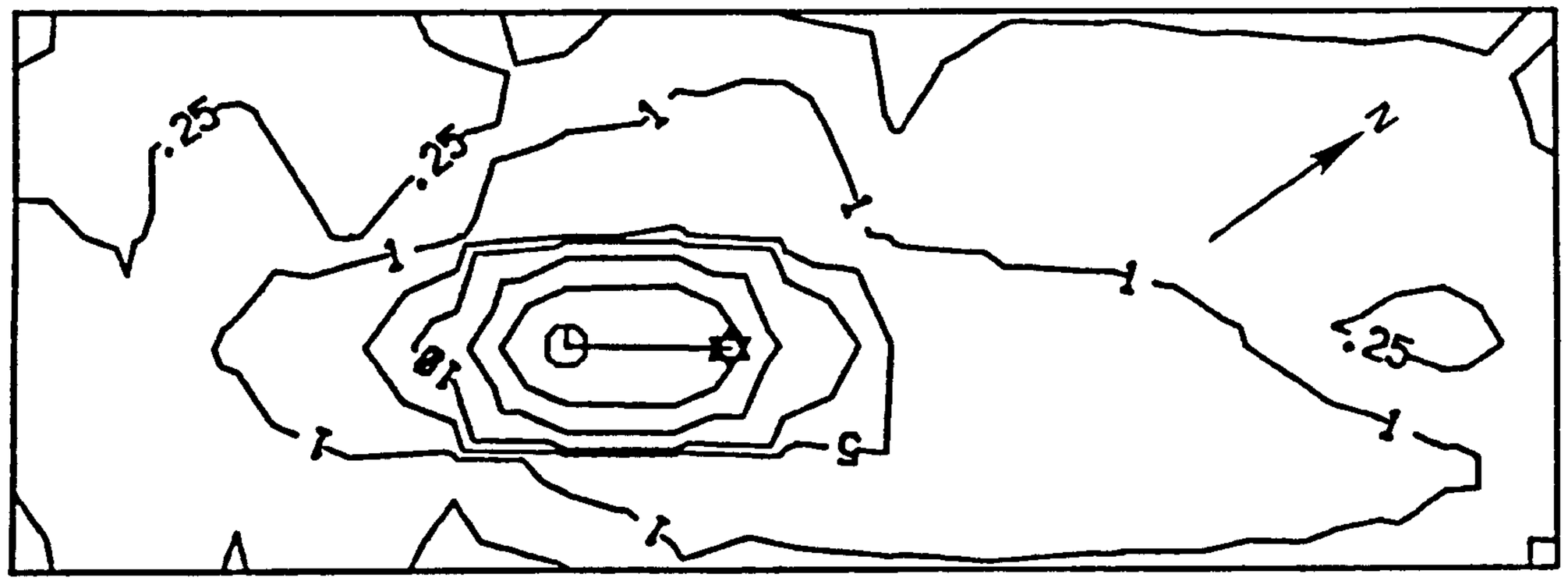
17 5 76 LOWER RIDGE H2 P (A)
.25
.25
.25
.1
5
2
20 METRES
INJECTION POINT
CENTRE OF GRAVITY

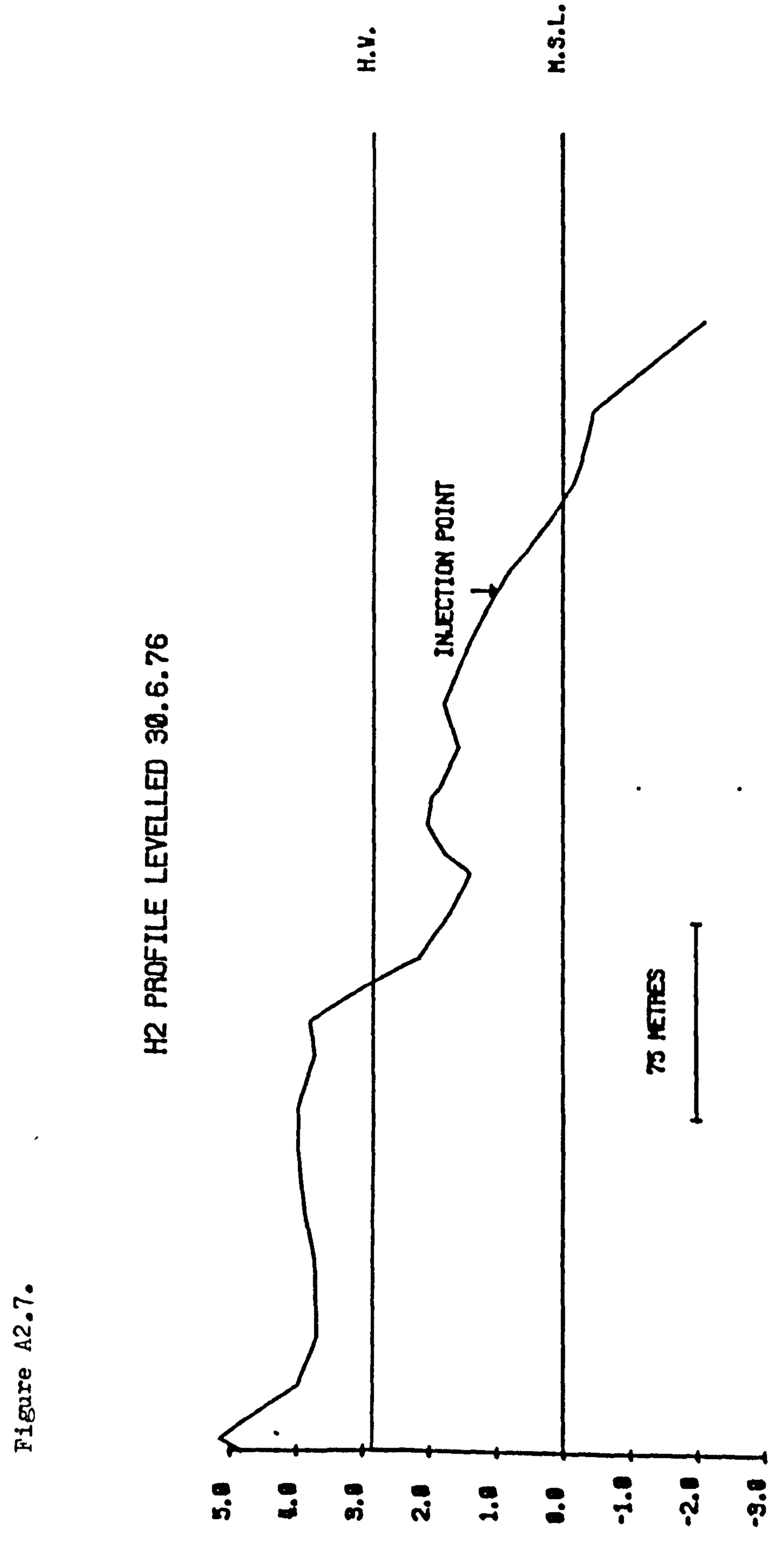
H.V.
M.S.L.
INJECTION POINT
H2 PROFILE LEVELLED 30.6.76
75 METRES
H.V. PREDICTED TIDE HEIGHT FOR EXPERIMENT
M.S.L. MEAN SEA LEVEL
5.0
4.0
3.0
2.0
1.0
0.0
-1.0
-2.0
-3.0
METRES O.D.NEWLYN

Figure A2.7.

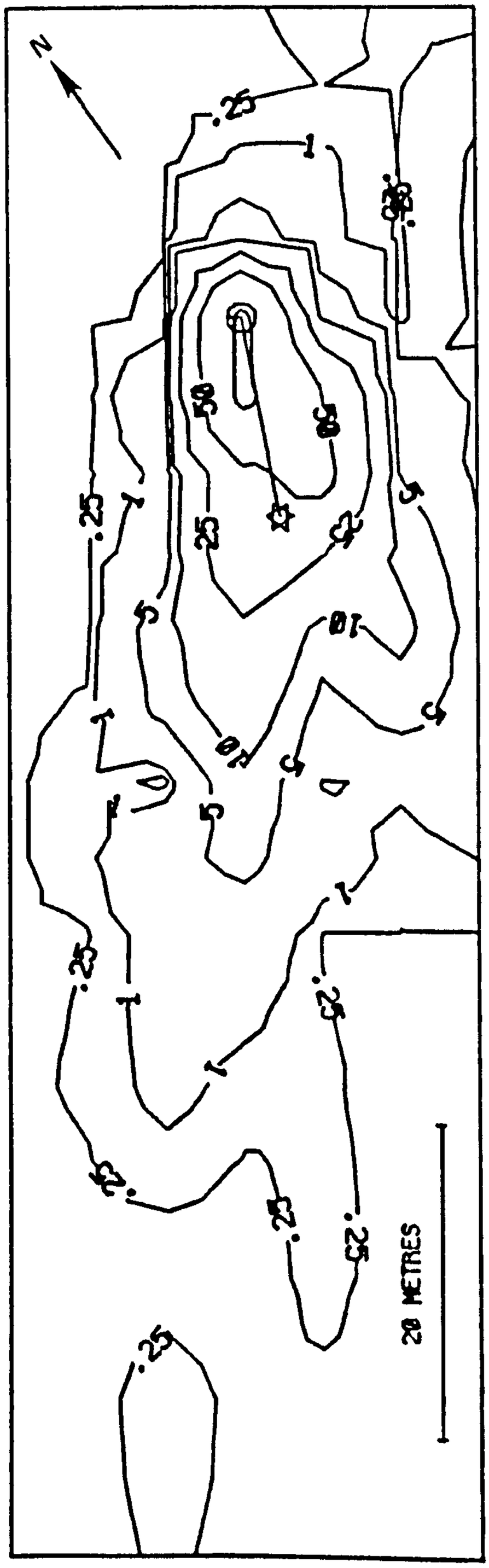

30 6 76 LOWER RIDGE H2 Y

INJECTION POINT ⊙ CENTRE OF GRAVITY ✡

Figure A2.8.

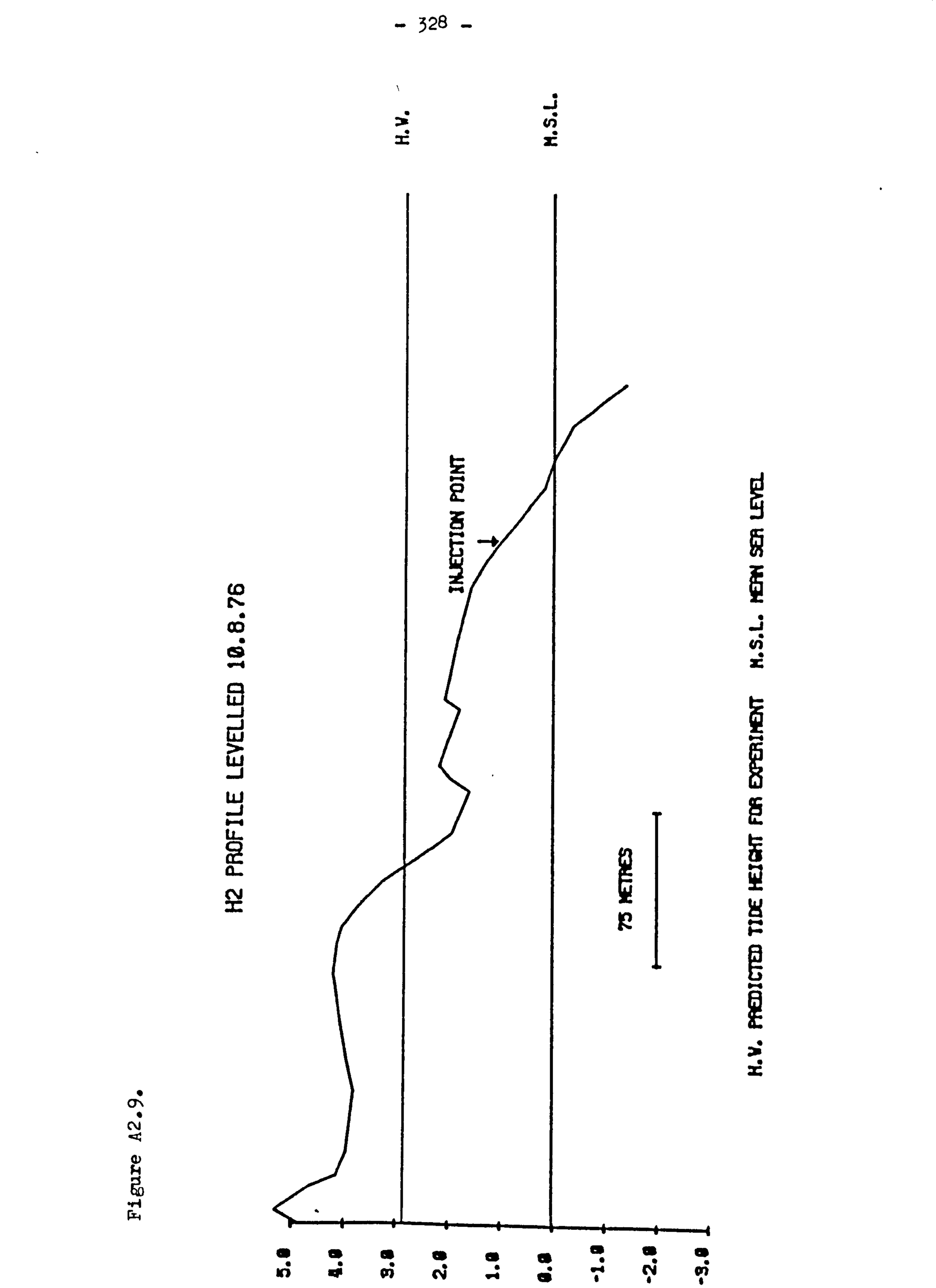
H.V.
M.S.L.
INJECTION POINT
H2 PROFILE LEVELLED 10.8.76
M.S.L. MEAN SEA LEVEL
75 METRES
H.V. PREDICTED TIDE HEIGHT FOR EXPERIMENT
5.0
4.0
3.0
2.0
1.0
0.0
-1.0
-2.0
-3.0
METRES O.D.NEWLYN

Figure A2.9.

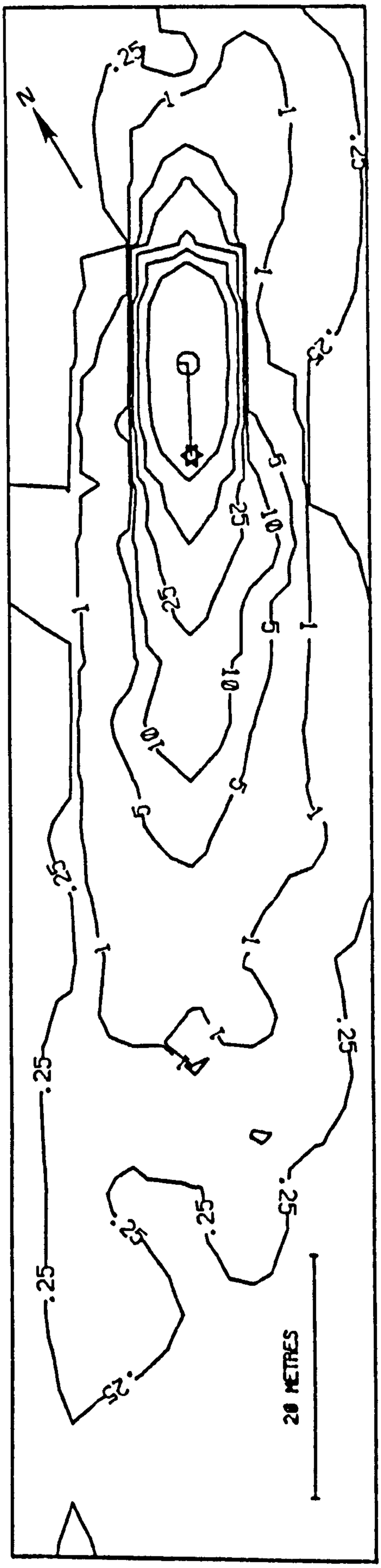
N
.25
1
5
10
25
52
0
20 METRES
INJECTION POINT
CENTRE OF GRAVITY
10 8 76 H2 LOWER RIDGE Y

Figure A2.10.

7·9·76 Lower Ridge First Sample Blue 0·46mm

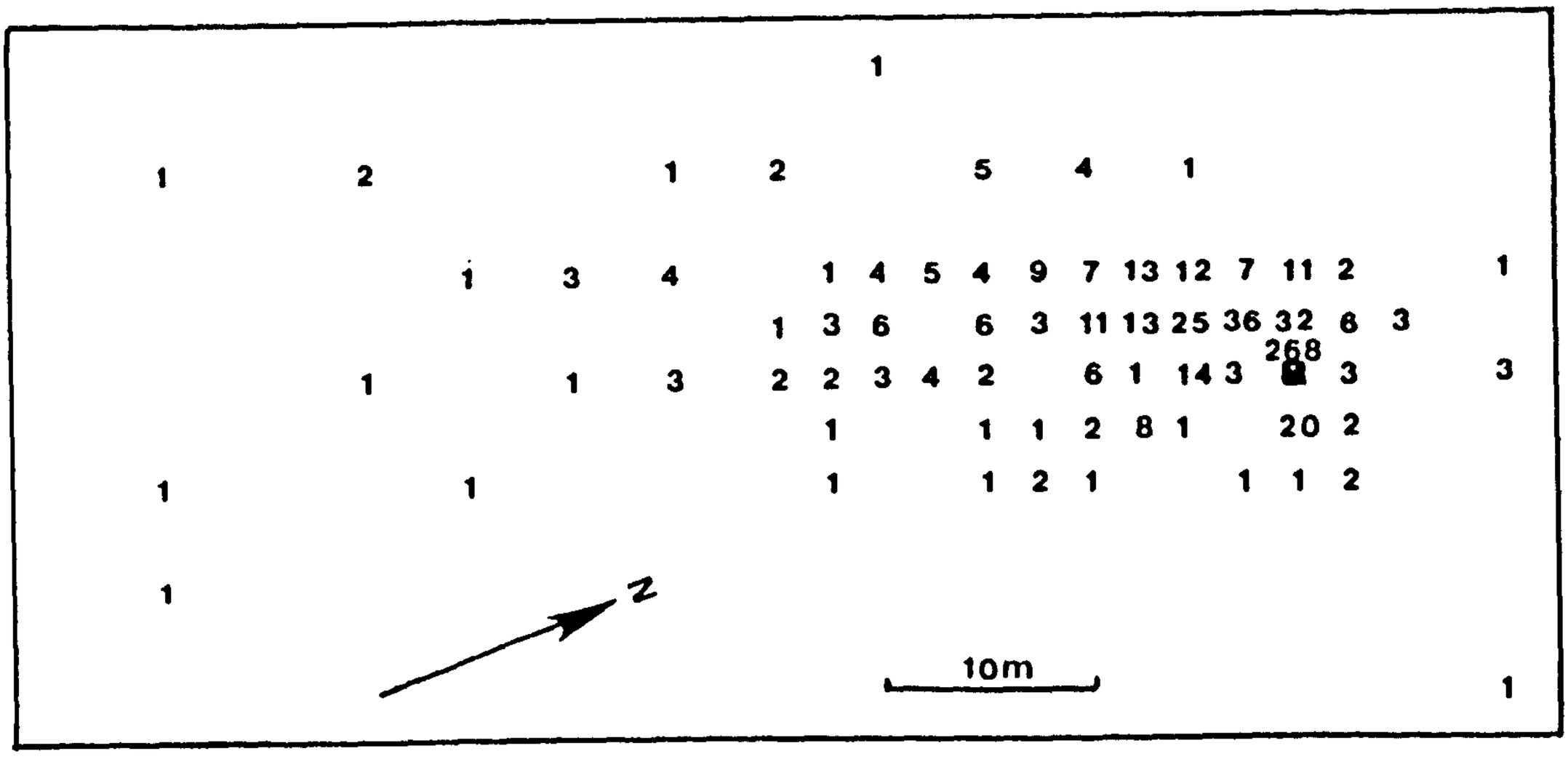

■ Tracer Release Point

7·9·76 Lower Ridge First Sample Pink 0·78mm

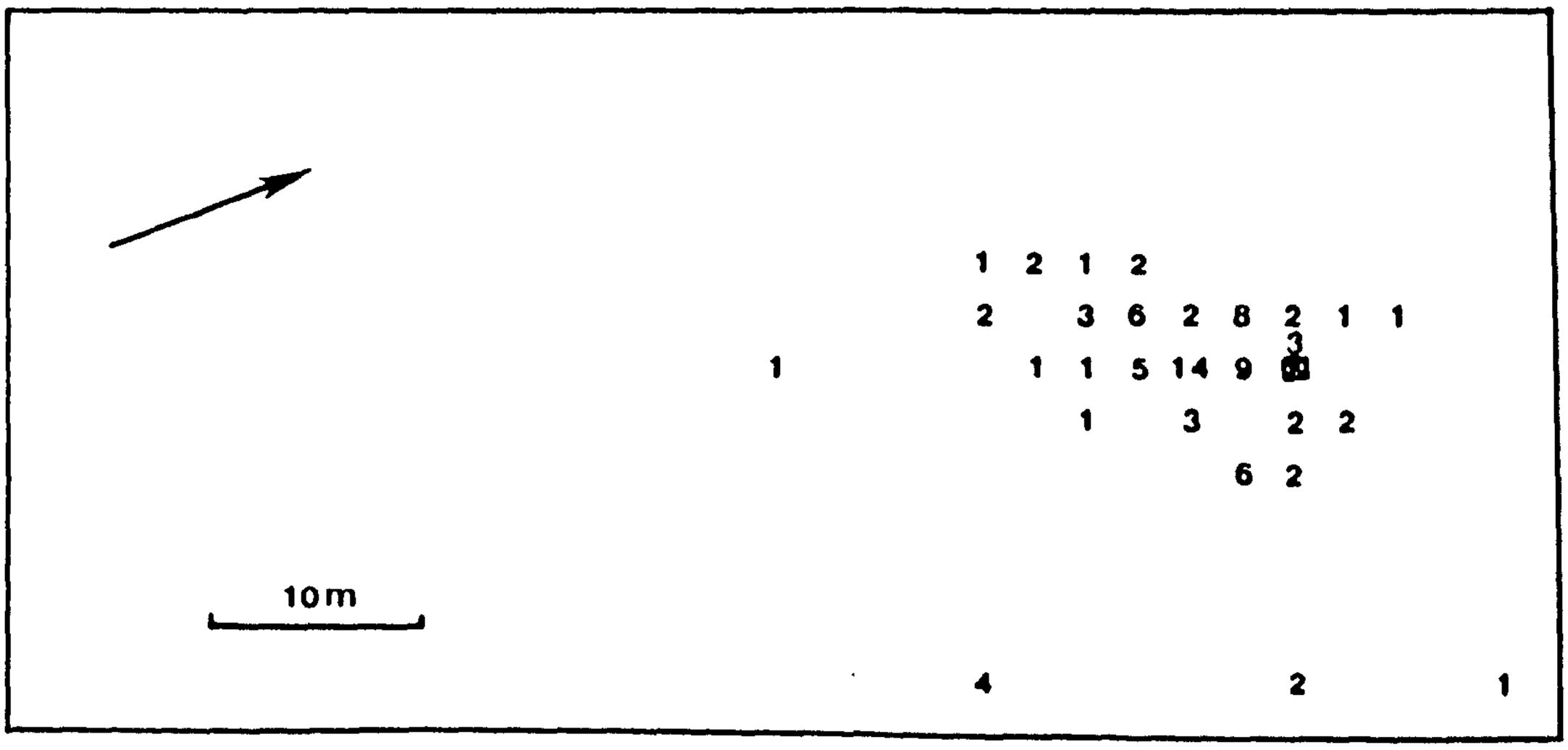

■ Tracer Release Point

Figure A2.11. Tracer maps for grain size test 7.9.76 lower ridge H3, first sample, one tidal cycle.

8·9·76 Lower Ridge 2nd Sample H3 Blue 0·46mm

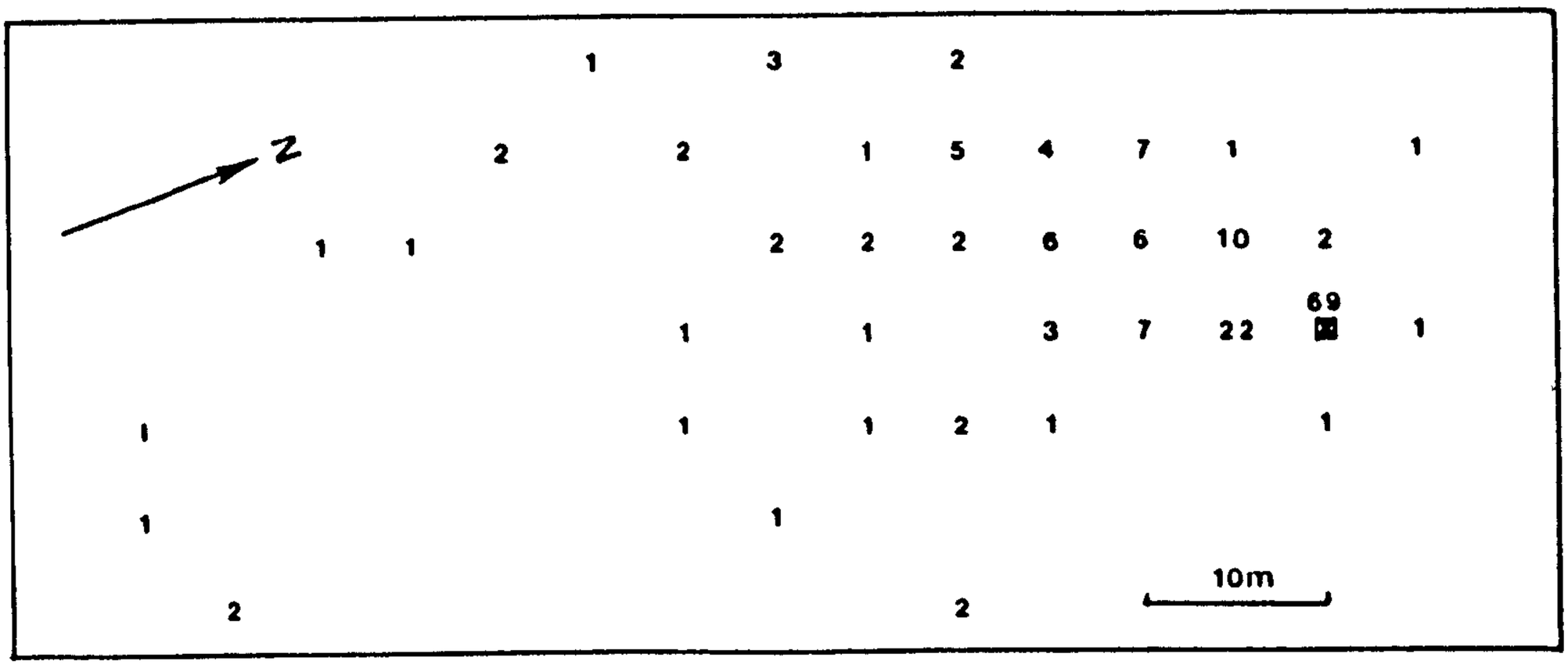

■ Tracer Release Point

8·9·76 Lower Ridge 2nd Sample H3 Pink 0·78mm

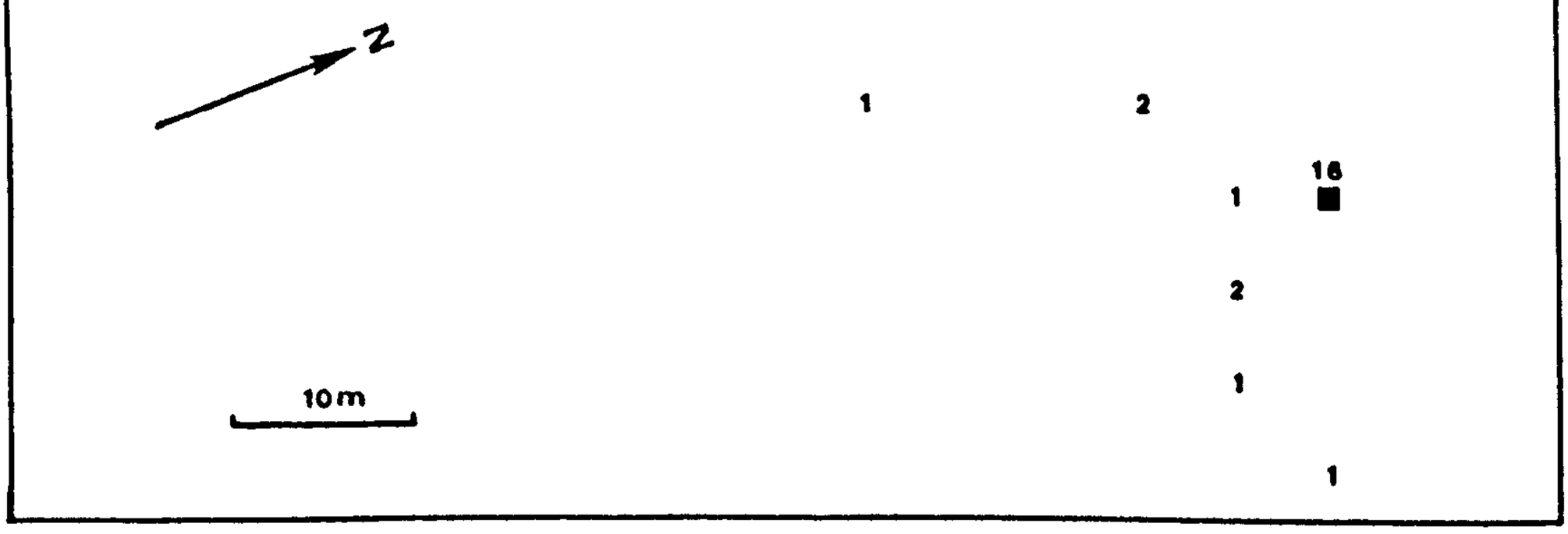

■ Tracer Release Point

Figure A2.12. Tracer maps for grain size test 8.9.76 lower ridge H3, second sample, two tidal cycles. Compare dispersions with Figure A2.11.

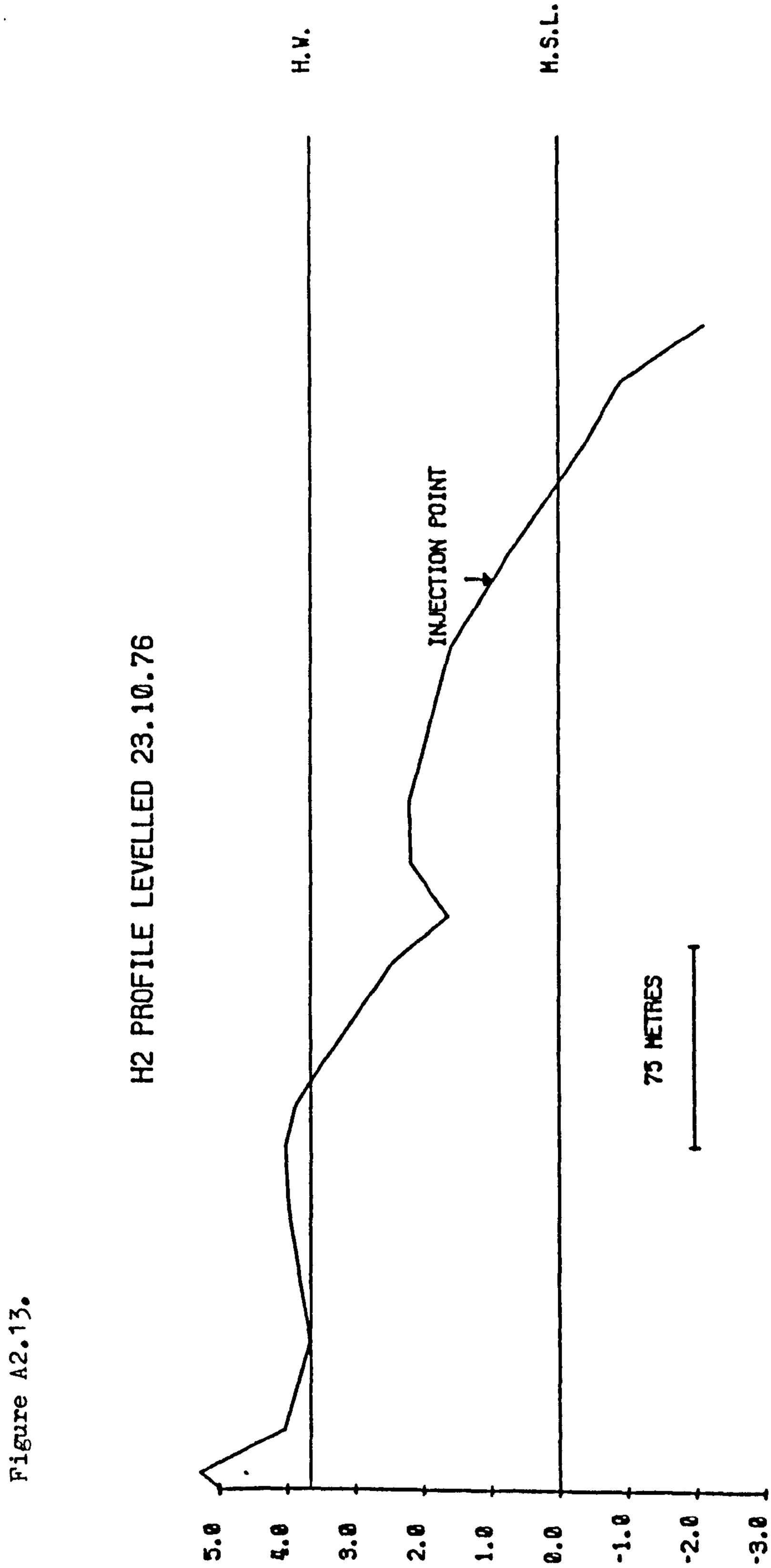
H.W.
M.S.L.
INJECTION POINT
H2 PROFILE LEVELLED 23.10.76
H.W.PREDICTED TIDE HEIGHT FOR EXPERIMENT
M.S.L. MEAN SEA LEVEL
75 METRES
5.0
4.0
3.0
2.0
1.0
0.0
-1.0
-2.0
-3.0
METRES O.D.NEWLYN

Figure A2.13.

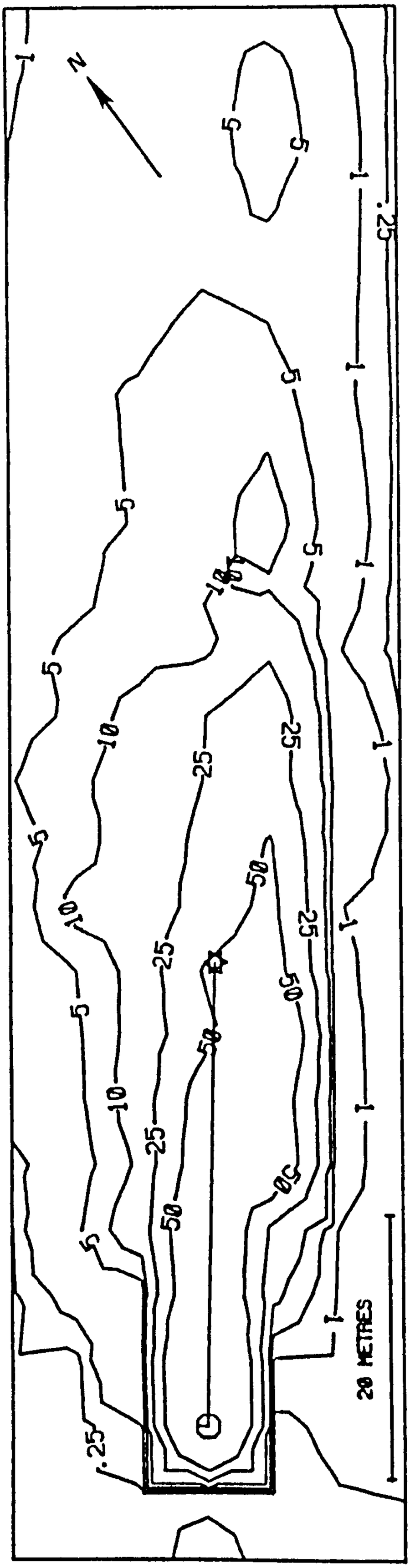
LOWER RIDGE P
23 10 76 H2
CENTRE OF GRAVITY
INJECTION POINT
20 METRES

Figure A2.14.

23·10·76 Lower Ridge H2 Blue 0·21mm

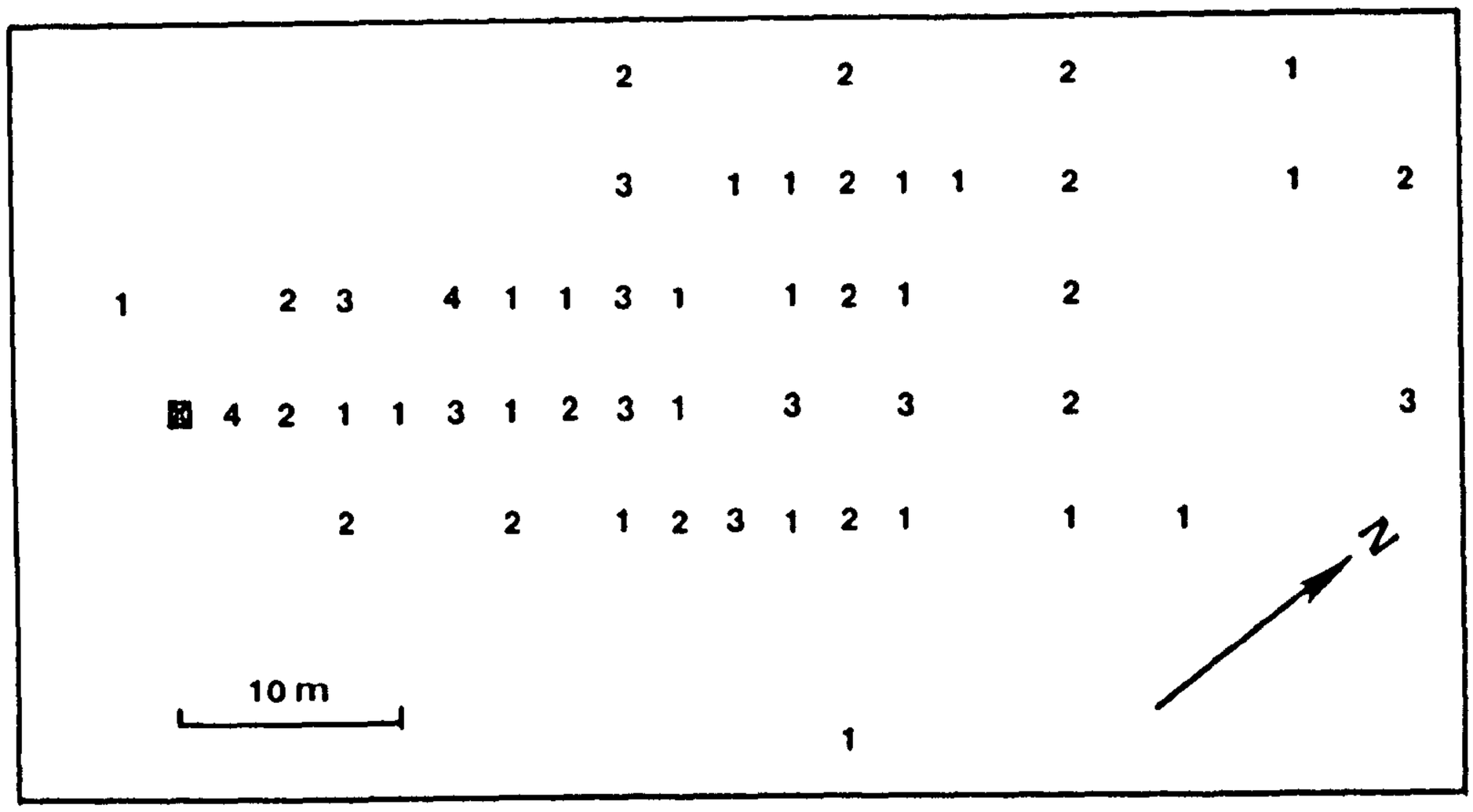

Tracer Release Point

23·10·76 Lower Ridge H2 Yellow 0·55mm

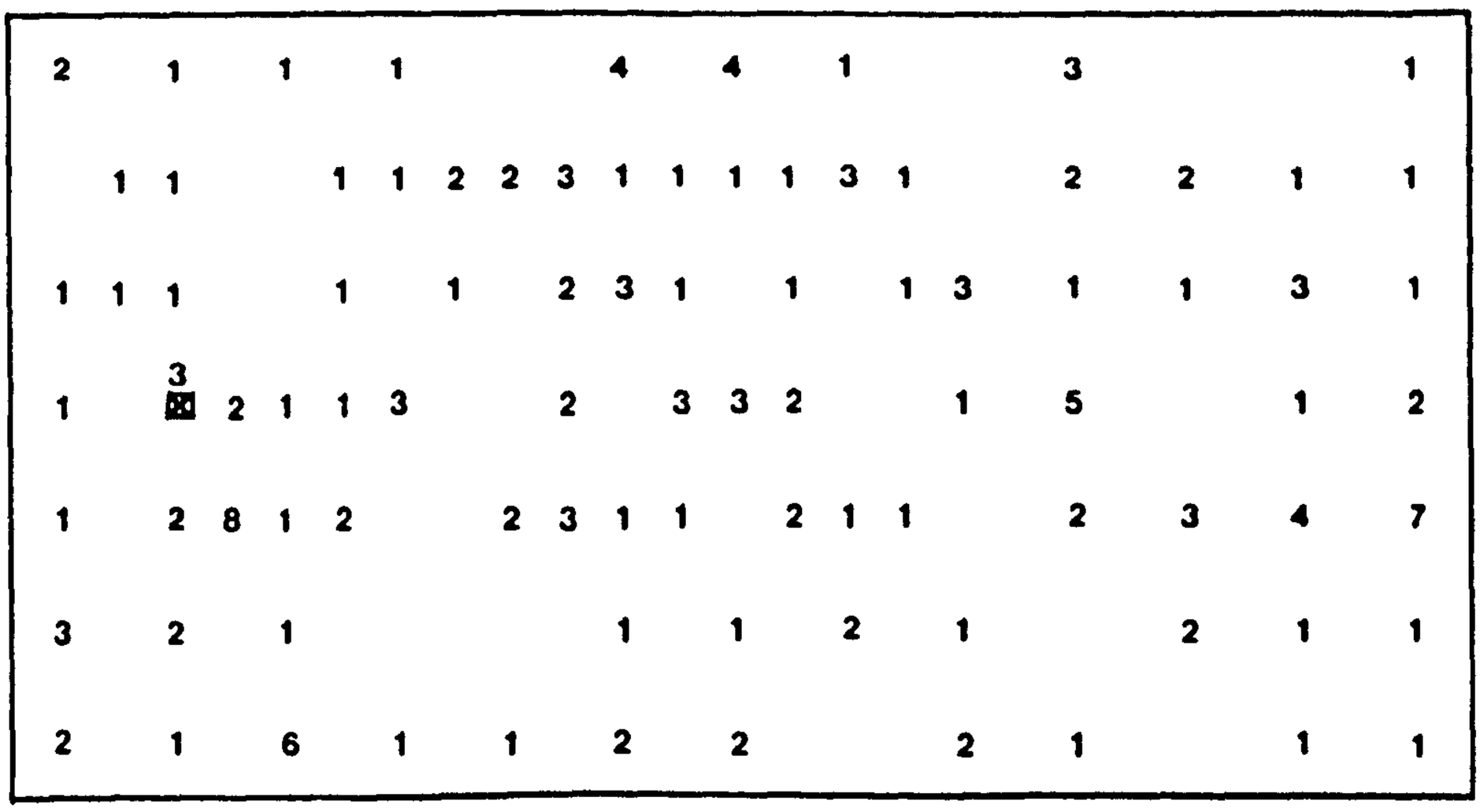

Tracer Release Point

Figure A2.15. Tracer maps for grain size test 23.10.76 lower ridge H2.

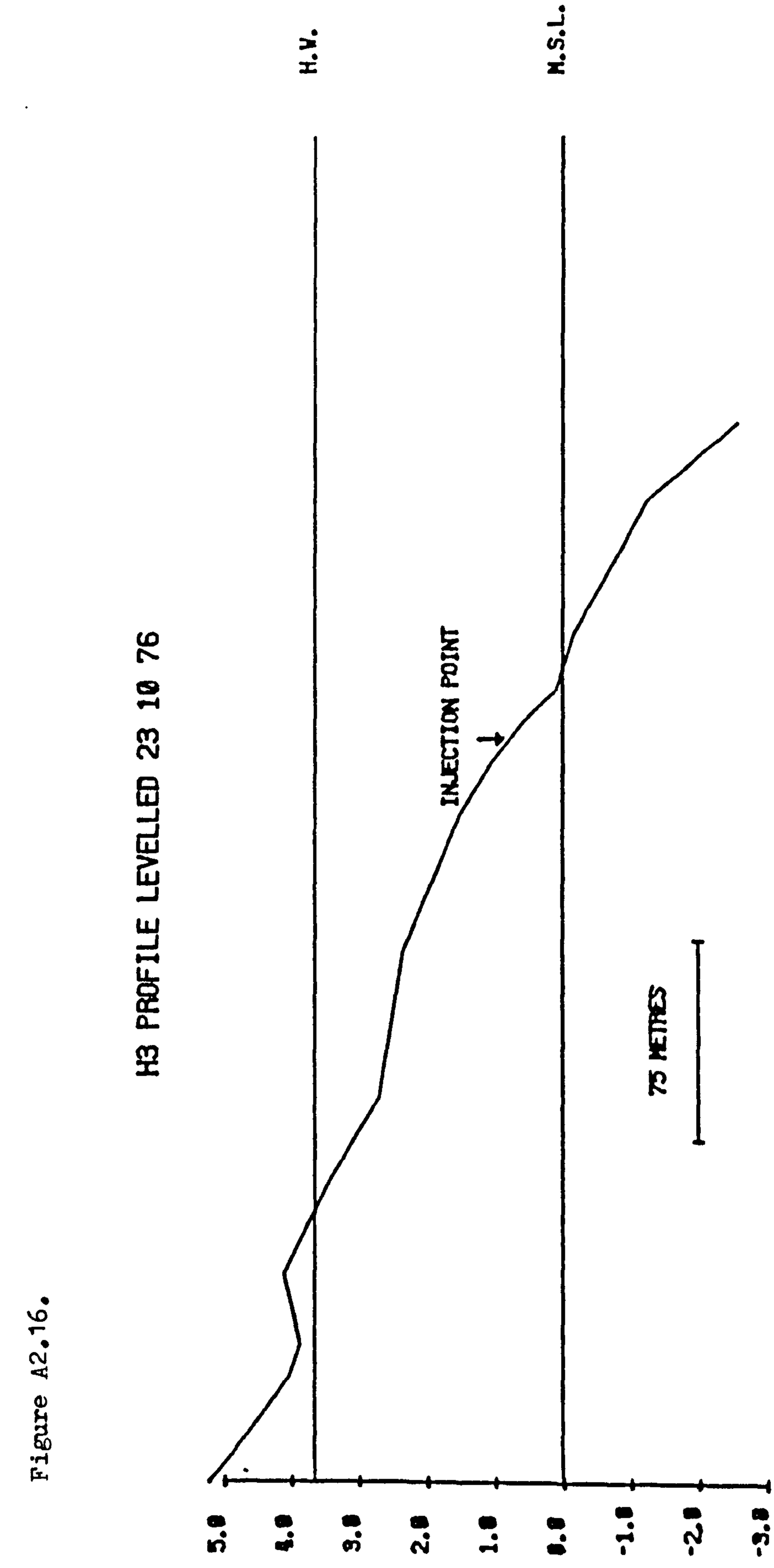
H.W.
M.S.L.
INJECTION POINT
H3 PROFILE LEVELLED 23 10 76
H.W. PREDICTED TIDE HEIGHT FOR EXPERIMENT
M.S.L. MEAN SEA LEVEL
75 METRES
5.0
4.0
3.0
2.0
1.0
0.0
-1.0
-2.0
-3.0
METRES O.D.NEWLYN

Figure A2.16.

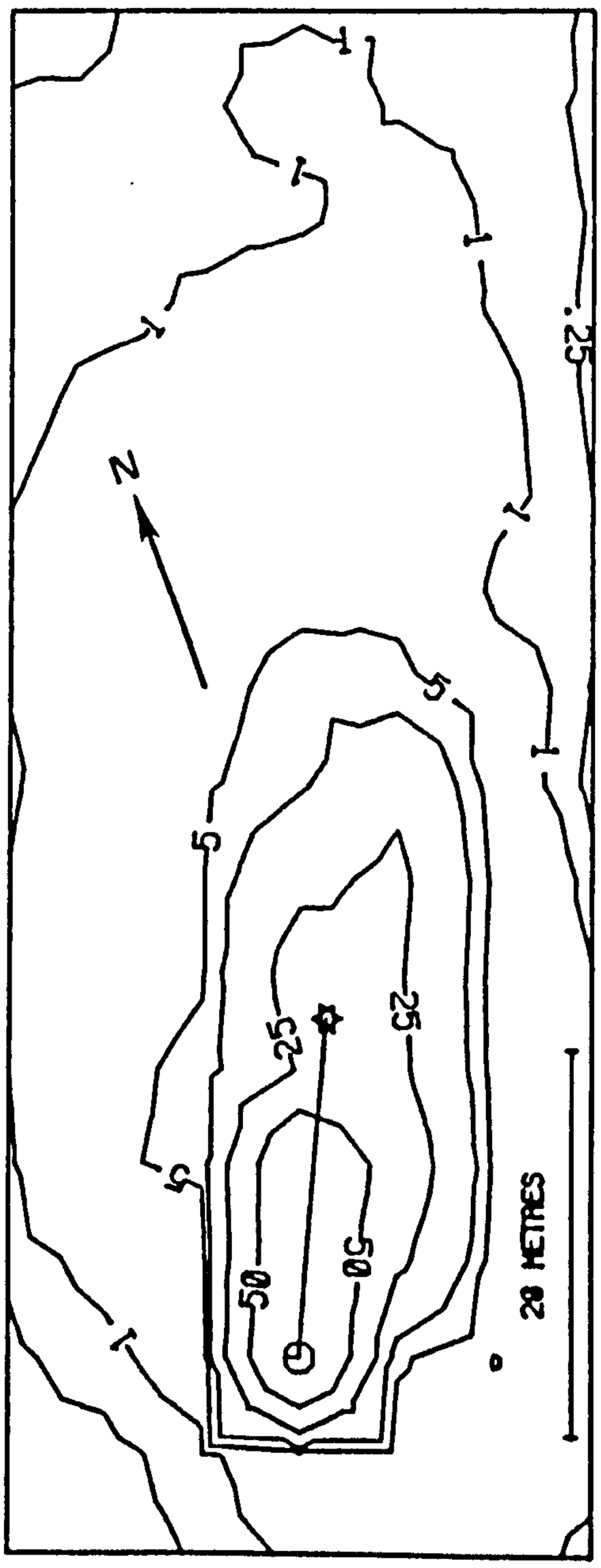

Figure A2.17.

INJECTION POINT

Compare with Figure A2.15. Shows contrast in sediment movement which can occur over short distance (500m Om) along beach.

CENTRE OF GRAVITY

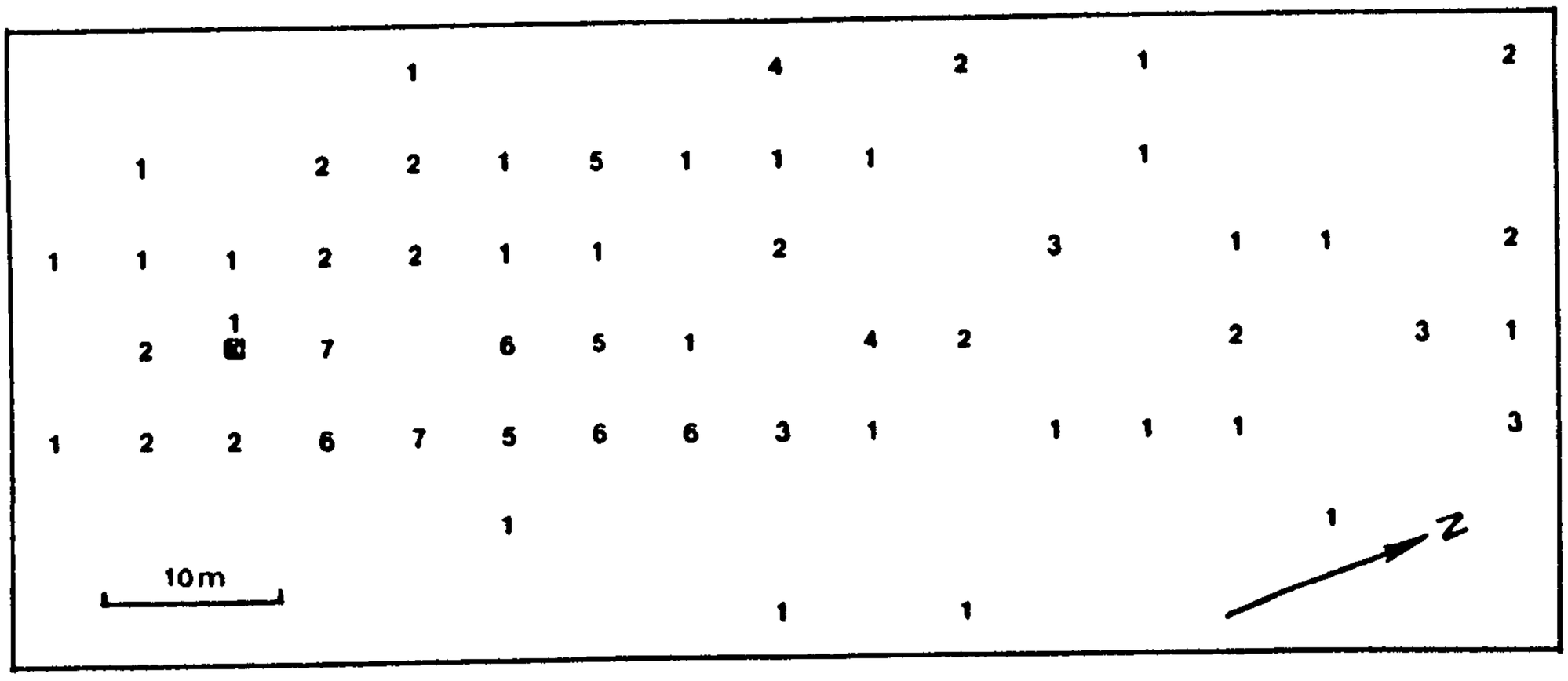

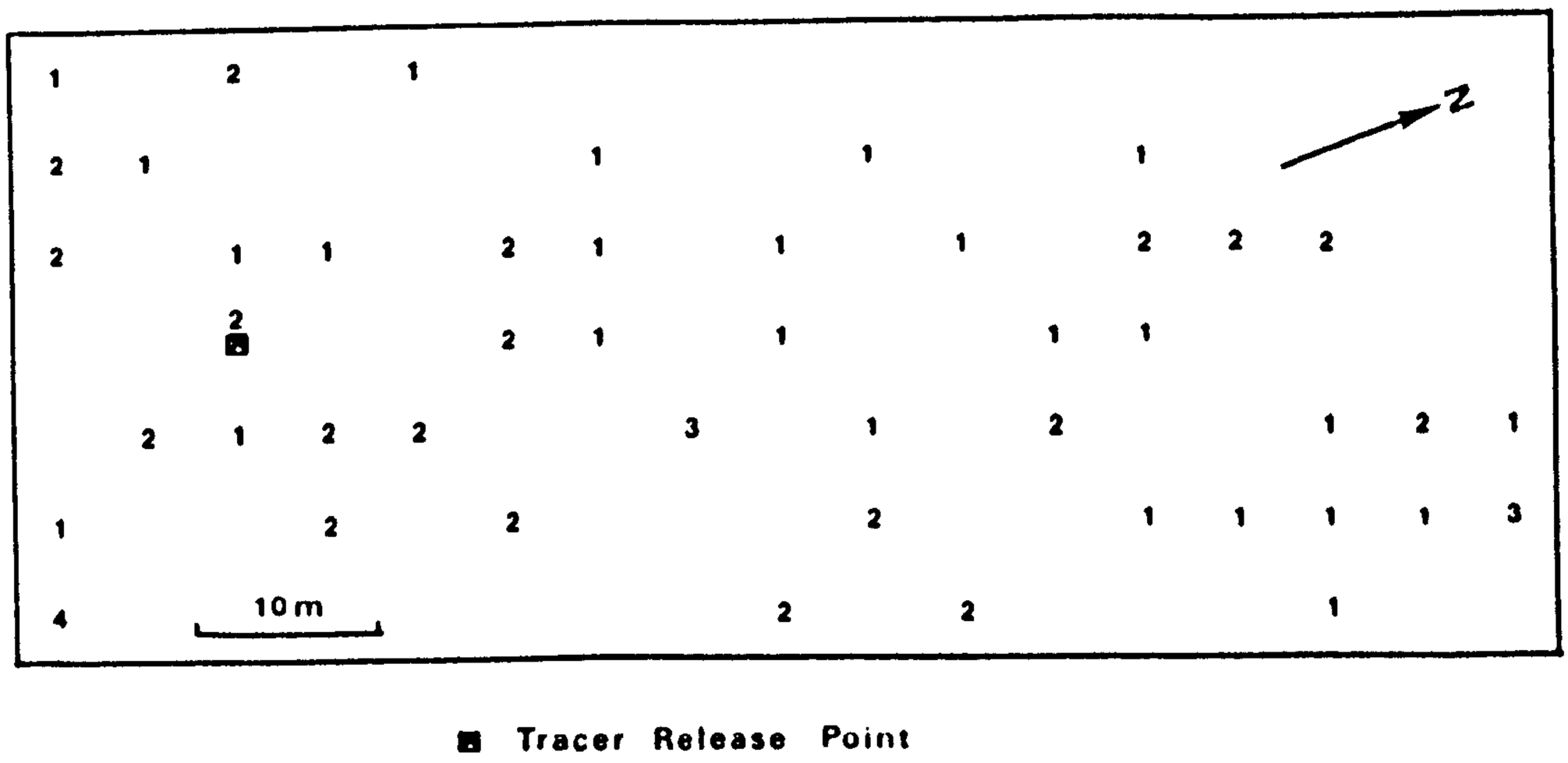

Figure A2.18. Tracer maps for grain size test 23.10.76 H3.

Profiles and tracer maps for experiments not specifically mentioned in text: Skegness (E1 profile).

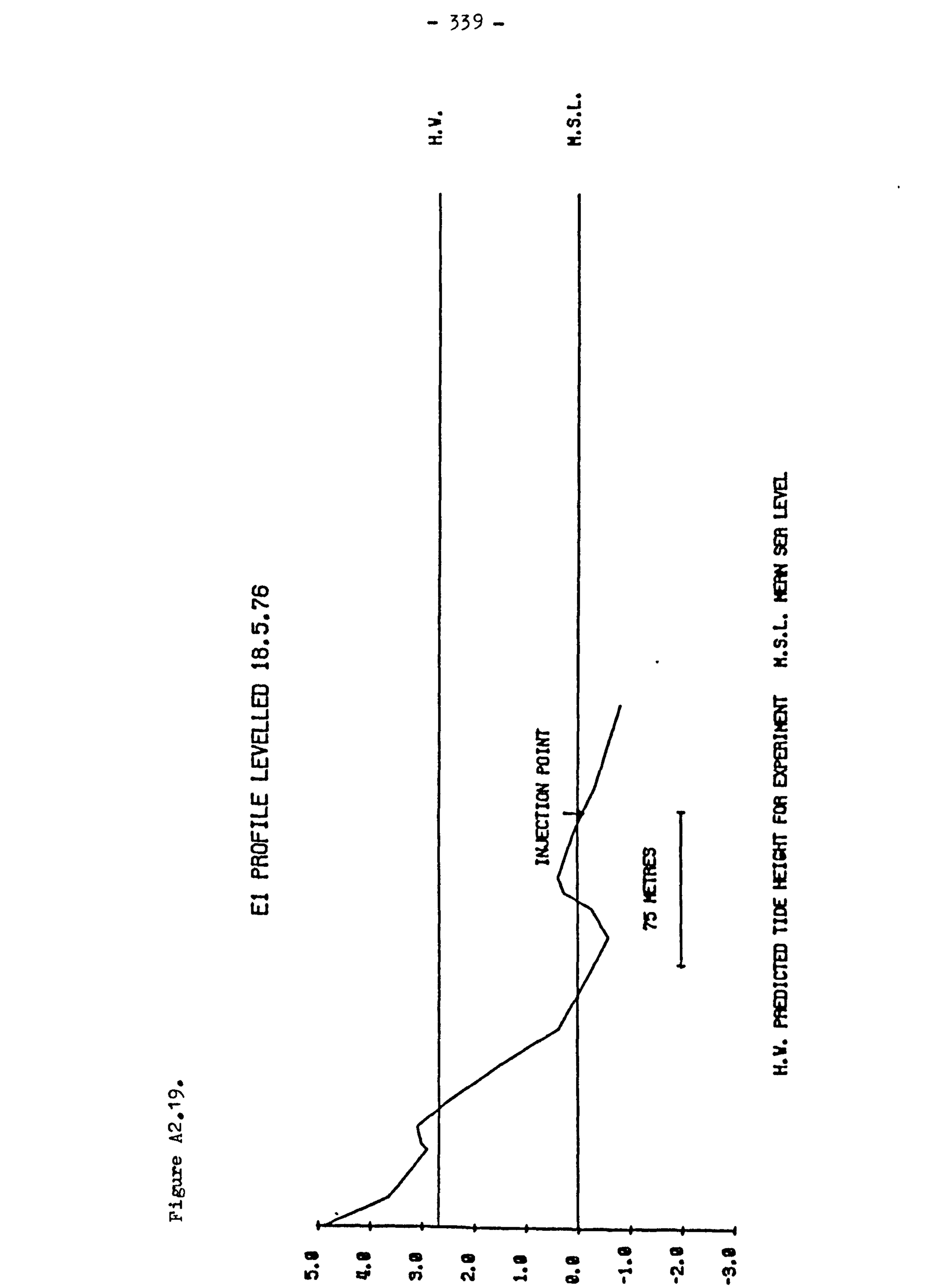
H.W.
M.S.L.
E1 PROFILE LEVELLED 18.5.76
INJECTION POINT
75 METRES
H.W. PREDICTED TIDE HEIGHT FOR EXPERIMENT
M.S.L. MEAN SEA LEVEL
5.0
4.0
3.0
2.0
1.0
0.0
-1.0
-2.0
-3.0
METRES O.D.NEWLYN

Figure A2.19.

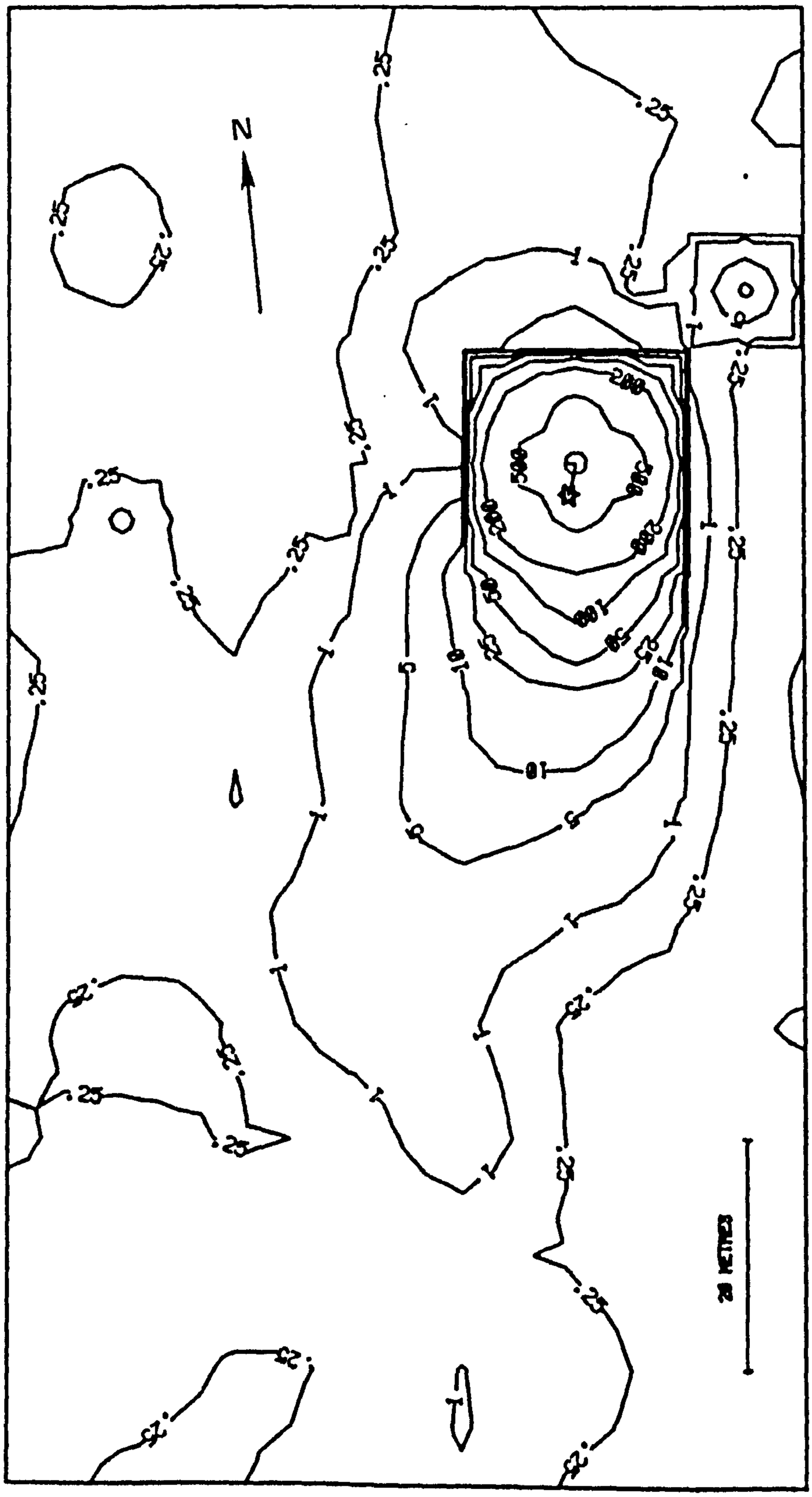
18 5 76 LOWER RIDGE E1 P
N
INJECTION POINT
CENTRE OF GRAVITY
25 METRES

Figure A2.20.

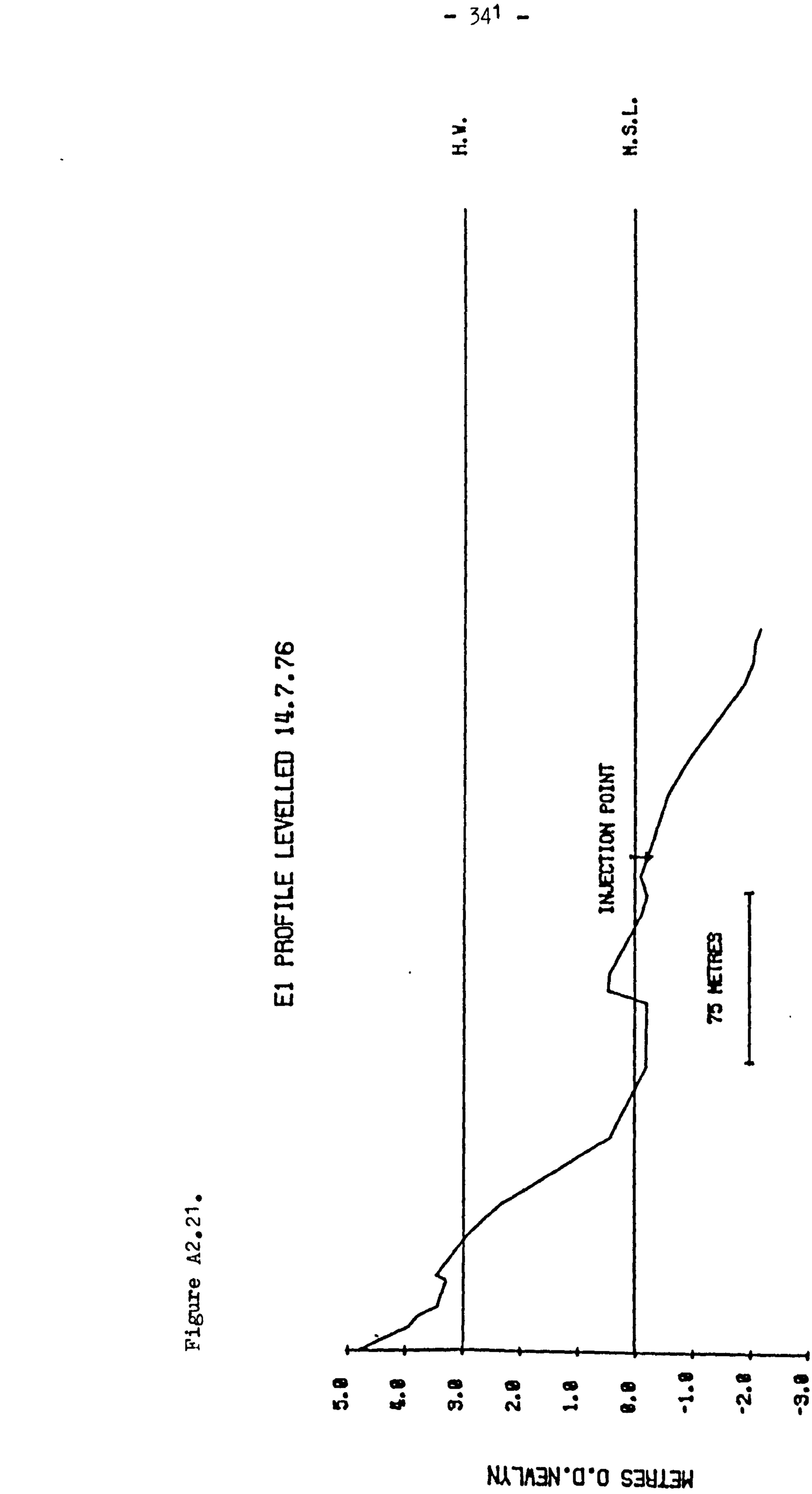

Figure A2.21. E1 PROFILE LEVELLED 14.7.76

H.W. PREDICTED TIDE HEIGHT FOR EXPERIMENT M.S.L. MEAN SEA LEVEL

Figure A2.22.

14 7 76 LOWER RIDGE E1 Y

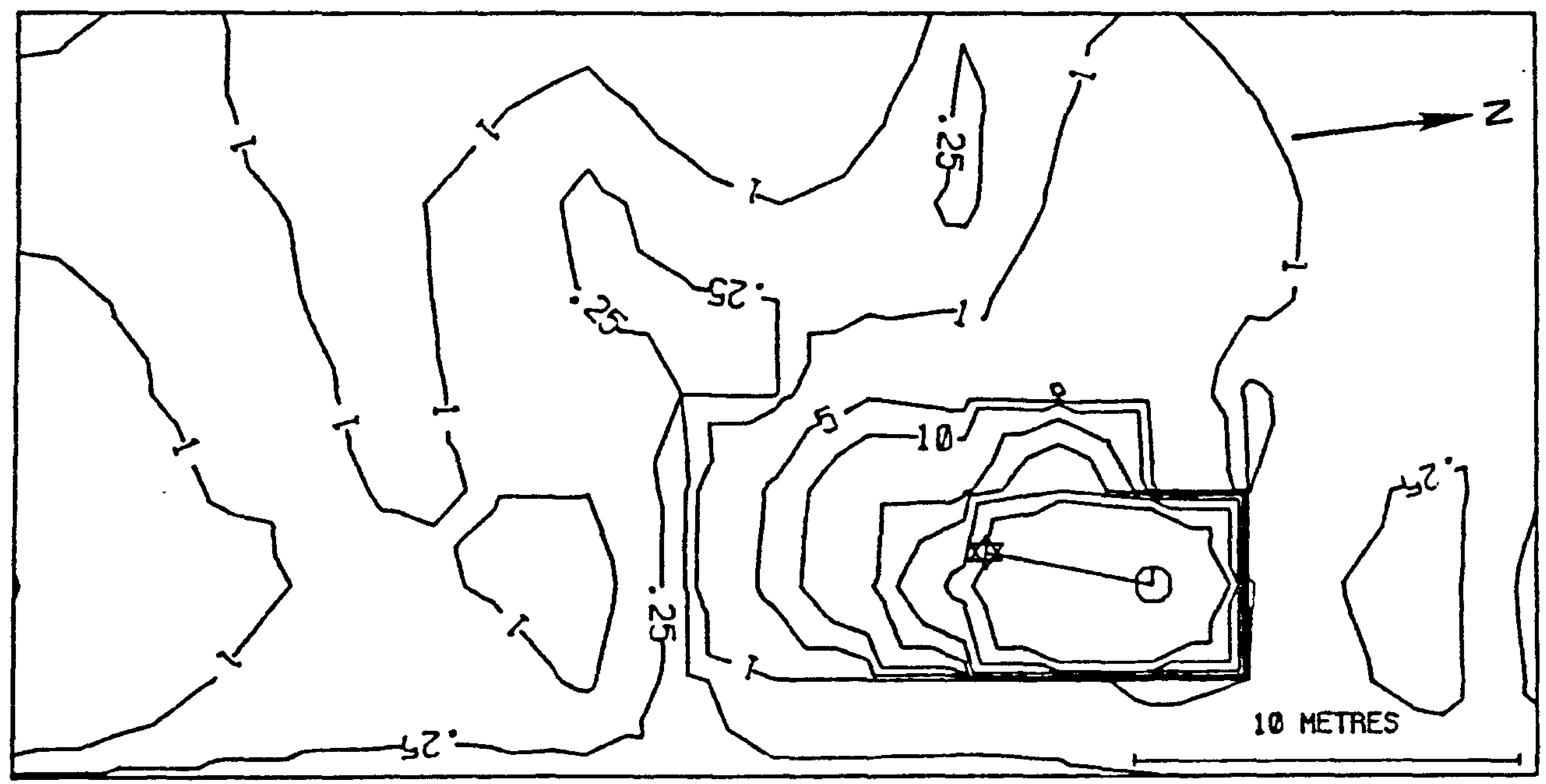

INJECTION POINT ⊙ CENTRE OF GRAVITY ✡

21·9·76 Upper Ridge E1 Orange 0·33mm

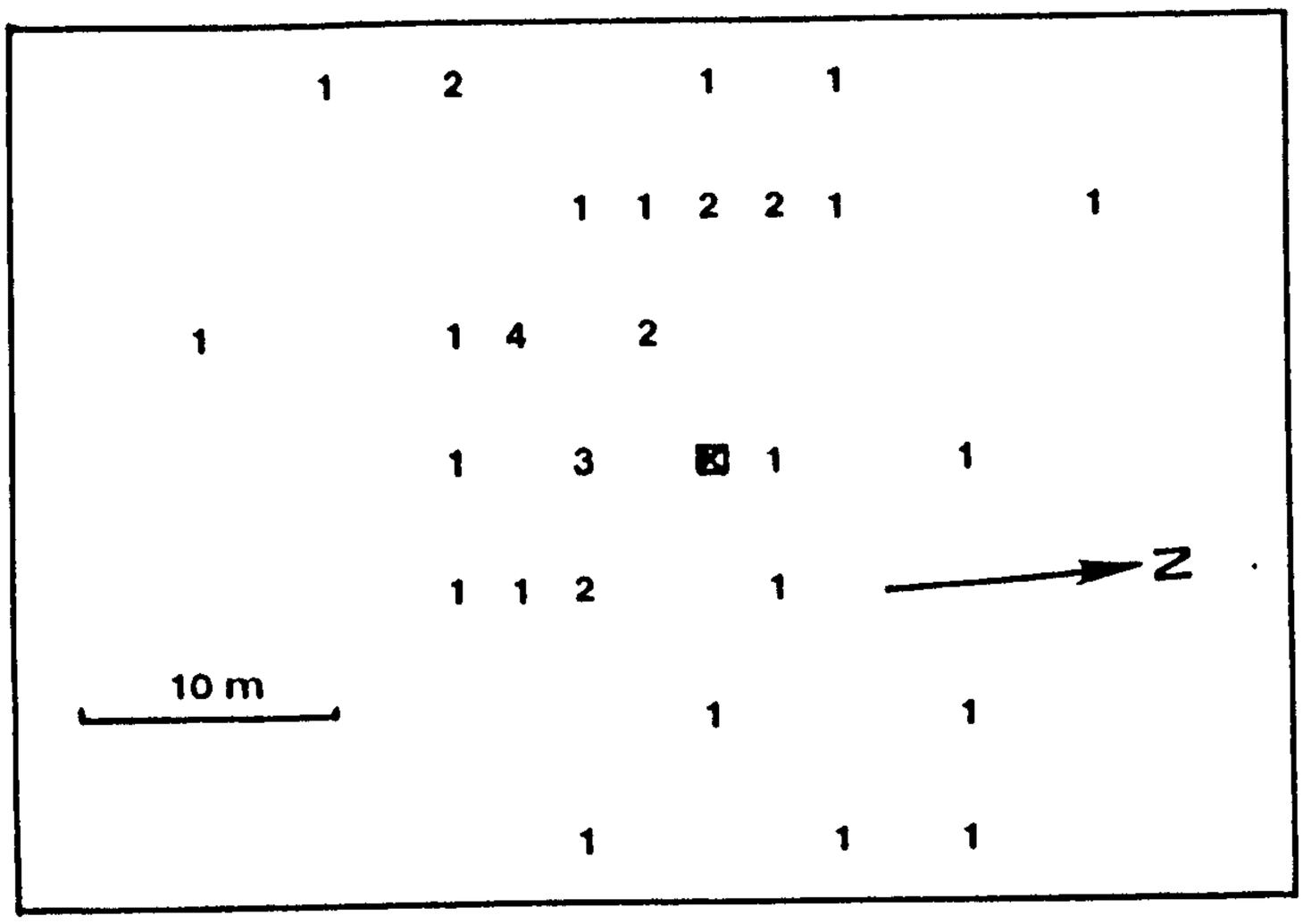

⊠ Tracer Release Point

21·9·76 Upper Ridge E1 Blue 0·45mm

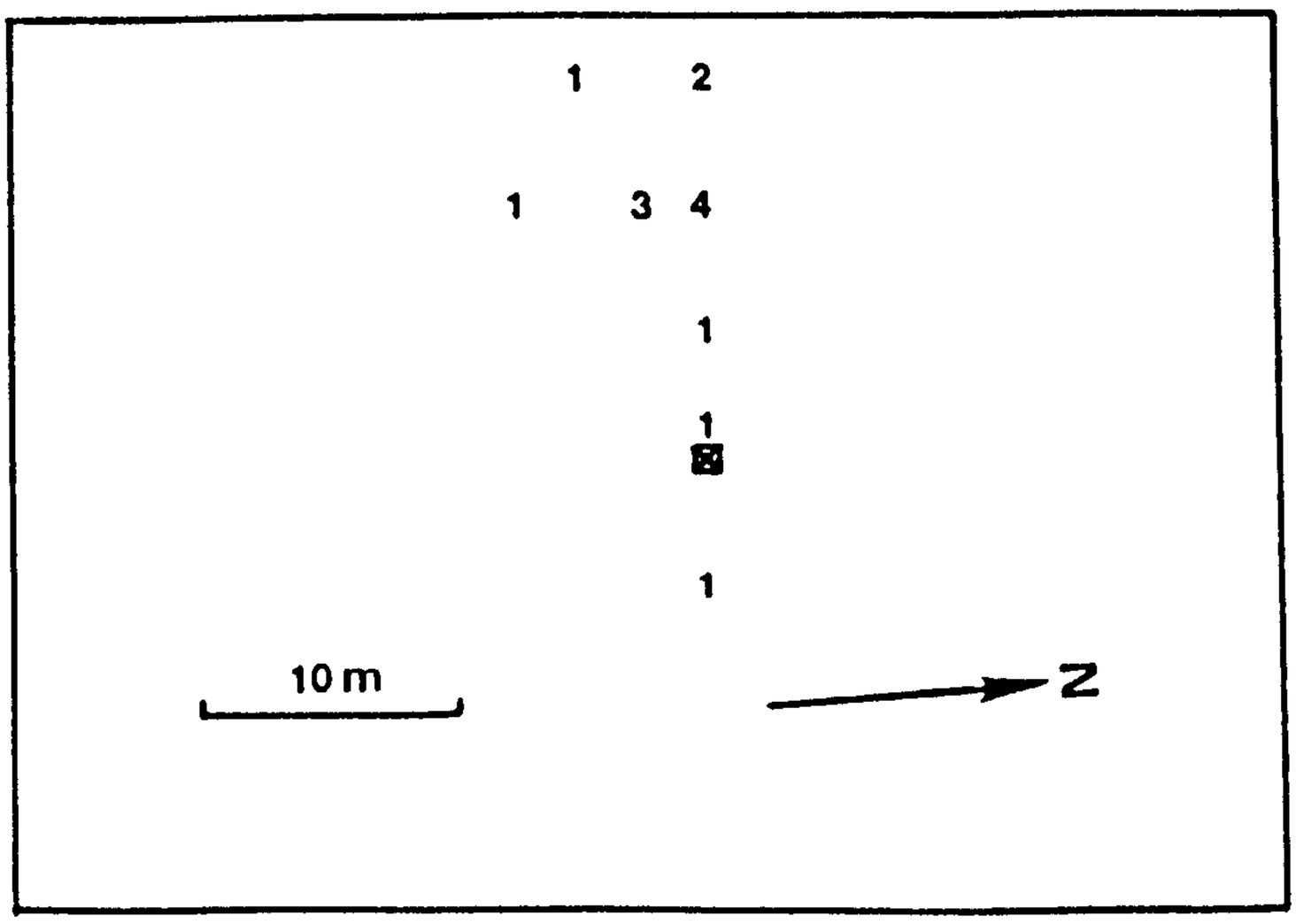

⊠ Tracer Release Point

Figure A2.23 Tracer maps for grain size test 21.9.76 upper ridge E1.

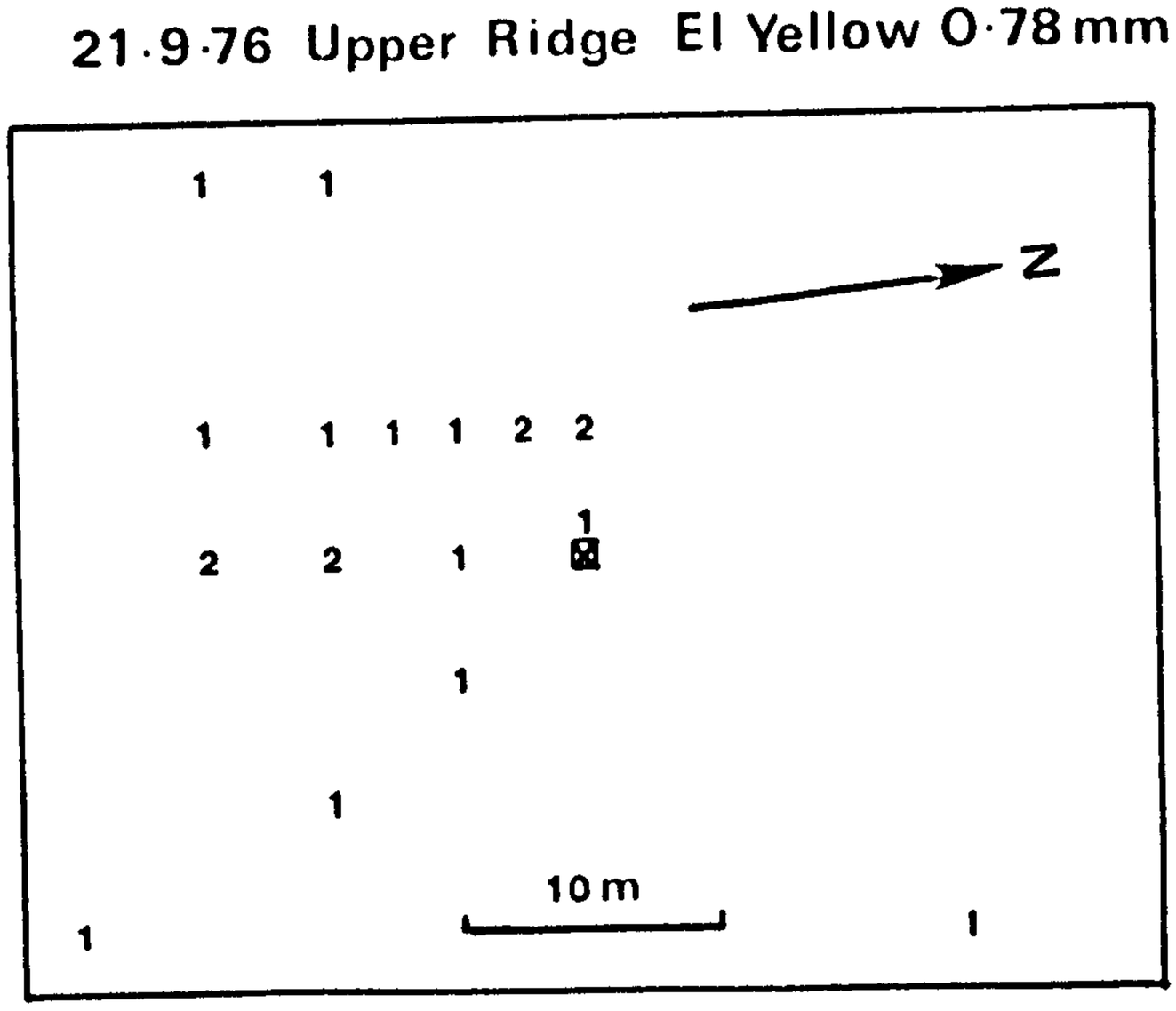

Figure A2.24. Tracer map for grain size test 21.9.76 upper ridge E1.

BIBLIOGRAPHY.

Akima, H. (1974): Bivariate interpolation and smooth surface fitting based on local procedures. Communications of A.C.M., 17, 26-27.

Akima, H. (1974): A method of bivariate interpolation and smooth surface fitting based on local procedures. Communications of A.C.M., 17, 18-20.

Bagnold, R.A. (1963): Mechanics of marine sedimentation. In: M.N. Hill (ed.) (1963), The Sea. Interscience, New York, Volume III, pp.507-528.

Bagnold, R.A. (1946): Motions of waves in shallow water, interactions between waves and sand bottoms. Proc. Royal Soc. London. Series A, 187, 1-185.

Bagnold, R.A. (1966): An approach to the sediment transport problem from general physics. U.S. Geological Survey, Washington D.C., Prof. Paper 422 I.

Barnes, F.A. and C.A.M. King (1955): Beach changes in Lincolnshire since 1953 storm surge. East Midland Geogr., 1, 18-28.

Barnes, F.A. and C.A.M. King, (1957): The spit at Gibraltar Point, Lincolnshire. East Midland Geogr., 8, 22-31.

Barnes, F.A., and C.A.M. King (1961): Salt marsh development at Gibraltar Pt. Lincs. East Midland Geogr., 15, 20-21.

Batschelet, E. (1965): Statistical methods for the analysis of problems of animal orientation and certain biological rhythms. American Institute of Biol. Sciences, Monograph.

Bijker, E.W., J.P. Kalkwijk, J. and S.T. Pieter (1974): Mass transport in gravity waves on a sloping bottom. Proceedings of 12th Conference on Coastal Engineering (ASCE), New York, 447-465.

Boon, J.D. III (1968): Trend surface analysis of sand tracer distribution on a carbonate beach, Bimini, British West Indies. Journ. Geol., 76, 71-87.

Boon, J.D. III (1969): Quantitative analysis of beach sand movement, Virginia Beach, Virginia. Sedimentology, 13, 85-103.

Bowen, A.J. and D.L. Inman (1969): Rip currents 2 laboratory and field observation. Journ. Geophysical Research, 74, 5477-90.

Caldwell, J.M. (1956): Wave action and sand movement near Anaheim Bay. California, U.S. U.S. Army Corps of Engineers, Beach Erosion Board, Tech. Memo. No.68, Washington D.C.

Camber, G. (1973): The retreat of unconsolidated Quaternary cliffs. Unpublished Ph.D. Thesis. Univ. of East Anglia.

Carstairs, M.R., F.M. Neilson and H.D. Altinbilek (1969): Bed forms generated under an oscillatory flow analytical and experimental study. U.S. Army Corps of Engineers Coastal Engineering Research Centre., Tech. Memo. 28.

Castanho, J. (1970): Influence of grain size on littoral drift. Proceedings of 12th Conference on Coastal Engineering, 891-898.

Cherry, J.A. (1966): Sand movement along equilibrium beaches north of San Francisco. Journ. Sedimentary Petrology, 36, 341-357.

Coastal Engineering Research Centre (1973): Shore protection manual. U.S. Army Corps of Engineers, Washington D.C., 3 vols.

Crain, I.K. (1970): Computer interpolation and contouring of two dimensional data: a review. Geoexploration, 8, 71-86.

Crawford, N.H. and R.K. Linsley (1966): Digital simulation in hydrology: Stanford watershed model IV. Dept. of Civ. Eng., Stanford Univ., Stanford, California. Tech. Report 39.

Crickmore, M.J. and G.H. Lean (1962,A): The measurement of sand transport by means of radioactive tracers. Proc. Royal Society, Maths. and Pure Science, Series A, 266, 402-421.

Crickmore, M.J. and G.H. Lean (1962,B): Sand transport by the time integration method with radioactive tracers. Proc. Royal Society, Maths. and Pure Science, Series A, 270, 27-47.

Davies, J.L. (1964): A morphogenetic approach to world shorelines. Zeits.für Geomorph., 8, 127-142.

Davis, W. (1962): Recent sediments of the Gibraltar Point area. Unpublished Ph.D. Thesis. Univ. of London.

de Vries, M. (1973): Applicability of fluorescent tracers. In: Tracer techniques in sediment transport. International Atomic Energy Authority, Vienna. Tech. Rept. 145, H.M.S.O. pp.105-124.

Draper, L. (1968): Waves at Smith's Knoll Light Vessel, North Sea. National Institute of Oceanography Internal Report A33.

Draper, N.D. and H. Smith (1966): Applied regression analysis. Wiley, New York.

Dugdale, R.E. (1977): Movement of sediment in the nearshore zone, Gibraltar Point, Lincolnshire. Unpublished Ph.D. Thesis.

Duncan, J.R. (1964): The effects of water table and tidal cycle on swash backwash sediment distribution and beach profile development. Marine Geology, 2, 186-197.

Eagleson, P.S. and R.G. Dean (1961): Wave induced motion of bottom sediment particles. Trans. American Soc. Civil Engineers, 126, 1162-1189.

Ebdon, D.E. (1977): Spatial statistics. Blackwell, Oxford.

Evans, O.F. (1939): Sorting and transportation of material in swash and backwash. Journ. of Sedimentary Petrology, 9, 28-31.

Galvin, C.J. (1968): Breaker type classification on three laboratory beaches. Journ. Geophysical Res., 12, 3651-3659.

Galvin, C.J. and S. Savage (1966): Longshore currents at Nags Head, North Carolina. U.S. Army Corps of Engineers, Coastal Engineering Research Centre. Bulletin 2.

Gould, A.L. (1969): A regression technique for angular variates. Biometrics, 25, 683-700.

Grosenbaugh, L.R. (1967): REX : Fortran 4 system for combinatorial screening or conventional analysis of multivariate regression. Berkeley, California Pacific S.W. Forest and Range Experimental Station U.S. Forest Service, Paper P.S.W. - 44.

Hama, F.R. (1954): Boundary-layer characteristics for smooth and rough surfaces. Soc. Naval Architects and Mar.Eng., 62, 322-58.

Harrison, W. (1969): Empirical equation for foreshore changes over a tidal cycle. Marine Geology, 7, 529-551.

Harrison, W. (1970): Prediction of beach changes. In: C. Board, R.J. Chorley, P. Haggett and D.R. Stoddart, Progress in Geography, 2, Edward Arnold, London, pp.207-235.

Harrison, W. and W.C. Krumbein (1964): Interaction of beach, ocean atmosphere system at Virginia Beach, Virginia. U.S. Army Coastal Engineering Research Centre. Tech. Memo. No.7, Washington D.C.

Harrison, W., E.W. Rayfield, J.D. Boon III, G. Reynolds, J.B. Grant and D. Tyler (1968): A time series from the beach environment. U.S. Dept. of Commerce Environmental Science Services Administration Research Laboratories, Atlantic Ocean Laboratories,Tech. Memo. 1.

Harrison, W., J.D. Boon III, C.S. Fang, S.N. Wang and L.E. Fausak (1971): Investigation of the water table in a tidal beach. Office of Naval Research Geography Branch, Special Scientific Rept. No.60, Virginia Instit. of Marine Science.

Hauser, D.P. (1974): Some problems in the use of stepwise regression techniques in geographical research. Canadian Geographer, 18, 148-158.

Harvey, D. (1969): Explanation in geography. Edward Arnold, London.

Heap, B.R. (1974,A): Two Fortran contouring routines. National Physical Laboratory. Rpt. NAC 47 Dept. of Trade and Industry.

Heap, B.R. (1974,B): A simple curve drawing algorithm. National Physical Laboratory. Rpt. NAC 49 Dept. of Trade and Industry.

Heap, B.R. and M.G. Pink, (1969): Three contouring algorithms. National Physical Laboratory, Division of Numerical and Applied Maths. Rpt. DNAM, 81.

Holtan, N.H., G.J. Stiltner, W.H. Henson and N.C. Lopez (1975): USDAHL - 74, Revised model of watershed hydrology. Agric. Res. Service, U.S. Dept. of Agriculture. Tech. Bull. 1518.

Ingle, J.C. (1966): Movement of beach sand. Developments in Sedimentology 5, Elsevier, Amsterdam.

Ingle, J.C. and D.S. Gorsline (1973): Use of fluorescent tracers in the nearshore environment. In: Tracer techniques in sediment transport. International Atomic Energy Authority Tech. Rept. 145. H.M.S.O., pp.125-148.

Ingle, J.C. and E.J. Schnack (1971): Sorting in the surf zone; new evidence from fluorescent tracer studies. Abstracts of 8th International Sedimentological Congress, Heidelberg, 47.

Inman, D.L. (1949): Sorting of sediments in the light of fluid mechanics. Journ. Sedimentary Petrology, 19, 51-70.

Inman, D.L. and R.A. Bagnold (1963): Littoral processes. In: M.N. Hill (ed.) 1963, The Sea. Interscience, New York, Volume III, 529-533.

Inman, D.L. and A.J. Bowen (1963) Flume experiments on sand transport by waves and currents. Proc. 8th Conference on Coastal Engineering, 137-50.

Ippen, A.T. and P.S. Eagleson (1955): A study of sediment sorting by waves shoaling on a plane beach. U.S. Army Corps of Engineers Beach Erosion Board. Tech. Memo. 63.

James, W.R. (1970): A class of probability models for littoral drift. Proc. 12th Conference on Coastal Engineering. 2. 83.

Jonsson, I.G. (1966): Wave boundary layers and friction factors. Proc. 10th Conference on Coastal Engineering, 127-148.

Kamphuis, J.W. (1973): Sediment transport by waves over a flat bed. Engineering Dynamics of the Coastal Zone, Sydney

King, C.A.M. (1951): Depth of disturbance of sand on sea beaches by waves. Journ. of Sedimentary Petrology, 21, 131-140.

King, C.A.M. (1953): Relationship between wave incidence, wind direction and beach changes at Marsden Bay, Co. Durham. Trans. Institute of Brit. Geographers, 19, 13-23.

King, C.A.M. (1964) The character of the offshore zone and its relationship to the foreshore near Gibraltar Point, Lincolnshire. East Midland Geographer, 3, 230-243.

King, C.A.M. (1968): Beach measurements at Gibraltar Point, Lincolnshire. East Midland Geographer, 4, 295-300.

King, C.A.M. (1970): Changes in the spit at Gibraltar Point, Lincolnshire. East Midland Geographer, 5, 19-30.

King, C.A.M. (1971): Techniques in Geomorphology. Edward Arnold, London.

King, C.A.M. (1972): Beaches and coasts, 2nd edition, Edward Arnold, London.

King, C.A.M. (1973): The dynamics of beach accretion in south Lincolnshire, England. In: D.A. Coates (ed.) (1973), Coastal geomorphology. Publication in Geomorphology Univ. of New York, Binghampton, 73-98.

King, C.A.M. and W.W. Williams (1949): The formation and movement of sand loss by wave action. Geographical Journ., 107, 70-84.

King, C.A.M. and F.A. Barnes (1964): Changes in the configuration of the inter tidal beach zone of part of the Lincolnshire coast since 1951. Zeits. für Geomorph., 8, 105-126.

Kmenta, J. (1971): Elements of econometrics. Macmillan, New York.

Komar, P.D. (1969): The longshore transport of sand on beaches. Unpublished Ph.D. thesis, University of California, San Diego.

Komar, P.D. (1971): The mechanics of sand transport on beaches. Journ. Geophys. Res., 76, 713-221.

Komar, P.D. (1976): Beach processes and sedimentation. Prentice-Hall, Englewood Cliffs, New Jersey.

Komar, P.D. and D.L. Inman (1970): Longshore sand transport on beaches. Journ. Geophys. Res., 75, 5914-5927.

Komar, P.D. and M.L. Miller (1973): The threshold of sediment movement under oscillatory water waves. Journ. Sedimentary Petrology, 43, 1101-1110.

Komar, P.D. and M.L. Miller (1975): On the comparison between the threshold of sediment motion under waves and unidirectional currents with a practical evaluation of the threshold. Journ. of Sedimentary Petrology, 45, 362-367.

Komar, P.D. (1977): Selective longshore transport rates of different grain size fractions within a beach. Journ. of Sedimentary Petrology, 47, 1444-1453.

Krumbein, W.C. (1961): The analysis of observational data from natural beaches. U.S. Army Crops of Engineers Beach Erosion Board, Tech. Memo. 130.

Krumbein, W.C. (1976): Probabilistic modelling in geology. In: D.F. Merriam (ed.) (1976), Random processes in geology, Springer-Berlag.

Langhaar, H.L. (1951): Dimensional analysis and the theory of models. Wiley, New York.

Lean, G.H. and M.J. Crickmore (1966): Dilution methods of measuring transport of sand from a point source. Journ. of Geophys. Res., 71, 5843-5855.

Longuet-Higgins, M.S. (1952): On the statistical distribution of the heights of sea waves. Journ. of Marine Research, 11, 245-6.

Longuet-Higgins, M.S. (1953): Mass transport in water waves. Phil. Trans. Royal Society (London), Series A, 245, 535-581.

Longuet-Higgins, M.S. (1970): Longshore currents generated by obliquely incident sea waves. Journ. Geophys. Res., 75, 6778-89.

Longuet-Higgins, M.S. (1972): Recent progress in the study of longshore currents. In: R.E. Meyer (1972) Waves on beaches and resulting sediment transport, Academic Press, New York, 203-248.

Longuet-Higgins, M.S. and R.S. Stewart (1963): A note on wave set up. Journ. of Marine Res., 21, 4-10.

Longuet-Higgins, M.S. and R.S. Stewart (1964): Radiation stress in water waves; a physical discussion with applications. Deep Sea Res., 11, 529-563.

Ludwick, J.C. (1974): Variations in boundary drag coefficient in the tidal entrance to Chesapeake Bay, Virginia. Inst. of Oceanography, Old Dominion Univ., Norfolk Virginia, Tech. Report, 19.

McBride, E.F. (1971): Mathematical treatment of size distribution data. In: R.F. Carver (ed.) Procedures in Sedimentary Petrology, Wiley-Interscience, New York.

McLain, D.M. (1972): Drawing contours from arbitrary data points. Computer Journal, 17, 318-324.

Maddala, G.S. (1977): Econometrics. McGraw Hill, New York.

Madsen, O.S. and W.D. Grant (1975): The threshold of sediment movement under oscillatory water waves: A discussion. Journ. of Sedimentary Petrology, 45, 360-361.

Madsen, O.S. and W.D. Grant (1976): Sediment transport in the coastal environment. Water resources and Hydrodynamics. Dept. of Civil Engineering, Massachusetts Institute of Technology, Internal Report 209.

Mather, P.M. (1975): Computational methods of multivariate analysis in physical geography. J. Wiley, London.

Melton, M.A. (1957): An analysis of the relations among elements of climate, surface properties and geomorphology. Office of Naval Research Project NR 389-042 Tech. Report 11.

Miller, R.L. and J.M. Zeigler (1958): A model relating dynamics and sediment pattern in equilibrium in the region of shoaling waves, breaker zone and foreshore. Journ. of Geology, 66, 417-441.

Mogridge, G.R. and J.W.Kamphuis (1973): Experiments on bed form generation by wave action. Proc. of 13th Conference on Coastal Engineering, 1123-1142.

Murray, S.P. (1967): Control of grain size dispersion by particle size and wave state. Journ. of Geology, 75, 612-634.

Niederoda, A.W. (1974): Transport at right angles to the littoral system. In: W.F. Tanner (ed.) (1974) Sediment transport in the nearshore zone. Proc. of Symposium, Florida State Univ. 81-103.

Norcliffe, G.B. (1977): Inferential statistics for geographers. Hutchinson, London.

Otvos, E.G. (1965): Sedimentation - erosion cycles of single tidal periods on Long Island Sound beaches. Journ. of Sedimentary Petrology, 35, 604-609.

Owen, A.E.B. (1952): Coast erosion in East Lincolnshire. Lincolnshire Historian, 9, 330-339.

Parker, W.R. (1971): Aspects of the marine environment at Formby Point, Lancs. Unpublished Ph.D. Thesis, Liverpool Univ.

Parker, W.R. (1976): Sediment mobility and erosion on a multibarred foreshore (S.W. Lancs. U.K.). In: J. Hails and A. Carr (ed.) (1976) Nearshore sediment dynamics and sedimentation, Wiley, London.

,

Patrick, D.A. and R.L. Wiegel (1954): Amphibian tractors in the surf. Conf. Ships Waves, 397.

Price, W.A. (1969): Variable dispersion and its effects on the movements of tracers on beaches. Proc. 11th Conf. on Coastal Engineering, 329-384.

Putnam, J.A., W.H. Munk and M.A. Trayler (1949): The prediction of longshore currents. Trans. American Geophysical Union, 30, 337-345.

Raudkivi, A.J. (1967): Loose boundary hydraulics Pergamon, Oxford.

Rector, R.L. (1954): Laboratory study of the equilibrium profiles of beaches. U.S. Army Corps of Engineers, Beach Erosion Board, Tech. Memo. 41.

Robinson, A.H.W. (1964): The inshore waters, sediment supply and coastal changes of part of Lincolnshire. East Midland Geographer, 6, 307-321.

Robinson, A.H.W. (1966): Residual currents in relation to the shoreline of the East Anglian coast. Marine Geology, 4, 57-84.

Robinson, A.H.W. (1968): The submerged glacial landscape of the Lincolnshire coast. Trans. Institute of British Geogrs., 44, 119-132.

Russell, J.R. (1978): Tidal currents and sediment movement in the nearshore zone at Gibraltar Point, Lincolnshire. Unpublished Ph.D. Thesis, Nottingham University.

Russell, R.C.H. and J.D.L. Osorio (1958): An experimental investigation of drift profiles in a closed channel. Proc. 6th Conf. on Coastal Engineering, 171-183.

Savage, R.P. (1959): Laboratory study of effects of grains on rate of littoral transport. U.S. Army Corps of Engineers, Beach Erosion Board, Tech. Memo. 68.

Schiffman, A. (1965): Energy measurements in the swash-surf zone. Limnol. and oceanog., 10, 255-260.

Schwartz, M.J. (1967): Littoral zone tidal cycle sedimentation. Journ. of Sedimentary Petrology, 37, 677-683.

Seber, G.A.F. (1977): Linear Regression Analysis. Wiley, New York.

Seibold, E. (1963): Geological investigation of nearshore sand transport. In: M. Sears (ed.) (1963): Progress in Oceanography 1, Pergamon Press, New York, 3-70.

Shepard, F.P. and D.L. Inman (1950): Nearshore circulation related to bottom topography and wave refraction. Trans. American Geophysical Union, 31, 555-565.

Shields, A. (1936): Anwerdung der Ahnlichkeits Mechanik und der Turbulenzferschung auf die Geschiebe Berwegung. Preuss. Versuchanstalt für Wasserbau und Schiffbau, Berlin.

Siegel, S. (1956): Non-parametric Statistics for the Behavioural Sciences. McGraw-Hill, New York.

Silvester, R. and G.R. Mogridge (1971): Reach of waves to the bed of the continental shelf. Proc. 12th Conf. on Coastal Engineering, 651-667.

Stiuver, M. and J.A. Purpura (1968): Application of fluorescent coated sand in littoral drift and inlet studies. Proc. 11th Conf. on Coastal Engineering, 307.

Strahler, A.H. (1966): Tidal cycle changes in an equilibrium beach, Sandy Hook, New Jersey. Journ. Geology, 74, 247-268.

Swinnerton, H.H. (1931): The post glacial deposits of the Lincolnshire Coast. Quart. Journ. Geological Society, London, 87, 360-375.

Swinnerton, H.H. (1936): The physical history of east Lincolnshire. Trans. Lincolnshire Naturalists Union, Presidential Address, 91-100.

Swinnerton, H.H. and P.E. Kent, (1949): The Geology of Lincolnshire. Lincolnshire Natural History Brochure, 1. Lincolnshire Naturalist Union, Lincoln.

Teleki, P.G. (1966): Fluorescent sand tracers. Journ. of Sedimentary Petrology, 36, 468.

Teleki, P.G. (1967): Automatic analysis of tracer sand. Journ. of Sedimentary Petrology, 37, 747.

Thornton, E.B. (1973): Distribution of sediment transport across the surf zone. Proc. 13th Conf. on Coastal Engineering, 1049-1068.

Tukey, J.W. (1969): Analysing data - sanctification or detective work? American Psychologist, 24, 83-91.

Vollbrecht, K. (1966): The relationship between wind records, energy of longshore drift and energy balance off the coast of a restricted water body as applied to the Baltic. Marine Geology, 4, 119-148.

Watts, G.M. (1953): Study of sand movement at South Lake Worth Inlet, Florida. U.S. Army Corps of Engineers, Beach Erosion Board, Tech. Memo. 42.

Yalin, M.S. (1972): Mechanics of sediment transport. Pergamon Press, Oxford.

Yasso, W.E. (1962): Fluorescent coatings on coarse sediments: an integrated system. U.S. Navy, Office of Naval Research, Tech. Report 1.

Yasso, W.E. (1966): Formulation and use of fluorescent tracer coatings in sediment transport studies. Sedimentology, 6, 287-301.

Yuill, R.S. (1971): Standard deviational ellipse: an updated tool for spatial analysis. Geografiska Annaler, 538, 28-39.

Zenkovitch, V.P. (1960): Fluorescent substances as tracers for studying the movement of sand on the sea bed; experiments conducted in the U.S.S.R. Dock Harbour Authority, 40, 280-283.

Zenkovitch, V.P. (1967) Processes of coastal development. Trans. R.G. Foy, ed. J.A. Steers. Oliver and Boyd, Edinburgh.

ADDITIONAL REFERENCES

HARPER, S. (1976): The dynamics of salt marsh development in south-east Lincolnshire. Unpublished Ph.D. Thesis, Nottingham University.

SONU, C. J. (1972): Comments on a paper by A. J. Bowen and D. L. Inman "Edge waves and crescentic bars", J. Geophys. Res., 77, 33, 6629-31.